

SPIN POLARIZATION AND MAGNETIC EFFECTS IN RADICAL REACTIONS

K. M. Salikhov, Yu. N. Molin,
R. Z. Sagdeev, A. L. Buchachenko

Edited by
Yu. N. Molin

Akadémiai Kiadó, Budapest



**SPIN POLARIZATION
AND
MAGNETIC EFFECTS
IN RADICAL REACTIONS**



SPIN POLARIZATION AND MAGNETIC EFFECTS IN RADICAL REACTIONS

K. M. Salikhov, Yu. N. Molin, R. Z. Sagdeev

*Institute of Chemical Kinetics and Combustion
USSR Academy of Sciences, Siberian Branch
Novosibirsk, USSR*

A. L. Buchachenko

*Institute of Chemical Physics
USSR Academy of Sciences
Moscow, USSR*

Edited by

Yu. N. Molin



Akadémiai Kiadó, Budapest 1984

Translated by

G. Z. RIBINA and L. Ya. YUZINA

Translation editor

P. W. ATKINS
University of Oxford

This monograph is published by Elsevier Science Publishers as volume 22 in the series of
'Studies in Physical and Theoretical Chemistry'.

ISBN 963 05 2948 3

© *Akadémiai Kiadó, Budapest 1984*

Joint edition published by Akadémiai Kiadó, The Publishing House of the Hungarian Academy
of Sciences, Budapest, Hungary and Elsevier Science Publishers, Amsterdam,
The Netherlands

Printed in Hungary

CONTENTS

Editor's Preface	9
Authors' Preface	11
1 Introduction	13
1.1 Radical pairs and their reactions	13
1.2 Mechanisms of RP singlet-triplet transitions	16
1.3 The origin of CIDNP and magnetic effects in radical reactions	22
1.4 Basic steps of investigations	29
2 The theory of radical recombination	32
2.1 The dynamics of molecular motions in solutions and the spin-independent theory of radical recombination	32
2.1.1 The statistics of radical encounters in solutions	32
2.1.2 Radical recombination	45
2.2 RP singlet-triplet evolution	57
2.2.1 Spin dependence of RP recombination	58
2.2.2 The spin-Hamiltonian and the equation of motion of RP spins	61
2.2.3 RP spin dynamics in high magnetic fields	65
2.2.4 RP spin dynamics in low magnetic fields	72
2.2.5 RP spin dynamics under random hf modulation	89
2.2.6 RP spin dynamics in microwave fields	93
2.3 Mathematical tools of the theory	96
2.3.1 Kinetic equations of RP geminate recombination	98
2.3.2 Radical recombination in homogeneous solutions	106
2.3.3 The method of summation of RP re-encounter contributions to the recombination	110
2.3.4 Methods of approximate calculations	113

3 The theory of magnetic effects in radical reactions	117
3.1 Radical recombination in high magnetic fields	117
3.1.1 The continuous diffusion model	118
3.1.2 The reaction equilibrium	124
3.1.3 Exchange interaction effects	125
3.1.4 Radical diffusion by jumps	128
3.1.5 Recombination in the presence of radical acceptors	131
3.1.6 Recombination of radicals with anisotropic reactivity	132
3.1.7 Radical-ion recombination	134
3.1.8 The exponential model	136
3.1.9 S-T ₊ , T ₋ transitions in high magnetic fields	138
3.1.10 The relaxation mechanism of S-T transitions	140
3.1.11 Sequence of radical pairs	142
3.1.12 Triplet RP recombination	146
3.2 Radical recombination in low magnetic fields	147
3.2.1 The relation between different RP recombination probabilities	148
3.2.2 One-nucleus radical pairs with spin $I = 1/2$	149
3.2.3 Other model systems	157
3.2.4 The semi-classical theory of magnetic effects in the recombination of radicals with a large number of magnetic nuclei	159
3.3 The magnetic isotope effect	162
3.3.1 Qualitative considerations	163
3.3.2 Magnetic isotope effect in zero magnetic field	163
3.3.3 Field dependence of the magnetic isotope effect	165
4 The theory of chemically induced dynamic nuclear and electron spin polarizations	168
4.1 Phenomenological description and spectroscopic manifestation of CIDNP and CIDEP	168
4.1.1 Net polarization effects	168
4.1.2 Multiplet polarization effects	170
4.2 CIDNP theory for high magnetic fields	172
4.2.1 Basic regularities of net CIDNP effects	172
4.2.2 Basic regularities of multiplet CIDNP effects	174
4.2.3 The Kaptein rules for CIDNP effects	175
4.2.4 The operator formalism in CIDNP theory	176
4.2.5 Quantitative CIDNP calculations; absolute values of nuclear polarization	179
4.2.6 The influence of radical acceptors on CIDNP	187
4.2.7 The influence of anisotropic radical reactivity on CIDNP	187
4.2.8 RP substitution	190
4.2.9 CIDNP kinetics	196
4.2.10 Concluding remarks	199
4.3 Low field CIDNP theory	199
4.3.1 Qualitative considerations	199
4.3.2 CIDNP effects in short-lived RPs	206
4.3.3 Approximate calculations	210
4.3.4 Precise calculations	213

4.4 CIDNP in biradical reactions	217
4.5 CIDEP theory in radical pairs	224
4.6 Spin polarizations in triplet molecule reactions	235
5 Experimental observations of magnetic field effects in radical reactions	243
5.1 Spin effects	243
5.2 Reactions of neutral radicals	245
5.3 Recombination of radical-ions	255
5.4 Optical detection of radical-ion pair ESR spectra	269
5.5 Radical reactions in solids	276
5.6 Biochemical reactions	277
5.7 Processes involving triplet molecules	281
5.8 Conclusion	288
6 Magnetic isotope effect	291
6.1 Introduction	291
6.2 Reactions of neutral radicals	292
6.3 Reactions of radical-ions	298
6.4 Conclusion	298
7 Chemically induced dynamic nuclear polarization	300
7.1 Experimental observations and detection of CIDNP	300
7.1.1 High magnetic fields	300
7.1.2 Low magnetic fields	304
7.2 Experimental basis of the CIDNP theory	307
7.2.1 High magnetic fields	307
7.2.2 Low magnetic fields	320
7.3 Chemical applications of CIDNP	328
7.3.1 Identification of radical stages	328
7.3.2 Radical transformation genealogy	330
7.3.3 CIDNP kinetics	332
7.3.4 Radical and nonradical reaction routes	332
7.3.5 Identification of crypto-radical pathways	342

7.3.6 Identification of unstable intermediates	345
7.3.7 Fast reaction kinetics in radical pairs	348
7.3.8 "Hot radicals"	358
7.3.9 CIDNP applications in structural chemistry	360
7.3.10 Chemical applications of low field CIDNP	369
7.4 CIDNP in the gas phase	373
7.4.1 CIDNP in biradical reactions	373
7.4.2 CIDNP in radical-ion reactions	375
7.5 CIDNP in biradicals	376
7.6 Technical applications of CIDNP	379
7.6.1 Nuclear magnetometry	379
7.6.2 Oriented polarized targets	380
7.6.3 Radio-frequency generation with chemical pumping (chemical RASER)	380
7.7 CIDNP detected magnetic resonance	383
8 Chemically induced dynamic electron polarization	387
8.1 Experimental methods of CIDEP observation and analysis	387
8.2 Experimental CIDEP investigations	389
8.2.1 CIDEP in radical pairs	390
8.2.2 CIDEP in reactions of triplet molecules	396
8.3 Conclusion	401
References	403
Subject index	417

Magnetic and spin polarization effects in radical reactions are a new and intensively developing field of chemical physics which has arisen on the borderline of magnetic radiospectroscopy and chemical kinetics. Although the rise of this field, which dates back to the discovery of chemically induced nuclear polarization (1967), was rather unexpected, its further rapid development can be considered as quite natural. The understanding of the physical principles of chemically induced nuclear and electron polarization (CIDNP and CIDEP), the development of their chemical applications, the prediction and discovery of the effects of magnetic fields and magnetic nuclear moments on radical reactions—all this was predetermined both by the intriguing peculiarity of the phenomena and the breadth of their application in chemistry, and by the high level of development of magnetic radiospectroscopy and radical reaction kinetics achieved at that time.

The material treated in this book is based on novel manifestations of the spin selection rule in radical reactions. The new manifestations are associated with the spin transitions in radical pairs induced by interactions of magnetic origin (Zeeman and hyperfine interactions). It is due to these transitions that magnetic interactions can affect the recombination probability of a radical pair. Since the energy of magnetic interactions in free radicals is several orders lower than that of thermal motion, the magnetic effects discussed in this book can be considered as one of the few examples of chemical kinetics 'controlled' by weak interactions. On the other hand, as a result of the spin transitions in radical pairs, a chemical reaction between radicals serves as a mechanism for sorting the nuclear and electron spins. CIDNP and CIDEP effects can therefore be considered as a mechanism of transformation of a chemical disequilibrium into that of nuclear and electron spin systems.

The idea for this book appeared at the moment when the underlying unity of all the phenomena considered became obvious and their basic applications in chemistry were established. The main aim of this book is to sum up the results of this stage of investigations. For the first time the physics and theory of spin polarization and magnetic effects are explored from a common viewpoint. The authors review in detail the papers on magnetic field effects in radical reactions, and vividly illustrate the basic principles of chemical applications of CIDNP and CIDEP.

Now, when the number of investigators engaged or interested in magnetic and spin polarization effects arising in chemical reactions is constantly growing, the present book will be indispensable.

Yu. N. Molin

AUTHORS' PREFACE

The present book is based on the monograph "Magnetic and Spin Effects in Chemical Reactions" by A. L. Buchachenko, R. Z. Sagdeev, and K. M. Salikhov (edited by Yu. N. Molin, "Nauka", Novosibirsk, 1978). We have substantially revised that book, supplied it with a number of new sections and up-to-date results recently obtained on physicochemical applications of the effects of spin polarizations, external fields, and magnetic isotope substitution on radical reactions in solutions.

The monograph consists of eight sections. The introduction deals with the physical principles of chemically induced spin polarizations and magnetic effects in radical reactions. This includes an historical review of the problems. The second section considers the molecular dynamics and the spin motion of radical pairs, and the mathematical tools of modern theory of radical recombination. The third section summarizes the data on the theoretical analysis of the effects of the external field and magnetic isotope substitution on radical recombination. The basic results on the theory of chemically induced nuclear and electron polarizations are discussed in the fourth section. The fifth section sums up experimental data on external field effects on radical reactions (including thermal, photochemical, radiation-chemical, and biochemical reactions). The sixth section is devoted to experiments on magnetic isotope effects. The seventh section reviews experimental results on chemically induced nuclear polarization and the possibilities of CIDNP applications in physics, chemistry, and biology. The main experimental data on chemically induced electron polarization are considered in the eighth Section.

The first Section is written by Yu. N. Molin; Sections 2, 3 and 4 by K. M. Salikhov; Section 5 by Yu. N. Molin and R. Z. Sagdeev; Sections 6 and 7 by A. L. Buchachenko and R. Z. Sagdeev; Section 8 by A. L. Buchachenko.

The authors are pleased to express their gratitude to O. A. Anisimov, Yu. A. Grishin, A. V. Dushkin, R. Kaptein, T. V. Leshina, A. V. Podoplelov, P. A. Purtoov and F. S. Sarvarov for cooperation in obtaining the data considered. We are especially indebted to all the authors and editors for allowing us to use their original material. We are also grateful to the pupils of the Young Programmist School headed by Prof. A. P. Ershov for assistance in preparing the figures to Section 2.2, and S. V. Camyshan for the help in the final preparing of the manuscript.

*K. M. Salikhov,
Yu. N. Molin,
R. Z. Sagdeev,
A. L. Buchachenko*

1 INTRODUCTION

Spin polarization and magnetic effects in free radical reactions are two closely interconnected phenomena based on common physical mechanisms. The phenomenon of spin polarization in chemical reactions embraces chemically induced dynamic nuclear polarization (CIDNP) and chemically induced dynamic electron polarization (CIDEP). The nuclear polarization is detected through anomalous line intensities in the NMR spectra of radical reaction products immediately after their formation (emission or enhanced absorption are observed). The electron spin polarization is detected by observing similar anomalies in the ESR spectra. The effects produced on radical reaction rates by either the external magnetic field or the internal (hyperfine) field induced by a magnetic nucleus are referred to as *magnetic effects*. The dependence of the radical reaction rate on the strength of the hyperfine interactions between a nucleus and an electron results in an isotope effect that is specific for radical reactions; this is the so-called *magnetic isotopic effect*.

All the above phenomena depend on the existence of a stage of interaction between the two radicals in a "cage", when they constitute a *radical pair* (RP). The effects are induced by singlet-triplet transitions occurring within the RP lifetime in the "cage".

There are a number of reviews and monographs exploring CIDNP [1.1-5], CIDEP [1.4-7], and magnetic effects [1.8-10] in radical reactions. The present book treats all these phenomena from a general viewpoint.

1.1 Radical pairs and their reactions

In the broad sense a "cage" is a region of effective recombination of two radicals forming a pair. As long as the radicals are in this region, the probability of their recombination with other particles is negligible as compared to their reaction with each other. Two radicals constituting a pair can diffuse with respect to each other, a reaction between them occurring at their direct contact at the Van der Waals radius. In the end, the radicals either recombine (the notion "recombination" will be further used in the broad sense including disproportionation), or diffuse ad infinitum, or react with some other particles.

In-cage RP lifetimes depend on many factors—radical reactivity, radical diffusion mobility, electrostatic interactions between radicals. Characteristic RP lifetimes are as a rule in the range 10^{-10} to 10^{-8} s.

RPs are usually divided into *correlated* and *uncorrelated* according to their spin state. In correlated RPs the electron spins are mutually orientated in a certain way. When the orientation is antiparallel, the overall spin of the pair is zero, i.e., the pair is *singlet* (S). Otherwise, when the orientation is parallel, the pair spin equals unity and the pair is *triplet* (T). In an external field the energy levels of a triplet RP are split by the Zeeman interaction into three sublevels $-T_+$, T_0 , and T_- in accordance with the three possible projections of the overall spin on the external field direction (+1, 0, -1). The magnitude of this splitting equals $g\beta H_0$ where g is the electron g -value, β is the Bohr magneton, and H_0 is the magnetic field strength. The energies of singlet and triplet RPs are in general unequal on account of the radical exchange interaction. The exchange interaction energy rapidly falls with interradsical distance, and for separations of about 1 nm or more the exchange interaction can be neglected. Figure 1.1 depicts the energy level diagram of singlet and triplet RPs and their splitting in an external field.

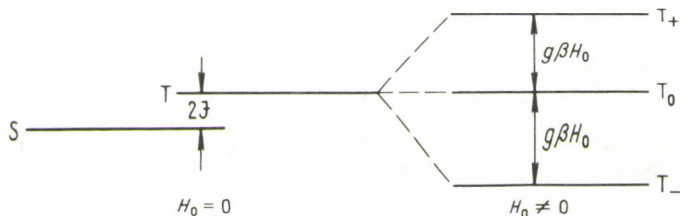


Fig. 1.1. RP energy level diagram. In an external magnetic field the triplet RP level is split into three sublevels

Correlated pairs result from decomposition of molecule-precursors which are in a certain spin state. An elementary decomposition step itself occurs so fast that the RP inherits the electron spin correlation of the molecule-precursor. For example, thermal decomposition, which results as a rule from vibrational excitation of the ground (singlet) state, affords singlet RPs. Photochemical molecular decomposition can occur both from the singlet excited and triplet states, giving singlet or triplet RPs respectively.

The electron spins of uncorrelated pairs are orientated in a random manner. The statistical weight of the singlet state of such pairs equals $1/4$, that of the triplet is $3/4$. Uncorrelated RPs result, for example, from a random encounter of two radicals in the bulk.

The elementary step of RP recombination, as well as the process of RP formation, takes place with overall electron spin conservation. This results in definite spin selection rules for RP recombination: singlet pairs yield recombination products in the singlet (ground or excited) state, while triplet pairs yield the triplet excited state.

In most cases the radical recombination energy is not sufficient for the product to be generated in an excited (triplet or singlet) state. The radical recombination is then possible only if it yields the product in the ground, singlet, state. In this case only singlet but not triplet RPs can recombine, a typical example being alkyl radical recombination. The triplet states of the recombination (alkane) or disproportionation (alkane + olefine) products lie too high in energy to be formed by the recombination energy. Hence, in the case of alkyl radicals, only singlet RPs are reactive.

There are however cases when RPs can recombine both in triplet and singlet states. The recombination of aromatic radical-ions in nonpolar or weakly-polar media can be considered as an example. The recombination energy in this case can exceed that of excitation to the triplet and the first excited singlet states. The triplet pairs then give triplet excited products, and the singlet pairs give singlet (ground or excited) states.

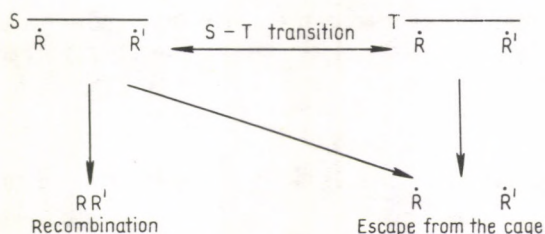


Fig. 1.2. Scheme of processes of in-cage RP recombination. The efficiency of singlet RP recombination reduces as a result of S-T transitions. A triplet RP can recombine only after a S-T transition

Let us now consider the effects of RP singlet-triplet transitions on reactions. Figure 1.2 depicts the reaction scheme for a pair of neutral radicals when recombination is possible only from the singlet state. In the case when the pair is in the correlated triplet state, the recombination is forbidden. However, if the pair turns into singlet within its lifetime, recombination becomes possible. Thus, T-S transitions increase the recombination probability of primary triplet RPs. On the contrary, if the primary pair is singlet, S-T transitions make it nonreactive triplet and thus reduce the recombination probability. Finally, in the case of uncorrelated RPs, a portion of singlet pairs recombine after the first contact, and as a result the RP distribution between singlet and triplet states is shifted towards triplet RPs as compared to the statistical distribution (1:3). In this case singlet-triplet transitions produce qualitatively the same effect as in correlated triplet RPs; i.e., they increase the recombination probability.

The scheme of radical-ion recombination in nonpolar solvents is shown in Fig. 1.3. In this case S-T transitions affect the ratio of singlet and triplet excited molecules. For instance, if the primary RP is correlated singlet-born, triplet-excited molecules can appear only as a consequence of S-T transitions.

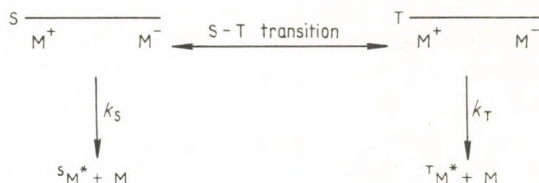


Fig. 1.3. Scheme of processes of aromatic radical-ion recombination. The ratio of singlet and triplet excited molecules depends on the S-T transition rate

The above examples demonstrate that S-T transitions in RPs violate the spin selection rule: because of these transitions a RP, initially in a definite correlated state, can give a product of some other multiplicity. It is however necessary to note that for the mechanism of S-T transitions considered below this violation is only apparent. The RP multiplicity variations occur in the intervals between the chemical interaction steps, and the elementary chemical steps themselves occur without change of spin.

1.2 Mechanisms of RP singlet-triplet transitions

Spin-orbit interactions have been shown by spectroscopic studies to be the basic factor inducing singlet-triplet transitions in molecules. In the case of RPs, however, this mechanism is ineffective. Spin-orbit interactions can be of great importance only if the orbitals of corresponding electrons appreciably overlap, i.e., when the electron spins are interconnected by strong exchange interactions. This is the situation with singlet-triplet transitions in molecules. In radical pairs, as we have noted, exchange interactions fall rapidly with increasing interradsical distances. According to all available data, singlet-triplet RP transitions are most effective at distances where exchange interactions can be neglected and radical electron spins precess independently in an external magnetic field.

However a RP containing a heavy atom can be an exception. The spin-orbital interaction at short distances can be of importance in this case.

Under usual conditions S-T transitions in a pair can be induced by three factors: the difference in the electron spin Larmor precession frequencies of the two radicals in an external magnetic field (*Δg-mechanism*), hyperfine interactions of unpaired electrons with radical nuclei (*hf-mechanism*), and electron spin orientation relaxation (*relaxation mechanism*). In the first two cases, S-T transitions are reversible since they have the character of quantum-mechanical oscillations between singlet and triplet states. To emphasize this feature, one speaks of *singlet-triplet RP evolution*. The relaxation mechanism results in irreversible losses of spin correlation. To consider the S-T transition mechanisms qualitatively, one may employ the vector model of RP spins.

The vector model of S-T transitions. In an external magnetic field H_0 the spin of an unpaired electron and its magnetic moment precess about the field direction with the Larmor frequency

$$\omega = g\beta\hbar^{-1} \cdot H_0,$$

where g is the electron g -value and β is the Bohr magneton. On the vector model, the unpaired electron spins of a singlet RP, \vec{S}_1 and \vec{S}_2 , precess so that their vector sum is always zero (Fig. 1.4 (a)). In the triplet state vector sum of \vec{S}_1 and \vec{S}_2 is non-zero and the total RP spin equals unity. Figures 1.4 (b), (c), (d) show schematically the mutual spin orientations in the three triplet states T_0 , T_+ , T_- conforming to the three values of the total spin projection 0, +1, -1 on to the external field direction.

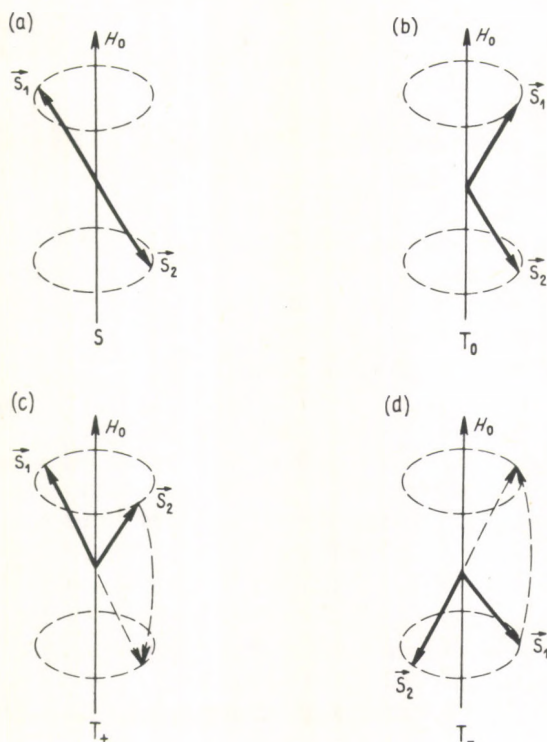


Fig. 1.4. Vector model of RP electron spin states

Figure 1.4 depicts graphically what types of spin motion are responsible for singlet-triplet transitions in RPs. Relative dephasing of the spin precessions is sufficient for transitions between S and T_0 states. Indeed, the only difference between S and T_0 states is that the \vec{S}_1 and \vec{S}_2 precession phases differ by 180° .

Therefore, any physical factors that can affect the relative precession phase of the two spins can induce S-T₀ transitions. The spin precession dephasing cannot, however, lead to T₊-S or T₋-S transitions, for these are possible only if one of the partners changes its spin projection on the quantization axis. Such spin flips are shown in Fig. 1.4 (c), (d) by dashed lines.

The Δg-mechanism. Consider a situation in which two radicals have no magnetic nuclei but their Larmor precession frequencies $\omega_i = g_i \beta \hbar^{-1} H_0$ differ in an external magnetic field H_0 . According to the vector model, the precession is accompanied with periodic transitions between the two vector configurations shown in Figs 1.4 (a) and 1.4 (b); i.e., there are S-T₀ transitions. The frequency of these transitions is determined by the difference of the Larmor precession frequencies,

$$\omega_{\text{ST}_0} = \omega_1 - \omega_2 = (g_1 - g_2) \beta \hbar^{-1} H_0 = \Delta g \beta \hbar^{-1} H_0, \quad (1.1)$$

where ω_1, ω_2 , and g_1, g_2 are the Larmor frequencies and g -values of the radicals. It is necessary to note that the Δg -mechanism of singlet-triplet transitions is effective only in the presence of an external magnetic field: the higher the field, the more frequent the singlet-triplet transitions.

To estimate the Δg -mechanism efficiency, assume the in-cage RP lifetime τ_D to be $\approx 10^{-9}$ s, and $\Delta g \approx 0.001$. This Δg value is typical of organic radicals containing no heavy atoms. An effective S-T₀ mixing occurs provided $\omega_{\text{ST}_0} \cdot \tau_D = 1$. This requirement is fulfilled when $\omega_{\text{ST}_0} = 10^9$ rad/s, i.e., when the external magnetic field is about 10^5 G. If one of the partners is either a radical involving heavy elements or a complex ion of a transition metal, Δg can attain very high values. In this case the Δg -mechanism is effective even in a lower external field.

The hf-mechanism. Manifestations of the hf-mechanism of singlet-triplet RP transitions depend on the external magnetic field strength.

In high fields, when H_0 exceeds that induced by the magnetic nuclei at the location of the unpaired electron ($H_0 > 100$ – 1000 G), the hf-mechanism manifests itself like the Δg -mechanism. In such fields the spins of the unpaired electrons and magnetic nuclei precess independently, and the hf-mechanism corresponds to the effect of an additional local magnetic field that changes the unpaired electron precession frequency. Consider, e.g., a RP with one of the radicals having no magnetic nuclei and the other possessing one nucleus with spin $I = 1/2$ and a hf constant equal to a . Let the g -values of both radicals be equal. The electron spin of the former radical will then precess about the external field with a frequency $\omega = g \cdot \beta \cdot \hbar^{-1} \cdot H_0$, while that of the latter precesses with frequencies $\omega + \frac{a}{2}$ and

$\omega - \frac{a}{2}$ depending on the nuclear spin orientation. Thus, the difference in the precession frequencies will result in S-T₀ transitions, their frequency being $\omega_{\text{ST}_0} = \frac{a}{2}$.

In low magnetic fields, fields comparable to the local hyperfine field, the hf- and Ag-mechanisms show a fundamental difference: the hf field induces transitions from the singlet to the *three* triplet states. The vector model attributes this behaviour to the fact that in the case of a hf interaction the unpaired electron precesses about a total field which is a vector sum of the external and hyperfine fields. In a sufficiently high external field the directions of the total and external fields practically coincide, and hence the electron spin projections on H_0 do not change. In low fields, in contrast, the total field does not coincide with the external one, and thus the precession about the total field affects the spin projection on the external field direction. As a result, transitions from S not only to T_0 but also to T_+ and T_- states become possible.

The above features of the radical spin dynamics obeying the hf-mechanism can be illustrated by considering what happens at zero external field. When $H_0=0$, the electron (S) and nuclear (I) spins of a one-nucleus radical precess about the total spin, making a mutual flip-flop motion (Fig. 1.5). The electron spin configuration corresponding to the triplet T_+ state is seen to turn into the configuration corresponding to the singlet state.

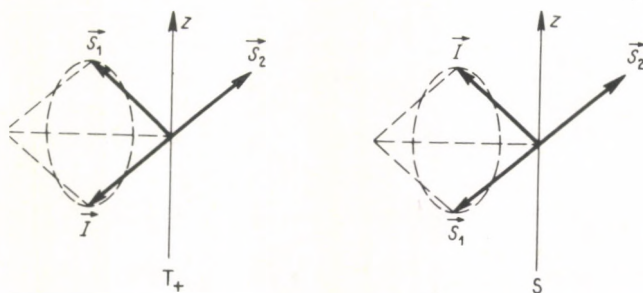


Fig. 1.5. Vector model of one-nucleus RP spin motion in zero field. The electron spin S_1 and nuclear spin I exchange their position as a result of precession about the total spin direction

The frequency of S-T transitions induced by the hf interactions of unpaired electrons with magnetic nuclei is determined by the hf constants obtained from ESR experiments on free radicals. Typical a values for organic free radicals are 10^8 – 10^9 rad/s. It means that the hf-mechanism of S-T transitions is effective at RP lifetimes around 10^{-8} to 10^{-9} s. In some cases hf constants of free radicals can reach much higher values, e.g., those of some organometallic radicals. The transitions then occur within times shorter than the above values.

The relaxation mechanism. The relaxation of spin orientation in an external magnetic field is described by two characteristic times: the *longitudinal relaxation time*, T_1 , characterizing the rate of attaining an equilibrium value of the spin projection on the field direction, and the *phase (or transverse) relaxation time*, T_2 , characterizing the decay rate of spin polarization component normal to H_0 . Phase

relaxation of the S_1 and S_2 spin precessions reduces the coherence, and thus induces $S-T_0$ transitions, the rate being $1/T_2$. The longitudinal spin relaxation leads to $S-T_+$ and $S-T_-$ transitions with the rate $1/T_1$.

In the case of free radicals, electron spin relaxation is caused chiefly by rotation-induced random modulation of anisotropic interactions—hyperfine (hf-anisotropy) and Zeeman (g -tensor anisotropy). When discussing the Δg - and hf-mechanisms, we implicitly took into account only the isotropic components of these interactions. This approximation to the Δg - and hf-mechanisms is justified since, on account of the fast, chaotic radical rotation with a characteristic time of the order of 10^{-11} s, the anisotropic interactions are averaged to zero and the electron spin can sense only an average local field arising from the isotropic component of the interaction. However, in the case of the relaxation mechanism, it is the anisotropic interaction component that induces $S-T$ transitions.

The relaxation due to the dipole-dipole anisotropic interaction of an electron and a spin I nucleus, in the point-dipole approximation, is described by the relations [1.11]

$$\begin{aligned} T_1^{-1} &= 2W/(1 + \gamma_e^2 H_0^2 \tau_0^2), \\ T_2^{-1} &= W[1 + 1/(1 + \gamma_e^2 H_0^2 \tau_0^2)], \end{aligned} \quad (1.2)$$

where

$$W = (2/3)I(I+1)\gamma_e^2\gamma_I^2\hbar^2 r^{-6}\tau_0,$$

r is the distance between the electron and the nucleus, γ_e and γ_I are electron and nuclear gyromagnetic ratios, τ_0 is the correlation time of the radicals rotational motion. The $S-T$ transition rate is seen from eq. (1.2) to decrease with increasing field.

If the relaxation is associated with the g -tensor anisotropy, we have [1.11]

$$\begin{aligned} T_1^{-1} &= (1/55)\overline{\Delta g^2} \beta_e^2 \hbar^{-2} H_0^2 \tau_0 / (1 + \gamma_e^2 H_0^2 \tau_0^2), \\ T_2^{-1} &= (1/30)\overline{\Delta g^2} \beta_e^2 \hbar^{-2} H_0^2 \tau_0 [4 + 3/(1 + \gamma_e^2 H_0^2 \tau_0^2)], \end{aligned} \quad (1.3)$$

where β_e is the Bohr magneton $\overline{\Delta g^2}$ characterizes the scale of the g -tensor anisotropy and is expressed through its principal values,

$$\overline{\Delta g^2} = g_1^2 + g_2^2 + g_3^2 - 3\bar{g}^2, \quad \bar{g} = (g_1 + g_2 + g_3)/3.$$

The $S-T$ transition rate is seen in this case to increase with the magnetic field.

Estimates obtained by eqs (1.2) and (1.3), and also experimental data, show typical values of organic radical relaxation times T_1 and T_2 to be in the range 10^{-6} to 10^{-5} s at a viscosity 1 cP. Hence, the relaxation mechanism is much less effective than the Δg - and hf-mechanisms, and thus can be neglected. However, sometimes RP partners have sufficiently short relaxation times for the relaxation mechanism to be predominant. Although rare in the case of free radicals, such cases are typical of

paramagnetic complex ions and triplet molecules since in them some other more effective spin relaxation mechanisms can occur.

Quantum-mechanical approach to singlet-triplet RP evolution. The description of singlet-triplet transitions in terms of the vector model gives a physical representation of the transition mechanism. To describe the S-T transitions and all related phenomena in detail, one must employ a quantum-mechanical approach. This will be done in theoretical sections of the present book. We now consider the general scheme and basic results of this approach.

In the language of the quantum-mechanical approach, singlet-triplet RP evolution is associated with the fact that neither the singlet nor the triplet states are RP eigenstates in the absence of strong exchange interactions between the unpaired electrons. Therefore, a spin-correlated-born RP must be described by a superposition of several eigenfunctions and hence must be subject to time evolution.

To describe the RP electron spin behaviour, one must solve the Schrödinger equation

$$i\hbar(\partial\psi/\partial t) = \hat{H}\psi, \quad (1.4)$$

where ψ is the RP spin wave function, \hat{H} is the spin-Hamiltonian including, in the general case, the interactions of the unpaired electrons with each other, with the external field, and with the magnetic nuclei.

When there is no exchange interaction between the unpaired electrons (a most important case, as we shall see) the Hamiltonian \hat{H} is

$$\hat{H} = \beta_e H_0 (g_1 \hat{S}_{1z} + g_2 \hat{S}_{2z}) + \sum_i \hbar a_{1i} \hat{S}_1 \hat{I}_{1i} + \sum_j \hbar a_{2j} \hat{S}_2 \hat{I}_{2j}. \quad (1.5)$$

Here the first term describes the Zeeman interaction of the unpaired electrons, and the second and the third terms are the hf interactions of the unpaired electron of each radical with its magnetic nuclei.

The solution of eq. (1.4) with spin-Hamiltonian (1.5) is very simple in the case of a high external field, $\gamma_e H_0 \gg |a_{1i}|, |a_{2j}|$. Then the wave functions T_+ and T_- and also the combinations $S + T_0$ and $S - T_0$ are stationary states of the system. This result means that the Zeeman and hyperfine interactions can induce transitions between S and T_0 states but cannot mix them with T_+ and T_- . This conclusion has already been illustrated in terms of the vector model.

If a primary RP is formed in a spin-correlated state, say S, then the time evolution of the spin wave function will consist of oscillations between S and T_0 states. The probability ρ_s of finding the system in the singlet state at a time t is determined by the relation

$$\rho_S = \cos^2 \{ \omega_{ST_0} \cdot t/2 \} \quad (1.6)$$

and the probability of the T_0 state, ρ_{T_0} , is

$$\rho_{T_0} = \sin^2 \{ \omega_{ST_0} \cdot t/2 \}, \quad (1.7)$$

where ω_{ST_0} is the $S-T_0$ transition frequency,

$$\omega_{ST_0} = |Ag \cdot \beta_e \cdot \hbar^{-1} \cdot H_0 + \sum_i a_{1i} \cdot m_{1i} - \sum_j a_{2j} \cdot m_{2j}|. \quad (1.8)$$

In full agreement with the vector model, $S-T_0$ transitions are seen to be induced both by the difference in the g -values and the differences in the local hyperfine fields. Formula (1.8) also demonstrates that the $S-T_0$ frequency can depend on a number of factors: the external field strength, the difference in the radical g -values, and the hf constants of both radicals. Moreover, the frequency also depends on the radical nuclear spin orientation. In other words, an ensemble of radical pairs of a certain type can be divided into RP subensembles with a definite set of quantum numbers m_{1i} and m_{2j} , each subensemble being characterized by its own frequency of singlet-triplet transitions. The last point is of fundamental importance in the description of CIDNP effects.

1.3 The origin of CIDNP and magnetic effects in radical reactions

Since they are simpler, magnetic effects are treated first.

Magnetic isotope effects. Assume that a radical pair can recombine only from the singlet state and that one of its atoms is either a magnetic or a nonmagnetic isotope, e.g., $^{12}\text{C}(I=0)/^{13}\text{C}(I=1/2)$ or $^{16}\text{O}(I=0)/^{17}\text{O}(I=5/2)$. Assume also that the magnetic moments of the other nuclei are zero. To make the example concrete, let the primary RP be correlated triplet-born (Fig. 1.6). A pair that has no magnetic isotope cannot turn into singlet. Such a pair cannot recombine. Therefore, its radicals diffuse apart and give escape products, e.g., by reacting with radical scavengers. A RP with a magnetic isotope can undergo singlet-triplet evolution and

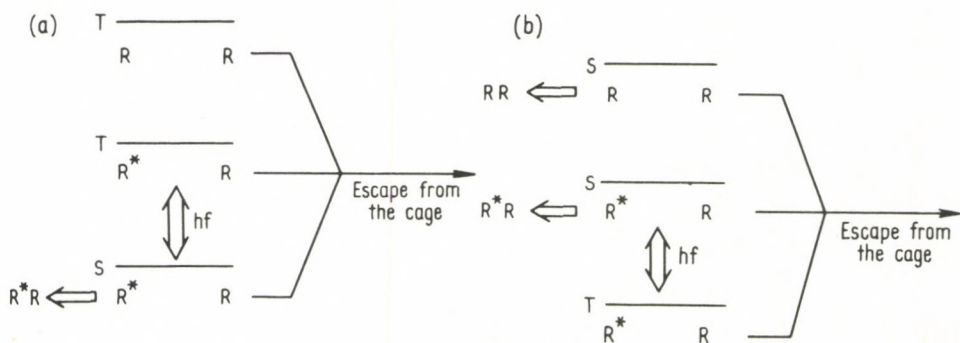


Fig. 1.6. Reaction scheme accounting for the origin of magnetic isotope effects in a triplet (a) and singlet (b) RP. R^* is a radical with a magnetic isotope

so it can give in-cage recombination products. Therefore, the in-cage recombination takes place only in those pairs having a magnetic isotope. In other words, the recombination product of a RP under discussion must show a 100 percent content of magnetic isotope, the escape product being depleted in it.

If the primary RP is singlet, the magnetic isotope effect will be opposite. Indeed, the pairs with a magnetic isotope will turn from reactive singlet into nonreactive triplet states. As a result, the cage recombination product will be depleted and the escape product enriched with magnetic isotopes. Note, however, that a 100 percent isotope content in each product cannot be achieved. Consequently, to obtain strong magnetic isotopic effects, it is expedient to start with triplet RPs.

Real RPs as a rule have some other isotopes together with those of interest to the investigators. The hyperfine interactions with these isotopes contribute to the singlet-triplet RP evolution and so reduce the scale of the observed magnetic isotope effects. However, even in these cases, the isotopic effect can be considerable provided the hf constant for the chosen magnetic isotope exceeds that with the other nuclei.

Magnetic isotopic effects must also arise in the recombination of uncorrelated RPs resulting from random radical encounters in the bulk. As stated above, the first radical encounters lead to recombination of only the singlet RPs, the recombination probability being independent of the nature of the RP isotopes. After the first contact, the system has mainly triplet RPs, and hence the sign of the magnetic isotopic effect corresponds to that predicted for triplet pairs. The scale of the effect is reduced owing to the recombination of the singlet RPs.

It is necessary to note that the nature of magnetic isotopic effects differs fundamentally from that of common kinetic isotopic effects in chemical reactions, the latter being associated with the isotopic mass differences and their effects on the reactions' activation free energy. Such effects can be observed in various reactions, including radical reactions. However, while greatest for hydrogen isotopes, the magnitude of the effect rapidly falls with increasing atomic mass. Magnetic isotopic effects, in contrast are induced by the difference in nuclear magnetic properties and manifest themselves only in radical pairs. Magnetic isotopic effects can considerably exceed kinetic isotopic effects, especially in the case of heavy elements.

Magnetic field effects on radical reactions. The rate of S-T transitions by any of the mechanisms considered in Sec. 1.2 is a function of the external magnetic field. For example, the Δg -mechanism induces S-T₀ oscillations, their frequency being proportional to the external field. The action of the hf-mechanism is also field-dependent: in a high field the hf interactions induce only S-T₀ transitions, whereas in a low field transitions between S and any of the three triplet sublevels are induced. As a result, the S-T rate in low fields exceeds that in high fields. At short times of S-T mixing the rate ratio is 3/1 according to the number of working channels (Fig. 1.7). Finally, the relaxation transition rates are also dependent on external fields. However, being of small importance in the case of free radicals, these transitions will henceforth be neglected.

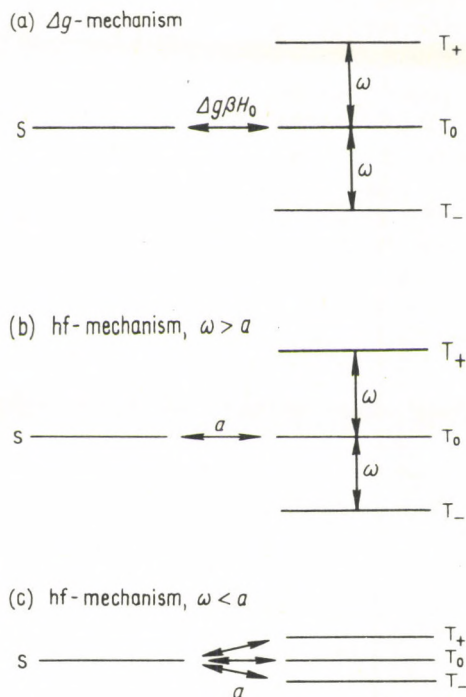


Fig. 1.7. Scheme accounting for the field dependence of S-T transition rates: (a) Δg -mechanism. S-T₀ transition frequency is proportional to the external field, (b), (c) hf-mechanism. In a low field, hf interaction induces transitions to all the three triplet states; in a high field eliminating the triplet level degeneracy, it results in transitions only to the T₀ state, which is in resonance with S

The above influence of external fields on S-T transitions can, under favourable conditions, result in an external field dependence of radical reaction rates. Consider, for example, the recombination of a correlated triplet-born RP, which can recombine only from the singlet state, and consider the initial stages of T-S evolution, i.e., at short times. In this case the RP recombination probability at a certain moment will be proportional to the singlet state population. One must take into account that in high fields the T₊ and T₋ levels do not interact with S and do not participate in S-T evolution. In the case of Δg -mechanism we have according to eqs (1.6—8)

$$\rho_S \approx \Delta g^2 \cdot \beta_e^2 \cdot \hbar^{-2} \cdot H_0^2 \cdot t^2 / 12. \quad (1.9)$$

Thus, the recombination probability is proportional to the square of the external magnetic field. In the case of hf-mechanism and high fields the same equations yield

$$\rho_S \approx \left[\sum_i a_{1i}^2 \cdot I_{1i} \cdot (I_{1i} + 1) + \sum_j a_{2j}^2 \cdot I_{2j} \cdot (I_{2j} + 1) \right] \cdot t^2 / 12. \quad (1.10)$$

In low magnetic fields, the analysis described in Section 2.2 gives

$$\rho_s \approx \left[\sum_i a_{1i}^2 \cdot I_{1i}(I_{1i} + 1) + \sum_j a_{2j}^2 \cdot I_{2j}(I_{2j} + 1) \right] \cdot t^2/4 \quad (1.11)$$

Thus, the recombination probability in high magnetic fields is one-third of that at low fields. The intermediate region is shown by a more detailed analysis to occur when the fields are comparable to the hf constants.

Figure 1.8 shows schematically the field dependence of the recombination probability according to the Δg - and hf-mechanisms individually, and also when

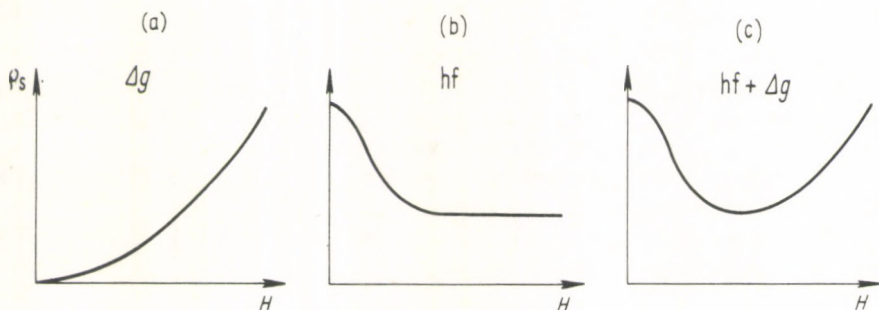


Fig. 1.8. Schematic representation of the field dependence of the probability of in-cage product formation for a triplet-born RP in the case of (a) Δg -mechanism; (b) hf-mechanism; (c) joint action of both

both mechanisms work simultaneously. It is clear that the character of this dependence gives information about the mechanism of S-T evolution in a radical pair, the sign of the magnetic field effect being dependent both on the initial pair multiplicity and the origin of the product; that is, whether it is in-cage or escape.

The above example of a small extent of S-T evolution is typical of uncharged radicals in solvents with normal viscosity. The characteristic evolution time in such systems exceeds as a rule the characteristic time for escaping from the cage. A contrary situation can be observed in the recombination of oppositely charged radicals initially separated by about 100 Å. The recombination time of radicals which diffuse in the field of their Coulomb interaction, can exceed the period of S-T evolution induced by the hyperfine interaction. However, magnetic field effects will manifest themselves in this case too. Indeed, in a high field, the hf mechanism results in equal average S and T_0 populations, while in a low field the T_+ and T_- levels will also be populated. Thus, at the moment of radical encounter the sublevel populations will be different, and that will influence the RP reactions.

Note, in conclusion, that the mechanism of magnetic field effects on radical reactions discussed here cannot be associated with changes in the reaction energetics. The energy of any magnetic interactions (Zeeman, hf) in the systems

under discussion is several orders of magnitude lower than the thermal energy at room temperature.

Chemically induced dynamic nuclear polarization. As seen from eq. (1.8), the RP singlet-triplet mixing rate depends on the quantum numbers m_{1i} and m_{2j} , i.e., on the nuclear spin orientation with respect to the external magnetic field. As a result, the RP recombination probability depends on the nuclear spin orientation; therefore the nuclear spins of recombination products will acquire a certain orientation. Radicals with other spin orientations, on the contrary, have a fair chance to escape from the cage and to yield bulk reaction products. Nuclear spin polarizations arise in both the in-cage and escape products.

Two types of CIDNP effect can be observed experimentally. The *net CIDNP* effect is either enhanced absorption (*A effect*) or emission (*E effect*) in the NMR spectrum of the reaction product. The *multiplet effect* can be observed in those NMR lines that are split by the spin-spin interaction of a given nucleus with other nuclei of the molecule. In the case of the multiplet effect the multiplet lines show enhanced absorption in a low field and emission in a high field (*A/E effect*) or vice versa (*E/A effect*). Sometimes both effects—net and multiplet—are observed in the same line simultaneously.

For a more detailed description of the origin of net and multiplet effects, consider two model triplet RPs in a high magnetic field.

1. *A one-nucleus RP* ($I=1/2$, $a_1 > 0$) with different *g-values*, $g_1 > g_2$. In a high magnetic field the RPs in T_+ and T_- states will not show time evolution of their spin state, those in T_0 state will evolve to singlet with the rate governed by eq. (1.8). If the radical nuclear spin is orientated along the field (α -orientation),

$$\omega_{ST_0}(\alpha) = |Ag \cdot \beta_e \cdot \hbar^{-1} \cdot H_0 + a_1/2|, \quad (1.12)$$

while in the case of opposite orientation (β -orientation)

$$\omega_{ST_0}(\beta) = |Ag \cdot \beta_e \cdot \hbar^{-1} \cdot H_0 - a_1/2|. \quad (1.13)$$

Compare eqs (1.12) and (1.13) and obtain

$$\omega_{ST_0}(\alpha) > \omega_{ST_0}(\beta).$$

Thus, RPs with α -projection of the nuclear spin become singlet more rapidly and thus have a better chance to recombine. Therefore, the in-cage product nuclei will be positively polarized and the NMR spectrum will demonstrate enhanced absorption (*A spectrum*). For the same reason the escape product nuclei will be negatively polarized, the NMR spectrum showing emission (*E spectrum*). The nuclear level populations and the NMR spectra are shown schematically in Fig. 1.9. Equations (1.12) and (1.13) show that the sign of CIDNP changes with those of Ag or a_1 and also when the primary pair changes from triplet to singlet.

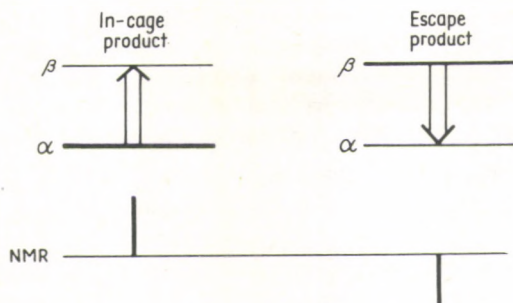


Fig. 1.9. Schematic representation of nuclear level populations and NMR spectrum for in-cage and escape products of a one-nuclear RP, $I = 1/2$, $\Delta g \neq 0$

2. A RP with equal g -values in which one of the radicals carries two nuclei ($I_1 = I_2 = 1/2$) with equal hf constants. The $S-T_0$ mixing rate in this pair is seen from eq. (1.8) to depend on the mutual spin orientation:

$$\omega_{ST_0}(\alpha\alpha) = \omega_{ST_0}(\beta\beta) = a, \quad (1.14)$$

$$\omega_{ST_0}(\alpha\beta) = \omega_{ST_0}(\beta\alpha) = 0. \quad (1.15)$$

Thus, no $S-T_0$ evolution can occur in a pair with oppositely orientated nuclear spins and hence this pair cannot recombine. On the contrary, a pair with both nuclei orientated either along ($\alpha\alpha$) or against ($\beta\beta$) the field will evolve from T_0 to S state. As a result, nuclear configurations ($\alpha\alpha$) and ($\beta\beta$) will be accumulated in the in-cage product and configurations ($\alpha\beta$) and ($\beta\alpha$) in the escape product. This nuclear selection cannot lead to net nuclear polarization. Indeed, in the in-cage product, for instance, the polarization due to ($\alpha\alpha$) configurations is entirely compensated by the opposite polarization due to ($\beta\beta$) configurations. However, it leads to a certain order in the mutual spin orientation which manifests itself in the NMR spectrum as multiplet effects.

Indeed, let us compare the unpolarized and polarized NMR spectrum of in-cage products. If two magnetic nuclei with different chemical shifts are spin-spin coupled, the corresponding unpolarized NMR spectrum is two doublets, one pertaining to flips of the nucleus a , the other to those of the nucleus b . This spectrum conforms to the energy level diagram depicted in Fig. 1.10(a), so that the four allowed transitions correspond to the four lines in the NMR spectrum. The equal spectral intensities correspond to the fact that the difference in the populations of any two levels involved in the transition are determined by the Boltzmann factor under equilibrium conditions.

Figure 1.10(b) shows the populations of the same levels for in-cage products under polarization effects: $\alpha\beta$ and $\beta\alpha$ levels are not populated, while $\alpha\alpha$ and $\beta\beta$ levels are equally populated. It is seen from the scheme that one of the transitions of each nucleus results in emission, the other in absorption. The transition intensities

considerably exceed in absolute value those in the equilibrium situation since the difference in the level populations exceeds that under equilibrium conditions. As a result, the NMR spectrum shows a multiplet effect (Fig. 1.10).

An important feature, common to both the cases considered, is that in the course of RP transformations the nuclear spin orientation does not vary with respect to the external field. The nuclear spin polarizations result from the spin-sorting process: the nuclei orientated in one way arrive in the in-cage product, those with the opposite orientation arrive in the escape product, the total polarization being zero. Detection of this polarization proves to be possible due to the fact that NMR signals from different products have unequal chemical shifts and so the polarization of each in the NMR spectrum can be detected independently.

The above feature characterizes the behaviour of radical pairs in high magnetic fields. In low fields, and in the case of essential radical exchange interactions, electron–nuclear flip–flop processes begin to play a role in inducing the polarization. These cases are outside the scope of the qualitative models considered in this section and will be explored in sections devoted to CIDNP theory (Section 4).

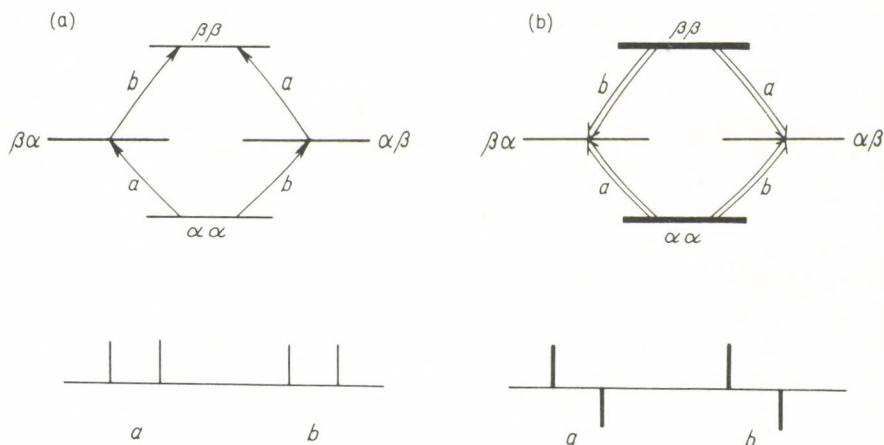


Fig. 1.10. Schematic representation of nuclear level populations and NMR spectrum for the in-cage product of a RP with two nuclei ($I = 1/2$, $\Delta g = 0$), under equilibrium (a) and polarization (b) conditions

Chemically induced dynamic electron polarization. Electron spin polarization of free radicals is detected by lines of anomalous intensity in their ESR spectra. CIDNP and CIDEP have much in common: CIDEP originates in radical pairs due to S–T mixing, and there exist net and multiplet CIDEP. However, there is also an appreciable difference between them. Unlike CIDNP and magnetic effects, no chemical RP transformation is required to induce CIDEP. Moreover, CIDEP can arise in RP only under radical exchange interactions, the maximum efficiency being attained at the distances when $J \approx a$. The nature of CIDEP, including the features

mentioned, will be discussed in Section 4 on the basis of the generalized vector model.

Note in conclusion that though of the same nature, the phenomena discussed can be detected under different conditions. For instance, appreciable field and magnetic isotope effects (of 10 percent and more) can arise at great degrees of S-T evolution. In other words, RP lifetimes and S-T mixing times must be comparable. To realize these conditions experimentally, one must take special measures: increase the RP lifetime by either enhancing the viscosity, by using radical-ions at large initial separation between them or by performing the reaction in micellar systems. Another way is to choose systems with short S-T mixing times. This can be ensured either by selecting systems with large hf constants or by increasing the external field (in the case of Δg -mechanism of S-T evolution). A careful choice of systems and experimental conditions is therefore necessary in order to ensure appreciable magnetic effects.

An important point is that CIDEP and, in particular, CIDNP can be observed at small amounts of S-T evolution because *equilibrium* values of electron polarizations in radicals and nuclear polarizations in molecules are not great. The degree of polarization for particles with spin-1/2 obeys the equation

$$P = (n_{\alpha} - n_{\beta}) / (n_{\alpha} + n_{\beta}), \quad (1.16)$$

where n_{α} and n_{β} are the numbers of spins at the lower and upper Zeeman levels, respectively. Under equilibrium conditions at room temperatures $P \approx 10^{-3}$ for electrons ($H_0 = 3000$ G) and $P \approx 10^{-5}$ for protons ($H_0 = 30,000$ G). In order to obtain appreciable effects, only a small nonequilibrium polarization is required, and this can be attained even in the early stages of S-T mixing. It is these CIDNP and CIDEP effects that are readily observed in a wide range of radical reactions.

1.4 Basic steps of investigations

The discovery of chemically induced dynamic nuclear polarization (CIDNP) in 1967 is regarded as an event of fundamental importance which encouraged rapid development of research in the field. This discovery was made simultaneously and independently by two groups of researchers. Bargon *et al.* [1.12] observed emission lines in NMR spectra taken during thermal decomposition of peroxide compounds in the probe of a NMR spectrometer. When studying reactions of lithium alkyls with alkyl halides, Ward and Lawler [1.13] found anomalously intensity lines corresponding to absorption and emission in the NMR spectra. Both groups realized that the emission and enhanced absorption observed in the reaction product NMR spectra were associated with free radicals involved in the reaction. The new phenomenon immediately attracted the attention of many researchers as a simple and highly sensitive method to detect radical involvement in chemical

reaction pathways. The most surprising feature is perhaps the fact that CIDNP was not discovered earlier despite the wide use of NMR spectroscopy in chemical investigations and a wide spread of CIDNP phenomena in chemical reactions.

It took about two years to understand the physical mechanism of CIDNP, Kaptein and Oosterhoff [1.14–15] and Closs [1.16–17] making the decisive contributions. They proposed the model based on the idea of a radical pair in a cage, and on the selection of nuclear spin orientation due to RP singlet–triplet evolution and recombination. Furthermore they carried out experiments that supported unambiguously the reliability of the model. The next important step in the development of the CIDNP theory was the work by Adrian [1.18] who was the first to realize the fundamental role of RP re-encounters at the recombination radius in inducing nuclear spin polarization.

Chronologically, CIDEP effects in radical ESR spectra were detected prior to CIDNP. In 1963 Fessenden and Schuler [1.19] observed unusual ESR spectra of hydrogen and deuterium atoms in methane and its mixtures with ethane under irradiation with fast electrons. It is obvious now that the spectral components presented showed emission in low fields and enhanced absorption in high fields, i.e., they show multiplet CIDEP effects. The authors, however, tried to assign the anomalies to instrumental effects. That perhaps, can account for the fact that the results did not attract much attention.

Only five years later, in 1968, when observing an analogous effect in the ESR spectra of alkyl radicals under pulse radiolysis, Smaller *et al.* [1.20] came to the conclusion that the anomalous spectra were due to electron spin polarization. The mechanism of multiplet CIDEP effects became clear still later, on the basis of models developed for CIDNP, and was reported by Kaptein, Oosterhoff [1.14] and Adrian [1.21]. The emission effects observed by Atkins *et al.* [1.22] and Livingstone and Zeldes [1.23], led Atkins and McLauchlan [1.24] and Wong *et al.* [1.25] to the idea that CIDEP can arise not only in radical pairs but also in their precursors–triplet excited molecules.

The first physically valid hypothesis on plausible external field effects was put forward in 1969 by Brocklehurst [1.26] who suggested that a magnetic field changing electron relaxation times can effect the ratio of singlet and triplet recombination channels of radical-ion pairs originating in solutions as a result of ionizing irradiation. Though important in some cases, this so-called *relaxation mechanism* proved to be negligible in the case of free radicals.

More substantiated hypotheses on the external magnetic field and magnetic isotope moment effects on radical pair reactions were put forward in 1971 by Lawler and Evans [1.27] on the basis of the CIDNP mechanism. The effects however were thought to be small and hardly accessible for detection.

In 1972 Sagdeev *et al.* [1.28] were the first to observe magnetic field effects in radical reactions of pentafluorobenzylchloride with *n*-butyllithium. The result obtained was interpreted by Salikhov *et al.* [1.28, 29] as a manifestation of RP S–T transitions induced by hyperfine interactions. Later on, Podoplelov *et al.* [1.30] and Tanimoto *et al.* [1.31] observed the manifestation of *Δg*-mechanism of S–T.

In 1976 the magnetic isotope effect was successfully detected simultaneously and independently by two research groups. Buchachenko *et al.* [1.32] observed magnetic isotope effects from carbon nuclei in the photochemical decomposition of dibenzyl ketone, while Molin *et al.* [1.33] detected the effects at the same nuclei in the triplet photosensitized photolysis of benzoyl peroxide.

In studies on magnetic effects the role of radical-ion pairs and micellar solutions were important as an example of systems with sufficient radical in-cage lifetimes. Brocklehurst *et al.* [1.34] were the first to observe magnetic effects in such pairs generated by ionizing radiation, and Schulten *et al.* [1.35] and Michel-Beyerle *et al.* [1.36] in photochemical reactions. Turro *et al.* [1.37] observed isotopic and magnetic field effects in micellar solutions.

A definite stage of investigations in this field can be considered as completed. The problems associated with physical mechanisms of spin polarization and magnetic effects have mainly been solved. Different chemical applications connected with a detailed understanding of RP reaction mechanisms have been well developed, especially for the case of CIDNP, which was applied to study a great number of reactions. In order to develop these applications and to elaborate the theory, numerical computations have grown in importance. They allow one to analyze the behaviour of real and fairly complex systems. This field has been contributed to by many investigators. The elaboration of special experimental techniques to conduct time-resolved experiments and to enhance the sensitivity of RP detection is now beginning to be of importance in CIDNP, CIDEP and magnetic effect applications. Finally, the attention of many researchers has been attracted by some purely applied aspects: the possibility of field-controlled chemical reactions, applications of magnetic isotope effects to isotope separation, and new ways of interpreting the biological action of magnetic fields.

2 THE THEORY OF RADICAL RECOMBINATION

In order to describe magnetic and spin polarization effects in radical reactions, one needs, first, the statistics of reactant collisions in solutions and the dynamics of molecular motion in the reaction zone, and, second, the reactant spin dynamics. As to the reactant molecular dynamics in solutions, they have been thoroughly studied in the traditional, spin-independent, radical recombination theory. The radical spin dynamics can be easily interpreted by the methods developed to describe electron spin resonance (ESR) phenomena. Thus, the theory of spin polarization and magnetic effects in radical recombination is developing on the borderline of chemical kinetics and ESR. Each of these fields is well established and provides a sound basis for further investigations of magnetic and spin polarization effects in radical chemical reactions.

2.1 The dynamics of molecular motions in solutions and the spin-independent theory of radical recombination

Spin polarization and magnetic effects in radical reactions are induced by singlet-triplet transitions in a pair of radicals which can recombine on their encounter in a solution. The efficiency of these transitions is strongly dependent on the dynamics of molecular motion of the reactants, i.e., their contact duration and the number of re-encounters. Therefore, we begin by discussing the theory of chemically induced spin polarization and magnetic effects in radical recombination with a brief survey of the theory of spin-independent radical recombination.

2.1.1 The statistics of radical encounters in solutions

The statistics of contacts between two radicals in solutions is characterized by a number of peculiarities arising from the influence of the condensed medium on the reactant molecular dynamics. The so-called *cage effect* is one vivid example of this influence. It is this effect that is responsible for spin polarization and magnetic effects

in bimolecular processes involving paramagnetic partners and free radicals in particular.

The cage effect. Franck and Rabinowitch [2.1] were the first to consider the cage effect. Two radicals, or molecule fragments, do not always separate. In condensed media the radicals can either recombine and yield the parent molecule again—the *precursor* of this radical pair—or disproportionate to molecular products of some other structure. This reaction is called a *geminate reaction* or *in-cage recombination* and its product is called a *geminate product* [2.2]. The recombination product can differ from the parent molecule provided the decay fragments include not only the pair of radicals but also a nonradical particle. The radicals can also leave the cage and react in the bulk, the products of this reaction being called the *escape products*. The reduced quantum yield of molecular photodecomposition in liquids as compared to gases, for example, is a striking manifestation of geminate recombination.

The phenomenon discussed above corresponds to the intuitive supposition that a sufficiently condensed medium prevents partners from diffusing apart by holding them in "a cage". Such a picture of cage effect was observed in model simulations made by Rabinowitch and Wood [2.3]. Several dozens of nonconductive balls were placed on a metallic zigzag-edged surface in order to imitate solvent molecules. Two conductive balls were also placed on the surface, one of them being fixed at the center of the plate and isolated from it. Voltage was applied both to the central metallic ball and the plate. A collision of the two metallic balls completed a current circuit. The plate was constantly shaken. As a result of the special choice of the surface the balls movement modelled Brownian motion in liquids. As a result, it was found that collisions of the two given partners were distributed in time nonuniformly and occurred in series. Each series reflected collisions of two neighbouring partners surrounded by the solvent molecules. To describe this phenomenon the notion of a cage composed of the medium molecules was introduced [2.3]. The cage ensured that the 'reactant' pair remained as partners for longer in condensed media than in gases.

However, theoretical and experimental investigations [2.4] have shown the physical background of the cage effect should be ascribed not only to this factor, but also to another of more importance, the *re-encounters* of the same radicals in condensed media.

From the foregoing, the movement of radicals involved in recombination in liquids can be represented as follows. Both in geminate recombination and in combination in homogeneous solutions, reaction can take place either at the first radical contact or at one of their re-encounters. Note that in the geminate recombination even the first contact of the reagents is in fact a re-encounter, i.e., the fragments of the initial molecule come back to the reaction zone. Thus two characteristic features of the reaction in condensed media can be traced in the cage effect: a comparatively long duration of a contact and the possibility of a re-encounter resulting from radical diffusion.

Nowadays the notion "cage" is interpreted in two ways. In its proper meaning it is a cage composed by the medium molecules which hold two reagents together in a direct contact [2.3]. Such a cage is sometimes called a *primary cage*. However, the primary cage does not fully describe the cage effect since even if the partners get to the second, the third, etc. coordination sphere by diffusion, they can again come back into direct contacts and give products. The notion of the *secondary, tertiary, etc. cages* for the reagent pairs in the second, the third, etc. coordination spheres respectively can be introduced to describe this phenomenon. Note that in some cases direct contacts of two partners are not necessary for reaction. E.g., an electron can be transferred at long distances, $\sim 10 \text{ \AA}$ [2.5]. Then the secondary and tertiary cages differ from the primary one only in the reaction (or electron transfer) probability. All these concepts can be collected under the term "cage", and a reagent pair can be considered to be in the "cage" not only at the moment of its direct contact but also between re-encounters. In this generalized sense a "cage" should be interpreted as a certain region of effective recombination of a given reactant pair. As long as the potential reactants are in this region the probability of their reaction with radicals of other pairs and with acceptors is low compared to the probability of their recombination with each other.

The "cage" radius and the in-cage lifetime of the reagents, τ_D , are effective parameters depending on such values as the radical jump length in an elementary diffusion step, the radical reactivity, and the concentration of the acceptor. In calculations of neutral radical reactions the "cage" radius can be set equal to about 1 nm [2.4]. Hence, for nonviscous liquids with the diffusion coefficient $D \sim 10^{-5} \text{ cm}^2 \cdot \text{s}^{-1}$ we obtain $\tau_D \sim 10^{-9} \text{ s}$.

The density of the medium is not the only factor that influences the relative diffusion of a molecule fragments. It can be also affected by the long-range attraction between the reactants. The Coulomb attraction between an electron and the parent ion is known [2.6] to ensure their re-encounter even in rarefied gases. Therefore, when discussing the cage effect for charged species one must take into account interactions between the partners. In the case of oppositely charged partners, the "cage" radius increases to hundreds of angstroms in nonpolar media. On the other hand, in the case of similarly charged partners the Coulomb repulsion can in fact reduce the cage effect to zero in nonpolar media.

Two radicals in a "cage" form a radical pair (RP). We can distinguish three different ways of RP formation: the decomposition of a molecule, the transformation of one RP into another, and as a result of radical encounters in solutions. In the last case the term "*diffusion pair*" is used. The term "RP" is sometimes employed in spectroscopy when the features resulting from the interaction of two radicals can be observed in spectra (e.g., [2.7]). However, the idea of RP in chemical kinetics does not necessarily correspond to that in spectroscopy. The reaction products of diffusion pairs are called *bulk recombination products*.

Radical motion in a cage. Geminate recombination is essentially dependent on kinematic factors, i.e., on the detailed picture of particle motion. It is of great importance for the reaction whether the reagent diffusion occurs via infrequent but

large jumps (in the sense of exceeding molecular sizes), or if it results from frequent but short particle displacements. The reaction can also be influenced by the orientational mobility of the partners. Therefore, the quantitative theory of the cage effect should be based upon various concepts of the structure and the nature of thermal molecular motion in liquids.

The models of *continuous media* and of *quasi-crystalline liquid structure* are the most widely used. The mobility of molecules in a quasi-crystalline liquid lattice was considered in detail by Frenkel [2.8]. The molecules vibrate elastically at the quasi-crystalline lattice points with the frequency of about 10^{13} s^{-1} . Occasionally as a result of environmental fluctuations, molecules jump to neighbouring vacant points. In liquids with viscosity $\eta \sim 1 \text{ cP}$ the "settled" lifetime of a particle at a given point is $\tau \sim 10^{-11} \text{ s}$. In highly viscous liquids, when $\eta \sim 1 \text{ P}$, τ can reach 10^{-9} s . In the model discussed we assume two reactants to be in a direct contact if they get to neighbouring points. When at neighbouring "points", the reagents can collide and recombine as a result of their vibrations or jumps towards each other.

In contrast to the previous model, that of the continuous medium assumes that molecules can travel in any directions and for any distance, not only to strictly determined, lattice points. If the reagents travel for infinitely small distances in an elementary step, we obtain the extreme situation of continuous diffusion in continuous media. Mathematical models of diffusion by jumps in continuous media have been developed by Chandrasekhar [2.9]. Below we give a brief description of one of his models. It is assumed that every single step occurs through a constant distance but in an arbitrary direction, i.e. a molecule can with equal probability jump from its present location to any point on a spherical surface with the radius equal to the jump length λ_D (Fig. 2.1(a)). This model was later on used by Noyes [2.10] in his numerical calculations of re-encounter statistics and called by him a *flight* model. Two partners can be in contact only if the distance between them is less than b , the radius of contact [2.10]. It is often assumed that the contact radius equals the sum of the van der Waals radii of the partners:

$$b = R_A + R_B = R_{AB}.$$

Assume the distance between the partners r_0 is in the range $b < r_0 < b + \lambda_D$ at the initial moment. That is, the reactants—are not initially in contact, but at the very first jump of one of them they can approach to the contact radius. Consider a contact sphere with radius b around one of the partners, say A. At a jump of the other reagent, B, the partners get into contact with a probability determined from Fig. 2.1(b) as a section of the surface of the B flights sphere with the solid angle Θ [2.10]. Note that in this case the characteristic volume of the reagents is not considered properly as, they are assumed to "penetrate" into each other, B can fly through A without coming into contact with the latter. As in the quasi-crystalline approximation, in the jump diffusion models in continuous media the "settled" lifetime of the reagents, in the vicinity of their temporarily stable position, is considered to be their contact time. The jump model seems to be in line with reality

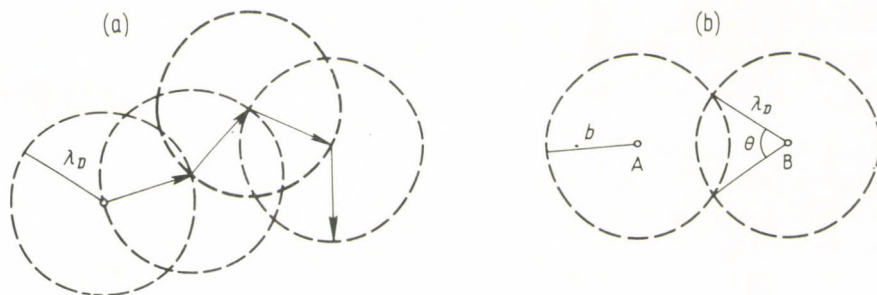


Fig. 2.1. Molecular diffusion (a) and contact (b) within the flight model; b is the distance of the closest approach of A and B, λ_D is the flight length of particles

provided the sizes of the reagents are either less or comparable to those of the solvent molecules. In this case one can expect the reagents to move by jumps through distances of the order of the solvent molecular size. If the sizes of the reagents exceed those of the solvent molecules, the diffusion of the former can be characterized by small steps and considered to be practically continuous. Within the limits of such an approximation to continuous diffusion in continuous media the particles are constantly changing their coordinates. This corresponds to the case when both the jump length and the settled lifetime tend to zero. Therefore the time of an individual contact is infinitely short. Note however that in the continuous diffusion model the number of re-encounters tends to infinity so that the total result of all re-encounters is a non-zero recombination probability of the partners. To be in contact, in this model, means to be as close as b . If there is no reaction, the contact sphere serves as a reflection surface for the mutual diffusion of the partners. Thus the reaction results in the fact that the contact sphere serves at the same time as an *absorption* surface.

RP contact statistics. Noyes described in detail the RP re-encounter statistics on the basis of neglect of radical-radical interactions [2.2, 10, 11]. The basic statistical characteristics are the following:

p is the probability of at least one re-encounter, $(1-p)$ being the probability that no re-encounters occur; $f(t)dt$ is the probability that the radicals of a pair will again approach as close as the contact radius within the time interval $(t, t+dt)$; p_0 is the probability of the first RP contact provided the radicals were separated by r_0 initially; $f_0(t)dt$ is the probability of the first approach as close as the contact radius provided initially the partners were separated by r_0 .

Note that $p=p_0$ if $r_0=b$. The full probabilities of the first contacts and their distribution functions are related by the equations (2.1).

$$p = \int_0^{\infty} f(t) dt,$$

$$p_0 = \int_0^{\infty} f_0(t) dt. \quad (2.1)$$

p values for various choices of contact radius and jump length of the partners in an individual diffusion step have been calculated [2.10] and the results obtained are listed in Table 2.1. The data fully confirm the expected strong dependence of p on the

Table 2.1. Re-encounter probabilities p for various ratios between the distance of the closest partners approach, b , and the mean length of one diffusion step, λ_D

b/λ_D	p^a	p^b	p^c
0.01	0.000720		
0.03	0.00500		
0.1	0.0370		
0.2	0.104		
0.5	0.308		0.333
1	0.527	0.600	0.500
2	0.719	0.750	0.666
5	0.875	0.8823	0.833
10	0.935	0.9375	0.909
100	0.99336	0.99338	0.990
1000	0.999334	0.999334	0.9990

^a according to ref. [2.10]

^b according to eq. (2.13)

^c according to eq. $p = b/(b + \lambda_D)$

parameters of the partners motion. Indeed, when $\lambda_D \gg b$ the situation is analogous to that of collisions in gases, and p must tend to zero as $(b/\lambda_D)^2$. With a decrease of jump length p increases and tends to unity in the extreme case of the continual diffusion. Thus when $\lambda_D \gg b$ one should use the gas-kinetic representation of collisions, and if $\lambda_D < b$, the continuous diffusion approximation can be used. Note that the re-encounter probability is equal to about 0.5 if molecules jump by steps approximating their contact radius. The latter case is perhaps of the greatest interest among the jump models of molecular motion in liquids. For example, only this type of molecular motion is considered in the quasi-crystalline liquid model.

The contact probability versus the number (N) of jumps between the first and the following encounter has been found for $b = \lambda_D$ [2.10]. It appears that starting with four jumps the re-encounter probability distribution can be approximated by the function

$$f(N) = 0.2390/(N + 0.442)^{3/2}. \quad (2.2)$$

Spin polarization and magnetic effects in radical recombination are mainly associated with the re-encounters occurring after a number of jumps. Therefore, to evaluate the scope of these effects, a precise form of $f(N)$ function at $N < 4$ is of no importance. With the above considerations and taking into account the fact that in the flight model, a re-encounter cannot occur before two jumps, the re-encounter distribution has been approximated [2.12] as

$$f(t) = \begin{cases} 0.24(dt/\tau)/(t/\tau + 0.44)^{3/2}, & \text{if } t \geq 2\tau, \\ 0, & \text{if } t < 2\tau. \end{cases} \quad (2.3)$$

Hence, using (2.2) we have $p=0.31$. In (2.3) $t=N\tau$, and τ —is the average time interval between two subsequent flights. The distribution (2.3) underestimates the re-encounter probability at small t when $2 \cdot \tau \geq t < 4 \cdot \tau$. Indeed, in this case $p=0.31$ and not 0.5 as expected according to the data listed in Table 2.1 for $\lambda_D=b$. Relation (2.3) is often used to estimate spin polarization and magnetic effects.

In a general case of an arbitrary ratio between the collision radius and the molecule jump length Noyes suggested the following distribution function [2.11]

$$f(t)dt = m \cdot t^{-3/2} \cdot \exp(-\pi \cdot m^2/p^2 \cdot t)dt \quad (2.4)$$

where the distribution parameter m is expressed via the full re-encounter probability p and molecular-kinetic parameters,

$$m = (27/8\pi)^{1/2} \cdot (1-p)^2 \cdot (b/\lambda_D)^2 \cdot \tau^{1/2}. \quad (2.5)$$

To compare it with (2.3), set $\lambda_D=b$ in eqs (2.4) and (2.5). Hence,

$$p = 0.527, \quad m = 0.224 \cdot \tau^{1/2},$$

$$f(t)dt = 0.224 \cdot \tau^{1/2} t^{-3/2} \cdot \exp(-0.18\pi\tau/t)dt. \quad (2.6)$$

According to (2.3) and (2.6) the contact distributions differ only if intervals between two subsequent contacts are short; for long intervals they coincide (see Fig. 2.2).

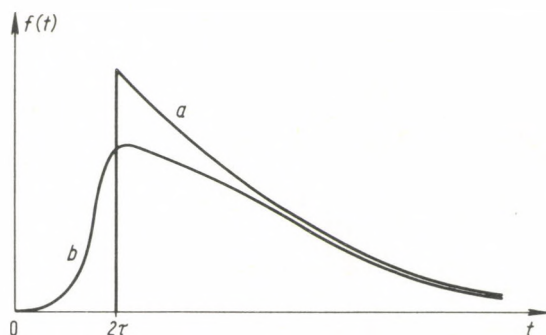


Fig. 2.2. Re-encounter distribution according to (2.3) — Curve *a* and (2.6) — Curve *b*. Two curves coincide at long time intervals between re-encounters

Note that picosecond spectroscopy experiments confirm that re-encounters are described by the distribution (2.3, 4) (see, e.g., [2.13]). Some re-encounters occurs with arbitrarily long time intervals between them, the mean time between subsequent contacts being $\bar{t} = \int t f(t) dt / p \rightarrow \infty$. According to eq. (2.4), the most probable time interval between two contacts is $t_{\max} = 2\pi m^2 / 3p^2$. In the continuous model, $t_{\max} \rightarrow b^2 / 6D$.

With the above results one can readily come to the following general conclusion on the role of kinematic factors in the re-encounter statistics. The contact probability over a long period of time can be described by the function $f(t) \sim t^{-3/2}$ irrespective of the molecule jump length in a diffusion step. This is the result that should be expected judging by the form of the fundamental solution of the diffusion equation in the continuous diffusion approximation. Indeed, for long time intervals the details of an elementary diffusion step do not greatly affect the statistics of the partners approaching at the contact radius. But at times comparable to the mean time of one or several elementary diffusion steps the contact distribution must depend, and does depend, on the detailed microscopic picture of the thermal particle motion.

The re-encounter probability should be independent of how many contacts a given pair has already had. Therefore, to know the first contact distribution is sufficient for the description of the statistics of all re-encounters. The re-encounter probability over the time intervals $(t_1, t_1 + dt_1), (t_2, t_2 + dt_2), \dots$ equals

$$dw(t_1, t_2, \dots) = f(t_1) \cdot f(t_2 - t_1) \dots f(t_n - t_{n-1}) dt_1 \dots dt_n. \quad (2.7)$$

Summing the contributions of all possible realizations of repeated contacts, we get the total number of contacts of a given pair as

$$n = 1 + p + p^2 + \dots = 1/(1 - p), \quad (2.8)$$

where $n - 1 = p/(1 - p)$ is the number of repeated contacts. As the diffusion jump length decreases, $p \rightarrow 1$ and hence the importance of re-encounters increases. In the continuous diffusion approach, the number of repeated contacts tends to infinity. In the intermediate case of $\lambda_D \approx b$ when $p = 0.5$ the average number of re-encounters equals unity and $n = 2$.

In the geminate recombination process, at the initial moment the radicals of a pair are not always in direct contact but can be separated by a distance $r_0 > b$. In the latter case the statistics of first contacts will differ from the re-encounter distribution. In the extreme model of the continuous diffusion, the distribution function $f_0(t)$ can be solved analytically [2.14]

$$f_0(t) dt = m_0 \cdot t^{-3/2} \cdot \exp(-\pi m_0^2 / p_0^2 \cdot t) dt, \quad (2.9)$$

where the distribution parameter m_0 is expressed through the mutual diffusion coefficient $D = D_A + D_B$ and geometrical parameters

$$m_0 = b \cdot (r_0 - b) / [2 \cdot r_0 \cdot (\pi \cdot D)^{1/2}] \quad (2.10)$$

The overall probability of the first contact is

$$p_0 = b/r_0. \quad (2.11)$$

The most probable time interval before the first contact is

$$t_{\max} = 2\pi \cdot m_0^2/3 \cdot p_0^2 = (r_0 - b)^2/6D. \quad (2.12)$$

It is the time of diffusion from the initial distance r_0 to the reaction radius b .

There is every reason to believe that relations (2.9–11) could be applied also to the jump mechanism of diffusion provided the jump length does not exceed the size of the particles, i.e. $\lambda_D \lesssim b$. The greater the initial distance between the partners, the less the error expected. Suppose the particles move by jumps and the initial distance between them is $r_0 = b + \lambda_D$. In this case the first contact probability coincides with that of re-encounters since the particles have to diffuse at a distance approximately equal to $b + \lambda_D$ before a re-encounter occurs. Therefore, p in Table 2.1 can be also interpreted as the first contact probability p_0 for pairs with the initial distance $r_0 \cong b + \lambda_D$. If in this case p_0 is calculated by formula (2.11), we obtain the result given in the last column of Table 2.1. The comparison of numerical results for the 'flight' model (the second column, Table 2.1) with those for the continuous model shows them to coincide not only for small jumps, $\lambda_D < b$, but also for $\lambda_D \cong b$. In the extreme case of diffusion by small jumps when $\lambda_D \ll b$, the re-encounter probability is described by the relation [2.15]

$$p = b/(b + 2\lambda_D/3). \quad (2.13)$$

Values calculated by these formulae are also listed in Table 2.1. The numerical results by Noyes are seen to agree with those obtained by eq. (2.13). Equations (2.9, 10) also reliably describe the encounter distribution of partners diffusing by jumps. Setting $r_0 = b + \lambda_D$ in eq. (2.9) we get practically the same first contact distribution as that obtained by eq. (2.4) for particles moving by jumps if $\lambda_D \lesssim b$. For example, when $\lambda_D = b$ eqs (2.9) and (2.10) result in a distribution which differs negligibly from (2.6):

$$f_0(t)dt = 0.345\tau^{1/2} \cdot t^{-3/2} \cdot \exp(-0.477 \cdot \pi \cdot \tau/t)dt, \\ p_0 = 0.5, \quad m_0 = 0.345 \cdot \tau^{1/2}.$$

In rare cases in liquids reactant species can travel by jumps exceeding molecular sizes, e.g., in reactions of such light particles as electrons, positronium, and hydrogen atoms. In these cases, when $\lambda_D > b$, the following way of evaluating p_0 can be suggested. If the initial distances between partners is $r_0 < b + \lambda_D$, then p_0 , as noted above, approximately equals the probability of the first re-encounter and can be evaluated with the data listed in Table 2.1. In the case when $r_0 > b + \lambda_D$, it is convenient to represent p_0 as the product of two quantities: the probability of reaching the spherical surface with the radius $b + \lambda_D$ and the probability of the first contact at the collision radius b for $b + \lambda_D$ separated partners. The latter value equals approximately the probability of the first re-encounters p (see the second column,

Table 2.1). As to the former probability, it can be evaluated using (2.11). This can be explained by the fact that the continuous diffusion model, as shown above, reliably describes the collision statistics until λ_D exceeds the encounter radius, which in this case is set equal to $b + \lambda_D$. As a result, we have the following expression of p_0 in terms of the jump model

$$p_0 = p, \quad \text{when } r_0 \leq \lambda_D + b,$$

$$p_0 = p \cdot (\lambda_D + b)/r_0, \quad \text{when } r_0 > \lambda_D + b.$$

The values of p for a number of relations between λ_D and b are given in Table 2.1.

Summarizing the above results one can infer that the statistics of the first contact is weakly dependent on the elementary diffusion jump length provided it does not exceed the molecule sizes (i.e., $\lambda_D \lesssim b$) and can be described by the continuous diffusion model. Some appreciable deviations can appear when $\lambda_D > b$. However, the latter case can be of interest to describe molecular motion in liquids only in some particular cases.

Contact statistics in the presence of radical acceptors. The above results can be readily generalized for the case when radicals can react with acceptors. The contact probability in the presence of acceptors equals the product of the encounter probability in the absence of acceptors and the probability that the radicals do not react with the acceptors before their collision. Let K' be the pseudo-first order rate constant for the reaction between a radical and an acceptor. The probability that the RP does not react with acceptors in an interval t is $\exp(-K_s t)$, where $K_s = 2K'$. As a result, we obtain the following expression for the distribution of re-encounters in the presence of acceptors:

$$f_s(t) dt = m \cdot t^{-3/2} \cdot \exp(-\pi \cdot m^2/p^2 \cdot t - K_s \cdot t) dt. \quad (2.14)$$

The full probability of repeated contacts is

$$p_s = p \cdot \exp[-2m \cdot (\pi \cdot K_s)^{1/2}/p] \quad (2.15)$$

and to express the probability of the first contact in the continuous diffusion model we have

$$p_0 = (b/r_0) \cdot \exp[-(K_s(r_0 - b)^2/D)^{1/2}]. \quad (2.16)$$

No radical encounters separated by long time intervals can occur in the presence of acceptors. Hence, the mean time interval before the first contact acquires a finite value,

$$\bar{t} = \int t f_s(t) dt = [(r_0 - b)^2/4D \cdot K_s]^{1/2}. \quad (2.17)$$

The rate constant K_s is proportional to the concentration of scavengers. Thus, according to (2.14–16), the re-encounter probability depends on the concentration of radical scavengers in a particular way. This fact can be used to confirm the reliability of the theory in question [2.15].

The influence of radical interaction on the encounter statistics. The collision probability can be affected by the partner interaction. Let $U(r)$ be the energy of this interaction. Within the continuous diffusion model the value of p_0 can be obtained with the data reported by Monchick [2.15]. With this data one can calculate the encounter probability at an arbitrary initial distance r_0 between the partners,

$$p_0 = S(r_0)/S(b), \quad (2.18)$$

where

$$S(r) = \int_r^{\infty} dx \cdot x^{-2} \cdot \exp(U(x)/k \cdot T).$$

Ion-radical recombination is of particular interest. The recombination of an electron with the parent cation in radiation-chemical reactions can serve as a typical example. If two oppositely-charged particles with the Coulomb attraction energy $U = -q_1 \cdot q_2/\varepsilon \cdot r$ are reacting (where q_1, q_2 are charges, ε is the relative permittivity of the medium), from (2.18) we have

$$p_0 = [1 - \exp(-q_1 \cdot q_2/\varepsilon \cdot r_0 \cdot k \cdot T)]/[1 - \exp(-q_1 \cdot q_2/\varepsilon \cdot b \cdot k \cdot T)]. \quad (2.19)$$

Hence, taking into account the fact that at the collision radius the Coulomb energy exceeds thermal energy even for water ($\varepsilon = 81$), we come to the results first obtained by Onsager [2.6]

$$p_0 \cong 1 - \exp(-r_c/r_0). \quad (2.20)$$

The sphere of influence of the Coulomb field on the reactant motion is characterized by the Onsager radius r_c found as the condition for the Coulomb interaction being equal to the thermal energy,

$$r_c = q_1 q_2 / \varepsilon k T. \quad (2.21)$$

In a non-polar medium the Onsager radius can reach several tens nanometers.

A remarkable result can be obtained if the initial distance between the reagents exceeds the Onsager radius. Then

$$p_0 \cong r_c/r_0. \quad (2.22)$$

It is clear that the Onsager radius acts as a contact radius in (2.11). It reflects the essence of the physical situation discussed above, for charged partners with high reactivity, once having got into the sphere of the Coulomb field, recombine practically without fail. The long-range Coulomb attraction enables two reagents to re-encounter even if they are separated by the Onsager radius.

The encounter probability is decreased if the reactants have the same sign of charge:

$$\begin{aligned} p_0 &= [\exp(r_c/r_0) - 1]/[\exp(r_c/b) - 1], \\ p_0 &\cong (r_c/r_0) \cdot \exp(-r_c/b), \quad \text{if } r_0 > r_c. \end{aligned} \quad (2.23)$$

The analytical form of the contact distribution function for charged particles is unknown. There are, however, some numerical calculations [2.16] for the recombination of oppositely charged radical ions. The distribution function was shown to be strongly dependent on the medium polarity. Polar solvents shield the Coulomb interactions and hence, for systems with large dielectric constants, $f(t)$ for charged partners tends to the encounter distribution function for uncharged ones. In weakly polar solvents, with $\epsilon = 10$, pairs are accumulated in the contact region. In more polar solvents, with $\epsilon = 20$, the pairs succeed in escaping beyond the Onsager radius of 2.8 nm in a time comparable to that of free diffusion of uncharged particles at the same distance.

The time of the first contact of oppositely charged partners can be evaluated as follows. Consider the case when the interparticle distance at the initial moment is less than half the Onsager radius. The flux of the particles in the electric field of their partners then exceeds their diffusion flux and, in the first approximation, one need take into account only their motion in the electric field. Then the flow rate of the particles is

$$v = q_1 \cdot q_2 \cdot D / \epsilon \cdot k \cdot T \cdot r^2$$

and the time interval before the first contact equals

$$t_1 = \int_b^{r_0} dr/v(r) = (r_0^3 - b^3)/3 \cdot D \cdot r_c. \quad (2.24)$$

Compare t_1 with the most probable time interval before the first contact of uncharged particles (2.12). We have

$$\begin{aligned} t_1/t_{\max} &= 2(r_0^3 - b^3)/r_c \cdot (r_0 - b)^2, \\ t_1/t_{\max} &= 2r_0/r_c, \quad \text{if } r_0 \gg b. \end{aligned} \quad (2.25)$$

Thus, when the interparticle distance is less than half the Onsager radius, the Coulomb attraction reduces the time passed before the first contact. If $r_0 > r_c/2$, this time can be estimated by eq. (2.12) up to the sphere with a radius $r_c/2$ and by eq. (2.22) beyond $r_c/2$.

Rate constants of diffusional encounters. The rate of bimolecular encounters is the most important kinetic characteristics of radicals in homogeneous solutions. According to the genetic criterion one distinguishes two types of collisions: the first contact of given partners and one of their re-encounters. The former leads to the formation of a diffusion pair. Reagent encounters in a solution are usually characterized by the rate of diffusion pair formation. The rate constant of this process is usually denoted as K_D and called the *rate constant of diffusional encounters*. The rate of diffusional encounters is associated with the reagent concentrations C_A and C_B through the well-known relation

$$w = K_D \cdot C_A \cdot C_B \quad (2.26)$$

In the extreme case, when the contact sphere serves for the partners as a fully absorbing surface, re-encounters are impossible and the rate of diffusion pair formation coincides with the frequency of encounters. The rate constant of diffusional encounters of uncharged particles in homogeneous solutions is given by the expression obtained by Smolukhovsky in the continuous diffusion approximation in connection with the problem of colloid particle coagulation (see, e.g., [2.9]).

$$K_D = 4\pi b \cdot D. \quad (2.27)$$

The rate constant of diffusional encounters, for interacting reagents was calculated by Waite [2.17]:

$$K_D = 4\pi D/S(b). \quad (2.28)$$

Thus, for charged partners we obtain the following results. If the reactants are oppositely charged, then

$$K_D = 4\pi D r_c / [1 - \exp(-r_c/b)] \cong 4\pi \cdot D \cdot r_c, \quad (2.29)$$

i.e., encounters occur with the same frequency as when uncharged particles collide at a contact radius equal to the Onsager radius of charged partners. The rate constant of diffusion encounters of like-charged reactants is less than that for collisions of uncharged particles:

$$K_D = 4\pi D r_c / [\exp(r_c/b) - 1] \cong 4\pi \cdot D \cdot r_c \cdot \exp(-r_c/b). \quad (2.30)$$

In the general case, the rate constant of diffusional encounters depends upon the character of the reactant motion. For example, in the gas-kinetic limit $\lambda_D \gg b$, for uncharged particles the Smolukhovsky equation would essentially overestimate the encounter rate constant. In fact, in the gas phase $K_D = \pi b^2 \cdot u$ where u is the mean relative speed of the encountering particles. Taking into consideration the fact that the molecular diffusion coefficient in gases is $(1/3)\lambda_D \cdot u$ we see that real encounters in gases are much more rare than those calculated by the Smolukhovsky formulas (2.27) in the gas-kinetic limit. However motion by such large jumps as $\lambda_D \gg b$ is not typical of liquids. For condensed media, in cases corresponding to $\lambda_D \lesssim b$, the Smolukhovsky equation can be used successfully to describe the rate of diffusional pair formation. This is confirmed, on the one hand, by comparison of the re-encounter statistics in the continuous diffusion model with that in the jump model and, on the other hand, by calculations of the rate of diffusional encounters within the quasi-crystalline model [2.18].

The exponential model of RP. Comparison with the diffusion model. The so-called RP exponential model (see, e.g. [2.19–21]) is widely used in cage effect theory. In this model the notion "cage" is identified with the primary cage. Two radicals are considered to form a pair—a certain intermediate quasi-particle—if they are in direct contact. The process of escaping from the cage is considered as RP unimolecular decomposition with the Poisson lifetime distribution

$$f(t)dt = \exp(-t/\tau_c) \cdot (dt/\tau_c). \quad (2.31)$$

Here τ_c is the mean in-cage RP lifetime. The RP recombination and its reaction with acceptors compete with the RP decomposition. Depending on the character of the reagent motion, the cage effect can be described by the exponential model.

The diffusion model reflects both basic aspects of the cage effect: the increasing contact time of the two partners and their re-encounters at the contact radius. The exponential model takes into account only the former factor. Hence, it describes the cage effect reliably only if the re-encounters contribute negligibly to the recombination. It is applicable to a number of physical situations, for example, to systems where reagents either diffuse by large jumps and in practice do not approach again as close as the contact radius or which certainly react at the very first contact. Furthermore, irrespective of the jump length, the re-encounter probability is negligible if there are many radical scavengers in the solution.

The exponential model can be of use when the radicals are held in contact by the Coulomb attraction, the formation of exciplexes, specific associations, etc. In these situations the cage effect is due principally to increasing contact time but not to repeated contacts.

In order to simplify calculations, the exponential model can be used instead of the diffusion model in cases when the former is, strictly speaking, invalid. In such cases the exponential model can be regarded as an equivalent scheme which reflects the main channels of in-cage RP transformations, and the mean time τ_c in (2.31) can be interpreted as the total time of all the RP contacts.

2.1.2 Radical recombination¹

Recombination of radical is possible only at their closest approach. That is why it is usually treated as a contact process. As a rule, two radicals in contact are assumed to give recombination products with the rate constant K , (see, [2.19–22]). According to this assumption, the probability of RP recombination at a time t in the primary cage is $1 - \exp(-Kt)$. In the extreme model of continuous diffusion, the reaction is introduced as a boundary condition of RP absorption on the contact sphere. It can be found by setting the rate of appearance of the radicals on the contact sphere surface equal to the RP diffusion flow towards it. As a result we have [2.17, 22]:

$$D \cdot (\partial n(r)/\partial r)|_{r=b} = n(b) \cdot W, \quad (2.32)$$

where $n(b)$ is the RP concentration on the contact sphere, D is the mutual radical diffusion coefficient, W is the rate of their appearance on the contact sphere and $n(r)$ is the concentration of RPs with r – distant partners. The quantity W can be

¹ Here we discuss the spin-independent radical recombination theory. Spin factors should be taken into account when discussing experimental data. The next sections consider the recombination with account taken of RP spin states.

expressed in terms of the RP recombination rate constant in the primary cage provided the reaction occurs not at a fixed distance between the radicals but in a layer of thickness a included between two spheres with the radii $b-a$ and b , respectively (see Fig. 2.3). This gives $W = aK$, and the boundary condition (2.32) reduces to [2.22]

$$D \cdot (\partial n / \partial r)|_{r=b} = a \cdot n(b) \cdot K. \quad (2.33)$$

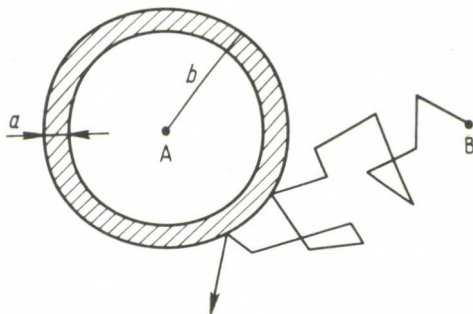


Fig. 2.3. Schematic presentation of the reaction layer; a is the thickness of the reaction zone

Note that in this approach the equation for mutual radical diffusion is solved in the region outside the reaction layer. Understanding of the significance of the reaction layer and the introduction of this layer width as an effective parameter allows us to calculate reasonably well the rate of particle appearance on the radical contact sphere.

The reaction between partners with so high reactivity that the very first contact results in their recombination is of particular interest. In this case, instead of (2.32) one can use the condition of full RP absorption on the contact sphere and set [2.9]

$$n(b) = 0. \quad (2.34)$$

Geminate RP recombination. We begin the discussion of cage effects in radical recombination with the simplest, exponential, RP model. In this case the RP is transformed by several parallel and independent channels. The probability of geminate RP recombination is equal to the ratio of the recombination rate K to the total rate of all RP processes given in Fig. 2.4

$$p_r = K / (K + K_s + \tau_c^{-1}).$$

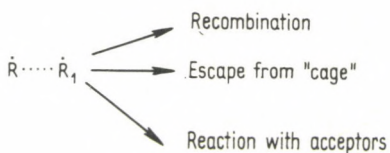


Fig. 2.4. Basic channels of RP in-cage transformations

It is expedient to introduce the effective time of geminate RP recombination. It is determined by the relation $\tau_r^{-1} = K_s + \tau_c^{-1}$ and equals

$$\tau_r = \tau_c / (1 + K_s \cdot \tau_c). \quad (2.35)$$

Hence, the geminate recombination probability can be presented as

$$p_r = K \tau_r / (1 + K \tau_r). \quad (2.36)$$

It follows that geminate recombination is determined by the quantity $K \cdot \tau_r$, i.e., the reagent reactivity and the effective reaction time. If $K \cdot \tau_r \gg 1$, then $p_r \rightarrow 1$ and the RP recombination probability becomes independent of the contact time and we observe a cage effect saturation: a further increase of the RP contact time with the viscosity does not influence the RP recombination. This is quite different from the case for radicals with lower reactivity, when $K \cdot \tau_r < 1$. Here the cage effect is vividly manifested by p_r increasing with the contact time.

A deficiency of the exponential model is that it neglects RP re-encounters. A more detailed quantitative analysis of the cage effect requires use of a diffusion RP model which takes into account all collisions of the reagents. The continuous diffusion model gives a satisfactory description of the reactant motion in liquids. That is why the majority of theories concerning radical recombination in liquids are based on this approach. Here we present some of the most important results obtained within the continuous model.

The contact character of the process allows us to present the geminate RP recombination probability p_g as the product of the probability of the first contact, p_0 , and the full reaction probability during all re-encounters (including the first contact) provided the first approach up to the contact radius did take place. If we express the latter probability as p_r , the geminate recombination probability equals

$$p_g = p_0 \cdot p_r, \quad (2.37)$$

p_0 was discussed in detail in the previous chapter. Here we shall consider only p_r , which can be expressed by eq. (2.36). The difference between the exponential and continuous models is that in the latter the effective geminate recombination time is not expressed by eq. (2.35). Here τ_r is the total time of all the RP contacts. Some practically important τ_r expressions are given in Table 2.2.

The analysis of these results shows that the effective RP recombination time depends on the molecular-kinetic radical parameters (b , D), the reactivity characteristics (a , K), and the interrational interaction parameters $U(r)$. Let us evaluate the scale of the cage recombination time for solutions with viscosity ≈ 1 cP where the mutual reagent diffusion is characterized by the coefficient $D \approx 10^{-5}$ cm² · s⁻¹. The distance at which the exchange attraction between the partners is e -fold reduced is taken as the width of the reaction layer. For real atomic interaction potentials $a \approx 0.01$ – 0.05 nm. Bearing in mind the fact that the contact radius is of the order of several angstroms, we obtain $\tau_r \sim 10^{-12}$ – 10^{-11} s for uncharged radicals.

Table 2.2. Recombination time τ_r of radicals with isotropic reactivity within the framework of the continuous diffusion model. RP parameters are: D , the coefficient of the mutual diffusion of the partners, b , the distance of their closest approach, a , the width of the reaction zone, r_c , the Onsager radius, q_k the charges of the partners, and ϵ the relative permittivity

K_s^a	$U(r)^b$	τ_r
$K_s = 0$	$U(r) = 0$	$a \cdot b/D$
$K_s \neq 0$	$U(r) = 0$	$(a \cdot b/D)/[1 + (K_s \cdot b^2/D)^{1/2}]$
$K_s = 0$	$U(r) \neq 0$	$(a \cdot b/D) \cdot b \cdot S(b) \cdot \exp(-U(b)/kT)$
$K_s = 0$	$U(r) = -q_1 \cdot q_2/\epsilon \cdot r$	$(a \cdot b/D) \cdot (b/r_c) \cdot [\exp(r_c/b) - 1]$
$K_s = 0$	$U(r) = +q_1 \cdot q_2/\epsilon \cdot r$	$(a \cdot b/D) \cdot (b/r_c) \cdot [1 - \exp(-r_c/b)]$

^a K_s is the rate of RP reaction with acceptors

^b $U(r)$ is the potential of interaction between two r -distant reagents

When they are present, acceptors reduce the effective recombination time (see Table 2.2). This can be explained as follows. The quantity τ_r is the total time of all contacts of a given radical pair at the reaction radius. Between the re-encounters the acceptors can capture some radicals thus preventing them from occurring at the recombination radius. As a result, the effective recombination time, or the total time of two radicals being at the reaction radius, is reduced. The recombination time also depends on the radical interaction. According to Table 2.2, in the case of radical-ion recombination in such highly polar solvents as water, the Coulomb interaction only slightly influences the effective recombination time, while in nonpolar solvents this influence is great.

Table 2.2 shows that the reagent interaction changes the reaction time by a factor of $\tau_r(U)/\tau_r(U=0) = b \cdot S(b) \cdot \exp(-U(b)/kT)$. Table 2.3 gives the factor $\chi = \tau_r(U)/\tau_r(U=0)$ calculated numerically for the potentials that are most interesting from the viewpoint of possible applications: (1) Coulomb interaction of charged partners in a polar medium with the Debye shielding effect taken into account; (2) the mutual reagent attraction due to exchange interaction. In the former case the interaction potential equals

$$U(r) = \pm(q_1 \cdot q_2/\epsilon \cdot r) \cdot \exp(-(r-b)/r_D)/(1+b/r_D), \quad (2.38)$$

where r_D is the shielding radius. The exchange interaction reduces with increasing distance between the reagents according to the exponential law

$$U(r) = -U_0 \cdot \exp[-(r-b)/r_e], \quad (2.39)$$

where r_e characterizes the width of the effective exchange interaction layer. In Table 2.3 are given numerical values of χ including values for the case when the Debye shielding effect is neglected, when $r_D \rightarrow \infty$.

Table 2.3. Values of $\chi = \tau_r(U \neq 0) / \tau_r(U = 0)$ at the following RP parameters: $T = 300$ K, $b = 4$ Å

		Coulomb interaction ^a							
		Attraction				Repulsion			
$r_D^c, \text{Å}$	ϵ^b	5	10	20	81	5	10	20	81
∞		$3.104 \cdot 10^{10}$	$6.638 \cdot 10^4$	$1.394 \cdot 10^2$	2.617	0.036	0.072	0.145	0.479
100		$1.967 \cdot 10^{10}$	$5.606 \cdot 10^4$	$1.318 \cdot 10^2$	2.601	0.036	0.072	0.145	0.480
10		$7.243 \cdot 10^7$	$4.891 \cdot 10^3$	$5.141 \cdot 10^1$	2.258	0.036	0.073	0.149	0.508
5		$1.369 \cdot 10^6$	$8.441 \cdot 10^2$	$2.243 \cdot 10^1$	1.974	0.036	0.075	0.161	0.549
1		$1.730 \cdot 10^2$	$1.217 \cdot 10^1$	3.472	1.336	0.045	0.135	0.332	0.748

^a charges of partners are equal, $|q_1| = |q_2| = e$, e is the charge of electron

^b ϵ is a dielectric constant

^c r_D is the Debye shielding radius

Exchange interaction $U(r)$ at $r_e = 0.5$ Å

U_0/kT	10^{-3}	10^{-2}	10^{-1}	1	10	20
χ	1.000	1.008	1.095	2.507	$1.656 \cdot 10^4$	$3.376 \cdot 10^8$

The data listed in Tables 2.2 and 2.3 show that the inter-reactant attraction can essentially increase the effective recombination time by holding the partners in the cage; the reactant repulsion decreases the effective reaction time by pushing the partners out of the cage. The influence of the radical interaction on the effective reaction time is negligible if even at the closest approach of the particles it remains small compared to the thermal energy of the translational motion of the reactants.

In Table 2.4 we compare the recombination probabilities p_r calculated with and without taking account of the exchange interaction between the reactants. As expected, an exchange interaction that exceeds the thermal energy increases the recombination probability of radicals with comparatively low reactivity and in fact does not influence that of more active partners. In the case of active radicals even without exchange interaction, $K \cdot \tau_r > 1$ and the recombination probability reaches its extreme value, $p_r \rightarrow 1$. Hence, an increase in τ_r due to exchange interaction hardly affects p_r . The situation is different in the case of low-active radicals when $K \cdot \tau_r < 1$ and $p_r \cong K \cdot \tau_r$. For such partners the recombination probability increases with the reaction time τ_r .

The results obtained by the continuous model, as has been noted, can be applied to the jump mechanism if the jump length is comparatively small, $\lambda_D \lesssim b$. For the general case of jump movement, the geminate recombination probability was found by Noyes by summing up the contributions of all re-encounters made to the reaction [2.11]. Let λ be the RP recombination probability on contact. Note an

Table 2.4. Radical recombination probability p_r and the values of χ (see Table 2.3) at different exchange interaction parameters (the first column) and various reactivity of partners to recombine within the reaction zone (the second column) ($D = 10^{-5}$ cm²/s, $b = 0.4$ nm, $a = 0.005$ nm, $r_e = 0.0347$ nm)

U_0/kT	K, s^{-1}	p_r	χ
0	10^{14}	0.992	1
	10^{12}	0.666	
	10^{10}	$1.96 \cdot 10^{-2}$	
	10^8	$1.97 \cdot 10^{-4}$	
0.0025	10^{14}	0.992	1.002
	10^{12}	0.666	
	10^{10}	$1.96 \cdot 10^{-2}$	
	10^8	$1.97 \cdot 10^{-4}$	
0.25	10^{14}	0.996	1.268
	10^{12}	0.716	
	10^{10}	$2.46 \cdot 10^{-2}$	
	10^8	$2.52 \cdot 10^{-4}$	
2.5	10^{14}	0.996	10.81
	10^{12}	0.956	
	10^{10}	$1.77 \cdot 10^{-1}$	
	10^8	$2.15 \cdot 10^{-3}$	
10	10^{14}	1	$1.766 \cdot 10^4$
	10^{12}	1	
	10^{10}	0.996	
	10^8	0.776	

important supposition which is usually assumed in the radical recombination theory: the reaction probability at a given contact is considered to be independent of whether the radicals have had any previous encounters. Note that the anisotropic density distribution of unpaired electrons and the spin selection rule in RP recombination show that this supposition is not always valid.

The geminate RP recombination probability can be expressed through the probabilities of the first, p_0 , and repeated, p , contacts,

$$p_g = p_0 \cdot \lambda / [1 - (1 - \lambda)p] = p_0 \cdot \lambda \cdot n / (1 + p \cdot \lambda \cdot n). \quad (2.40)$$

Hence, in the general case of jump mechanism

$$p_r = \lambda \cdot n / (1 + p \cdot \lambda \cdot n), \quad (2.41)$$

where n is the number of all encounters, $n = 1/(1 - p)$. The comparison of (2.41) with the result of the continuous approach presented above shows that when the jump length decreases, the following relations are valid

$$\begin{aligned} \lambda \cdot n &\rightarrow K \cdot \tau_r, \\ p \cdot \lambda \cdot n &\rightarrow K \cdot \tau_r, \end{aligned} \quad (2.42)$$

i.e., $p \rightarrow 1$, $n \rightarrow \infty$. Although the RP recombination probability in an individual contact tends to zero as a result of assuming an infinitely small encounter time in the continuous approach, the total effect of all re-encounters is a definite geminate recombination probability. In this extreme case of continuous diffusion, when an individual contact contributes negligibly to the reaction, the effect of RP re-encounters on the radical recombination is appreciable.

In the case of the jump mechanism, the role of re-encounters depends on the reactivity of partners. Indeed, for radicals with high reactivity, when $\lambda = 1$, the very first contact results in a product, the radicals cannot diffuse apart and thus do not re-encounter at all. For low-reactive radicals, when $\lambda \ll 1$, re-encounters contribute the better half of the geminate product. This follows from the fact that in liquids radicals move by small jumps, $\lambda_D \lesssim b$, the re-encounter probability p is within the range 0.5 to 1 (Table 2.1) and thus the total number of RP contacts either equals or exceeds 2.

Biradicals are of interest as a particular case of RPs. Only their reaction with acceptors can prevent them from recombining. Hence, in the absence of radical acceptors, $p = 1$, radical re-encounters do occur and yield a product unless this biradical is stable.

In chemical kinetics the cage effect is usually characterized by the RP escape probability (see, e.g., [2.23]), i.e. by the quantity

$$e = 1 - p_g = 1 - p_0 \cdot p_r \quad (2.43)$$

This relation is sometimes used to evaluate the quantum yield of molecular photodecomposition and, vice versa, to evaluate the geminate recombination probability p_g from experimental data on the quantum photodecomposition yield. However, one should bear in mind that in a general case the value calculated by (2.43) must not be identified with the actual quantum photodecomposition yield. Relation (2.43) gives the RP escape probability provided an excited molecule dissociates and generates an RP. When absorbing a photon, the molecule either can or cannot dissociate, because it may be deactivated as a result of its collisions with some unexcited molecules. Such excitation relaxation can take place in gas reactions too, but in a condensed medium it is much more effective, and competes successfully with the molecular decomposition process, so decreasing the quantum yield of RP formation.

Radical recombination in homogeneous solutions. In radical reactions in homogeneous solutions (*bulk recombination*) we can distinguish two basic stages: the formation of diffusion RPs as a result of the first contacts, and their subsequent recombination. According to this classification, the radical recombination rate constant can be presented as

$$K_r = K_D \cdot p_r \quad (2.44)$$

where K_D is the rate constant of diffusion RP formation and p_r is the RP recombination probability. The diffusion encounter constant is given, e.g., by (2.27, 28). The recombination probability of two colliding radicals p_r in (2.44) is analogous

to that for the geminate recombination discussed above (see (2.36, 41)). For example, in the continual approach we have

$$K_r = K_D \cdot K\tau_r / (1 + K\tau_r). \quad (2.45)$$

The quantity $q = K \cdot \tau_r$ is a characteristic parameter determining the kinetic regularities of radical recombination in solutions. If the radical reactivity is sufficiently high, so that $q > 1$, and the diffusion pair practically always recombines without leaving the cage, then the diffusion pair formation can be treated as a limiting stage of the reaction. Under these conditions the reaction rate equals that of the first diffusion contacts and $K_r = K_D$. Otherwise, when $q < 1$, the diffusion RP recombination in the cage becomes the limiting stage itself.

Non-stationary recombination. In a number of experiments the reaction proceeds as a nonstationary process. The kinetics of geminate RP recombination induced by light or ionizing radiation serves as an example. Analysis of the geminate RP recombination kinetics under nonstationary conditions can yield some valuable information on the character of the in-cage reactant diffusion and allow one to measure experimentally the time distribution of re-encounters (see, e.g., [2.13, 24]).

The contact distribution functions (2.1–10) allow one to calculate the RP recombination kinetics. The simplest results are obtained for the recombination of uncharged radicals with a reactivity sufficiently high for the very first contact to yield a product. The rate of the RP recombination is

$$W = -\dot{n}(t) = n(o) \cdot m_0 \cdot t^{-3/2} \cdot \exp(-\pi \cdot m_0^2 / p_0^2 \cdot t) = n(o) f_0(t),$$

where $n(t)$ is the RP concentration and $f_0(t)$ is the first contact distribution for RPs which start from a specified interradsical distance r_0 (2.9).

Up to a moment t_{\max} (2.12) the reaction rate increases and then reduces by the law $W \sim t^{-3/2}$. The total recombination product yield kinetics is described by the equation

$$C(t) = \int_0^t W(t) dt = n(o) \cdot p_0 \cdot \operatorname{erfc}[(\pi \cdot m_0^2 / p_0^2 \cdot t)^{1/2}], \quad (2.46)$$

where $\operatorname{erfc}(x)$ is a complementary error function,

$$\operatorname{erfc}(x) = (2/\sqrt{\pi}) \cdot \int_x^\infty \exp(-x^2) dx \equiv 1 - \operatorname{erf}(x).$$

At small times when $t < t_{\max}$ the product yield kinetics follows the law

$$C(t) \approx n(o)(p_0^2/\pi \cdot m_0) \cdot t^{1/2} \cdot \exp(-\pi \cdot m_0^2/p_0^2 \cdot t).$$

At long times, when $t > t_{\max}$ the product yield kinetics follows

$$C(t) \cong n(o) \cdot p_0 \cdot (1 - 2m_0/p_0 \cdot \sqrt{t}).$$

In the case of radicals with a finite reactivity, the recombination product yield kinetics can be found by summing up the contributions of all the contacts [2.11]

$$C(t) = n(o) \cdot \lambda \sum_{n=0}^{\infty} (1-\lambda)^n \cdot \int_0^t dt_{n+1} \cdot \int_0^{t_{n+1}} dt_n \dots \int_0^{t_2} dt_1 \times \\ \times f_0(t_1) \cdot f(t_2-t_1) \dots f(t_{n+1}-t_n),$$

where $f_0(t)$ and $f(t)$ are the distribution functions of the first and the second contacts respectively, λ is the recombination probability at a single contact.

In terms of the continuous diffusion model the recombination kinetics are described by the following relations. For RPs starting from the recombination radius the reaction rate and the total product yield kinetics are (see, e.g. [2.16])

$$W = [a \cdot K / (\pi D t)^{1/2}] \cdot [1 - \sqrt{\pi} \cdot z \cdot \exp(z^2) \cdot \operatorname{erfc}(z)] \cdot n(o), \\ C(t) = [K \cdot \tau_r / (1 + K \cdot \tau_r)] \cdot [1 - \exp(z^2) \cdot \operatorname{erfc}(z)] \cdot n(o), \quad (2.47)$$

where

$$z = (1 + K \cdot \tau_r) \cdot (t / \tau_D)^{1/2}, \quad \tau_D = b^2 / D.$$

At small times, when $t < \tau_D$,

$$C(t) \cong n(o) \cdot 2K\tau_r(t/\pi \cdot \tau_D)^{1/2}$$

At great times $t > \tau_D$

$$C(t) \cong n(o) \cdot [K \cdot \tau_r / (1 + K \cdot \tau_r)] \cdot [1 - (\tau_D / \pi \cdot t)^{1/2} / (1 + K \cdot \tau_r)].$$

If the radicals start from an arbitrary distance r_0 the reaction rate and the total product yield kinetics are set by the relations

$$W(t) = n(o) \cdot a \cdot K \int_0^t d\tau \cdot f_0(\tau) \cdot [1 - \sqrt{\pi} \cdot z_1 \cdot \\ \cdot \exp(z_1^2) \cdot \operatorname{erfc}(z_1)] / [(\pi D(t-\tau))^{1/2}], \\ C(t) = n(o) [K\tau_r / (1 + K\tau_r)] \cdot [p_0 - \int_0^t d\tau \cdot f_0(\tau) \exp(z_1^2) \operatorname{erfc}(z_1)], \quad (2.48)$$

where

$$z_1 = (1 + K\tau_r) \cdot [(t-\tau)/\tau_D]^{1/2}.$$

The recombination kinetics are therefore characterized by two times: t_{\max} and τ_D . If the radicals start from the recombination radius, the RP in-cage lifetime τ_D serves as a characteristic time of the process.

In the presence of radical acceptors the product yield rate is reduced by an amount proportional to $\exp(-K_a t)$ (cf. (2.14)).

The nonstationary stage is also observed in the process of radical recombination in homogeneous solutions.

Below we give the well-known relation which describes the recombination kinetics in homogeneous solutions (see, e.g., [2.22]). Let us assume that at the initial moment we have a homogeneous solution of radicals A and B . At the very first moment only those radical pairs react that happen to be in contact at the moment when the solution is being prepared. The reaction becomes steady-state as the RPs,

whose radicals at the initial moment occur at a sufficiently close distance, vanish. For example,

$$\begin{aligned} dC_A/dt = dC_B/dt &= -K_D \cdot \lambda [1 + \lambda \cdot b / (\pi \cdot D \cdot t)^{1/2}] C_A \cdot C_B; \\ \lambda &= K \cdot \tau_r / (1 + K \tau_r), \end{aligned} \quad (2.49)$$

describes the recombination kinetics of uncharged radicals. Thus we can see that at a time of the order of $\tau_D = b^2/D \sim 10^{-9}$ s the reaction becomes stationary.

Reactivity anisotropy and its averaging by rotation and RP translational diffusion in a cage. In most cases radical reactivity must be anisotropic, since the density distribution of an unpaired electron is as a rule also anisotropic. It means that a RP can recombine not at any contact but at definite mutual radical orientations favourable for overlapping the unpaired electron orbitals. The anisotropy of reactivity can be characterized by a steric factor f , i.e. the statistical weight of the mutual orientation of two colliding radicals which ensures the overlap of their electron orbitals necessary for the reaction.

The way in which the anisotropy of the unpaired electron distribution manifests itself in radical recombination depends strongly on the relaxation of the mutual orientation of the partners in the cage. If during the in-cage RP lifetime the mutual orientation cannot change, the steric factor f should be introduced as a multiplier into the above relations for the RP recombination probability. In fact, the mutual orientation of RP partners changes. There are two relaxation mechanisms of mutual reagent orientation. First, the radical rotation that occurs in the cage either during the RP contact or between two subsequent contacts. Second, even if the rotation is completely "frozen", the mutual orientation of the partners will vary in re-encounters: when at the contact radius, the radicals can touch on different sides. The former mechanism is of primary importance in averaging the anisotropy of RP reactivity. The latter mechanism is effective only for re-encounters which take place after several steps of spatial diffusion. However the statistical weight of such re-encounters is small, and during long spatial travels the mutual partner orientation can become completely random due to their rotation. If so, the recombination occurs as if the reaction is independent of radical mutual orientation and the RP recombination on immediate contact is characterized by an average rate constant $K_{\text{eff}} = f \cdot K$.

The role of orientation in radical recombination has not been studied in detail yet, but it has been shown [2.25] to be very important. Note that an analogous problem is also provided by bimolecular spin exchange between paramagnetic particles. The spin exchange, like radical recombination, results from the orbital overlapping of unpaired electrons and, generally speaking, depends on the mutual particle orientation. This problem has been discussed in detail in ref. [2.26].

A number of new problems, which are irrelevant to the isotropic case arise, in reactions of radicals with anisotropic properties. In the latter case the recombination probability depends on all preceding contacts. Geminate and bulk recombinations follow different schemes. In a diffusion pair, orientations favourable

for the reaction are realized at the moment of the first collision with the probability f . In geminate recombination, at the moment of the first collision, the partners can still "remember" their mutual orientation in the parent molecule. As in the case of isotropic reactivity explored above, the reaction of radicals with anisotropic properties can be characterized by the geminate recombination probability $p_g = p_0 \cdot \tilde{p}_r$, and the constant $K_r = K_A \cdot p_r$; however p_g and K_r cannot be expressed in a general case via the same cage recombination probability, $p_r \neq \tilde{p}_r$ (cf. eq. (2.37, 44)).

The radical reactivity anisotropy averaged by rotation has been considered theoretically [2.27]. RP recombination was calculated with account being taken of the orientational relaxation both at a collision moment and, what is of a particular interest, between re-encounters. The data obtained confirm the above qualitative considerations. Thus, for the diffusion RP recombination probability we have

$$p_r = f \cdot K \cdot \tau_c \cdot n [1 + n(n'_0 + w)] \cdot \{1 + n(n'_0 + w) + K \cdot \tau_c \cdot n [1 + f n(n'_0 + w)]\}^{-1}, \quad (2.50)$$

where f is the portion of mutual radical orientations favourable for the reaction, n is the number of RP contacts in the cage, K is the RP recombination rate constant given contacts favourable for the reaction, $n'_0 = \tau_c / \tau'_0$ is the number of flips of the partners at their contact time (τ'_0 is the time of RP mutual orientation relaxation in a contact), and w/p expresses the probability of a radical flip between re-encounters:

$$w = \int dt \cdot f(t) \cdot [1 - \exp(-t/\tau_0)].$$

Here τ_0 is the relaxation time of the mutual radical orientation between re-encounters. With eq. (2.4) we obtain

$$w = p \cdot [1 - \exp(-(4\pi m^2/p^2 \cdot \tau_0)^{1/2})]. \quad (2.51)$$

From (2.50) it follows that the recombination probability is enhanced by rotation. If the in-cage radical rotation was "frozen" the reaction would be characterized by the steric factor f and

$$p_r = f \cdot K \cdot \tau_c \cdot n / (1 + K \cdot \tau_c \cdot n). \quad (2.52)$$

When anisotropy is averaged by rotation the general expression (2.50) can be represented in the form (2.52) provided the effective quantities

$$f_{\text{eff}} = f \cdot [1 + n(n'_0 + w)] / [1 + f n(n'_0 + w)], \\ K_{\text{eff}} = K \cdot [1 + f n(n'_0 + w)] / [1 + n(n'_0 + w)] \quad (2.53)$$

are substituted for f and K . Hence, the radical rotation increases f_{eff} to unity. Simultaneously, the radical recombination rate constant in a contact, K_{eff} , decreases. Under rapid rotation of the radicals $K_{\text{eff}} \rightarrow fK$. For low-reactive radicals, when $K \cdot \tau_c \cdot n < 1$, increasing f_{eff} and decreasing K_{eff} compensate each other, $p_r \cong f_{\text{eff}} \cdot K_{\text{eff}} \cdot \tau_c \cdot n = f \cdot K \cdot \tau_c \cdot n$, i.e., the in-cage rotation of the radicals does not practically influence their recombination. For sufficiently active radicals $fK\tau_c n > 1$,

$p_r \cong f_{\text{eff}}$ so that due to the in-cage reagent rotation the steric hindrances are less than in gas-phase reactions between the same partners.

RP recombination probability in the presence of acceptors and the long-range interaction between reagents can be calculated by eq. (2.50). In the presence of acceptors the re-encounter statistics are described by eqs (2.14) and the effective reaction time is

$$\tau_r = \tau_c \cdot n_s.$$

The total number of encounters is

$$n_s = 1/(1 - p_s) = 1/[1 - p \cdot \exp(-(4\pi \cdot m^2 K_s/p^2)^{1/2})]. \quad (2.54)$$

The quantity w averaged by eq. (2.14) takes the form

$$w_s = p \cdot \{\exp(-\mu K_s^{1/2}) - \exp[-\mu(K_s + 1/\tau_0)^{1/2}]\} \quad (2.55)$$

where

$$\mu = 2\sqrt{\pi} \cdot m/p.$$

Acceptors reduce the reaction time τ_r and the radical lifetime. This results in a decrease of the time available for the relaxation of the mutual radical orientation. Hence acceptors reduce the orientation relaxation effect in radical recombination.

We have already mentioned that for radicals with anisotropic properties RP geminate and bulk recombinations occur, generally speaking, under different conditions. The following example illustrates this statement. Let the molecular decomposition fragments remain in the primary cage and their mutual orientation in the parent molecule be preserved at the moment of decomposition. Then the recombination probability equals [2.27]

$$\tilde{p}_r = K_{\text{eff}} \cdot \tau_c \cdot n / (1 + K_{\text{eff}} \cdot \tau_c \cdot n). \quad (2.56)$$

The analysis of this formula leads to completely opposite conclusions as compared to the diffusion pair recombination. According to (2.56) the orientation relaxation decreases the reaction probability which is most readily observed in low-reactive radical recombinations. For sufficiently active radicals, under the conditions in question, rotation of radicals can be neglected as they are quicker to react than to rotate.

The extreme situation of continuous diffusion is then of interest. In this case the results are simplified and become applicable for practical use. Under these conditions

$$\begin{aligned} \tau_c \cdot n_s = \tau_r &\Rightarrow a \cdot b/D \cdot [1 + (K_s \cdot \tau_D)^{1/2}], \\ n_s \cdot n'_0 &\Rightarrow \tau_r/\tau'_0, \\ n_s \cdot w_s &\Rightarrow \{(K_s \cdot \tau_D + \tau_D/\tau_0)^{1/2} - (K_s \cdot \tau_D)^{1/2}\} \cdot \\ &\cdot [1 + (K_s \cdot \tau_D)^{1/2}]^{-1}; \quad \tau_D = b^2/D, \end{aligned} \quad (2.57)$$

τ_D is the effective in-cage RP lifetime in the absence of acceptors.

To simplify the case consider RP recombination in the absence of acceptors. Substitute eq. (2.57) into eq. (2.53) and obtain the following expressions for effective values of the steric factor and the RP recombination rate constant

$$\begin{aligned} f_{\text{eff}} &= f \cdot (1+d)/(1+f \cdot d) \geq f, \\ K_{\text{eff}} &= K \cdot (1+f \cdot d)/(1+d) \leq K, \end{aligned} \quad (2.58)$$

where

$$d = n \cdot n'_0 + n \cdot w = a \cdot b/D \cdot \tau'_0 + (b^2/D \cdot \tau_0)^{1/2}. \quad (2.59)$$

For quantitative evaluation assume that the orientation relaxation both in contacts and between them occurs with the same rate, i.e. $\tau'_0 = \tau_0$. The relaxation time of the mutual radical orientation can be estimated by the Debye formula for molecular rotational relaxation in liquids. Assume both partners have anisotropic reactivity. Then τ_0 can be presented as

$$\tau_0 = b^2/6 \cdot D. \quad (2.60)$$

If one of the radicals has isotropic distribution of the unpaired electron then

$$\tau_0 = b^2/3D.$$

Substitute eq. (2.60) into eq. (2.59) and obtain

$$d = 6a/b + \sqrt{6}. \quad (2.61)$$

The reaction layer width is an order of magnitude less than the reaction radius, $a \ll b$. Hence $(6a/b) < \sqrt{6}$. Therefore, the basic contribution to the averaging of the radical reactivity anisotropy is made by the orientation relaxation between re-encounters. Equations (2.58, 61) show that in the case of high anisotropy of radical reactivity, i.e. at $f \lesssim 0.1$, the effective steric factor increases by a factor of 3–4, K_{eff} showing the same decrease.

From the foregoing we can come to the conclusion that the theory of RP molecular dynamics has been developed in detail. Now consider the theory of spin-dependent RP recombination which is the basis of interpretation of experiments on chemically induced spin polarization and magnetic effects in radical reactions.

2.2 RP singlet-triplet evolution

The theory set forth in the previous section neglects the role of RP spin state in RP recombination. Therefore, it fails to account for the experimentally observed chemically induced spin polarization and magnetic effects.

2.2.1 Spin dependence of RP recombination

The dependence of the recombination probability on the electron state multiplicity and the changes of this multiplicity due to RP spin motion are the basis of the magnetic effects and spin polarizations under discussion.

The spin selection rule. A RP can be found in two spin states: either *singlet* with the total spin of unpaired electrons being zero, or *triplet*, with the total spin being unity. The RP recombination probabilities in these states are usually different. Indeed, for the overwhelming majority of molecules, singlet is the ground electron state, whereas triplet is their excited state. To illustrate the foregoing Fig. 2.5 shows plots of the energy of the ground singlet and excited triplet RP terms vs. the distance between the partners. According to Fig. 2.5, a stable product will result from singlet

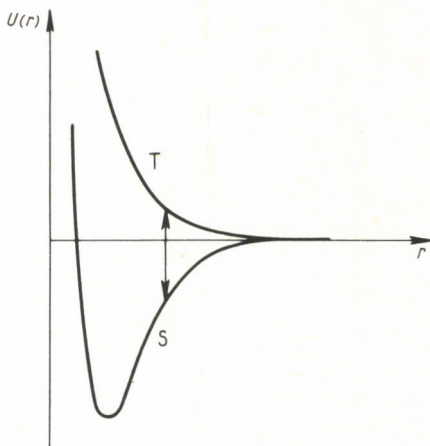


Fig. 2.5. Schematic diagram of RP singlet (S) and triplet (T) terms as a function of interradical distance, r .
 $U_S - U_T = 2\hbar J$, $J(r)$ is an exchange integral

RPs. In fact RP multiplicity can vary at the moment of encounter, and so formation of singlet molecules becomes possible even for triplet RPs. However, RP recombination in the triplet state is much less effective than that in the singlet state. Therefore in what follows if not mentioned explicitly, RP recombination will be assumed to occur provided the mutual orientation of the unpaired electrons conforms to the singlet state, and to be impossible for triplet RPs. Note that for some molecules the ground term is triplet. For these the RP recombination in the singlet state is less probable. In the general case, recombination of triplet RPs is also possible. This gives a product in an electronically-excited triplet state which then makes a transition to the ground singlet state as a result either of radiationless intramolecular intersystem crossing or of radiative decay.

Even in the case when recombination of triplet and singlet RPs is equally probable the spin selection rule with respect to RP multiplicity can have

experimental consequences. Indeed, assume that a RP can recombine both from the singlet and triplet states with equal probability. In the former case it gives, a molecule in the singlet (ground or excited) state. If the recombination product is in the singlet excited state, it can be detected by its fluorescence. A triplet RP recombination yields a triplet-excited molecule which can be detected either by phosphorescence or triplet-triplet absorption. Thus, one can investigate singlet and triplet RP recombination products separately. The spin selection rule can thus be applied to each of these products.

RPs are usually classified as *correlated* or *uncorrelated* according to their spin states. In geminate recombination RPs are correlated. The spin alignment cannot change during the molecule decomposition time and thus the RP is formed in the spin state of the precursor-molecule. In a diffusion pair the unpaired electron spins have a random orientation — it is an uncorrelated RP. At the moment of the first contact a diffusion RP is in S and T states with the statistical weights 1/4 and 3/4. A fraction of singlet RPs recombine at the very first contact and hence the statistical weight of triplet diffusion pairs grows.

Singlet-triplet transitions in the RP. The cage effect ensures conditions favourable for eliminating selectivity in RP recombination. For example, even in a solution of low viscosity the period two neutral radicals reside in a cage is comparatively long and equal to $b^2/D \sim 10^{-9}$ s. During this time even weak interactions of unpaired electrons, e.g., with the external magnetic field or with the magnetic nuclei, which make up only one hundred-thousandth of the thermal energy, can effectively mix the singlet and triplet terms. Re-encounters and the Coulomb attraction of the partners are important for elimination of the spin selection rule: on the one hand, the time intervals between the re-encounters are sufficiently long for a singlet-triplet (S-T) transition, on the other hand, the separation between the partners reaches tens of angströms so that S and T term energies practically coincide (see Fig. 2.5) and the S-T transition is a resonant process. In the case of charged particles the Coulomb interaction can influence S-T evolution markedly. The Coulomb attraction essentially increases the in-cage RP lifetime. Therefore, it is in ion-radical reactions that RP singlet-triplet evolution is manifested most clearly.

We have seen that the magnetic effects in radical recombination are caused by the spin selection rule and S-T transitions in RPs. The main channels of RP transformations including the RP multiplicity changes, are shown in Fig. 1.2. Of these processes, only intersystem S-T transitions depend on the interaction of RP unpaired electrons with external magnetic fields. This is the physical basis of magnetic effects in radical recombination which are to be discussed in the present book. At the same time, the singlet-triplet evolution in an RP also depends on the internal magnetic fields induced by the nuclear spins at the locations of unpaired electrons. It gives rise to magnetic isotopic effects. Singlet-triplet transitions are different in RPs with different configurations of nuclear spins. This leads ultimately to nuclear polarizations both in the recombination products and in the radicals which have not yet recombined.

The analogy between the spin dependence of the reaction and the reactivity anisotropy. Attention should be paid to the fact that, from the viewpoint of formal kinetics, RP multiplicity manifests itself like anisotropy in unpaired electron distribution. The spin selection rule permits the reaction only for a certain mutual orientation of radical spins and because of the steric restrictions the reaction can occur only at certain mutual orientations of the reactants themselves. The S-T transitions remove the spin restrictions and the reactant rotation averages the anisotropic effects and thus removes the steric hindrances. This analogy between the two effects is observed in all their kinetic manifestations. As a result of both effects, the geminate RP recombination probability depends on the manner of RP formation, and on the mutual orientation of the reactants or spins at the moment of the very first contact between the partners. These are responsible for the dependence of the RP recombination probability in a contact on the number of previous contacts and also for the differences between the recombinations of geminate and diffusion pairs.

Note the following manifestations of the spin-state dependence of radical recombination. This dependence can be easily taken into account in two extreme situations: no S-T transitions; a very strong S-T mixing. If S-T transitions cannot occur during the in-cage RP lifetime, we have:

(a) Geminate recombination of triplet RPs is impossible, whereas no spin selection rule is against singlet RP recombination, hence the recombination probability of a singlet-born RP is described by the spin-independent theory given in Section 2.1.

(b) The recombination rate constant in homogeneous solutions is one-quarter that of the spin-independent theory according to the statistical weight of singlet diffusion uncorrelated pairs.

The other situation is realized if S-T transitions are so effective that they occur during the "settled" radical lifetime ($\approx 10^{-11}$ s). Then the spin correlation in the RP is relaxed so fast that at any moment the spins can be considered uncorrelated. In this situation the RP recombination probability must be independent of the initial spin state of the pair and the occurrence of the reaction at a given contact becomes independent of the previous contacts. As a result, the geminate and bulk radical recombinations would be described by the spin-independent theory with a rate constant averaged over all RP spin states, $K_{\text{eff}} = (1/4)K$. Here K is the recombination constant of singlet RPs at the moment of contact. It was used in the formulas of Section 2.1 as a monomolecular rate constant of RP recombination inside the reaction layer (see Fig. 2.3). Thus, in the two extreme situations (when during the in-cage radical lifetime either (a) no S-T transition occurs or (b), an effective S-T mixing occurs, one can use the spin-independent theory with the above modifications to analyze radical recombinations. In a general case, the RP spin dynamics must be considered in detail.

2.2.2 The spin-Hamiltonian and the equation of motion of RP spins

Singlet-triplet transitions in a RP result from a fairly complex spin motion of the unpaired electrons and magnetic nuclei. This section is a brief analysis of interactions which determine RP spin motion. A more detailed information on this problem can be found in monographs on electron spin resonance, ESR (see, e.g. [2.28]).

The RP spin energy is contributed by the energies of the partners and the spin-spin interaction between them:

$$\hat{H} = \hat{H}_1 + \hat{H}_2 + \hat{V}. \quad (2.62)$$

Here \hat{H} is the RP spin-Hamiltonian, \hat{H}_1 and \hat{H}_2 are the spin-Hamiltonians of two isolated radicals, \hat{V} describes radical interactions.

The spin-Hamiltonian of an isolated radical. A radical spin energy can be regarded as arising from isotropic and anisotropic components. The isotropic component is contributed to by the Zeeman interaction of the spins with the external magnetic field H_0 averaged over all possible radical orientations and also by the contact hf interaction of the unpaired electrons with the magnetic nuclei

$$\hat{H} = \hat{H}_z + \hat{H}_{\text{hf}} \quad (2.63)$$

The Zeeman radical energy is

$$\hat{H}_z = g\beta\hat{H}_0\hat{S} + \hat{H}_{zn} \quad (2.64)$$

where g is the g -value of an unpaired electron with spin S , β is the Bohr magneton. The second term in eq. (2.64) describes the Zeeman nuclear energy. As a rule, \hat{H}_{zn} is of no importance in the radical electron spin dynamics and hence we shall neglect it. In a constant magnetic field H_0 , the Zeeman energy of an unpaired electron is ($\hat{H}_0 \parallel z$)

$$\hat{H}_z = g\beta H_0 \cdot \hat{S}_z. \quad (2.65)$$

The isotropic hf of the unpaired electron with the k -th magnetic nucleus is characterized by a constant a_k . As a result,

$$\hat{H}_{\text{hf}} = \hbar \sum_k a_k \cdot \hat{S} \cdot \hat{I}_k \quad (2.66)$$

and the overall radical spin-Hamiltonian is

$$\hat{H} = g\beta H_0 \hat{S}_z + \hbar \sum_k a_k \cdot \hat{S} \cdot \hat{I}_k \quad (2.67)$$

(the hf constant will be denoted as a when expressed as a frequency (rad/s), and A when expressed as a field (G)). The spin-Hamiltonian parameters g and a_k can be found from ESR spectra. The Zeeman splitting of the energy levels of the unpaired

electron which is equal to $g\beta H_0$, determines the mean frequency of the radical ESR spectrum

$$\omega_0 = g\beta\hbar^{-1} \cdot H_0. \quad (2.68)$$

Isotropic hf interaction splits the energy levels and causes the hyperfine structure of the ESR spectrum. The g -values and the hf constants for a number of radicals are added in Section 5 (see Tables 5.5 and 5.6). For instance, in the case of organic free radicals, the g -value is close to that of free electrons ($g = 2.002322$). Variations of g for different radicals are associated with different spin-orbital interactions. Typical hf constants in the case of organic radicals with a localized unpaired electron are $A \approx 10\text{--}100$ G.

The anisotropic term of the radical spin-Hamiltonian is contributed by the dipole-dipole interaction of the unpaired electron with the magnetic nuclei (*anisotropic hf interaction*), the anisotropic spin-orbital interaction of the unpaired electron (*g -tensor anisotropy*) and also by the spin-rotation interaction. In liquids molecules tumble quickly from one orientation to another, the time of their orientational relaxation being of the order of 10^{-11} s. The rotational diffusion averages the anisotropic component of the radical spin energy to zero. These anisotropic interactions are responsible for the process of radical paramagnetic relaxation. The scale of the paramagnetic relaxation rate of unpaired electrons is determined by the magnitude of the product of the mean square value of the anisotropic interaction and the time of the radical rotational relaxation, τ_0 , (see eqs 1.2, 3).

$$W_{\text{relax}} \approx \langle \hat{H}_{\text{anisotr.}}^2 \rangle \hbar^{-2} \cdot \tau_0. \quad (2.69)$$

In the case of organic free radicals in liquids with the viscosity about 1 cP, the paramagnetic relaxation times lie within the range $10^{-5}\text{--}10^{-6}$ s. It means that paramagnetic relaxation processes in such systems cannot as a rule manifest themselves during radical in-cage lifetimes which have been estimated in Section 2.1 to be within the nanosecond range.

The equation of motion of isolated radical spins. A radical spin state is expressed by the density matrix σ . It obeys the equation of motion

$$\partial\sigma/\partial t = -i\hbar^{-1}[\hat{H}, \sigma] + \hat{R}\sigma. \quad (2.70)$$

Here \hat{R} is a linear operator describing relaxation changes in σ , while the term with the commutator describes the spin motion due to the isotropic component of the radical spin-Hamiltonian. Relaxation processes neglected, we have for radicals in a constant magnetic field

$$\begin{aligned} \partial\sigma/\partial t &= -i\hbar^{-1}[\hat{H}, \sigma], \\ \hat{H} &= \hbar\omega_0 \hat{S}_z + \hbar \sum_k a_k \hat{S} \hat{I}_k. \end{aligned} \quad (2.71)$$

This equation expresses the spin motion at times less than those of radical paramagnetic relaxation. According to eq. (2.71) the density matrix is related to its initial value $\sigma(o)$ as

$$\sigma(t) = \exp(-i\hbar^{-1}\hat{H}t) \cdot \sigma(o) \cdot \exp(i\hbar^{-1}\hat{H}t). \quad (2.72)$$

The density matrix known, one can obtain mean values of the spin moment projections. For instance,

$$\langle \hat{S}_z \rangle = Tr\{\sigma \hat{S}_z\} \quad (2.73)$$

where Tr means the trace over all the spin states.

To illustrate the foregoing, consider the spin motion of the unpaired electron of a one-nucleus radical with $I=1/2$. At the initial moment take

$$\langle S_z \rangle = 1/2, \langle S_y \rangle = \langle S_x \rangle = 0, \langle I_x \rangle = \langle I_y \rangle = \langle I_z \rangle = 0,$$

i.e. the electron spin is in its eigenstate with $S_z=1/2$. Later we have from eqs (2.72, 73)

$$\begin{aligned} \langle S_z \rangle &= (1/2)[1 - (a^2/R^2) \cdot \sin^2 \{R \cdot t/2\}], \\ \langle I_z \rangle &= (a^2/2 \cdot R^2) \cdot \sin^2 \{Rt/2\}, \\ R^2 &= a^2 + \omega_0^2. \end{aligned}$$

In low fields, when the Zeeman level splitting is less than the hf interaction energy, i.e., $\omega_0 < a$, we obtain

$$\begin{aligned} \langle S_z \rangle &\approx (1/2) \cdot \cos^2 \{a \cdot t/2\}, \\ \langle I_z \rangle &\approx (1/2) \cdot \sin^2 \{a \cdot t/2\}. \end{aligned}$$

The electron spin projection varies because its motion is correlated with that of the nuclear spin. In high fields, when $\omega_0 > a$, the hf interaction cannot compensate the Zeeman energy changes caused by the spin flips and hence the spin projections conserve their initial values.

If the spins started from some other initial state, their projections would vary qualitatively in the same manner as in the above case. For instance, if at the starting moment the spins are in the $S_z=1/2$ and $I_z=-1/2$ states, then at the following moments

$$\begin{aligned} \langle S_z \rangle &= 1/2 - (a^2/R^2) \cdot \sin^2 \{Rt/2\}, \\ \langle I_z \rangle &= -1/2 + (a^2/R^2) \cdot \sin^2 \{Rt/2\}. \end{aligned}$$

Hence, in low fields the sign of the spin projection periodically alters, the motion of S and I is a 'flip-flop',

$$\begin{aligned} \langle S_z \rangle &\approx 1/2 - \sin^2 \{at/2\}, \\ \langle I_z \rangle &\approx -1/2 + \sin^2 \{at/2\}. \end{aligned} \quad (2.74)$$

Note that in both cases the overall spin projection of the electron and nucleus does not vary in time, this property being typical of all radicals. Indeed, in the case of radicals with an arbitrary number of magnetic nuclei, the overall spin projection operator,

$$\hat{S}_z = \hat{S}_z + \sum_k \hat{I}_{kz},$$

commutes with the Hamiltonian \hat{H} (2.67)

$$[\hat{H}, \hat{S}_z] = 0 \quad (2.75)$$

and hence does not vary at times less than those of the paramagnetic relaxation.

Radical spin-spin interactions. These include exchange and dipole-dipole interactions of unpaired electrons. The dipole-dipole interaction is averaged to zero as a result of the relative reorientational diffusion of the two in-cage radicals. The radical exchange interaction is described by the spin-Hamiltonian

$$\hat{V} = -\hbar J(1/2 + 2\hat{S}_1 \cdot \hat{S}_2). \quad (2.76)$$

The interaction scale is determined by the *exchange integral* J which depends upon the interradsical distance and the mutual radical orientation [2.26]. J decreases approximately exponentially with the interradsical distance r . Data on radical spin exchange show $J \approx 10^{13}$ rad/s at the Van der Waals interradsical distance R_{AB} . The exchange integral reduces by orders of magnitude for a 0.1 nm increase in r . Therefore, the exchange interaction is of fundamental importance in RP spin dynamics only over a comparatively narrow range of r , while at $r \gg R_{AB}$ it is negligible.

Exchange interactions split the RP singlet and triplet terms, the energy separation being $2J$. At great interradsical distances J is negligible, and the singlet and triplet terms are degenerate. When the radicals approach, the terms diverge (see Fig. 2.5).

RP spin-Hamiltonian; RP singlet and triplet populations. A RP spin-Hamiltonian

$$\begin{aligned} \hat{H} = & g_1 \beta H_0 \hat{S}_{1z} + g_2 \beta H_0 \hat{S}_{2z} + \hbar \sum_i a_{1i} \hat{S}_1 \cdot \hat{I}_{1i} + \\ & + \hbar \sum_k a_{2k} \hat{S}_2 \cdot \hat{I}_{2k} - \hbar J(r) \cdot (1/2 + 2\hat{S}_1 \cdot \hat{S}_2) \end{aligned} \quad (2.77)$$

includes the Zeeman energy, and the hf and exchange interactions of the radicals. The exchange interaction depends upon the interradsical distance. Therefore, in a general case the spin and molecular dynamics cannot be considered separately. However, when speaking of spin evolution at comparatively large interradsical distances, when $J(r) < a_{1i}, a_{2k}$ (between re-encounters), the exchange interaction is negligible. The spin evolution can thus be studied irrespective of the reactant molecular motion. In this approximation the RP spin-Hamiltonian takes the form

$$\begin{aligned} \hat{H} = & g_1 \beta H_0 \hat{S}_{1z} + g_2 \beta H_0 \hat{S}_{2z} + \\ & + \hbar \sum_i a_{1i} \hat{S}_1 \cdot \hat{I}_{1i} + \hbar \sum_k a_{2k} \hat{S}_2 \cdot \hat{I}_{2k}. \end{aligned} \quad (2.78)$$

At a time t the density matrix is related to its initial value $\rho(0)$ as

$$\rho(t) = \exp(-i\hbar^{-1}\hat{H}t) \cdot \rho(0) \cdot \exp(i\hbar^{-1}\hat{H}t). \quad (2.79)$$

Let $\{m\}$ be a set of quantum numbers characterizing the nuclear spin projections. Assume that at the initial instant the RP is singlet. The singlet term population at any later time is

$$\rho_S(t) = \left[1 / \prod_{i,k} (2I_{1i} + 1)(2I_{2k} + 1) \right] \cdot \sum_{(m,m')} \left| \langle S, m | \exp(-i\hbar^{-1}\hat{H}t) | S, m' \rangle \right|^2. \quad (2.80)$$

The probability of the RP being triplet at the moment of detection equals the triplet term population

$$\rho_T(t) = 1 - \rho_S(t). \quad (2.81)$$

The populations of singlet (2.80) and triplet (2.81) RP terms can be readily found provided the eigenfunctions $|q\rangle$ and the eigenvalues E_q of the Hamiltonian (2.78) are known. Indeed, eq. (2.81) can be presented as

$$\rho_T(t) = 1 - \left[1 / \prod_{i,k} (2I_{1i} + 1)(2I_{2k} + 1) \right] \cdot \sum_{(m,m')} \left| \sum_q \langle S, m | q \rangle \cdot \langle q | S, m' \rangle \cdot \exp(-i\hbar^{-1}E_q \cdot t) \right|^2 \quad (2.82)$$

where $\langle S, m | q \rangle$ is the projection of $|q\rangle$ on to the state $|S, m\rangle$, the singlet state of a RP with a specified nuclear spin configuration.

In the general case this calculation runs into considerable difficulties and sometimes cannot be realized even by computers. Analytical solutions, however, can be obtained in some concrete situations: e.g., in high magnetic fields for arbitrary radicals, in low fields for radicals with equivalent magnetic nuclei etc.

2.2.3 RP spin dynamics in high magnetic fields

The fields in which the Zeeman energy of an unpaired electron exceeds the hf energy, $g\beta H_0 \gg \hbar a$ will henceforth be referred to as 'high'. The Zeeman interaction splits RP triplet terms into three sublevels, T_+ , T_0 , and T_- corresponding to three projections, $+1.0$ and -1 , of the total spin of the unpaired electrons of a triplet RP. Figure 2.6 depicts the scheme of RP energy levels in high fields.

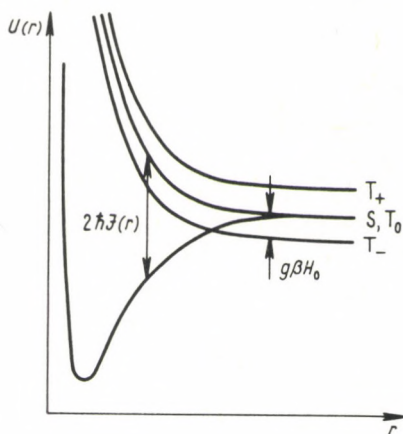


Fig. 2.6. Scheme of RP level splitting in high magnetic fields. At great interradical distances the exchange interaction can be neglected

In high magnetic fields the triplet states T_+ and T_- are no longer in resonance with the singlet state S . That is why the intersystem transitions occur only between the S and T_0 states, and why it is sufficient to consider only the *adiabatic* or *secular* component of the RP spin-Hamiltonian

$$\begin{aligned} \hat{H} = & g_1 \beta H_0 \hat{S}_{1z} + g_2 \beta H_0 \hat{S}_{2z} + \\ & + \hbar \sum_i a_{1i} \hat{S}_{1z} \hat{I}_{1iz} + \hbar \sum_k a_{2k} \hat{S}_{2z} \hat{I}_{2kz}. \end{aligned} \quad (2.83)$$

Substitute (2.83) into (2.81) for any RPs in high magnetic fields and obtain the following triplet state population for a singlet-born RP,

$$\rho_{T_0}(t) = \left[1 / \prod_{i,k} (2I_{1i} + 1)(2I_{2k} + 1) \right] \cdot \sum_{\{m\}} \sin^2 \{ \varepsilon(m) \cdot t \}, \quad (2.84)$$

where summation is carried out over all possible nuclear spin configurations and $\varepsilon(m) = [(g_1 - g_2)\beta\hbar^{-1}H_0 + \sum_i a_{1i}m_{1i} - \sum_k a_{2k}m_{2k}]/2$ is the matrix element of transition between S and T_0 states.

According to eq. (2.84), $S-T_0$ transitions are induced by the difference of Zeeman radical frequencies (the Δg -mechanism) and the difference of spin resonance frequencies belonging to different hf components of radical ESR spectra (the hf-mechanism).

If unpaired electrons do not interact with magnetic nuclei and the Δg -value is the only mechanism of singlet-triplet evolution, then, in full agreements with the

qualitative picture discussed in the introduction, there occur oscillations between S and T_0 states with the frequency $(g_1 - g_2)\beta\hbar^{-1}H_0$ (see (1.7)):

$$\rho_{T_0}(t) = \sin^2 \{(g_1 - g_2)\beta\hbar^{-1}H_0 t/2\}. \quad (2.85)$$

Equation (2.84) can be simplified provided all the magnetic nuclei have 1/2 spins. In this case, as it has been shown by Brocklehurst [2.29], eq. (2.84) takes the form

$$\rho_{T_0}(t) = (1/2) \cdot \left[1 - \cos \{(g_1 - g_2)\beta\hbar^{-1}H_0 t\} \cdot \prod_{k=1}^n \cos \{a_k \cdot t/2\} \right], \quad (2.86)$$

where n is the number of the magnetic nuclei and a_k stands for hf constants. For radicals with equal g -values we have

$$\rho_{T_0}(t) = (1/2) \cdot \left[1 - \prod_{k=1}^n \cos \{a_k \cdot t/2\} \right]. \quad (2.87)$$

Equation (2.84) for a RP triplet term population can be further simplified if we limit our interest in spin evolution to only small time intervals. In this case the influence of all magnetic nuclei on RP singlet-triplet evolution is determined by a single effective parameter [2.30-32]

$$a_{\text{eff}} = \left\{ (1/3) \cdot \sum_i a_{1i}^2 \cdot I_{1i} \cdot (I_{1i} + 1) + (1/3) \cdot \sum_k a_{2k}^2 \cdot I_{2k} \cdot (I_{2k} + 1) \right\}^{1/2} \quad (2.88)$$

From (2.84) we have at small time intervals

$$\rho_{T_0}(t) \cong [(g_1 - g_2)^2 \beta^2 \hbar^{-2} H_0^2 + a_{\text{eff}}^2] \cdot t^2/4. \quad (2.89)$$

For radicals with equal g -values

$$\rho_{T_0}(t) \cong a_{\text{eff}}^2 \cdot t^2/4. \quad (2.90)$$

In high magnetic fields, different nuclear spin configurations correspond to a definite component in the hyperfine structure (hfs) of the radical ESR spectrum. Therefore, a RP ensemble is divided into subensembles, radicals in each belonging to a given hf component of their ESR spectrum. If none of the hfs components of one radical coincides with that of its partner, then in all the subensembles S- T_0 oscillations will occur with frequencies equal to the difference between the positions of the corresponding hfs components of the RP spectra. In RP subensembles with both radicals giving a line in the ESR spectrum at the same resonance frequency (hfs components of both radicals coinciding), no S- T_0 transition occurs. Such situations are always observed when two identical radicals recombine, while in the case of two different radicals some of their hfs components can either accidentally coincide or be close enough to be considered as such.

The foregoing can be illustrated by the following examples. Let one of the radicals have a doublet ESR spectrum with a splitting a , the ESR spectrum of the other

giving a single line in the centre. S-T₀ mixing then takes place in all RPs and

$$\rho_{T_0}(t) = \sin^2 \{a \cdot t/4\}. \quad (2.91)$$

In general, at sufficiently long times, RPs spend approximately equal time intervals in S and T₀ states. If a pair is formed by two identical radicals, each having one proton and a doublet ESR spectrum with *a*-splitting, then in accord with eq. (2.84)

$$\rho_{T_0}(t) = (1/2) \cdot \sin^2 \{a \cdot t/2\}. \quad (2.92)$$

It is thus clear that on the average only 1/4 of the RPs are in the triplet state, half of them not participating in S-T₀ evolution at all.

On the recombination of different radicals with a fairly complex hfs in their ESR spectra, the probability of a random coincidence of the spectral components is negligible, and none of the terms in eq. (2.84) for the triplet population becomes zero, S-T₀ oscillations occurring in all the RPs. In this case $\rho_{T_0}(t)$ (2.84) is a superposition of a great number of oscillating functions. One can therefore expect the oscillations $\rho_{T_0}(t)$ to be detected only in the initial step until the dephasing between different oscillating terms is negligible. This function will further remain practically unchanged and equal to 1/2. For two identical radicals recombining, the time dependence of ρ_{T_0} behaves qualitatively in the same way as it does in the case of different radicals. However, the average level it reaches will be somewhat less than 1/2 since a fraction of RPs radicals have identical nuclear spin configurations.

Figure 2.7 shows the way the triplet term population varies for several RPs. Oscillations in S-T evolution are seen to decay for RPs with a great number of nuclei.

The singlet-triplet transition probability in high magnetic fields can be expressed in terms of the frequencies and intensities of hfs components of the radical ESR spectra, the latter being expressed by the distribution

$$\tilde{g}(\omega) = \sum_{\{m\}} \delta(\omega - \omega_0 - \sum_k a_k \cdot m_k) = \sum_k I_k \cdot \delta(\omega - \omega_k) \quad (2.93)$$

where δ is the delta function, ω_k and I_k are the frequency and the relative intensity of the *k*-th spectral component. The isotropic hf interaction gives an ESR spectrum symmetrical with respect to the Zeeman frequency ω_0 . Introducing the hfs distribution $g(\omega)$ for both radicals we have from eq. (2.84)

$$\begin{aligned} \rho_{T_0}(t) &= (1/2) \cdot [1 - \text{Re} \{ \exp [i(g_1 - g_2)\beta\hbar^{-1}H_0t] \cdot \\ &\cdot \int \int d\omega \cdot d\omega' \cdot g_1(\omega) \cdot g_2(\omega') \cdot \exp [i(\omega - \omega')t] \}] = \\ &= (1/2) \cdot [1 - \cos \{ (g_1 - g_2)\beta\hbar^{-1}H_0t \} \cdot g_1(t) \cdot g_2(t)], \end{aligned} \quad (2.94)$$

where $g(t)$ is the Fourier transform of the ESR spectrum

$$g(t) = \int d\omega \cdot g(\omega) \cdot \exp(i\omega t).$$

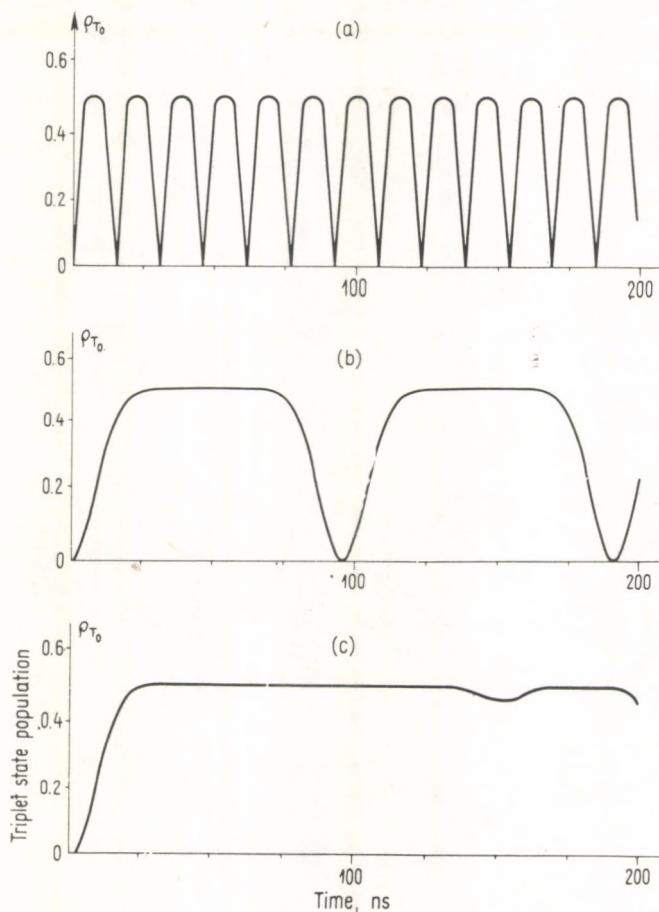


Fig. 2.7. Triplet term populations in high magnetic fields for some singlet-born RPs: (a) $\text{CH}_3 \dots \text{CH}_3$ ($A = -23.04$ G); (b) $\text{C}_6\text{H}_6 \dots \text{C}_6\text{H}_6^-$ ($A = -3.75$ G); (c) $\text{C}_{10}\text{H}_8 \dots \text{C}_{10}\text{H}_8^-$ ($A_\alpha = -4.95$ G, $A_\beta = -1.83$ G)

Equation (2.94) is useful when the number of radical magnetic nuclei is great. In this case the ESR spectrum can be approximated by the Gaussian distribution

$$g(\omega) = [1/(2\pi \cdot a_{\text{eff}}^2)^{1/2}] \cdot \exp(-(\omega - \omega_0)^2/2 \cdot a_{\text{eff}}^2) \quad (2.95)$$

Substitute eq. (2.95) into (2.94) and obtain in the limits of a great number of magnetic nuclei [2.33]

$$\rho_{T_0}(t) = (1/2) \cdot [1 - \cos \{(g_1 - g_2)\beta\hbar^{-1}H_0t\} \cdot \exp(-a_{\text{eff}}^2 \cdot t^2/2)]. \quad (2.96)$$

It is obvious that for RPs with few magnetic nuclei eq. (2.96) greatly obscures the S-T transition dynamics. Note, however, that as the number of magnetic nuclei grows,

the accuracy of eq. (2.96) increases. For instance, Fig. 2.8 depicts the singlet-triplet transition dynamics in terms of this approximation and compares it with exact calculations. The actual dynamics is seen to differ slightly from the approximate formula (2.96) since the RP considered contains a large number of magnetic nuclei.

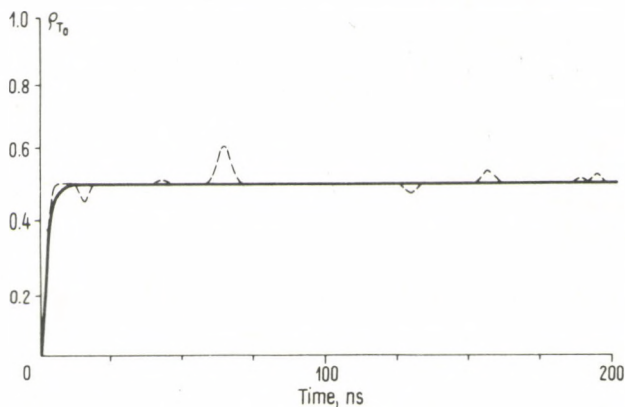
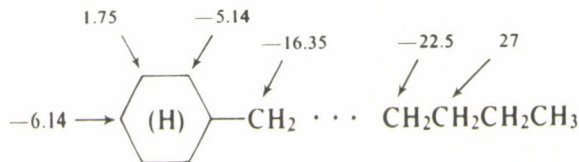


Fig. 2.8. Comparison of exact (dashed line) (2.84) and approximate (solid line) (2.96) calculations of triplet term populations for a singlet-born pair of benzyl and alkyl radicals in high fields ($g_1 = g_2 = 2.0025$)



Hyperfine interaction constants are given in gauss

If one of the radicals, say 1, contains few magnetic nuclei with spin $I = 1/2$, whereas the other has a large number, then

$$\rho_{T_0}(t) = (1/2) \cdot [1 - \cos \{(g_1 - g_2)\beta\hbar H_0 t\}] \cdot \prod_i \cos \{a_{1i} \cdot t/2\} \cdot \exp(-a_{2, \text{eff}}^2 \cdot t^2/2), \quad (2.97)$$

where

$$a_{2, \text{eff}}^2 = (1/3) \sum_k a_{2k}^2 \cdot I_{2k} \cdot (I_{2k} + 1).$$

Finally consider the effect of interradical exchange interaction on the S-T transition dynamics. The exchange interaction removes the resonance of S and T_0 states, thus decreasing the efficiency of S-T₀ transitions. Indeed, for a system with the Hamiltonian

$$\hat{H} = g_1 \beta H_0 \hat{S}_{1z} + g_2 \beta H_0 \hat{S}_{2z} + \hbar \sum_i a_{1i} \hat{S}_{1z} \hat{I}_{1iz} + \hbar \sum_k a_{2k} \hat{S}_{2z} \hat{I}_{2kz} - \hbar J(1/2 + 2\hat{S}_1 \cdot \hat{S}_2) \quad (2.98)$$

the probability of these transitions is set by the relation

$$\rho_{T_0}(t) = \left[1 / \prod_{i,k} (2I_{1i} + 1)(2I_{2k} + 1) \right] \cdot \sum_{(m)} [\varepsilon^2(m) / (\varepsilon^2(m) + J^2)] \cdot \sin^2 \{ (\varepsilon^2(m) + J^2)^{1/2} \cdot t \} \quad (2.99)$$

instead of eq. (2.84). Hence, $\rho_{T_0} \rightarrow 0$ when $J \gg \varepsilon(m)$.

As radicals approach as close as the Van der Waals distances, $J \gg \varepsilon(m)$ and hence S-T₀ transitions are practically impossible. S-T₀ mixing is effective only if the interradical distance is sufficiently large, of the order of 10 Å.

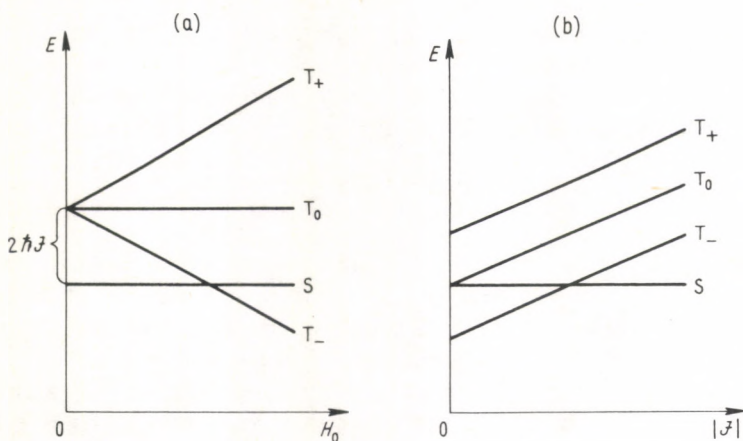


Fig. 2.9. Scheme of RP energy levels: (a) field dependence at a fixed J ; (b) J dependence at a fixed H_0 (set $J < 0$)

However, S-T₊ or S-T₋ transitions can occur due to exchange splitting of the S and T terms in high magnetic fields. Consider the level scheme (Fig. 2.9) of the Hamiltonian of the Zeeman and exchange interactions. The S and T₋ terms cross in fields $g\beta H_0 \sim 2\hbar J$. In the vicinity of their crossing point the radical hf interaction induces S-T₋ transitions. For instance, under strong resonance

$$g\beta H_0 = 2\hbar |J| \quad (2.100)$$

in a one-nuclear RP with $I = 1/2$

$$p_{S \rightarrow T_-} = (1/2) \cdot \sin^2 \{ a \cdot t / 2\sqrt{2} \}. \quad (2.101)$$

In the case of positive J , S-T₊ transitions will take place.

The above results show that the RP spin dynamics can be exhaustively described in high magnetic fields. We can estimate characteristic frequencies of S-T₀ transitions. If radical g -values differ, S-T₀ transitions occur with the frequencies

$(g_1 - g_2)\beta\hbar^{-1}H_0$. For instance, even for $g_1 - g_2 = 0.001$ this frequency reaches about 10^8 rad/s in a field $H_0 = 10^4$ G. At still greater difference of the g -values, effective S-T₀ transitions can arise in lower fields. Induced by hyperfine interactions the frequency of S-T₀ transitions is about a . For instance, $A = 10$ G results in S-T₀ transitions frequency equal to approximately 10^8 rad/s.

2.2.4 RP spin dynamics in low magnetic fields

The fields in which the Zeeman energy of an unpaired electron is either less or comparable with the hf energy will henceforth be referred to as 'low'. RP spin dynamics in low fields differs qualitatively from that in high fields. In the former case all the three channels of S-T transitions are open: S-T₊, T₀, T₋.

As noted, in low fields the S-T transition probability can be found analytically only in the simplest cases. First of all, it can be done for sufficiently short times, when $a_{\text{eff}} \cdot t < 1$. Then [2.30-32]

$$\rho_T(t) \approx (3/4) \cdot a_{\text{eff}}^2 \cdot t^2. \quad (2.102)$$

Comparing this result with the S-T₀ transition probability in high fields we see that for sufficiently short-lived RPs, i.e. when $a_{\text{eff}} \cdot t < 1$, the ratio of the S-T transition probabilities in low and high fields is 3, which corresponds precisely to the relative numbers of conversion channels effective in low and high fields.

The triplet term population at an arbitrary external field strength in the case of short-lived RPs and $\Delta g = 0$ ($g_1 = g_2 = g$) has been obtained by Haberkorn [2.32]

$$\rho_T \approx (a_{\text{eff}}^2 \cdot t^2 / 4) \cdot [1 + 2 \cdot \sin^2 \{g\beta\hbar^{-1}H_0 t / 2\} / (g\beta\hbar^{-1}H_0 t / 2)^2]. \quad (2.103)$$

A precise expression for $\rho_T(t)$ can be found for a RP with each partner having either a single nucleus or several equivalent nuclei. In the latter case the RP can be divided into subensembles, each having radicals with an effective single nucleus with spin equal to the total spin of all equivalent nuclei. However, even such comparatively simple situations are described by rather cumbersome expressions.

Consider some results obtained for a one-nucleus RP with an arbitrary spin I and a spin-Hamiltonian

$$\hat{H} = \hbar\omega_1 \hat{S}_{1z} + \hbar\omega_2 \hat{S}_{2z} + \hbar a \hat{S}_i \hat{I}. \quad (2.104)$$

Let the RP be in the singlet state at the starting moment. The probability of finding it in the triplet state at any later time is

$$\begin{aligned} \rho_T(I, t) = & 1 - [1/4 \cdot (2I + 1)] \cdot \sum_{m=-I}^I |\exp(i\omega_2 \cdot t) \cdot \\ & \cdot [\exp(-iR_m t) \cdot \cos^2 \varphi_m + \exp(iR_m t) \cdot \sin^2 \varphi_m] + \\ & + \exp(-iR_{m-1} t) \cdot \sin^2 \varphi_{m-1} + \exp(iR_{m-1} t) \cdot \cos^2 \varphi_{m-1}|^2, \end{aligned} \quad (2.105)$$

where

$$R_m = (1/2) \cdot [\omega_1^2 + a \cdot \omega_1(1+2m) + a^2(I+1/2)^2]^{1/2},$$

$$\cos^2 \varphi_m = [R_m + \omega_1/2 + a \cdot (1+2m)/4]/2 \cdot R_m.$$

In low fields the difference in radical g -values is of no importance for the S-T transition dynamics and hence the g -values can be considered equal.

Consider some examples. In the case of one-nucleus RPs with $1/2$ spin we have from eq. (2.105)

$$\begin{aligned} \rho_T(t) = & (1/4) \cdot [3 - \sin^4 \varphi - \cos^4 \varphi - \\ & - 2 \cdot \sin^2 \varphi \cdot \cos \{at/2\} \cdot \cos \{(\omega_1/2 - \omega_2 - R)t\} - \\ & - 2 \cdot \cos^2 \varphi \cdot \cos \{at/2\} \cdot \cos \{(\omega_1/2 - \omega_2 + R)t\} - \\ & - 2 \cdot \sin^2 \varphi \cdot \cos^2 \varphi \cdot \cos \{2Rt\}], \end{aligned} \quad (2.106)$$

$$R = (\omega_1^2 + a^2)^{1/2}/2,$$

$$\cos^2 \varphi = (R + \omega_1/2)/2 \cdot R.$$

In extreme cases of $H_0 \ll A$ and $H_0 \gg A$ eq. (2.106) gives for $\omega_1 = \omega_2 = \omega$ ($g_1 = g_2$)

$$\rho_T(H_0 < A) \cong (3/4) \cdot \sin^2 \{at/2\} + (1/2) \cdot \cos^2 \{at/2\} \cdot \sin^2 \{\omega t/4\}, \quad (2.107)$$

$$\rho_T(H_0 \gg A) = \sin^2 \{at/4\}.$$

The g -values being equal, $\rho_T(t)$ depends on two dimensionless parameters, $a \cdot t$ and H_0/A . Figure 2.10 depicts the triplet term population calculated by eq. (2.106) at several values of these parameters. (Remember that A and a denote the hf constant measured in G and rad/s respectively.) S-T transition dynamics is seen to be extremely sensitive to changes of hf interaction and external fields.

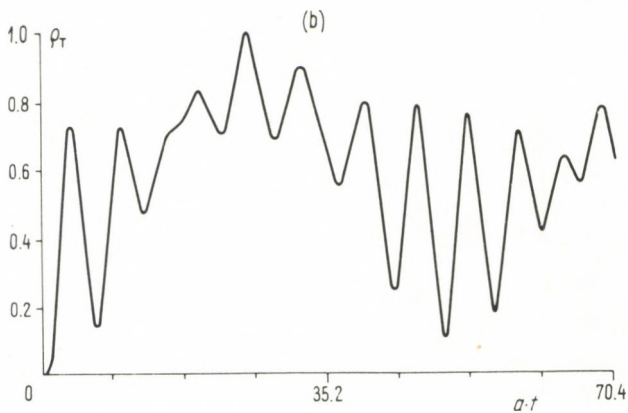
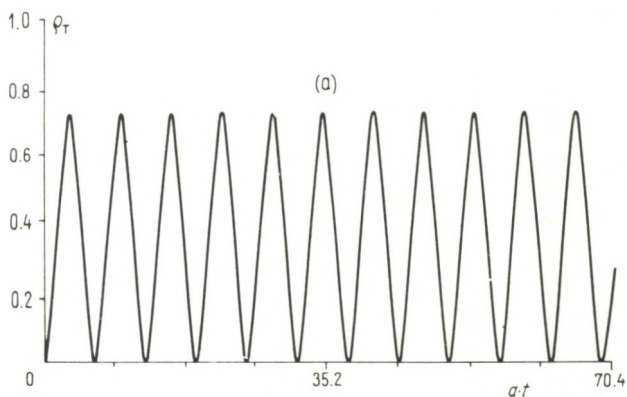
Within a sufficiently long time interval when oscillating terms are averaged to zero, the S-T transition efficiency falls with an increase in the external field strength. According to (2.106)

$$\bar{\rho}_T = 1/2 + a^2/8 \cdot (a^2 + \omega_1^2) \quad \text{for } \omega_1 \neq 0 \text{ (} H_0 \neq 0 \text{)}.$$

Zero field is an exception. In a field $H_0 = 0$ the mean efficiency of intersystem transitions is less than that in high fields and is equal to only 0.375 (see eq. (2.107)). These peculiarities are seen from Fig. 2.10 and Fig. 2.12. Another example is a one-nucleus RP with $I = 1$

$$\begin{aligned} \rho_T(t) = & (1/6) \cdot [5 - \sin^4 \varphi_- - \cos^4 \varphi_- - \sin^4 \varphi_+ - \cos^4 \varphi_+ - \\ & - \sin^2 \varphi_+ \cdot \cos \{(\omega_2 - \omega_1/2 - 3a/4 + R_+)t\} - \\ & - \cos^2 \varphi_+ \cdot \cos \{(\omega_2 - \omega_1/2 - 3a/4 - R_+)t\} - \\ & - 2 \cdot \sin^2 \varphi_+ \cdot \cos^2 \varphi_+ \cdot \cos \{2R_+t\} - \end{aligned}$$

$$\begin{aligned}
 & -\sin^2 \varphi_- \cdot \cos \{(\omega_2 - \omega_1/2 + 3a/4 + R_-)t\} - \\
 & -\cos^2 \varphi_- \cdot \cos \{(\omega_2 - \omega_1/2 + 3a/4 - R_-)t\} - \\
 & -2 \cdot \sin^2 \varphi_- \cdot \cos^2 \varphi_- \cdot \cos \{2R_-t\} - \\
 & -\sin^2 \varphi_- \cdot \cos^2 \varphi_+ \cdot \cos \{(\omega_2 + R_- - R_+)t\} - \\
 & -\sin^2 \varphi_- \cdot \sin^2 \varphi_+ \cdot \cos \{(\omega_2 + R_- + R_+)t\} - \\
 & -\cos^2 \varphi_- \cdot \cos^2 \varphi_+ \cdot \cos \{(\omega_2 - R_- - R_+)t\} - \\
 & -\sin^2 \varphi_+ \cdot \cos^2 \varphi_- \cdot \cos \{(\omega_2 - R_- + R_+)t\}],
 \end{aligned}
 \tag{2.108}$$



where

$$R_{\pm} = (1/2) \cdot [\omega_1^2 \pm \omega_1 \cdot a + 9a^2/4]^{1/2},$$

$$\cos^2 \varphi_+ = (R_+ + \omega_1/2 + a/4)/2R_+,$$

$$\cos^2 \varphi_- = (R_- + \omega_1/2 - a/4)/2R_-.$$

Hence in very low ($H_0 \ll A$) and high fields at $g_1 = g_2$

$$\rho_T(H_0 < A) \cong (1/54) \cdot [35 - 10 \cdot \cos \{2 \cdot \omega \cdot t/3\} - \cos \{4 \cdot \omega \cdot t/3\} - 4 \cdot \cos \{3at/2\} \cdot [\cos \{\omega \cdot t\} + 5 \cdot \cos \{\omega \cdot t/3\}]], \quad (2.109)$$

$$\rho_T(H_0 \gg A) = (2/3) \cdot \sin^2 \{at/2\}.$$

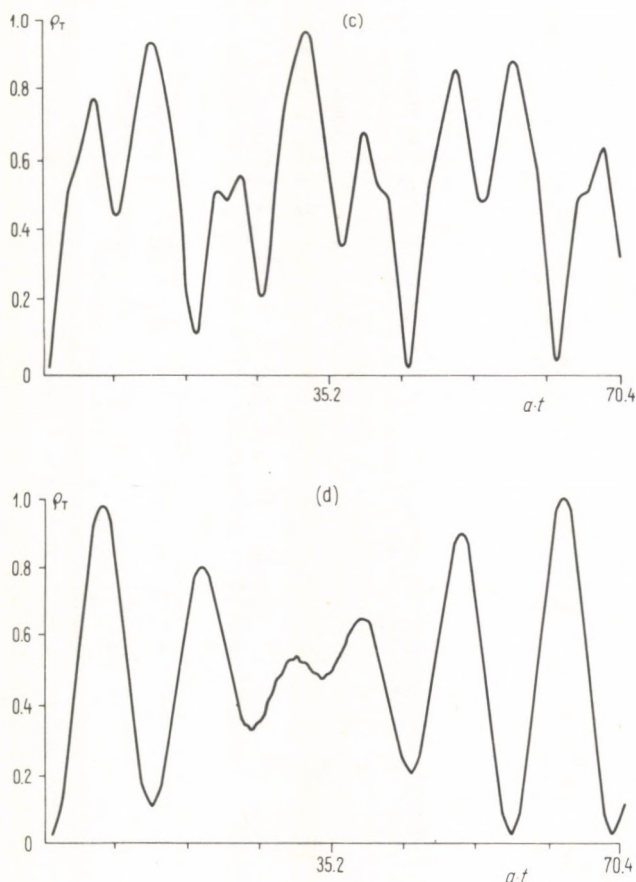


Fig. 2.10. S-T transition dynamics for a one-nuclear singlet-born RP ($I = 1/2, Ag = 0$) at various ratios H_0/A : (a) 0; (b) 0.25; (c) 1; (d) 5

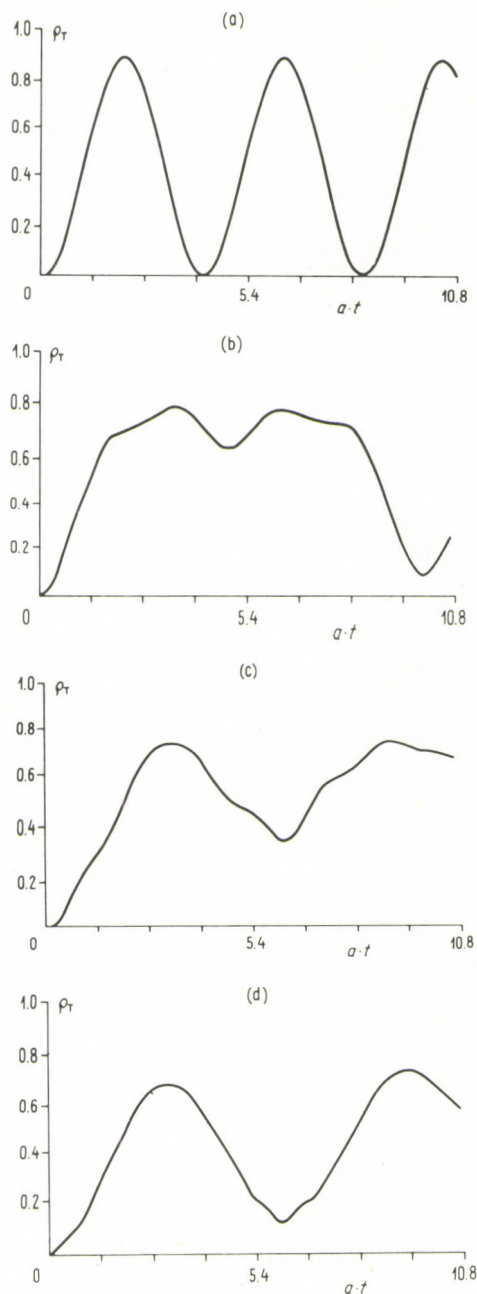


Fig. 2.11. S-T transition dynamics for a one-nucleus singlet-born RP ($I=1$, $\Delta g=0$) at various ratios H_0/A : (a) 0; (b) 1.63; (c) 3.26; (d) 6.51

Figure 2.11 shows the RP triplet state population calculated by eq. (2.108). The S-T transition falls with increasing field intensity as in the case of a one-nucleus pair with $I = 1/2$, zero field being an exception.

Figure 2.12 gives the field dependence of S-T transitions averaged over a long time interval. When averaging, we assume the values $\sin^2 \times t$ and $\cos^2 \times t$ to be $1/2$. In zero magnetic fields and at an arbitrary I [2.30]

$$\rho_T^0 = [4I(I+1)/(2I+1)^2] \cdot \sin^2 \{(2I+1)a \cdot t/4\}. \quad (2.110)$$

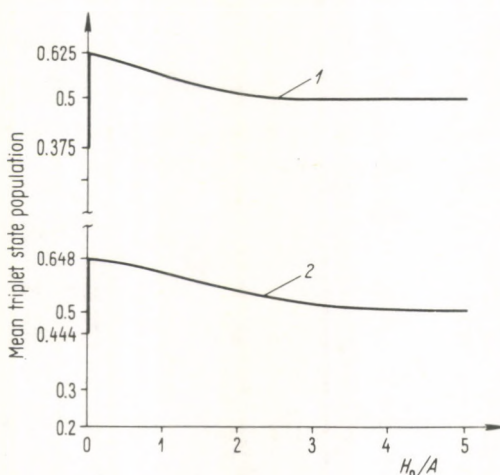


Fig. 2.12. Triplet term population of a one-nucleus singlet-born RP averaged over a long time interval. 1 - $I = 1/2$; 2 - $I = 1$

The RP spin dynamics in low fields reveal an interesting feature: the contributions made by different channels of S-T transitions can interfere and are therefore not additive. Indeed, for instance, eq. (2.107) shows that in zero field, when all the three channels are effective, the maximum triplet population reaches 0.75, whereas in high fields the single S-T₀ channel affords a maximum population equal to 1. A similar effect of interference of S-T channels can also arise in other RPs. This problem has already been exhaustively studied [2.31, 60]. Crossings of RP spin levels affect substantially the interference of S-T channels [2.74, 75]. Figures 2.10, 2.11 illustrate S-T evolution for some concrete RPs. The S-T transition dynamics are seen to be strongly dependent on the values of the nuclear spin, the hf constant and the magnetic field strength.

RPs with two magnetic nuclei. The S-T transition dynamics can be found in the case of a RP with each partner having one magnetic nucleus with I_1 and I_2 spins respectively. The triplet term population is

$$\begin{aligned}
 \rho_T(I_1, I_2, t) = & 1 - [1/4 \cdot (2I_1 + 1) \cdot (2I_2 + 1)] \sum_{m_1 = -I_1}^{I_1} \cdot \\
 & \sum_{m_2 = -I_2}^{I_2} \{ \sin^2 \{2 \cdot \varphi_{m_1-1}\} \cdot \sin^2 \{2 \cdot \varphi_{m_2}\} \cdot \sin^2 \{R_{m_1-1} \cdot t\} \cdot \sin^2 \{R_{m_2} \cdot t\} + \\
 & + \sin^2 \{2 \cdot \varphi_{m_1}\} \cdot \sin^2 \{2 \cdot \varphi_{m_2-1}\} \cdot \sin^2 \{R_{m_1} \cdot t\} \cdot \sin^2 \{R_{m_2-1} \cdot t\} + \\
 & + [\exp(-iR_{m_1} \cdot t) \cdot \cos^2 \{\varphi_{m_1}\} + \exp(iR_{m_1} \cdot t) \cdot \sin^2 \{\varphi_{m_1}\}] \cdot \\
 & \cdot [\exp(-iR_{m_2-1} \cdot t) \cdot \sin^2 \{\varphi_{m_2-1}\} + \exp(iR_{m_2-1} \cdot t) \cdot \cos^2 \{\varphi_{m_2-1}\}] + \\
 & + [\exp(-iR_{m_1-1} \cdot t) \cdot \sin^2 \{\varphi_{m_1-1}\} + \exp(iR_{m_1-1} \cdot t) \cdot \cos^2 \{\varphi_{m_1-1}\}] \cdot \\
 & \cdot [\exp(-iR_{m_2} \cdot t) \cdot \cos^2 \{\varphi_{m_2}\} + \exp(iR_{m_2} \cdot t) \cdot \sin^2 \{\varphi_{m_2}\}]^2 \}. \quad (2.111)
 \end{aligned}$$

The symbols of this expression are the same as those in eq. (2.105). The quantities with subscripts 1 and 2 refer to different RP partners. This expression takes a much simpler form in zero field:

$$\begin{aligned}
 \rho_T^0(I_1, I_2, t) = & [4/(2I_1 + 1)^2 \cdot (2I_2 + 1)^2] \cdot \\
 & \cdot \{ I_1(I_1 + 1) \cdot [1 + 4 \cdot I_2 \cdot (I_2 + 1)/3] \cdot \sin^2 \{(2I_1 + 1)a_1 \cdot t/4\} + \\
 & + I_2(I_2 + 1) \cdot [1 + 4 \cdot I_1 \cdot (I_1 + 1)/3] \cdot \sin^2 \{(2I_2 + 1)a_2 \cdot t/4\} + \\
 & + (4/3) \cdot I_1 \cdot I_2 \cdot (I_1 + 1) \cdot (I_2 + 1) \cdot [\sin^2 \{((2I_1 + 1)a_1 + (2I_2 + 1)a_2)t/4\} + \\
 & + \sin^2 \{((2I_1 + 1)a_1 - (2I_2 + 1)a_2)t/4\}] \}, \quad (2.112)
 \end{aligned}$$

$\rho_T(I_1, I_2, t)$ values are reported in refs [2.31, 34–36] for a number of systems. For example, for two radicals with equal g -values, $A_1 = A_2 = A$, $I_1 = I_2 = 1/2$, we have

$$\begin{aligned}
 \rho_T(1/2, 1/2, t) = & (1/2) \cdot \sin^2 \{at/2\} - \lambda \cdot [\sin^2 \{at/2\} - \\
 & - (1/2) \cdot \sin^2 \{(a/2 + R)t\} - (1/2) \cdot \sin^2 \{(a/2 - R)t\} - \\
 & - 3 \cdot \sin^2 \{Rt\}] - \lambda^2 \cdot [4 \cdot \sin^2 \{Rt\} - \sin^2 \{2Rt\}], \quad (2.113)
 \end{aligned}$$

where

$$R = (\omega^2 + a^2)^{1/2}/2, \quad \lambda = a^2/4 \cdot (a^2 + \omega^2).$$

Hence, in zero fields

$$\rho_T^0(1/2, 1/2, t) = (3/4) \cdot \sin^2 \{at/2\} + (3/16) \cdot \sin^2 \{at\}.$$

Figure 2.13 shows the triplet term population for this case. The calculations were made for various ratios of magnetic field strength and hf constant. The maximum triplet term population is seen to be 0.75 in zero field and 0.5 in high fields.

RPs with many nuclei. The above results can give the S–T transition dynamics in the case of a RP with many nuclei provided the magnetic nuclei of each radical are equivalent. For instance, all protons are equivalent in a methyl radical. A RP with partners having many equivalent nuclei can be divided into RP subensembles. Each subensemble is assumed to have a magnetic nucleus with one of the possible values

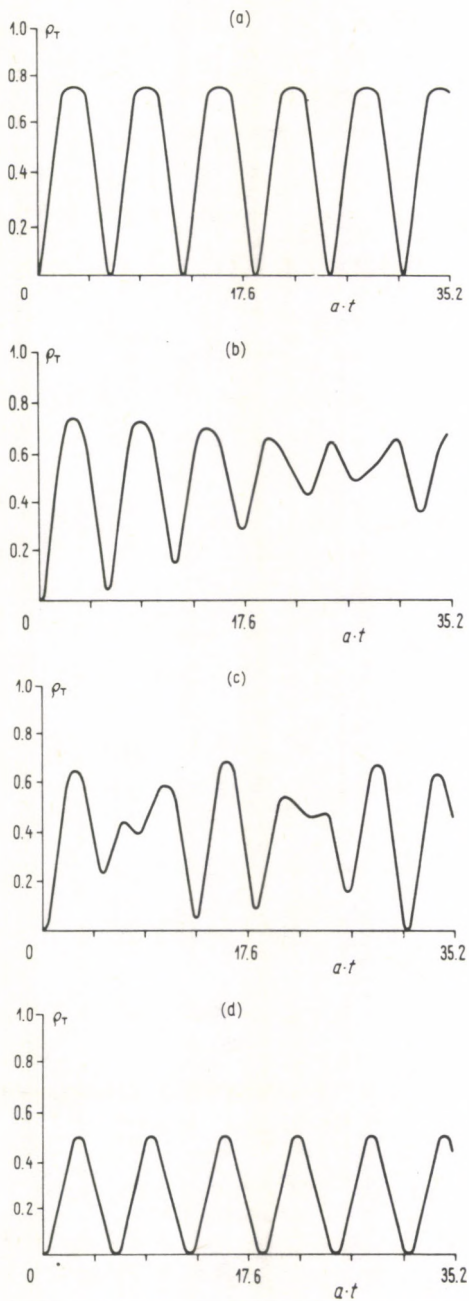
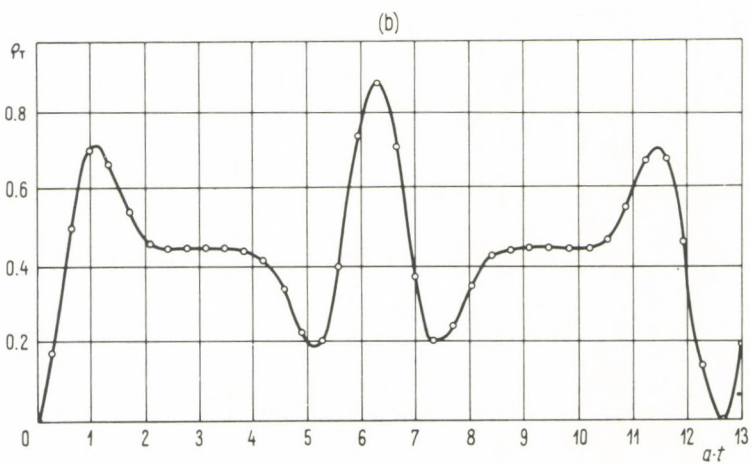
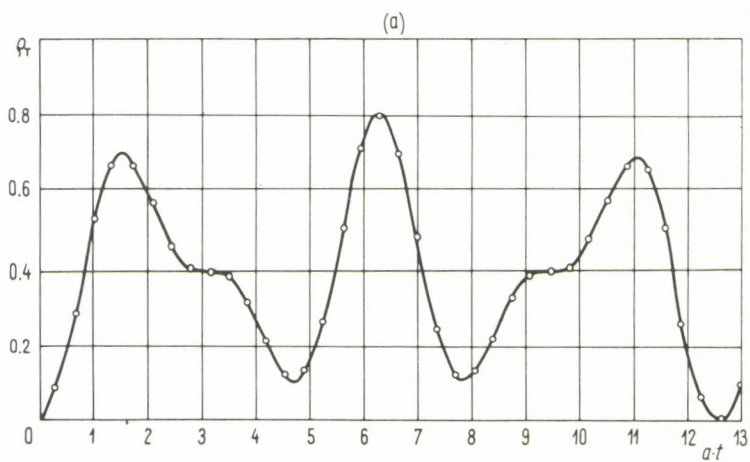


Fig. 2.13. S-T transition dynamics for a two-nucleus singlet-born RP for various ratios H_0/A : (a) 0; (b) 0.5; (c) 1; (d) 10



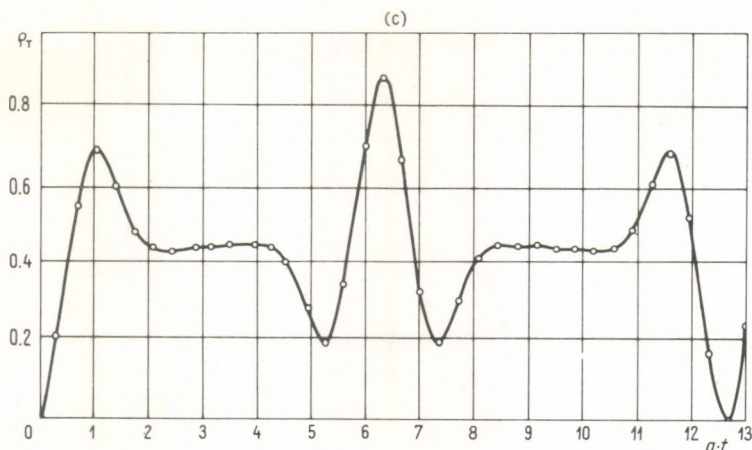


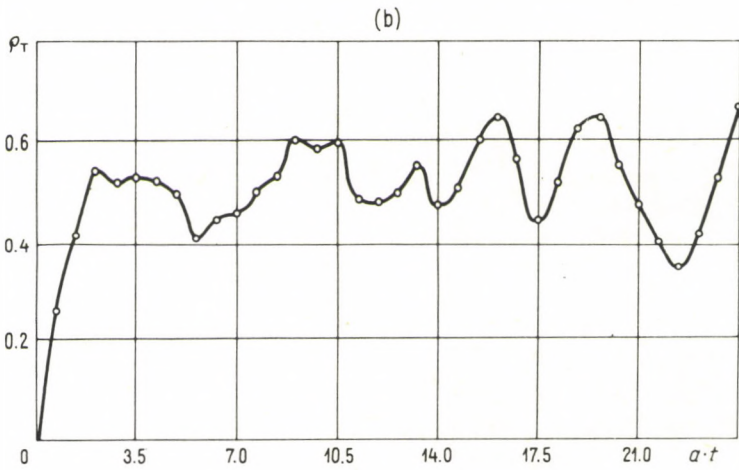
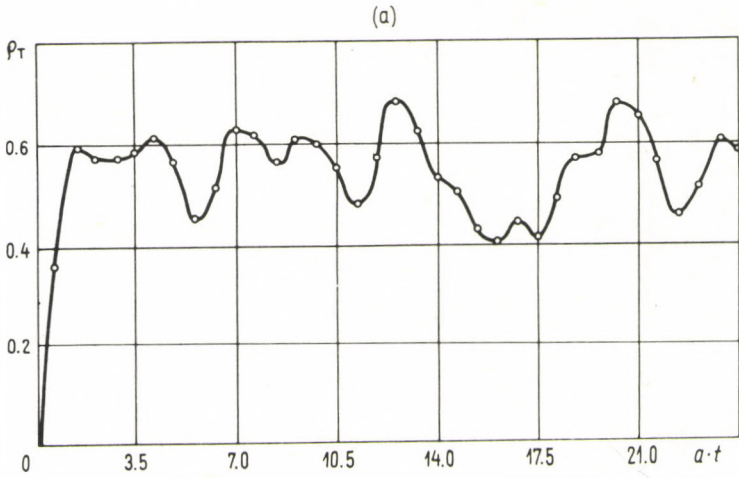
Fig. 2.14. S-T transition dynamics for a singlet-born RP with one of the partners having several equivalent nuclei with $I = 1/2$ in zero field: (a) 4 nuclei; (b) 8 nuclei, (c) 10 nuclei

of the total spin of all the equivalent nuclei. For example, if one of the radicals has 2 protons and the other has no magnetic nucleus, the whole RP ensemble can be divided into two subensembles. In one none of the radicals has a magnetic nucleus, in the other one of the radicals has a $I = 1$ nucleus, the statistical weight of the latter pairs being $3/4$. As a result, in this case

$$\rho_T(t) = (3/4) \cdot \rho_T(1, t),$$

where $\rho_T(1, t)$ is given by the relation (2.105). The S-T transition dynamics for more complex systems with equivalent nuclei can be found in a similar way. Figures 2.14 and 2.15 show triplet state populations calculated for a number of model RPs. The dynamics is seen to be rather complex. They depend on the number of nuclei and the magnetic field strength. It is interesting to compare the initial stages of the S-T dynamics. For all RPs, at times of the order of 10^{-8} s, the triplet state population goes through a maximum equal to 0.7. Then the curves become saturated at $p_{S-T} \approx 0.4-0.45$, this region lengthening as the number of magnetic nuclei increases. These data are interesting for their qualitative agreement with the S-T transition dynamics obtained within the semiclassical approximation (see below).

RPs with nonequivalent nuclei. In a general case, when the radical have nonequivalent nuclei, the spin state population has to be found numerically. The problem is to find the eigenvalues and the eigenstates of Hamiltonian (2.78). Such numerical calculations have been made by Werner *et al.* [2.37] who computed the time evolution of the triplet term population for two RPs at several values of the field strength ($H_0 = 0, 5, 10, 40, 80, \infty$ G). In one RP, one of the radicals had 2 groups of 4 equivalent protons with hf constants 2.3 and 5.2 G, the other had 6 and 3 equivalent protons with hf constants 12.0 and 6.25 G respectively and also a



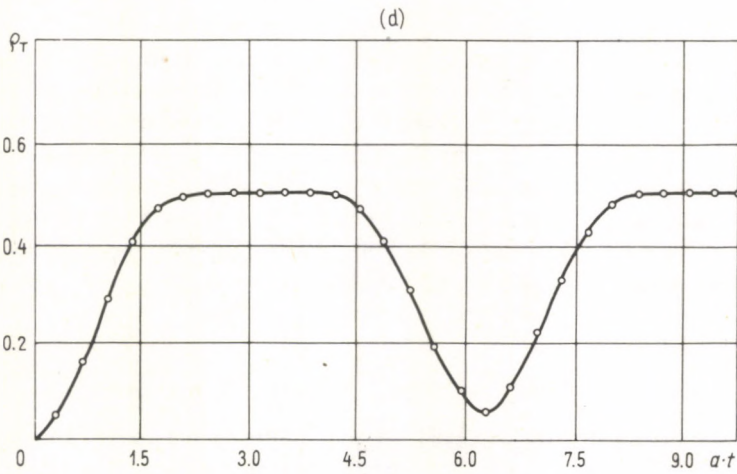
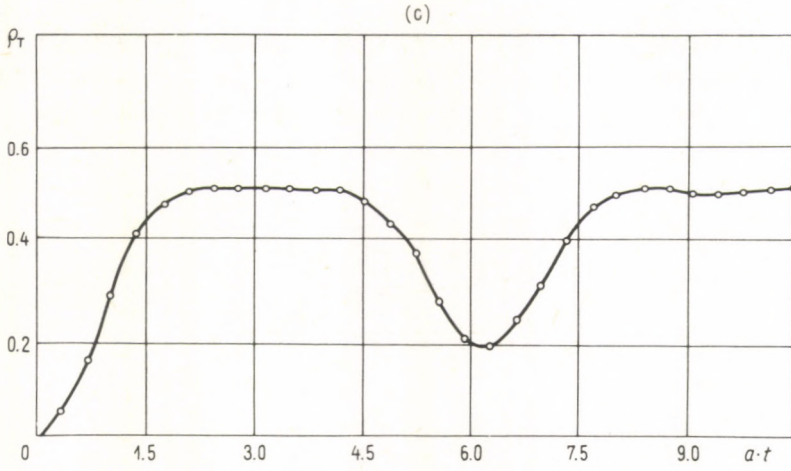


Fig. 2.15. Time dependence of triplet term populations for a singlet-born RP with one of the radicals having 6 equivalent nuclei, $I = 1/2$, for various ratios H_0/A : (a) 2.51; (b) 5.03; (c) 12.57, (d) 25.14

nitrogen nucleus with a hf constant 12.0 G. The results of their calculations are given in Fig. 2.16. At times about 5 ns, the triplet state population reaches a definite level which then changes negligibly up to 50 ns. In fields $H_0 \approx A$, $\rho_T(t)$ reaches about 2/3, in high fields the limiting value of $\rho_T(t)$ falls to 0.5 with increasing field.

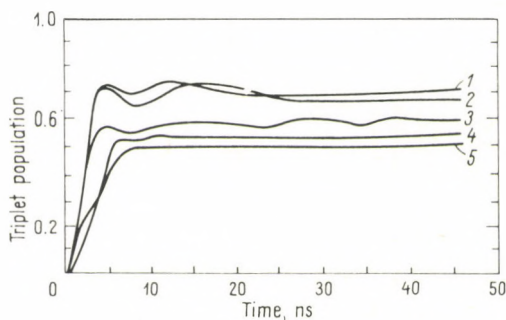


Fig. 2.16. Time evolution of the hyperfine-induced triplet probability for the radical pair system ${}^2P_y^- + {}^2DMA^+$ for different magnetic field strengths: 1-10 G; 2-0; 3-40 G; 4-80 G; 5- ∞ [2.37]

The semi-classical approximation. Calculations of the S-T transition dynamics in arbitrary fields are rather cumbersome. Moreover, if the number of magnetic nuclei is great and they are not equivalent, precise calculations, even numerical, become impossible. To describe S-T transitions in complex RPs with a great number of nuclei, Schulten and Wolynes proposed the following approximate approach [2.33]. They considered the hf effect on the electron spin motion in a semiclassical way. Classical vectors were substituted for nuclear spin moment operators. Mutually correlated motion of the electron and nuclear spins of each radical was replaced by electron spin precession in a local nuclear field

$$\vec{H}_l = \sum_k A_k \vec{I}_k. \quad (2.114)$$

In the approximation, the back effect of the electron spin on the nuclear spin motion is neglected and the nuclear spin configuration of each radical is considered to remain unchanged in some set state. In a point of fact, the nuclear and electron spins can undergo flip-flop transitions. However, if the number of nuclei is great, the variation of the nuclear spin configuration can be assumed negligible for the electron spin motion during the not very long time intervals.

All the radicals are divided into subensembles with a specified configuration of nuclear spins, i.e., the local field of each subensemble has a certain magnitude H_l and a certain orientation specified by the angles ϑ and φ ,

$$\vec{H}_l (H_l \cdot \sin \vartheta \cdot \cos \varphi, H_l \cdot \sin \vartheta \cdot \sin \varphi, H_l \cdot \cos \vartheta) \quad (2.115)$$

It is assumed that all \vec{H}_l orientations are equally probable and that the magnitude of the field H_l (2.114) follows the distribution law for the sum of a great number of independent vectors

$$\begin{aligned} \varrho(H_l, \vartheta) dH_l \cdot d\vartheta &= [1/(2\pi)^{1/2} \cdot \langle H_l^2 \rangle^{3/2}] \cdot \\ &\cdot \exp(-H_l^2/2 \cdot \langle H_l^2 \rangle) \cdot H_l^2 \cdot \sin \vartheta \cdot dH_l \cdot d\vartheta, \end{aligned} \quad (2.116)$$

where $\langle H_l^2 \rangle$ is the mean square value of the local field created by hf interactions,

$$\langle H_l^2 \rangle = (1/3) \cdot \sum_k A_k^2 I_k(I_k + 1) = A_{\text{eff}}^2. \quad (2.117)$$

The total magnetic field strength is

$$H = [(H_0 + H_l \cdot \cos \vartheta)^2 + H_l^2 \cdot \sin^2 \vartheta]^{1/2} \quad (2.118)$$

and its unit vector has the following components

$$\begin{aligned} n_x &= H_l \cdot \sin \vartheta \cdot \cos \varphi / H, & n_y &= H_l \cdot \sin \vartheta \cdot \sin \varphi / H, \\ n_z &= (H_0 + H_l \cdot \cos \vartheta) / H. \end{aligned} \quad (2.119)$$

The unpaired electron spin-Hamiltonian in the semi-classical approximation is

$$\hat{H} = g\beta H \vec{n} \hat{S} \quad (2.120)$$

and the RP spin-Hamiltonian is

$$\hat{H} = g_1 \beta H_1 \vec{n}_1 \cdot \hat{S}_1 + g_2 \beta H_2 \vec{n}_2 \cdot \hat{S}_2 = \hat{H}_1 + \hat{H}_2. \quad (2.121)$$

The triplet state population of a RP with set radical local magnetic fields equal

$$\rho_T = 1 - |\langle S | \exp(-i\hbar^{-1} \hat{H}_1 t) \cdot \exp(-i\hbar^{-1} \hat{H}_2 t) | S \rangle|^2. \quad (2.122)$$

Taking into account the fact that the evolution operator $\exp(-i\vec{c}\vec{n} \cdot \hat{S})$ for particles with $S=1/2$ can be taken in the form

$$\exp(-i\vec{c}\vec{n} \cdot \hat{S}) = \cos \{c/2\} - i2(\vec{n} \cdot \hat{S}) \cdot \sin \{c/2\} \quad (2.123)$$

and substituting this expression into eq. (2.122), one can find the unknown triplet population. For the ensemble of all RPs, $\rho_T(t)$ must be averaged over all values and orientations of the local field. As a result,

$$\begin{aligned} \rho_T(t) &= 1 - F_1(1) \cdot F_1(2) - 2 \cdot F_2(1) \cdot F_2(2) - \\ &- F_3(1) \cdot F_3(2) - F_4(1) \cdot F_4(2)/2. \end{aligned} \quad (2.124)$$

where

$$F_1(k) = \langle \cos^2 \{B(k) \cdot t/2\} \rangle, \quad (2.125)$$

$$F_2(k) = (1/2) \cdot \langle n_z(k) \cdot \sin \{B(k) \cdot t\} \rangle, \quad (2.126)$$

$$F_3(k) = \langle n_x^2(k) \cdot \sin^2 \{B(k) \cdot t/2\} \rangle, \quad (2.127)$$

$$F_4(k) = \langle [n_x^2(k) + n_y^2(k)] \cdot \sin^2 \{B(k) \cdot t/2\} \rangle, \quad (2.128)$$

$B(k) = g_k \beta \cdot \hbar^{-1} \cdot H(k)$ is the S_k Larmor precession frequency, here $k = 1, 2$, is the number of the RP radical, $\langle \dots \rangle$ means averaging with the distribution function (2.116). This averaging can be done analytically in both zero and high magnetic fields. In the latter case, we obtain the above mentioned equation (2.96). In zero fields [2.33]

$$\rho_T(t) = (3/4) \cdot [1 - g_1^0(t) \cdot g_2^0(t)], \quad (2.129)$$

where

$$g_k^0 = (1/3) \cdot [1 + 2 \cdot C_k(t)],$$

$$C_k(t) = (1 - t^2 \cdot a_{k,\text{eff}}^2) \cdot \exp(-t^2 \cdot a_{k,\text{eff}}^2/2).$$

Consider an extreme value of RP triplet state population at $t \rightarrow \infty$. Remember that in high magnetic fields S-T₀ transitions result in equal populations of S and T₀ states. In zero fields three-quarters of RPs might be expected to be triplet, which in fact is not the case. According to eq. (2.129) $\rho_T \rightarrow 1/2$ at $t \rightarrow \infty$ provided only one of the radicals has magnetic nuclei. In this case the asymptotes of $\rho_T(t)$ coincide in zero and high fields. However, in the initial stage of S-T evolution its efficiency in zero field exceeds that in high fields. The extreme value of triplet population in zero field reaches 2/3 (see (2.129)) provided both radicals have magnetic nuclei.

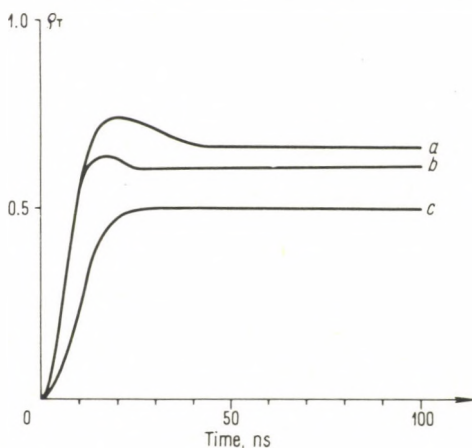


Fig. 2.17. S-T transition probability calculated in the semiclassical approximation for a RP with $\Delta g = 0$ and effective hf constants $A_{1,\text{eff}} = A_{2,\text{eff}} = 4.85$ G in different magnetic fields: a — 0 G; b — 10 G; c — 100 G

In arbitrary magnetic fields $\rho_T(t)$ has to be calculated numerically. For instance, Fig. 2.17 shows the S-T transition dynamics calculated by eq. (2.124) for some concrete situations. ρ_T is seen to run via one or two maxima which lie in the region of $a_{\text{eff}}^2 \cdot t^2 \approx 1$.

The maxima are due to S-T₊ and S-T₋ transitions. In the semi-classical approximation S-T₀ and S-T_{+, -} channels contribute to the total probability of S-T transitions as follows

$$P_{S \rightarrow T_+ + T_-} = F_4(1) \cdot [F_1(2) + F_3(2)] + F_4(2) \cdot [F_1(1) + F_3(1)],$$

$$P_{S \rightarrow T_0} = \rho_T - P_{S \rightarrow T_+ + T_-}. \quad (2.130)$$

Here the total probabilities of S-T transitions, ρ_T , and F_k are determined by eq. (2.121). The time dependences of S-T transition probabilities along different channels are plotted in Fig. 2.18. The S-T₀ transition probability is seen to reach a plateau, while those of S-T₊, T₋ are characterized by a maximum; when the external field increases, S-T₊, T₋ channels are closed.

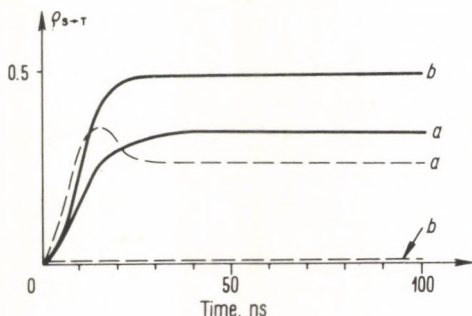


Fig. 2.18. Contributions of S-T₀ (solid lines) and S-T₊, T₋ (dashed lines) transitions to the total probability of S-T evolution: $A_{1, \text{eff}} = A_{2, \text{eff}} = 4.85$ G, $\Delta g = 0$: a - $H_0 = 10$ G; b - $H_0 = 100$ G

The semi-classical approximation smooths the S-T transition dynamics (see Fig. 2.19). However, one is almost forced to employ it in the case of complex radicals with a great number of magnetic nuclei, and it is the only viable approach to complex RP spin dynamics in arbitrary fields.

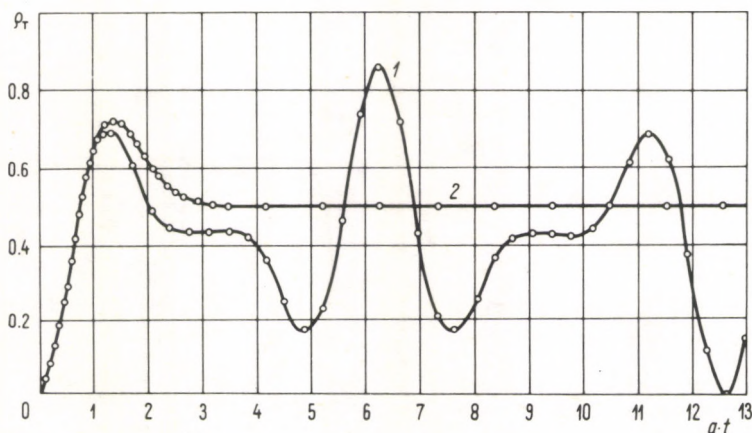


Fig. 2.19. Triplet term population of a singlet-born RP with one of the partners having six equivalent nuclei ($I = 1/2$) in zero field. 1 — exact theory; 2 — semi-classical approximation

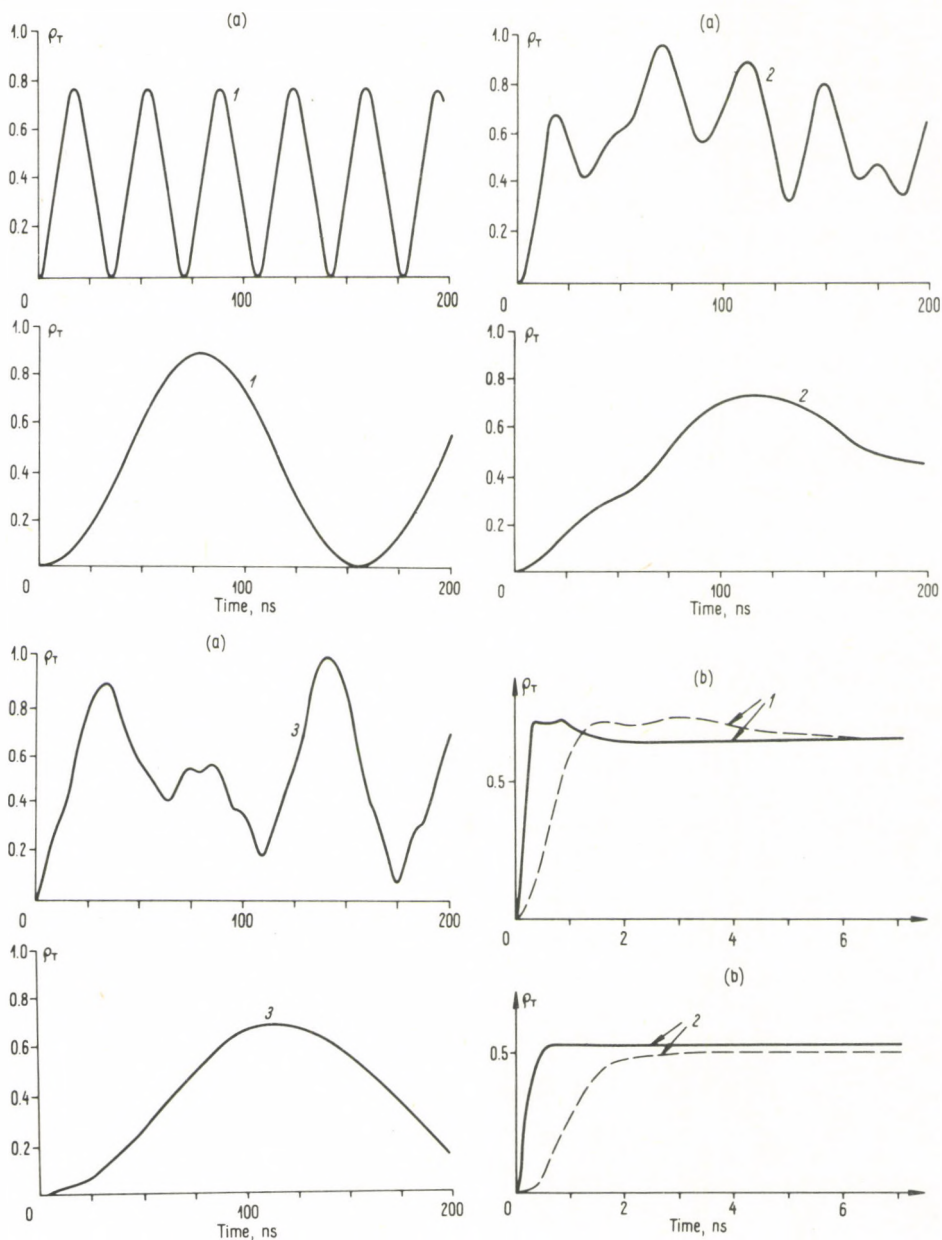


Fig. 2.20. Changes in RP S-T dynamics with D substituted for H . (a) A one-nuclear RP, $A_H = 10$ G, $A_D = 1.535$ G. Upper curves for a protonated RP, lower curves for a deuterated RP. 1 - $H_0 = 0$; 2 - $H_0 = 5$ G; 3 - $H_0 = 20$ G; (b) A pair of benzyl and alkyl radicals (see Fig. 2.8); solid lines—completely protonated radicals; dashed lines—completely deuterated radicals: 1 - $H_0 = 0$; 2 - $H_0 = 100$ G

The role of exchange interactions. In low magnetic fields the exchange interactions between terms reduce the S-T transition efficiency provided the exchange energy exceeds that of the hf interaction. If $J \approx a$, the low-field spin dynamics become much more complex. For example, consider the spin dynamics of a one-nucleus RP with spin I in zero field. The triplet term population is [2.30]

$$\rho_T^0(t) = I \cdot (I + 1) \cdot (a^2/R^2) \cdot \sin^2 \{Rt/2\}, \quad (2.131)$$

$$R^2 = I \cdot (I + 1) \cdot a^2 + (2J + a/2)^2. \quad (2.132)$$

The function

$$f = a^2/R^2 \quad (2.133)$$

can have a maximum with increasing J provided a and J are of opposite signs.

The influence of magnetic isotope substitution. The above results unambiguously demonstrate RP spin dynamics to be strongly dependent on the nuclear spins and the hf constants. In the case of isotopic substitution, both the nuclear spin and the hf constant, and thus singlet-triplet dynamics, change.

To illustrate the magnetic isotope effect in the spin dynamics let us consider the simplest case: a one-proton RP, the proton spin being $1/2$. On substituting D for H , the nuclear spin increases by a factor of 2 accompanied with a simultaneous 6.5-fold decrease in the hf constant. The effective hf constant reduces in this case approximately by a factor of 4. The spin dynamics for a RP with one proton and one deuteron, for a number of concrete values of hf and magnetic field, are shown in Fig. 2.20 (a). The spin dynamics is seen to be very sensitive to isotopic substitution.

In real experiments a pair usually contains many magnetic nuclei, especially protons. For the isotope substitution to affect S-T transition dynamics appreciably, the hf energy must change sufficiently too, the greatest effects taking place for complete isotope substitution. To illustrate variations of singlet-triplet evolution in complex systems induced by isotope substitution, Fig. 2.20b depicts semi-classical calculations for a pair of benzyl and alkyl radicals. Particularly large changes of spin evolution in protonated and deuterated systems are seen in the initial parts of the curves: in a deuterated pair, S-T transitions are much less effective.

2.2.5 RP spin dynamics under random hf modulation

The above considerations assume the unpaired electrons to belong always to the same particles, and the electron spins, during the S-T evolution, to interact with the same magnetic nuclei with fixed hf constants. However, there are situations when the hf interaction is modulated in a random manner. An example of processes resulting in random hf modulation is internal rotation in radicals leading to the magnetic nuclear exchange between nonequivalent positions. Consider, e.g., a radical with two magnetic nuclei which can be in two nonequivalent positions. If the

nuclei can exchange their positions, the hf spin-Hamiltonian would certainly acquire one of the two values:

$$\hat{H}_a = \hbar a_1 \hat{S} \cdot \hat{I}_1 + \hbar a_2 \hat{S} \cdot \hat{I}_2 \quad (2.134)$$

or

$$\hat{H}_b = \hbar a_2 \hat{S} \cdot \hat{I}_1 + \hbar a_1 \hat{S} \cdot \hat{I}_2. \quad (2.135)$$

Thus, the position interchange of the magnetic nuclei modulates the hf randomly. Another process of random hf modulation is electron jumps between molecules. As a result, the electron finds itself in different nuclear environments.

Random hf modulation causes significant effects on ESR spectra. When the modulation is slow, the ESR spectral components broaden as a result of a decrease in the radical lifetime at a specified magnetic nuclear configuration. When the characteristic frequency of the random hf modulation exceeds the scale of the hyperfine splitting of the radical ESR spectrum, the interchanged spectral components merge to a single narrow line.

The random hf modulation effect on the S-T transition dynamics has been first considered by Schulten and Wolynes [2.33]. This problem becomes comparatively simple in the case of high magnetic fields and the semi-classical approach to the RP spin dynamics. The effect of random hf modulation induced by an electron or hole jumps in radical-ion pairs upon CIDEP and CIDNP was considered by Hore and McLauchlan [2.76], Salikhov and Sarvarov [2.77], and by Kruppa *et al.* [2.78].

High magnetic fields. In high fields the random hf modulation corresponds to a random jump of the unpaired electron from one hfs component of the ESR spectrum to another, that in turn results in a random migration of the electron spin precession frequency. The matrix element of S-T₀ transitions, $\varepsilon(m)$, equals half the difference between the resonance frequencies of the partners (see eq. (2.84)). Because of the electron spin frequency migration, $\varepsilon(m)$ is characterized by a random time evolution,

$$\varepsilon(t) = (g_1 - g_2)\beta\hbar^{-1}H_0/2 + \varepsilon_{\text{hf}}(t), \quad (2.136)$$

$$\varepsilon_{\text{hf}}(t) = \sum_i a_{1i} \cdot m_{1i}(t)/2 - \sum_k a_{2k} \cdot m_{2k}/2. \quad (2.137)$$

The S-T₀ transition probability is described by the expression (cf. eq. (2.84))

$$\rho_{T_0}(t) = (1/2) \cdot [1 - \text{Re} \{ \exp [i(g_1 - g_2)\beta\hbar^{-1}H_0 t] \cdot \langle \exp [i \int_0^t 2\varepsilon_{\text{hf}}(t) dt] \rangle \}]. \quad (2.138)$$

Here $\langle \dots \rangle$ means averaging over all realizations of the random process $\varepsilon_{\text{hf}}(t)$. Since the hf interaction results in a frequency distribution which is symmetrical with respect to the centre and the hf interaction of the partners varies independently, we have

$$\rho_{T_0}(t) = (1/2) \cdot [1 - \cos \{(g_1 - g_2)\beta\hbar^{-1}H_0 t\} \cdot \langle \exp [i \int_0^t 2 \cdot \varepsilon_{1, \text{hf}}(t) dt] \rangle \cdot \langle \exp [i \int_0^t 2 \cdot \varepsilon_{2, \text{hf}}(t) dt] \rangle]. \quad (2.139)$$

The theory of magnetic resonance has a well developed technique for averaging quantities of the type $\exp [i\int e(t)dt]$, the results being available for a number of random processes (see, e.g. [2.38]). Consider, e.g., a pair of radical-ions, A^+ and B^- . Assume an electron can jump from molecule to molecule with a frequency K and interact with one magnetic nucleus. Let A have no magnetic nucleus. In this case

$$\rho_{T_0}(t) = (1/2) \cdot [1 - \cos \{(g_1 - g_2)\beta\hbar^{-1}H_0t\}] \cdot \langle \exp \left[ia \int_0^t m(t)dt \right] \rangle. \quad (2.140)$$

When jumping to a new molecule, the electron meets, with equal probability, either a $+1/2$ or $-1/2$ spin nucleus. Thus, the sign of the spin projection of the nucleus, in whose field the electron spin precesses, alters on average in a time $\tau = 2/K$. According to ref. [2.39],

$$g(t) = \langle \exp \left[ia \int_0^t m(t)dt \right] \rangle = \exp(-Kt/2) \cdot [\text{ch} \{Rt\} + (K/2 \cdot R) \cdot \text{sh} \{Rt\}], \quad (2.141)$$

where $R^2 = (K^2 - a^2)/4$. Substitution of this result into eq. (2.140) gives

$$\rho_{T_0}(t) = (1/2) \cdot [1 - \cos \{Ag \cdot \beta\hbar^{-1}H_0t\}] \cdot g(t). \quad (2.142)$$

To simplify the formulas, consider a RP with equal g -values of the partners. The $S-T_0$ transition probability is strongly dependent on the electron migration rate. When it is low, i.e., $K \ll a$, $Kt < 1$,

$$g(t) \approx \cos \{a \cdot t/2\}$$

we obtain a result coinciding in fact with the above equation (2.87) for a system without random hf modulation. In the other extreme case of fast electron migration, when $K \gg a$

$$g(t) \approx \exp(-a^2 \cdot t/4 \cdot K), \quad (2.143)$$

$$\rho_{T_0}(t) \approx (1/2) \cdot [1 - \exp(-a^2 \cdot t/4 \cdot K)].$$

The dependence of $S-T$ transitions on the electron migration rate is plotted in Fig. 2.21. The example shows that when the rate of the electron transfer increases, the hf interaction is effectively averaged to zero and the singlet-triplet transition probability due to the hf-mechanism is reduced. At a very fast hf modulation, the hf-mechanism affects the singlet-triplet dynamics negligibly. This conclusion is valid for RPs with any number of magnetic nuclei.

The semi-classical approximation. In arbitrary fields the effect of random hf modulation on RP spin dynamics has been studied by Schulten and Wolynes [2.33]. They considered this problem in the semi-classical approximation (see the preceding section). A random intermolecular jump of an electron results in a random change of the magnitude and the orientation of the local magnetic field in

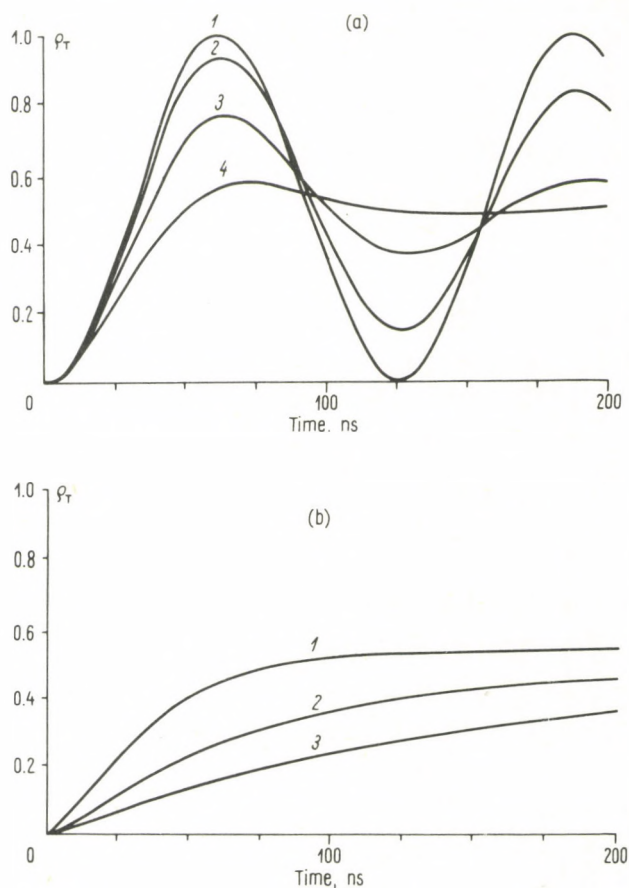


Fig 2.21. S-T transition probability at different rates K of random hf modulation, $a = 10^8$ rad/s. (a) $-K < a$: 1 — $K = 0$; 2 — $K = 5 \cdot 10^6$ s $^{-1}$; 3 — $K = 2 \cdot 10^7$ s $^{-1}$; 4 — $K = 5 \cdot 10^7$ s $^{-1}$; (b) $-K \geq a$: 1 — $K = 10^8$ s $^{-1}$; 2 — $K = 2 \cdot 10^8$ s $^{-1}$; 3 — $K = 4 \cdot 10^8$ s $^{-1}$

which the unpaired electron spin precesses. The electron spin motion can be described in this case as follows. All the radicals are divided into subensembles, each having a local nuclear field of a definite magnitude and orientation. The spin density matrix of a subensemble varies due to the Larmor precession of the unpaired electron and random electron transitions between the subensembles. Let $\sigma(\vec{H}_i)$ and $\hat{H}(\vec{H}_i)$ be the density matrix and the spin-Hamiltonian of a radical subensemble with a set local field. The electron lifetime on a molecule is assumed to be τ . The density matrix obeys the equation

$$\partial\sigma(\vec{H}_i)/\partial t = -i\hbar^{-1} \cdot [\hat{H}(\vec{H}_i), \sigma(\vec{H}_i)] - [\sigma(\vec{H}_i) - \sigma]/\tau \quad (2.144)$$

where σ is the density matrix of all the radicals averaged over all possible \vec{H}_1 (see (2.116)),

$$\sigma = \int \sigma(\vec{H}_1) \cdot \varphi(\vec{H}_1) \cdot dH_1 \cdot d\vartheta. \quad (2.145)$$

The density matrix of a RP subensemble with the radical 1 having the local field $H_{1,1}$ and the radical 2 with the field $H_{1,2}$ also obeys an equation of type (2.144),

$$\begin{aligned} \partial \rho(\vec{H}_{1,1}, \vec{H}_{1,2}) / \partial t = & -i\hbar^{-1} [\hat{H}_1(\vec{H}_{1,1}) + \hat{H}_2(\vec{H}_{1,2}), \rho(\vec{H}_{1,1}, \vec{H}_{1,2})] - \\ & -(1/\tau_1 + 1/\tau_2) \cdot [\rho(\vec{H}_{1,1}, \vec{H}_{1,2}) - \bar{\rho}] \end{aligned} \quad (2.146)$$

where

$$\bar{\rho} = \int \dots \int \rho(\vec{H}_{1,1}, \vec{H}_{1,2}) \cdot \varphi(\vec{H}_{1,1}) \cdot \varphi(\vec{H}_{1,2}) \cdot dH_{1,1} \cdot dH_{1,2} \cdot d\vartheta_1 \cdot d\vartheta_2$$

is the RP density matrix averaged over the entire subensemble. The system of equations (2.146) gives the singlet and triplet populations at any time. If initially all the RPs were singlet, the probability of finding them in the triplet state is

$$\rho_T(t) = 1 - \langle S | \bar{\rho}(t) | S \rangle.$$

This approximation has been used to calculate the S-T transition dynamics for some particular cases [2.33, 40]. Random changes of the local fields of unpaired electrons have been shown to reduce the efficiency of singlet-triplet transitions in RPs.

2.2.6 RP spin dynamics in microwave fields

The effects of the microwave field on RP spin dynamics is an interesting problem. Theoretically this problem has been first studied by Kubarev *et al.* [2.41, 42]. Consider the electron spin motion of two radicals with different Zeeman frequencies in a constant magnetic field \vec{H}_0 and an oscillating field \vec{H}_1 normal to \vec{H}_0 . The spin-Hamiltonian of the pair is the sum of those of the partners,

$$\hat{H} = \hat{H}_1 + \hat{H}_2$$

where

$$\hat{H}_k = g_k \cdot \beta [H_0 \hat{S}_{kz} + H_1 (\hat{S}_{kx} \cdot \cos \{\omega t\} + \hat{S}_{ky} \cdot \sin \{\omega t\})].$$

To calculate the spin dynamics it is expedient to employ a co-ordinate system rotating about \vec{H}_0 (defining the z-axis) with a frequency ω . The spin-Hamiltonian then takes the form

$$\hat{H}_k = (g_k \cdot \beta H_0 - \hbar \omega) \hat{S}_{kz} + g_k \beta H_1 \hat{S}_{kx}. \quad (2.147)$$

The spin precesses in the effective magnetic field with a frequency

$$\begin{aligned} \omega_{\text{eff}}(k) = & [(\gamma_k \cdot H_0 - \omega)^2 + \gamma_k^2 \cdot H_1^2]^{1/2}, \\ \gamma_k = & g_k \cdot \beta \cdot \hbar^{-1}. \end{aligned} \quad (2.148)$$

The direction cosines of the effective field are

$$\begin{aligned}n_{kx} &= \gamma_k \cdot H_1 / \omega_{\text{eff}}(k), \\n_{ky} &= 0, \\n_{kz} &= (\gamma_k \cdot H_0 - \omega) / \omega_{\text{eff}}(k).\end{aligned}\quad (2.149)$$

Calculations, similar to those done for the spin dynamics under the influence of a local nuclear field in the semi-classical approximation, give the following result. The triplet term population is

$$\begin{aligned}\rho_T(t) &= 1 - [\cos \{ \omega_{\text{eff}}(1)t/2 \} \cdot \cos \{ \omega_{\text{eff}}(2) \cdot t/2 \} + \\&+ (\vec{n}_1 \cdot \vec{n}_2) \cdot \sin \{ \omega_{\text{eff}}(1) \cdot t/2 \} \cdot \sin \{ \omega_{\text{eff}}(2) \cdot t/2 \}]^2,\end{aligned}\quad (2.150)$$

where $(\vec{n}_1 \cdot \vec{n}_2)$ is the scalar product of the unit vectors setting the directions of the spin effective fields (see (2.149)).

In order to elucidate the role of an oscillating magnetic field in the S-T transitions, consider some examples. In two extreme situations the effective spin fields are co-linear, $\vec{n}_1 \parallel \vec{n}_2$. This is the case, firstly, when there is no variable field, $H_1 = 0$; and, secondly, in very strong microwave fields, when $g\beta H_1 \gg \Delta g \cdot \beta H_0$. In both cases $(\vec{n}_1 \cdot \vec{n}_2) = 1$ and

$$\rho_T(t) = \sin^2 \{ [\omega_{\text{eff}}(1) - \omega_{\text{eff}}(2)] \cdot t/2 \} \quad (2.151)$$

or

$$\rho_T = \sin^2 \{ \Delta g \cdot \beta \hbar^{-1} \cdot H_0 t/2 \} \text{ when } H_1 = 0 \quad (2.152)$$

and

$$\rho_T = \sin^2 \{ \Delta g \cdot \beta \hbar^{-1} H_1 t/2 \} \text{ when } H_1 \text{ is high.} \quad (2.153)$$

Here $\Delta g = g_1 - g_2$ is the difference in the radical g -values. In point of fact, in this case the S-T transitions follow the Δg -mechanism in both the laboratory (2.152) and the rotating (2.153) coordinate systems. Intermediate values of H_1 give more complex dynamics of S-T transitions.

As an example, Fig. 2.22 illustrates the S-T transition dynamics for several values of the microwave field intensity, the latter being in resonance with one of the spins of the pair. At small H_1 , S-T transitions obey eq. (2.152). Their efficiency first increases with H_1 , then falls. Later on, in very high microwave fields, the efficiency of S-T transitions increases again due to the Δg -mechanism in the rotational coordinate system (in line with eq. (2.153)).

In practice it is extremely difficult to obtain microwave fields appreciably exceeding $H_1 \approx 10$ G. It means that the extreme case (2.153) can be realized practically only if the radicals possess a very small Δg -value, $\Delta g < gH_1/H_0 \lesssim 0.01$. However, even if this requirement is fulfilled, one can hardly expect to observe S-T transitions experimentally with the frequency

$$\Delta g \cdot \beta \cdot \hbar^{-1} H_1 \approx 10^6 \text{ rad/s at } \Delta g \approx 0.01, H_1 \approx 10 \text{ G,}$$

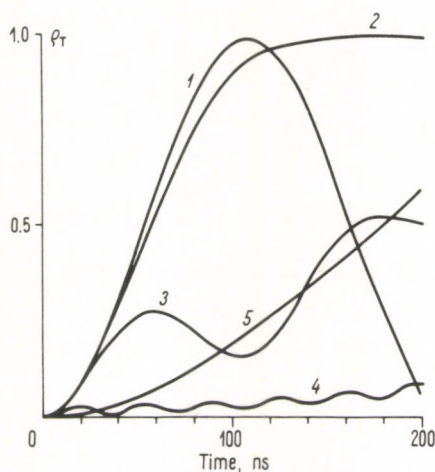


Fig. 2.22. Microwave field effects on S-T transition probability. RP parameters: $g_1=2.000$; $g_2=2.001$; $H_0=3300$ G. H_1 values: 1 — 0.01 G; 2 — 1 G; 3 — 3 G; 4 — 10 G; 5 — 10^3 G

which is comparable with the rate of paramagnetic relaxation processes. These considerations taken into account, one can neglect the Δg -value in the energy of interactions between the radicals and the microwave field. Then

$$\begin{aligned}\omega_{\text{eff}}(k) &\cong [(\gamma_k \cdot H_0 - \omega)^2 + \gamma^2 H_1^2]^{1/2}, \\ n_{kx} &\cong \gamma H_1 / \omega_{\text{eff}}(k), \\ n_{ky} &= 0, \\ n_{kz} &\cong (\gamma_k \cdot H_0 - \omega) / \omega_{\text{eff}}(k).\end{aligned}\quad (2.154)$$

The expression for the S-T transition probability can be simplified if the microwave field is tuned to resonate with one of the spins, say S_1 . In this case

$$\begin{aligned}\rho_T(t) &= 1 - [\cos \{\omega_1 \cdot t/2\} \cdot \cos \{\omega_2 \cdot t/2\}] + \\ &\quad + n \cdot \sin \{\omega_1 \cdot t/2\} \cdot \sin \{\omega_2 \cdot t/2\}]^2, \\ \omega_1 &= \gamma H_1, \quad \omega_2 = [(\gamma_1 - \gamma_2)^2 \cdot H_0^2 + \gamma^2 \cdot H_1^2]^{1/2}, \\ n &= \gamma H_1 / \omega_2.\end{aligned}\quad (2.155)$$

Without a microwave field, in a high H_0 , the S-T₀ mixing is induced by the difference in the spin resonance frequencies. On switching on a variable field $H_1(\vec{H}_1 \perp \vec{H}_0)$, S-T₊, T₋ transitions arise together with S-T₀ transitions. Note that if the resonance frequencies are equal, the microwave field does not induce S-T transitions but only those between the triplet sublevels.

The above results on spin dynamics in microwave fields can be readily generalized to the case of a pair with the partners having hfs ESR spectra. This situation is of great practical interest. Let $\omega_k(1)$, $\varphi_k(1)$; $\omega_n(2)$, $\varphi_n(2)$ be the resonance frequencies and the hfs component intensities of the radical ESR spectra. The triplet state population changes then as

$$\begin{aligned} \rho_T(t) = & 1 - \sum_{k,n} \varphi_k(1) \cdot \varphi_n(2) \cdot [\cos \{\tilde{\omega}_k(1) \cdot t/2\} \cdot \cos \{\tilde{\omega}_n(2) \cdot t/2\} + \\ & + (\vec{n}_k(1) \cdot \vec{n}_n(2)) \cdot \sin \{\tilde{\omega}_k(1) \cdot t/2\} \cdot \sin \{\tilde{\omega}_n(2) \cdot t/2\}]^2, \quad (2.156) \\ & \tilde{\omega}_k(1) = [\omega_k^2(1) + \gamma_1^2 H_1^2]^{1/2}, \\ & \tilde{\omega}_n(2) = [\omega_n^2(2) + \gamma_2^2 H_1^2]^{1/2}, \\ & \vec{n}_k(1) = (\gamma_1 H_1 / \tilde{\omega}_k(1), 0, (\omega_k(1) - \omega) / \tilde{\omega}_k(1)), \\ & \vec{n}_n(2) = (\gamma_2 H_1 / \tilde{\omega}_n(2), 0, (\omega_n(2) - \omega) / \tilde{\omega}_n(2)). \end{aligned}$$

In conclusion it can be noted that at present the RP spin dynamics has been sufficiently well described. The basic mechanisms of S-T transitions are the difference in radical g -values (Δg -mechanism) and the isotropic hf interaction of unpaired electrons with magnetic nuclei (hf-mechanism). The S-T dynamics in high fields can be calculated for the case of arbitrary RPs with any magnetic nuclei. In low fields, the S-T dynamics has been adequately described only for the simplest systems including radicals with equivalent magnetic nuclei. For those with a great number of magnetic nuclei, the spin dynamics can be calculated at arbitrary fields in the semi-classical approximation.

2.3 Mathematical tools of the theory

In the spin-independent theory of radical recombination in liquids, two methods have been elaborated to calculate the RP recombination probability and to find the recombination rate constant. One of them involves solving the kinetic equation for the concentration of RPs with different distances between the partners (see, e.g., [2.17, 22]). This approach gives the total effect of all contacts of a given pair during its in-cage lifetime. The other method is a direct summation of the contributions to the recombination made by a sequence of RP contacts at the reaction radius [2.2]. When it became necessary to include spin polarization and magnetic effects into the theory, both methods were generalized. That, however, resulted in a complication of the theory. On the one hand, the number of degrees of freedom which should be explicitly considered in the course of recombination increased greatly. Indeed, the spin-independent theory of RP recombination usually considers only the mutual spatial diffusion of two radicals. Even account taken of the rotational diffusion of the reactants in the presence of reactivity anisotropy effects complicates the theory (see, e.g. [2.27]). In the theory of spin polarization and magnetic effects in radical reactions we have to distinguish RPs with various configurations of electron and

nuclear spins. In fact, instead of one RP ensemble in the spin-independent theory, when considering spin polarization and magnetic effects one has to deal with a great number of RP subensembles, each corresponding to a certain spin configuration. The interaction of RP spins with external magnetic fields and that between the spins interchange RPs between the subensembles. As a result, we have a large set of coupled kinetic equations for the RP subensembles in a cage. On the other hand, the RP spin state representation requires quantum mechanical tools as well. In order to consider molecular motion and RP spin dynamics simultaneously the density matrix is the most appropriate technique [2.43, 44].

A consistent theory of radical recombination which considers both spatial and spin reagent coordinates has been formulated and developed independently by two research groups: Pedersen and Freed [2.45–47] and Salikhov *et al.* [2.30, 48–51]. The contribution made by Evans *et al.* [2.52] and Schulten *et al.* [2.16, 37] as well as the data obtained by Harberkorn [2.32, 53] are also of importance. In the literature there are many approximate evaluations of spin polarization effects, both CIDNP and CIDEP, and also magnetic field effects on the yield of radical recombination products (see, e.g. [2.12, 14, 20, 29–31, 51, 54–64]).

The problem is to describe changes of spin and spatial reagent coordinates simultaneously, bearing in mind that these changes are interrelated. Indeed, a RP spin state is essentially dependent upon the thermal motion of the partners. The mutual radical diffusion in a pair, on the one hand, determines the time interval between subsequent RP contacts when singlet–triplet transitions occur and, on the other hand, affects the exchange and dipolar spin interactions of the unpaired electrons in a random manner. If the exchange interaction is anisotropic, it can also be modulated by rotational diffusion. Furthermore, radical rotation averages the anisotropic hyperfine interaction of the unpaired electrons with the magnetic nuclei, etc. Therefore, the state of the electron and nuclear spins at the moment of radical contact depends both on the parameters determining spin interactions and on the trajectory followed by the radicals in the course of their random walk in a cage. However, a RP spin state not only depends on the thermal motion of the partners but can, in a general case, itself influence the character of their random walk. The partners are, as a rule, attracted in the singlet term and repulsed in the triplet. Singlet RPs are therefore kept in contact longer than triplets.

Theoretical evaluations of the exchange integral and experimental data on spin exchange between free radicals show [2.26] that when the radicals are as close as the sum of their Van der Waals radii the exchange interaction is of order of magnitude $\approx 10^{13}$ rad/s, i.e. at room temperature it does not exceed the thermal energy of the reagents translational motion. From the foregoing, in most cases the influence of the RP spin state upon the mutual diffusion of the partners can be neglected right up to collisions at the Van der Waals radii. At small distances, when radicals get into the recombination zone, the exchange interaction is, of course, of great importance. It is due to the exchange interaction that the formation of stable products becomes possible. Unfortunately, so far the process of formation of a molecule from two colliding radicals has not been described in detail and the recombination is usually

introduced phenomenologically². In this case the exchange interaction at small distances is expressed in terms of phenomenological parameters such as the RP recombination rate constant, the reaction layer width, and the effective recombination time. From the foregoing, in most cases the in-cage thermal motion of species between re-encounters at the recombination radius can be considered to be independent of their spin state.

This section investigates formal features of the radical recombination theory. First consider geminate RP recombination.

2.3.1 Kinetic equations of RP geminate recombination

Consider the dynamics of spin and spatial coordinates of a RP in a cage. It is convenient to divide all RPs into subensembles, each having partners separated by a certain radius-vector \vec{r} at a given moment. The spin state of a particular RP subensemble is completely determined by the partial spin density matrix $\rho(\vec{r}, t)$. Note that the diagonal matrix elements give RP populations in the respective spin states. For example, $\rho_{SS}(\vec{r}, t)$ is the fraction of a particular subensemble in the singlet state. The off-diagonal elements of the density matrix characterize the relation between the phases of the RP spin states. Suppose that the RP wave function represents a superposition of the singlet S and triplet T_0 states $\Psi = a_S|S\rangle + a_T|T_0\rangle$. The state amplitudes in a general case are complex, $a_S = |a_S| \cdot \exp(i\varphi_S)$, $a_T = |a_T| \cdot \exp(i\varphi_T)$. An off-diagonal matrix element equals $\rho_{ST_0} = |a_S \cdot a_T| \cdot \exp[i(\varphi_T - \varphi_S)]$. If in a RP subensemble the phases of S and T_0 states become completely random, the mean value of $\exp[i(\varphi_T - \varphi_S)]$ and thus the off-diagonal matrix element become zero.

Changes of the partial density matrix are governed by several factors: (1) the RP spin evolution induced by the interactions between the RP spins or those of the spins with the orbital and rotational radical moments and with external magnetic fields; (2) radical mutual diffusion; (3) radical recombination, (4) reactions of radicals with acceptors etc. We discuss these factors.

The singlet-triplet in-cage evolution of RP spins, as stated in the preceding section, is determined mainly by the interaction of electron spins with magnetic fields and the isotropic hf interactions of unpaired electrons with magnetic nuclei. The spin-Hamiltonian of the Zeeman and isotropic hf interactions of the unpaired electrons of an RP have the form (2.78). In the general case one should remember that an unpaired electron of one radical can interact with the magnetic nucleus of its partner and, when necessary, it should be included in eq. (2.78). Besides, in RP spin

² Furthermore it would be desirable to develop a theory free of purely phenomenological approach to recombination of the two colliding reactants. A detailed microscopic description of an elementary chemical transformation step of two colliding species can in fact reveal some additional mechanisms and manifestations of spin dynamics and magnetic effects. In fact, two radicals colliding at the recombination radius represent a certain intermediate complex, a quasi-molecule, where intramolecular singlet-triplet intersystem crossing can be effectively realized.

dynamics the exchange interaction between the unpaired electrons is of great importance. It is the exchange interaction that splits RP terms into singlets and triplets, $2J$ being their difference in energy. Hence, changes of the RP partial density matrix due to the RP spin evolution can be expressed in the form

$$(\partial\rho(\vec{r}, t)/\partial t)_s = -i\hbar^{-1}[\hat{H}_0 + \hat{V}(\vec{r}), \rho(\vec{r}, t)]. \quad (2.157)$$

Another source of the partial density matrix changes is the mutual radical diffusion. This can be described in terms of the conditional probability $P(\vec{r}, t|\vec{r}', t')$ that the radius-vector between them will equal \vec{r} at a time t provided the separation was \vec{r}' at some preceding moment t' . It obeys the equation

$$\partial P(\vec{r}, t|\vec{r}', t')/\partial t = \hat{L}(\vec{r}) \cdot P(\vec{r}, t|\vec{r}', t'), \quad (2.158)$$

where the explicit form of the linear operator \hat{L} is determined by the character of the particle diffusion. For example, if the radical motion between the temporarily stable states is jump-like, then the conditional probability obeys the *Feller equation*

$$\begin{aligned} \partial P(\vec{r}, t|\vec{r}', t')/\partial t = & -[P(\vec{r}, t|\vec{r}', t') - \\ & - \int d^3\vec{r}'' \cdot f(\vec{r}, \vec{r}'') \cdot P(\vec{r}'', t|\vec{r}'', t')]/\tau_c, \end{aligned} \quad (2.159)$$

where $1/\tau_c$ is the mean frequency of the interrational distance changes due to radical jumps, $f(\vec{r}, \vec{r}'')$ is the probability that the intermolecular distance in the pair changes from \vec{r}'' to \vec{r} as a result of a single jump of one of the partners. In the extreme case of continuous diffusion, the kinematic operator \hat{L} is an ordinary diffusion differential operator,

$$\hat{L}\hat{P} = D \cdot \Delta P(\vec{r}, t|\vec{r}', t'), \quad (2.160)$$

where $\Delta = \partial^2/\partial x^2 + \partial^2/\partial y^2 + \partial^2/\partial z^2$ is the Laplace operator. If the radical diffusion is influenced by spin-independent forces of interrational interactions $U(r)$, then the kinematic operator is

$$\hat{L}(U) \cdot P = D[\Delta \cdot P + \nabla \cdot (P \cdot \nabla U(\vec{r}))/kT]. \quad (2.161)$$

Changes of the partial density matrix owing to radical mutual diffusion are determined by the kinematic operator from the equation

$$(\partial\rho(\vec{r}, t)/\partial t)_d = \hat{L}\rho(\vec{r}, t). \quad (2.162)$$

The total change of the partial density matrix due to the RP spin evolution and the mutual diffusion of the partners is described by the kinetic equation [2.30, 45–48]

$$\partial\rho(\vec{r}, t)/\partial t = -i\hbar^{-1}[\hat{H}_0 + \hat{V}(\vec{r}), \rho(\vec{r}, t)] + \hat{L}\rho(\vec{r}, t). \quad (2.163)$$

Moreover, one should take into account the RP decay due to recombination reactions. It can be done in two ways: either introducing an additional term into (2.163) [2.45–47] or choosing appropriate boundary conditions at the recom-

bination radius [2.30, 48–51]. Let $K(\vec{r})$ be the pseudo first order rate constant of RP recombination, the radius-vector between the partners being \vec{r} (to be explicit, we assume that only singlet RPs can recombine). The RP recombination can be allowed for by an additional term:

$$(\partial\rho(\vec{r}, t)/\partial t)_r = -(K(\vec{r})/2) \cdot [\hat{P}_S \cdot \rho(\vec{r}, t) + \rho(\vec{r}, t) \cdot \hat{P}_S] \quad (2.164)$$

inserted into (2.163). Here $\hat{P}_S = |S\rangle \cdot \langle S|$ is the projection operator on to the singlet RP state. This relation reflects the fact that owing to the RP recombination the singlet state population decreases with the rate constant K , the triplet state populations do not vary and the off-diagonal elements of the density matrix, which connect the singlet and triplet states, decrease with the constant $K/2$.

Equation (2.164) can be illustrated by the following example. Assume that the RP wave function is a superposition of S and T_0 , $\Psi = a_S|S\rangle + a_T|T_0\rangle$. The singlet state amplitude decreases as a result of recombination and thus the wave function can be written as

$$\Psi = a_S \cdot \exp(-Kt/2) \cdot |S\rangle + a_T \cdot |T_0\rangle.$$

Hence,

$$\rho_{SS} = |a_S|^2 \cdot \exp(-Kt); \quad \rho_{T_0T_0} = |a_T|^2;$$

$$\rho_{ST_0} = a_S^* \cdot a_T \cdot \exp(-Kt/2).$$

It is these changes of the RP density matrix induced by the recombination that are described by eq. (2.164) in operator form.

We now establish the appropriate boundary conditions. The characteristic volumes of the radicals prevent them from penetrating into each other. Therefore, at small radii r the reagent mutual diffusion must be restricted. As a result, on closest approach of the partners the boundary condition must equal zero kinematic flow. Note that the operator \hat{L} introduced above represents the divergence of the kinematic particle flux. For example, in the limit of continuous diffusion in the absence of interaction, the kinematic flow operator is $\hat{\Pi} = -D \cdot \nabla$, where ∇ is the gradient operator.

Valence forces are of short-range character. Therefore, $K(r)$ differs from zero only in a very narrow layer. That is why RP recombination is usually treated as a contact process. In this approach no addend of the type (2.164) is introduced into the kinetic equation, but as a boundary condition one considers the RP decay at the recombination radius to be compensated by the radical diffusion flux towards the boundary. As a result, at the recombination radius, one obtains the boundary condition

$$\hat{\Pi} \cdot \rho(\vec{r}, t)|_{r=b} = -(K \cdot a/2) \cdot [\hat{P}_S \cdot \rho(b, t) + \rho(b, t) \cdot \hat{P}_S], \quad (2.165)$$

where $\hat{\Pi}$ is the kinematic flux operator of the partners mutual diffusion, K is the recombination rate constant of singlet RPs at the moment of contact at the recombination radius, a is the reaction layer width (see Fig. 2.3). The boundary condition (2.164) directly generalizes eq. (2.33). Both ways of allowing for recombination, (2.164) and (2.165), are in fact equivalent, and the choice between

them is often imposed by calculational requirements. The adequacy of the approaches is violated only when the RP recombination reaction takes place in quite a thick reaction layer, as, for example, in the case of electron transfer [2.5], when the contact consideration of the reaction becomes invalid and one must use eq. (2.164). To solve the kinetic equation for the density matrix (2.163) the boundary condition at large interpartner distances, as well as the initial state of RP ensemble, must be specified. For the solution to be finite, one gets the boundary condition

$$\rho(r, t) \xrightarrow[r \rightarrow \infty]{} 0. \quad (2.166)$$

The initial RP state depends on the spin state of the RP precursor and the conditions of RP formation. In the parent molecule the nuclear spins are in equilibrium and, as a result of the small value of the nuclear Zeeman energy, they are orientated along and against the direction of the external magnetic field with nearly equal probability. Therefore, at the initial moment, immediately after the molecule dissociation, the populations of all the nuclear spin states are practically the same. If the molecule precursor is in the pure singlet electron state, the initial conditions take the form

$$\begin{aligned} \hat{P}_S \rho(\vec{r}, 0) \hat{P}_S &= \varphi(\vec{r}) \cdot \hat{E}(I_k) / \prod_k (2I_k + 1), \\ \hat{P}_T \rho(\vec{r}, 0) \hat{P}_T &= 0, \end{aligned} \quad (2.167)$$

where \hat{P}_S and \hat{P}_T are projection operators on the singlet and triplet terms, $\hat{E}(I_k)$ is a unit operator in the space of nuclear spin states I_k , $\varphi(\vec{r})$ is the statistical weight of those RPs whose interpartner radius-vector is \vec{r} initially. From the RP formation conditions, the initial distribution $\varphi(\vec{r})$ can often be described to a good approximation with the help of the delta function

$$\varphi(r) = (1/4 \cdot \pi \cdot r^2) \cdot \delta(r - r_0). \quad (2.168)$$

If the molecule-precursor is in the pure triplet state, the initial condition takes the form

$$\hat{P}_S \rho(r, 0) \hat{P}_S = 0, \quad (2.169)$$

$$\hat{P}_T \rho(r, 0) \hat{P}_T = (1/3) \cdot \varphi(\vec{r}) \cdot \hat{E}(I_k) / \prod_k (2I_k + 1).$$

When deriving the above kinetic equation, we assumed the spatial radical motion to be independent of the spin state. Pedersen and Freed [2.46] proposed the way of eliminating this limitation. Let the energy of the radical interaction in the singlet term be $U_S(\vec{r}) = U(\vec{r}) + \hbar J(\vec{r})$ and in the triplet term $U_T(\vec{r}) = U(\vec{r}) - \hbar J(\vec{r})$. Here $U(r)$ is the part of the radical interaction potential which is independent of the RP spin state

(see (2.161)). According to [2.46], changes of the RP partial density matrix due to the mutual diffusion of the partners is determined by the equations

$$\begin{aligned}(\partial \rho_{SS}(\vec{r}, t) / \partial t)_d &= \hat{L}(U_S) \cdot \rho_{SS}(\vec{r}, t), \\(\partial \rho_{TT}(\vec{r}, t) / \partial t)_d &= \hat{L}(U_T) \cdot \rho_{TT}(\vec{r}, t), \\(\partial \rho_{ST}(\vec{r}, t) / \partial t)_d &= \hat{L}((U_S + U_T) / 2) \cdot \rho_{ST}(\vec{r}, t).\end{aligned}\quad (2.170)$$

Here T and T' assume the values T₊, T₋, T₀. The above equations generalize (2.163). Note that these are not derived directly from the consideration of the reverse influence of the spin state on the radical random walk but are obtained from plausible but a priori suppositions, and some analogies with the theory of paramagnetic relaxation. It would be desirable to substantiate more precisely the validity of the generalized kinetic equations (2.170) for RP partial density matrix.

The kinetic equations above describe in detail spin polarization and magnetic effects in radical reactions. They allow one to calculate chemical spin polarization effects, the external field dependence of radical recombination, and the effects of magnetic isotopic effects on RP recombination. They also permit the analysis of both geminate recombination kinetics and the total recombination yield. Magnetic effects in geminate recombination (including magnetic isotopic effects) are described by the overall recombination probability

$$p_g = Tr_I \left\{ \int_0^\infty dt \int_V d^3 \vec{r} \cdot K(\vec{r}) \cdot \rho_{SS}(\vec{r}, t) \right\}, \quad (2.171)$$

where V is the total volume of the solution and Tr_I means the summation over diagonal matrix elements of all configurations of the RP nuclear spins.

CIDNP effects are determined by the nuclear spin density matrix of the radical recombination products. Geminate recombination occurs in times of the order of 10^{-9} s and is followed by bulk radical recombination. The populations of nuclear spin states relax towards equilibrium values at times of the order of microseconds in RPs and of seconds in their diamagnetic recombination products. The important point is that nuclear spin relaxation requires much more time than geminate RP recombination.

From the foregoing it follows that RP recombination results in molecules with the following density matrix

$$\sigma = \int_0^\infty dt \int_V d^3 \vec{r} \cdot K(\vec{r}) \cdot \rho_{SS}(\vec{r}, t). \quad (2.172)$$

The matrix σ fully characterizes the nuclear spin states of the recombination products. The total RP recombination probability, with no account taken of the nuclear spin state of the product, equals the sum of the diagonal elements of σ , i.e.

$$p_g = Tr_I \{ \sigma \}. \quad (2.173)$$

CIDEP effects are associated with spin polarizations of the escaping radicals, they are also fully described by the RP density matrix. Moreover, it is enough to know the density matrix at times exceeding those of geminate recombination. CIDEP effects are studied by observing the ESR spectra of the escaping radicals. However, the RP density matrix being known, one can readily find the density matrix of each radical of the pair by convolution of the RP density matrix with respect to spin variables of the radical partner. Thus, if a RP is formed by two radicals A and B , CIDEP effects of these radicals are determined by their density matrices

$$\begin{aligned} \sigma_A &= Tr_B \left\{ \lim_{t \rightarrow \infty} \int_V d^3\vec{r} \cdot \rho(\vec{r}, t) \right\}, \\ \sigma_B &= Tr_A \left\{ \lim_{t \rightarrow \infty} \int_V d^3\vec{r} \cdot \rho(\vec{r}, t) \right\}, \end{aligned} \quad (2.174)$$

where Tr_A and Tr_B are traces over the spin states of A and B (the unpaired electron and magnetic nuclei).

As noted in Section 2.1, in the radical recombination theory, two extreme and complementary models are widely used which reflect different aspects of cage effects in bimolecular reactions in liquids: these are increasing contact time as compared to the duration of reactant contacts in gases, and re-encounters of the same partners at the recombination radius.

In the so-called *exponential model* re-encounters are neglected. It is assumed that once in contact, the partners separate at a certain time, which is not less than the settled lifetime of the particles. An alternative model is that of *radical continuous diffusion*. Within this model the duration of a single contact is infinitely short, but the number of re-encounters at the recombination radius tends to infinity. The problem of applicability of these models to the description of radical recombination was discussed in detail in Section 2.1. It is interesting to consider the general formalism of the theory as applied to these extreme cases.

The kinetic equation for the density matrix in terms of the exponential model of RP recombination. In the general case of jumping motion of radicals the RP partial density matrix obeys the equation

$$\begin{aligned} \partial \rho(\vec{r}, t) / \partial t &= -i\hbar^{-1} [\hat{H}_0 + \hat{V}(\vec{r}), \rho(\vec{r}, t)] - \\ &\quad - (K(\vec{r})/2) \cdot [\hat{P}_s \rho(\vec{r}, t) + \rho(\vec{r}, t) \cdot \hat{P}_s] - \\ &\quad - (1/\tau_c) \cdot [\rho(\vec{r}, t) - \int d^3\vec{r}' \cdot f(\vec{r}, \vec{r}') \cdot \rho(\vec{r}', t)]. \end{aligned} \quad (2.175)$$

Assume the primary cage for a RP to be a narrow layer restricted by two spheres with radii $b-a$ and b . Let V_r be the volume of the primary cage. The RP density matrix in the primary cage is

$$\rho(t) = \int_{V_r} \rho(\vec{r}, t) d^3\vec{r}. \quad (2.176)$$

The recombination rate constant and the exchange integral can be characterized by certain average quantities K and J_0 . Neglecting re-encounters, one can obtain from (2.175) the following kinetic equation for $\rho(t)$ [2.30, 65–67]

$$\begin{aligned} \partial\rho(t)/\partial t = & -i\hbar^{-1}[\hat{H}_0 + \hat{V}_0, \rho(t)] - \\ & -(K/2) \cdot [\hat{P}_S \cdot \rho(t) + \rho(t) \cdot \hat{P}_S] - \rho(t)/\tau_c, \end{aligned} \quad (2.177)$$

where

$$\begin{aligned} \hat{V}_0 = & -\hbar \cdot J_0 \cdot (1/2 + 2 \cdot \hat{S}_1 \cdot \hat{S}_2), \\ 1/\tau_c^1 = & (1/\tau_c) \cdot \left[1 - V_r^{-1} \cdot \int_{V_r} f(\vec{r}, \vec{r}') d^3\vec{r} \cdot d^3\vec{r}' \right] \approx 1/\tau_c. \end{aligned}$$

The rate of product yield is expressed through $\dot{p}_g = K \cdot \text{Tr}_I \{ \rho_{SS}(t) \}$. The geminate recombination probability, and CIDNP and CIDEP in the exponential model are described by the following equations

$$\begin{aligned} p_g = & K \cdot \text{Tr}_I \left\{ \int_0^\infty \rho_{SS}(t) dt \right\}; \\ \sigma = & K \cdot \int_0^\infty \rho_{SS}(t) \cdot dt; \\ \sigma_A = & \text{Tr}_B \left\{ \int_0^\infty \rho(t) dt / \tau_c \right\}; \\ \sigma_B = & \text{Tr}_A \left\{ \int_0^\infty \rho(t) dt / \tau_c \right\}, \end{aligned} \quad (2.178)$$

respectively. From the foregoing one comes to the conclusion that in order to calculate p_g , σ and $\sigma_{A(B)}$ it is unnecessary to solve the time-dependent equation (2.177) but sufficient is to know the average value $\bar{\rho} = \int_0^\infty \rho(t) dt$. Integrating (2.177) with respect to time gives

$$-\rho(0) = -i\hbar^{-1} \cdot [\hat{H}_0 + \hat{V}_0, \bar{\rho}] - (K/2) \cdot (\hat{P}_S \cdot \bar{\rho} + \bar{\rho} \cdot \hat{P}_S) - \bar{\rho}/\tau_c, \quad (2.179)$$

where the initial RP state in the primary cage, $\rho(0)$, is determined by the multiplicity of the RP precursor. According to (2.179) the elements of the RP density matrix $\bar{\rho}$ satisfy the system of algebraic equations with constant coefficients. Hence, these equations can be comparatively easily solved for RPs with any number of magnetic nuclei.

The kinetic equation for the continuous diffusion model. In this case the kinetic equation for the partial density matrix takes the form [2.30, 45–53]

$$\partial\rho(\vec{r}, t)/\partial t = -i\hbar^{-1}[\hat{H}_0 + \hat{V}(\vec{r}), \rho(\vec{r}, t)] + D \cdot \Delta\rho(\vec{r}, t), \quad (2.180)$$

where D is the mutual diffusion coefficient of the partners. The boundary conditions at the recombination radius (2.165) take the form

$$D \cdot \nabla \rho(\vec{r}, t)|_{r=b} = (Ka/2) \cdot [\hat{P}_S \cdot \rho(b, t) + \rho(b, t) \cdot \hat{P}_S] \quad (2.181)$$

The initial and the boundary at infinity conditions are given by relations (2.166–169).

CIDNP, CIDEF, and magnetic effects in geminate recombination are determined by the values of

$$\begin{aligned} p_g &= 4 \cdot \pi \cdot b^2 \cdot a \cdot K \cdot Tr_I \left\{ \int_0^\infty dt \cdot \rho_{SS}(b, t) \right\}, \\ \sigma &= 4 \cdot \pi \cdot b^2 \cdot a \cdot K \cdot \int_0^\infty dt \cdot \rho_{SS}(b, t), \\ \sigma_A &= Tr_B \left\{ \lim_{t \rightarrow \infty} \int d^3\vec{r} \cdot \rho(\vec{r}, t) \right\}, \\ \sigma_B &= Tr_A \left\{ \lim_{t \rightarrow \infty} \int d^3\vec{r} \cdot \rho(\vec{r}, t) \right\}. \end{aligned} \quad (2.182)$$

The rate of the product yield is $\dot{p}_g = 4 \cdot \pi \cdot b^2 \cdot a \cdot K \cdot Tr_I \{ \rho_{SS}(b, t) \}$. As in the case of exponential model, it follows from (2.182) that to calculate magnetic and spin polarization effects it is sufficient to know the density matrix of the RP subensemble averaged over an infinite time interval with r -distant partners

$$\bar{\rho}(\vec{r}) = \int_0^\infty \rho(\vec{r}, t) dt.$$

Integrating eq. (2.180) by time we have for $\bar{\rho}(\vec{r})$

$$-\rho(\vec{r}, 0) = -i\hbar^{-1} [\hat{H}_0 + \hat{V}(\vec{r}), \bar{\rho}(\vec{r})] + D \cdot \Delta \bar{\rho}(\vec{r}), \quad (2.183)$$

which must be solved with the boundary conditions (2.166–169, 181). In keeping with (2.181) the boundary condition at the recombination radius for off-diagonal matrix elements ρ_{ST} ($T = T_+, T_0, T_-$) is given by

$$D \cdot \nabla \bar{\rho}_{ST}(\vec{r})|_{r=b} = (Ka/2) \cdot \bar{\rho}_{ST}(b). \quad (2.184)$$

This equation reflects changes of the off-diagonal matrix elements at the recombination radius as a result of the reaction of singlet RPs. One can, however, expect an additional change of ρ_{ST} in the reaction layer caused by dephasing between singlet and triplet RP states resulting from the essential exchange interaction at the very moment of the closest particle approach. In view of the possibility of this additional phase relaxation at the recombination radius one can take

$$D \cdot \nabla \bar{\rho}_{ST}(\vec{r})|_{r=b} = K' \cdot a \cdot \bar{\rho}_{ST}(b), \quad K' \geq K/2, \quad (2.185)$$

as the boundary condition for $\bar{\rho}_{ST}$ [2.30, 48–51, 68]. This condition can be replaced by an equivalent but much simpler one in the limiting case, when $K' \cdot \tau_r \gg 1$, where τ_r is the effective recombination time. In this situation of complete spin dephasing at the contact moment one can use the boundary condition [2.48–51]

$$\bar{\rho}_{ST}(b) = 0. \quad (2.186)$$

Thus, the whole system of equations presented above can describe the problem of geminate recombination in detail. If necessary, these kinetic equations can easily be extended to include, for example, the relaxation mechanism of RP singlet–triplet evolution in a cage or the anisotropic effects of radical reactivity. For that purpose one more term either allowing for the additional spin evolution mechanisms, or describing the kinematics of the mutual orientation of the partners due to their rotation [2.26], should be introduced into the kinetic equation. If the system has radical scavengers, then an additional term conforming to the RP decay induced by the scavengers,

$$\partial \rho(\vec{r}, t) / \partial t)_a = -K_s \cdot \rho(\vec{r}, t) \quad (2.187)$$

must be added to eq. (2.163). Here K_s is the rate constant of RP recombination with acceptors. The process of transformation of one RP into another due to isomerization or chemical reactions can be allowed for by the kinetic equation in a similar way (see, e.g., Section 3.1).

2.3.2 Radical recombination in homogeneous solutions

With the above kinetic equations one can also find the rate constant of bulk radical recombination. It can be done as follows. Consider a sphere with a sufficiently large radius r_0 . On the assumption that a RP can recombine within this sphere only, $K(r) = 0$, if $r \geq r_0$. The radical recombination rate constant in homogeneous solutions under steady state conditions can be expressed as the product of the first encounter rate constant of diffusion pairs at the sphere with radius r_0

$$K_D(r_0) = 4 \cdot \pi \cdot r_0 \cdot D,$$

and the diffusion RP recombination probability, which can be found by solving the above kinetic equations under the initial conditions

$$\rho(r, 0) = (1/4) \hat{E}(I_k) \delta(r - r_0) / 4\pi r^2 \cdot \prod_K (2I_k + 1)$$

which holds for the uncorrelated state of RP spins. Hence, the recombination rate constant in homogeneous solutions (cf. (2.44)) is

$$K_r = 4\pi r_0 D \cdot p_r(r_0). \quad (2.188)$$

This is one way of calculating radical steady-state recombination constants in solutions. A more logical way is, however, to find the kinetic equations for radical recombination in homogeneous solutions. These kinetic equations describe radical encounters with different partners and allow, for example, for changes of radical spin states between the encounters, etc. The kinetic equations for radical recombination in solutions were formulated in [2.30, 50]. Consider a homogeneous solution including radicals of two types, A and B , with the concentrations C_A and C_B respectively. Let the one-particle density matrices of these radicals be σ_A and σ_B . Their time evolution is

$$\partial\sigma/\partial t = (\partial\sigma/\partial t)_0 + (\partial\sigma/\partial t)_{\text{col.}}, \quad (2.189)$$

where the first term describes the changes of radical spin states between encounters. For example, if account is taken of the Zeeman interaction of an unpaired electron, the isotropic hf interaction of an unpaired electron with magnetic nuclei and the process of paramagnetic radical relaxation, then the one-particle density matrices obey a kinetic equation of the kind (2.70). In the general case, the spin dynamics of individual, isolated, bulk radicals are given by a certain linear operator \hat{Q}_A or \hat{Q}_B for A and B particles respectively. These operators can be easily found (see below) and thus considered known; we can therefore write

$$(\partial\sigma_A/\partial t)_0 = \hat{Q}_A \cdot \sigma_A, \quad (\partial\sigma_B/\partial t)_0 = \hat{Q}_B \cdot \sigma_B. \quad (2.190)$$

The second term in (2.189) describes the one-particle matrix changes as a result of binary encounters. It can be written as [2.26, 69]

$$\begin{aligned} (\partial\sigma_A/\partial t)_{\text{col.}} &= C_B(0) \cdot Tr_B \{ -i\hbar^{-1} \int d^3\vec{r} [\hat{V}(\vec{r}), \rho(\vec{r}, t)] - \\ &\quad - (1/2) \int d^3\vec{r} \cdot K(\vec{r}) \cdot [\hat{P}_S \cdot \rho(\vec{r}, t) + \rho(\vec{r}, t) \cdot \hat{P}_S] \}, \\ (\partial\sigma_B/\partial t)_{\text{col.}} &= C_A(0) \cdot Tr_A \{ -i\hbar^{-1} \int d^3\vec{r} [\hat{V}(\vec{r}), \rho(\vec{r}, t)] - \\ &\quad - (1/2) \int d^3\vec{r} \cdot K(\vec{r}) \cdot [\hat{P}_S \rho(\vec{r}, t) + \rho(\vec{r}, t) \hat{P}_S] \}, \end{aligned} \quad (2.191)$$

where Tr_A and Tr_B denote the trace over spin states of A and B radicals respectively and $\rho(\vec{r}, t)$ is the two-particle density matrix. The first terms in the right-hand sides of eqs (2.191) are responsible for the bimolecular spin exchange process discussed in detail in [2.26]. Here we dwell upon the last terms of (2.191) only, since they describe the radical recombination

$$\begin{aligned} (\partial\sigma_A/\partial t)_r &= -C_B(0) \cdot Tr_B \{ \int d^3\vec{r} \cdot K(\vec{r}) \cdot [\hat{P}_S \cdot \rho(\vec{r}, t) + \rho(\vec{r}, t) \cdot \hat{P}_S] / 2 \}, \\ (\partial\sigma_B/\partial t)_r &= -C_A(0) \cdot Tr_A \{ \int d^3\vec{r} \cdot K(\vec{r}) \cdot [\hat{P}_S \cdot \rho(\vec{r}, t) + \rho(\vec{r}, t) \cdot \hat{P}_S] / 2 \}. \end{aligned} \quad (2.192)$$

Kinetic equations for the two-particle density matrix $\rho(\vec{r}, t)$ have already been cited above when discussing geminate recombination. However, in this case they must be solved using different boundary conditions, only that at the recombination radius being the same. In a homogeneous solution, at the initial moment the spin

states of any RP are uncorrelated, hence, the initial two-particle density matrix is the direct (or exterior) product of the one-particle matrices,

$$\rho(\vec{r}, 0) = \sigma_A \times \sigma_B. \quad (2.193)$$

Under the assumption of weakening correlation [2.70], the boundary condition at infinity is

$$\rho(\vec{r}, t) \xrightarrow{r \rightarrow \infty} \sigma_A(t) \times \sigma_B(t). \quad (2.194)$$

The bimolecular recombination is characterized by two times: the effective in-cage lifetime of two partners, τ_D , and the time interval between encounters of different partners $1/K_D \cdot C$; $K_D \cdot C \cdot \tau_D \ll 1$ holds for reagent concentrations C_A , $C_B \lesssim 10^{20} \text{ cm}^{-3}$. Such time scale hierarchy leads to the fact that at times $t > \tau_D$ the solution of the kinetic equation for the two-particle density matrix stops depending on the initial conditions, and the reaction becomes steady-state. This type of reaction kinetics are of special practical interest. Under these conditions, equations (2.192) can be simplified so that the problem of finding the reaction rate constant is reduced to solving the steady-state equations for the operators of the interaction efficiency of two partners when they are in the same cage. For that purpose the kinetic equation for the partial density matrix should be written in the form

$$\begin{aligned} \partial \rho(\vec{r}, t) / \partial t = & (\hat{Q}_A + \hat{Q}_B) \rho(\vec{r}, t) - \\ & - i \hbar^{-1} [\hat{V}(\vec{r}), \rho(\vec{r}, t)] + \hat{L} \cdot \rho(\vec{r}, t) + \hat{K}(\vec{r}) \cdot \rho(\vec{r}, t), \end{aligned} \quad (2.195)$$

where the operators \hat{Q}_A and \hat{Q}_B describe the free motion of two radicals isolated in the solution. To make the equation more compact we introduce the operator $\hat{K}(\vec{r})$ which describes changes of the density matrix due to the recombination

$$\hat{K}(\vec{r}) \rho \equiv -(K(\vec{r})/2) \cdot (\hat{P}_S \cdot \rho + \rho \cdot \hat{P}_S). \quad (2.196)$$

In keeping with [2.70] under steady-state conditions, the pair density matrix must depend on time, not explicitly but through the relation

$$\rho(\vec{r}, t) \approx \hat{T}(\vec{r}) \sigma_A(t) \times \sigma_B(t). \quad (2.197)$$

Here the tensor $\hat{T}(\vec{r})$ characterizes the effects of radical interaction (in particular, spin exchange) and recombination. If we substitute (2.197) into (2.195) and take into consideration the fact that one-particle density matrices change according to equations (2.190), then accurate to values as small as $\tau_D \cdot K_D \cdot C$, we obtain the following equation for $\hat{T}(\vec{r})$ [2.30, 50]

$$[\hat{T}, \hat{Q}_A + \hat{Q}_B] = \hat{\Omega} \cdot \hat{T} + \hat{L} \cdot \hat{T} + \hat{K} \cdot \hat{T} \quad (2.198)$$

where

$$\Omega_{mn,kl} = -i \hbar^{-1} \cdot (V_{mk} \delta_{nl} - V_{ln} \delta_{mk})$$

and δ_{mn} are the Kronecker symbols.

If the free motion of unpaired electron spins is controlled by only their Zeeman interaction and the isotropic hf interaction with magnetic nuclei, the components $\hat{Q}_A + \hat{Q}_B$ are expressed through the matrix elements of the Hamiltonian \hat{H}_0

$$(\hat{Q}_A + \hat{Q}_B)_{mn,kl} = -i\hbar^{-1}(H_{0_{mk}} \cdot \delta_{nl} - H_{0_{ln}} \cdot \delta_{mk}). \quad (2.199)$$

Equation (2.198) for the tensor of the interaction efficiency of two partners must be solved with the following boundary conditions: at infinity $\hat{T}(\vec{r})$ tends to a unit operator and at the closest approach of the particles the kinematic flux $\hat{T}(\vec{r})$ must be zero.

Substitution of (2.197) into (2.192) gives the required kinetic equations for recombination-induced changes of the density matrix

$$\begin{aligned} (\partial\sigma_A/\partial t)_r &= -C_B(0) \cdot Tr_B\{\hat{K}_1\sigma_A \times \sigma_B\}, \\ (\partial\sigma_B/\partial t)_r &= -C_A(0) \cdot Tr_A\{\hat{K}_1\sigma_A \times \sigma_B\}, \end{aligned} \quad (2.200)$$

where the operator \hat{K}_1 is defined by

$$\hat{K}_1 \equiv \int d^3\vec{r} \cdot \hat{K}(\vec{r}) \cdot \hat{T}(\vec{r}). \quad (2.201)$$

With eq. (2.200) one can obtain the usual equations of chemical kinetics in terms of reagent concentration, the radical concentration at any moment being expressed via the initial concentration and the density matrix,

$$\begin{aligned} C_A(t) &= C_A(0) \cdot Tr_A\{\sigma_A(t)\}, \\ C_B(t) &= C_B(0) \cdot Tr_B\{\sigma_B(t)\}. \end{aligned}$$

Solving the above kinetic equations we obtain the density matrices of A and B radicals which, as mentioned, fully describe A and B spin states, including CIDNP effects and possible anomalies in the ESR spectra (CIDEP). These equations also describe magnetic effects arising in radical recombination. The reaction rate constant obtained from eq. (2.201) depends on the external field strength. Information on the magnetic isotopic effect can be obtained by solving eqs (2.198–201) for two cases which differ only in the presence or absence of some magnetic isotope. And, finally, the nuclear spin polarization kinetics in recombination products are determined by the following equation for the nuclear spin density matrix,

$$(\partial\sigma/\partial t)_r = Tr_S\{\hat{K}_1\sigma_A(t) \times \sigma_B(t)\} \cdot C_A(0) C_B(0), \quad (2.202)$$

where Tr_S denotes the trace over A and B electron spin states only, the rate of the product yield being $v = Tr_I\{(\partial\sigma/\partial t)_r\}$. The above equations provide a complete basis for the solution of the problem of interpretation of spin polarization and magnetic effects in radical chemical reactions.

As noted in connection with geminate recombination it is interesting to apply the general equations to the so-called exponential recombination model and to the model of continuous diffusion.

Within the exponential model the components of the encounter efficiency tensor, \hat{T} , obeys a system of algebraic equations with constant coefficients [2.30]

$$[\hat{T}(b), \hat{Q}_A + \hat{Q}_B] = \hat{\Omega}(b) \cdot \hat{T}(b) - [\hat{T}(b) - \hat{E}]/\tau_c + \hat{K}(b) \cdot \hat{T}(b). \quad (2.203)$$

Here the tensors $\hat{\Omega}$ and \hat{K} characterizing radical interaction and recombination refer to the reaction radius and the reagent contact. The overall change of the one-particle density matrix as a result of the bimolecular spin exchange and radical recombination is determined by the equations

$$\begin{aligned} (\partial\sigma_A/\partial t)_{\text{col.}} &= -V_r \cdot \tau_c^{-1} \cdot C_B(0) [\sigma_A - Tr_B\{(b)\sigma_A \times \sigma_B\}], \\ (\partial\sigma_B/\partial t)_{\text{col.}} &= -V_r \cdot \tau_c^{-1} \cdot C_A(0) [\sigma_B - Tr_A\{\hat{T}(b)\sigma_A \times \sigma_B\}], \end{aligned} \quad (2.204)$$

where V_r is the reaction layer volume, $V_r = 4\pi b^2 a$. The recombination-induced changes are determined by an equation of the type (2.200) where

$$\hat{K}_1 = -V_r \cdot \hat{K}(b) \cdot \hat{T}(b).$$

Within the continuous diffusion model, we obtain the following results under the same suppositions as those used for (2.180–184). The contribution of recombination to the radical kinetic equation is

$$\begin{aligned} (\partial\sigma_A/\partial t)_r &= -C_B(0) \cdot D \cdot Tr_B\left\{ \int_{S(b)} d\vec{s} \cdot \nabla \hat{T}(\vec{r}) \sigma_A \times \sigma_B \right\}, \\ (\partial\sigma_B/\partial t)_r &= -C_A(0) \cdot D \cdot Tr_A\left\{ \int_{S(b)} d\vec{s} \cdot \nabla \hat{T}(\vec{r}) \sigma_A \times \sigma_B \right\}, \end{aligned} \quad (2.205)$$

where $S(b)$ is the reaction sphere surface, and the encounter efficiency tensor obeys the equation

$$[\hat{T}(\vec{r}), \hat{Q}_A + \hat{Q}_B] = \hat{\Omega}(\vec{r}) \hat{T}(\vec{r}) + D \cdot \Delta \hat{T}(\vec{r}) \quad (2.206)$$

which is to be solved at the boundary conditions specified by eqs (2.181, 184, 194).

2.3.3 The method of summation of RP re-encounter contributions to the recombination

The above method of dealing with kinetic equations is convenient for practical applications only in the extreme cases of the models of exponential recombination and continuous diffusion. In the general case of jump radical motion, another method, the summation of RP re-encounter contributions to the recombination, is preferable [2.27, 58, 64, 71, 72] since the statistics of re-encounters at the recombination radius has been thoroughly studied by Noyes (see Section 2.1). The RP recombination theory can take into account the kinematic factors very easily. One more merit of the theory in question is worth mentioning. It creates the basis for the approximate evaluation of the spin polarization and magnetic effects in radical

recombination, and clarifies the role of subsequent contacts at the recombination radius.

However, the method has an important limitation. The spin evolution between re-encounters is assumed to be independent of the actual trajectories of the reagents and determined only by the time interval between the contacts (as well as by the parameters of spin interactions, which are considered to be constant and independent of the interradsical distance). Thus, it is assumed that one can distinguish between the spin and molecular RP dynamics. This approach yields reliable results if the radical exchange interaction makes a negligible contribution to the process of spin and molecular motion between re-encounters. Furthermore, calculations show that this interaction can indeed sometimes be neglected.

The main steps of RP recombination probability calculations by the method are the following. Consider a RP ensemble. Let the initial RP density matrix be $\rho(0)$. The RP spin state between contacts obeys the equation

$$\partial\rho/\partial t = -i\hbar^{-1}[\hat{H}_0, \rho], \quad (2.207)$$

where \hat{H}_0 is the RP spin-Hamiltonian. The solution of the equation can be presented as

$$\rho(t) = \hat{F}(t)\rho(0). \quad (2.208)$$

The explicit form of the RP spin evolution operator $\hat{F}(t)$ is determined by the number of magnetic nuclei, the hf constants, the external magnetic field strength, and the g -values. For a given RP the operator $\hat{F}(t)$ can be determined by eq. (2.207). Analysing the RP spin motion at the moment of the closest approach, one can describe the changes in $\rho(t)$ induced by a single contact.

In the simplest case it is possible to consider that a single contact results in the following changes. The RP singlet term population decreases by the value of $\lambda \cdot \rho_{SS}$, where λ is the probability of a singlet RP recombination at a single contact, ρ_{SS} is the singlet term population at the contact moment. It follows from Section 2.1 that

$$\lambda = K\tau_c/(1 + K\tau_c) \quad (2.209)$$

where K is the pseudo-first order recombination constant of a singlet RP in contact, and τ_c is the mean duration of a single contact. Furthermore, there is every reason to believe that at the contact moment the singlet and triplet states dephase considerably as a result of the radical exchange interaction at the moment of their closest approach. As a result of the contact, the off-diagonal matrix elements become zero (cf. eq. (2.186)). To simplify calculations the operators \hat{P} and \hat{Q} are introduced

$$\hat{P}\rho = \begin{pmatrix} \lambda\rho_{SS} & 0 \\ 0 & 0 \end{pmatrix}, \quad \hat{Q}\rho = \begin{pmatrix} (1-\lambda)\rho_{SS} & 0 \\ 0 & \rho_{TT'} \end{pmatrix}. \quad (2.210)$$

Hence it is clear that $Tr\{\hat{P}\rho\}$ is the RP recombination probability at a given contact, $\hat{Q}\rho$ is the density matrix of the RP immediately after the contact, $\rho_{TT'}$ is the RP density matrix in the triplet state subspace of the unpaired electrons.

In order to determine the RP recombination probability, assume that at a moment t_1 a radical pair gets into its first contact. By this time its density matrix is $\rho(t_1) = \hat{F}(t_1)\rho(0)$. The first contact yields a product with the probability

$$p^{(1)} = Tr\{\hat{P}\hat{F}(t_1)\rho(0)\}. \quad (2.211)$$

Just after the contact the RP is characterized by the density matrix $\rho = \hat{Q}\hat{F}(t_1)\rho(0)$, and at the moment of the next contact, t_2 , the density matrix becomes $\rho(t_2, t_1) = \hat{F}(t_2 - t_1)\hat{Q}\hat{F}(t_1)\rho(0)$. After the second contact the recombination probability is $p^{(2)} = Tr\{\hat{P}\hat{F}(t_2 - t_1)\hat{Q}\hat{F}(t_1)\rho(0)\}$. Going on in this manner we find the contribution of all re-encounters to recombination at moments t_3, t_4 , etc. Summing these contributions gives the following recombination probability of encountering radicals at given moments

$$\begin{aligned} p(t_1, t_2, \dots) &= Tr\{\hat{P} \sum_{n=1}^{\infty} \rho(t_1, t_2, \dots)\} = \\ &= Tr\{\hat{P}[1 + \hat{F}(t_2 - t_1)\hat{Q} + \hat{F}(t_3 - t_2)\hat{Q}\hat{F}(t_2 - t_1)\hat{Q} + \dots]\hat{F}(t_1)\rho(0)\}. \end{aligned} \quad (2.212)$$

This result must be averaged over all possible RP contacts. For this purpose eq. (2.212) is multiplied by the probability of the specified realization of RP contacts (2.7) and integrated over the entire infinite time interval. As a result, the recombination probability is

$$\begin{aligned} p &= Tr\{\hat{P}[1 + \hat{F}\hat{Q} + (\hat{F}\hat{Q})^2 + \dots]\hat{F}_0\rho(0)\} = Tr\{\hat{P} \cdot (1 - \hat{F}\hat{Q})^{-1} \cdot \hat{F}_0\rho(0)\}, \\ \hat{F} &= \int dt \cdot \hat{F}(t)f(t), \\ \hat{F}_0 &= \int dt \cdot \hat{F}(t)f_0(t), \end{aligned} \quad (2.213)$$

where $f(t)$ and $f_0(t)$ are the contact distribution functions: $f_0(t)dt$ is the probability of the first contact occurring within the time interval $(t, t + dt)$ given by eq. (2.9); $f(t)dt$ is the probability of a re-encounter within the range $(t, t + dt)$ provided the previous contact occurred at the initial moment (it is given by eq. (2.4)).

With (2.213) established, one can calculate the geminate recombination probability for arbitrary initial conditions as well as the recombination probability of diffusion RPs. In the latter case, at the initial moment of the first contact the RP density matrix is a direct product of the one-particle matrices of the partners. Hence, the recombination probability of diffusion RPs is

$$p_r = Tr\{\hat{P} \cdot (1 - \hat{F}\hat{Q})^{-1} \cdot \sigma_A \times \sigma_B\}. \quad (2.214)$$

Note that in eqs (2.212, 213) each term corresponds to one of the subsequent contacts. If the radicals have magnetic nuclei, the above results must be additionally summed over all possible configurations of the nuclear spins, which means taking the trace over the RP nuclear spins. It can also be noted that the above formalism can be easily generalized, if necessary, to include anisotropic effects of radical reactivity, the recombination both from singlet and triplet RP states, and RP spin

state changes at the contact moment, or to add to eq. (2.207) some other spin interactions, e.g., paramagnetic relaxation processes or reactions of radicals with acceptors [2.71, 72].

2.3.4 Methods of approximate calculations

The analysis of low field effects and of chemical nuclear polarizations by the general kinetic equations is a rather difficult problem; such calculations being almost impracticable in the case of RPs with many magnetic nuclei. Therefore, one has to use approximate calculations and estimates.

The *CKO model* [2.20, 21]. An approximate scheme to calculate chemical spin polarization and magnetic effects, known as CKO model (Closs-Kaptein-Oosterhoff), is widely used. It is a simplified version of the exponential model, and is as follows. One investigates the spin evolution and obtains the spin state population at a moment t , $\rho_{ss}(t)$, for a pair of radicals with fixed spin-Hamiltonian parameters. The RP 'decomposition' into two escaping radicals is described in terms of the exponential model. The RP is assumed to decompose with a mean rate $1/\tau_c$ and its lifetime distribution is governed by eq. (2.31). The mean singlet state population for the whole RP ensemble is

$$\bar{\rho}_{ss} = \int_0^{\infty} (dt/\tau_c) \cdot \rho_{ss}(t) \cdot \exp(-t/\tau_c). \quad (2.215)$$

The RP recombination probability is assumed to be proportional to the mean singlet state population

$$p = \lambda \cdot \bar{\rho}_{ss}. \quad (2.216)$$

For example, the singlet state population for a singlet-born RP in the case of the Δg -mechanism of S-T₀ transition is

$$\rho_{ss}(t) = \cos^2\{\varepsilon t\}, \quad \varepsilon = \Delta g \cdot \beta H_0 / 2 \cdot \hbar.$$

Average this value by RP lifetimes and obtain according to (2.215, 216) [2.56]

$${}^s p_g = (\lambda/2) \cdot (1 + 1/(1 + \Delta g^2 \cdot \beta^2 \hbar^{-2} \cdot H_0^2 \cdot \tau_c^2)). \quad (2.217)$$

The CKO model assumes that RP recombination does not affect the RP spin dynamics. This approximation can be justified if the radical reactivity is so low that only a small portion of RPs can react during their in-cage lifetime. [This can be readily proved by comparing (2.217) with more consistent calculations within the exponential model (2.66).] If $K\tau_c \ll 1$ the CKO model can be used successfully instead of the exponential model. If during the in-cage lifetime a RP can react with high probability, then a more general exponential recombination model, allowing for both spin dynamics and RP recombination, must be applied.

The exponential model in general, however, fails to describe all in-cage processes since it neglects re-encounters, yet time intervals between them are sufficiently long for intersystem S-T transitions to occur.

The diffusion model in the one re-encounter approximation. Adrian [2.12] and Kaptein [2.58] were the first to evaluate spin polarization effects in radical recombination with one re-encounter. For this purpose only the first terms of eqs (2.212, 213) are used. Consider geminate RP recombination. The singlet state population at any instant is determined for some fixed RP parameters. Then this population is averaged over all possible time intervals up to the first contact at the reaction radius,

$$\bar{\rho}_{SS} = \int dt \cdot \rho_{SS}(t) f_0(t). \quad (2.218)$$

Adrian employed eq. (2.3) as the first contact distribution function, $f_0(t)$, while Kaptein used eq. (2.4). It is perhaps better justified to use in (2.218) the first contact distribution function (2.9) obtained by Deutch. However, all these distributions yield approximately the same result for the average population (2.218). The geminate recombination probability according to eq. (2.216), within the approach discussed, is equal to the product of $\bar{\rho}_{SS}$ and the singlet RP recombination probability at a single contact λ . In the case of diffusion RPs, 1/4 of pairs are in the singlet state and can recombine at the moment of the first contact, intersystem transitions occurring until the next contact. The total recombination probability, as a result of the first and the second contacts, would be determined by the first two terms of eqs (2.212, 213).

The applicability of the one re-encounter approximation depends above all on the kinematics of in-cage radical motion. In the case of continuous diffusion the recombination probability is the combined effect of a number of re-encounters, the contribution of a single contact to the reaction being negligible. Therefore, the approximation allowing for only one re-encounter is invalid in this case. However, if radical diffusion occurs by jumps that are long compared with van der Waals molecular sizes, the total number of re-encounters is small and the approximate relations (2.215–218) can be expected to yield satisfactory estimates of spin polarization and magnetic effects. Thus, approximate estimations of magnetic and spin polarization effects by formulas (2.215–218) are applicable under the following conditions: the radicals move by comparatively large jumps and the number of re-encounters is thus small, the interaction inducing intersystem S-T transitions must be sufficiently small; and, finally, the radicals must be sufficiently active.

The approximation of reaction-independent spin dynamics. Z. Schulten and K. Schulten [2.16] have proposed an approximate method to calculate the radical recombination probability taking into consideration all re-encounters. First of all, one studies the RP spin dynamics, i.e., S-T evolution, then finds the singlet, $n_S^0(t)$, and triplet, $n_T^0(t)$, populations:

$$\begin{aligned} n_S^0(t) &= Tr\{\hat{P}_S \rho^0(t) \hat{P}_S\} = Tr_I\{\rho_{SS}^0(t)\}, \\ n_T^0(t) &= Tr\{\hat{P}_T \rho^0(t) \hat{P}_T\} = Tr_I\{\sum_T \rho_{TT}^0(t)\}. \end{aligned} \quad (2.219)$$

Here Tr is the trace over the spin variables (electron, S , and nuclear, I), $\rho^0(t)$ is the spin density matrix. The operators \hat{P}_S and \hat{P}_T are projection operators for the states S and T . On introducing the distribution function $P(r, t)$ of RPs with an interradsical distance r at a moment t which are either in a singlet ($P_S(r, t)$) or a triplet ($P_T(r, t)$) state, in accord with [2.16], the time evolution of these functions can be written as (cf. (2.175))

$$\begin{aligned}\partial P_S/\partial t &= \hat{L}P_S + \dot{n}_S^0(P_S + P_T) - K_S \cdot P_S, \\ \partial P_T/\partial t &= \hat{L}P_T + \dot{n}_T^0(P_S + P_T) - K_T \cdot P_T.\end{aligned}\quad (2.220)$$

Here the first terms describe changes in P induced by radical diffusion and molecular dynamics, the second terms are meant to describe P_S and P_T changes due to S–T mixing, and the last terms allow for RP recombination and radical reactions with acceptors. This system of two equations allows one to calculate the recombination probability and to study magnetic field and magnetic isotope effects. This approximation appreciably simplifies the problem and allows calculations for fairly complex RPs. The data on RP recombination probability obtained by precise (2.180) and approximate (2.220) kinetic equations have been compared for the case of a RP with two magnetic nuclei [2.16, 37], the agreement being satisfactory.

This model, as well as the CKO model, neglects the effect of the recombination process on the S–T mixing. The latter is assumed to be independent of molecular motion and radical reactions. Nevertheless, radical recombination can, in a general case, appreciably affect the spin dynamics. For example, let S–T transitions occur with a frequency ω , their probability being $p_{S-T} = \sin^2\{\omega t\}$. Assume that a singlet RP recombines at a moment t_1 , $0 < t_1 < t$. The probability that the RP is in the T state at the moment t then obeys the equation $p_{S-T} = \sin^2\{\omega t_1\} \cdot \cos^2\{\omega(t - t_1)\}$, but not $\sin^2\{\omega t\}$. Note also that the approximate equations (2.220) fail to accommodate nuclear polarization effects since they describe the RP subensemble behaviour averaged over all the nuclear spin states.

Within the approximation discussed, one must first calculate the S–T dynamics. In the case of complex radicals in low fields, such calculations can be done in the semi-classical approximation: substitute (2.124) into (2.220) and, as a result, obtain the recombination probability. This calculation program has been realized by Schulten and Epshtein [2.40] and includes one more, additional, approximation. Equation (2.124) gives the S–T transition dynamics averaged all over the RP ensemble and all possible values and orientations of the local field induced by the nuclear spins. It would be more reasonable to find the recombination probability at a set local field of the unpaired electron, and then to average this over all possible nuclear spin configurations.

Such a program has been carried through in ref. [2.73]. First the spin dynamics of a subensemble of RPs with definite nuclear spin configurations was calculated. The S–T transition dynamics was then averaged over all possible values of the azimuthal angle characterizing the local nuclear field orientation at the location of the electron spins. The re-encounter contributions to the recombination were summed up at set

values of the local field strength and the polar angle for a RP subensemble. Finally, the contributions of all the subensembles with all plausible values of field strength and polar angle were summed. This approach employs two approximations: (1) RP spin dynamics are calculated in the semi-classical approximation and (2) the averaging over the azimuthal angle is performed before summing the re-encounter contributions to recombination. Both approximations appreciably simplify the calculations. The approach affords perhaps more precise values of RP recombination probability than calculations based on the spin dynamics averaged over all nuclear spin configurations [2.40]. Note that the averaging of RP spin dynamics over the azimuthal angle of the local nuclear field reduces to zero the off-diagonal elements of a density matrix that connect triplet sublevels.

At this stage, mechanisms of nuclear and electron spin polarization in the course of radical chemical reactions as well as possible mechanisms of external magnetic field and magnetic isotopic effects on these reactions have been formulated. The central feature of the physical theory of these phenomena is the concept of a radical pair in a 'cage' and its singlet-triplet evolution. On this basis, general mathematical tools of the theory of radical recombination in solutions have been formulated. They allow a consistent consideration of coupled changes of spin and spatial coordinates of the reagents in a 'cage' between re-encounters at the reaction radius. The above results make the basis of the modern theory of spin polarization and magnetic effects in radical reactions. The detailed theory of these effects is developed in the following sections.

In conclusion it is necessary to note that the formalism of the theory, developed as applied to radical recombination, can be readily generalized and applied to other bimolecular processes with some minor modifications. Indeed, the comparison of the formal tool of the recombination theory with the theory of bimolecular processes such as triplet-triplet exciton annihilation in crystals and triplet molecule quenching by paramagnetic admixtures demonstrates their similarity [2.65, 66].

3 THE THEORY OF MAGNETIC EFFECTS IN RADICAL REACTIONS

Radical reactions show magnetic effects of two types: external magnetic field effects on radical recombination and magnetic isotopic effects. The origin of the magnetic effects has been discussed in Section 2.2.1. They are induced by magnetosensitive nonradiative singlet-triplet transitions in a radical pair. Section 2.3 gives the basic kinetic equations for the radical density matrix under recombination. These general equations allow one to develop a quantitative theory of magnetic effects in radical reactions.

Magnetic effects in radical reactions have been studied theoretically (see, e.g., [3.1-12]). Investigations on chemical spin polarization effects incidentally afford some data also on magnetic effects (see, e.g., [3.13-17]). In a high magnetic field, $H_0 \gg A$, the external field effect on radical recombination is associated mainly with the Δg -mechanism of singlet-triplet mixing: if $\Delta g \neq 0$ the frequency of S-T₀ transitions grows with the field (see Fig. 1.7a). In low fields the hf interaction of unpaired electrons with magnetic nuclei is the principal mechanism of S-T mixing. In this case the magnetic field effect is conditioned by the fact that the number of effective S-T channels changes with the external field (see Fig. 1.7b). The hf energy can be modified by isotope substitution. As a result, magnetic isotope effects can arise both in high and in low fields.

In high fields both mechanisms of S-T₀ transitions can work simultaneously. In this case, on the one hand, the Δg -mechanism will either partially or entirely mask the changes in S-T₀ transition efficiency induced by isotope substitution, i.e., reduce the magnetic isotopic effect; on the other hand, the hf-mechanism will influence the magnetic field effect arising by the Δg -mechanism.

3.1 Radical recombination in high magnetic fields

The present subsection explores the magnetic field effect only. Therefore, the Δg -mechanism will be the main object of discussion. At the same time, we are going to adduce some theoretical results on RP recombination in high fields with the hf-mechanism in operation. These results will be used when discussing magnetic isotope effects and in CIDNP theory.

The program of radical recombination probability calculations formulated in the above section has been realized in detail only for magnetic fields exceeding local hyperfine fields, $H_0 \gtrsim 10^3$ G. In this case the problem is simplified because only one channel of singlet-triplet transitions, intersystem S-T₀ mixing, operates.

The S-T₀ approximation. RP terms in a high magnetic field are depicted in Fig. 2.6. Between re-encounters, the singlet and triplet terms with zero projection of the total electron spin are seen to merge at sufficiently great radical separations and thus S-T₀ is the only channel. As the radicals approach, the S and T₀ terms split which results in the S-T₀ transitions switching off. At a distance r^* , when the exchange integral becomes comparable to the Zeeman electron energy, the singlet term crosses either T₋ or T₊ depending on the sign of J (see Fig. 2.6). Over this region of interradsical distances, the S-T₋ (or S-T₊) channels are the most effective. However, the S-T₀ mixing is still of fundamental importance in singlet-triplet evolutions between re-encounters in high magnetic fields.

In the S-T₀ approximation, a RP spin Hamiltonian includes the Zeeman energy of the unpaired electrons, the adiabatic part of the isotropic hf interaction, and the exchange interaction (2.77, 83). This spin Hamiltonian leads to S-T₀ transitions with z -projections of the nuclear spins conserved. Denote the nuclear spin configuration with a set z -projection as $m = \{m_i, m_k\}$. In the basis $|Sm\rangle, |T_0m\rangle$ the matrix element of S-T₀ mixing is

$$\langle Sm | \hat{H}_0 | T_0m \rangle \equiv \hbar \varepsilon(m), \quad (3.1)$$

$$\varepsilon(m) = [(g_1 - g_2)\beta\hbar^{-1}H_0 + \sum_i a_{1i} \cdot m_{1i} - \sum_k a_{2k} \cdot m_{2k}]/2.$$

Radical recombination has been studied for several model situations using the above formalism in the S-T₀ approximation [3.1-15].

3.1.1 The continuous diffusion model

In the S-T₀ approximation, with exchange interaction neglected, the kinetic equations (2.180) of the density matrix for a pair of uncharged particles have an exact solution [3.4-7].

Geminate recombination. The geminate recombination probability for a singlet-born RP is

$$\begin{aligned} {}^s p_g &= \sum_m {}^s \sigma_{mm}, \\ {}^s \sigma_{mm} &= (b/r_0) \cdot A(m) \cdot \{1 + \delta(m) + \\ &+ \cos \{ \delta(m) \cdot (r_0/b - 1) \} \cdot \exp [- \delta(m) \cdot (r_0/b - 1)] \} \end{aligned} \quad (3.2)$$

and for a triplet-born RP

$${}^T p_g = (1/3) \cdot \sum_m {}^T \sigma_{mm},$$

$${}^T \sigma_m = (b/r_0) \cdot A(m) \cdot \{1 + \delta(m) - \cos \{ \delta(m) \cdot (r_0/b - 1) \} \cdot \exp [- \delta(m) \cdot (r_0/b - 1)] \} \quad (3.3)$$

where b is the recombination radius, r_0 is the initial interpartner distance,

$$\delta(m) = (|\varepsilon(m)| \cdot \tau_D)^{1/2}; \quad \tau_D = b^2/D; \quad \tau_r = a \cdot b/D,$$

$$A(m) = K \tau_r / \{ [2(1 + K \tau_r) + \delta(m) \cdot (2 + K \tau_r)] \cdot \prod_k (2I_k + 1) \}.$$

The summation in (3.2, 3), is carried out over all possible nuclear spin configurations.³ If the partners have no magnetic nuclei or the isotropic hf constants are negligible, the singlet-triplet evolution follows the Δg -mechanism only. In this case, only the term with

$$\delta = (|g_1 - g_2| \beta \hbar^{-1} \cdot H_0 \cdot \tau_D/2)^{1/2} \quad (3.4)$$

remains in (3.2, 3).

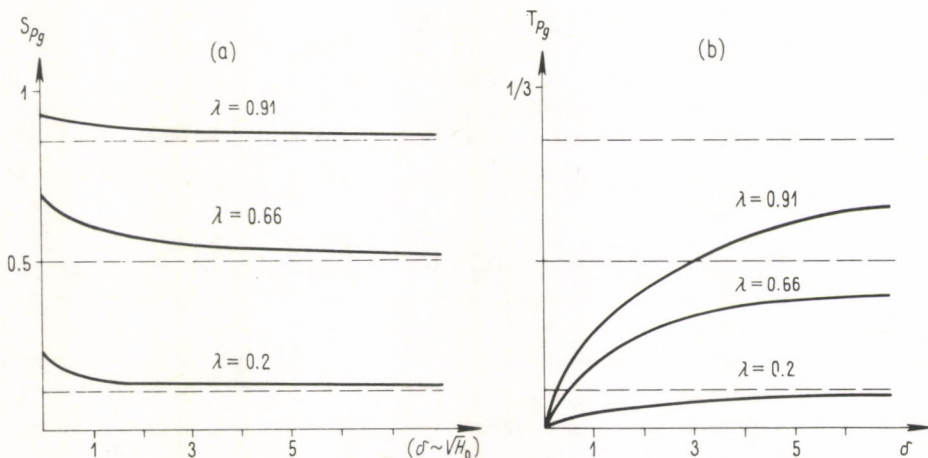


Fig. 3.1. Magnetic field dependence of geminate recombination probability within the Δg -mechanism of S - T_0 mixing: (a) for a singlet-born RP; (b) for a triplet-born RP

³ Note that (3.2) and (3.3) contain information on the nuclear spin state populations in the recombination products. Each term in the sums is the probability of formation of a molecule with a nuclear spin configuration characterized by a given set of $\{m\}$ spin projections on the field direction. Thus the quantities $\sigma_{m,m}$ can be used to interpret CIDNP effects in radical recombination products (see Section 4).

The above results allow one to analyze constant magnetic field and magnetic isotopic effects in radical recombination.

To simplify the situation, consider an ensemble of RPs at the recombination radius at the initial moment, i.e. $r_0 = b$. In this case formulas (3.2) and (3.3) as applied to the Δg -mechanism of S-T₀ transitions take the form

$$\begin{aligned} {}^S p_g &= (2 + \delta) \cdot K \cdot \tau_r / A, \\ {}^T p_g &= \delta \cdot K \cdot \tau_r / 3 \cdot A, \\ A &= 2 \cdot (1 + K\tau_r) + \delta \cdot (2 + K\tau_r), \end{aligned} \quad (3.5)$$

where δ is determined by eq. (3.4). The RP recombination probabilities calculated by eq. (3.5) are shown in Fig. 3.1. The curves conform to different values of λ equal to the RP recombination probability provided there is no spin selection rule, $\lambda = K\tau_r / (1 + K\tau_r)$. It is seen that if the Δg -value is the basic mechanism of S-T₀ transitions, then the recombination probability of singlet-born RPs reduces monotonically, and that of triplet-born pairs increases with the magnetic field strength. The conditions for field effect detection are especially favourable in the case of a triplet precursor. The scale of the effect depends strongly on the value of λ . As the radical reactivity or the solution viscosity increases, i.e. with an increase in λ , the magnetic field effect on the singlet-born RP recombination reduces, while that on the triplet-born RP recombination increases.

The scale of plausible field effects in radical recombination, when S-T transitions follow only the Δg -mechanism is given in Table 3.1 which lists recombination probabilities for several RPs calculated by eq. (3.5). The table shows that for the chosen molecular-kinetic RP parameters, at fields intensities as high as 10^4 – 10^5 Gauss, the magnetic field can change the recombination probability by the value of about 10^{-2} – 10^{-1} .

If singlet-triplet transitions are induced not only by the Δg -mechanism but also the isotropic hyperfine interactions, the field dependence of the recombination probability would have a more complex character. Hf-induced singlet-triplet transitions can mask those by the Δg -mechanism, the combined action of both mechanisms giving a nonmonotonic magnetic field dependence of radical reactions. As for some nuclear spin configurations, the matrix element of the singlet-triplet mixing passes through zero with increasing magnetic field (see (3.1)). For instance, Table 3.2 shows the field dependence of the recombination probability for one of the unpaired electrons interacting with a magnetic nucleus with spin 1/2 and a constant. In fields of about H_0^* , ($\Delta g \cdot \beta \hbar^{-1} H_0 \approx a$), the RP recombination probability passes through an extremum. For radicals with a larger number of magnetic nuclei the recombination probability can have several maxima and minima with changing magnetic field.

The geminate recombination probability (3.2, 3) contains oscillating terms. To observe these oscillations experimentally, the intersystem S-T transitions must occur at times of diffusion to the reaction radius. It is facilitated by an increase of the solution viscosity, Δg , and the magnetic field strength. Furthermore, when born, the

Table 3.1. Recombination probability of geminate and diffusion RPs for the Δg -mechanism of singlet-triplet transitions (RP parameters: $\Delta g = 10^{-2}$, $D = 10^{-5}$ cm²/s, $b = 0.4$ nm, $r_0 = b$)

$K \cdot \tau_r$	λ	H_0, G	$^s p_g$	$^T p_g$	p_r
0.5	0.333	0	0.333	0	0.0833
		10 ²	0.330	0.00432	0.0837
		10 ³	0.324	0.00435	0.0844
		10 ⁴	0.309	0.0120	0.0863
		10 ⁵	0.278	0.0274	0.0902
		10 ⁶	0.241	0.0459	0.0948
		∞	0.200	0.0666	0.100
1	0.500	0	0.500	0	0.125
		10 ²	0.496	0.00225	0.125
		10 ³	0.490	0.00656	0.127
		10 ⁴	0.472	0.0183	0.132
		10 ⁵	0.435	0.043	0.141
		10 ⁶	0.389	0.073	0.152
		∞	0.333	0.111	0.166
2	0.666	0	0.666	0	0.166
		10 ²	0.663	0.00289	0.167
		10 ³	0.657	0.00879	0.170
		10 ⁴	0.641	0.0249	0.178
		10 ⁵	0.606	0.0597	0.196
		10 ⁶	0.560	0.106	0.219
		∞	0.500	0.166	0.250
10	0.909	0	0.909	0	0.227
		10 ²	0.908	0.00395	0.229
		10 ³	0.905	0.0121	0.235
		10 ⁴	0.899	0.0351	0.251
		10 ⁵	0.885	0.0871	0.286
		10 ⁶	0.864	0.164	0.339
		∞	0.833	0.277	0.416
100	0.990	0	0.990	0	0.247
		10 ²	0.990	0.00431	0.250
		10 ³	0.989	0.0132	0.257
		10 ⁴	0.988	0.0385	0.276
		10 ⁵	0.986	0.0971	0.319
		10 ⁶	0.984	0.186	0.386
		∞	0.980	0.326	0.490

Table 3.2. Field dependence of recombination probability for geminate and diffusion RPs for the following parameters: $\Delta g = 10^{-2}$, $D = 10^{-5}$ cm²/s, $r_0 = b = 0.4$ nm, $K \cdot \tau_r = 0.5$, $a = 4 \cdot 10^9$ rad/s, $H_0^* = \hbar \cdot a / 2 \cdot \beta_e \cdot \Delta g = 2.274 \cdot 10^4$ G

H_0	$(1/2)H_0^*$	H_0^*	$(3/2)H_0^*$	$2H_0^*$	$5H_0^*$	∞
$^s p_g$	0.301	0.312	0.297	0.292	0.277	0.200
$^T p_g$	0.0160	0.0106	0.0178	0.0205	0.0283	0.0666
p_r	0.0873	0.0860	0.0788	0.0781	0.0904	0.100

RP must not be at the reaction radius, i.e., r_0 must exceed b . A serious obstacle in detecting the oscillations lies in the fact that the RP distribution at the initial moment can differ from the delta-type (2.168), in which case (3.2, 3) must be averaged over different initial distances. Such averaging [3.8] damps the oscillations in the field dependence of the geminate recombination probability.

Bulk recombination. The radical recombination rate constant in homogeneous solutions is defined by the equation [3.7]

$$K_r = 4\pi b D p_r, \quad (3.6)$$

$$p_r = (1/2) \cdot \sum_m A(m) \cdot [1 + \delta(m)].$$

Hence, for the Δg -mechanism of S-T₀ transitions we obtain

$$p_r = (1 + \delta) K \tau_r / 2 \cdot A, \quad (3.7)$$

which shows that the radical recombination rate constant grows with the external field.

If $\Delta g = 0$ and the isotropic hf constants are negligible, then according to the singlet state statistical weight, only 1/4 of diffusive RPs can recombine. In this case from (3.6) we have

$$p_r = K \tau_r / 4 \cdot (1 + K \tau_r) = \lambda / 4. \quad (3.8)$$

On the other hand, when the S-T₀ mixing is extremely effective, we obtain from (3.6)

$$p_r = (1/2) \cdot (K \tau_r / 2) / [1 + (K \tau_r / 2)]. \quad (3.9)$$

This result is demonstrative of the fact that when S-T₀ transitions are fast only half the diffusive pairs can recombine, and at the contact moment the reaction must be characterized by the average constant $K_{\text{eff}} = K/2$. We have already come across this problem while discussing the radical reactivity anisotropy averaged by rotation.

As in the case of geminate recombination, the scale of the recombination rate constant variations induced by S-T₀ transitions depends on λ . Intersystem transitions manifest themselves most strongly in diffusion-controlled reactions where $K \tau_r > 1$ and $\lambda \rightarrow 1$. In these reactions S-T₀ transitions can change the reaction rate constant by a factor of two. Figure 3.2 and Table 3.1 list the p_r values calculated by eq. (3.7). The analysis of these data and those given in Fig. 3.1 shows that the field dependence of a diffusion RP recombination probability coincides qualitatively with the field dependence of a triplet-born RP recombination. If the Δg - and hf-mechanisms of S-T₀ transitions operate simultaneously, the p_r field dependence can be nonmonotonic (see, e.g., Table 3.2).

Radical recombination probabilities for a number of parameters characterizing diffusion, recombination and exchange interactions have been calculated numerically [3.13]. With exchange interactions neglected, the numerical calculations show a pleasing fit to the exact relations (3.2-7).

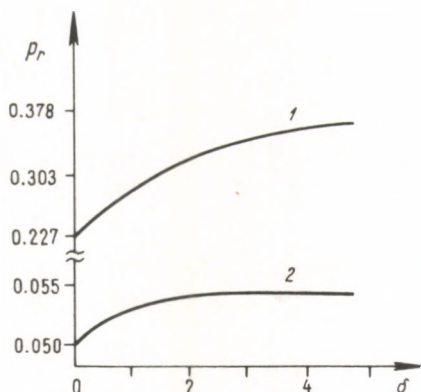


Fig. 3.2. Magnetic field dependence of diffusion pair recombination probability in the Δg -mechanism of S-T₀ mixing: 1 — $\lambda=0.91$; 2 — $\lambda=0.80$

Nonstationary recombination. The initial recombination stage of radicals formed at random in solutions takes place by nonstationary kinetics (see eq. 2.49), and singlet-triplet transitions affect the time at which steady-state kinetics are attained. For instance, for the Δg -mechanism, the nonstationary kinetics is characterized by the time-dependent rate constant

$$K_r(t) = 4\pi b D p_r [1 + 2p_r(\tau_D/\pi \cdot t)^{1/2}]. \quad (3.10)$$

The comparison of this relation for two cases, when $\delta=0$ and $\delta \neq 0$, shows that the singlet-triplet transition increases the time of attaining the steady-state reaction kinetics.

The geminate recombination kinetics are described by more complex dependences. For instance, consider the recombination of a pair of highly reactive radicals, so that the very first contact results in recombination provided the pair is singlet. Assume that the initial interradsical separation is r_0 and that the pair is triplet-born. The recombination kinetics then obey the equation

$$W(t) \sim \sum_{n=0}^{\infty} \sum_m \int_0^t dt_{n+1} \int_0^{t_{n+1}} dt_n \dots \int_0^{t_2} dt_1 \cdot f_0(t_1) f(t_2 - t_1) \dots f(t_{n+1} - t_n) \cdot \sin^2 \{ \varepsilon(m) \cdot (t_{n+1} - t_n) \} \cdot \prod_{k=1}^n \cos^2 \{ \varepsilon(m) \cdot (t_k - t_{k-1}) \},$$

where f_0 and f are distribution functions of the first and the following contacts respectively (see eqs (2.1-9)), the summation is performed over all nuclear spin configurations and all re-encounters. However, the nonstationary geminate recombination kinetics has not been thoroughly investigated.

3.1.2 The reaction equilibrium

In the case of a pair with initial interradsical distance $r_0 = b$, $^S p_g$ and $^T p_g$ are related. Substitute $r_0 = b$ into eq. (3.2, 3) and see that the relation

$$\lambda - ^S p_g = 3 \cdot ^T p_g \cdot (1 - \lambda) \quad (3.11)$$

with

$$\lambda = K \tau_r / (1 + K \tau_r)$$

is valid. The diffusion RP recombination probability can also be expressed in terms of the probability of geminate RPs occurring at the initial moment at the reaction radius:

$$p_r = (1/4) \cdot [^S p_g(r_0 = b) + 3 \cdot ^T p_g(r_0 = b)] = (\lambda/4) \cdot [1 + 3 \cdot ^T p_g(r_0 = b)]. \quad (3.12)$$

Thus, in the systems where $r_0 = b$ at the moment of a geminate pair formation, it is sufficient to calculate the recombination probability of a triplet-born RP, whereas the probability for singlet-born and diffusion pairs can be obtained from (3.11, 12). Relations (3.11, 12) are neither unexpected nor connected with the model approximation, but follow directly from general statistical considerations. Singlet-triplet mixing accelerates (or decelerates) the radical recombination and the back reaction of radical formation, but it does not affect the state of reaction equilibrium. Relations (3.11, 12) exactly reflect the fact that the magnetic effects do not influence the equilibrium state. Indeed, the ratio of the diffusion RP recombination probability, p_r , to the probability of generating and escaping of two radicals due to singlet molecule (or activated complex) decomposition must obey

$$p_r / (1 - ^S p_g) = \lambda / 4 \cdot (1 - \lambda) = K \tau_r / 4 \quad (3.13)$$

and does not depend on the singlet-triplet evolution. Hence, eqs (3.11, 12) must hold irrespective of the RP spin dynamics and the radical motion kinematics. Calculations within the jump model and also those using the exponential recombination model do result in relations of type (3.11, 12) (see below).

Relations (3.11, 12) have been corroborated numerically [3.13], $^T p_g$ calculations being approximated by the formula

$$^T p_g = (\lambda/3) \cdot \sum_m F^*(m) / [1 + F^*(m) \cdot (1 - \lambda)] \cdot \prod_k (2I_k + 1) \quad (3.14)$$

which coincides with eq. (3.3) provided

$$F^*(m) = \delta(m) / (2 + \delta(m)), \quad (3.15)$$

$$\lambda = K \tau_r / (1 + K \tau_r).$$

3.1.3 Exchange interaction effects

Exchange interaction effects can be of two kinds. On the one hand, the exchange interactions influence the RP spin dynamics (see, e.g., Section 2.2) by splitting S and T terms and thus preventing S-T₀ mixing. As a result, the singlet-triplet transitions are manifested to a less extent than they would in the absence of these interactions. On the other hand, exchange interactions can affect RP molecular dynamics [see eq. (2.170)]. The exchange attraction between the partners of a singlet RP increases the in-cage RP lifetime and the recombination time. It can thus increase the geminate recombination probability. Table 2.3 lists data characterizing the scale of the recombination time increase due to exchange interactions. The way this increase manifests itself in the RP recombination probability must greatly depend upon the radical reactivity. If the RP recombination rate constant is sufficiently great and $K\tau_r > 1$ without exchange attraction, an additional increase in the effective RP recombination time will change the recombination probability by a small value of the order of $1/K\tau_r$. In the other extreme case, when the reactions are not controlled by the diffusion of the partners but by their recombination at the contact moment, for $K\tau_r < 1$, the RP recombination probability will increase proportionally to the effective recombination time.

The RP molecular dynamics can be appreciably affected only by comparatively strong exchange interactions, $\hbar J > kT$. According to the data on spin exchange [3.18] the exchange integral at the Van der Waals distances between the radicals usually does not exceed kT at room temperatures. In this situation the exchange interaction effect on the partners diffusion must be negligible. However, in the RP spin dynamics even such weak interactions ($J \approx 10^8 - 10^{10}$ rad/s) can be of great importance.

The radical recombination probability has been calculated numerically with account taken of the exchange interaction [3.13]. The calculations were of two kinds. First, the exchange interaction was assumed to affect only the spin dynamics, i.e., this interaction was included in the spin-Hamiltonian, while no exchange potential was in the diffusion operator (exchange forces absent, or EFA approach). Second, the exchange interaction was assumed to affect both spin and molecular dynamics (exchange forces present, or EFP approach). Note that the exchange interaction is partially allowed for in eqs (3.2-6) too. It is expressed in the choice of the boundary condition for the off-diagonal matrix elements ρ_{ST} at the reaction radius in the form (2.186) that reflects an additional dephasing of the off-diagonal density matrix elements associated with the exchange integral at the moment of closest approach of the particles.

Table 3.3 lists data on diffusion RP recombination probabilities obtained by Pedersen and Freed in the EFA approximation, calculated by eq. (3.7) and also by (3.8) when no singlet-triplet mixing occurs. Numerical calculations demonstrate that the exchange interaction in RP spin dynamics does not affect p_r . It disagrees, however, with the expected exchange interaction effect. Perhaps it was the bad

Table 3.3. Diffusion RP recombination probability for the Δg -mechanism of singlet-triplet transitions. RP parameters: $b=0.4$ nm, $r_e=0.4$ nm, $a=0.0025$ nm, $D=10^{-5}$ cm²/s

$\hbar J_0/kT$	K, s^{-1}	p_r^a	p_r^b	p_r^c
0	10^{14}		0.247	0.262
	10^{12}		0.125	0.128
	10^{10}		$2.47 \cdot 10^{-3}$	$2.47 \cdot 10^{-3}$
	10^8		$2.49 \cdot 10^{-5}$	$2.49 \cdot 10^{-5}$
	10^{14}	0.259		
$2.5 \cdot 10^{-3}$	10^{12}	0.127		
	10^{10}	$2.43 \cdot 10^{-3}$		
	10^8	$2.45 \cdot 10^{-5}$		
	10^{14}	0.259		
0.25; 2.5	10^{12}	0.126		
	10^{10}	$2.43 \cdot 10^{-3}$		
	10^8	$2.45 \cdot 10^{-5}$		
	10^{14}	0.259		

^a according to ref. [3.13, b], p_r calculated for the singlet-triplet mixing frequency $\varepsilon=10^8$ rad/s

^b according to eq. (3.8) for $\varepsilon=0$

^c according to eq. (3.7) for $\varepsilon=10^8$ rad/s

choice of parameters used for calculations that resulted in the invalid interpretation of the exchange interaction effect on p_r [3.13]. Indeed, comparison of the last two columns in Table 3.3 shows that the singlet-triplet transitions induced by the matrix transition element $\varepsilon=10^8$ rad/s play no appreciable role in the recombination of radicals with $K \lesssim 10^{10} s^{-1}$. No wonder, therefore, that Pedersen and Freed failed to observe the exchange interaction effect at $K=10^8$ and $K=10^{10} s^{-1}$. Singlet-triplet transitions considerably change the RP recombination probability at $K=10^{14} s^{-1}$ (see the first line in Table 3.3). Here the exchange splitting of S and T_0 terms might be expected to be manifested in p_r , but in fact is not. One of possible interpretations of this phenomenon is that at $K=10^{14} s^{-1}$ the singlet term is extremely broad due to the lifetime broadening, so that the S and T_0 terms are in fact still in resonance even when the exchange interaction is of the order of 10^{14} rad/s.

Table 3.4 compares the numerical calculations of Freed and Pedersen with those obtained by eqs (3.2-6). p_r values calculated for the absence of the singlet-triplet transitions are compared in the second and the third columns, the fourth and fifth ones listing values with S- T_0 transitions being present. It is thus seen that at $\varepsilon=10^8$ rad/s the RP term splitting has practically no influence on the p_r values. It may be associated with the fact that the broadening of the RP singlet term exceeds the exchange splitting for K values listed in Table 3.4.

Calculations in the EFP approximation reveal an appreciable effect of strong exchange interactions, $\hbar J_0 > kT$, on the radical recombination owing to the increase in the recombination time and also in the in-cage RP lifetime.

Table 3.4. Diffusion RP recombination probability for the Δg -mechanism of singlet-triplet transitions. RP parameters: $b=r_c=0.4$ nm, $D=10^{-5}$ cm²/s, $a=0.0125$ nm, $J_0=10^8$ rad/s

K, s^{-1}	$\varepsilon=0$		$\varepsilon=10^8$ rad/s	
	p_r^a	p_r^b	p_r^a	p_r^c
10^9	$1.2428 \cdot 10^{-3}$	$1.2437 \cdot 10^{-3}$	$1.2431 \cdot 10^{-3}$	$1.2441 \cdot 10^{-3}$
10^{10}	$1.1895 \cdot 10^{-2}$	$1.1904 \cdot 10^{-2}$	$1.1929 \cdot 10^{-2}$	$1.1936 \cdot 10^{-2}$
10^{11}	$8.329 \cdot 10^{-2}$	$8.333 \cdot 10^{-2}$	$8.346 \cdot 10^{-2}$	$8.492 \cdot 10^{-2}$
10^{12}	0.20830	0.20833	0.21955	0.21856
10^{14}	0.24950	0.24950	0.26580	0.26431
10^{18}	0.25	0.25	0.26638	0.26487

^a according to ref. [3.13, c]

^b according to eq. (3.8)

^c according to eq. (3.7)

Numerical calculations of the recombination probability at different values of the exchange integral allowed Pedersen and Freed to come to the general conclusion that at $\hbar J \lesssim 10 \cdot kT$ the exchange interaction influences two parameters characterizing RP recombination, namely τ_r and F^* . The exchange interactions being neglected, the effective recombination time $\tau_r = ab/D$ and F^* is given by eq. (3.15). Otherwise τ_r and F^* are [3.13, c]

$$\tau_r^* = \tau_r \cdot \chi = (ab/D) \cdot b \cdot S(b) \cdot \exp[-U_{ss}(b)/kT],$$

$$F^{**}(m) = F^*(m)/b \cdot S(b), \quad (3.16)$$

$$S(b) = \int_b^{\infty} dr \cdot r^{-2} \cdot \exp[U_{ss}(r)/kT],$$

where U_{ss} is the singlet RP term energy. Thus, eqs (3.14, 15) give the RP recombination probability at any values of the exchange integral provided τ_r^* and F^{**} are substituted for τ_r and F^* . Physically τ_r^* represents an effective time of RP recombination in the field of exchange attraction forces (see Tables 2.2-4), whereas the physical sense of F^{**} is unclear. Note, however, that $1/(b S(b))$ is the ratio of the effective radius of a RP encounters in the presence of exchange interactions to the contact radius b (see (2.28)).

Table 3.5 compares RP recombination probabilities calculated in the EFA and EFP approximations [3.13, b]. At $\hbar J_0 > kT$ the exchange interaction, as expected, is seen to increase the recombination probability of radicals with a comparatively low reactivity ($K = 10^8 - 10^{10} s^{-1}$) orders of magnitude. In the case of active radicals, an increase in the reaction time caused by the exchange attraction affects their recombination negligibly.

As it has been noted in the case of free radicals, a typical situation is $\hbar J_0 < kT$. Thus, one can conclude that in quite a range of RP molecular-kinetic parameters the participation of the exchange interaction in the RP spin dynamics affects the

Table 3.5. Effect of exchange forces on diffusion RP recombination probability [3.13] ($J = J_0 \cdot \exp(-(r-b)/r_e)$, $r_e = 0.4$ nm, the other parameters are as given in Table 3.3

$\hbar J_0/kT$	K, s^{-1}	p_r^a	p_r^b
0.0025	10^{14}	0.260	0.259
	10^{12}	0.127	0.127
	10^{10}	$2.44 \cdot 10^{-3}$	$2.43 \cdot 10^{-3}$
	10^8	$2.96 \cdot 10^{-5}$	$2.45 \cdot 10^{-5}$
0.25	10^{14}	0.264	0.259
	10^{12}	0.144	0.126
	10^{10}	$3.1 \cdot 10^{-3}$	$2.43 \cdot 10^{-3}$
	10^8	$3.1 \cdot 10^{-5}$	$2.45 \cdot 10^{-5}$
2.5	10^{14}	0.296	0.259
	10^{12}	0.269	0.126
	10^{10}	$2.7 \cdot 10^{-2}$	$2.43 \cdot 10^{-3}$
	10^8	$3.0 \cdot 10^{-4}$	$2.45 \cdot 10^{-5}$
10	10^{14}	0.329	0.258
	10^{12}	0.329	0.126
	10^{10}	0.328	$2.43 \cdot 10^{-3}$
	10^8	0.233	$2.45 \cdot 10^{-5}$

^a calculated in EFP approach

^b calculated in EFA approximation

recombination probability only negligibly. As a rule, the radical exchange interaction is of small importance in the process of diffusion of the partners between re-encounters at the reaction radius. However, in some case the exchange interaction at the Van der Waals distances between particles can exceed the thermal energy; it then becomes necessary to take into account the fact that singlet and triplet RPs are mutually diffusive in the fields of exchange attraction and repulsion forces. For instance, the exchange attraction between hydrogen and oxygen atoms at Van der Waals distances, $J_0 \gtrsim kT \cdot \hbar^{-1}$, can increase the effective recombination time by an order of magnitude.

3.1.4 Radical diffusion by jumps

The kinetic equations for the RP density matrix (2.175) have not been solved for radical motion by jumps. The RP recombination probability in this case was found by summing up the contributions of all subsequent radical contacts at the reaction radius [3.9, 19]. Remember that in this approach distance-dependent radical exchange interactions cannot be introduced into the theory subsequently. However, the above considerations on the effects of exchange interaction in radical

recombination within the model of continuous diffusion prove that in most cases the exchange interaction negligibly influences the spin dynamics between contacts.

Consider a RP ensemble with the spin Hamiltonian (2.83). Within the time of radical diffusion between two contacts, a S-T₀ transition occurs in the RP subensemble with a given spin-nuclear configuration with the probability (see eq. (2.84))

$$p_{S-T_0} = \sin^2 \{ \varepsilon(m) \cdot t \}.$$

The contribution of all re-encounters to the recombination can be summarized by (2.211–214), the Liouville representation being the most convenient for this purpose. The RP density matrix can be expressed as a vector with components ($\rho_{SS}, \rho_{ST_0}, \rho_{T_0S}, \rho_{T_0T_0}$). The considerations given in the above section enable one to believe that the off-diagonal matrix element ρ_{ST_0} becomes zero at the moment when the partners are at the reaction radius (see eq. (2.186)). Under this condition it is sufficient to consider the vector $\vec{\rho}$ with two components ($\rho_{SS}, \rho_{T_0T_0}$), i.e. the populations of the singlet and triplet terms only. The operators $\hat{F}, \hat{F}\hat{Q}$ (2.211–214) describing changes of S and T₀ state populations are determined by the equations

$$\hat{F}(t)\rho = \begin{pmatrix} \cos^2 \{ \varepsilon t \} & \sin^2 \{ \varepsilon t \} \\ \sin^2 \{ \varepsilon t \} & \cos^2 \{ \varepsilon t \} \end{pmatrix} \begin{pmatrix} \rho_{SS} \\ \rho_{T_0T_0} \end{pmatrix}, \quad \hat{F}\hat{Q} = \begin{pmatrix} (1-\lambda) \cos^2 \{ \varepsilon t \} & \sin^2 \{ \varepsilon t \} \\ (1-\lambda) \sin^2 \{ \varepsilon t \} & \cos^2 \{ \varepsilon t \} \end{pmatrix}.$$

Substitution of these expressions into eqs (2.213) and (2.214) leads to the RP recombination probability.

For a *singlet RP precursor*

$${}^S p_g = p_0 \cdot \sum_m (\lambda n / 2 \cdot \Delta(m)) \cdot [1 + 2 \cdot z(m) \cdot n + (p_0 - 2 \cdot z_0(m)) / p_0]. \quad (3.17)$$

For a *triplet RP precursor*

$${}^T p_g = (p_0 / 3) \cdot \sum_m (\lambda n / 2 \cdot \Delta(m)) \cdot [1 + 2 \cdot z(m) \cdot n - (p_0 - 2 \cdot z_0(m)) / p_0]. \quad (3.18)$$

For a *diffusion RP*

$$p_r = (1/4) \cdot \sum_m (\lambda n / \Delta(m)) \cdot [1 + 2 \cdot z(m) \cdot n], \quad (3.19)$$

$$\Delta(m) = \{ 1 + \lambda p n + 2 \cdot z(m) \cdot n [1 + \lambda n \cdot (p - 1/2)] \} \prod_k (2I_k + 1).$$

In these equations the summation is performed over all possible nuclear spin configurations and the notation is as follows: p_0 and p are the probabilities of the first contact and the re-encounter at the reaction radius, n is the total number of all contacts of the RP, $n = 1/(1-p)$ and $\lambda = K\tau_c/(1+K\tau_c)$ is the singlet RP recombination probability at a single contact, z_0/p_0 and z/p are the mean probabilities of S-T₀ transitions before the first contact and between two re-encounters

$$\begin{aligned} z_0(m) &= \int dt \cdot f_0(t) \cdot \sin^2 \{ \varepsilon(m)t \}, \\ z(m) &= \int dt \cdot f(t) \cdot \sin^2 \{ \varepsilon(m)t \}. \end{aligned} \quad (3.20)$$

The re-encounter distribution function is described by eqs (2.2–4). The distribution function of the first contacts has not been found yet in an arbitrary jump model but it can be approximated using either eq. (2.3), if the initial interradical distance exceeds the recombination radius by the radical jump length in a single diffusion step, i.e. $r_0 \approx b + \lambda_D$, or eq. (2.9) if the initial interradical distance exceeds the recombination radius, i.e. $r_0 \gg b$.

The contact distribution functions (2.4) and (2.9) are of the same form. Averaging the S–T₀ mixing probability using them gives

$$\begin{aligned} z &= (p/2) \cdot [1 - \cos \{c\} \cdot \exp(-c)], \\ z_0 &= (p_0/2) \cdot [1 - \cos \{c_0\} \cdot \exp(-c_0)], \\ c &= (2m/p) \cdot (\pi \cdot |\varepsilon|)^{1/2}, \quad c_0 = (2m_0/p_0) \cdot (\pi \cdot |\varepsilon|)^{1/2}, \end{aligned} \quad (3.21)$$

where the distribution parameters are given by relations (2.5, 6, 10, 11). On substituting (3.21) into (3.17–19) we obtain the results that predict qualitatively the same dependence of the radical recombination probability on the field strength and magnetic isotopic effect as that obtained in the continuous diffusion model (3.2–6). Moreover, in the continuous diffusion limit one has expressions (3.2–6) obtained from eqs (3.17–19). Indeed, according to (2.42) and (3.21) in the continuous limit

$$\begin{aligned} \lambda n &\Rightarrow K \tau_r, \\ 2 \cdot z \cdot n &\Rightarrow (b^2 |\varepsilon| / D)^{1/2} = (|\varepsilon| \tau_D)^{1/2}. \end{aligned} \quad (3.22)$$

Comparing (3.17–19) with (3.2–6) we obtain a limiting value of $2zn$ which exactly equals that given by (3.22).

To compare quantitatively the data obtained in the jump model and those in the continual approximation consider the situation when, in an elementary diffusion step, particles diffuse by distances comparable to their Van der Waals sizes and set $\lambda_D = b$. Then $p \approx 0.5$, $m \approx 0.224 \cdot (b^2/6D)^{1/2} = 0.224 \cdot (\tau_D/6)^{1/2}$. For the sake of simplicity consider diffusion RPs and assume that S–T₀ transitions are induced by the difference in the g -values. For the case discussed, from (3.20, 21) we obtain

$$\begin{aligned} p_r &= (\lambda/2) \cdot [2 - \cos \{\delta \cdot (\pi/6)^{1/2}\} \cdot \exp(-\delta \cdot (\pi/6)^{1/2})] \cdot \\ &\quad \cdot [2 + \lambda - \cos \{\delta \cdot (\pi/6)^{1/2}\} \cdot \exp(-\delta \cdot (\pi/6)^{1/2})]^{-1}, \\ p_r &\approx (\lambda/2) \cdot [1 + \delta/\sqrt{2}] \cdot [1 + \lambda + \delta/\sqrt{2}]^{-1}, \quad \text{if } \delta < 1, \\ \delta &= (|\varepsilon| \cdot \tau_D)^{1/2}. \end{aligned} \quad (3.23)$$

Intersystem transitions are manifested most strongly in diffusion-controlled reactions when $\lambda \rightarrow 1$. Here according to eq. (3.23) S–T₀ transitions may result in a 4/3-fold increase of p_r . Under the same conditions S–T₀ transitions in the continual model increase p_r by a factor of 2 (cf. (3.8) and (3.9)). This quantitative difference in the field effect scale for two diffusion models is attributed to the fact that the

contribution of re-encounters to the reaction decreases with increasing radical displacement in an elementary diffusion step.

As stated above, from the viewpoint of formal kinetics the spin selection rule in recombination reactions must manifest itself in the same way as the steric restrictions or the anisotropy in unpaired electron distributions. To make this point definite, compare eqs (3.19) with (2.50) under compatible conditions: assume that S-T₀ transitions follow only the Δg-mechanism, the anisotropic effects are averaged by rotation only between re-encounters, and the portion of mutual orientations favourable for the reaction is $f = 1/2$. Then eqs (2.50) and (3.19) take the forms

$$p_r = (1/2)K\tau_c n \cdot (1 + nw) / [1 + nw + K\tau_c n \cdot (1 + nw/2)], \quad (3.24)$$

$$p_r = (1/4)K\tau_c n(1 + 2zn) / [1 + 2zn + K\tau_c n(1 + zn)], \quad (3.25)$$

respectively. These expressions are obviously of an identical form. An additional factor (1/2) in eq. (3.25) arises due to the fact that in the S-T₀ approximation half the RPs, namely those in triplet states T₊ and T₋, do not participate in the reaction at all. The difference between (3.24) and (3.25) is that in the former w/p is the average radical flip probability, while in the latter z/p is the average S-T₀ transition probability between two re-encounters.

3.1.5 Recombination in the presence of radical acceptors

If there are radical acceptors in the solution or the solvent molecules themselves can react with the radicals, then the necessity arises to take into consideration these additional parallel channels of RP transformation. Under these conditions the re-encounter statistics are expressed by eqs (2.14, 15). The RP recombination probability is described by the same relations (3.17-19), whereas the contact probabilities p , p_0 as well as the mean values of singlet-triplet transitions in a RP must be found with the account taken of possible parallel RP transformation channels, i.e. using eq. (2.14, 15).

Below we set out results for the continual diffusion model in the case when the initial interradical distance equals the recombination radius, $r_0 = b$. In the general case of $r_0 > b$, as well as in the case of jump particle diffusion, data are available in ref. [3.9].

$${}^S p_g = \sum_m (1 + F(m)) \cdot K\tau_r / A(m),$$

$${}^T p_g = \sum_m (1 - F(m)) \cdot K\tau_r / 3 \cdot A(m),$$

$$p_r = \sum_m K\tau_r / 2 \cdot A(m),$$

$$A(m) = [2 + K\tau_r(1 + F(m))] \cdot \prod_k (2I_k + 1),$$

$$F(m) = [1 + (K_s \cdot \tau_D)^{1/2}] / \{1 + [K_s \cdot \tau_D / 2 + (\tau_D / 2) \cdot (K_s^2 + 4e^2(m))^{1/2}]^{1/2}\}, \quad (3.26)$$

$$\tau_r = ab/D[1 + (K_s \tau_D)^{1/2}]$$

the recombination probabilities (3.26) obey relations (3.11, 13). These formulas show that acceptors ($K_s \neq 0$) reduce the role of S-T transitions in recombination and, in general, the recombination probability and the scale of magnetic effects due to decrease of the recombination time and the re-encounter probability (see Fig. 3.3).

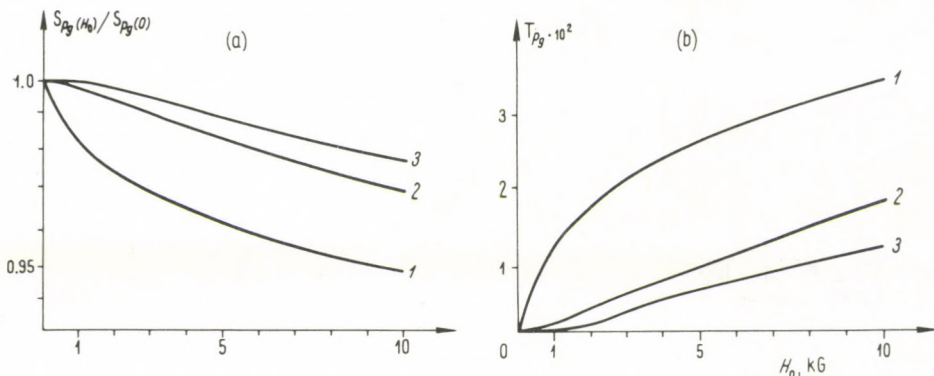


Fig. 3.3. Field dependence of radical recombination probability for a singlet- (a) and triplet- (b) born RP at $\tau_D = 0.36$ ns, $K \cdot a \cdot b/D = 2$, $\Delta g = 0.01$ and at various reaction rates with acceptors: 1 — $K_s = 0$; 2 — $K_s = 10^8$ s $^{-1}$; 3 — $K_s = 2 \cdot 10^8$ s $^{-1}$

3.1.6 Recombination of radicals with anisotropic reactivity

As a rule, the unpaired electron distribution in radicals is anisotropic and the reaction occurs thus only at favourable mutual orientations of the reagents, when the overlap of unpaired electron orbitals is sufficiently great. In this case, radical rotation is of fundamental importance. Orientational relaxation averages radical anisotropic properties. Recombination of radicals with anisotropic reactivity has been calculated using the following model [3.20]. Anisotropic reactivity is characterized by a steric factor f equal to the statistical weight of favourable mutual orientations. The radical orientation relaxation is assumed to occur both at the contact moment and between encounters, the orientational relaxation kinetics being described by the simplest model: the fraction of RPs with favourable [$\rho(I)$] and unfavourable [$\rho(II)$] mutual orientations obeys the equation

$$\partial \rho(I) / \partial t = -\partial \rho(II) / \partial t = -(1-f) \cdot \rho(I) / \tau_0 + f \cdot \rho(II) / \tau_0.$$

The recombination probability is calculated at arbitrary values of the initial interradsical separation and jump length in an elementary diffusion step [3.9].

Below are the results for recombination of radicals starting from the reaction zone, i.e., $r_0 = b$, and diffusing by small jumps (continuous diffusion).

$$\begin{aligned}
 {}^S p_g &= \sum_m K \tau_r \cdot [F_1(m) + F_2(m)] / A(m), \\
 {}^T p_g &= \sum_m K \tau_r \cdot [F_1(m) - F_2(m)] / 3 \cdot A(m), \quad (3.27) \\
 p_r &= \sum_m f K \tau_r / 4 \cdot A(m), \\
 \tau_r &= (a \cdot b / D) \cdot [1 + (K_s \cdot \tau_D)^{1/2}]^{-1}, \quad \tau_D = b^2 / D, \\
 A(m) &= \{1 + K \tau_r \cdot [F_1(m) + F_2(m)]\} \cdot \prod_m (2I_k + 1), \\
 F_1(m) &= (1/2) \cdot \{f + (1 - f) \cdot [1 + (K_s \cdot \tau_D)^{1/2}] / \\
 &\quad [1 + (K_s \cdot \tau_D + \tau_D / \tau_0)^{1/2} + a \cdot b / D \cdot \tau'_0]\}, \\
 F_2(m) &= (1/2) \cdot [1 + (K_s \cdot \tau_D)^{1/2}] \cdot \{f \cdot [1 + (K_s \cdot \tau_D / 2 + \\
 &\quad + (K_s^2 \tau_D^2 / 4 + \varepsilon^2(m) \cdot \tau_D^2)^{1/2})^{1/2}]^{-1} + \\
 &\quad + (1 - f) \cdot [1 + a \cdot b / D \cdot \tau'_0 + (K_s \cdot \tau_D / 2 + \tau_D / 2 \cdot \tau_0 + \\
 &\quad + ((K_s \cdot \tau_D / 2 + \tau_D / 2 \cdot \tau_0)^2 + \varepsilon^2(m) \cdot \tau_D^2)^{1/2})^{1/2}]^{-1}\}.
 \end{aligned}$$

when radical acceptors are absent, these expressions reduce to

$$\begin{aligned}
 F_1(m) &= (1/2) \cdot \{f + (1 - f) \cdot [1 + a \cdot b / D \cdot \tau'_0 + (\tau_D / \tau_0)^{1/2}]^{-1}\} \\
 F_2(m) &= (1/2) \cdot \{f \cdot [1 + (|\varepsilon(m)| \tau_D)^{1/2}]^{-1} + (1 - f) \cdot [1 + \\
 &\quad + a \cdot b / D \cdot \tau'_0 + (\tau_D / 2 \tau_0 + (\tau_D^2 / 4 \tau_0^2 + \varepsilon^2(m) \cdot \tau_D^2)^{1/2})^{1/2}]^{-1}\}. \quad (3.28)
 \end{aligned}$$

Here τ_0 and τ'_0 are times of mutual radical orientation relaxation between re-encounters and at a contact moment. Let $\tau_0 = \tau'_0$, then τ_0 , estimated by the Debye theory of rotational molecular relaxation in liquids, is (see also (2.60))

$$\tau_0 = \pi \eta b^3 / 4kT. \quad (3.29)$$

Expressing the mutual radical diffusion coefficient via η by the Stokes formula

$$D = 2kT / 3\pi b \eta$$

we have (see eq. (2.61))

$$\tau_D / \tau_0 = 6, \quad a \cdot b / D \cdot \tau_0 = 6a / b. \quad (3.30)$$

The quantities τ_D / τ_0 and $ab / D \tau'_0$ characterize the orientational relaxation efficiencies between re-encounters and at a contact moment respectively. As a rule, the reaction layer width is small compared to the Van der Waals particle sizes, $a \ll b$.

Hence, it follows from eq. (3.30) that the radical rotation between re-encounters makes the basic contribution to the averaging of anisotropy of the radical reactivity.

In real systems, as a rule, $|\varepsilon(m)| \cdot \tau_D < 1$. By expanding eq. (3.28) in this small parameter, we have

$$F_1(m) \cong 1 - (1/2) \cdot (|\varepsilon(m)| \cdot \tau_D)^{1/2},$$

$$F_2(m) \cong [1 + a \cdot b/D \cdot \tau_0 + (\tau_D/\tau_0)^{1/2}]^{-1} \approx 0.3,$$

$$S_{p_g} \cong \sum_m K \tau_r \cdot [0.3 + 0.7f - 0.5f \cdot (|\varepsilon(m)| \tau_D)^{1/2}] \cdot \{ [1 + K \tau_r (0.3 + 0.7f - 0.5f \cdot (|\varepsilon(m)| \tau_D)^{1/2})] \prod_k (2I_k + 1) \}^{-1}.$$

In the case of geminate recombination, the radical orientation of the primary pair favours the reaction. Therefore, radical rotation reduces the reaction probability. In the case of diffusion pairs, the orientational relaxation increases the recombination probability of radicals with anisotropic reactivity.

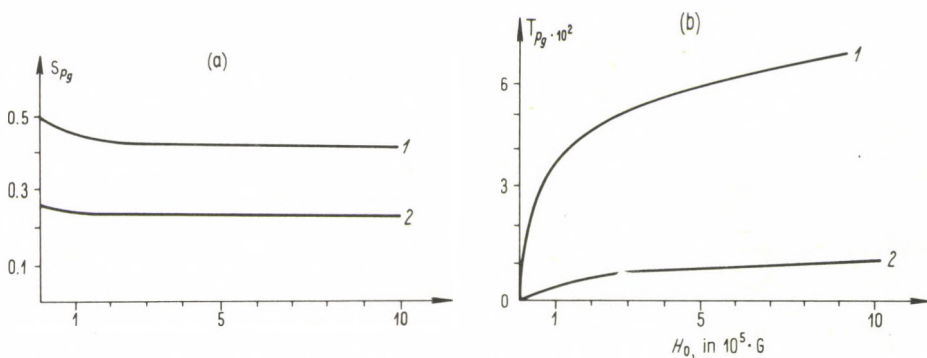


Fig. 3.4. Field dependence of radical recombination probability for a singlet- (a) and triplet- (b) born RP at $K \cdot \tau_r = 1$, $\tau_D = 1$ ns, $f = 0.1$, $\Delta g = 10^{-3}$ at various orientational relaxation rates: 1 — $\tau_D/\tau_0 = 0$; 2 — $\tau_D/\tau_0 = 6$

Figure 3.4 depicts the recombination probabilities, for singlet and triplet RP precursors and for diffusion pairs, calculated with and without account taken of the orientational relaxation. Radical rotation is seen to influence the magnetic field effect strongly.

3.1.7 Radical-ion recombination

The influence of Coulomb radical interactions on magnetic effects depends on the solvent polarity. In highly polar solvents the Coulomb interactions are effectively shielded by the medium polarization and hence the reaction between radical-ions

must resemble the situation of uncharged reagents. For example, in water ($\epsilon = 81$) the Coulomb interaction negligibly affects the recombination time (see Table 2.3) and the Onsager radius does not exceed 0.7 nm at 298 K. Note that outside the Onsager radius, the Coulomb interaction is negligible.

Thus, in reactions of radical-ions in polar solvents, one should expect magnetic effects to be of the same order as those in uncharged particle reactions, the role of the Coulomb interaction being important in nonpolar solvents. In the case of partners of like charge, the probabilities of the first and the following contacts reduce with a simultaneous decrease in the effective recombination time (see Tables 2.2–4). Hence, the scale of magnetic effects must also reduce. In the case of oppositely charged partners in nonpolar solvents, the recombination time increases sharply (see Tables 2.2–4) and re-encounters with long time intervals between them become possible. Indeed, the Coulomb attraction returns the partners at the recombination radius with the probability $p_0 = 1 - e^{-1} = 0.6$ even if the latter were at the Onsager radius r_c . For instance at $\epsilon = 2$, $T = 298$ K we have $r_c = 28$ nm. With a typical value of the mutual diffusion coefficient, $D = 10^{-5}$ cm²/s, the particles return from the Onsager radius within a time $t_c \approx r_c^2/6D \approx \frac{500}{\epsilon^2}$ (ns). Thus, the above estimates indicate a large re-encounter probability for particles after their long diffusion travel in nonpolar solvents.

It should be noted, that the re-encounters are clearly shown only in recombination of radicals with sufficiently low reactivity in singlet or triplet (or both) states of radical pairs. Indeed, highly reactive particles react at the very first collision and thus would not start a diffusion travel to re-encounter. In this case, appreciable magnetic effects due to the Δg -mechanism can be expected only in geminate recombination of the pairs that at the starting moment, on the one hand, are outside the reaction layer, with S–T₀ transitions being possible, and, on the other hand, have not too great interpartner distances and thus the S–T₀ mixing before the first contact is incomplete. In this case, magnetic effects in diffusion pair recombination must be rather weak since the RP spins are uncorrelated at the moment of the first contact and the radicals do not diffuse to re-encounter as a result of their high reactivity in both singlet and triplet states.

Providing the RP reactivity, either in S and T states or at least one of them, is not very high, the re-encounters can make appreciable contributions to the recombination and the magnetic effects.

Numerical calculations [3.13 c] show the magnetic effects in high field reactions of radical-ions can be obtained from eq. (3.14) modified as follows. As the recombination time τ_r , one must use the corresponding quantity for interacting partners (see Table 2.2),

$$\tau_r = (a \cdot b/D) \cdot b \cdot S(b) \cdot \exp(-U(b)/kT) \quad (3.31)$$

and the quantity

$$F^{**} \simeq F^* \cdot (b \cdot S(b))^{-(1+\epsilon)}$$

instead of F^* , where $\varepsilon \approx 1/4$ for a Coulomb attraction and $0 \leq \varepsilon \leq 1/4$ for a Coulomb repulsion. In electrolytes the Coulomb interaction can be reduced by the Debye shielding. If the Debye shielding length is small, the Coulomb potential has a short range. Coulomb interaction effect on particle diffusion is then qualitatively the same as those of exchange interactions and hence the magnetic effects in radical-ion recombination can be calculated by eqs (3.14, 16).

3.1.8 The exponential model

The exponential model is widely used in radical recombination theory. In this approach the kinetic equations for the RP density matrix have the form (2.175) and (2.204) for geminate and diffusion RP recombinations respectively. The RP recombination probability is determined by solving the system of algebraic equations (2.177) and (2.203) with constant coefficients. Solving them in the S-T₀ approximation, we obtain for the recombination probability [3.8, 17] the following results.

For a *singlet RP precursor*

$${}^s p_g = \sum_m [K\tau_c/\Delta(m)] \cdot \{(1 + K\tau_c/2)^2 + 4J_0^2\tau_c^2 + 2\varepsilon^2(m) \cdot \tau_c^2 \cdot (1 + K\tau_c/2)\}. \quad (3.32)$$

For a *triplet RP precursor*

$${}^t p_g = \sum_m [2K\tau_c/3 \cdot \Delta(m)] \cdot \varepsilon^2(m) \cdot \tau_c^2 \cdot (1 + K\tau_c/2). \quad (3.33)$$

For a *diffusion RP*

$$p_r = \sum_m [K\tau_c/4 \cdot \Delta(m)] \cdot \{(1 + K\tau_c/2)^2 + 4J_0^2\tau_c^2 + 4\varepsilon^2(m) \cdot \tau_c^2 \cdot (1 + K\tau_c/2)\}, \quad (3.34)$$

where

$$\Delta(m) = \{(1 + K\tau_c) \cdot [(1 + K\tau_c/2)^2 + 4J_0^2 \cdot \tau_c^2] + 4\varepsilon^2(m) \cdot \tau_c^2 \cdot (1 + K\tau_c/2)^2\} \cdot \prod_K (2I_K + 1).$$

In the case of charged particle recombination, these expressions must include, as τ_c , the recombination time taking into account the Coulomb interaction (3.31).

As in the diffusion model (see (3.11, 12)), the recombination probabilities for singlet-born and diffusion pairs are expressed via that for triplet-born RPs

$${}^s p_g = \lambda - 3(1 - \lambda) \cdot {}^t p_g, \\ p_r = ({}^s p_g + 3 \cdot {}^t p_g)/4 = \lambda(1 + 3 \cdot {}^t p_g)/4; \quad \lambda = K\tau_c/(1 + K\tau_c).$$

In all these formulas the summation is carried out over all possible nuclear spin configurations.

The strongest magnetic effects are expected in the geminate recombination from the initial triplet state. Therefore, we discuss in detail only expression (3.33). Set $J_0=0$ and obtain for the Δg -mechanism of S-T₀ transitions

$${}^T p_g = (2/3) \cdot K\tau_c \cdot \varepsilon^2 \cdot \tau_c^2 \cdot \{(1 + K\tau_c/2) \cdot (1 + K\tau_c + 4\varepsilon^2 \cdot \tau_c^2)\}^{-1} \quad (3.35)$$

where $\varepsilon = \Delta g \cdot \beta \hbar^{-1} H_0/2$ (see (3.1)). If $\Delta g=0$, for a one-nucleus RP

$${}^T p_g = (1/24) \cdot K\tau_c \cdot a^2 \tau_c^2 \cdot \{(1 + K\tau_c/2)(1 + K\tau_c + a^2 \tau_c^2/4)\}^{-1}. \quad (3.36)$$

It follows from eq. (3.35) that as the field strength grows, ${}^T p_g$ varies from zero to

$${}^T p_g \Rightarrow (1/3) \cdot (K\tau_c/2) \cdot [1 + K\tau_c/2]^{-1}, \quad (3.37)$$

$${}^T p_g \Rightarrow K\tau_c/6, \quad \text{if } K\tau_c < 1,$$

$${}^T p_g \Rightarrow 1/3, \quad \text{if } K\tau_c > 1.$$

In a triplet-born RP recombination the field effects are stronger the higher the reactivity of the partners or the longer the time the partners reside in a cage. Similar conclusions follow from eq. (3.36) for magnetic isotopic effects: the bigger the parameters A , K and τ_c , the stronger the effects.

Spin polarization and magnetic effects for arbitrary RPs can be calculated by (3.32–34). However, their comparison with those calculated by the diffusion model shows that the influence of magnetic fields, magnetic isotopic substitution, radical reactivity and mobility on radical recombination is independent of the RP model chosen for calculations. The only difference between the diffusion and exponential models is in the functional dependence of the RP recombination probability on the above parameters. To illustrate this statement, compare eqs (3.35, 36) with (3.5) in a case of practical interest when a full singlet-triplet mixing cannot occur during the RP lifetime in a cage. According to the exponential model

$${}^T p_g \approx 2\lambda \varepsilon^2 \tau_c^2 / 3 \sim H_0^2 \tau_c^2, \quad (3.38)$$

$${}^T p_g \approx \lambda a^2 \tau_c^2 / 24 \sim a^2 \cdot \tau_c^2; \quad \lambda = K\tau_c / (1 + K\tau_c) \cdot (1 + K\tau_c/2),$$

whereas within the diffusion model

$${}^T p_g \approx \lambda \delta / 6 \sim \sqrt{H_0 \cdot \tau_D}, \quad (3.39)$$

$${}^T p_g \approx \lambda (|a| \tau_D)^{1/2} / 12 \sim (|a| \cdot \tau_D)^{1/2}; \quad \lambda = K\tau_r / (1 + K\tau_r).$$

Note that the difference in the functional dependences of the RP recombination probability on the parameters characterizing spin interactions— H_0 and A —can be used to verify the applicability of this or that model. As noted in Sec. 2.1, a typical physical situation, when the exponential model can be applied instead of the diffusion model, is RP recombination in the presence of a number of effective radical acceptors. The latter capture, in fact, all radicals that did not recombine on their first

contacts, therefore, re-encounters stop contributing to recombination. Indeed, from eq. (3.26) it follows that as the radical reaction with acceptors grows in importance in the time interval between the re-encounters, dependences of the type (3.38) are substituted for (3.39) (see Fig. 3.3).

Relations (3.32–34) allow one to analyze the effect of the radical exchange interaction on the recombination. The equations demonstrate that the exchange interaction decreases the S– T_0 mixing efficiency. This is the expected effect of the exchange integral J_0 , because it splits S and T_0 terms and destroys their resonance. At the same time, quantitatively the exchange interaction effect on the RP recombination probability is negligible if $|J_0| \ll K$, since the singlet term is broadened by the quantity K because of the lifetime effect. Hence, the splitting of S and T_0 terms suppresses the intersystem transitions only if it exceeds the broadening of the levels. This statement is exemplified by the triplet-born RP recombination probability at large K values. In this case from eq. (3.33)

$${}^T p_g \approx (4/3) \cdot \varepsilon^2 \cdot K^{-1} \tau_c < 1.$$

This is the result obtained if the transition probability between two terms, one having the broadening K , is calculated by perturbation theory. The broadening of the levels due to a finite RP lifetime in a cage produces the same effect.

The above discussion of magnetic effects in radical recombination shows that in comparatively high magnetic fields, $H_0 \gtrsim A$, the difference in radical g -values and the isotropic hf interactions of unpaired electrons with magnetic nuclei can effectively mix S and T_0 states and thus influence appreciably the radical reaction kinetics. However, the above data were obtained in the S– T_0 approximation. RPs in two triplet states T_+ and T_- did not participate in the reaction at all. The intersystem transitions S– T_+ , T_- are of fundamental importance in low magnetic fields comparable with local hyperfine fields. However, in high magnetic fields we can come across some situations when, S– T_+ , T_- channels can also be effective, as well as the S– T_0 channel.

3.1.9 S– T_+ , T_- transitions in high magnetic fields

Between RP re-encounters, when the partners are at a certain distance from each other, S and T_0 terms are in resonance taking part in the intersystem transitions alone. Figure 3.5 shows that S and T_- terms are in resonance due to the exchange splitting at a distance r^* . Within this distance S– T_- transitions must be taken into account in the general case. Unpaired electron interactions, either isotropic or anisotropic, split the crossing terms S and T_- . For free radicals the value of the splitting is $V \approx 10^8$ – 10^9 rad/s. Hence, magnetic isotopic effects can also be expected for S– T_+ , T_- transitions. The probability of S– T_- transitions when the radicals pass through the region of term crossing, is determined by the parameter $V \cdot \tau$ where τ is the effective time of this crossing [3.21]. For radical recombination in solutions

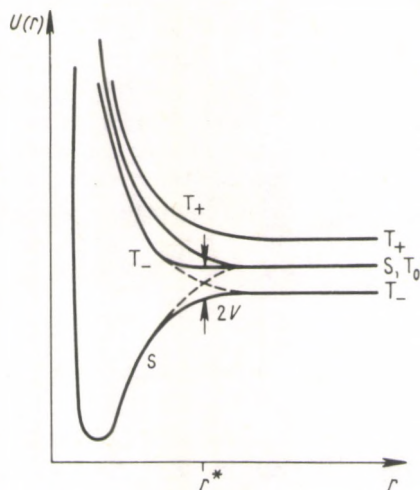


Fig. 3.5. Adiabatic passage of the region of S and T_- terms crossing

$\tau \approx 10^{-11} - 10^{-13}$ s, so that $V\tau \ll 1$ and $S-T_-$ transitions must be of small importance in RP recombination in high fields. If the time the radicals reside in the region of term crossing could somehow be increased, e.g. either by increasing the solution viscosity or by interradsical attraction, the $S-T_-$ mixing would become an essential factor in RP recombination. In a limiting case of $V\tau > 1$, the radical motion would occur only at the lowest term depicted in Fig. 3.5 and this would result in the following. A singlet precursor would yield a RP in T_- state. Only 1/4 of diffusion RPs, namely those in the T_- state at the moment when the partners are close to each other, would yield the reaction product. The greater the slope of the potential terms, the smaller the transition probability [3.21]. Thus, the $S-T_-$ transition probability can be expected to reduce with growing field intensity since the crossing point of the terms shifts towards lower values of interradsical distances, where the slope of the potential terms increases.

$S-T_+$, T_- transitions can also take place if the RP singlet term broadening induced by the RP recombination is so great that the singlet state would overlap the three triplet states simultaneously.

Although in high fields $S-T_+$, T_- transitions can sometimes take place alongside with $S-T_0$ transitions, at present no experimental data interpreted by intersystem $S-T_+$ or $S-T_-$ transitions in high fields are available. This suggests that $S-T_+$, T_- transitions play, as a rule, a negligible role in radical recombination in high fields, biradicals being an exception [3.22]. Suppose a biradical can possess two configurations: in one it can recombine, in the other it cannot, the unpaired electron interaction in the latter case being characterized by the exchange integral J and the singlet-triplet transitions occurring. Under these conditions the singlet-triplet transition efficiency would have its maximum with growing magnetic field, since at

intermediate fields the S and T₋ terms are in resonance and the singlet-triplet mixing is a maximum. The singlet-triplet transitions can influence radical recombination provided the latter is accompanied by some competitive process. The escape of radicals can serve as such in the case of RP recombination. A peculiarity of biradicals is that the radical centres cannot diverge completely, being connected by a chain of chemical bonds. The reaction of radical centres with either acceptors or solvent molecules can be a competitive process in the case of biradicals. If so, the biradical recombination probability in the above example passes through a maximum with growing field strength.

3.1.10 The relaxation mechanism of S-T transitions

Paramagnetic relaxation tends to randomize the mutual orientation, the spin state correlation, of unpaired electrons. Therefore, the relaxation mechanism of intersystem transitions is characterized by simultaneous transitions from the singlet to the three triplet states. For this mechanism the field dependence of RP recombination probability, as well as magnetic isotopic effects, result from the longitudinal and transverse relaxation rates ($1/T_1$ and $1/T_2$ respectively) varying with the external constant field and depending on the electron-nuclear hf interaction (see eqs (1.2, 3)). The paramagnetic relaxation induced by hf-anisotropy varies appreciably in fields $H_0 \approx \hbar/g \cdot \beta \cdot \tau_0$, where τ_0 is the radical rotational correlation time, equal as a rule to some 10^{-11} s. Hence, for this mechanism, the field dependence of radical recombination must manifest itself in high magnetic fields of thousands of gauss. Such high fields are unnecessary for the observation of magnetic isotopic effects. In the case when paramagnetic relaxation is mainly induced by rotational modulation of the g -tensor anisotropy, the paramagnetic relaxation rate, according to (1.3), reaches about 10^8 s^{-1} in fields of around 10^5 Gauss. With account taken of these factors, it is expedient to consider the effect of the relaxation mechanism on RP recombination in this section, dwelling upon the field dependence of radical recombination in high fields, $H_0 \gtrsim 10^3$ G.

Consider the recombination of two radicals *A* and *B*. Assume *B* to be a free hydrocarbon radical characterized by a comparably slow paramagnetic relaxation, $T_1, T_2 \approx 10^{-6}$ s, while *A* has shorter relaxation times, $T_{1A}, T_{2A} \lesssim 10^{-8}$ s. Oxygen-containing radicals of the type OH, HO₂ or sulphur-containing radicals can serve as *A* radicals. The RP state population relaxation is described by the kinetic equations

$$(\partial \rho_{SS} / \partial t)_{\text{rel.}} = -w_1 \cdot \rho_{SS} + w_2 \cdot \rho_{T_0 T_0} + w \cdot (\rho_{T_+ T_+} + \rho_{T_- T_-}),$$

$$(\partial \rho_{T_0 T_0} / \partial t)_{\text{rel.}} = w_2 \cdot \rho_{SS} - w_1 \cdot \rho_{T_0 T_0} + w \cdot (\rho_{T_+ T_+} + \rho_{T_- T_-}),$$

$$(\partial \rho_{T_+ T_+} / \partial t)_{\text{rel.}} = w(\rho_{SS} + \rho_{T_0 T_0} - 2\rho_{T_+ T_+} - 2R),$$

$$(\partial \rho_{T_- T_-} / \partial t)_{\text{rel.}} = w(\rho_{SS} + \rho_{T_0 T_0} - 2\rho_{T_- T_-} + 2R),$$

$$(\partial R/\partial t)_{\text{rel.}} = w(\rho_{T-T-} - \rho_{T+T+} - 2R),$$

$$R = \text{Re}\{\rho_{\text{ST}0}\},$$

$$w = 1/4 \cdot T_{1A}, \quad w_1 = w + 1/2 \cdot T_{2A}, \quad w_2 = -w + 1/2 \cdot T_{2A}. \quad (3.40)$$

The recombination probability for the relaxation mechanism of S-T transitions has been calculated on the exponential model [3.8, 19], the kinetic equation for the RP density matrix (2.174) taking the form

$$\partial \rho / \partial t = (\partial \rho / \partial t)_{\text{rel.}} - K(\hat{P}\rho + \rho\hat{P})/2 - \rho/\tau_c. \quad (3.41)$$

Here the first term describes the RP density matrix evolution by paramagnetic radical relaxation and is expressed by eqs (3.40). Solving (3.41) and using eqs (2.178, 179) we have the following recombination probabilities.

For a *singlet-born RP*

$${}^S p_g = (K\tau_c/4 \cdot \Delta) \cdot [4 + 3\tau_c/T_{1A} + 2\tau_c/T_{2A} + \tau_c^2/T_{1A} \cdot T_{2A}]. \quad (3.42)$$

For a *triplet-born RP*

$${}^T p_g = (K\tau_c/4 \cdot \Delta) \cdot [\tau_c/3 T_{1A} + 2\tau_c/3 \cdot T_{2A} + \tau_c^2/T_{1A} \cdot T_{2A}]. \quad (3.43)$$

For a *diffusion RP*

$$p_r = (K\tau_c/4 \cdot \Delta) \cdot [1 + \tau_c/T_{1A} + \tau_c/T_{2A} + \tau_c^2/T_{1A} \cdot T_{2A}]. \quad (3.44)$$

where

$$\begin{aligned} \Delta = & (1 + \tau_c/T_{1A}) \cdot (1 + \tau_c/T_{2A}) + \\ & + K\tau_c(1 + 3\tau_c/4 \cdot T_{1A} + \tau_c/2 \cdot T_{2A} + \tau_c^2/4 \cdot T_{1A} \cdot T_{2A}). \end{aligned}$$

The singlet-triplet transitions induced by radical paramagnetic relaxation are seen from these formulas to increase ${}^T p_g$ and p_r and to reduce ${}^S p_g$. Note the results obtained for the recombination of radicals with extremely short relaxation times, when $T_{1A}, T_{2A} < \tau_c$. Then (3.42-44) yield the same results

$${}^S p_g \approx {}^T p_g \approx p_r \approx K_{\text{eff}} \cdot \tau_c / (1 + K_{\text{eff}} \cdot \tau_c); \quad K_{\text{eff}} = K/4. \quad (3.45)$$

Thus, for the case of fast paramagnetic relaxation, i.e., for a fast singlet-triplet mixing, formally radicals recombine in the same manner as if there were no spin selection rule for the reaction (cf. (3.45) with (2.36)). The spin selection rule is reflected in the fact that unlike the spin independent theory (2.36), eq. (3.45) includes the effective recombination rate constant. The paramagnetic relaxation times can be affected either by magnetic isotopic substitution or varying field intensity. The maximum magnetic effect possible for diffusion RP recombination equals 4, while that expected in geminate recombination of a triplet-born pair is somewhat greater.

3.1.11 Sequence of radical pairs

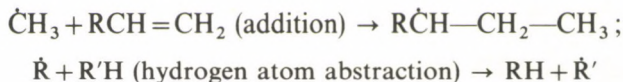
Prior to recombination a radical pair can experience changes induced by radical rearrangements, addition reactions, atom abstractions, etc. (see, e.g., [3.23]). It is therefore interesting to discuss magnetic effects in reactions proceeding via a succession of RPs. From the standpoint of the dynamics of S-T transitions and magnetic effects, there are several types of successive RPs.

(a) When one RP turns into another, the unpaired electrons of the latter can continue their interactions with the same magnetic nuclei as in the former. This process can be illustrated by the reactions of radical isomerization or rearrangement,



In this case the transformation of one RP into another results in changes of the pair spin-Hamiltonian, radical g -values and hf constants. It is also possible that, being negligible in one pair, the interaction with the same magnetic nucleus contributes appreciably to the S-T evolution of the other pair.

(b) Reactions of addition, substitution, atom transfer, etc. can produce new radicals. For example,



In this case an unpaired electron of the newly formed radical can interact with the magnetic nuclei that were in the primary radical as well as with new ones.

Consider a sequence of two RPs. Assume the equilibrium in the reaction of RP transformation to be shifted towards the second pair. Figure 3.6 depicts the reaction scheme for the case discussed. With respect to the first pair, the transformation into the second one plays the same role as the RP reaction with acceptors. Hence, the recombination probability of the first RP can be calculated by eqs (3.26, 27) where K_s is substituted either by K_{12} (no radical acceptors), or $K_{12} + K_s$ (with radical acceptors). Magnetic effects of the first pair would qualitatively coincide with those observed in a RP without transformation into another pair. Being analogous to the reaction with acceptors, this transformation decreases the scale of magnetic effects in the primary pair. As to the second pair, the case is much more complex because of the distributions of interrational distances and spin states observed at the moment of its generation. Assume that RP_1 is singlet-born and its partners are in contact at the starting moment. At the instant of transformation into RP_2 , the interrational separation can acquire any value and the spins would not be in a pure singlet state

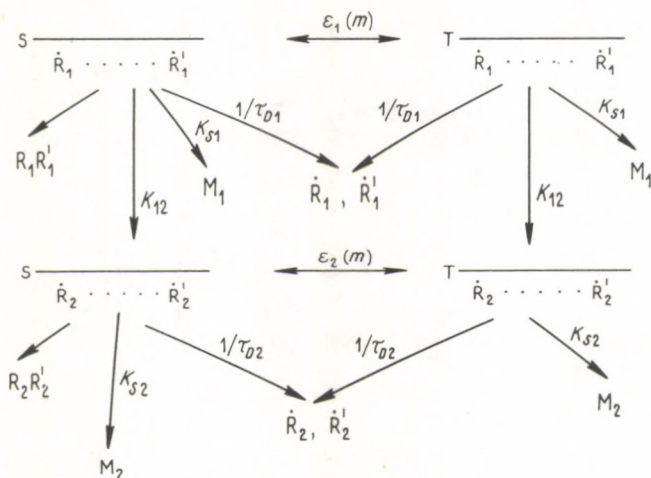


Fig. 3.6. Scheme of processes in two successive RPs

but in a mixed state of superposition of S and T. Situations are also possible when the triplet state population would exceed that of the singlet. At the instant of RP_2 generation, the off-diagonal element of the density matrix ρ_{ST_0} can differ from zero, which also affects the RP_2 spin dynamics. As a result, magnetic effects in the recombination of successive pairs can manifest certain peculiarities. If RP_1 is assumed, as before, to be singlet-born, then the magnetic effect in RP_2 can correspond to either S- or T-precursor. Indeed, if RP_1 s show effective S-T₀ mixing and singlet RP_1 s recombine quickly, then RP_2 s would be formed mainly from triplet pairs. The RP_2 magnetic effect would conform to the case of geminate RP recombination from a T-precursor. However, if the S-T₀ mixing and singlet RP_1 recombination are less effective, then RP_2 would be singlet-born. The RP_2 magnetic effects, as well as those of RP_1 , would correspond to geminate RP recombination from the initial S-state. If RP_1 is triplet-born and, as before, only singlet RP_1 s can recombine, then RP_2 s would be produced mainly from triplet RP_1 s. The magnetic effects of both pairs will confirm to the situation of geminate RP recombination from the initial T state.

The radical recombination probability in a sequence of pairs can be found by solving a set of coupled kinetic equations of the density matrices. When averaged in time, the kinetic equations take the form (see eq. (2.183))

$$\begin{aligned}
 -\rho_1(\vec{r}, 0) &= -i\hbar^{-1}[\hat{H}_1, \bar{\rho}_1(\vec{r})] + D_1 \cdot \Delta \bar{\rho}_1(\vec{r}) - (K_{12} + K_{s1})\bar{\rho}_1(\vec{r}), \\
 -K_{12} \cdot \bar{\rho}_1(\vec{r}) &= -i\hbar^{-1}[\hat{H}_2, \bar{\rho}_2(\vec{r})] + D_2 \cdot \Delta \bar{\rho}_2(\vec{r}) - K_{s2} \cdot \bar{\rho}_2(\vec{r}).
 \end{aligned}$$

The average density matrix of RP_1 serves as the initial condition for the second pair. The matrices $\bar{\rho}_1$ and $\bar{\rho}_2$ obey the boundary conditions of type (2.184-186). Prior to solving these equations, we introduce some notation. Let all the magnetic nuclei be

divided into three groups. The first group includes solely the nuclei of RP_1 , the second one those of RP_2 , the third group the common nuclei of both pairs, the nuclear spin configurations of these groups being $\{m_1\}$, $\{m_2\}$ and $\{m\}$ respectively. The matrix elements of S-T₀ transitions in the RP_1 and RP_2 are $\varepsilon_1(m_1, m)$ and $\varepsilon_2(m, m_2)$ (see (3.1)). For the sake of definiteness, assume the primary pair to be at the recombination radius at the starting moment, $r_0 = b$. The recombination probability of the RP_1 subensemble with a set nuclear configuration is [3.24]

$$p_1(m_1, m) = (K_1 \cdot \tau_{r1} / \Delta_1) \cdot \{(n_S + n_{T_0})(1 + x_1) + (n_S - n_{T_0}) \cdot [1 + (\tilde{K}_{12} \cdot \tau_{D1})^{1/2}]\}, \quad (3.46)$$

while that of RP_2 subensemble with the nuclear spin configuration $\{m, m_2\}$ is

$$p_2(m, m_2) = \sum_{m_1} K_2 \cdot \tau_{r2} \cdot K_{12} \cdot \tau_{D1} \cdot \{(1 + x_2) \cdot [(n_S + n_{T_0}) \cdot (2 + K_1 \cdot \tau_{r1} + 2 \cdot x_1) + (n_{T_0} - n_S) \cdot K_1 \cdot \tau_{r1}] \cdot [(\tilde{K}_{12} \cdot \tau_{D1})^{1/2} + (K_{S2} \cdot \tau_{D2})^{1/2}]^{-1} - (x_1 + x_2) \cdot [1 + (K_{S2} \cdot \tau_{D2})^{1/2}] \cdot [(n_S + n_{T_0}) \cdot K_1 \cdot \tau_{r1} + (n_{T_0} - n_S) \cdot (2 + K_1 \cdot \tau_{r1} + 2 \cdot (\tilde{K}_{12} \cdot \tau_{D1})^{1/2})] \cdot [(x_1 + x_2)^2 + F^2]^{-1}\} / \Delta_1 \cdot \Delta_2 \cdot \prod_n^{(m_2)} (2I_n + 1), \quad (3.47)$$

where

$$\begin{aligned} \tau_{ri} &= a_i \cdot b_i / D_i, \quad \tau_{Di} = b_i^2 / D_i, \quad i = 1, 2; \\ x_1 &= \{[\tilde{K}_{12} \cdot \tau_{D1} + (\tilde{K}_{12}^2 \cdot \tau_{D1}^2 + 4 \cdot \varepsilon_1^2 \cdot \tau_{D1}^2)^{1/2}] / 2\}^{1/2}, \\ \Delta_1 &= (1 + x_1) \cdot [1 + K_1 \cdot \tau_{r1} + (\tilde{K}_{12} \cdot \tau_{D1})^{1/2}] + \\ &\quad + (1 + K_1 \cdot \tau_{r1} + x_1) \cdot [1 + (\tilde{K}_{12} \cdot \tau_{D1})^{1/2}], \\ x_2 &= \{[K_{S2} \cdot \tau_{D2} + (K_{S2}^2 \cdot \tau_{D2}^2 + 4 \cdot \varepsilon_2^2 \cdot \tau_{D2}^2)^{1/2}] / 2\}^{1/2}, \\ \Delta_2 &= (1 + x_2) \cdot [1 + K_2 \cdot \tau_{r2} + (K_{S2} \cdot \tau_{D2})^{1/2}] + \\ &\quad + (1 + K_2 \cdot \tau_{r2} + x_2) \cdot [1 + (K_{S2} \cdot \tau_{D2})^{1/2}], \\ F &= \varepsilon_1 \cdot \tau_{D1} / x_1 + \varepsilon_2 \cdot \tau_{D2} / x_2, \\ \tilde{K}_{12} &= K_{12} + K_{S1}, \end{aligned}$$

$n_S(m_1, m)$ and $n_{T_0}(m_1, m)$ are statistical weights of RP_1 subensembles in S and T₀ states with a set nuclear spin configuration at the moment of RP_1 generation. For the case of an S-precursor

$$n_S(m_1, m) = 1 / \prod_k (2I_k + 1),$$

$$n_{T_0}(m_1, m) = 0$$

and for the case of a T-precursor

$$n_S(m_1, m) = 0,$$

$$n_{T_0}(m_1, m) = 1/3 \cdot \prod_k (2I_k + 1),$$

where the product is over all the nuclei of the RP_1 . The recombination probability of the whole RP ensemble is

$$p_1 = \sum_{m, m_1} p_1(m_1, m),$$

$$p_2 = \sum_{m, m_2} p_2(m, m_2). \quad (3.48)$$

Note that the above formulas estimate CIDNP also in successive RPs.

Figure 3.7 illustrates the recombination probabilities in a succession of two pairs calculated by eqs (3.46–48) for the case of the Δg -mechanism of $S-T_0$ transitions. When the field strength grows, changes of the RP_2 recombination probability are relatively greater than those of RP_1 . In accordance with the qualitative considerations, in the case of a primary singlet pair, an increase in the field intensity, i.e., in the $S-T_0$ transition rate, results in the magnetic effect sign alteration (see, Fig. 3.7(b)). In the case of a triplet RP_1 , the sign is the same in both pairs.

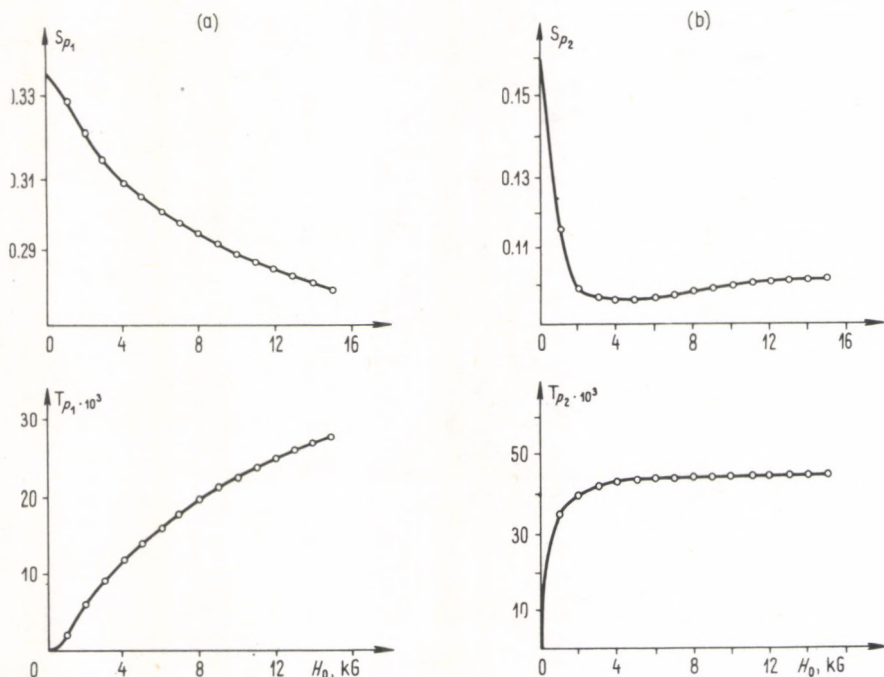


Fig. 3.7. Field dependence of radical recombination probability in the first (p_1) — (a) and the second (p_2) — (b) RP for a singlet and triplet-born RP_1 . RP parameters: $\tau_{D1} = \tau_{D2} = 1$ ns, $\tau_{r1} = \tau_{r2} = 0.1$ ns, $K_{12} = 10^9$ s^{-1} , $K_{s1} = K_{s2} = 0$, $K_1 = K_2 = 10^{10}$ s^{-1} , $\Delta g_1 = \Delta g_2 = 0.1$, $r_0 = b$

3.1.12 Triplet RP recombination

As a rule, a pair recombines only if the radical electrons are in a singlet state. Therefore, the formulas of the present section describe the case of this recombination according to the spin selection rule. However, there are cases when RPs recombine from the triplet state. If only triplet pairs recombine, singlet ones yielding no molecules, all the above formulas are also valid. The only thing one has to do is to exchange the roles of S and T states. For instance, eq. (3.2) gives the geminate recombination probability for a singlet RP precursor in the case of reactive S state. Otherwise, when the T state is reactive, the same eq. (3.2) describes the recombination probability of a triplet-born RP. Such a simple reduction of the equations is possible since in high magnetic fields the singlet RP state can mix only with one of the triplets, T_0 .

In some cases RPs can recombine both in S and T states, it being possible to detect the recombination products separately. For example, sometimes the RP recombination energy is sufficiently high for the molecule to be formed in an electronically-excited singlet or triplet state depending on the RP multiplicity in the reaction layer. The molecule would either fluoresce or phosphoresce respectively. The triplet-excited molecules can have enough time to give their energy to other particles and thus initiate further transformations. Hence, the RP recombination products from singlet and triplet states can be distinguished experimentally.

Below we give the recombination probability of a pair with radicals starting from the recombination radius, i.e., $r_0 = b$. Let the recombination rate constants at the encounter moment in the singlet and triplet states be $K(S)$ and $K(T)$ respectively. When the contributions of all re-encounters by eqs (2.211–214) are summed we obtain the singlet ($p(S)$) and triplet ($p(T)$) product generation probabilities:

$$\begin{aligned}
 p(S) &= \sum_m K(S) \cdot \tau_r \cdot \{ [1 + K(T) \cdot \tau_r] \cdot n_S(m) + \\
 &\quad + z(m) \cdot n \cdot [n_S(m) + n_{T_0}(m)] \} / \Delta(m) \\
 p(T) &= \sum_m K(T) \cdot \tau_r \cdot \{ [1 + K(S) \cdot \tau_r] \cdot n_{T_0}(m) + \\
 &\quad + z(m) \cdot n \cdot [n_S(m) + n_{T_0}(m)] \} / \Delta(m) \\
 &\quad + (n_{T_+} + n_{T_-}) \cdot \frac{K(T) \tau_r}{1 + K(T) \tau_r}, \quad (3.49)
 \end{aligned}$$

where

$$\Delta(m) = [1 + K(S) \cdot \tau_r] \cdot [1 + K(T) \cdot \tau_r] + z(m) \cdot n \cdot [2 + K(S) \cdot \tau_r + K(T) \cdot \tau_r],$$

n is the number of all contacts, $n_S(m)$ and $n_{T_0}(m)$ are the initial state populations of a RP with the nuclear spin configuration $\{m\}$, $z(m)n$ characterizes the efficiency of S– T_0 transitions between all re-encounters and is given by eqs (3.20–32).

For a singlet RP precursor $n_S(m) = 1/\prod_k (2I_k + 1)$, $n_T(m) = 0$, while for a triplet precursor $n_S(m) = 0$, $n_{T_0}(m) = 1/3 \prod_k (2I_k + 1)$. In the case of diffusion pairs $n_S(m) = n_{T_0}(m) = 1/4 \cdot \prod_k (2I_k + 1)$. If $K(T) = 0$, then eq. (3.49) reduces to (3.2, 3, 6, 16–17). Thus, with eq. (3.49) one can analyse magnetic effects and spin polarizations when there are parallel reaction channels both from singlet and triplet RP states.

By way of conclusion, one may say that the theory of magnetic effects in radical recombination has been thoroughly developed for magnetic fields high enough to exceed local hyperfine fields. It predicts the scale and the character of field and magnetic isotopic effects and also the optimum conditions for their experimental observation.

3.2 Radical recombination in low magnetic fields

The in-cage RP singlet–triplet evolution in low fields differs greatly from that in high fields (see Sec. 2.2). In low fields comparable with a local hyperfine field the hf-mechanism is basic for S–T mixing while the Δg -mechanism can manifest itself only in the extreme cases: when either the difference in radical g -values or the hf constants are anomalously great ($\Delta g \approx 1$ or $A \approx 10^3$ G respectively). In low fields the three channels of S–T mixing (S–T₀, T₊, T₋) operate simultaneously, while in high fields only S–T₀ transitions are possible as a rule (Fig. 1.7). Hence, the S–T mixing efficiency in low fields can be expected to decrease with increasing field strength. However, the situation proves to be much more complex. In Section 2.2.4 we have already pointed to the fact that the contributions of S–T mixing channels are nonadditive in a general case [3.3, 25]. In some cases, owing to their interference, the three channels can be even less effective than one S–T₀ channel (see, e.g., eq. (2.107)). The S–T transition efficiency does not then fall continuously with the magnetic field strength but has a maximum. Figure 3.8 depicts such field dependencies of S–T

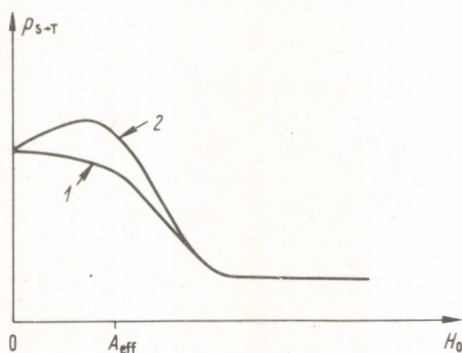


Fig. 3.8. Field dependence of S–T mixing efficiency. Low fields, qualitative picture. 1 — no appreciable effects of S–T channel interference, 2 — pronounced interference effects

transitions in the region of low fields (see also Fig. 2.12). The S-T transitions are less effective at the points of RP energy level crossing, e.g., in a zero magnetic field some levels are crossed.

The channel interference effect is pronounced in the recombination of the simplest RPs with a few magnetic nuclei. In those with a great number of nuclei the interference may become indistinct, and does not appear in radical recombination.

In low fields the kinetic equations for the RP density matrix become much more complex compared with those in high fields (Section 3.1) since in the former case one

has to take into account the transitions between all $4 \cdot \prod_k (2I_k + 1)$ spin states simultaneously because the hf interaction mixes all of them. So far RP recombination has been calculated only for the simplest RPs with one [3.7, 26-28] or two [3.12] magnetic nuclei with 1/2 spins. RPs with a great number of nuclei have been calculated for several concrete systems in the approximations of reaction-independent spin dynamics [3.12] and the semi-classical approach to unpaired electron spin motion [3.29, 30]. Magnetic effects have been estimated for a number of systems by the CKO model and in the one-reencounter approximation [3.5, 25, 31].

3.2.1 The relation between different RP recombination probabilities

As stressed in the preceding section, S-T transitions either accelerate or decelerate the reactions of radical formation and back recombination but do not affect the state of chemical equilibrium. It means that a ratio of type (3.13) must always hold. Thus in low fields, as well as in high ones, the diffusion pair recombination probability, p_r , and the geminate recombination probabilities for singlet, ${}^S p_g$, and triplet, ${}^T p_g$, precursors are interconnected provided the geminate pair is formed at the reaction radius ($r_0 = b$). Hence we have

$${}^S p_g(r_0 = b) = \lambda - 3 \cdot (1 - \lambda) \cdot {}^T p_g(r_0 = b), \quad (3.50)$$

$$\begin{aligned} p_r &= (1/4) \cdot [{}^S p_g(r_0 = b) + 3 \cdot {}^T p_g(r_0 = b)] = \\ &= (\lambda/4) \cdot [1 + 3 \cdot {}^T p_g(r_0 = b)], \end{aligned} \quad (3.51)$$

where $\lambda = K\tau_r / (1 + K\tau_r)$, which are analogous to (3.11, 12). These relations pertain to the situation of the singlet RP state being reactive. Such relations can be readily obtained also for the case of triplet RP recombination. The chemical equilibrium condition then gives

$$p_r / [1 - {}^T p_g(r_0 = b)] = 3 \cdot \lambda_T / 4 \cdot (1 - \lambda_T) = 3 \cdot K_T \cdot \tau_r / 4 \quad (3.52)$$

and for the case of diffusional RP recombination

$$p_r = (1/4) \cdot [{}^S p_g(r_0 = b) + 3 \cdot {}^T p_g(r_0 = b)] = (\lambda_T/4) \cdot [3 + {}^S p_g(r_0 = b)]$$

In eq. (3.52) $\lambda_T = K_T \cdot \tau_r / (1 + K_T \cdot \tau_r)$, K_T is a triplet pair recombination rate constant in the reaction layer. The above relations hold for any kinematics of the in-cage reagent motion and for any values of the exchange integral both for the diffusion and exponential recombination models. With these relations one can calculate, e.g., p_r and ${}^S p_g(r_0 = b)$ using the known values of ${}^T p_g(r_0 = b)$. These allow one to judge the character of the magnetic field dependence upon the RP precursor. Magnetic effects in triplet- and singlet-born RPs must be of opposite in sign. If a magnetic field or the magnetic isotope substitution enhances the recombination probability for a triplet-born RP, then in the case of a singlet-born RP the recombination probability will fall. The sign of the magnetic effect in a diffusion pair recombination must coincide with that of the field effect in geminate recombination products of either triplet or singlet RPs depending on the multiplicity of the state, singlet or triplet leading to recombination.

The scale of magnetic effects must be reactivity dependent. Assume the singlet state to be reactive and geminate pairs to be formed at the recombination radius. In the case of a singlet precursor the magnetic effect must then be the less the higher the reactivity: the radicals are quick to recombine and the S-T evolution cannot occur. However, one must remember an important factor: the recombination probability diminishes with decreasing radical reactivity. Hence though increasing at $K\tau_r$, $\lambda \rightarrow 0$, the magnetic effect is difficult to detect owing to the small product yield.

This is not the case for triplet precursors and diffusion pairs. To understand it, consider eq. (3.50). Remember that λ is the RP recombination probability in the case of a singlet precursor provided there are no S-T transitions. Hence, ${}^S p_g$ is convenient to be presented as a sum of two terms,

$${}^S p_g(r_0 = b) = \lambda + \Delta^S p \quad (3.53)$$

where the second describes the effect of S-T transitions on the reaction. Substitute eq. (3.53) into (3.50, 51) and obtain

$$\begin{aligned} {}^T p_g(r_0 = b) &= -\Delta^S p / 3 \cdot (1 - \lambda), \\ p_r &= \lambda / 4 - \lambda \cdot \Delta^S p / 4 \cdot (1 - \lambda). \end{aligned} \quad (3.54)$$

Hence the magnetic effect in the case of triplet precursors and diffusion pairs may be large enough for highly reactive radicals, when $K\tau_r \gtrsim 1$, $\lambda \rightarrow 1$.

3.2.2 One-nucleus radical pairs with spin $I = 1/2$

This simplest system has been exhaustively studied theoretically. The kinetic equations for the density matrix of this RP have been solved numerically within the continuous diffusion model [3.7, 26-28]. The recombination probability of this RP has been calculated analytically neglecting radical exchange interactions [3.32]. The problem has also been solved by the exponential model of RP recombination [3.8, 17].

The recombination probability neglecting the exchange interactions between re-encounters has been computed by summing up the contributions of all re-encounters [3.32]. Calculations were carried out for arbitrary travel of radicals in an elementary diffusion step. To sum the contributions of all re-encounters to recombination, one must solve the equation of spin motion between these re-encounters and find the operator \hat{F} (2.208). The spin Hamiltonian

$$\hat{H} = \hbar\omega_1 \hat{S}_{1z} + \hbar\omega_2 \hat{S}_{2z} + \hbar a \hat{S}_1 \hat{I} \quad (3.55)$$

mixes the states within the two groups $|S\alpha_n\rangle, |T_0\alpha_n\rangle, |T_+\beta_n\rangle$ and $|S\beta_n\rangle, |T_0\beta_n\rangle, |T_-\alpha_n\rangle$ (here α_n and β_n denote two nuclear spin states). Assume that only singlet RPs can recombine. Eqs (2.207–214) give the formation probability of the product with α_n and β_n nuclear spin orientations. Consider the results for a singlet-born RP in the extreme case of continuous diffusion. The formation probability of β_n -orientated product is

$${}^S p_g(r_0=b, H_0|\beta_n) = (K\tau_r/2) \cdot [3 - A/B + K\tau_r]^{-1}, \quad (3.56)$$

where K is the recombination rate constant of a contact RP, τ_r is the recombination time, A and B are expressed through the parameters of the spin Hamiltonian (3.55) and the in-cage RP lifetime, τ_D :

$$\begin{aligned} A = & 2 + (1/2)\{(4 + \cos^2 \varphi \cdot \sin^2 \varphi) \cdot \vartheta_2 + (1 + 3 \cdot \cos^2 \varphi) \cdot \vartheta_3 + \\ & + (1 + 3 \cdot \sin^2 \varphi) \cdot \vartheta_1 + (2 + \cos^2 \varphi \cdot \sin^2 \varphi) \cdot \vartheta_2^2 + \\ & + (1 + \sin^2 \varphi) \cdot \sin^2 \varphi \cdot \vartheta_1^2 + (1 + \cos^2 \varphi) \cdot \cos^2 \varphi \cdot \vartheta_3^2 + \\ & + (1 + \sin^2 \varphi) \cdot (1 + \sin^2 \varphi \cdot \cos^2 \varphi - \sin^2 \varphi \cdot \text{sign}(H_0)) \cdot \vartheta_1 \cdot \vartheta_2 + \\ & + (1 + 3 \cdot \cos^2 \varphi + \sin^2 \varphi \cdot \cos^4 \varphi) \cdot \vartheta_2 \cdot \vartheta_3 + \\ & + [1 + \sin^2 \varphi \cdot \cos^2 \varphi \cdot (1 + \text{sign}(H_0))] \cdot \vartheta_1 \cdot \vartheta_3 + \\ & + (\vartheta_2 + \cos^2 \varphi \cdot \vartheta_3) \cdot [\vartheta_1 + (1 + \cos^2 \varphi)^2 \cdot \sin^2 \varphi \cdot \vartheta_2] \cdot \vartheta_3/2 + \\ & + (\vartheta_2 + \sin^2 \varphi \cdot \vartheta_1) \cdot [\vartheta_3 + (1 + \sin^2 \varphi)^2 \cdot \cos^2 \varphi \cdot \vartheta_2] \cdot \vartheta_1/2 - \\ & - \sin^6 \varphi \cdot (1 + \cos^2 \varphi) \cdot (1 + \text{sign}(H_0)) \cdot \vartheta_1 \cdot \vartheta_2 \cdot \vartheta_3/2\}; \\ B = & 1 + (2 + \cos^2 \varphi \cdot \sin^2 \varphi) \cdot \vartheta_2/2 + (1 + \sin^2 \varphi) \cdot \vartheta_1/2 + \\ & + (1 + \cos^2 \varphi) \cdot \vartheta_3/2 + (1/2) \cdot \{(1 + \cos^2 \varphi \cdot \sin^2 \varphi) \cdot \vartheta_2^2 + \\ & + \sin^2 \varphi \cdot \vartheta_1^2 + \cos^2 \varphi \cdot \vartheta_3^2 + \vartheta_1 \cdot \vartheta_3 + (1 + \sin^2 \varphi - \sin^6 \varphi - \\ & - \sin^4 \varphi \cdot \text{sign}(H_0)) \cdot \vartheta_1 \cdot \vartheta_2 + (1 + \cos^2 \varphi + \cos^4 \varphi \cdot \sin^2 \varphi) \cdot \vartheta_2 \cdot \vartheta_3\} + \\ & + \cos^2 \varphi \cdot (1 + \sin^2 \varphi)^2 \cdot \vartheta_1 \cdot \vartheta_2^2/4 + \sin^2 \varphi \cdot (1 + \cos^2 \varphi)^2 \cdot \vartheta_2 \cdot \vartheta_3/4 + \\ & + \cos^2 \varphi \cdot \sin^2 \varphi \cdot (1 + \sin^2 \varphi)^2 \cdot \vartheta_1^2 \cdot \vartheta_2/4 + \\ & + \cos^2 \varphi \cdot \sin^2 \varphi \cdot (1 + \cos^2 \varphi)^2 \cdot \vartheta_2 \cdot \vartheta_3^2/4 + \end{aligned} \quad (3.57)$$

$$\begin{aligned}
 & + \sin^2 \varphi \cdot \vartheta_1^2 \cdot \vartheta_3/4 + \cos^2 \varphi \cdot \vartheta_1 \cdot \vartheta_3^2/4 + \\
 & + [1 - \sin^6 \varphi \cdot (1 + \cos^2 \varphi) (1 + \text{sign}(H_0))/2] \cdot \vartheta_1 \cdot \vartheta_2 \cdot \vartheta_3/2 + \\
 & + \cos^2 \varphi \cdot \sin^2 \varphi \cdot \vartheta_2 \cdot \{ \cos^2 \varphi \cdot \vartheta_1 \cdot \vartheta_3^2/2 + \sin^2 \varphi \cdot \vartheta_1^2 \cdot \vartheta_3/2 + \\
 & + \vartheta_1 \cdot \vartheta_2 \cdot \vartheta_3/2 + \cos 2\varphi \cdot \cos^2 \varphi \cdot \sin^2 \varphi \cdot \vartheta_2(\vartheta_3^2 - \vartheta_1^2) \},
 \end{aligned}$$

where

$$\begin{aligned}
 \cos^2 \varphi &= (1/2) \cdot [1 + \omega_1/(\omega_1^2 + a^2)^{1/2}], \\
 \vartheta_1 &= n \cdot \langle 1 - \cos \{ (E_1 - E_2) \hbar^{-1} \cdot t \} \rangle, \\
 \vartheta_2 &= n \cdot \langle 1 - \cos \{ (E_1 - E_3) \hbar^{-1} \cdot t \} \rangle, \\
 \vartheta_3 &= n \cdot \langle 1 - \cos \{ (E_2 - E_3) \hbar^{-1} \cdot t \} \rangle, \\
 \langle \Phi(t) \rangle &\equiv \int \Phi(t) \cdot f(t) dt.
 \end{aligned}$$

Here n is the overall number and $f(t)$ is the distribution function of re-encounters (2.4), E_1, E_2, E_3 are eigenvalues of the spin Hamiltonian (3.55),

$$\begin{aligned}
 E_1 &= -(\hbar/2) \cdot [\omega_2 + a/2 - (\omega_1^2 + a^2)^{1/2}], \\
 E_2 &= -(\hbar/2) \cdot [(\omega_1 - \omega_2)/2 - a/4], \\
 E_3 &= -(\hbar/2) \cdot [\omega_2 + a/2 + (\omega_1^2 + a^2)^{1/2}].
 \end{aligned}$$

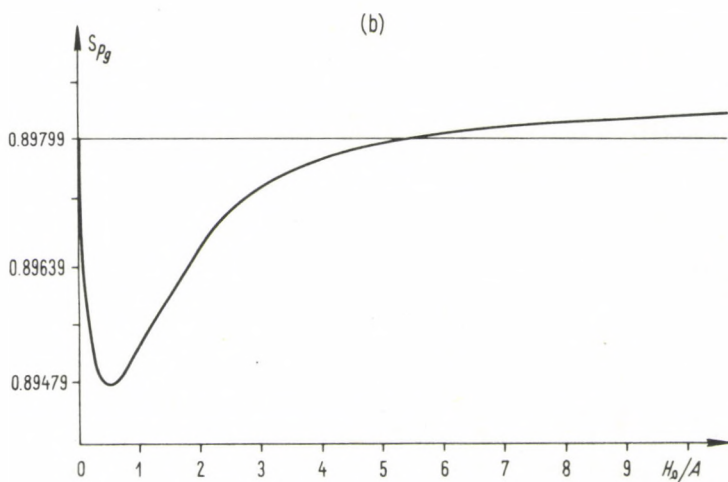
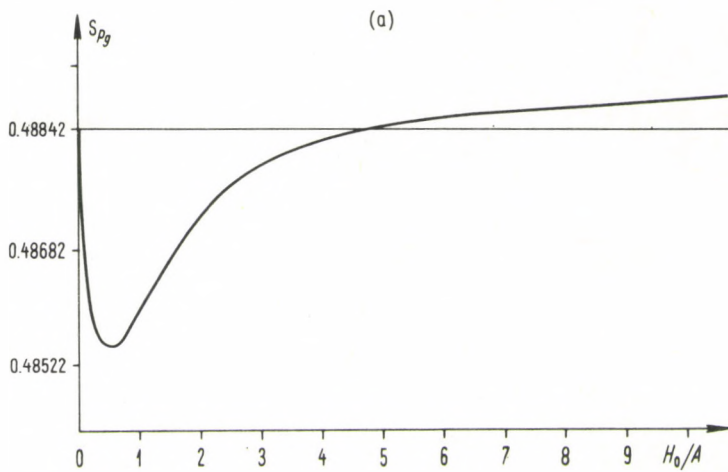
The formation probability of α_n -orientated product is given by relations of type (3.56, 57) with $-H_0$ substituted for H_0 (or $\omega_1 \rightarrow -\omega_1, \omega_2 \rightarrow -\omega_2$):

$${}^S p_g(r_0 = b, H_0 | \alpha_n) = {}^S p_g(r_0 = b, -H_0 | \beta_n). \quad (3.58)$$

The total RP recombination probability is

$${}^S p_g = {}^S p_g(\alpha_n) + {}^S p_g(\beta_n). \quad (3.59)$$

According to eqs (3.56–59) the recombination of a one-nucleus RP depends on the following dimensionless parameters characterizing radical reactivity, hf energy, and external fields: $K\tau_r, H_0/A$, and $|a|\tau_D$. The reaction is independent of the sign of the hf constant. The recombination probability varies with the external field strength. Figure 3.9 depicts the field dependence of the recombination probability of one-nucleus RPs in the case of a singlet precursor for several values of the radical reactivity and the hf constants. It follows that with increasing H_0 the recombination probability first decreases, passes through a minimum, then, with a further increase of the field strength, reaches its extreme value ${}^S p_g(\infty)$ in fields $H_0 \gg A$ which exceeds that in zero magnetic fields. This difference is much smaller than that expected when the field increases from zero to $H_0 \gg A$. Indeed, the hf interaction induces S–T transitions to all the triplet states in zero fields and to only one of these, T_0 , when $H_0 \gg A$. Thus, when the field changes from zero to a thousand gauss, two of the three



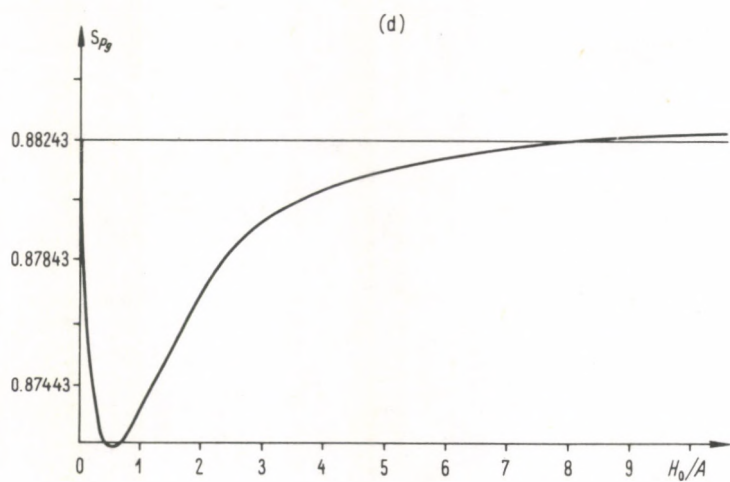
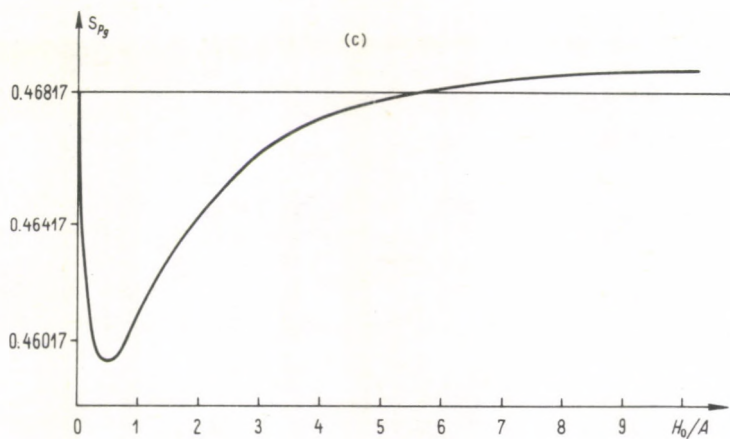


Fig. 3.9. Field dependence of $S_{P_3}(r_0=b)$ for a one-nucleus RP ($I=1/2$) at $\Delta g=10^{-3}$. (a) $a \cdot \tau_D=3.52 \cdot 10^{-2}$, $K \cdot \tau_r=1$; (b) $a \cdot \tau_D=3.52 \cdot 10^{-1}$, $K \cdot \tau_r=10$; (c) $a \cdot \tau_D=3.52 \cdot 10^{-1}$, $K \cdot \tau_r=1$; (d) $a \cdot \tau_D=3.52$, $K \cdot \tau_r=10$

intersystem transition channels are closed. For a singlet-born RP the probability of remaining in the initial state and recombine might be expected to increase. However, this might be not the case. For instance, if $K \cdot \tau_r = 1$ the geminate recombination probability of a singlet-born RP, regardless of S-T transitions, is $S_{p_g} = 0.5$, while if $a \cdot \tau_D = 0.352$ and $H_0 = 0$ we have $S_{p_g} = 0.468$, i.e., S-T transitions cause a 6% reduce in the recombination probability. However, as the field increases, S_{p_g} varies slightly, approximately by 1% (see Fig. 3.9). This can be accounted for by the fact that different S-T channels manifest themselves nonadditively, interfering with each other so that an increase in the number of parallel channels of intersystem transitions does not always add to give the total efficiency of these transitions. This nonadditivity of different S-T channels in low fields has been discussed in detail in ref. [3.25].

Another interesting feature of the field dependence of the one-nucleus RP recombination probability in low magnetic fields is that S_{p_g} changes nonmonotonously with growing field H_0 and has a minimum. This minimum results from the interference of different S-T channels. The field strength at which S_{p_g} is minimum is

Table 3.6. Values of $10^3 \cdot T_{p_g}(r_0 = b)$ [3.28]

H_0, G	$J_0 = 0$	$J_0 \cdot \tau_D = 0.16$	$J_0 \cdot \tau_D = 1.6$	$J_0 \cdot \tau_D = 160$	$J_0 \cdot \tau_D = -1.6$	$J_0 \cdot \tau_D = -160$
0	22.9	22.8	21.8	20.1	23.8	21.0
1	25.4	25.3	24.4	22.4	26.2	23.2
5	28.1	28.1	27.3	24.8	28.7	25.5
10	29.1	29.1	28.4	25.7	29.5	26.2
15	29.0	29.0	28.4	25.7	29.3	26.1
20	28.4	28.4	27.9	25.2	28.6	25.6
25	27.7	27.7	27.3	24.7	27.8	24.9
30	27.0	27.0	26.7	24.1	27.0	24.3
35	26.4	26.4	26.1	23.6	26.4	23.7
40	25.8	25.8	25.6	23.1	25.8	23.2
45	25.4	25.4	25.2	22.7	25.3	22.8
50	25.0	25.0	24.8	22.4	24.9	22.5
55	24.7	24.7	24.5	22.1	24.6	22.2
60	24.4	24.4	24.2	21.9	24.3	21.9
65	24.2	24.2	24.0	21.6	24.1	21.7
70	24.0	24.0	23.8	21.5	23.9	21.5
75	23.8	23.8	23.6	21.3	23.7	21.3
80	23.6	23.6	23.5	21.2	23.5	21.2
85	23.5	23.5	23.3	21.0	23.4	21.1
90	23.4	23.4	23.2	20.9	23.3	21.0
95	23.3	23.3	23.1	20.8	23.2	20.9
100	23.2	23.2	23.0	20.7	23.1	20.8
150	22.7	22.7	22.5	20.2	22.5	20.2

related to the hf constant: $H_{\min} \approx A/2$. The quantity H_{\min} is weakly dependent on the medium viscosity.

In the case of triplet-born and diffusion RPs the recombination probability has a maximum as the field increases to $H_0 \approx A/2$.

The role of the exchange interaction. Kinetic equations for one-nucleus RPs ($I = 1/2$) have been computed numerically with account taken of exchange interactions [3.27, 28]. Table 3.6 lists recombination probabilities of triplet-born RPs with the singlet state reactive. Calculations were performed at $\Delta g = 0$, $a \cdot \tau_D = 0.064$ and $\lambda \approx 1$. The exchange integral depends on the interradsical distance according to

$$J(r) = J_0 \cdot \exp[-5 \cdot \ln 10 \cdot (r-b)/r_e]. \quad (3.60)$$

Calculations were made at $r_e = b$. The comparison of the data obtained at various values of J_0 shows that the exchange interaction does not qualitatively affect the field dependence of the recombination probability (position of the maximum, approximate equality of S-T efficiencies in zero and high fields). The effect is quantitative: the recombination probability changes by 10% compared to the case of $J_0 = 0$. Thus, the exchange interaction in S-T mixing can be neglected accurate to 10% when analyzing magnetic effects since the basic contribution to these effects is made by the re-encounters of radicals after their long diffusion walk at great distances at which the exchange interaction becomes negligible. Note that account taken of the exchange interaction leads to more substantial results in the theory of spin polarization (see below).

The exponential model. The recombination probability for a RP with a spin 1/2 magnetic nucleus has been found by the exponential model in ref. [3.5]. For instance, in zero fields eqs (2.177, 203) yield the following recombination probability for a singlet-born RP

$$\begin{aligned} {}^s p_g(H_0 = 0) = & K\tau_c \cdot [(1 + K\tau_c/2)^2 + (2J_0 + a/2)^2 \tau_c^2 + \\ & + 3 \cdot a^2 \tau_c^2 (1 + K\tau_c/2)/8] / \{ (1 + K\tau_c) \cdot [(1 + K\tau_c/2)^2 + \\ & + (2J_0 + a/2)^2 \tau_c^2] + 3a^2 \tau_c^2 (1 + K\tau_c/2)^2 / 4 \}. \end{aligned} \quad (3.61)$$

For comparison note that the recombination probability for the same RP in fields $H_0 \gg A$ is described by relation (3.32) and equal to

$$\begin{aligned} {}^s p_g(H_0 \gg A) = & K\tau_c \{ 1 + K\tau_c/2 \}^2 + 4J_0^2 \tau_c^2 + \\ & + a^2 \tau_c^2 (1 + K\tau_c/2)/8 \} / \{ (1 + K\tau_c) \cdot [(1 + \\ & + K\tau_c/2)^2 + 4J_0^2 \tau_c^2] + a^2 \tau_c^2 (1 + K\tau_c/2)^2 / 4 \}. \end{aligned} \quad (3.62)$$

The recombination probability in high fields (3.62) increases monotonically with the exchange integral, which corresponds to decreasing efficiency of S-T₀ transitions with growing exchange splitting of the RP terms. In zero field, when J_0 increases, the probability ${}^s p_g$ passes through a minimum at the point $J_0 = -a/4$ if

the hf constant and the exchange integral are of opposite signs. This is associated with the fact that the two RP terms occur at the minimum distance, i.e. their splitting is minimum at this ratio of J_0 and a . Indeed the energy levels of a RP with a spin 1/2 nucleus are

$$\begin{aligned} E_1 &= -J_0\hbar + a\hbar/4, \\ E_2 &= -a\hbar/4 + R\hbar/2, \\ E_3 &= -a\hbar/4 - R\hbar/2; \quad R^2 = 3J_0^2 + (a + J_0)^2. \end{aligned} \quad (3.63)$$

Two two-fold degenerated levels E_2 and E_3 are split by the quantity R which is minimum at $J_0 = -a/4$. As the levels are approaching, when J_0 grows, the efficiency of S-T mixing increases, and this results in a minimum RP recombination probability of a singlet-born RP.

The comparison of eqs (3.61) and (3.62) allows an interpretation of the above field dependence of the recombination probability for one-nucleus RPs (see Fig. 3.9). In zero and high magnetic fields the efficiencies of S-T mixing differ slightly. To simplify the case, set $J_0 = 0$ and assume the radical reactivity to be comparatively low, i.e. $K\tau_c < 1$. Then (3.61) and (3.62) take the form

$$\begin{aligned} {}^s p_g(H_0 = 0) &\approx K\tau_c \cdot [1 - (3/8) \cdot a^2\tau_c^2 / (1 + a^2\tau_c^2)], \\ {}^s p_g(H_0 \gg A) &\approx K\tau_c \cdot [1 - (1/8) \cdot a^2\tau_c^2 / (1 + a^2\tau_c^2/4)], \end{aligned} \quad (3.64)$$

respectively.

The field dependence of intersystem transition effects is of contrary character for short-lived RPs, when $a\tau_c < 1$, and for comparatively long-lived RPs, when $a\tau_c > 1$. Eq. (3.64) shows that for $a\tau_c < 1$ intersystem transitions in zero field are three times more effective than those in high fields. It means that for short-lived RPs S-T transitions to the three triplet states are additive and increase the intensity of S-T mixing with growing number of S-T channels. However, for $a\tau_c > 1$ the three S-T channels in zero field prove to be less effective than one in high fields. In the case of strong interactions, different channels of intersystem transitions are manifested nonadditively, they interfere in a complex manner.

Bearing in mind the above results, consider the diffusion model of RP recombination in a cage characterized by a wide spectrum of in-cage RP lifetimes. When the field changes from zero to high values, the intersystem transition efficiency increases for some RPs and decreases for others, the total change of S-T transition efficiency for the whole RP ensemble being small (see Fig. 3.9).

Thus the weak field dependence of the recombination within the radical free diffusion model is associated with the peculiarities of the simplest RP spin dynamics and those of RP re-encounter statistics (2.4). The increase in the re-encounter probability after a long period of diffusion, e.g., due to the Coulomb radical-ion attraction, can appreciably change the situation and enhance the scale of the magnetic effects.

3.2.3 Other model systems

Werner *et al.* [3.12], using exact kinetic equations have calculated the probabilities of singlet and triplet excited state yields for a RP with each radical carrying a proton at $A=20$ G and 50 G and several values of the magnetic field strength. In the case of a singlet-born RP, the triplet state yield has been shown to decrease by a factor of two in high fields as compared to zero field. For instance, at $A=50$ G, $D=10^{-5}$ cm²/s, $K\tau_r=1$ the probability of triplet product yield is approximately 0.045 in zero field and 0.025 in a field of 200 G.

In the case of a system with an arbitrary number of magnetic nuclei, the spin dynamics can be readily calculated for short-lived RPs (see Sec. 2.2). The efficiency of S-T transitions of these pairs in high fields is one-third of that in zero fields, according to the number of intersystem transition channels working in high and low fields (cf. eqs (2.90) and (2.102)). The S-T mixing is determined by the effective hf constant defined as

$$a_{\text{eff}} = \left\{ (1/3) \cdot \sum_K a_k^2 \cdot I_k \cdot (I_k + 1) \right\}^{1/2}$$

where the summation is performed over all magnetic nuclei. In the case of short-lived RPs the contributions of different channels to S-T transitions are additive. The precise calculation of magnetic effects in low fields in the case of multinuclear systems is very complicated. One therefore has to refer to approximate estimates of the expected effect scale. One approximation that is widely used takes into consideration only one re-encounter at the recombination radius. Table 3.7 lists the values of $^s p_g$ calculated in this way. The magnetic effect is seen to be least for a one-nucleus RP with spin 1/2. For other RPs, the relative change in the recombination probability is of the order of $(a \cdot \tau)^{1/2}$ in high fields as compared to zero one. In common liquids $\tau \approx 10^{-11}$ s. Hence, the relative change of $^s p_g$ is about 10% if $A \approx 100$ G. It is also seen from the table that the singlet-triplet conversion probability is approximately halved (except for one-nucleus RPs with spin 1/2) when the field increases from $H_0=0$ to high values, so for triplet-born RPs the magnetic field effect can be about 100%.

The field dependence of the product yield of radical-ion recombination has been calculated for the system of pyrene-N, N-dimethylaniline in the approximation of assuming reaction-independent RP spin dynamics in a cage [3.12]. Figure 3.10 gives these results. The efficiency of S-T mixing is seen to be twice as low at $H > A_{\text{eff}}$ as compared to zero field. It corresponds to a decreasing number of S-T channels with increasing magnetic field intensity. The effect of interference of different S-T channels is here of less importance than in the case of one-nucleus RPs. Indeed, though nonmonotonic in the vicinity of zero fields, the S-T mixing efficiency shows a less pronounced maximum (Fig. 3.10) than that in the case of a one-nucleus RP (Fig. 3.9).

The effects of the exchange and Coulomb interactions on S-T mixing efficiency within the in-cage radical-ion lifetime have been studied for a RP with each radical

Table 3.7. Recombination probability of model singlet-born RPs in the one-reencounter approximation (see eq. (2.218)). s_{p_0} and s_{p_∞} refer to zero and high magnetic fields respectively. S-T transitions are induced by the hf interaction, $a \cdot \tau < 1$ and λ is singlet RP recombination probability at a single contact

RP	Nuclear spin	s_{p_0}	s_{p_∞}	$1 - s_{p_\infty}/s_{p_0}$
$I^a - R \dots R_1$	arbitrary	$\lambda \cdot (0.31 - [1.20 \cdot I \cdot (I+1)/(2I+1)^2]) \cdot [(2I+1) \cdot a \cdot \tau/2]^{1/2}$	$\lambda \cdot (0.31 - [0.30/(2I+1)]) \cdot \sum_m (a \cdot m \cdot \tau)^{1/2}$	—
$I^a - R \dots R_1$	1/2	$\lambda \cdot (0.31 - 0.22 \cdot (a \cdot \tau)^{1/2})$	$\lambda \cdot (0.31 - 0.21 \cdot (a \cdot \tau)^{1/2})$	$\sim 0.03 \cdot (a \cdot \tau)^{1/2}$
$I^a - R \dots R_1$	1	$\lambda \cdot (0.31 - 0.32 \cdot (a \cdot \tau)^{1/2})$	$\lambda \cdot (0.31 - 0.20 \cdot (a \cdot \tau)^{1/2})$	$\sim 0.4 \cdot (a \cdot \tau)^{1/2}$
$I_1^a - R^a - I_2 \dots R_1$	1/2	$\lambda \cdot (0.31 - 0.24 \cdot (a \cdot \tau)^{1/2})$	$\lambda \cdot (0.31 - 0.15 \cdot (a \cdot \tau)^{1/2})$	$\sim 0.3 \cdot (a \cdot \tau)^{1/2}$
$I_1 \begin{matrix} a \\ \searrow \\ R \\ \nearrow \\ a \end{matrix} - I_3 \dots R_1$	1/2	$\lambda \cdot (0.31 - 0.31 \cdot (a \cdot \tau)^{1/2})$	$\lambda \cdot (0.31 - 0.24 \cdot (a \cdot \tau)^{1/2})$	$\sim 0.2 \cdot (a \cdot \tau)^{1/2}$
$I_1^a - R \begin{matrix} -a \\ \searrow \\ I_2 \\ \nearrow \\ a \end{matrix} \dots R_1$	1/2	$\lambda \cdot (0.31 - 0.30 \cdot (a \cdot \tau)^{1/2})$	$\lambda \cdot (0.31 - 0.15 \cdot (a \cdot \tau)^{1/2})$	$\sim 0.5 \cdot (a \cdot \tau)^{1/2}$
$I_1^a - R \dots R_1 - I_2^a$	1/2	$\lambda \cdot (0.31 - 0.30 \cdot (a \cdot \tau)^{1/2})$	$\lambda \cdot (0.31 - 0.15 \cdot (a \cdot \tau)^{1/2})$	$\sim 0.5 \cdot (a \cdot \tau)^{1/2}$
$I_1 \begin{matrix} a \\ \searrow \\ R \\ \nearrow \\ a \end{matrix} \dots R_1 \begin{matrix} a \\ \searrow \\ I_3 \\ \nearrow \\ a \end{matrix}$	1/2	$\lambda \cdot (0.31 - 0.34 \cdot (a \cdot \tau)^{1/2})$	$\lambda \cdot (0.31 - 0.20 \cdot (a \cdot \tau)^{1/2})$	$\sim 0.5 \cdot (a \cdot \tau)^{1/2}$

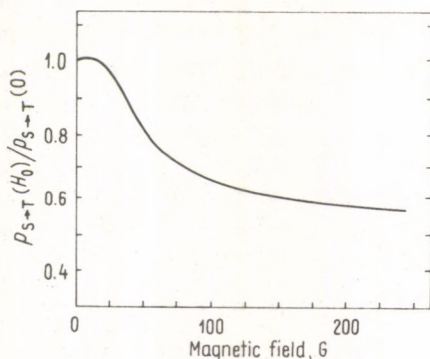


Fig. 3.10. Magnetic field dependence of the relative S-T mixing efficiency in the pair ${}^2\text{P}_y^{\pm} + {}^2\text{DMA}^{\pm}$ [3.12]

carrying one proton [3.12]. The exchange interaction was shown to reduce (to 30%) the S-T mixing efficiency, the exchange interaction effect increasing with diminishing solvent polarity. This can be attributed to the fact that in nonpolar media the Coulomb radical-ion attraction enhances the time the partners reside in the region of strong exchange interaction. In polar solvents ($\epsilon \gtrsim 30$) the exchange interaction effect is negligible. Hence one can conclude that the exchange interaction must not influence magnetic effects in neutral (uncharged) radical recombination. It agrees also with the data on a one-proton RP (see Table 3.6).

3.2.4 The semi-classical theory of magnetic effects in the recombination of radicals with a large number of magnetic nuclei

An exact solution of the density matrix for a RP with a large number of magnetic nuclei in low fields practically cannot be obtained in practice even with a computer. Therefore, to study magnetic effects in such systems, one has to use the semiclassical approximation proposed by Schulten and Wolynes [3.33]. With this technique it is possible to calculate singlet-triplet transition dynamics in any magnetic field.

The RP recombination probability has been calculated numerically in the semiclassical description of S-T transition dynamics under the assumption of recombination-independent spin dynamics [3.29].

The foregoing discussion shows the exchange interaction to be of small importance for magnetic effects and thus can be neglected. It allows one to calculate magnetic effects by summing up all the re-encounter contributions (see (2.213, 214)).

Summation of all re-encounter contributions [3.30]. First of all one must find the spin evolution operator \hat{F} (2.208) between radical re-encounters. The whole RP

ensemble is divided into subensembles corresponding to different nuclear spin configurations. In a given subensemble each radical has a definite longitudinal (along the external field direction) and transverse projections of the local hf field (2.115–121). $\hat{F}(t)$ is found for each subensemble from equations (2.121–129). The operator $\hat{F}(t)$ depends on the value and orientation of the local hf field of both partners ($H_{11}, \vartheta_1, \varphi_1$) and ($H_{12}, \vartheta_2, \varphi_2$). One averages $\hat{F}(t)$ over the azimuthal angles φ_1 and φ_2 and obtains $\hat{F}(t)$ for a RP subensemble with specified H_{11}, H_{12} and ϑ_1, ϑ_2 (see (2.115)). The S and T state populations in a RP subensemble between re-encounters (after averaging over φ_1, φ_2) obey the relations

$$\begin{pmatrix} \rho_{SS}(t) \\ \rho_{T_0T_0}(t) \\ \rho_{T_+T_+}(t) \\ \rho_{T_-T_-}(t) \end{pmatrix} = \begin{pmatrix} F_{11} & F_1 & F_2 & F_2 \\ F_1 & F_{11} & F_2 & F_2 \\ F_2 & F_2 & F_{33} & F_3 \\ F_2 & F_2 & F_3 & F_{33} \end{pmatrix} \begin{pmatrix} \rho_{SS}(0) \\ \rho_{T_0T_0}(0) \\ \rho_{T_+T_+}(0) \\ \rho_{T_-T_-}(0) \end{pmatrix} \quad (3.65)$$

where F_1, F_2 and F_3 are probabilities of S–T₀, S–T₊, T₋ and T₊–T₋ transitions respectively, $F_{11} = 1 - F_1 - 2F_2$, $F_{33} = 1 - 2F_2 - F_3$,

$$F_1 = n_{1z}^2 \cdot s_1^2 \cdot c_2^2 + n_{2z}^2 \cdot c_1^2 \cdot s_2^2 + n_1^2 \cdot n_2^2 \cdot s_1^2 \cdot s_2^2 / 2 - 2 \cdot n_{1z} \cdot n_{2z} \cdot c_1 \cdot s_1 \cdot c_2 \cdot s_2,$$

$$F_2 = (1/2) \cdot [n_1^2 \cdot s_1^2 \cdot (c_2^2 + n_{2z}^2 \cdot s_2^2) + n_2^2 \cdot s_2^2 \cdot (c_1^2 + n_{1z}^2 \cdot s_1^2)],$$

$$F_3 = n_1^2 \cdot n_2^2 \cdot s_1^2 \cdot s_2^2;$$

and

$$s_k = \sin \{ \omega_k \cdot t / 2 \}, \quad c_k = \cos \{ \omega_k \cdot t / 2 \},$$

$$n_{kz} = (\omega_{0k} + \omega_{lk} \cdot \cos \Theta_k) / \omega_k, \quad n_k = \omega_{lk} \cdot \sin \Theta_k / \omega_k,$$

$$\omega_k = [(\omega_{0k} + \omega_{lk} \cdot \cos \Theta_k)^2 + \omega_{lk}^2 \cdot \sin^2 \Theta_k]^{1/2},$$

ω_{0k} is the Zeeman frequency of unpaired electrons, ω_{lk} is the precession frequency in a local hf field, ω_k is the precession frequency in the total external and local fields (cf. (2.118)).

Substituting (3.65) into (2.213, 214) and averaging it over all possible values of H_{lk} , Θ_k with the distribution function (2.116) gives the recombination probability. For the sake of simplicity assume the radicals to be in a contact at the starting moment, i.e. the initial interradical distance equals the recombination radius b . Below are the final expressions pertaining to the following cases: a triplet-born RP with the singlet state being reactive, ${}^1p_g(S)$, and vice versa a singlet-born RP with a reactive triplet state, ${}^3p_g(T)$. The recombination probability for other plausible situations can be found by relations (3.50–52).

Thus, we obtain the following results [3.30]

$${}^1p_g(S) = \langle {}^1p_g(\vec{H}_{11}, \vec{H}_{12} | S) \rangle,$$

$${}^3p_g(T) = \langle {}^3p_g(\vec{H}_{11}, \vec{H}_{12} | T) \rangle; \quad (3.66)$$

$$\langle \Phi \rangle = \int \dots \int \Phi \cdot \varphi(H_{11}) \cdot \varphi(H_{12}) \cdot \sin \Theta_1 \cdot \sin \Theta_2 \cdot dH_{11} \cdot dH_{12} \cdot d\Theta_1 \cdot d\Theta_2$$

where the corresponding recombination probabilities for a RP subensemble are governed by the expressions

$$\begin{aligned}
 {}^1P_g(\vec{H}_{11}, \vec{H}_{12}|S) &= (1/3) \cdot K\tau_r \cdot (1-F)/(1+K\tau_r F), \\
 F &= (1/4) \cdot \{1 + 1/(1+4\bar{F}_2) + 2/[1+2(\bar{F}_1 + \bar{F}_2)]\}, \\
 {}^3P_g(\vec{H}_{11}, \vec{H}_{12}|T) &= K\tau_r \cdot (1-\tilde{F})/[1+K\tau_r \cdot (1-\tilde{F})], \\
 \tilde{F} &= (1/4) \cdot \{1 + 1/(1+4\tilde{F}_2) + 2/[1+2(\tilde{F}_1 + \tilde{F}_2)]\}, \\
 \tilde{F}_k &= F_k/(1+K\tau_r).
 \end{aligned} \tag{3.67}$$

Here \bar{F}_1 and \bar{F}_2 are the probabilities of S-T₀ and S-T₊, T₋ transitions averaged over time intervals between re-encounters,

$$\begin{aligned}
 4 \cdot \bar{F}_2 &= n_1^2 \cdot n_{2z}^2 \cdot b_1 + n_2^2 \cdot n_{1z}^2 \cdot b_2 + n_1^2 \cdot n_2^2 \cdot (b_3 + b_4)/2, \\
 2 \cdot (\bar{F}_1 + \bar{F}_2) &= [n_2^2 \cdot (1 + n_{1z}^2) \cdot b_1 + n_1^2 \cdot (1 + n_{2z}^2) \cdot b_2]/4 + \\
 &+ (1 + n_{1z}^2) \cdot (1 + n_{2z}^2) \cdot (b_3 + b_4)/8 + n_{1z} \cdot n_{2z} \cdot (b_3 - b_4)/2, \\
 b_1 &= (\omega_1 \cdot \tau_D/2)^{1/2}, & b_2 &= (\omega_2 \cdot \tau_D/2)^{1/2}, \\
 b_3 &= (|\omega_1 - \omega_2| \tau_D/2)^{1/2}, & b_4 &= ((\omega_1 + \omega_2) \cdot \tau_D/2)^{1/2}.
 \end{aligned}$$

The recombination probabilities depend on the overall time of all re-encounters, τ_r , and the in-cage RP lifetime, τ_D .

In that way the recombination probability of RPs with a large number of magnetic nuclei in any magnetic field can be presented in terms of the semi-classical approximation as definite integrals. As an example, Fig. 3.11 gives field dependencies of RP recombination probabilities calculated by the above formulas. In low fields the S-T transition efficiency is seen to reduce continuously with the external field strength. It is attributed to the reduction of the number of intersystem transition channels (cf. Fig. 3.8, curve 1). Figure 3.11 also shows that the interference of transition channels is not so effective in complex RPs with a large number of magnetic nuclei. In high fields, $H_0 \gg H_l$, the efficiency of S-T transitions begins increasing again (see Fig. 3.11b), this being associated with the Δg -mechanism.

The foregoing results allow one to state the basic principles of the low field magnetic effect theory. When the external field begins to exceed local hf fields, the S-T₊, T₋ channels are closed and only the S-T₀ channel is effective if there is a further increase in the external field strength. In fields $H_0 \gtrsim H_{loc}$ the efficiency of S-T transitions due to the hf-mechanism decreases. When $H_0 < H_{loc}$ the radical recombination probability of complex RPs with a large number of magnetic nuclei is virtually field independent. However, in simple systems with few magnetic nuclei in fields $H_0 \lesssim H_{loc}$ the singlet-triplet evolution is appreciably affected by the interference of different S-T channels. As a result, the S-T mixing efficiency has a maximum in fields $H_0 \approx H_{loc}$. The above calculations demonstrate that in low fields

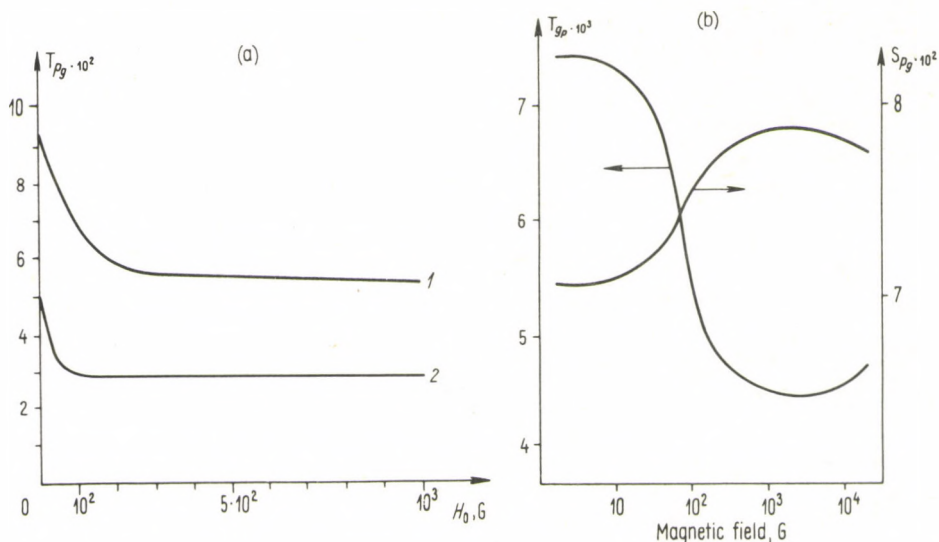


Fig. 3.11. Field dependence of recombination probability. The singlet RP state is assumed to be reactive. (a) A triplet-born pair of completely protonated, 1, and deuterated, 2, benzyl and alkyl radicals ($K \cdot \tau_r = 10$, $\tau_D = 1$ ns, hf constants given in Fig. 2.8); (b) a triplet and singlet-born pair of radicals with $\Delta g = 2 \cdot 10^{-3}$; $A_{1,\text{eff}} = 9.5$ G; $A_{2,\text{eff}} = 24.85$ G; $K \cdot \tau_r = 0.1$, $\lambda = 0.09090$; $\tau_D = 1$ ns

the recombination probability of a singlet-born RP can increase approximately by 1–10% with the external field intensity at typical values of molecular kinetic parameters. The field effects can be especially high (about 10–100%) in the case of a triplet-born RP.

3.3 The magnetic isotope effect

The theory presented in the above two sections shows that magnetic isotope effects must arise in radical recombinations. Indeed, the hf interaction of unpaired electrons with magnetic nuclei is one of the basic (in low fields practically the only) mechanisms of RP singlet–triplet transitions. Isotope substitution can change the hf interaction and consequently the recombination probability. For instance, with *D* substituted for *H*, the hf energy is reduced to approximately one-quarter and the S–T transition efficiency reduces. One more example is the pair of isotopes ^{12}C and ^{13}C ; the former is nonmagnetic, the latter has a magnetic moment ($I = 1/2$). Hence, S–T transitions will occur only in pairs containing the ^{13}C isotope (assuming the RP does not contain any other nuclei and the Δg -mechanism is ineffective: either $\Delta g = 0$ or $H_0 \lesssim A$).

3.3.1 Qualitative considerations

Magnetic isotope effects depend upon many factors. Above all, the most important is the change in the hf energy (the hf constants and the nuclear spin value) induced by isotope substitution. The greater the hf energy change, the stronger the isotope effect. At the same time, the scale of the magnetic effect is strongly dependent on parameters characterizing radical reactivity and mobility and also on the RP precursor multiplicity. The probabilities of geminate and diffusion RP recombinations are connected by relations (3.50–52). An increase in the medium viscosity enhances the RP in-cage lifetime, τ_D . As a result, the S–T mixing efficiency during random diffusion walk of the partners between re-encounters and thus the scale of magnetic isotope effect is expected to grow. This is however not always the case. The fact is that radical recombination time increases with the medium viscosity too, which is formally equivalent to an increase of radical reactivity since the recombination probability depends on the product of τ_r and the pseudo first-order rate constant, K , of the RP reaction in the recombination layer. Relations (3.50–52) show that S–T transition effects on radical recombination depend on RP recombination probability, with spin effects neglected, i.e. on

$$\lambda = K\tau_r / (1 + K\tau_r).$$

For instance, the singlet RP state being reactive, the isotope effect in the case of a triplet-born RP must be stronger for radicals with high enough reactivity.

The effect under discussion is determined by changes of the total hf energy induced by isotope substitution. It is strong under isotope substitution of either all the nuclei of a RP (for instance, the total deuteration of molecules) or one or several nuclei making the principal contribution to the hf interaction. The effect will be small provided the hf interaction is negligibly affected by isotope substitution.

Magnetic effects are also dependent on the external field strength. However, the problem of the scale of the magnetic isotope effect in the earth's field, the field in which chemical reactions are commonly carried out in, is of particular interest. From the viewpoint of the magnetic phenomenon discussed, the earth's magnetic field can be set equal to zero to a good approximation.

3.3.2 Magnetic isotope effect in zero magnetic field

Magnetic effects observed in one-nucleus RPs with $I = 1/2$ are most exhaustively studied. Table 3.8 lists the recombination probabilities of this simplest system in zero field, the singlet RP state being considered reactive. The quantity λ (the fourth column) is the recombination probability of a singlet-born RP having no magnetic isotope. The quantity $(\lambda - s_p)/\lambda$ characterizes relative changes of a singlet-born RP recombination probability under isotope substitution (the fifth column). In the case of a triplet precursor, a pair of radicals with a nonmagnetic isotope does not

Table 3.8. Magnetic isotope substitution effects on one-nucleus ($I=1/2$) RP recombination in zero magnetic field

$ a \cdot \tau_D$	$K \cdot \tau_r$	s_{p_g}	λ	$(1 - \frac{s_{p_g}}{\lambda}) \cdot 100\%$	τ_{p_g}	p_r
$3.52 \cdot 10^{-2}$	1	0.48842	0.5	2.3164	$7.720 \cdot 10^{-3}$	0.12789
$3.52 \cdot 10^{-1}$	10	0.89799	0.909091	1.2211	$4.0703 \cdot 10^{-2}$	0.25502
$3.52 \cdot 10^{-1}$	0.01	0.0087263	$9.90099 \cdot 10^{-3}$	11.864	$3.9548 \cdot 10^{-4}$	$2.4782 \cdot 10^{-3}$
$3.52 \cdot 10^{-1}$	1	0.46817	0.5	6.366	0.02122	0.13296
$3.52 \cdot 10^{-1}$	10	0.89799	0.90909	1.2211	$4.0703 \cdot 10^{-2}$	0.25502
$3.52 \cdot 10^{-1}$	10,000	0.99989	0.9999	$1.0014 \cdot 10^{-3}$	$3.3373 \cdot 10^{-2}$	0.27500
3.52	10	0.88243	0.90909	2.9327	$9.7757 \cdot 10^{-2}$	0.29392
3.52	100	0.98685	0.990099	0.32815	0.10938	0.32875
5.6	1	0.41906	0.5	16.188	0.05396	0.14523
5.6	10	0.87825	0.90909	3.3925	0.11308	0.30437
35.2	1000	0.99839	0.99900	$6.1166 \cdot 10^{-2}$	0.20390	0.40252
56	10	0.85722	0.90909	5.7058	0.19020	0.35695
56	100	0.98362	0.990099	0.65438	0.21812	0.40949
560	1000	0.99814	0.99900	$8.6188 \cdot 10^{-2}$	0.28731	0.46502

recombine at all. Hence, τ_{p_g} (the sixth column) shows the magnitude of the isotope effects.

The isotope effect of a one-nucleus RP in zero field is determined by two parameters, $|a| \cdot \tau_D$ and $K \cdot \tau_r$. The data of Table 3.8 confirm the above considerations on the influence of reactivity, viscosity, and hf constants upon magnetic isotope effects.

Table 3.8 shows that the isotope effect can reach about 10% in the case of a singlet-born RP. The isotope substitution effect on RP recombination is especially strong in the case of a triplet precursor.

Magnetic isotope effects in more complex systems can be estimated by the exponential recombination model or the diffusion model taking into consideration one re-encounter. Similar estimates can be made for any RP provided it is possible to solve the dynamic equations for its singlet-triplet transitions. An example of such systems is a RP with both radicals having equivalent magnetic nuclei (see Sec. 2.2). The isotope effects can thus be evaluated by, e.g., the formulas given in Table 3.7. In a singlet-born RP recombination these are seen to reach some 10% at quite realistic values of the parameters, $A \approx 10$ G, $\tau \approx 10^{-11}$ s.

In the case of a RP with many magnetic nuclei, isotope effects can be calculated by the semi-classical theory. Table 3.9 lists some of these calculations. In the semi-classical approximation the hf interaction with all radical nuclei is characterized by an effective constant A_{eff} . For instance, A_{eff} is reduced to one-quarter when D is substituted for H . When the deuteration is partial, A_{eff} reduces to a smaller extent. Table 3.9 gives the recombination probabilities for a number of effective hf constants, and they confirm the reliability of qualitative conclusions on the dependence of magnetic isotope effects upon radical molecular kinetic parameters.

Table 3.9. Effects of the hf interaction on RP recombination probability in zero magnetic field in the case of multinuclear radicals

$(a_{\text{eff}})_1 \cdot \tau_D$	$(a_{\text{eff}})_2 \cdot \tau_D$	$K \cdot \tau_r(\lambda)$	${}^S p_g(r_0=b)$	${}^T p_g(r_0=b)$	$p_r(\lambda/4)$
0.29	0.5	5 (0.833)	0.788	0.0901	0.265 (0.208)
0.18	0.09	1 (0.5)	0.452	0.0320	0.137 (0.125)
0.22	0.01	10 (0.909)	0.890	0.0691	0.274 (0.227)
0.22	3.97	10 (0.909)	0.853	0.205	0.367 (0.227)
5.8	5	5 (0.833)	0.727	0.211	0.340 (0.208)
11.6	10	5 (0.833)	0.705	0.256	0.368 (0.208)
0.17	0.44	0.1 (9.09 · 10 ⁻²)	7.07 · 10 ⁻²	7.39 · 10 ⁻³	2.32 · 10 ⁻² (2.27 · 10 ⁻²)
0.29	0.44	0.1 (9.09 · 10 ⁻²)	7.00 · 10 ⁻²	7.66 · 10 ⁻³	2.32 · 10 ⁻² (2.27 · 10 ⁻²)
0.25	0.44	10 (0.909)	0.883	9.54 · 10 ⁻²	0.292 (0.227)

3.3.3 Field dependence of the magnetic isotope effect

When the reaction is carried out in a magnetic field, the effects of external and local hf fields manifest themselves simultaneously, both effects overlapping.

In high magnetic fields ($H_0 > A_{\text{eff}}$) the theory described in Section 3.1 allows one to make precise calculations of the magnetic isotope effect. For example, let us consider a RP with coinciding radical Larmor frequencies, the hf interaction, e.g., with one nucleus, being the only S-T₀ mechanism. Then from (3.6) we obtain

$$p_r = K\tau_r \cdot [1 + (|a| \cdot \tau_D/4)^{1/2}]/2 \cdot \{2(1 + K\tau_r) + [2 + K\tau_r \cdot (|a| \cdot \tau_D/4)^{1/2}]\}.$$

Using this relation one can calculate the magnetic isotope effect. High external fields have no influence on the isotope effect if the radical g -values are equal. Otherwise, the role of the Δg -mechanism of S-T transitions increases with the field and thus the hf mechanism becomes of less importance in the RP recombination. Accordingly, magnetic isotope effects reduce with increasing H_0 .

The situation is more complex in low fields, fields comparable to the hf interaction. In the case of a one-nuclear RP with $I = 1/2$, the magnetic isotope effect is practically field independent since the external field only weakly affects radical recombination (see Section 3.2). Consider, for instance, the data given in Fig. 3.9 (a). A magnetic isotope is seen to reduce by 0.01158 ($\approx 2\%$) the recombination probability in zero field. As the field increases, S-T mixing in a RP with a magnetic isotope is maximum in fields $H_0 \approx A/2$, changes of the isotope effects at a varying external field being, however, one order of magnitude less than the magnitude of the effect itself. The recombination probability in fields $H_0 \approx A/2$ differs from that at $H_0 = 0$ by a small quantity of the order of 10^{-3} .

An external field can sometimes influence the magnetic isotope effect even in the case of a one-nucleus RP with $I = 1/2$ in the framework of free diffusion of radicals. For illustration, Fig. 3.12 compares recombination probabilities of RPs with nonmagnetic and magnetic isotopes with large hf constants.

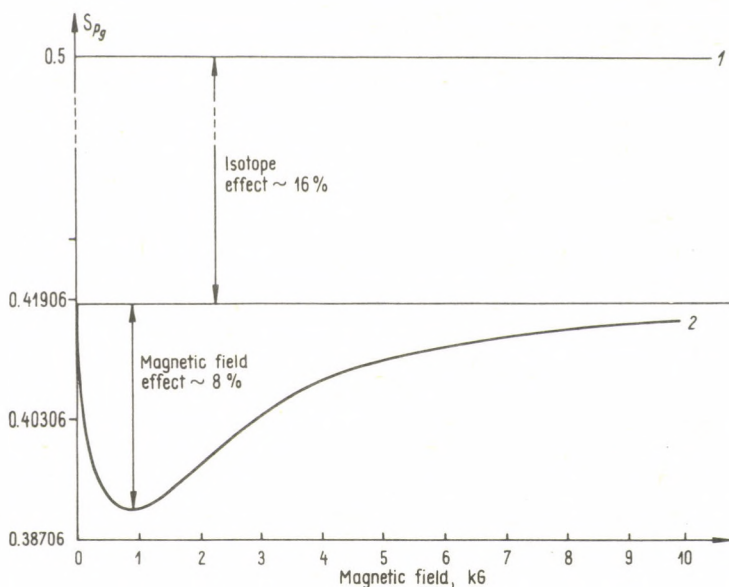


Fig. 3.12. Field dependence of radical recombination probability for a RP with nonmagnetic, 1, and magnetic, 2, isotope. $A = 1600$ G, $I = 1/2$, $K \cdot \tau_r = 1$, $\tau_D = 10^{-10}$ s, $\Delta g = 10^{-3}$

In the case of a multinuclear or even one-nucleus RP (with $I > 1/2$), an external field appreciably affects RP recombination. Therefore, the magnetic isotope effects in these systems can be strongly dependent on the external field strength (see Section 3.2).

The earth's field or that comparable to a local hf field can be optimum for revealing isotope effects, depending on the reaction. Consider some possibilities. Suppose there is a RP with negligibly small hf interaction. The combination probability of this RP is field independent. (Remember that we are speaking of comparatively low fields when the Δg -mechanism is not effective.) Assume isotope substitution takes place either in one or both radicals and results in an appreciable increase in the hf interaction. In this pair the S-T transitions become field dependent. S-T transitions in multinuclear RPs are most effective in zero field. As a result, in the case the strongest isotope effect is observed in zero field.

Figure 3.12 illustrates another possibility when the isotope effect is strongest not in zero but in some intermediate fields.

Consider one more example in which the magnetic isotope effect manifests itself more strongly in moderate fields. For instance, Fig. 3.11 (a) and 13 depict changes in the recombination probability of a pair of benzyl and alkyl radicals with D substituted for H . The isotope effect is seen to reach a maximum with increasing external field. This can be interpreted as follows⁴. The effective hf interaction in a

⁴ Haberkorn [3.34] pointed to the appearance of this type maximum.

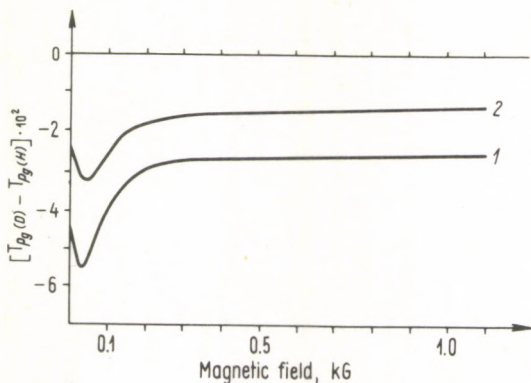


Fig. 3.13. H - D substitution effects on benzyl and alkyl radicals recombination probability. Effective hf constants A_{eff} in protonated radicals are 12.5 and 24.8 G, respectively. The other RP parameters: $K \cdot \tau_r = 10$, $\tau_D = 10^{-9}$ s, $\Delta g = 0$. Curves 1 and 2 are referred to completely deuterated radicals and deuterated alkyl radical of the pair respectively. The recombination probability of the completely protonated RP is shown in Fig. 3.11

deuterated radical is one-quarter of that in a protonated one. Therefore fields H_0 can be subdivided into three regions. In fields $H_0 < (A_{\text{eff}})_D$ the effective S - T mixing takes place in all the three S - T_0 , T_+ , T_- channels in protonated and deuterated pairs. In fields $(A_{\text{eff}})_D < H_0 < (A_{\text{eff}})_H$ all the three S - T channels still work in a protonated pair, while in a deuterated one we observe the situation of high fields, i.e. the only the S - T_0 channel remains. As a result, the difference in S - T transition efficiencies of protonated and deuterated pairs is higher in this region of H_0 than in zero fields, i.e. the isotope effect increases. With a further increase in the field, when $H_0 > (A_{\text{eff}})_H$, the S - T_+ , T_- channels of a protonated pair are closed. In this region both pairs obey the conditions of high fields, S - T transition efficiencies of both RPs being less than those in zero fields. As a result, in high fields the isotope effect is also less than that in zero field.

Thus, in systems with a sufficiently great number of magnetic nuclei the greatest isotope effect is to be expected in moderate fields either smaller than or of the order of a local hf field.

Let us try to briefly summarize the results on the theory of magnetic effects in radical recombination. Important qualitative results have been obtained and appreciable progress has been made in the development of a quantitative theory. Theory predicts that an external magnetic field and magnetic isotope substitution will change the RP recombination probability by an order of 0.01-0.1 with typical values of molecular kinetic and spin parameters of radicals. Of course, much is still to be done in the development of the quantitative theory, especially in the case of radicals with few magnetic nuclei, and with charged particles. However, the present state of the theory can serve as a good basis for development of both theoretical and experimental studies of magnetic effects both in radical recombination and in reactions involving other paramagnetic particles.

4 THE THEORY OF CHEMICALLY INDUCED DYNAMIC NUCLEAR AND ELECTRON SPIN POLARIZATIONS

Spin polarization in reactions originates from the same singlet-triplet transitions during a RP in-cage lifetime that are responsible for the external and local magnetic field effects on radical recombination (see Section 3). The present section treats the basic data of CIDNP and CIDEF theories.

4.1 Phenomenological description and spectroscopic manifestation of CIDNP and CIDEF

The appearance of NMR or ESR spectra from chemical reactions shows that in diamagnetic reaction products or in reactive intermediates—free radicals—the spin state population is in disequilibrium. Spin polarizations can be observed in chemical reactions proceeding under either pulse initiation of reaction or steady-state conditions. In reactions under flash irradiation CIDNP and CIDEF effects can be observed immediately after the light is switched off. Relaxation times of the nuclear spin state populations are of the order of seconds for diamagnetic molecules and of the order of microseconds for radicals in liquids. Within these times, either nuclear or electron polarizations respectively, are conserved. If the reaction proceeds under stationary conditions then, on the one hand, chemically induced spin polarizations arise and, on the other hand, paramagnetic relaxation processes tend to restore the equilibrium polarization values. It results in a certain steady-state level of nuclear and electron spin polarizations.

There are two types of chemically induced spin polarization effects: net and multiplet. In concrete systems they are manifested either separately or simultaneously.

4.1.1 Net polarization effects

Net CIDNP and CIDEF effects arise if there is a predominance of orientations of the nuclear spins in the reaction products (or those of electron spins in radicals) either along or opposite the external field direction. The Zeeman spin energy can serve as a measure of the net effect. When in thermodynamic equilibrium, spins

occupy preferably the more favourable states, therefore, the Zeeman spin energy is negative. If this energy becomes positive during the reaction, the spin system can later on release the accumulated energy. In this case one can observe induced or spontaneous radiation at the magnetic resonance frequency. If during the reaction the Zeeman spin energy reduces, i.e., the reservoir of the Zeeman spin interaction is cooled, then in order to heat the spin system up to the thermostat temperature, it should be supplied with some additional energy. Certain lines conforming to an anomalously large absorption would be then observed in the magnetic resonance spectra.

In Section 2.3 we have introduced density matrices of the nuclear spins in the radical recombination products, σ (see, e.g., eqs (2.172, 178, 182)) and those of the unpaired electrons of A and B radicals escaping the in-cage recombination, σ_A , σ_B (see e.g., eqs (2.174, 178, 182)). With these matrices the Zeeman energy of the nuclear spin, I , and that of the electron spins of two partners, the radicals A and B , are calculated by the formulas

$$\begin{aligned} E_{zI} &= -g_I \cdot \beta_I \cdot H_0 \cdot \text{Tr}_I \{ \sigma \hat{I}_z \} \equiv -g_I \cdot \beta_I \cdot H_0 \cdot \langle \hat{I}_z \rangle, \\ E_{zS_A} &= g_{eA} \cdot \beta_e \cdot H_0 \cdot \text{Tr}_{S_A, I} \{ \sigma_A \hat{S}_{Az} \} \equiv g_{eA} \cdot \beta_e \cdot H_0 \cdot \langle \hat{S}_{Az} \rangle, \\ E_{zS_B} &= g_{eB} \cdot \beta_e \cdot H_0 \cdot \text{Tr}_{S_B, I} \{ \sigma_B \hat{S}_{Bz} \} \equiv g_{eB} \cdot \beta_e \cdot H_0 \cdot \langle \hat{S}_{Bz} \rangle. \end{aligned} \quad (4.1)$$

If the Zeeman energy remains negative during the process of chemical polarization, as in the equilibrium situation, this polarization is called *positive*. In terms of spin level populations it corresponds to an increase in the populations difference of the lower and the upper levels. If the Zeeman energy becomes positive, the spin polarization is *negative*, the spin levels are inversely populated: the upper excited spin states are more populated than the lower ones. Figure 1.9 shows spectra of E and A types conforming to negative and positive polarizations. In radical reactions one observes anomalously large population differences as compared to the equilibrium case. For example, in a magnetic field of about 10^4 G at room temperatures, the number of nuclear spins orientated in the direction of the external field exceeds that of oppositely orientated spins by the factor of 10^{-5} as compared to the total number of spins. In the reaction products this magnitude becomes several orders of magnitude greater: the number of spins orientated along the field can differ from that of oppositely orientated ones by 1–10%.

Another convenient characteristics of net spin polarizations is the *magnetization*

$$\begin{aligned} M_{zI} &= g_I \cdot \beta_I \cdot \langle \hat{I}_z \rangle, \\ M_{zS} &= -g_e \cdot \beta_e \cdot \langle \hat{S}_z \rangle. \end{aligned} \quad (4.2)$$

The sign of spin polarization is determined by the following relations. For positive polarizations

$$\text{or} \quad \left. \begin{aligned} E_z - E_0 < 0 \\ M_z - M_0 > 0 \end{aligned} \right\} A \text{ type (absorption) spectra,} \quad (4.3)$$

and for negative polarizations

$$\text{or} \quad \left. \begin{array}{l} E_z - E_0 > 0 \\ M_z - M_0 < 0 \end{array} \right\} E \text{ type (emission) spectra.} \quad (4.4)$$

Under CIDN(E)P conditions the equilibrium polarizations (E_0, M_0) contribute negligibly, thus below in eqs (4.3, 4) we shall omit these equilibrium quantities.

4.1.2 Multiplet polarization effects

Multiplet effects are mutual spin orientations in radicals and their recombination products. In the case of the multiplet effect, each spin has no preferential orientation with respect to the external field. The essence of the phenomenon is that two spins—belonging to the electron and the nucleus in a radical, or to two nuclei in the reaction products—appear to be favourably orientated either parallel or antiparallel to each other. The quantitative measure of the multiplet effect, i.e., of the mutual spin orientation, can be presented in terms of spin–spin interaction energies: hyperfine interactions of the unpaired electron with the magnetic nucleus in a radical or spin–spin interactions between nuclei in recombination products. Thus, the energy of the spin–spin interaction reservoir resulting from chemically induced spin polarizations either increases or decreases. It is well known in the magnetic resonance that the energy of the spin–spin interaction reservoir can be substantially changed by the means of radiospectroscopy practically without changing the Zeeman spin energy. In the problem discussed chemical reactions create an analogous situation.

The energy of spin–spin interaction between nuclei in the recombination product and the energy of hyperfine interaction between the unpaired electrons and the magnetic nuclei of A and B radicals escaping the in-cage recombination, can be calculated with relations analogous to (4.1)

$$\begin{aligned} E_{II} &= \hbar \cdot j_{12} \cdot \text{Tr}_I \{ \sigma \hat{I}_{1z} \hat{I}_{2z} \} \equiv \hbar \cdot j_{12} \cdot \langle \hat{I}_{1z} \cdot \hat{I}_{2z} \rangle, \\ E_{SAI} &= \hbar \cdot a_A \cdot \text{Tr}_{SA,I} \{ \sigma_A \hat{S}_{Az} \hat{I}_z \} \equiv \hbar \cdot a_A \cdot \langle \hat{S}_{Az} \hat{I}_z \rangle, \\ E_{SBI} &= \hbar \cdot a_B \cdot \text{Tr}_{SB,I} \{ \sigma_B \hat{S}_{Bz} \hat{I}_z \} \equiv \hbar \cdot a_B \cdot \langle \hat{S}_{Bz} \hat{I}_z \rangle. \end{aligned} \quad (4.5)$$

The mutual spin orientation is manifested spectroscopically in oppositely polarized multiplet structure components of the product NMR spectra, or in oppositely polarized hyperfine structure components of the radical ESR spectra. From the viewpoint of spectroscopic manifestation, one distinguishes two types of multiplet effects: EA and AE . If the spectral component radiates in a low field and absorbs in a high field, it is a spectrum of EA type, AE corresponds to opposite polarization of the spectral components (see Fig. 1.10).

It should be stressed that interactions between nuclear spins are of no importance in the process of spin orientation, even those nuclear spins that do not directly interact with each other but both interact with radical unpaired electrons, can be mutually orientated during CIDNP generation. In this case the mutual spin

orientation cannot be characterized by the average energy of the spin-spin interactions since $E_{II}=0$, though $\langle \hat{I}_1 \hat{I}_2 \rangle \neq 0$. The spin-spin interaction splits the lines in the magnetic resonance spectrum and thus manifests the mutual spin orientation. The orientational correlation of two non-interacting spins is not manifested spectroscopically.

The type of spin polarizations is determined by the type of nonequilibrium population of spin levels that is formed in radical chemical reactions. In the case of multiplet effect, the type of magnetic resonance spectrum observed experimentally also depends on the sign of the spin-spin interaction constant j_{nk} and a . The spectrum of EA or AE type can originate from the same type of nonequilibrium spin level populations depending on the sign of j_{nk} or a . This statement follows directly

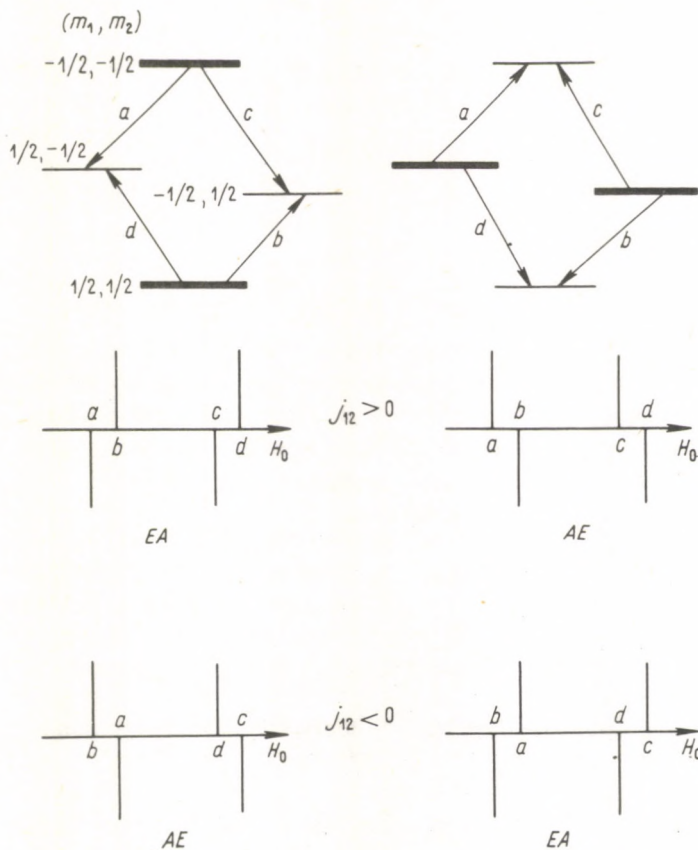


Fig. 4.1. Schematic diagram of nuclear spin level populations conforming to multiplet CIDNP effects (m_1 and m_2 are spin projections to the field direction). The nonequilibrium level population being the same, the multiplet CIDNP effect of either AE or EA type is observed depending on the sign of the nuclear interaction constant j_{12}

from eq. (4.5). To illustrate it, consider a molecule with two protons. Suppose that chemical shifts of the protons are different, hence, their resonance frequencies differ too. Because of the spin-spin interactions between the nuclei, each proton gives two resonance transitions corresponding to two possible spin orientations of the other proton. For each proton a resonance transition at a lower field corresponds to the other proton spin orientation along the external field provided $j_{12} > 0$. If $j_{12} < 0$, a resonance transition at a higher field corresponds to the same spin orientation of the partner. Figure 4.1 shows two possible populations of spin states corresponding to prevailing parallel or antiparallel mutual orientations of two spins. Each of the above distributions corresponds to either *AE* or *EA* spectrum depending upon the sign of the spin-spin interaction constant.

The type of multiplet spin polarization is unambiguously connected with the sign of the mean spin-spin interaction energy (note that at equilibrium, the spin correlation is negligible)

$$E_{II}, E_{SI} > 0, \text{ EA type NMR and ESR spectra;} \quad (4.6)$$

$$E_{II}, E_{SI} < 0, \text{ AE type NMR and ESR spectra.}$$

The microscopic theory of chemically induced spin polarization will be explored in the following sections.

4.2 CIDNP theory for high magnetic fields

Chemically induced nuclear polarization in radical recombination products is based on RP singlet-triplet transitions. The hf interaction taking part in inducing these transitions results in different recombination probabilities of RPs with different nuclear spin configurations. In high magnetic fields, when $H_0 > A_{\text{eff}}$, the main channel of intersystem transitions is *S-T₀*. In this situation the nuclear spin projection on to the field direction has no time to change during the RP in-cage lifetime. Nuclear polarizations in RP recombination products result from a certain RP selection with respect to the nuclear spin configuration which is realized by the reaction. This qualitative description of RP recombination probability as a function of nuclear spin states has been discussed in Section 1, 2.2.1, and in Section 3 this dependence has been calculated.

We begin the discussion of CIDNP theory with the basic qualitative results.

4.2.1 Basic regularities of net CIDNP effects

The origin and the basic regularities of net CIDNP can be analyzed considering the recombination of a RP with a spin 1/2 nucleus. Let g_1 and g_2 be the radical g -values, the magnetic nucleus belonging to the radical labelled 1. According to *S-T₀* transition efficiency, RPs are divided into two subensembles. First, the nuclear spin

is orientated parallel to the external field (positive polarization) and according to eq. (3.1), the matrix element of the intersystem transition is

$$\varepsilon^+(m_I = 1/2) = (g_1 - g_2) \cdot \beta \cdot H_0/2\hbar + a/4. \quad (4.7)$$

Second, the nuclear spin is polarized antiparallel to the field (negative polarization) and the matrix element of S-T₀ transition is

$$\varepsilon^-(m_I = -1/2) = (g_1 - g_2) \cdot \beta \cdot H_0/2\hbar - a/4. \quad (4.8)$$

Depending on the relationship between ε^+ and ε^- , singlet-triplet transitions would occur more often for RPs with either positive or negative nuclear polarizations.

Consider nuclear polarizations in geminate recombination products for the case of a singlet RP precursor. There are three possible ways of transformation for such a pair (the scheme of RP transformation channels is given in Fig. 1.2): recombination, escape from the cage (or radical reactions with acceptors) and intersystem transitions to the triplet state. Those pairs that occur in the triplet state do not recombine. The transition of a singlet RP to T₀ state increases the probability of its escape. Therefore, a RP subensemble with a smaller matrix element of S-T₀ transition gives a greater portion of the recombination product than that with a higher value of $|\varepsilon|$. As a result, the geminate recombination product shows nuclear polarization. The sign of the net CIDNP corresponds to the nuclear orientation having the smaller value of $|\varepsilon|$. Thus, we can come to the conclusion that the net polarization of the in-cage recombination product is positive if $|\varepsilon^+| < |\varepsilon^-|$. Therefore the differences of the g -values and the hf constants must be of opposite sign: $(g_1 - g_2) \cdot a < 0$. Otherwise the net CIDNP is negative.

In the case of a triplet-born RP the CIDNP must be of an opposite sign to the recombination of a singlet-born RP. From the initial triplet state the radicals can either leave the cage or react with acceptors. The intersystem transition to the singlet state allows them to recombine and to give in-cage products. Hence, unlike the situation with a singlet precursor, the RP subensemble with a greater $|\varepsilon|$ gives more in-cage products. Thus, the net polarization in the in-cage product is positive if $(g_1 - g_2) \cdot a > 0$, and negative if $(g_1 - g_2) \cdot a < 0$.

In the case of a diffusional RP recombination, the polarization observed has the sign coinciding with that in the case of geminate recombination for a triplet-born RP. This can be interpreted as follows. At the first contact at the recombination radius in the ensemble of F -pairs (note that in CIDNP theory diffusion pairs are usually called F -pairs or uncorrelated U -pairs) the singlet pairs recombine independently of the nuclear state, and no nuclear polarization arises in the molecules resulting from the first contact. However, after the first contact the fraction of triplet RPs in the F -pair ensemble increases. Later on, the RP singlet-triplet mixing occurs between the re-encounters and nuclear polarization arises in the recombination product in the same way as that in the case of geminate recombination from the initial triplet state.

In the course of geminate recombination, the radicals with certain nuclear spin orientations have advantage in giving the final product. Hence, the nuclear spins of

those radicals that avoided the in-cage recombination and either escape the cage or react with acceptors, must be oppositely orientated. Indeed, in high magnetic fields the nuclear spins conserve their orientations during the RP in-cage lifetime. Therefore, if the radicals with a certain nuclear spin orientation recombine, then the rest of them will have oppositely orientated nuclear spins. As a result, the escape products, e.g. radical-acceptor reactions products, must be oppositely polarized as compared to the in-cage product.

This simple consideration proves that net nuclear polarizations are observed only in the case when both mechanisms of S-T₀ transition— Δg and hf—are involved simultaneously. Polarization depends on magnetic fields and reaches its maximum at the magnetic field strength H_0 when $|\Delta g| \cdot \beta \cdot \hbar^{-1} \cdot H_0 \sim |a|/2$, i.e., when the efficiencies of both intersystem transition mechanisms become comparable. In this region of field strength, the matrix elements of S-T₀ transitions (4.7) and (4.8), differ most of all.

4.2.2 Basic regularities of multiplet CIDNP effects

The origin and the basic regularities of multiplet CIDNP can be analyzed considering the recombination of a RP with one of the partners having two magnetic nuclei with spin 1/2. The multiplet polarization is associated only with the hf mechanism of S-T₀ transitions in RPs. Consider the recombination of two radicals with the same g -values. According to the efficiency of S-T₀ transitions the RP ensemble is divided into two subensembles: in one the nuclear spins have the same orientations and in the other they are oppositely orientated. For these subensembles the matrix elements of intersystem transitions are, according to (3.1),

$$\varepsilon(m_1 = m_2) = \pm(a_1 + a_2)/4,$$

$$\varepsilon(m_1 = -m_2) = \pm(a_1 - a_2)/4.$$

Thus, we have two types of RPs with different mutual configurations of nuclear spins varying by the efficiency of S-T₀ transitions. As a result, like in the above case of a one-nuclear RP, recombination realizes a certain selection of radicals with respect to mutual orientation of nuclear spins and thus the nuclear spins in the reaction products appear mutually ordered. In the case of a singlet precursor, recombination products possess spins with chiefly parallel orientation provided $|\varepsilon(m_1 = m_2)| < |\varepsilon(m_1 = -m_2)|$, i.e. a_1 and a_2 are of opposite signs. If the signs of a_1 and a_2 are the same, the nuclear spins of the in-cage products are mainly antiparallel. As in the case of net CIDNP, when the RP precursor multiplicity changes, the spin polarization sign becomes opposite and F -pairs give products with the same polarization as in the case of triplet-born geminate pairs. The in-cage and escape products are oppositely polarized.

4.2.3 The Kaptein rules for CIDNP effects

The basic qualitative regularities of CIDNP for two concrete RPs have been formulated above. Analogous considerations can be used for RPs with an arbitrary number of magnetic nuclei of both radicals. As a result, Kaptein [4.1] has formulated the rules characterizing the basic qualitative regularities of CIDNP effects for short-lived RPs. In accord with [4.1] the sign of net CIDNP is determined by the sign of the product of the following quantities

$$\Gamma_{NE} = \mu \cdot \varepsilon \cdot \Delta g \cdot a_k \quad (4.9)$$

and in the case of multiplet effect

$$\Gamma_{ME} = \mu \cdot \varepsilon \cdot a_i \cdot a_k \cdot j_{ik} \cdot \sigma_{ik} \quad (4.10)$$

Here $\mu = +1$ or $\mu = -1$ for triplet or singlet RP precursors respectively; $\varepsilon = +1$ or $\varepsilon = -1$ for in-cage or escape products, Δg is the difference in g -values of the radical which possesses the k -th magnetic nucleus in question and of the radical-partner; a_k is the isotropic hf constant with the nucleus whose polarization is involved; a_i and a_j are the constants for nuclei i and j , $\sigma_{i,j} = +1$ if these nuclei belong to the same radical, $\sigma_{i,j} = -1$ if they belong to different radicals; j_{ij} is the spin-spin interaction constant.

If $\Gamma_{NE} > 0$, the net CIDNP is positive, if $\Gamma_{NE} < 0$, it is negative. The NMR spectra must be either of A or E type respectively. The multiplet effect of EA type corresponds to $\Gamma_{ME} > 0$, and AE to $\Gamma_{ME} < 0$. For F -pairs the CIDNP sign coincides with that in the case of geminate pairs with the initial triplet state.

The comparison of eqs (4.9) with (4.3) and (4.10) with (4.6) shows the parameter Γ_{NE} is opposite in sign to the Zeeman spin energy and the sign of parameter Γ_{ME} coincides to that of the spin-spin j - j interaction energy.

Thus, the CIDNP sign is determined, on the one hand, by the signs of magnetic resonance parameters and, on the other by the origin of the molecule. If the g -values and hf constants of radicals participating in the reaction, and also spin-spin interaction constants in the molecule, are obtained from ESR and NMR studies, then the CIDNP sign allows us to determine, e.g., the precursor multiplicity of the RP which formed the molecule considered. And vice versa, knowing the origin of the molecule and using the CIDNP data one can obtain information on the magnetic resonance parameters of active intermediate radicals.

The Kaptein rules determine the CIDNP sign without setting the scale of the effect. Nuclear spin polarizations in chemical reactions can be described quantitatively by solving the kinetic equations given in Section 2.3. Detailed studies of CIDNP show that in some, perhaps rare, situations the Kaptein rules fail to predict even the CIDNP sign. Deviations from these rules can be expected, for example, in recombination of a RP whose partners at the initial moment, at the moment of the RP formation, are not at the recombination radius but comparatively far apart from each other. Suppose that at the initial moment the RP

is in the singlet state. Before the first contact at the reaction radius the RP can have time to change its state into triplet. As a result, the polarization sign in the recombination products will be the same as if at the initial moment a triplet RP were formed at the recombination radius.

4.2.4 The operator formalism in CIDNP theory

To solve many problems of chemical polarization, in particular, to determine qualitative regularities of the Kaptein rule type, the operator method is convenient [4.2]. This method is based on the idea that to calculate CIDNP and CIDEP effects the full information on the system containing in the spin density matrix is not necessary. For example, according to eqs (4.2-5) to interpret CIDNP one needs the mean Zeeman spin energy E_{zI} (or the mean value of the projection of a given spin on to the external magnetic field direction $\langle \hat{I}_{nz} \rangle$) in the case of net CIDNP, and the mean energy of spin-spin interactions between two given nuclei E_{ij} (or the correlation function of the mutual orientation of two spins ($\langle \hat{I}_{iz} \hat{I}_{jz} \rangle$) in the case of multiplet effects. It is expedient, therefore, to solve the equations of motion with respect to these quantities measured experimentally.

Consider a RP with the spin-Hamiltonian \hat{H} which is given by eq. (2.83) for high magnetic fields. The projection of a certain nuclear spin on to the field direction is $\langle \hat{I}_{nz} \rangle = Tr_{S,I} \{ \rho(t) \hat{I}_{nz} \}$, where ρ is the RP density matrix, and the trace is carried out over electron and nuclear spin variables. Only the singlet RP state affords recombination products. Therefore, the nuclear polarization in the recombination product is proportional not to the total value of $\langle \hat{I}_{nz}(t) \rangle$ in the whole of RP ensemble, but to only the mean nuclear polarization in the singlet RP subensemble at the moment of their recombination. Thus, the net CIDNP in the recombination product is determined by the mean value of (cf. with (4.2))

$$\hat{K}_{NE} = -g_I \cdot \beta_I \cdot H_0 \cdot \hat{P} \cdot \hat{I}_{nz} \cdot \hat{P} \quad (4.11)$$

where \hat{P} is the projection operator to the singlet RP subspace. It can be expressed via the operator of the total spin $\hat{S} = \hat{S}_1 + \hat{S}_2$ of both unpaired electrons in the RP

$$\hat{P} = 1 - \hat{S}^2/2. \quad (4.12)$$

Substituting (4.12) into (4.11) and taking into account the relations of spin operator commutations, we obtain

$$\hat{K}_{NE} = -g_I \cdot \beta_I \cdot H_0 \cdot \hat{I}_{nz} \cdot (1/4 - \hat{S}_1 \cdot \hat{S}_2). \quad (4.13)$$

Triplet RPs cannot recombine. That is why in the escape products we observe such nuclear polarization which arises in a subensemble of triplet RPs and is determined by the mean value of the projection \hat{I}_{zn} to the triplet RP state

$$\hat{K}'_{NE} = -g_I \cdot \beta_I \cdot H_0 \cdot \hat{I}_{nz} \cdot (3/4 + \hat{S}_1 \cdot \hat{S}_2). \quad (4.14)$$

Note that the net polarization can be also characterized by the total spin magnetization

$$\hat{K}_{NE} = g_I \cdot \beta_I \cdot \hat{I}_z \cdot (1/4 - \hat{S}_1 \cdot \hat{S}_2), \quad (4.15)$$

$$\hat{K}'_{NE} = g_I \cdot \beta_I \cdot \hat{I}_z \cdot (3/4 + \hat{S}_1 \cdot \hat{S}_2). \quad (4.16)$$

Note that quantities \hat{K} and \hat{K}' have opposite signs (see also eqs (4.3, 4)).

RP recombination products inherit the spin orientations observed in the singlet RP subensemble. The multiplet effect in recombination products is thus determined by the mean value of spin-spin nuclear interactions in the singlet RP subensemble at the moment of recombination (see (4.5)).

$$\hat{K}_{ME} = \hbar j_{nk} \cdot \hat{I}_{nz} \cdot \hat{I}_{kz} \cdot (1/4 - \hat{S}_1 \cdot \hat{S}_2). \quad (4.17)$$

In the escape products or in those of radical reactions with acceptors the multiplet effect reflects the mutual nuclear spin orientations observed in the triplet RP subensemble

$$\hat{K}'_{ME} = \hbar j_{nk} \cdot \hat{I}_{nz} \cdot \hat{I}_{kz} \cdot (3/4 + \hat{S}_1 \cdot \hat{S}_2). \quad (4.18)$$

The mean values of spin ordering operators can be calculated by the relations $\langle K \rangle = \langle \hat{K}(t) \cdot \rho(0) \rangle$, $\hat{K} = \hat{K}_{NE}$, \hat{K}_{ME} , \hat{K}'_{NE} , \hat{K}'_{ME} where $\rho(0)$ is the RP density matrix at the initial moment and the function $\hat{K}(t)$ is determined by the equations of motion

$$\partial \hat{K} / \partial t = -i \hbar^{-1} \cdot [\hat{K}, \hat{H}]. \quad (4.19)$$

To obtain a complete system of equations, repeated differentiations must be carried out.

The spin ordering operators \hat{K}_{NE} , \hat{K}'_{NE} , \hat{K}_{ME} , \hat{K}'_{ME} are zero at the moment of RP formation. However, if the singlet or triplet T_0 state is the RP precursor, then at the initial moment the unpaired electron spins are correlated. In these states the electron spin correlation functions

$$\hat{P}_0 = \hat{S}_1^+ \cdot \hat{S}_2^- + \hat{S}_1^- \cdot \hat{S}_2^+, \quad (\hat{S}^\pm = \hat{S}_x \pm i \hat{S}_y), \quad (4.20)$$

$$\hat{P}_1 = 1/2 + 2 \hat{S}_1 \cdot \hat{S}_2$$

differ from zero. P_0 and P_1 equal -1 in the singlet state and $+1$ in the triplet state T_0 . The RP spin dynamics is as follows. The initial mutual spin orientation of two unpaired electrons turns into either the spin orientation with respect to the external magnetic field direction or the mutual spin orientation in the singlet or triplet RP subensembles. As a result, the mean values of K characterizing the spin ordering differ from zero.

To illustrate the method, consider a one-nucleus RP. Its spin Hamiltonian in high magnetic fields is

$$\begin{aligned} \hat{H} &= g_1 \cdot \beta_e \cdot H_0 \cdot \hat{S}_{1z} + g_2 \cdot \beta_e \cdot H_0 \cdot \hat{S}_{2z} + \hbar a \hat{S}_{1z} \hat{I}_z \equiv \\ &\equiv \hbar \omega_1 \hat{S}_{1z} + \hbar \omega_2 \hat{S}_{2z} + \hbar a \hat{S}_{1z} \hat{I}_z. \end{aligned} \quad (4.21)$$

Net polarization of the in-cage recombination products are determined by the quantity K_{NE} which is found from the following set of equations [4.2]

$$\begin{aligned}\partial K_{NE}/\partial t &= g_I \cdot \beta_I \cdot H_0 [(\omega_1 - \omega_2) \cdot Q_1 + a \cdot Q_2/4], \\ \partial Q_1/\partial t &= (\omega_1 - \omega_2) \cdot Q - a \cdot P_0/8, \\ \partial Q_2/\partial t &= -(\omega_1 - \omega_2) \cdot P_0/2 + a \cdot Q, \\ \partial Q/\partial t &= -(\omega_1 - \omega_2) \cdot Q_1 - a \cdot Q_2/4, \\ \partial P_0/\partial t &= 2 \cdot (\omega_1 - \omega_2) \cdot Q_2 + 2a \cdot Q_1,\end{aligned}\quad (4.22)$$

where

$$\begin{aligned}Q &= \langle \hat{Q} \rangle = -(1/2) \cdot \langle \hat{I}_z \cdot \hat{P}_0 \rangle = -\langle \hat{I}_z \cdot (\hat{S}_{1x} \cdot \hat{S}_{2x} + \hat{S}_{1y} \cdot \hat{S}_{2y}) \rangle, \\ Q_1 &= \langle \hat{Q}_1 \rangle = \langle \hat{I}_z \cdot (\hat{S}_{1x} \hat{S}_{2y} - \hat{S}_{1y} \hat{S}_{2x}) \rangle, \\ Q_2 &= \langle \hat{Q}_2 \rangle = \langle \hat{S}_{1x} \hat{S}_{2y} - \hat{S}_{1y} \hat{S}_{2x} \rangle,\end{aligned}$$

$$\omega_1 - \omega_2 = (g_1 - g_2) \cdot \beta_e \cdot \hbar^{-1} \cdot H_0 = \Delta g \cdot \beta_e \cdot \hbar^{-1} \cdot H_0.$$

$\hat{Q}, \hat{Q}_1, \hat{Q}_2$ operators characterize the correlation of nuclear and electron spins. At the initial moment only the quantity P_0 differs from zero. Eqs (4.22) can be given in another equivalent form which reveal net CIDNP effects. Indeed, from (4.22) we obtain

$$\partial^2 K_{NE}/\partial t^2 = -g_I \cdot \beta_I \cdot H_0 \cdot \{(\omega_1 - \omega_2) \cdot a \cdot P_0/4 + [a^2/4 + (\omega_1 - \omega_2)^2] \cdot Q\}.$$

Hence it follows that $(\omega_1 - \omega_2) \cdot a$ is the parameter responsible for the net CIDNP. When the characteristic times of spin ordering redistribution are large when compared to the RP lifetimes, eq. (4.22) can be solved by expanding in powers of small parameters $a \cdot t < 1$, $\Delta g \cdot \beta_e \cdot \hbar^{-1} H_0 t < 1$.

Solving (4.22) by the iteration method and with the greatest term retained, we get

$$\begin{aligned}K_{NE} &\approx -(g_1 - g_2) a \cdot P_0 \cdot g_I \beta_I \beta_e \hbar^{-1} H_0^2 t^2 / 8 \sim \\ &\sim -(g_1 - g_2) \cdot a \cdot P_0.\end{aligned}\quad (4.23)$$

Hence, we obtain the Kaptein rule for the net CIDNP sign in RP recombination products. The relations obtained also evaluate the scale of the effect for short-lived RPs. Note that $K_{NE} < 0$ corresponds to the polarization of *A* type, and $K_{NE} > 0$ to *E* type.

Multiplet CIDNP effects can be considered in a similar way. For example, for RPs with two magnetic nuclei with spin 1/2 belonging to different radicals, one finds [4.2]

$$K_{ME} \approx -\hbar j_{12} a_1 a_2 P_0 t^2 / 32 \sim -j_{12} \cdot a_1 \cdot a_2 \cdot P_0. \quad (4.24)$$

This result corresponds to the Kaptein rule for the multiplet CIDNP. The relations (4.23, 24) result, in fact, from the application of the time perturbation theory. Therefore, they hold only for comparatively small times, until RP spin changes are

negligible in the process of singlet-triplet evolution. Thus, for comparatively short-lived RPs the Kaptein rule must predict the CIDNP effect sign correctly.

It is seen from the above considerations that the operator method allows one to get chemically induced spin polarization data for short-lived RPs quite readily. This method proved to be fruitful as applied to the theory of CIDEP and low field CIDNP.

4.2.5 Quantitative CIDNP calculations; absolute values of nuclear polarization

In the preceding section, in connection with the discussion of magnetic effects in radical recombination in high magnetic fields, some data for RP density matrices were obtained by kinetic equations which can be used to calculate absolute values of nuclear polarizations in recombination products. Eqs (3.2, 3, 6, 17-19, 26-28, 32-34, 47) give necessary data for different models of radical recombination and motion kinematics.

Continuous model. Consider the model of continuous radical diffusion and analyze the CIDNP effects. Let us discuss a one-nuclear RP with a spin-Hamiltonian (4.21) and find the population difference between the state with nuclear spins orientated along the magnetic field and that with the opposite orientation, $\Delta n = n(m_I = 1/2) - n(m_I = -1/2)$. According to eqs (3.2, 3, 6) for a singlet RP precursor it equals

$${}^S\Delta n_g = 2 \cdot \sum_m m \cdot {}^S\sigma_{mm} = (2b/r_0) \cdot \sum_m m \cdot A(m) \cdot \{1 + \delta(m) + \cos \{ \delta(m) \cdot (r_0/b - 1) \} \cdot \exp [- \delta(m) \cdot (r_0/b - 1)] \}, \quad (4.25)$$

for a triplet RP precursor

$${}^T\Delta n_g = (2/3) \cdot \sum_m m \cdot {}^T\sigma_{mm} = (2b/3r_0) \cdot \sum_m m \cdot A(m) \cdot \{1 + \delta(m) - \cos \{ \delta(m) \cdot (r_0/b - 1) \} \cdot \exp [- \delta(m) \cdot (r_0/b - 1)] \}, \quad (4.26)$$

and in the case of diffusion pair recombination,

$${}^F\Delta n = 2 \cdot \sum_m m \cdot {}^F\sigma_{mm} = \sum_m m \cdot A(m) \cdot [1 + \delta(m)], \quad (4.27)$$

where the symbols are the same as in eqs (3.2, 3)

$$\delta(m) = (|\varepsilon(m)| \cdot \tau_D)^{1/2}, \quad \tau_D = b^2/D,$$

$$\varepsilon(m) = \Delta g \cdot \beta_e \cdot H_0/2\hbar + a \cdot m/2,$$

$$A(m) = (K\tau_r/2)/[2(1 + K\tau_r) + \delta(m) \cdot (2 + K\tau_r)].$$

Note that the Zeeman nuclear energy equals $E_{zI} = -g_I \cdot \beta_I \cdot H_0 \cdot \Delta n/2$. Equations (4.25-27) characterize nuclear polarization calculated per radical pair. The nuclear

spin polarization calculated per molecule—the RP recombination product—is also of a particular interest. The difference in the nuclear state populations calculated per recombination product will be denoted by an asterisk:

$${}^S\Delta n_g^* = {}^S\Delta n_g / {}^S p_g, \quad {}^T\Delta n_g^* = {}^T\Delta n_g / {}^T p_g, \quad {}^F\Delta n^* = {}^F\Delta n / p_r.$$

Equations (4.25, 26) show the nuclear polarization in geminate recombination products to be essentially dependent on the initial distance between the radicals, r_0 . The simplest results are obtained if at the initial moment the RP is at the recombination radius, i.e., $r_0 = b$. In this case at any values of the other RP parameters eqs (4.25–27) predict for mononuclear RP the polarization sign which coincides with that predicted by the Kaptein rule for the net CIDNP. For mononuclear F -pairs the net CIDNP sign, according to (4.27), always coincides with that obtained by the Kaptein rule. Recently it has been shown [4.50] that in multinuclear systems the Kaptein rules can be violated owing to the mutual influence of the RP nuclei upon the CIDNP. Figure 4.2 presents plots of nuclear

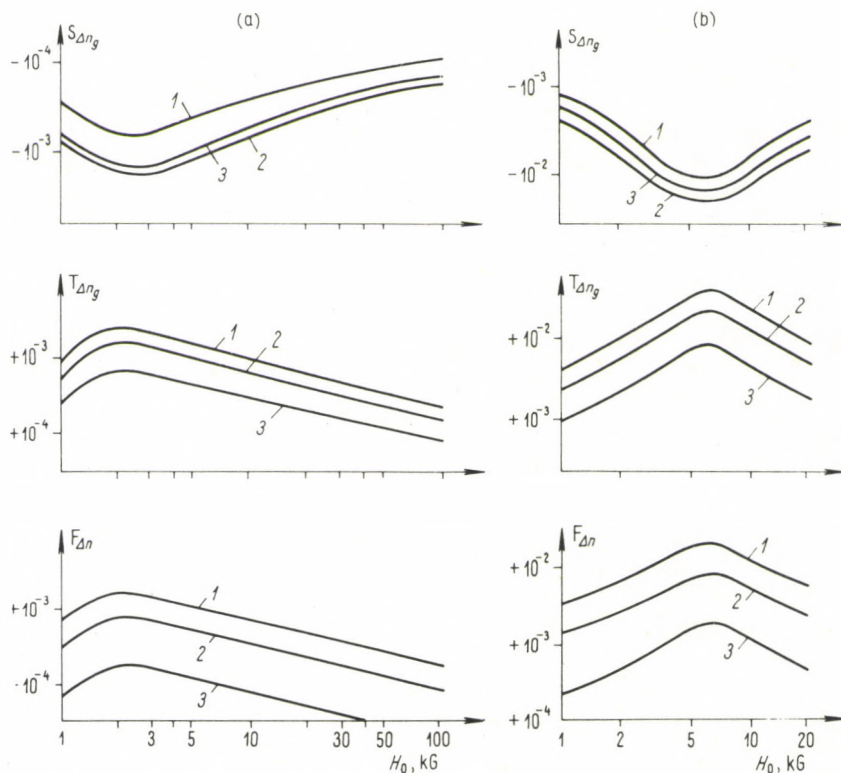


Fig. 4.2. Field dependence of the nuclear sublevel populations in recombination products per RP at varying $\lambda = K \cdot \tau_r / (1 + K \cdot \tau_r)$: 1, 0.909; 2, 0.625; 3, 0.294 (RP parameters: (a) $a \cdot \tau_D = 4 \cdot 10^{-3}$; $\Delta g \cdot \tau_D = 10^{-13}$ s; (b) $a \cdot \tau_D = 0.439$; $\Delta g \cdot \tau_D = 2.5 \cdot 10^{-11}$ s)

polarizations vs. the external magnetic field strength for singlet, triplet and uncorrelated initial spin states of the unpaired electrons. As expected from the qualitative data on net CIDNP, the polarization effect reaches its maximum in the fields when the efficiencies of the Δg - and hf-mechanisms of singlet-triplet transitions become equal. The value of Δn increases with the parameter λ for triplet RP precursors and F -pairs. It means that for diffusion controlled reactions the CIDNP effect must be greater. For singlet RP precursors the CIDNP effect is the greatest in the case of intermediate case, $K\tau_r \sim 1$. Figure 4.3 presents nuclear polarizations calculated per molecule resulted from RP recombination. It is clear that in fields as high as several kG, chemically induced polarizations exceed steady-state polarizations (equal approximately to 10^{-5}) by two to four orders of magnitude. It is interesting to note that, when calculated per molecule, nuclear polarizations in RP recombination from the initial triplet state are nearly

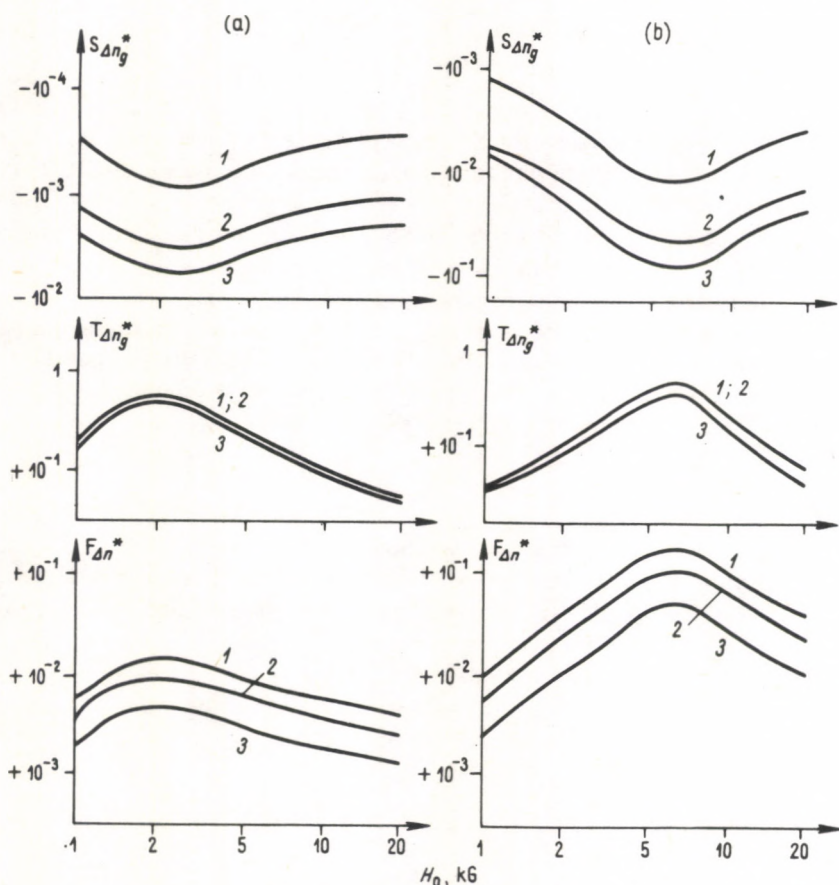


Fig. 4.3. Field dependence of nuclear polarization per molecule resulting from RP recombination. Symbols and parameters are the same as in Fig. 4.2

independent on the reactivity of the reagents. When calculated per molecule, the nuclear polarization in RP recombination from the initial singlet state depends monotonically on the parameter λ : the polarization increases with decreasing λ and becomes maximum for reactions controlled by the in-cage RP recombination.

The multiplet CIDNP effect in RP recombination products can be analyzed in a similar way using eqs (3.2, 3, 6). The mean energy of spin-spin interactions between nuclei with indices 1 and 2 is, in the case of singlet RP precursors,

$${}^S E_{I_1 I_2} = \hbar j_{12} \cdot \sum_m m_1 \cdot m_2 \cdot {}^S \sigma_{mm}, \quad (4.28)$$

in the case of triplet RP precursors

$${}^T E_{I_1 I_2} = (1/3) \cdot \hbar j_{12} \cdot \sum_m m_1 \cdot m_2 \cdot {}^T \sigma_{mm}, \quad (4.29)$$

and in the case of diffusion pair recombination

$${}^F E_{I_1 I_2} = \hbar j_{12} \cdot \sum_m m_1 \cdot m_2 \cdot {}^F \sigma_{mm}. \quad (4.30)$$

According to (4.30), the CIDNP sign for F -pairs with two magnetic nuclei always coincides with that predicted by the Kaptein rules. In geminate recombination, the CIDNP sign can be dependent on the initial distance between the radicals. If at the initial moment the radicals are at the reaction radius, the sign of multiplet CIDNP as well as that of net CIDNP is determined by the Kaptein rules. Some deviations from the Kaptein rules are possible at $r_0 > b$. In multi-nuclear systems the Kaptein rules for multiplet CIDNP can be sometimes violated [4.50].

In the case of geminate RPs occurring at the reaction radius at the initial moment, the recombination probabilities for RPs with a given nuclear spin configuration are interconnected by a relation of the type (3.11) in the cases of singlet and triplet precursors. Thus, for singlet and triplet RP precursors, at $r_0 = b$, we have

$$\lambda / \prod_k (2I_k + 1) - {}^S \sigma_{mm} = (1 - \lambda) \cdot {}^T \sigma_{mm} \quad (4.31)$$

where $\lambda = K\tau_r / (1 + K\tau_r)$ and the other symbols are the same as in eqs (3.2, 3). The recombination probability of diffusion RP subensemble with a given nuclear spin configuration is described by eq. (3.6) and can be expressed by the explicit relation

$${}^F \sigma_{mm} = ({}^S \sigma_{mm} + {}^T \sigma_{mm}) / 4. \quad (4.32)$$

Using eqs (4.31, 32) we obtain the following relations which connect net and multiplet nuclear polarizations for RPs of different origin ($r_0 = b$):

$$\begin{aligned} {}^T E_{zI_k} &= -(1/3) \cdot g_I \beta_I H_0 \cdot \sum_m m_k \cdot {}^T \sigma_{mm}, \\ {}^T E_{I_1 I_2} &= (1/3) \cdot \hbar j_{12} \cdot \sum_m m_1 \cdot m_2 \cdot {}^T \sigma_{mm}, \\ {}^S E_{zI_k} &= -3 \cdot (1 - \lambda) \cdot {}^T E_{zI_k}, \end{aligned} \quad (4.33)$$

$${}^S E_{I_1 I_2} = -3 \cdot (1 - \lambda) \cdot {}^T E_{I_1 I_2},$$

$${}^F E_{z I_k} = (3/4) \cdot \lambda \cdot {}^T E_{z I_k},$$

$${}^F E_{I_1 I_2} = (3/4) \cdot \lambda \cdot {}^T E_{I_1 I_2}.$$

To show the scale of possible multiplet CIDNP effects, consider RPs with two magnetic nuclei with spins 1/2 and the same g -values. Let $r_0 = b$. In this case we obtain from eqs (4.28–30) and (4.33)

$$\begin{aligned} {}^T E_{I_1 I_2} &= (1/6) \cdot \hbar j_{12} \cdot [{}^T \sigma(|a_1 + a_2|/4) - {}^T \sigma(|a_1 - a_2|/4)] \equiv \hbar \cdot j_{12} \cdot {}^T \Delta N / 6, \\ {}^S E_{I_1 I_2} &= -(1 - \lambda) \cdot {}^T \Delta N / 2, \end{aligned} \quad (4.34)$$

$${}^F E_{I_1 I_2} = \lambda \cdot {}^T \Delta N / 8; \quad \delta(x) \equiv (|x| \cdot \tau_D)^{1/2},$$

$$\sigma(x) \equiv (K \tau_r / 4) \cdot [1 + \delta(x)] / [2(1 + K \tau_r) + \delta(x) \cdot (2 + K \tau_r)].$$

In eq. (4.34) we introduced the population differences of states with parallel and antiparallel mutual orientation of two nuclear spins, ΔN . Table 4.1 lists some

Table 4.1. ΔN values for singlet-born, triplet-born, and diffusion RPs (recombination probabilities are given in parenthesis). It is supposed that radicals are close at the initial moment ($r_0 = b$); λ is the probability of a singlet-born RP recombination without any S–T transitions, A_1 and A_2 are hf constants of two radicals, τ_D is the in-cage RP life-time, $a_2 \cdot \tau_D = 4 \cdot 10^{-3}$

λ	$a_1 \cdot \tau_D$	${}^S \Delta N$	${}^T \Delta N$	${}^F \Delta N$
0.8331	$8.7944 \cdot 10^{-4}$	$-1.0836 \cdot 10^{-3}$ (0.79510)	$2.1674 \cdot 10^{-3}$ (0.07646)	$1.3546 \cdot 10^{-3}$ (0.14338)
	$4.3972 \cdot 10^{-3}$	$-5.6468 \cdot 10^{-3}$ (0.79605)	$1.1293 \cdot 10^{-2}$ (0.074555)	$7.0586 \cdot 10^{-3}$ (0.13883)
	$1.8468 \cdot 10^{-2}$	$-8.8720 \cdot 10^{-3}$ (0.78982)	$1.7744 \cdot 10^{-2}$ (0.087011)	$1.1090 \cdot 10^{-2}$ (0.14104)
	$3.6057 \cdot 10^{-2}$	$-4.4514 \cdot 10^{-3}$ (0.77839)	$0.89028 \cdot 10^{-2}$ (0.10988)	$5.5642 \cdot 10^{-3}$ (0.15293)
0.294	$8.7944 \cdot 10^{-4}$	$-1.2282 \cdot 10^{-3}$ (0.24436)	$0.58001 \cdot 10^{-3}$ ($2.3497 \cdot 10^{-2}$)	$1.2794 \cdot 10^{-4}$ (0.040798)
	$4.3972 \cdot 10^{-3}$	$-6.4439 \cdot 10^{-3}$ (0.24556)	$3.0429 \cdot 10^{-3}$ ($2.2928 \cdot 10^{-2}$)	$6.7124 \cdot 10^{-4}$ (0.040344)
	$1.8468 \cdot 10^{-2}$	$-9.7147 \cdot 10^{-3}$ (0.23876)	$0.45875 \cdot 10^{-2}$ ($2.6137 \cdot 10^{-2}$)	$1.01198 \cdot 10^{-3}$ (0.040483)
	$3.6057 \cdot 10^{-2}$	$-4.5209 \cdot 10^{-3}$ (0.22649)	$2.1349 \cdot 10^{-3}$ ($3.1934 \cdot 10^{-2}$)	$4.7093 \cdot 10^{-4}$ (0.041485)
0.0769	$8.7944 \cdot 10^{-4}$	$-3.7954 \cdot 10^{-4}$ ($6.0747 \cdot 10^{-2}$)	$1.3705 \cdot 10^{-4}$ ($0.58411 \cdot 10^{-2}$)	$7.9069 \cdot 10^{-6}$ ($9.8728 \cdot 10^{-3}$)
	$4.3972 \cdot 10^{-3}$	$-1.9960 \cdot 10^{-3}$ ($6.1132 \cdot 10^{-2}$)	$0.72080 \cdot 10^{-3}$ ($0.57021 \cdot 10^{-2}$)	$4.1583 \cdot 10^{-5}$ ($9.8443 \cdot 10^{-3}$)
	$1.8468 \cdot 10^{-2}$	$-2.9690 \cdot 10^{-3}$ ($5.9057 \cdot 10^{-2}$)	$1.0721 \cdot 10^{-3}$ ($0.64514 \cdot 10^{-2}$)	$6.1854 \cdot 10^{-5}$ ($9.8516 \cdot 10^{-3}$)
	$3.6057 \cdot 10^{-2}$	$-1.3486 \cdot 10^{-3}$ ($5.5328 \cdot 10^{-2}$)	$0.38702 \cdot 10^{-3}$ (0.007798)	$2.8098 \cdot 10^{-5}$ ($9.9114 \cdot 10^{-3}$)

possible values of RP parameters calculated by (4.34). The multiplet effect appears, according to the Table, to be the highest when the radical hf constants, A_1 and A_2 , are compatible.

In a number of cases, RPs are formed when molecules decompose into three fragments: two radicals and a diamagnetic molecule. Then, at the moment of radical pair formation, the radicals do not occur at the recombination radius, $r_0 > b$. Such systems can show some 'anomaly' in CIDNP—deviations from the Kaptein rule. Indeed, CIDNP effects in the geminate recombination products include oscillating terms. They are accounted for by the fact that in the time interval between RP formation and first contact at the reaction radius there occurs a singlet–triplet evolution in the RP, and at the moment of first contact the initial, e.g., singlet, pair can turn into a triplet pair. As a result, the nuclear polarization in the reaction product will be the same as if at the initial moment a triplet RP occurs at the recombination radius. If before the first contact the probability of intersystem transitions is high, the CIDNP sign can be opposite to that predicted by the Kaptein rules.

To obtain reliable data, one needs precise calculations. Figure 4.4 depicts the population difference of states with parallel and antiparallel nuclear spin orientations in the case of a one-nucleus RP recombination. This illustrates possible CIDNP features of the geminate recombination products. The polarization sign behaves in quite a complex manner depending on the initial distance between the reagents, their reactivity, and the magnetic field strength. It is, however, necessary to note that these CIDNP features can be observed only in the case when a geminate pair radicals can realize one or several singlet–triplet transitions within the time of a diffusional encounter. Some deviations from the Kaptein rules can thus be expected on increasing the viscosity of solutions or in systems with comparably high hf constants or the difference in g -values. For instance, a possible set of RP parameters corresponding to the plots of Fig. 4.4 is: $\Delta g = 0.01$, $\tau_D = 2.5 \cdot 10^{-9}$ s, $a = 4.39 \cdot 10^8$ rad/s (or $A = 25$ G).

Radical interactions. Exchange interactions as well as Coulomb attraction or repulsion between radicals can influence CIDNP effects. However, the role of exchange interaction in singlet–triplet mixing efficiency appears to be negligible for normal values of RP parameters. The repulsion between radical-ions reduces the intersystem transition effect on the RP recombination, whereas the attraction increases it [4.3]. The role of interaction between radicals in RP recombination has been discussed in more detail in Sec. 3.1.

The jump model. When radicals move by jumping, and in the extreme situation of passing through the cage with a jump (exponential recombination model), CIDNP effects can be analyzed using eqs (3.26–28) and (3.32–34). Qualitatively, the results coincide with those obtained within the continuous diffusion model. Eqs (4.33) hold for all recombination models provided $r_0 = b$. Note that (4.33) hold at an arbitrary value of the exchange integral.

Comments on approximate calculations of CIDNP effects. In the theory of nuclear polarization and magnetic effects, the approximation of only one encounter in the

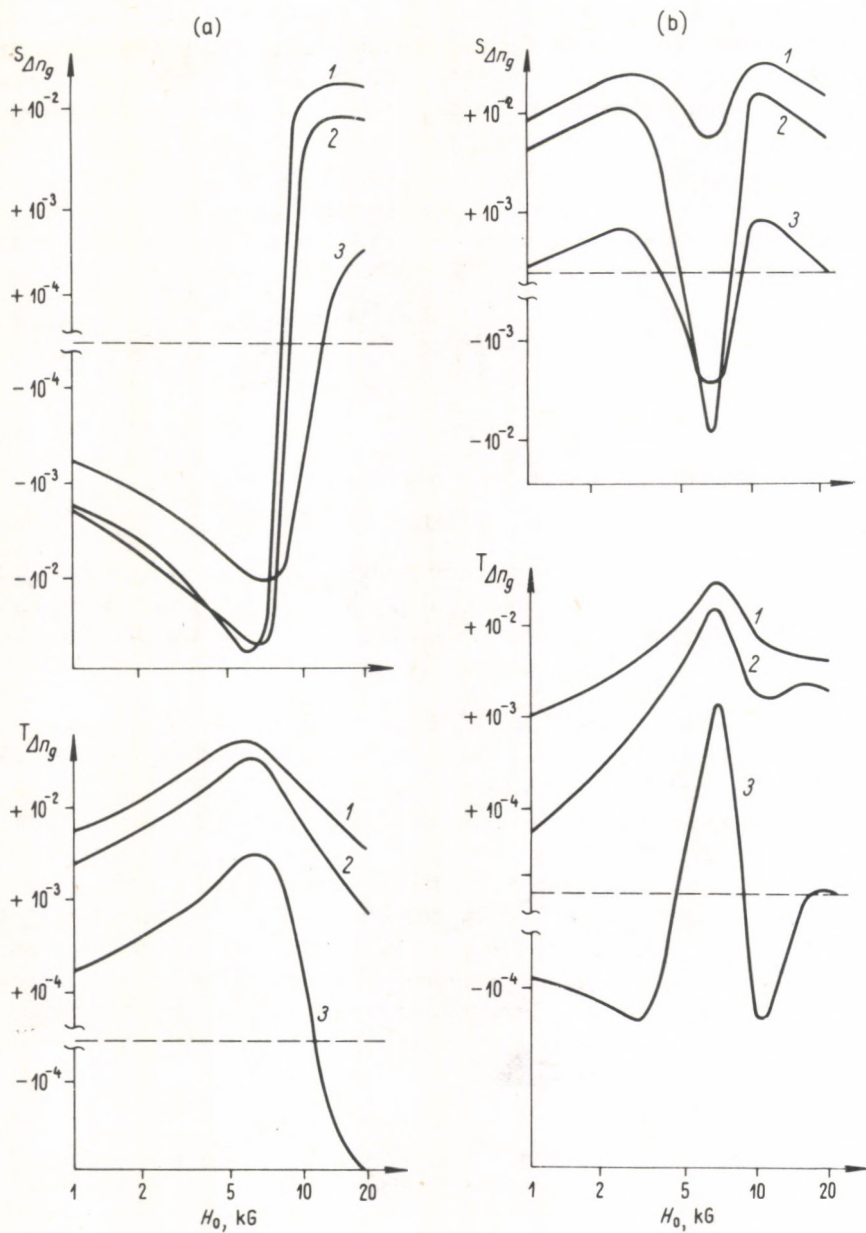


Fig. 4.4. Population difference in geminate recombination products: (a) $r_0 = 3 \cdot b$; (b) $r_0 = 5 \cdot b$; 1 — $\lambda = 0.909$; 2 — $\lambda = 0.625$; 3 — $\lambda = 0.0769$ (RP parameters: $a \cdot \tau_D = 0.439$, $\Delta g \cdot \tau_D = 2.5 \cdot 10^{-11}$ s. As the field increases, the nuclear polarization sign can change and no longer coincide with the Kaptein rules

reaction zone is widely used. However, in the extreme case of continuous diffusion, to consider only one re-encounter is not meaningful. Even if radical diffusion occurs by comparatively large jumps, jumps comparable to molecular sizes, taking all the re-encounters into consideration can lead to results which differ essentially from those obtained in the approximation of one re-encounter. To illustrate this statement, consider the recombination of a diffusion one-nucleus RP with spin 1/2 and spin-Hamiltonian specified by eq. (4.21). Using eq. (3.19), we have for the population difference of states with parallel and antiparallel nuclear spin orientations

$${}^F\Delta n = (\lambda n/8) \cdot \{1 + 2z_+ \cdot n/\Delta_+ - (1 + 2z_- \cdot n/\Delta_-)\},$$

where

$$z_{\pm} = \int dt \cdot f(t) \cdot \sin^2 \{(\Delta g \cdot \beta_e \cdot H_0/2\hbar \pm a/4)t\},$$

$$\Delta_{\pm} = 1 + \lambda p n + 2nz_{\pm} \cdot [1 + \lambda n(p - 1/2)].$$

With account taken of only one re-encounter we obtain

$${}^F\Delta n^{(1)} = \lambda^2 \cdot (z_+ - z_-)/8.$$

In these equations p is a re-encounter probability, n is the number of all RP contacts, λ is a singlet RP recombination probability in a single contact. The average probability of intersystem transitions can be evaluated by the Adrian formula [4.4]

$$z_{\pm} \approx 0.42 [|\Delta g \cdot \beta_e \cdot H_0/2\hbar \pm a/4| \cdot \tau]^{1/2}.$$

Assume $\Delta g > 0$ and $a > 0$. Table 4.2, where the data refer to a magnetic field $H_0^* = \hbar a/2 \cdot \Delta g \cdot \beta_e$ with $z_- = 0$, lists values of ${}^F\Delta n$ and ${}^F\Delta n^{(1)}$ for two values of the parameter $a \cdot \tau$ (note that in the Adrian model $p = 0.31$). Table 4.2 shows that in the above cases net CIDNP effects increase by a factor of two if all re-encounters are taken into consideration. At other RP parameters, this increase can be even greater. Hence, values of a , Δg or τ can be several-fold overestimated (up to an order of magnitude) provided these are determined from CIDNP data processed by the approximate model of Adrian and Kaptein taking into account only one re-encounter at the reaction radius. Therefore, to get some quantitative information from CIDNP data one needs to appeal to the precise theory taking into account all re-encounters. For high magnetic fields there are precise and sufficiently simple relations describing CIDNP effects (see, e.g. eqs (4.25–34)).

Table 4.2. Comparison of contributions to polarization made by all the contacts (Δn) and by a single re-encounter ($\Delta n^{(1)}$)

λ	$a \cdot \tau = 0.040$		$a \cdot \tau = 0.16$	
	${}^F\Delta n$	${}^F\Delta n^{(1)}$	${}^F\Delta n$	${}^F\Delta n^{(1)}$
0.1	$3.46 \cdot 10^{-4}$	$1.50 \cdot 10^{-4}$	$6.09 \cdot 10^{-4}$	$3.00 \cdot 10^{-4}$
0.3	$2.71 \cdot 10^{-3}$	$1.35 \cdot 10^{-3}$	$4.80 \cdot 10^{-3}$	$2.70 \cdot 10^{-3}$
0.6	$8.95 \cdot 10^{-3}$	$5.40 \cdot 10^{-3}$	$1.62 \cdot 10^{-2}$	$1.08 \cdot 10^{-2}$

4.2.6 The influence of radical acceptors on CIDNP

The reaction of radicals with acceptors effectively reduces the in-cage lifetime of a RP and the re-encounter probability. As a result, the CIDNP effects also decrease in the presence of radical acceptors. In this case nuclear polarizations can be precisely calculated by eqs (3.26). The Zeeman energy of a given nucleus as well as the energy of interaction of two nuclei in the product of a triplet-born RP recombination are described by the relations [4.5]

$${}^T E_{zI_k} = -g_I \cdot \beta_I \cdot H_0 \cdot \sum_m m_k \cdot [1 - F(m)] \cdot K \tau_r / 3 \cdot \Lambda(m), \quad (4.35)$$

$${}^T E_{I_1, I_2} = \hbar \cdot j_{12} \sum_m m_1 \cdot m_2 \cdot [1 - F(m)] \cdot K \tau_r / 3 \cdot \Lambda(m),$$

where $F(m)$ and $\Lambda(m)$ are given by eqs (3.26). For singlet-born RPs and F -pairs the CIDNP effects are expressed by (4.35) using general relations (4.33).

Under typical experimental conditions the average probability of $S-T_0$ transitions during the RP lifetime is small, i.e. $|\varepsilon(m)| \cdot \tau_D < 1$ ($\varepsilon(m)$ is the matrix element of a $S-T_0$ transition (3.1) and τ_D is the RP lifetime). For this case, which is of practical importance, compare CIDNP effects in two extreme situations: no radical acceptors, effective radical capture by acceptors. Eqs (3.26) and (4.35) give the following results at $|\varepsilon(m)| \cdot \tau_D < 1$.

In the absence of acceptors when $K_s = 0$,

$${}^T E_{zI_k} \approx -g_I \cdot \beta_I \cdot H_0 \cdot \lambda \sum_m m_k \cdot (|\varepsilon(m)| \cdot \tau_D)^{1/2} / 6 \cdot \prod_k (2I_k + 1). \quad (4.36)$$

Otherwise, when $K_s \cdot \tau_D > 1$,

$${}^T E_{zI_k} \approx -g_I \cdot \beta_I \cdot H_0 \cdot \lambda \sum_m m_k \cdot \varepsilon^2(m) \cdot K_s^{-2} / 12 \cdot \prod_k (2I_k + 1). \quad (4.37)$$

Eqs (4.36, 37) show that the reaction with acceptors reduces the scale of the effect but also qualitatively changes the functional dependence of nuclear polarizations on molecular-kinetic parameters. When the radical capture rate increases the square root dependence on $\varepsilon(m)$ at $K_s = 0$ which is (4.36) characteristic of the diffusion recombination model is replaced by the quadratic dependence of CIDNP on $\varepsilon(m)$ (4.37) [4.6] typical of the exponential recombination model. In the latter case the mean recombination time $1/K_s$ serves as the time of $S-T$ mixing.

4.2.7 The influence of anisotropic radical reactivity on CIDNP

When discussing CIDNP effects one must take into account the anisotropic character of unpaired electron distribution. The theory of recombination of RPs with such anisotropic properties has been discussed in Section 3.1.6. The orientational relaxation of radicals at contact moment and especially between re-

encounters has been shown to be of great importance in the recombination process [4.3, 5, 7].

In this case the CIDNP effects can be exactly calculated by eqs (3.27). For instance, according to the model described in Section 3.1.6 the net polarization can be found as [4.5]

$$\begin{aligned} {}^S E_{zIk} &= -g_I \cdot \beta_I \cdot H_0 \cdot \sum_m m_k \cdot [F_1(m) + F_2(m)] \cdot K\tau_r / \Lambda(m), \\ {}^F E_{zIk} &= -g_I \cdot \beta_I \cdot H_0 \cdot \sum_m m_k \cdot f K\tau_r / 4 \cdot \Lambda(m), \\ {}^T E_{zIk} &= -g_I \cdot \beta_I \cdot H_0 \cdot \sum_m m_k \cdot [F_1(m) - F_2(m)] \cdot K\tau_r / 3 \cdot \Lambda(m), \end{aligned} \quad (4.38)$$

where $F_k(m)$ and $\Lambda(m)$ are the same as in eq. (3.27).

Of the greatest practical interest is the case of weak S-T₀ mixing when $|\varepsilon(m)|\tau_D < 1$. From eq. (4.38) we have then

$$\begin{aligned} {}^S E_{zIk} &\approx g_I \cdot \beta_I H_0 \cdot f \cdot K \cdot \tau_r \sum_m m_k \cdot (|\varepsilon(m)| \cdot \tau_D)^{1/2} \cdot \\ &\cdot [2 \cdot \prod_k (2I_k + 1) \cdot (1 + 2F_1 K\tau_r)^2]^{-1}, \end{aligned} \quad (4.39)$$

$${}^T E_{zIk} \approx -{}^S E_{zIk} \cdot (1 + 2F_1 K\tau_r) / 3,$$

$${}^F E_{zIk} \approx -{}^S E_{zIk} \cdot f K\tau_r / 4,$$

where

$$2F_1 = f + (1 - f) / [1 + \tau_r / \tau_0 + (\tau_D / \tau_0)^{1/2}].$$

Here f is a geometrical steric factor, τ_0 is the relaxation time of mutual radical orientation. As estimated in Section 3.1.6, $\tau_D / \tau_0 = 6$. Multiplet CIDNP effects can be described by similar relations (see [4.5]).

For comparison, we calculate CIDNP effects neglecting radical orientational relaxation. Assume $\tau_0 \rightarrow \infty$ and obtain from eq. (4.38)

$$\begin{aligned} {}^S E_{zIk} &\approx g_I \cdot \beta_I \cdot H_0 \cdot K\tau_r \cdot \sum_m m_k \cdot (|\varepsilon(m)| \cdot \tau_D)^{1/2} \cdot \\ &\cdot [2 \cdot \prod_k (2I_k + 1) \cdot (1 + K \cdot \tau_r)^2]^{-1}, \end{aligned} \quad (4.40)$$

$${}^T E_{zIk} \approx -{}^S E_{zIk} \cdot (1 + K \cdot \tau_r) / 3,$$

$${}^F E_{zIk} \approx -f \cdot K \cdot \tau_r \cdot {}^S E_{zIk} / 4.$$

The analysis of the above relations shows that the rotation of radicals with anisotropic reactivity influences the CIDNP effects. In the case of geminate and diffusion RPs the character of rotational influence is the same; therefore we confine our discussion to diffusion pairs.

The influence of radical rotation on the scale of CIDNP effects is strongly dependent on radical reactivity. For radicals with low reactivity, when $K\tau_r < 1$, neglecting their rotation (see (4.40))

$${}^F E_{zIk} \sim f K^2 \tau_r^2 \cdot \sum_m m_k \cdot (|\varrho(m)| \cdot \tau_D)^{1/2}$$

while the rotational relaxation reduces nuclear polarization and, according to (4.39),

$${}^F E_{zIk} \sim f^2 K^2 \tau_r^2 \cdot \sum_m m_k \cdot (|\varrho(m)| \cdot \tau_D)^{1/2}.$$

Thus, for radicals with $K\tau_r < 1$ the CIDNP effect can be f^{-1} -fold overestimated provided no account is taken of the radical orientational relaxation.

For radicals with $fK\tau_r > 1$, the CIDNP effects are also strongly dependent on the rate of radical orientational relaxation. A comparatively slow orientational relaxation, $\tau_D/\tau_0 \approx 1$, results in a $1/f$ -fold decrease of the CIDNP effects as compared to those that would be erroneously calculated neglecting orientational relaxation. On the other hand, a very fast relaxation, when $\tau_D \gg \tau_0$, leads to $1/f$ -fold increase in the CIDNP effects as compared to those obtained neglecting radical rotation. Table 4.3 illustrates the above statements showing the data on CIDNP effects calculated at different values of the parameter τ_D/τ_0 . The CIDNP effect is seen to have a minimum as the parameter τ_D/τ_0 (i.e., the orientational relaxation rate) grows.

Table 4.3. Values of $\Delta(E_{zI} = -\hbar \cdot \gamma_1 \cdot H_0 \cdot A/16)$ for a one-nucleus RP with spin 1/2 and $Aq = 10^{-3}$, $H_0 = 10^4$ G, $f = 0.1$, $\tau_D = 10^{-10}$ s

$K\tau_r \backslash \tau_D/\tau_0$	0	0.1	1	5	100	∞
0.1	$1.7 \cdot 10^{-5}$	$1.9 \cdot 10^{-6}$	$1.9 \cdot 10^{-6}$	$1.9 \cdot 10^{-6}$	$2.0 \cdot 10^{-6}$	$2.0 \cdot 10^{-6}$
1	$5.4 \cdot 10^{-4}$	$6.8 \cdot 10^{-5}$	$8.9 \cdot 10^{-5}$	$1.1 \cdot 10^{-4}$	$1.5 \cdot 10^{-4}$	$1.7 \cdot 10^{-3}$
10	$1.8 \cdot 10^{-3}$	$2.8 \cdot 10^{-4}$	$5.0 \cdot 10^{-4}$	$9.4 \cdot 10^{-4}$	$2.7 \cdot 10^{-3}$	$5.0 \cdot 10^{-3}$
100	$2.2 \cdot 10^{-3}$	$3.4 \cdot 10^{-4}$	$6.9 \cdot 10^{-4}$	$1.4 \cdot 10^{-3}$	$5.9 \cdot 10^{-3}$	$1.8 \cdot 10^{-2}$

The parameter τ_D/τ_0 cannot be varied arbitrarily in any concrete system. This parameter will be viscosity independent provided that the rotational and translation radical mobilities are equally dependent on the solvent viscosity. For instance, radicals with equal van der Waals radii have $\tau_D/\tau_0 = 6$ if τ_0 is determined by the Debye rotational relaxation theory (3.30). The relaxation of mutual unpaired electron orientation can be associated with the rotation of radical fragments, which can increase τ_D/τ_0 .

We now compare CIDNP effects at $\tau_D/\tau_0 > 1$ with those calculated neglecting orientational relaxation. The ratio of these values is

$$\begin{aligned} \chi &= E_{zI}(\tau_D > \tau_0) / E_{zI}(\tau_0 \rightarrow \infty) \approx \\ &\approx f \cdot (1 + K \cdot \tau_r)^2 / [1 + K \cdot \tau_r (f + (1 - f) / (1 + (\tau_D/\tau_0)^{1/2}))]. \end{aligned}$$

Table 4.4 lists numerical values of χ and shows that fast orientational relaxation reduces the CIDNP effects in practically all reactions of radicals with anisotropic reactivity as compared to those that would be obtained without account taken of radical rotation. Thus, quantitative calculations of CIDNP effects demand that anisotropic character of radical reactivity as well as its averaging due to mutual radical orientational relaxation should be taken into consideration.

Table 4.4. χ values at $\tau_D/\tau_0 = 6$ and 12 (χ values at $\tau_D/\tau_0 = 12$ given in parenthesis). K is the rate constant of a singlet RP recombination at a contact, τ_r is the total time of all the contacts, f is the geometric steric factor, τ_D/τ_0 is the effective number of radical reorientations during the in-cage RP life-time

$f \backslash K\tau_r$	0.111	1.00	9.00	∞
0.5	0.21 (0.22)	0.38 (0.40)	0.90 (0.98)	1.2 (1.3)
0.1	0.062 (0.070)	0.12 (0.15)	0.47 (0.62)	0.76 (1.1)
0.05	0.032 (0.094)	0.073 (0.20)	0.27 (0.37)	0.47 (0.72)
0.01	0.0069 (0.0077)	0.016 (0.018)	0.063 (0.091)	0.11 (0.18)

4.2.8 RP substitution

In-cage reactions can proceed via a number of subsequent RPs. CIDNP analysis enables one to consider chemical RP transformations in a cage [4.1,8]. For example, acetyl peroxide decomposition follows the scheme presented in Fig. 4.5 where three successive RPs are seen to form. In this case net CIDNP is observed in the ethane molecules [4.1]. Ethane results from the recombination of two methyl radicals. Since the g -values of the two methyl radicals are equal, net polarization, according to the above theory, cannot result from the spin dynamics of a $\dot{\text{C}}\text{H}_3 + \dot{\text{C}}\text{H}_3$ pair. Similarly cannot the net polarization occur in the initial pair consisting of two identical radicals (see Fig. 4.5). Data on the net CIDNP in ethane leads to the

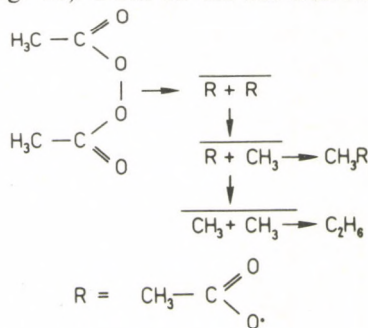


Fig. 4.5. Scheme of acetylperoxide decomposition

conclusion that the stage $\dot{R} + \dot{C}H_3$ is followed by ethane formation. Thus, nuclear polarizations in RP recombination products depend, in general, on the spin dynamics of not only the pair precursor but also all the preceding pairs. den Hollander was the first who paid attention to an important feature of nuclear polarizations in successive RPs [4.8]: the spin polarization effects cannot be treated simply as a sum of those arising in different stages and in different RPs. The effects of interference of spin dynamics of different RPs (called by den Hollander *cooperative effects*) can be of great importance.

To illustrate it, consider a succession of two RPs with the following characteristics. In the first pair (RP₁) the radical g -values are different and the hf constant with the magnetic nucleus equals zero. This pair then turns into RP₂ with equal g -values and a nonzero hf constant with spin 1/2 nucleus. No nuclear polarization will be observed in recombination products of each pair. However, when the same RPs are formed in succession, i.e. one RP turns into another, then the final recombination product shows nuclear polarization.

This can be illustrated by the vector RP model (see Fig. 1.4). Let both RPs be divided into two subensembles: in one the nuclear spins are orientated in the direction of the magnetic field and in the other against it. In RP₁ in both subensembles the spin precession phases of the unpaired electrons (S_1 and S_2 in Fig. 1.4 (a), (b)) differ by $\Delta g \cdot \beta_e \cdot H_0 \cdot t/\hbar$ due to the difference between the g -values. At a time t_1 RP₁ turns into RP₂. By the moment of RP₂ recombination, in one subensemble S_1 and S_2 spin dephasing is $\Delta g \cdot \beta_e \cdot \hbar^{-1} \cdot H_0 \cdot t_1 + a \cdot t_2/2$ and in the other subensemble $\Delta g \cdot \beta_e \cdot \hbar^{-1} \cdot H_0 \cdot t_1 - a \cdot t_2/2$. As a result, the RP recombination probability depends on the nuclear orientation. The situation is in fact the same as if there were only one RP with $\Delta g \neq 0$ and $A \neq 0$. The only difference is that the spin dephasings due to the Δg - and hf-mechanisms in the case of successive RPs are separated in time. This shows that the CIDNP effects in the case of successive RPs does not reduce to a simple summation of nuclear spin polarizations in different stages of chemical RP transformations. This fact impedes a detailed quantitative analysis of CIDNP effects for successive RPs.

In order to interpret CIDNP effects correctly for successive RPs, the following point is of importance. An elementary chemical step of transformation of one RP into another occurs too fast for the reagent spin states to change. Therefore, the spin state of the preceding RP is the initial state for the following RP spin dynamics. den Hollander [4.8] evaluated quantitatively the CIDNP effects in reactions proceeding through successive RPs. The scheme of his calculations is the following. Suppose that RP₁ turns into RP₂ with a mean rate $1/\tau_1$. Consider an RP subensemble with a certain nuclear spin orientation $\{m\}$. Let the matrix element for the singlet-triplet mixing of RP states be $\varepsilon_1(m) = \varepsilon_1$ and $\varepsilon_2(m) = \varepsilon_2$ for RP₁ and RP₂ respectively (see (3.1)). To simplify the case, suppose that at the initial moment the RP₁ is in the singlet state. The probability that RP₂ will be in the singlet state by a time t is

$$\rho_s(t) = \int_0^t (dt'/\tau_1) \cdot \exp(-t'/\tau_1) \cdot \cos^2 \{ \varepsilon_1 t' + \varepsilon_2(t-t') \}, \quad (4.41)$$

where $(dt'/\tau_1) \cdot \exp(-t'/\tau_1)$ is the probability that RP_1 turns into RP_2 within the range $(t', t' + dt')$. If RP_2 can in its turn transform into a new pair then the integrand in (4.41) must be multiplied by the probability that RP_2 is not subjected to chemical transformations within the range (t', t) . With account taken of only one re-encounter at the recombination radius we obtain the following recombination probability for RP_2 with a set configuration of nuclear spins

$$s_p \approx \lambda_2 \int_0^{\infty} dt \cdot f(t) \cdot \rho_S(t) \quad (4.42)$$

where $f(t) \cdot dt$ is the distribution function for first re-encounters and, λ_2 is RP_2 recombination probability from the singlet state at a contact.

The above consideration can be generalized by taking into account further RP transformations. For example, den Hollander calculated three successive RPs. The methods discussed in Section 2.3 make it possible to summarize the contributions of all the re-encounters of a RP to the reaction. However, the results become very cumbersome.

Sufficiently simple results on CIDNP effects in reactions proceeding through successive RPs can be obtained when the lifetimes of individual pairs are comparatively small, so that the singlet-triplet transitions have enough time to be realized but with a very small probability. We consider some examples before making generalizations.

Let RP_1 and RP_2 be two successive RPs with the spin-Hamiltonian of eq. (4.21). The parameters referring to the first and the second RPs will be denoted by superscripts. At a time t_1 , RP_1 transforms into RP_2 which then recombines and yields a product. Solving eqs (4.22) and considering only the terms of the order at_1 , $a^2 t_1^2$, $\Delta g \cdot t_1$, $\Delta g^2 \cdot t_1^2$ we have that by the moment of RP_1 transformation into RP_2 the quantities characterizing the spin state ordering are

$$\begin{aligned} K_{NE}(t_1) &\approx -g_I \cdot \beta_I \cdot H_0 \cdot (\omega_1^{(1)} - \omega_2^{(1)}) \cdot a^{(1)} \cdot P_0(0) \cdot t_1^2/8, \\ Q_1(t_1) &\approx -a^{(1)} \cdot P_0(0) \cdot t_1/8, \\ Q_2(t_1) &\approx -(\omega_1^{(1)} - \omega_2^{(1)}) \cdot P_0(0) \cdot t_1/2, \\ P_0(t_1) &\approx P_0(0) \cdot \{1 - [(\omega_1^{(1)} - \omega_2^{(1)})^2 + (a^{(1)}/2)^2] \cdot t_1^2\}. \end{aligned} \quad (4.43)$$

For RP_1 only the quantity $P_0(0)$ differs from zero at the initial moment; however, it is not the case for RP_2 at the moment of its formation. The spin dynamics in RP_2 goes on developing under the initial condition determined by eqs (4.43). By the moment of RP_2 recombination, polarization is observed in the singlet RP subensemble,

$$\begin{aligned} K_{NE}(t_1 + t_2) &\approx -(g_I \cdot \beta_I \cdot H_0/8) \cdot \{(\omega_1^{(1)} - \omega_2^{(1)}) \cdot a^{(1)} \cdot t_1^2 + \\ &+ (\omega_1^{(1)} - \omega_2^{(1)}) \cdot a^{(2)} \cdot t_1 t_2 + (\omega_1^{(2)} - \omega_2^{(2)}) \cdot a^{(1)} \cdot t_1 t_2 + \\ &+ (\omega_1^{(2)} - \omega_2^{(2)}) \cdot a^{(2)} \cdot t_2^2\} \cdot P_0(0). \end{aligned} \quad (4.44)$$

It follows from this equation that interference of spin dynamics in successive RPs contributes to the CIDNP effect.

The last result can be readily generalized for the case when the reaction proceeds through n successive RPs

$$K_{NE}(t_1 + t_2 + \dots + t_n) \approx -(g_I \cdot \beta_I \cdot \beta_e \cdot \hbar^{-1} \cdot H_0^2/8) \cdot P_0(0) \cdot \sum_{k=1}^n \sum_{l=1}^n (g_1^{(k)} - g_2^{(k)}) \cdot a^{(l)} \cdot t_k \cdot t_l. \quad (4.45)$$

Thus net CIDNP is determined by the effective parameters

$$\Delta g_{\text{eff}} = \sum_{k=1}^n (g_1^{(k)} - g_2^{(k)}) \cdot t_k / \sum_{k=1}^n t_k \quad (4.46)$$

and

$$a_{\text{eff}} = \sum_{k=1}^n a^{(k)} \cdot t_k / \sum_{k=1}^n t_k. \quad (4.47)$$

Analogous regularities can also be obtained for multiplet CIDNP effects in reactions proceeding via successive RPs:

$$K_{ME} \approx -(1/32) \cdot \hbar \cdot j_{12} \cdot P_0(0) \cdot \sum_{k=1}^n a_1^{(k)} \cdot t_k \cdot \sum_{l=1}^n a_2^{(l)} \cdot t_l. \quad (4.48)$$

According to eqs (4.44–48) the CIDNP effects for a succession of short-lived radical pairs obey the well-known Kaptein rules provided the effective quantities (4.46) and (4.47) are substituted to eqs (4.9, 10) for the radical Δg -values and hf constants. When deriving (4.44–48) we assume that only the last pair of the RP succession can recombine, while each of the preceding pairs transforms into a new RP rather than recombine. If the preceding RPs can also recombine, the nuclear polarization arising in the recombination product of a given pair can differ essentially from that described by eqs (4.44–48).

To illustrate this statement consider the following example. Let RP_1 be singlet-born. Assume that it can either recombine (with the rate K) or transform into a triplet state (with the rate ε). The S–T mixing being sufficiently effective ($\varepsilon \gtrsim K$), RP_2 is chiefly triplet-born. Hence, the CIDNP effects originate in RP_2 as in a triplet-born pair even though the initial state of the primary pair was singlet. In the case when the primary pair is also triplet-born, no multiplicity alterations of the initial RP_1 and RP_2 states of the type take place.

The CIDNP effects originating in reactions running via successive RPs can be calculated quantitatively by corresponding kinetic equations. So far such calculations have only been performed for two successive pairs [4.9]. The recombination probability of the primary and the secondary RPs with specified nuclear spin configurations, $p_1(m)$ and $p_2(m)$ have already been cited in Section 3.1.11 when discussing the field effects on such reactions (see eqs (3.46, 47)).

The net polarizations arising in the primary and secondary RP recombination products follow the equations

$$E_{zIk}(1) = -g_I \cdot \beta_I \cdot H_0 \cdot \sum_m m_k \cdot p_1(m) = -g_I \cdot \beta_I \cdot H_0 \cdot \langle m_k(1) \rangle,$$

$$E_{zIk}(2) = -g_I \cdot \beta_I \cdot H_0 \cdot \sum_m m_k \cdot p_2(m) = -g_I \cdot \beta_I \cdot H_0 \cdot \langle m_k(2) \rangle. \quad (4.49)$$

The mean values of the nuclear spin projection in the RP_1 and RP_2 recombination products are calculated by relations (3.46, 47). Likewise, the multiplet polarization is governed by the quantities

$$\sum_m m_1 \cdot m_2 \cdot p_1(m) \text{ and } \sum_m m_1 \cdot m_2 \cdot p_2(m).$$

Figures 4.6 and 4.7 give the nuclear polarizations calculated by eq. (4.49). The recombination of both pairs is assumed to occur only from a singlet state.

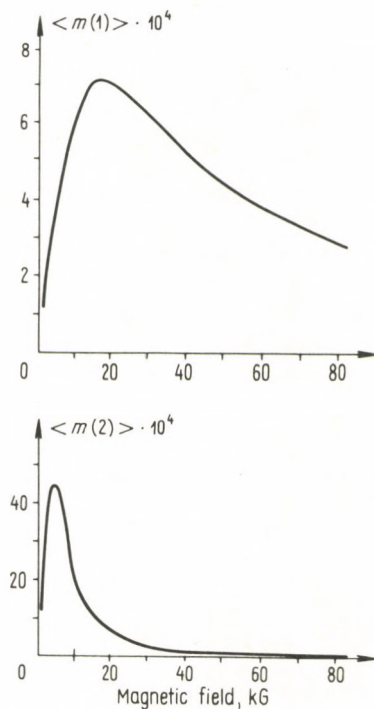


Fig. 4.6. Field dependence of nuclear spin polarizations in the primary and secondary pair recombination products for a triplet-born RP_1 . Both RPs are assumed to have one magnetic nucleus with the hf constant equal to 40 G; the difference in the g -values in both pairs is 0.01. The other RP parameters are the same as in Fig. 3.7. The nuclear polarization signs in the recombination products of the primary and secondary pairs coincide

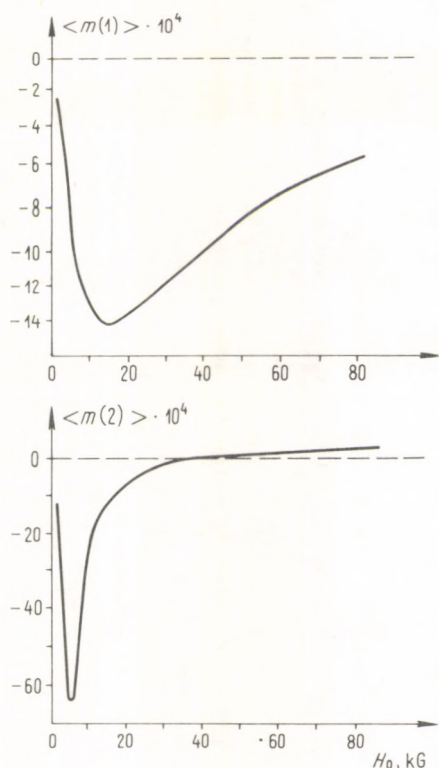


Fig. 4.7. Field dependence of nuclear spin polarizations in the primary and secondary pair recombination product in the case of a singlet-born RP_1 . All the parameters are the same as in Fig. 4.6. In very high fields the nuclear polarization sign in the recombination products of the primary and secondary pairs are opposite

As a rule, the net polarization has a maximum. The CIDNP maximum is usually reached in fields H_0 when the efficiencies of the Δg - and hf-mechanisms become comparable. This is just the case for RP_1 . The maximum polarization observed in RP_2 recombination product arises however at a much lower strength of the external field.

The maximum in $\langle m(2) \rangle$ correlates with the extremum in the field dependence of RP_2 recombination probability (cf. Figs 4.6 and 4.8).

When the RP_1 is triplet-born, the nuclear polarization sign of both RP_1 and RP_2 recombination products obeys the Kaptein rules. However, according to the foregoing considerations, in the case of a singlet-born RP_1 the nuclear polarization arising in the secondary pair recombination product shows an anomaly: the polarization sign alters with growing magnetic field. However the sign alteration occurs at considerable field strengths and the absolute value of the polarization is small; this makes it difficult to observe the anomaly experimentally.

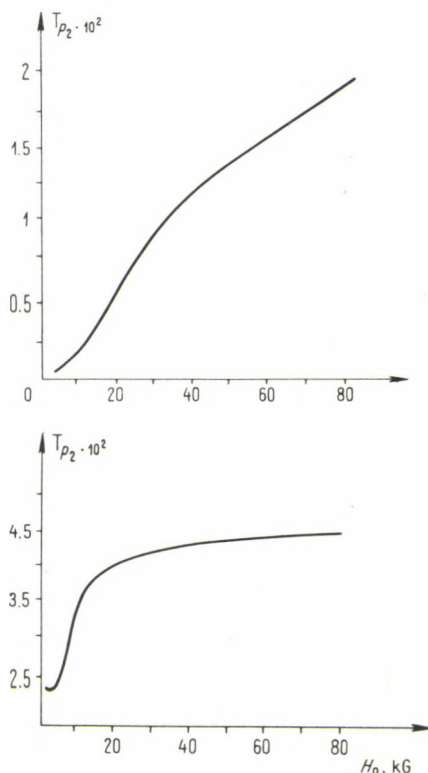


Fig. 4.8. Field dependence of the recombination probability of two successive RPs in the case of triplet-born RP_1 . RP parameters are the same as in Fig. 4.6. The product generation probability in the secondary RPs is minimum in fields $H_0 \approx 4$ kG

An interesting case of two successive RPs occurs when one of RP_1 partners has short paramagnetic relaxation times $T_1, T_2 \lesssim 10^{-10}$ s [4.8]. During RP_1 lifetime the relaxation randomizes the spin orientations of the reagents and, independently of the RP_1 precursor multiplicity, the electron spins become uncorrelated by the time of RP_2 formation. The nuclear polarization of RP_2 recombination products then has the same sign as for CIDNP in diffusion RP_2 recombination products.

CIDNP analysis in reactions running through successive pairs is a somewhat cumbersome problem. This analysis, however, can be carried out, and it provides unique information on the intermediate elementary steps of radical reactions (see, e.g., [4.8])

4.2.9 CIDNP kinetics

We have already discussed nuclear polarizations in reaction products calculated per RP. The number of RPs participating in a specific reaction and the kinetics of their formation are determined by concrete experimental conditions. However

experimental value of nuclear polarization depends not only on chemical reaction kinetics, but also on the nuclear spin relaxation in the recombination products. Thus to interpret experimental CIDNP data quantitatively one must analyze the kinetics of CIDNP formation and its relaxation in the diamagnetic products.

Nuclear polarization kinetics in the course of chemical reactions. Consider nuclear polarizations in the case of geminate recombination. Suppose that radical pairs are generated in a system with the rate $v(t)$. The value of $v(t)$ depends on the specific system and the experimental conditions. With the above data on nuclear polarizations in the recombination product of one RP we can write the following kinetic equations describing CIDNP formation

$$\begin{aligned} (\partial^{S,T} E_{zIk}/\partial t)_r &= v(t) \cdot \left\{ -g_I \cdot \beta_I \cdot H_0 \cdot \sum_m m_k \cdot {}^{S,T} \sigma_{mm} \right\}, \\ (\partial^{S,T} E_{I_1 I_2}/\partial t)_r &= v(t) \cdot \hbar j_{12} \cdot \sum_m m_1 \cdot m_2 \cdot {}^{S,T} \sigma_{mm}, \end{aligned} \quad (4.50)$$

where superscripts S and T characterize the values referring to singlet and triplet RP precursors, σ_{mm} is the population of the state with the nuclear spin configuration $m = (m_1, m_2, \dots)$. The quantities in braces have been discussed above in detail.

Using eq. (2.202) we have the following equations

$$\begin{aligned} (\partial^F E_{zIk}/\partial t)_r &= -g_I \cdot \beta_I \cdot H_0 \cdot \text{Tr}_{S,I} \{ \hat{I}_{kz} \cdot \hat{R} \}, \\ (\partial^F E_{I_1 I_2}/\partial t)_r &= \hbar \cdot j_{12} \cdot \text{Tr}_{S,I} \{ \hat{I}_{1z} \cdot \hat{I}_{2z} \cdot \hat{R} \}, \\ \hat{R} &= \hat{K}_1 \sigma_A(t) \times \sigma_B(t) \cdot C_A(0) \cdot C_B(0) \end{aligned} \quad (4.51)$$

for CIDNP induced by radical recombination in homogeneous solutions. The quantities in these relations have been determined in eqs (2.200–202). Note, that $\text{Tr}_{S,I}$ means the trace over all spin variables of radical pairs. Equation (4.51) can be written in a more convenient form using the above data on nuclear polarization in diffusion RP recombination products:

$$\begin{aligned} (\partial^F E_{zIk}/\partial t)_r &= -g_I \cdot \beta_I \cdot H_0 \cdot K_D \cdot C_A(t) \cdot C_B(t) \cdot \sum_m m_k \cdot {}^F \sigma_{mm}, \\ (\partial^F E_{I_1 I_2}/\partial t)_r &= \hbar \cdot j_{12} \cdot K_D \cdot C_A(t) \cdot C_B(t) \cdot \sum_m m_1 \cdot m_2 \cdot {}^F \sigma_{mm}. \end{aligned} \quad (4.52)$$

Here K_D is the rate constant of diffusion radical encounters, C_A and C_B are concentrations of A and B radicals.

CIDNP effect relaxation. The nuclear polarization relaxation occurring in diamagnetic molecules can be of two types: spin–lattice relaxation and polarization redistribution, i.e. polarization transfer between nuclei. All these processes and the corresponding kinetic equations have been thoroughly studied and the detailed information on them can be found in a number of monographs on NMR (see, e.g., [4.10]). Therefore, here we confine ourselves to a brief discussion of the problem.

In most cases nuclear spin-lattice relaxation can be described in terms of a time T_1 [4.10]. Under this condition we get

$$\begin{aligned} (\partial E_{zI}/\partial t)_{s-l} &= -(E_{zI} - E_{zI}^0)/T_1, \\ (\partial E_{I_1 I_2}/\partial t)_{s-l} &= -[1/T_1(1) + 1/T_1(2)] \cdot (E_{I_1 I_2} - E_{I_1 I_2}^0), \end{aligned} \quad (4.53)$$

where E_{zI}^0 and E_{II}^0 are the Zeeman energy and the energy of spin-spin nuclear interaction under equilibrium conditions. Equations (4.53) describe changes in the nuclear polarization induced by the nuclear binding with the thermal reservoir (lattice).

In real systems, CIDNP relaxation can be hampered by the processes of polarization redistribution among different nuclei. As a result of spin-spin interaction, the Zeeman energy can be transferred from some nuclei to others. As a result, one can observe the polarization of even those nuclei that are not directly polarized in the RP recombination.

Polarization transfer is caused either by dipole-dipole or scalar (j - j) nuclear interactions. Consider, for example, two nuclei, I_1 and I_2 . Assume the j - j interaction to be negligible. The thermal molecular motion (rotational diffusion, in particular) modulates the dipolar interaction of the said nuclei in a random manner. The kinetic equations describing the polarization transfer between two spins induced by dipolar interactions are well known (see, [4.10] eqs (VIII. 87))

$$\begin{aligned} \partial \langle I_{z1} \rangle / \partial t &= -(\langle I_{z1} \rangle - I_1^0) / T_1(1) - (\langle I_{z2} \rangle - I_2^0) / T_1(12), \\ \partial \langle I_{z2} \rangle / \partial t &= -(\langle I_{z1} \rangle - I_1^0) / T_1(21) - (\langle I_{z2} \rangle - I_2^0) / T_1(2). \end{aligned} \quad (4.54)$$

The quantities $1/T_1(12)$ and $1/T_1(21)$ characterize the polarization transfer rate between the spins. The kinetic parameters in eqs (4.54) are known from NMR theory to depend strongly upon molecule mobility. The molecule rotation being comparatively slow, the excitation is transferred by flip-flops of the spin-partners. Therefore, the polarization of one spin is transferred to its partner without sign alteration. In the case of fast molecule rotation, the polarization transfer between the partners occurs with sign alteration (see [4.10], eq. (VIII. 88 a)).

The Zeeman spin frequency difference slightly exceeding the j - j interaction constant, the latter can also result in the interspin polarization transfer. In this case the transfer mechanism is a mutual flip-flop of two spins and hence no sign alteration is observed.

The processes of nuclear polarization relaxation and redistribution in diamagnetic products complicate the interpretation of the CIDNP effect. These difficulties can be overcome successfully by performing experiments not under stationary but under pulse conditions, and by measuring CIDNP effects in either nanosecond or submicrosecond time scales, when the processes of nuclear polarization relaxation and transfer cannot manifest themselves [4.11].

4.2.10 Concluding remarks

Recombination of two radicals is one of the most important and frequent reactions among reactions between paramagnetic particles. The theory of spin effects in chemical reactions is therefore being developed, first of all, in relation to this phenomenon. However, spin polarization effects can take place in some other bimolecular (or trimolecular, etc.) reactions involving paramagnetic partners. In fact, the underlying mechanism of CIDNP effects is similar to that in the case of radical recombination.

For example, consider the possibility of nuclear polarization in the products of biradical recombination [4.12]. When encountering, two biradicals can occur in the state with the total spin of four unpaired electrons equal to 2, 1, or 0. The isotropic hyperfine interaction of the unpaired electrons with their magnetic nuclei induces intersystem transitions. As a result, the nuclear spins of the products are polarized as in the case of radical recombination. Two biradicals will usually recombine provided that at the moment of their contact they are in an overall singlet state. There is, however, one more plausible mechanism of CIDNP effects in such reactions [4.12]. Two biradicals can recombine even from the triplet state. In this case they give a new biradical in which singlet-triplet transitions are quite possible.

Summarizing, then, one may say that at the present time the basic regularities of CIDNP effects in high magnetic fields have been found and a quantitative theory of nuclear polarizations in radical reaction products has been elaborated. The Kaptein rules are the most important results in the CIDNP theory for high magnetic fields. One must remember, however, that in a number of cases the nuclear polarization sign observed experimentally does not agree with that predicted by the Kaptein rules. For instance, reactions running through successive RPs, geminate RP recombination with the partners not in a direct contact at the initial moment and with fast singlet-triplet mixing before the first encounter, etc. are possible exceptions. To interpret CIDNP effects quantitatively, it is necessary, on the one hand, to calculate precisely the nuclear polarization in radical recombination and, on the other hand, to analyze the nuclear polarization kinetics in the final products using experimental and theoretical data about nuclear magnetic relaxation.

4.3 Low field CIDNP theory

4.3.1 Qualitative considerations

The in-cage RP spin dynamics is essentially dependent on the magnetic field strength. In high magnetic fields the basic channels of RP intersystem transitions are S-T transitions induced by either the difference in the g -values of the collision partners or the hf interactions of the unpaired electrons with the magnetic nuclei (or by both mechanisms), orientation of each spin being constant with respect to the

external magnetic field direction. However, as a result of the spin selection rule, the chemical reaction sorts RPs according to their nuclear spin configurations, so that the reaction products are formed with a particular nuclear spin polarization.

In low fields the spin dynamics are quite different. First of all, the difference in g -values is no longer important. Indeed, the matrix element of $S-T_0$ mixing for the Δg -mechanism is $\varepsilon_{ST_0} = 0.44 \cdot 10^7 \cdot \Delta g \cdot H_0$ rad/s (if H_0 is in Gauss). Hence, for a typical Δg -value, $\Delta g \approx 0.01-0.001$, in low magnetic fields of some 10–100 G, ε_{ST_0} is too small values to manifest itself during the in-cage RP lifetimes. The only exception is reactions between partners with Δg of the order of unity, for example, those involving paramagnetic ion complexes (see, e.g., [4.13]).

The basic mechanism of intersystem transitions in low fields is the hf-mechanism, the hf effects on RP spin motion in low and high fields being quite different. As the field strength decreases, some additional channels of intersystem transitions are opened (see e.g. Fig. 1.7 (b), (c)). The Zeeman splitting of the triplet term becomes comparable to the hf interaction and, hence, $S-T_+$, T_- transitions become possible together with $S-T_0$. The peculiarity of the latter transitions is that they allow mutual electron and nuclear spin flips (see, e.g., Fig. 1.5). Thus, unlike high magnetic fields, in low fields nuclear polarizations result not only from the RP selection during the reaction, the nuclear spin configuration being constant, but also from the RP nuclear spin flips.

When the field is changed from high to low, the role of radical exchange interactions in the CIDNP effects increases. To consider this problem qualitatively, see the RP term scheme (Fig. 4.9) where shaded regions show interrational distances at which hf interactions can mix singlet and triplet RP terms efficiently. It is obvious from the scheme that at high magnetic fields, $S-T_-$ transitions can occur only over a

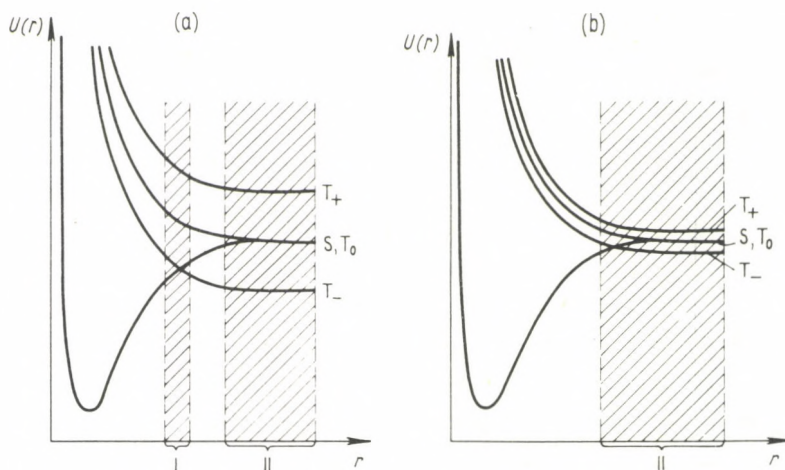


Fig. 4.9. Comparison of RP terms in high (a) and low (b) magnetic fields. In case of high fields S and T_- terms are in resonance only within a very narrow layer I

narrow region of interradical distances (region I). The time of passing via the region of S and T crossing is of the order of that of an elementary radical diffusion step, that is about 10^{-11} s. Within this time the hf interaction practically does not mix the S and T₋ terms. The S-T₀ channel is thus the basic one (region II in Fig. 4.9 (a)), the RP residing in region II for a comparatively long time between the re-encounters. The exchange interactions split the S and T₀ terms thus hampering intersystem transitions. In conclusion it is possible to say that in high magnetic fields the exchange interactions do not qualitatively affect singlet-triplet mixing but result only in quantitative changes of S-T₀ transition efficiency. In low fields all the three types of transitions occur simultaneously. Different transition channels interfere, this interference sometimes being a determining factor for CIDNP effects. As a result, even a weak radical exchange interaction in region II (Fig. 4.9 (b)) can affect the coupled motion of RP electron and nuclear spins qualitatively.

During the thermal motion of a RP, the exchange integral varies in a random manner. It increases sharply when the radicals approach, the singlet-triplet transitions ceasing. When the RP is out of contact, the singlet-triplet mixing resumes. At the encounter moment the singlet and triplet states are being dephased by strong exchange interactions which can be expressed in the choice of the boundary conditions at the reaction radius (see eq. (2.186)). In high fields, when only the S-T₀ channel is open, this dephasing can affect the RP intersystem transition probability only quantitatively. In low fields, with the channels interfering, the S and T state dephasing at the encounter moment can influence the RP spin dynamics qualitatively. Adrian [4.14] has considered an interesting example of the post-encounter spin dynamics affected by an exchange interaction at the encounter moment.

An increase in the number of S-T transition channels, as well as exchange interaction effects on the RP spin dynamics, greatly complicates the CIDNP theory in low fields. Therefore, though the mathematical methods described in Sec. 2.3 allows one to analyze chemical spin polarizations in any magnetic field, the low field CIDNP theory has hitherto been much less elaborated than that for high fields.

Some attempts were made to interpret the low field CIDNP phenomenon qualitatively on the basis of diagram representations [4.1,14]. In general, those attempts proved to be a failure. Nevertheless, it is expedient to discuss them since, first there are situations (e.g., in biradicals [4.1,15]) for which the model representations describe the CIDNP mechanism reliably. Second, graphic models provide better understanding of the difficulties the low field CIDNP theory is faced with.

The Kaptein diagram. Kaptein proposed the graphic model to interpret low field CIDNP qualitatively [4.1]. Consider a RP with a spin 1/2 nucleus and assume it is characterized by some constant, time-independent, exchange integral. The spin Hamiltonian of this RP is

$$\begin{aligned} \hat{H} = & \hbar\omega_0 \cdot (\hat{S}_{1z} + \hat{S}_{2z}) + \hbar a \hat{S}_{1z} \hat{I}_z + \hbar b \cdot (\hat{S}_{1x} \hat{I}_x + \\ & + \hat{S}_{1y} \hat{I}_y) - \hbar J_0 \cdot (1/2 + 2\hat{S}_1 \hat{S}_2); \quad \omega_0 = g \cdot \beta_e \cdot \hbar^{-1} \cdot H_0, \end{aligned} \quad (4.55)$$

where $b \equiv a$. Equation (4.55) is used to identify the role of the secular, $a \cdot \hat{S}_{1z} \cdot \hat{S}_{2z}$, and non-secular, $b \cdot (\hat{S}_{1x} \cdot \hat{I}_x + S_{1y} \cdot \hat{I}_y)$, portions of the hf. Assume that the RP is singlet-born. The hf interaction induces intersystem transitions; the total projection of all spins, electron and nuclear, must be constant in a system with Hamiltonian (4.55). Hence, the matrix elements of the following transitions

$$\begin{aligned} \langle S, 1/2 | \hat{H} | T_0, 1/2 \rangle &= \hbar a / 4, \\ \langle S, -1/2 | \hat{H} | T_0, -1/2 \rangle &= -\hbar a / 4, \\ \langle S, 1/2 | \hat{H} | T_+, -1/2 \rangle &= -\hbar b / 2 \sqrt{2}, \\ \langle S, -1/2 | \hat{H} | T_-, 1/2 \rangle &= \hbar b / 2 \sqrt{2} \end{aligned} \tag{4.56}$$

differ from zero. Here $|1/2\rangle$ and $|-1/2\rangle$ are the states when the nuclear spins are orientated either along or opposite the magnetic field, respectively. At the initial moment, the number of RPs in states $|S, +1/2\rangle$ and $|S, -1/2\rangle$ are equal. From both states a pair can turn into two triplet terms, the matrix transition elements with and without spin flips coinciding respectively for both RP subensembles. According to Kaptein, nuclear polarizations in RP recombination products arise due to different rates of the processes $|S, +1/2\rangle \rightarrow |T_+, -1/2\rangle$ and $|S, -1/2\rangle \rightarrow |T_-, +1/2\rangle$. The matrix elements of both transitions are equal (see (4.56)). The difference in the efficiencies of the intersystem transitions has been attributed by Kaptein to the difference in their energy separations. His idea is based on the scheme of RP levels depicted in Fig. 4.10(a), where the level $|T_+, -1/2\rangle$ is closer to the singlet term than the level $|T_-, +1/2\rangle$. Hence, at $J_0 = 0$ and $a > 0$ transitions $|S, 1/2\rangle \rightarrow |T_+, -1/2\rangle$ seem to be more effective than $|S, -1/2\rangle \rightarrow |T_-, 1/2\rangle$. As a result, in the singlet and triplet RP states, nuclear spins are expected to be preferably oriented opposed to the field direction. Both in geminate and escape recombination products, nuclear spins are negatively polarized. In the situations depicted in Fig. 4.10 (b), (c), (d) the energy

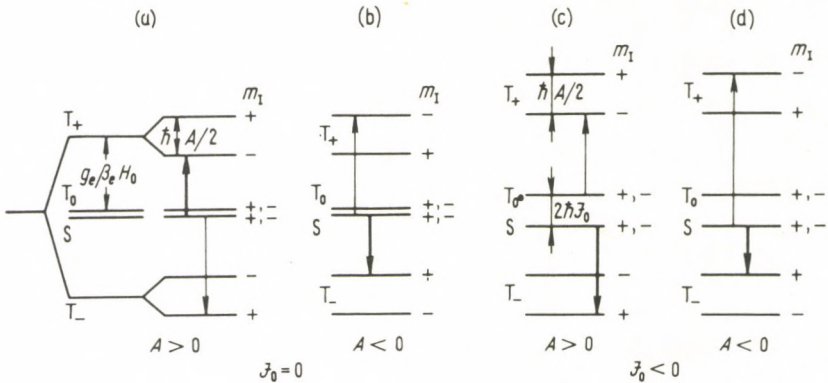


Fig. 4.10. Energy level diagram of one-nuclear RP [4.1]. The scheme neglects the splitting of S and T₀ terms induced by the adiabatic part of the hf interaction

separation is less for the transition $|S, -1/2\rangle \rightarrow |T_-, 1/2\rangle$. As a result, the geminate and escape products are expected to be positively polarized.

Thus, the basic postulates and conclusions of the graphic model are as follows. $S-T_0$ transitions are considered unimportant in CIDNP arising in low fields. Nuclear polarizations are associated with different efficiencies of $|S, 1/2\rangle \rightarrow |T_+, -1/2\rangle$ and $|S, -1/2\rangle \rightarrow |T_-, 1/2\rangle$ transitions accompanied by nuclear spin flips. The diagram depicted in Fig. 4.10 shows the CIDNP sign to be the same both in geminate and escape recombination products. If $|J_0| > |a|/4$, then the nuclear polarization sign must be independent of the sign of the hf constant. At lower values of the exchange integral the polarization is opposite in sign to the hf constant. Considerations analogous to those given above lead to the conclusion that the polarization sign alters if the RP has a triplet but not a singlet precursor.

The graphic model interprets CIDNP as a result of competition between two intersystem transition channels in which the nuclei are oppositely polarized. This model, however, is valid, with respect to spin dynamics, only for RPs with comparatively strong exchange interaction, when $|J_0| > |a|/4$. Indeed in this case in fields $g_e \beta_e H_0 \sim 2hJ_0$ the singlet RP state is in resonance with the triplet state T_- if $J_0 < 0$ or T_+ if $J_0 > 0$. Near the resonance conditions, only one of channels, either $S-T_-$ or $S-T_+$, is of importance. At lower values of the exchange integral, in particular at $J_0 = 0$, the Kaptein model and thus the level scheme given in Fig. 4.10 are invalid. In the general case, in the low field CIDNP both $S-T_0$ and $S-T_+$, T_- must be taken into account [4.16, 17].

The role of interference of different intersystem transition channels in low field CIDNP. Consider the spin dynamics of a RP with a nuclear spin 1/2 under the supposition that the exchange integral equals zero and the RP is singlet-born.

The secular portion of the hf interaction splits the T_- and T_+ levels into two sublevels conforming to different nuclear spin orientations. At the same time, it mixes S and T_0 states. The efficiency of singlet-triplet transitions induced by the secular hf interaction is equal for both nuclear spin orientations. It is due to this fact that $S-T_0$ mixing is not considered in the graphic model. However, a consistent account of $S-T_0$ mixing is necessary to describe reliably the transitions to T_- , T_+ states. Indeed, the $a \cdot \hat{S}_{Iz} \hat{I}_z$ contribution splits the S and T_0 terms (see Fig. 4.11 (b)). With account taken of this interaction the stationary RP states are

$$\begin{aligned} |\Psi_1\rangle &= (|S, 1/2\rangle + |T_0, 1/2\rangle)/\sqrt{2}, \\ |\Psi_2\rangle &= (|S, -1/2\rangle - |T_0, -1/2\rangle)/\sqrt{2}, \\ |\Psi_3\rangle &= (-|S, 1/2\rangle + |T_0, 1/2\rangle)/\sqrt{2}, \\ |\Psi_4\rangle &= (|S, -1/2\rangle + |T_0, -1/2\rangle)/\sqrt{2}. \end{aligned}$$

The non-secular hf interaction does not change the $|\Psi_1\rangle$ and $|\Psi_2\rangle$ states, inducing transitions from $|\Psi_3\rangle$ and $|\Psi_4\rangle$ to $|T_+, -1/2\rangle$ and $|T_-, 1/2\rangle$ respectively. These are shown by arrows in Fig. 4.11 (b). The energy separations and matrix elements for these transitions are equal. Therefore, equal numbers of RPs are transformed into

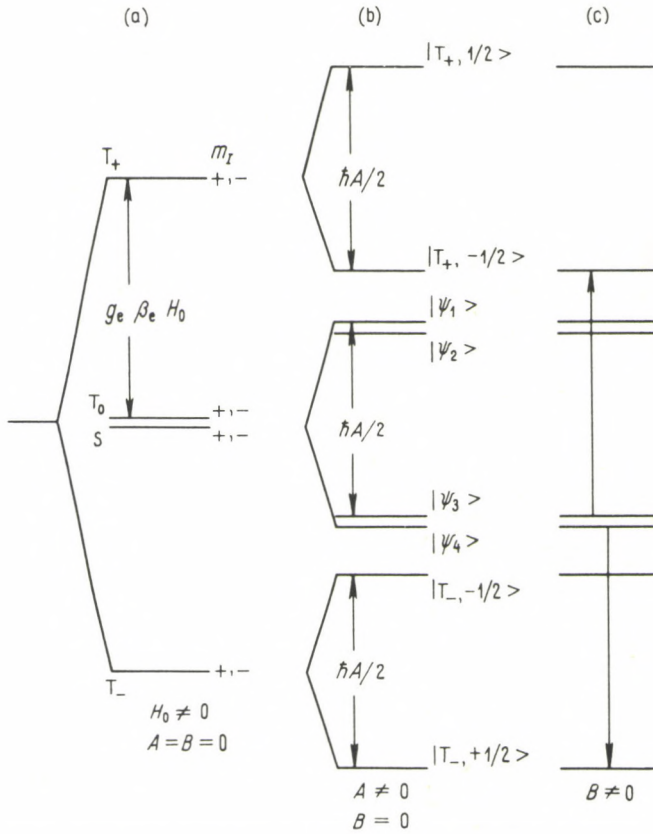


Fig. 4.11. Exact energy levels and transitions in one-nuclear RPs ($A > 0, J = 0$)

the triplet states $|T_+, -1/2\rangle$ and $|T_-, 1/2\rangle$. Thus, in the case discussed, the channels of intersystem transition to $|T_+, -1/2\rangle$ and $|T_-, 1/2\rangle$ states are equal in efficiency.

At the same time, a precise solution of the density matrix equation shows the possibility of the CIDNP effects. For a singlet precursor the probability of finding a RP in the singlet state by a time t depends on the nuclear spin orientation and equals

$$\begin{aligned}
 {}^S p(1/2, \omega_0) &= (1/8) \cdot [2 - (b^2/2 \cdot \Delta^2) \cdot (1 - \cos \{\Delta \cdot t\}) + \\
 &+ (1 - \omega_0/\Delta) \cdot \cos \{(a - \omega_0 - \Delta) \cdot t/2\} + (1 + \omega_0/\Delta) \cdot \cos \{(a - \omega_0 + \Delta) \cdot t/2\}], \\
 {}^S p(-1/2, \omega_0) &= {}^S p(1/2, -\omega_0), \\
 \Delta &\equiv (\omega_0^2 + b^2)^{1/2},
 \end{aligned}$$

for positive and negative nuclear polarizations respectively [4.18]. Hence, no nuclear polarization arises if account is taken only either of $S-T_0$ transitions with $A \neq 0, B = 0$, or of $S-T_-, T_+$ transitions with $A = 0, B \neq 0$. However, CIDNP is

nonzero if all intersystem transition channels are taken into account simultaneously since nuclear polarization results from the quantum-mechanical interference of RP transformation channels which, considered separately, induce no predominant nuclear spin orientation in RP recombination products.

In the theory of magnetic effects in radical recombination attention has been paid to the non-additivity of different intersystem transition channels. Deviations from additivity have been observed in the case of long-lived RPs. The following considerations can be put forward: the additive scheme of intersystem transitions along different channels affords a qualitatively reliable description of spin polarization and magnetic effects in radical recombination only when second order of perturbation theory, with respect to spin interactions, yields a non-zero result and a reasonable estimate of the scale of the effect. As soon as this approximation becomes insufficient, the interference of different channels of S-T transitions becomes of fundamental importance. This is the case for long-lived RP recombination in the theory of magnetic effects. The same can be said of the net CIDNP effect in low fields, which arises only in the fourth order of the perturbation theory [4.2], and thus the additive scheme appears to be inapplicable. The above discussion proves that in the theory of spin polarization and magnetic effects in chemical reactions one must be especially careful with approximate evaluations and the graphic model as they can lead to errors.

The graphic model allows one to determine correctly the nuclear polarization sign in chemical reactions provided the exchange integral is high in comparison to the hf constant. However, between RP re-encounters the exchange integral changes in a random manner and becomes less than the hf constant when the interradsical distance reaches tens of angstroms. High field CIDNP studies show that intersystem transitions are most effective at these interspecies distances. It leads to the conclusion that the graphic model seems to be more helpful for biradical systems rather than for describing CIDNP effects in case of RPs. The exchange integral in biradicals, despite the particle thermal motion, can be sufficiently high throughout the process.

According to graphic model the exchange integral maintains some fixed value. An attempt to overcome this limitation was made by Adrian [4.14] who suggested the idea of using the approximation of a sudden switching on of the exchange interaction at the contact moment [4.19]. The exchange integral is considered to take some fixed value $|J| \gg |a|$ at the encounter moment, while between re-encounters $J=0$. Adrian uses the additive scheme of S-T transitions neglecting S-T₀ mixing and expresses nuclear polarizations as a result of different efficiencies of S-T₋ and S-T₊ channels. As shown above, between re-encounters the approximation based only on S-T₋, T₊ transitions is invalid. Therefore, we will not discuss the conclusions published in ref. [4.14]. Note that according to Adrian, nuclear polarizations reveal a fairly complex spin dynamics interference both at the contact moment and between re-encounters.

4.3.2 CIDNP effects in short-lived RPs

CIDNP effects in reactions of short-lived RPs have been studied in most detail. The results obtained allow the sign of net and multiplet CIDNP effects to be determined [4.1, 4.2, 4.8].

The net CIDNP for the simplest system. Consider, first, a RP with a nuclear spin 1/2 and a spin Hamiltonian as in eq. (4.55). The exchange integral is fixed and time-independent.

We first show that at $J_0=0$ the total nuclear polarization in the geminate and escape products is zero. The mean nuclear polarization obeys the following set of equations

$$\begin{aligned} M_z &= g_I \cdot \beta_I \cdot \langle \hat{I}_z \rangle, \\ \partial^2 M_z / \partial t^2 &= -g_I \cdot \beta_I \cdot \{(\omega_0 \cdot b/2) \cdot Q_2 + (b^2/2) \cdot Q_3\}, \\ \partial^2 Q_2 / \partial t^2 &= -\omega_0^2 \cdot Q_2 - \omega_0 \cdot b \cdot Q_3, \\ \partial^2 Q_3 / \partial t^2 &= -\omega_0 \cdot b \cdot Q_2 - b^2 \cdot Q_3. \end{aligned} \quad (4.57)$$

Here Q_2 and Q_3 are the mean values of the operators, $\hat{Q}_2 = 2 \cdot (\hat{S}_{1x} \hat{I}_x + \hat{S}_{1y} \hat{I}_y)$, $\hat{Q}_3 = \hat{I}_z - \hat{S}_{1z}$. At the initial moment M_z , Q_2 and Q_3 equal zero for singlet and triplet RPs. Therefore, as follows from eqs (4.57), the total nuclear polarization is zero at all subsequent times. Note that the nuclear spin moment operator \hat{I}_z does not commute with the RP Hamiltonian. Nevertheless, under certain initial conditions, $\langle \hat{I}_z \rangle$ preserves its initial zero value. According to (4.57) the total nuclear polarization is associated with only those RP spin characteristics that equal zero at the initial moment.

Thus, at $J_0=0$ CIDNP in the geminate and escape products, unlike the consequence of the graphic model, must be opposite in sign.

Nuclear polarizations in geminate products are governed by the operator \hat{K}_{NE} (4.15). Differentiate $\tilde{K}_{NE}(t)$ and find that at $t=0$

$$\partial^4 \tilde{K}_{NE} / \partial t^4 |_{t=0} = g_I \cdot \beta_I \cdot \omega_0 \cdot a \cdot b^2 \cdot P_0(0) / 8$$

is the lowest non-zero derivative. Hence, for short-lived RPs

$$\tilde{K}_{NE} \approx g_I \cdot \beta_I \cdot g_e \cdot \beta_e \cdot \hbar^{-1} \cdot H_0 \cdot a \cdot b^2 \cdot P_0(0) \cdot t^4 / 8 \cdot 4! \sim H_0 \cdot a^3 \cdot P_0(0). \quad (4.58)$$

This expression for a RP with a 1/2 spin nucleus and $J_0=0$ leads us to the following conclusions.

1. Nuclear net polarization signs depend on the multiplicity of a RP precursor and the sign of the hf constant. In geminate recombination products polarizations are positive at $a < 0$ for a singlet RP precursor and at $a > 0$ for a triplet RP precursor.
2. Geminate and escape products are oppositely polarized.
3. Nuclear polarization is a fourth-order effect with respect to the spin interaction parameters and results from the interference of the Zeeman unpaired electron

interactions and both secular and non-secular hf contributions. There is every reason to believe, then, that net CIDNP effects in low fields cannot be reduced to the additive contribution of singlet-triplet transitions initiated by both secular and non-secular hf contributions.

Summing up these results, it can be emphasized that the sign of nuclear polarization is dominated by that of the value

$$\Gamma_{NE} = \mu \cdot \varepsilon \cdot a. \quad (4.59)$$

The symbols are the same as in eq. (4.9).

A strong exchange interaction, as compared to hf, qualitatively changes the nuclear net polarizations in low fields. If the exchange integral differs from zero, the total nuclear polarization is observed in geminate and escape products. Differentiate the whole nuclear polarization M_z and obtain

$$M_z \approx g_I \cdot \beta_I \cdot g_e \cdot \beta_e \cdot \hbar^{-1} \cdot H_0 \cdot b^2 \cdot J_0 \cdot P_0(0) t^4 / 4! \sim H_0 \cdot a^2 \cdot J_0 \cdot P_0(0). \quad (4.60)$$

For net polarizations in geminate products

$$\partial^4 \tilde{K}_{NE} / \partial t^4 |_{t=0} = g_I \cdot \beta_I \cdot \omega_0 \cdot b^2 \cdot (J_0 + a/4) \cdot P_0(0) / 2, \quad (4.61)$$

$$\tilde{K}_{NE} \sim H_0 \cdot a^2 \cdot (J_0 + a/4) \cdot P_0(0).$$

Net polarizations in escape products are

$$\tilde{K}'_{NE} = M_z - \tilde{K}_{NE} \sim H_0 \cdot a^2 \cdot (J_0 - a/4) \cdot P_0(0). \quad (4.62)$$

These relations suggest that at comparatively weak radical exchange interactions, when $|J_0| < |a|/4$, the CIDNP effect sign is set by eq. (4.59) derived at $J_0 = 0$. The CIDNP effect sign stops depending on the hf constant sign when $|J_0| > |a|/4$. Moreover, in this case the signs of geminate and escape recombination products coincide. Thus, for $|J_0| > |a|/4$ the polarization sign is determined by

$$\Gamma_{NE} = \mu \cdot J_0. \quad (4.63)$$

The last result coincides with that suggested by the Kaptein model since at sufficiently high values of the exchange integral the principal channel of singlet-triplet transitions is either S-T₋ or S-T₊ depending on J_0 sign, and the graphic model then provides a reliable description of RP spin dynamics.

It is interesting to note that if $J_0 = -a/4$, eq. (4.61) reduces to zero. In this case nuclear polarization in geminate recombination products are manifested only in the sixth-order perturbation theory and equal [4.2]

$$\tilde{K}_{NE} \approx -g_I \cdot \beta_I \cdot \omega_0 \cdot a^3 \cdot (a^2 - \omega_0^2) \cdot P_0(0) \cdot t^6 / 2^4 \cdot 6!. \quad (4.64)$$

Hence, in fields $g_e \cdot \beta_e \cdot \hbar^{-1} \cdot H_0 \sim 4 \cdot |J_0|$ polarizations change sign. Note that the polarization sign in escape products can remain constant. Indeed, at $J_0 = -a/4$ \tilde{K}'_{NE} (4.62) does not reduce to zero.

Some generalizations. The above results are readily generalized for the case of a RP with one magnetic nucleus and an arbitrary spin. All qualitative conclusions being the same, the CIDNP effect shows $(4/3)I \cdot (I + 1)$ -fold increase [4.18].

For short-lived RPs with any number of magnetic nuclei, CIDNP effects can be formally reduced to the case of a RP with one or both radicals possessing one nucleus. Therefore, we shall consider net CIDNP effects for a RP with two magnetic nuclei belonging to different radicals. With arguments analogous to those used for a one-nucleus RP, we obtain the following results [4.2]. I_1 and I_2 spin nuclear polarizations in geminate recombination products with $I_1 = I_2 = 1/2$ are

$$\begin{aligned}\tilde{K}_{NE}(I_1) &\approx g_I \cdot \beta_I \cdot \omega_0 \cdot P_0(0) \cdot \{b_1^2 \cdot (J_0 + a_1/4) - a_1 \cdot b_2^2/4\} \cdot t^4/2 \cdot 4!, \\ \tilde{K}_{NE}(I_2) &\approx g_I \cdot \beta_I \cdot \omega_0 \cdot P_0(0) \cdot \{b_2^2 \cdot (J_0 + a_2/4) - a_2 \cdot b_1^2/4\} \cdot t^4/2 \cdot 4!\end{aligned}\quad (4.65)$$

where $A_1 = B_1$ and $A_2 = B_2$ are the hf constants for I_1 and I_2 nuclei respectively. Eq. (4.65) proves exchange interactions to be, in some cases, of primary importance in giving rise to spin polarizations. Indeed, in the case of equivalent nuclei, when $A_1 = A_2$, nuclear polarizations are detected only when exchange interactions take place. At $J_0 = 0$ the total polarization sign of both nuclei depends on the sign of the hf constant sum:

$$\tilde{K}_{NE}(I_1) + \tilde{K}_{NE}(I_2) \approx P_0(0) \cdot (a_1 + a_2) \cdot (a_1 - a_2)^2. \quad (4.66)$$

The polarization signs for both nuclei coincide and are determined, as in the case of a one-nucleus RP, by eq. (4.63) provided the exchange intergal exceeds the hf constant.

The above results on CIDNP in short-lived RPs have been generalized to RPs with an arbitrary number of magnetic nuclei [4.2, 20]. We first introduce some notation $A_{1n} = B_{1n}$ and $A_{2k} = B_{2k}$ are the hf constants of the unpaired electron of one radical with its n th nucleus and that of the other radical with its k th nucleus respectively.

The net polarization of an arbitrary nucleus I_{1n} is: in geminate recombination products

$$\begin{aligned}\tilde{K}_{NE}(I_{1n}) &\approx g_I \cdot \beta_I \cdot \omega_0 \cdot P_0(0) \cdot \{(4/3) \cdot I_{1n} \cdot (I_{1n} + 1) \cdot b_{1n}^2 \cdot \\ &(J_0 + a_{1n}/4) - (a_{1n}/4) \cdot \sum_k (4/3) \cdot I_{2k} \cdot (I_{2k} + 1) \cdot b_{2k}^2\} \cdot t^4/2 \cdot 4!\end{aligned}\quad (4.67)$$

and in escape products

$$\begin{aligned}\tilde{K}'_{NE}(I_{1n}) &\approx g_I \cdot \beta_I \cdot \omega_0 \cdot P_0(0) \cdot \{(4/3) \cdot I_{1n} \cdot (I_{1n} + 1) \cdot b_{1n}^2 \cdot (J_0 - a_{1n}/4) + \\ &+ (a_{1n}/4) \cdot \sum_k (4/3) \cdot I_{2k} \cdot (I_{2k} + 1) \cdot b_{2k}^2\} \cdot t^4/2 \cdot 4!\end{aligned}\quad (4.68)$$

The net CIDNP contains two types of contribution: one contribution is connected with exchange interaction and it gives a polarization of the same sign in both cage and escape products; another contribution arises from interference of secular and

non-secular parts of the hf interaction, i.e. from the interference of the $S-T_0$, $S-T_{\pm}$; channels of intersystem crossing. This interference term gives polarizations of opposite signs for in-cage and escape products. The total polarization in both products is

$$M_z = \tilde{K}_{NE}(I_{1n}) + \tilde{K}'_{NE}(I_{1n}) \sim H_0 \cdot J_0 \cdot a_{1n}^2 \cdot P_0(0). \quad (4.69)$$

Comparing eqs (4.67) with corresponding results on RPs with one or two magnetic nuclei belonging to different partners makes it possible to arrive at the following conclusions.

1. Net polarization analysis of a RP with any number of magnetic nuclei can be formally reduced to that of a RP with one or two nuclei. For this purpose in one radical we consider the nucleus whose polarization is being analyzed, while in its partner all the nuclei can be substituted by one with the effective hf constant A_{eff}

$$= \left\{ \sum_k A_k^2 \right\}^{1/2}$$

2. No nuclear net polarization is observed in zero field.

3. The polarization of any nucleus does not depend on the hf of the unpaired electron with the other nuclei of the same radical.

4. When there is no exchange interaction, net polarizations of geminate recombination and escape products are of the opposite signs. At fairly large values of the exchange integral, when $|J_0| > |a|/4$, all radical reaction products have CIDNP of the same sign.

5. When exchange interactions exceed the hf constants, the polarization of any nucleus follows the pattern of that of a one-nucleus RP. In this case the nuclear polarization sign in all reaction products is determined by eq. (4.63).

Multiplet CIDNP effects. Multiplet polarization analysis demonstrates [4.2] the CIDNP effect sign for short-lived RPs in any magnetic field to be dominated by the Kaptein rule (4.10). Indeed, in any field, for values characterizing the mutual spin orientation, K_{ME} (see eqs (4.17, 18)), the lowest non-zero derivative is

$$\partial^2 K_{ME} / \partial t^2 |_{t=0} = \hbar \cdot j_{nk} \cdot a_{1n} \cdot a_{1k} \cdot P_0(0) / 16$$

if both nuclei belong to the same radical, and

$$\partial^2 K_{ME} / \partial t^2 |_{t=0} = -\hbar \cdot j_{nk} \cdot a_{1n} \cdot a_{2k} \cdot P_0(0) / 16$$

if the nuclei belong to different radicals. Here j_{nk} is the nuclear spin-spin interaction constant. Hence, the Kaptein rule for multiplet CIDNP effects (4.10) can be derived directly. So, for short-lived RPs, multiplet CIDNP is field-independent.

When they are compared, the results on net and multiplet polarizations demonstrate that for short-lived RPs the scale of net CIDNP effects in low fields can be much less than that of multiplet effects, the effects being observed in different orders of perturbation theory. Net polarization is more sensitive to exchange interactions than multiplet polarization. Therefore, net CIDNP studies in low fields are much more informative on exchange interactions between radicals.

The above data have been obtained for RPs with a fixed exchange integral. However, the exchange integral varies in fact in a random way during radical diffusion in a cage. By letting the exchange integral to vary in time in a certain way and by solving the equations of motion for the spin orientation operator \tilde{K} , we have instead of (4.67)

$$\begin{aligned} \tilde{K}_{NE}(I_{1n}) \approx & g_I \cdot \beta_I \cdot \omega_0 \cdot P_0(0) \cdot \left\{ a_{1n} \cdot (b_{1n}^2 - b_{2,\text{eff}}^2) \cdot t^4 / 8 \cdot 4! + \right. \\ & \left. + b_{1n}^2 \cdot \left[\int_0^t dt_1 \int_0^{t_1} d\tau \cdot \tau^2 \cdot J(\tau) + 2 \int_0^t dt_1 \int_0^{t_1} dt_2 \int_0^{t_2} d\tau \cdot \tau \cdot J(\tau) \right] / 8 \right\} \end{aligned} \quad (4.70)$$

for RPs with an arbitrary number of magnetic nuclei. Compare (4.70) with (4.67) and see that J_0 in (4.60–68) is an effective parameter which is some average value of the exchange integral

$$J_0 \Rightarrow (3!/t^4) \int_0^t dt_1 \int_0^{t_1} d\tau \left[\tau^2 \cdot J(\tau) + 2 \int_0^\tau dx \cdot x \cdot J(x) \right]. \quad (4.71)$$

Unfortunately, it is difficult to explain why it is the average value of the type in (4.71) that is an effective parameter for determining nuclear net polarizations in radical reaction products.

4.3.3 Approximate calculations

Net CIDNP effect. Within the framework of the one re-encounter approximation [4.1] and the CKO model [4.16] the net polarization effect has been calculated in one-nucleus RP recombination products.

In Section 2.3 we have already discussed the method of approximate evaluation of spin polarization effects. The essence of the method is that the populations of singlet RPs with nuclear spins orientated along and against the external field direction are determined by solving the equation of motion for the RP density matrix with spin-Hamiltonian (4.55). Then these populations are averaged by either the re-encounter distribution function (see eq. (2.218)) or the exponential function of contact times of the RP distribution for the CKO model (see eq. (2.215)), the results being qualitatively independent of the way of averaging. That is why we explore only Kaptein's results [4.1]; he calculated the polarizations within the diffusion model in the approximation of one re-encounter.

Figure 4.12 presents nuclear polarizations in a singlet-born RP recombination product calculated for several values of the RP parameters: the y-axis represents the ratio of differences in the state populations with the nuclear spins parallel and antiparallel to the external field under CIDNP and equilibrium conditions, the x-axis represents the external magnetic field strength. All the schemes presented refer to antiferromagnetic type of radical exchange interactions. Kaptein has averaged RP state populations by eq. (2.218) and the re-encounter distribution function (2.4) using the parameters $p=0.5$, $m=10^{-6}\text{s}^{1/2}$. The figure shows nuclear polarizations to depend on the sign of the hf constant, the exchange integral, and the field strength.

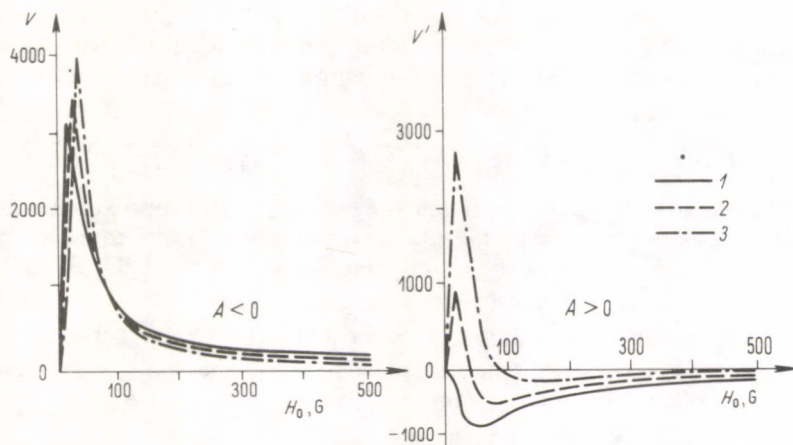


Fig. 4.12. Nuclear net polarization coefficient in geminate recombination products [4.1]. For all curves $|A| = +4.4 \cdot 10^8$ rad/s; 1 — $J_0 = -1.0 \cdot 10^8$ rad/s; 2 — $J_0 = -1.5 \cdot 10^8$ rad/s; 3 — $J_0 = -2.5 \cdot 10^8$ rad/s

At negative values of the hf constant and exchange integral, nuclear polarizations are positive at any field strength. When the hf constant is positive and the exchange integral negative, the polarization can change sign with growing magnetic field. As a rule, the exchange integral of two interacting radicals should be expected to be negative. Indeed, for the majority of molecules singlet but not triplet are the ground terms. Calculations for RPs with positive exchange integrals yield the following results [4.1]. If the hf constant is positive, nuclear polarizations are negative at any value of the exchange integral and field strength. Both positive and negative nuclear polarizations, depending on the field strength and exchange integral, can arise from negative values of the hf constant.

In the low field region, approximate calculations predict the same sign of the net CIDNP effect as follows from the rules obtained for short-lived RPs (compare the sign of polarization according to data of Fig. 4.12 and eq. (4.59, 63)).

Multiplet CIDNP effect. Both in high and in low fields, nuclear spins of radical recombination products appear to be mutually orientated, either parallel or antiparallel to each other. There are two ways to detect NMR signals from the reaction products in low fields: either in the same low field, or by transferring the system under investigation to the probe of a high field NMR spectrometer. In the former case the multiplet effect can be detected only for nuclei of different types, with different Zeeman frequencies, e.g., H and D or H and F , etc. In the latter case it is also observed for nuclei of the same type provided they have different chemical shifts. Theoretical analysis of low field multiplet nuclear polarizations is, in general, fairly complex, since the coupled motion of not less than four spins has to be analyzed. Comparatively simple results have been obtained only for short-lived RPs and for RP recombination in zero magnetic fields [4.1, 4.6, 4.17].

Consider multiplet polarization in zero fields for an RP consisting of two identical radicals [4.17]. Suppose each radical has a spin 1/2 nucleus. Table 4.5 lists state populations for different nuclear spin configurations for a singlet-born RP. The spin-Hamiltonian is

$$\hat{H} = \hbar a \cdot (\hat{S}_{1z} \hat{I}_{1z} + \hat{S}_{2z} \hat{I}_{2z}) + \hbar b \cdot (\hat{S}_{1x} \hat{I}_{1x} + \hat{S}_{1y} \hat{I}_{1y} + \hat{S}_{2x} \hat{I}_{2x} + \hat{S}_{2y} \hat{I}_{2y})$$

Table 4.5 also lists data obtained in the S-T₀ and S-T₊, T₋ approximations. These indicate that in the general case, the nuclear sublevel populations cannot be reliably obtained by a summation of the results obtained within the S-T₀ and S-T₊, T₋ models. As expected, the additive scheme gives reliable results accurate to the second-order perturbation theory with respect to the hf interaction when $a \cdot t < 1$. At large values of $a \cdot t$, because of interference of the S-T₀ and S-T₊, T₋ channels, the result might differ qualitatively from that given by the additive scheme.

Table 4.5. Nuclear sublevel populations in two-nuclear geminate recombination products

Approximation	Nuclear state population
$b=0$ $a \neq 0$ } S-T ₀ model	$n_{1/2, 1/2} = n_{-1/2, -1/2} = 1/4,$ $n_{1/2, -1/2} = n_{-1/2, 1/2} = (1/4) \cdot \cos^2 \{a \cdot t/2\}.$
$a=0$ $b \neq 0$ } S-T _± model	$n_{1/2, 1/2} = n_{-1/2, -1/2} = (1/4) \cdot \cos^2 \{b \cdot t/2\},$ $n_{1/2, -1/2} = n_{-1/2, 1/2} = (1/32) \cdot [8 - 4 \cdot \sin^2 \{b \cdot t/2\} - \sin^2 \{b \cdot t\}].$
$a = b \neq 0$ exact solution	$n_{1/2, 1/2} = n_{-1/2, -1/2} = (1/4) \cdot \cos^2 \{a \cdot t/2\},$ $n_{1/2, -1/2} = n_{-1/2, 1/2} = (1/32) \cdot [8 - 4 \cdot \sin^2 \{a \cdot t/2\} - 3 \cdot \sin^2 \{a \cdot t\}].$
$a = b \neq 0$ additive scheme: S-T ₀ +S-T _±	$n_{1/2, 1/2} = n_{-1/2, -1/2} = (1/4) \cdot \cos^2 \{a \cdot t/2\},$ $n_{1/2, -1/2} = n_{-1/2, 1/2} = (1/32) \cdot [8 - 12 \cdot \sin^2 \{a \cdot t/2\} - \sin^2 \{a \cdot t\}].$

Multiplet polarizations are characterized by the difference in state populations with parallel and anti-parallel mutual orientations of two nuclear spins, $\Delta n_{1,2} = n_{1/2, 1/2} - n_{1/2, -1/2}$. Table 4.6 lists $\Delta n_{1,2}$ values for this case and, to compare, for the case of high magnetic fields. For short-lived RPs, within the approximate model allowing for one re-encounter, the polarization signs coincide in high and zero field. In the case of long-lived RPs, polarizations may alter their signs when the field falls to zero.

Table 4.6. $\Delta n_{1,2}$ values

Approximation	Magnetic field strength	
	$g_e \cdot \beta_e \cdot H_0 \gg \hbar \cdot a$	$H_0 = 0$
Exact solution	$(1/4) \cdot \sin^2 (at/2)$	$-(1/8) \cdot [\sin^2 (at/2) - (3/4) \cdot \sin^2 (at)]$
Short-lived RPs, $a \cdot t < 1$	$+0.06 \cdot a^2 \cdot t^2$	$+0.06 \cdot a^2 \cdot t^2$
Diffusion model, $a \cdot \tau < 1$	$+0.07 \cdot (a \cdot \tau)^{1/2}$	$+0.003 \cdot (a \cdot \tau)^{1/2}$
Long-lived RPs, $a \cdot t < 1$	$+0.12$	-0.016
$\Delta n_{1/2}$ sign	$\Delta n_{1,2} > 0$	$\Delta n_{1,2} \geq 0$

4.3.4 Precise calculations

Low-field CIDNP calculations on the basis of precise kinetic eqs (see Sec. 2.3) so far have been carried out for a one-nucleus RP with a spin $1/2$ [4.21–23] and an arbitrary spin I [4.24].

The kinetic equations for the density matrix have been calculated numerically [4.21, 22] with account taken of radical exchange interactions. The exchange integral is assumed to drop off with increasing interradsical distance r according to the law

$$J = J_0 \cdot \exp(-\lambda \cdot (r - b)) \quad (4.72)$$

where b is the distance of the closest approach of the radicals.

Precise calculations of a one-nucleus RP with $I = 1/2$ in nonviscous liquids [4.21, 22] predict the net CIDNP sign to be the same as in the case of short-lived RPs, the exchange interaction being zero. Figure 4.13 depicts the difference in the

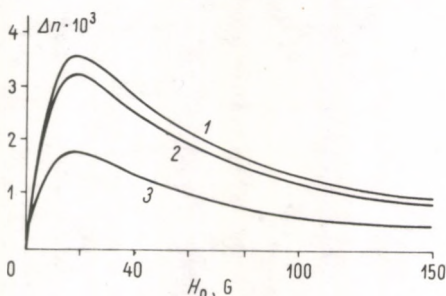


Fig. 4.13. Nuclear spin state population difference for triplet-born RPs as a function of the magnetic field applied during the reaction [4.22]. $\Delta n > 0$ implies an absorption signal. All the curves exhibit results for $a \cdot \tau_D = 0.064$. Curve 1 represents results for $J_0 \cdot \tau_D = 1.6$, Curve 2 for $J_0 = 0$ and Curve 3 for $J_0 \cdot \tau_D = -16.0$. Other parameters are $A g = 0$, $\tau_D = 1.6 \cdot 10^{-10}$ s, $K \cdot \tau_r \gg 1$, $\lambda = 5 \cdot \ln(10)/b$

populations of positively and negatively polarized nuclei in a triplet-born RP recombination product. The net CIDNP polarization sign is seen to agree with that predicted by rule (4.59) derived for short-lived RPs, the exchange interaction being neglected. Precise calculations show in this way that in nonpolar liquids when account is taken of the exchange interaction dropping off by the exponential law with increasing interradsical distance, there is no effect in the net CIDNP sign in freely diffusing radical recombination products. This result disagrees with those obtained above (see, e.g., eq. (4.63) and Fig. 4.12) under the supposition of a constant effective exchange interaction within RPs. The results obtained by the theory allowing for the exchange interaction of type (4.72) can be accounted for by the fact that CIDNP effects are associated mainly with singlet–triplet transitions in RPs between re-encounters when the interradsical distances are sufficiently great and the exponentially decreasing exchange integral is negligible.

The foresaid, however, does not imply that the exchange interaction is never of importance for CIDNP, and never qualitatively affects theoretical results. If the radicals do not freely diffuse but form some associates or weakly coupled complexes, certain constant exchange interactions arise in the RPs. In this case according to eq. (4.63) and numerical calculations (see Fig. 4.12) the exchange interactions are of fundamental importance in the process of CIDNP: the CIDNP sign then depends on the magnitude of the exchange interaction (cf. eqs (4.59) and (4.63)). The situation, when exchange interactions work in RPs for sufficiently long times, is realized, for example, in biradicals. The CIDNP in biradicals is discussed in detail in Section 4.4.

The low field CIDNP is greatly affected by the medium viscosity [4.21, 23]; the CIDNP sign can alter with increasing viscosity.

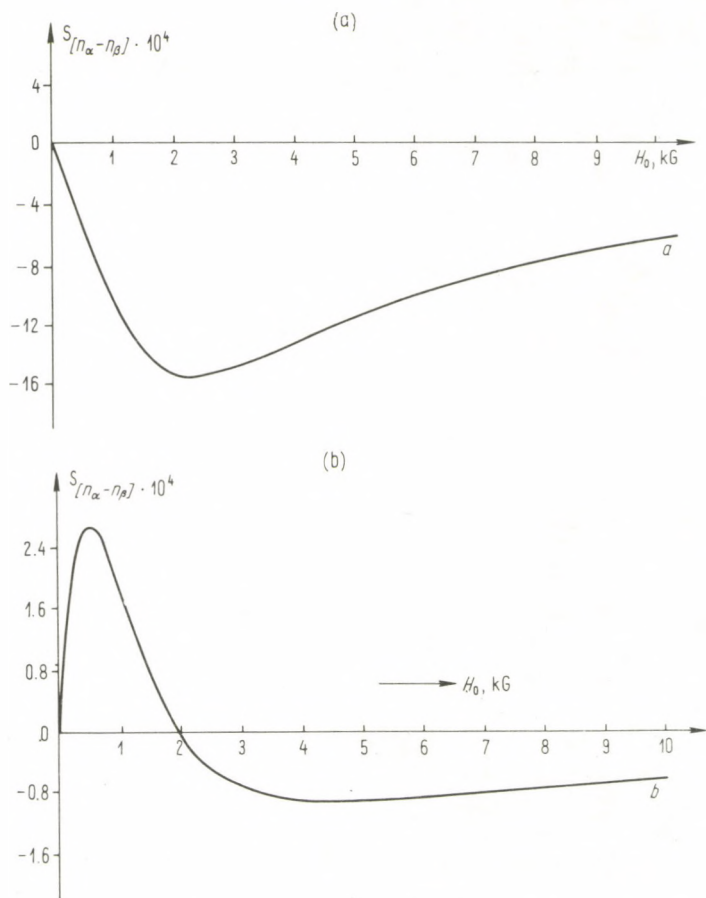


Fig. 4.14. Nuclear polarization sign alternation in low fields and a simultaneous change in the absolute value of nuclear polarization with increasing solution viscosity. (a) Curve *a* is the field dependence of CIDNP at $a \cdot \tau_D = 5.63$, $K \cdot \tau_r = 10$, $\Delta g = 0.001$; (b) Curve *b* is that at $a \cdot \tau_D = 56.3$, $K \cdot \tau_r = 100$, $\Delta g = 0.001$. The exchange integral is assumed zero, the RP singlet-born

Figure 4.14 gives the field dependence of nuclear polarization calculated at $J_0 = 0$ for two viscosities [4.23]. At a ten-fold increase in viscosity (cf. curves *a* and *b*) in low fields the nuclear polarization is seen to alter in sign. In highly viscous solutions, when $a \cdot \tau_D \gg 1$, the results obtained within the strict theory naturally do not fit those for short-lived RPs. When speaking about low-field effects in radical recombination, it has been described in detail that in long-lived RPs, when $a \cdot \tau_D \gg 1$, the RP spin dynamics reveal substantial differences from that observed at small times.

Medium viscosity also affects the shape of the field dependence of net CIDNP (see, e.g., Fig. 4.15). With viscosity growing, the maximum CIDNP has a tendency of shifting towards high magnetic fields, the whole curve broadening. The polarization sign change in Fig. 4.15 (c) in the range of high magnetic fields $H_0/A \approx 20$ is associated with a change of the polarization mechanism when low fields are replaced by high ones. In high fields $H_0 > 20A$ the Δg -mechanism of singlet-triplet transitions operates together with the hf-mechanism.

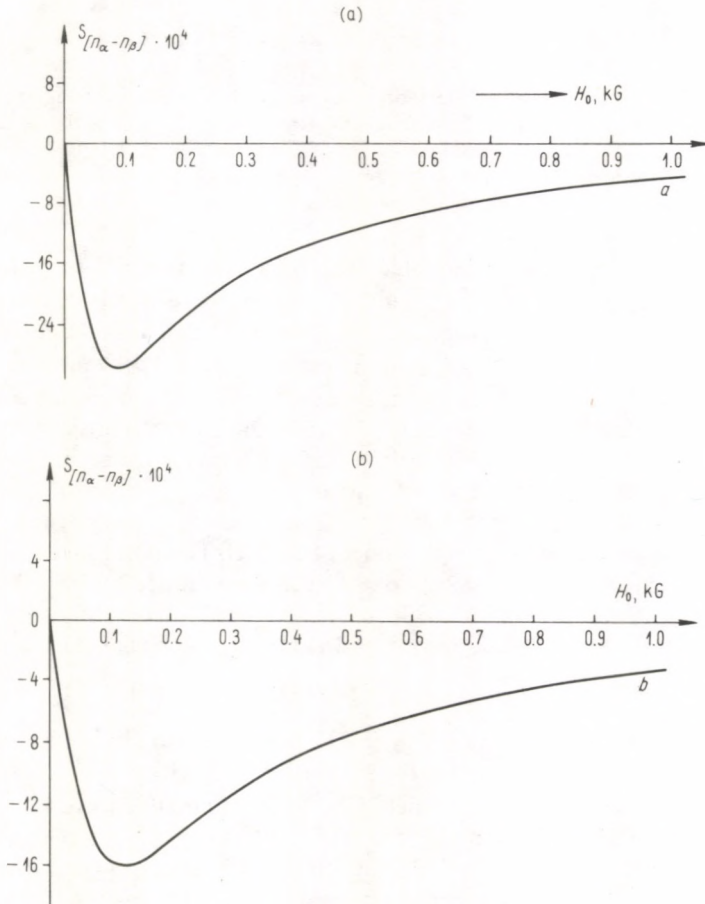


Fig. 4.15. (a), (b)

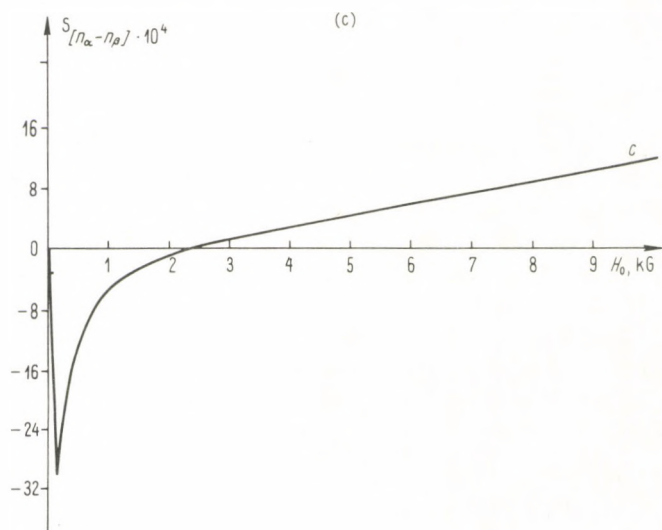


Fig. 4.15. The field dependence of net CIDNP for one-nuclear RP with a spin 1/2. Figs (a) (b) show the influence of the solution viscosity on the position of maximum and the width of the field dependence curve. RP parameters for Curves *a* and *b*: (a), $a \cdot \tau_D = 0.352$; $K \cdot \tau_r = 1$, $\Delta g = 0.001$; (b), $a \cdot \tau_D = 3.52$, $K \cdot \tau_r = 10$, $\Delta g = 0.001$. The figure (c) illustrates polarization changes within a wide range of field intensities with increasing magnetic field. RP parameters are the same as those in Fig. 4.15 (a)

Evans and Lawler [4.24] investigated the CIDNP effects in one-nuclear RPs with an arbitrary spin I . Their theory predicts two interesting effects: (1) in low fields, when $H_0 < I \cdot |A|$, the polarization of nuclei with 1/2 and 1 spins must be of the opposite sign compared to that arising in nuclei with $I > 1$ spins; (2) in fields $H_0 \approx I \cdot |A|$, the polarization originating in nuclei with $I > 1$ spins must change sign. It is desirable, however, to investigate by independent calculations the way the nuclear spin value affects the polarization sign. Such investigation has already been done and interrelations between different theories have been established. It was shown that for RPs with $I \geq 1$ net polarization can change sign twice when the strength of low magnetic fields is growing, [4.51, 52]. The point is that in the case of spin 1/2 nuclei the results [4.24] do not fit those obtained by the other authors [4.1, 2, 8, 21–23]. Indeed, in line with [4.24], the net CIDNP sign in the geminate recombination product is determined by the sign of the parameter

$$\Gamma_{NE} = \mu \cdot a \cdot (I - 1.1).$$

Hence, for 1/2 spin nuclei we have $\Gamma_{NE} = -\mu \cdot a$. This relation has a sign opposite to that predicted for Γ_{NE} , e.g., by eq. (4.59) or Figs 4.12–13.

Summarizing the results on low-field CIDNP, it is possible to state that nuclear polarization in low-field chemical reactions is the result of a fairly complex and correlated electron and nuclear RP spin motion. The theory gives comparatively simple results when applied only to short-lived RP recombinations. For nonviscous

solutions and in the absence of radical association, complexing, etc. the theoretical results on short-lived radicals with no exchange interaction taken into account (see eq. (4.59)) seem to predict correctly the experimentally observed CIDNP signs. In some extremely rare cases, however, the nuclear polarization sign can differ from that by eq. (4.59). The CIDNP sign alternation can be induced by a great change in the radical mobility (e.g., with increasing solution viscosity) and by the formation of weakly coupled complexes, when some fixed exchange interaction occurs in RPs.

4.4 CIDNP in biradical reactions

Biradicals are an extreme case of RPs whose radical centres do not separate but are coupled by a chain of chemical bonds. The scheme of possible biradical transformations is given in Fig. 4.16. The mechanisms and physical picture of CIDNP effects in biradical products are the same as in RP reactions: spin selection rules in recombination; singlet-triplet evolution due to hf- and Δg -mechanisms; dependence of S-T transitions on nuclear spin configuration.

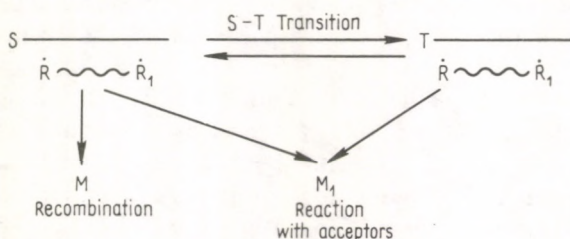


Fig. 4.16. Scheme of biradical transformations. Unlike the common RP model (Fig. 1.2, 2.4) no radicals escape into the bulk of solution

However, as compared to RPs, biradicals have a number of peculiarities. Note first of all the difference in exchange interactions.

The exchange interaction. RP partners reside a greater part of their in-cage lifetime at a comparatively large separation ($r \approx 1$ nm), when the exchange interaction is negligible, i.e., exceeded by the hf energy. In biradicals the exchange interaction is strongly dependent on the length of the chain between the radical centres. Provided the chain is sufficiently long (aliphatic chains composed of several dozens of C—C bonds), the biradicals will spend a greater part of time in conformations with negligible exchange interaction. In this case the situation in biradicals is similar to the model of a pair of freely diffusing radicals. It means that CIDNP effects can be as a rule qualitatively described with the exchange interaction entirely neglected. Hence one can conclude that for biradicals with sufficiently long chains between paramagnetic centres the net CIDNP sign is governed by rules (4.9)

and (4.59) in high and low fields respectively, while the multiplet polarization in any field is determined by rule (4.10). Note that in the case discussed, the nuclei in the biradical recombination products and in the products of biradical reactions with acceptors are oppositely polarized, the polarization sign of each nucleus depending upon the sign of its hf constant.

This is not the case for biradicals with comparatively short chains (e.g., aliphatic chains composed of 5–10 C—C bonds) when the exchange interaction can appreciably exceed the hf energy in the majority, if not in all, biradical conformations. In this case the CIDNP sign can be predicted by the CIDNP theory within the RP model with the exchange integral fixed. When the exchange integral is sufficiently large, the CIDNP sign can be determined, e.g., by the Kaptein diagram model (see Fig. 4.12, c, d). In the case under discussion, the net nuclear polarization sign must be the same in all biradical reaction products and determined by relation (4.63)

$$\Gamma_{NE} = \mu \cdot J \quad (4.73)$$

where $\mu = +1$ and $\mu = -1$ for a triplet and singlet biradical precursor, J is a certain exchange integral averaged over all biradical conformations. In most cases $J < 0$ and hence the net CIDNP sign is determined solely by the precursor multiplicity. According to eq. (4.73) the nuclear polarization sign is independent of the sign of the hf constant. If a biradical has several magnetic nuclei, they will all be equally polarized.

To illustrate the above qualitative regularities of CIDNP arising in biradicals with sufficiently strong exchange integral, consider the simplest case, of a one-nucleus biradical with spin 1/2. We set $J < 0$. Fig. 2.9 depicts the biradical terms. In low fields the singlet and triplet terms are separated by $2 \cdot J$. This splitting is assumed to be great enough for the hf energy to be insufficient for effective S–T mixing. The triplet sublevels split with increasing external magnetic field. In fields

$$H_0^* = 2|J|/\gamma_e \quad (4.74)$$

(γ_e is a magnetogyric ratio for electrons) the S and T_- states prove to be in resonance (see Figs 2.9 (a) and 4.17) and effectively mixed by the hf interaction. In the case under consideration the only nonzero matrix element of S–T transition is (see eqs (4.56))

$$\langle S, \beta_n | \hat{H}_{hf} | T_-, \alpha_n \rangle = \hbar a / 2 \cdot \sqrt{2}. \quad (4.75)$$

Assume the biradicals to be singlet-born. The S–T transitions lead to a decrease in the fraction of singlet biradicals with negative (β_n) nuclear polarizations while triplet biradicals are formed with positively (α_n) polarized nuclei. One will therefore observe positive nuclear polarizations in all the biradical reaction products and absorption in their NMR spectra. The polarization scheme given in Fig. 4.17 is in full agreement with the Kaptein diagram model (see Fig. 4.12 (c) (d)). The polarization sign is governed by rule (4.73).

In biradicals with large exchange interactions, nuclear polarizations result from mutual electron and nuclear spin flip-flops. It is interesting to note that within this

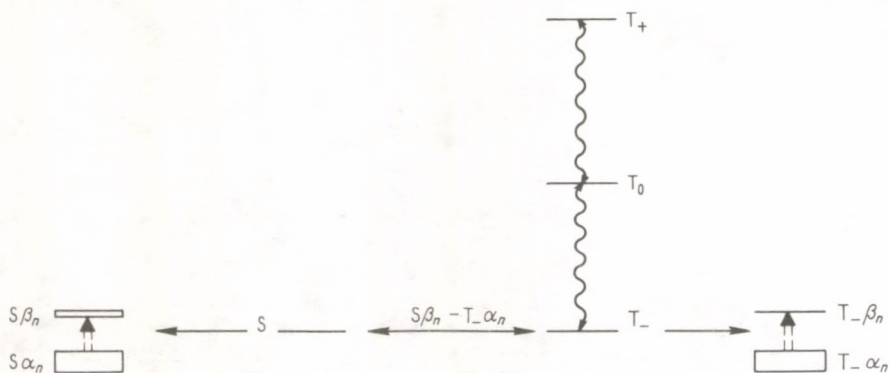


Fig. 4.17. Scheme of nuclear polarizations in biradical reaction products. The initial state is singlet, nuclear polarizations are positive in all products. Relaxation transitions between triplet sublevels are shown by wavy lines

mechanism of nuclear polarization induced only by $S-T_-$ transitions (no $S-T_0$ transitions), multiplet CIDNP effect does not arise. Consider, e.g., a biradical with two $1/2$ spin nuclei with hf constants a_1 and a_2 . In the region of crossing S and T_- terms, the following transition matrix elements are nonzero

$$\langle S, \alpha_1 \beta_2 | \hat{H}_{\text{hf}} | T_-, \alpha_1 \alpha_2 \rangle = \hbar a_2 / 2 \cdot \sqrt{2},$$

$$\langle S, \beta_1 \alpha_2 | \hat{H}_{\text{hf}} | T_-, \alpha_1 \alpha_2 \rangle = \hbar a_1 / 2 \cdot \sqrt{2},$$

$$\langle S, \beta_1 \beta_2 | \hat{H}_{\text{hf}} | T_-, \alpha_1 \beta_2 \rangle = \hbar a_1 / 2 \cdot \sqrt{2},$$

$$\langle S, \beta_1 \beta_2 | \hat{H}_{\text{hf}} | T_-, \beta_1 \alpha_2 \rangle = \hbar a_2 / 2 \cdot \sqrt{2}.$$

The fraction of singlet-born biradicals does not change in the subensemble with positive ($\alpha_1 \alpha_2$) nuclear spin orientation, while that of singlet biradicals with other nuclear configurations ($\alpha_1 \beta_2$, $\beta_1 \alpha_2$, $\beta_1 \beta_2$) reduces, biradicals with ($\beta_1 \beta_2$) nuclear configuration being the least in number.

Figure 4.18 shows state populations with different nuclear configurations and the NMR spectrum. The $S-T$ transitions are seen to lead to no multiplet CIDNP effect.

Note that similar considerations are also valid for the case of $J > 0$. The only difference is in the fact that the $S-T_+$ channel becomes important at $J > 0$.

The field dependence of CIDNP in short biradicals. The above considerations reveal one more interesting feature of CIDNP in reactions occurring through biradicals. In the case of comparatively short biradicals with sufficiently large exchange integral, the field dependence of CIDNP must be of resonance character: a maximum $S-T_-$ (or $S-T_+$ at $J > 0$) mixing and hence a maximum nuclear polarization must arise in fields when $S-T_-$ or S and T_+ terms appear in resonance depending on the sign of J (see Fig. 2.9 (a), eq. (4.74)). The greater the effective mean value of the exchange integral, the higher the field strength at which the polarization

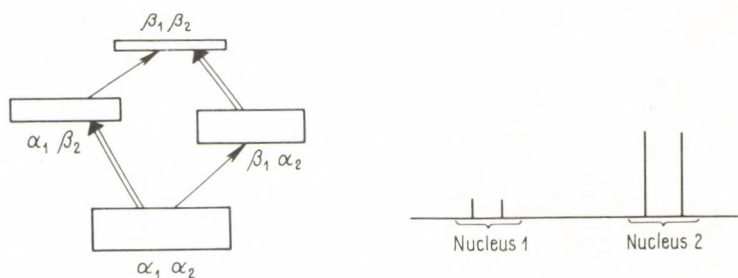


Fig. 4.18. Scheme of nuclear sublevel populations and NMR spectrum in the recombination product of a singlet-born biradical under the assumption that $|a_2| > |a_1|$. Nuclear polarizations result from electron and nuclear spin flip-flops. No multiplet but net CIDNP effects are observed. The higher the hf constant, the greater the nuclear polarization

reaches a maximum [4.15] (see Fig. 4.19). Thus, with growing length of the biradical chain, maximum CIDNP must shift towards the region of lower field strengths.

The width ΔH of the field dependence of CIDNP (see Fig. 4.19) depends upon a number of factors. It can be conditioned by broadening of the singlet and triplet RP terms. The broadening of levels due to the recombination and the reaction with acceptors is an important mechanism of this broadening [4.15]. Closs and Doubleday [4.15] pointed out that within this mechanism the broadening must increase with reducing biradical length. Indeed, a biradical lifetime should be expected to decrease (the level width increases) with reducing distance between the biradical reaction centres. de Kanter *et al.* [4.25] proposed one more possible mechanism of the field dependent broadening ΔH . A biradical can occur in different conformations, in each the S and T₋ levels crossing in different fields. In principle, not one but several maxima corresponding to the subensembles of biradicals with different exchange integrals can be observed in the field dependence of CIDNP. These conformations however do not remain unchanged, intersystem transitions taking place in the process of thermal motion. Sufficiently fast conformation transitions must result in averaging the exchange integral.

The two mechanisms of the field curve broadening ΔH (Fig. 4.19) must depend on the medium viscosity in an opposite manner. The intramolecular mobility of a

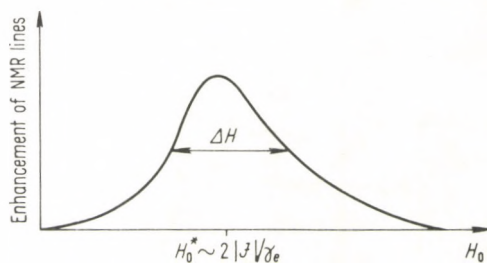


Fig. 4.19. Qualitative picture of field dependence of CIDNP in reaction products of biradicals with sufficiently large mean value of the exchange integral

biradical increases with reducing viscosity. As a result, the exchange integrals in various configurations are averaged; in this case, only the average exchange integral manifests itself and thus ΔH must reduce. At the same time, as the mobility of the biradical chain increases, the encounter rate of the biradical centres grows, the biradical lifetime shortens and ΔH increases.

The ΔH can be contributed to by the relaxation broadening of triplet sublevels. Moreover, ΔH must be the greater, the higher the hf constant.

Short rigid biradicals. While in sufficiently long biradicals the conditions for the singlet-triplet evolution are in fact the same as in free-diffusing RPs, then in short rigid biradicals we come to the well-known case of intramolecular nonradiative intersystem transitions. In this case, S-T transitions can be quite effective despite large values of the exchange integral. During an intramolecular transition the energy of S-T splitting is compensated by the reservoir of the vibrational molecular energy (see Fig. 4.20). The same transitions in a RP are not effective when the exchange integral exceeds the hf energy: the reservoirs of electron (exchange) energy and vibrational degrees of freedom of a RP are weakly coupled due to extremely small values of Frank-Condon factors. In the case of short rigid biradicals, the Frank-Condon factors of S-T transitions can be sufficiently great. Hence, the hf interaction can contribute to S-T transitions and result in nuclear polarizations of biradical reaction products, all the S-T channels (S-T₀, T₊, T₋) working, since among a great number of vibrational states one can practically always find those T₀, T₊ and T₋ levels that are in resonance with the S state (see Fig. 4.20). This means that the picture of S-T transitions in short rigid biradicals is similar with that in RPs with zero exchange integrals in low fields. Therefore, in this case the nuclear polarization sign in biradical reaction products can be assumed determined by the sign of $\Gamma_{NE} = \mu \cdot \epsilon \cdot a$ (see eq. (4.59)).

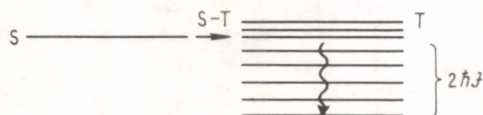


Fig. 4.20. Scheme of nonradiative intersystem transitions. The exchange interaction energy is compensated by the reservoir of vibrational degrees of freedom of biradicals

The above qualitative discussion demonstrates the existence of two types of biradicals which differ in their CIDNP mechanism. In sufficiently long biradicals with negligible average exchange integral the nuclear polarization mechanism is similar to that in a RP with zero exchange integral: in high fields S-T₀ transitions are prevalent while in low fields CIDNP effects are associated with the interference of S-T₀ and S-T₊, T₋ transitions. In the case of short biradicals, the basic mechanism of CIDNP formation is S-T₋ (or S-T₊) transitions.

The role of reaction with acceptors. In sufficiently long biradicals with negligible exchange interactions the nuclei are oppositely polarized at any moment of singlet-triplet evolution induced by the hf interaction in the singlet and triplet biradical

subensembles: when in singlet biradicals the nuclear polarization is positive, it is negative in triplet biradicals and vice versa. Thus at any instant the total nuclear polarization in both subensembles is zero (see, e.g., eq. (4.61) and eq. (4.62)). To distinguish the nuclear polarization in different subensembles, biradical transformations must follow competing channels, the biradical recombinations and reactions with acceptors serving as such (see Fig. 4.16). Remember that in the case of RPs there is always one more channel, that is radical escape into the bulk (see Fig. 2.4).

To illustrate the role of acceptors, consider a one-nucleus biradical with a spin $1/2$. Assume the biradical to be singlet-born and $S-T_0$ transitions to be the basic mechanism of singlet-triplet evolution. There are then two subensembles of biradicals with α_n and β_n nuclear spin orientations, the $S-T$ transitions occurring with different frequencies (see eq. (4.7, 8)). Let the singlet biradical recombination be the only channel of chemical transformations. Then, despite biradical oscillations between S and T_0 states, all the biradicals with α_n and β_n nuclear orientations will in the long run recombine and the nuclei of the reaction product will thus be unpolarized. If biradicals not only recombine but also react with acceptors, the situation dramatically changes: it is the biradicals with nuclear orientation characterized by lower frequency of $\hat{S}-T_0$ transitions that preferentially recombine. As a result, nuclear polarizations arise in the reaction product. At the same time, the higher the $S-T$ transition frequency, the greater the product of the reaction between biradicals and acceptors.

Thus, in long biradicals the reaction with acceptors can be of principal importance for the CIDNP observation.

In comparatively short biradicals, when the hf interaction mixes the S and T_- (or S and T_+) states, the nuclear polarization is of the same sign in the singlet and triplet subensembles. In this case the role of the reaction with acceptors depends on the multiplicity of the primary state. If the primary state is singlet, then, in the absence of acceptors, all the biradicals recombine in the long run and the nuclei are unpolarized. In this case CIDNP effects arise provided there are some competitive reactions, e.g., reaction with acceptors. When the primary state is triplet the hf interaction induces transitions to the singlet state only for biradicals with a certain nuclear orientation. For instance, in the case of a single nucleus the transitions would be of the type $|T_-, \alpha_n\rangle \rightarrow |S, \beta_n\rangle$ (see eq. (4.75)). As a result, not all biradicals would recombine but those with initially α_n -orientated nuclear spins do recombine. Nuclear polarizations then arise in the recombination products. In this case the reaction with acceptors is not necessary for the observation of CIDNP effects in biradical recombination products.

The above qualitative reasoning shows that the biradical reactions with acceptors can sometimes be used as a method to study the peculiarities of singlet-triplet evolution in biradicals.

Paramagnetic relaxation. Paramagnetic relaxation can be of great importance for biradical recombination. Consider, for instance, the scheme given in Fig. 4.17. Let the biradicals be triplet-born. The biradicals in a $|T_-, \alpha_n\rangle$ state can turn into the

singlet state and recombine. (In cases when the spin-orbital or spin rotational interactions mix the S and T states more effectively than the hf interaction, the CIDNP effects are negligible). In our example, when the hf interaction is the basic mechanism of singlet-triplet evolution, $|T_+, \alpha_n\rangle$, $|T_+, \beta_n\rangle$, $|T_0, \alpha_n\rangle$, $|T_0, \beta_n\rangle$ and $|T_-, \beta_n\rangle$ biradicals would always remain in the primary state without recombination. However, owing to relaxation transitions (see Fig. 4.17) the biradicals in any state can turn into a $|T_-, \alpha_n\rangle$ state and then to any reactive singlet state by the hf mechanism. Relaxation transitions clearly play an essential role in recombination only if S-T₀, S-T₋, S-T₊ transitions differ greatly in efficiency. In this case, the processes of paramagnetic relaxation in a triplet biradical ensure the transition of triplet biradicals to the states most strongly coupled with the singlet state.

In some cases the role of the paramagnetic relaxation in CIDNP formation in biradical recombination products is the same as that of the competitive reactions which are independent of the biradical multiplicity (reactions with acceptors). In illustration, consider a spin 1/2 one-nucleus biradical and assume it to be singlet-born. Let the recombination of singlet biradicals be the only reaction channel. As stated above, no CIDNP effects arise, with relaxation transitions between the triplet sublevels neglected. Let us consider the way the relaxation transitions change the situation. The hf mechanism induces $|S, \beta_n\rangle \rightarrow |T_-, \alpha_n\rangle$ transitions. The relaxation distributes the biradicals over all triplet sublevels which violates the balance between $|S, \beta_n\rangle \rightarrow |T_-, \alpha_n\rangle$ and $|T_-, \alpha_n\rangle \rightarrow |S, \beta_n\rangle$ channels induced by the hf interaction, provided the T₀→S and T₊→S transitions are not associated with the hf interaction. The latter transitions can be induced by either spin-orbital or spin-rotational interaction. As a result, the biradical recombination products can be positively polarized.

The paramagnetic relaxation times of biradicals lie in a microsecond range. The relaxation transitions must therefore be taken into account when analysing the CIDNP effects in biradical reaction products, if the biradical lifetimes are also in the microsecond range. In long-lived biradicals, the paramagnetic relaxation randomizes the spins entirely, and thus no CIDNP effect arises.

A quantitative theory of CIDNP in biradical reactions. A precise quantitative theory of CIDNP in biradical reactions can be developed by the mathematical tools discussed in Section 2.3. For this purpose it is sufficient to modify the results of Section 2.3 slightly. Divide the biradical ensemble into subensembles pertaining to different conformations. The biradical density matrix for a given subensemble, $\rho(k)$, varies for several reasons. First, the spin-Hamiltonians of the Zeeman, exchange and hyperfine interaction, $\hat{H}(k)$, with the value of the exchange integral $J(k)$ corresponding to this conformation, induce reversible spin evolution. Second, changes due to irreversible processes of paramagnetic relaxation. Third, the changes induced by chemical transformations of the biradical. And, finally, the biradical oscillates between different conformations. Hence, we have

$$\partial\rho(k)/\partial t = -i\hbar^{-1} \cdot [\hat{H}(k), \rho(k)] + \hat{R}_k\rho(k) + \hat{K}_k\rho(k) + \hat{L}\rho(k) \quad (4.76)$$

where \hat{R}_k is the relaxation operator (see, e.g., eq. (3.40)), \hat{K}_k is the operator describing the biradical reactions in the k -th conformation under study (see, e.g., eq. (2.196)). The last term in eq. (4.76) describes the conformation changes of the biradical.

If the conformation transitions are of jump-like then, by analogy with eq. (2.175) for the RP model, we have

$$\hat{L}\rho(k) = -W_k \cdot \rho(k) + \sum_{n(\neq k)} W_{n \rightarrow k} \cdot \rho(n). \quad (4.77)$$

Here W_k is the transition rate from the k -th conformation, $W_{n \rightarrow k}$ is the transition rate from the n -th to the k -th conformation. The case when there are just two biradical conformations was considered by Atkins and Evans [4.26]. CIDNP effects for biradicals with several conformations were computed by de Kanter *et al.* [4.25]. Equation (4.77), as applied to very long biradicals, can be simplified [4.25]. In this case a biradical ensemble can be divided into subensembles with a fixed separation of the radical centres, and the conformation transitions can be considered in terms of the continuous diffusion model by setting

$$\hat{L}\rho(r) = D \cdot \Delta\rho(r). \quad (4.78)$$

The kinetic equations (4.76, 78) coincide with the corresponding eqs (2.180) for RPs. The only difference is in the boundary conditions at great interradical distances r . In the RP model, this condition is $\rho(r) \rightarrow 0$ at $r \rightarrow \infty$ (see eq. (2.166)). In the case of biradicals, the radical centres remain always coupled and hence the boundary condition is the equality of the diffusion flow to zero at a distance l conforming to the most prolonged biradical conformation

$$\partial\rho(r)/\partial r|_{r=l} = 0. \quad (4.79)$$

The above kinetic equations have been solved numerically by de Kanter [4.27] for a number of one-nucleus biradicals with a $1/2$ spin. These exact calculations have confirmed the qualitative conclusions. The CIDNP analysis has been shown to be informative about the intramolecular mobility of biradicals and the mechanism of exchange interactions (both direct exchange due to the orbital overlap of unpaired electrons and, indirect exchange via either the chain of C—C bonds in a biradical or the diamagnetic molecules of the solvent).

4.5 CIDEP theory in radical pairs

The principles of the theory of unpaired electron spin polarizations in radical chemical reactions were put forward by Kaptein and Oosterhoff [4.28]. Later on the CIDEP theory was developed within the framework of the RP model by Adrian [4.14, 29], Atkins [4.30, 31], Pedersen and Freed [4.32], and others.

The mathematical tools discussed in Sec. 2.3 allow one to analyze radical spin states to calculate CIDEP effects. The program of radical CIDEP calculations has

been realized only as applied to the reactions in high magnetic fields in the $S-T_0$ approximation. A quantitative theory of CIDEP effects taking into account $S-T_-$, T_+ transitions has not yet been elaborated, only qualitative data being available. This can be explained, first of all, by the fact that so far experimental data on CIDEP have been interpreted in $S-T_0$ terms only [4.33]. Besides, there are some theoretical considerations that prove $S-T_0$ transitions to be the main channel of RP singlet-triplet evolution.

CIDEP induced by $S-T_-$, T_+ transitions. The efficiencies of $S-T_-$ and $S-T_+$ channels can be different in high fields which results in different populations of the T_- and T_+ states. As a result, the unpaired electron spins are polarized proportionally to the population difference of these states.

Consider the scheme of RP terms in high fields depicted in Fig. 2.6. Assume a singlet molecule to give two radicals. A $S-T_-$ transition becomes possible at the interradsical distance at which the singlet-triplet splitting is comparable to the Zeeman splitting of triplet levels. In this case both radicals must have a negative spin density, their ESR spectra showing enhanced absorption. If the molecule decomposes from the electronically excited triplet state, then within the region of $S-T_-$ mixing a portion of triplet RPs becomes singlet and can recombine. As a result, the T_- level becomes less populated and the radical ESR spectra must reveal emission. In some cases when the exchange integral is positive, the singlet term can mix with T_+ . Spin polarizations of unpaired electrons induced by $S-T_-$ and $S-T_+$ transitions are opposite in sign.

Thus $S-T_-$ (or $S-T_+$) transitions create equal electron polarizations in both radicals, their sign being determined by that of the product

$$\Gamma_{NE} = \mu \cdot J, \quad (4.80)$$

where $\mu = +1$ or $\mu = -1$ for a triplet- or singlet-born RP, J is the exchange integral. $\Gamma_{NE} > 0$ corresponds to enhanced absorption, A -type spectrum, $\Gamma_{NE} < 0$ corresponds to emission, E -type spectrum.

Intersystem $S-T_-$, $S-T_+$ transitions, in the general case, can be induced by both isotropic and anisotropic hf interactions as well as by spin-rotational and spin-spin dipolar interactions. In liquids anisotropic interactions are as a rule effectively averaged to zero by the fast radical orientational relaxation, their possible participation in inducing CIDEP effects having not yet been experimentally confirmed [4.33].

For $S-T_-$, T_+ transitions induced by isotropic hf interactions one must expect the CIDEP effects to depend on the number of the hyperfine structure component of the radical ESR spectra [4.30]. For instance, if a one-nucleus molecule with spin 1/2 decomposes, then $S-T_-$ transitions are possible only if the nuclear spin in S is antiparallel to the external field. In the case of the opposite nuclear orientation such transitions are forbidden by the rule of conservation of the total spin of a RP electron and nucleus. As a result, the radical ESR spectral component that corresponds to the parallel nuclear spin orientation must be polarized, while the other component is not expected to be polarized.

As a rule, the efficiency of $S-T_-, T_+$ transitions in high fields will be negligible. In the region of term crossing ($S-T_-$ or $S-T_+$) the radicals reside for a time of the order of 10^{-11} s which is comparable to that of an elementary diffusion step. In most radicals this time is not sufficient for the hf mechanism to manifest itself. As noted, the only exception is in biradicals in which the condition of S and T_- (or T_+) resonance can be preserved throughout their lifetime. $S-T_-, T_+$ transitions can manifest themselves in high fields in reactions involving radicals with large hf constants, e.g., hydrogen atoms [4.34] for which $A_n = 8.5 \cdot 10^9$ rad/s.

The vector model of CIDEP in the $S-T_0$ approximation developed by Adrian, Monchick [4.35] and Salikhov [4.36]. In singlet and triplet RP T_0 states the radical electron spins are not polarized. RP unpaired electron spin polarizations due to $S-T_0$ mixing then require a special analysis. To discuss this problem qualitatively it is convenient to compare the motion of a certain effective spin with the RP spin dynamics and to consider its vector model. Assume a RP has the spin-Hamiltonian

$$\hat{H} = \hbar\omega_1 \hat{S}_{1z} + \hbar\omega_2 \hat{S}_{2z} - \hbar J \cdot (1/2 + 2\hat{S}_1 \hat{S}_2). \quad (4.81)$$

In the $S-T_0$ approximation the spin dynamics allows for two states: S and T_0 . It is known (see, e.g. [4.10]) that any two-level system can be presented by some effective spin $F=1/2$. Let S and T_0 be eigenstates of the operator \hat{F}_z

$$\hat{F}_z |T_0\rangle = (1/2) \cdot |T_0\rangle, \quad \hat{F}_z |S\rangle = -(1/2) \cdot |S\rangle.$$

Then the eigenstates of the x -projection of the F spin moment are

$$\hat{F}_x |\psi_+\rangle = (1/2) \cdot |\psi_+\rangle,$$

$$\hat{F}_x |\psi_-\rangle = -(1/2) \cdot |\psi_-\rangle,$$

$$|\psi_+\rangle = (|S\rangle + |T_0\rangle) / \sqrt{2} \equiv |m_1 = 1/2, m_2 = -1/2\rangle,$$

$$|\psi_-\rangle = (|S\rangle - |T_0\rangle) / \sqrt{2} \equiv |m_1 = -1/2, m_2 = 1/2\rangle,$$

where $m = \pm 1/2$ denote the states of unpaired electrons with positive and negative spin densities. Thus different states of the effective spin are in one-to-one correspondence with the RP spin states (as shown in Fig. 4.21 (a)). The motion of the F spin is a one-to-one model of the total spin dynamics of the unpaired electrons provided the conditions of $S-T_0$ approximation applicability are not violated⁵.

⁵ The problems of external field effect on singlet-triplet transitions and CIDNP effects in radical reactions are qualitatively discussed in the conventional vector model of S and T_0 states (see Fig. 1.4). Note that the schemes like those depicted in Fig. 1.4 inadequately reflect S and T_0 states of two unpaired electrons. No wonder, then, that these rough schemes fail to interpret all the features of RP spin dynamics, in particular, CIDEP effects. The vector model using the effective spin gives an adequate and strict description of RP spin dynamics in the $S-T_0$ approximation. The effective vector \vec{F} allows one fairly well to interpret all magnetic and spin polarization effects in radical reactions including electron polarizations, magnetic field effects on RP recombination, magnetic isotope effects. However, giving due to the tradition, we employ the vector schemes like those shown in Fig. 1.4, c, d when discussing magnetic and CIDNP effects.

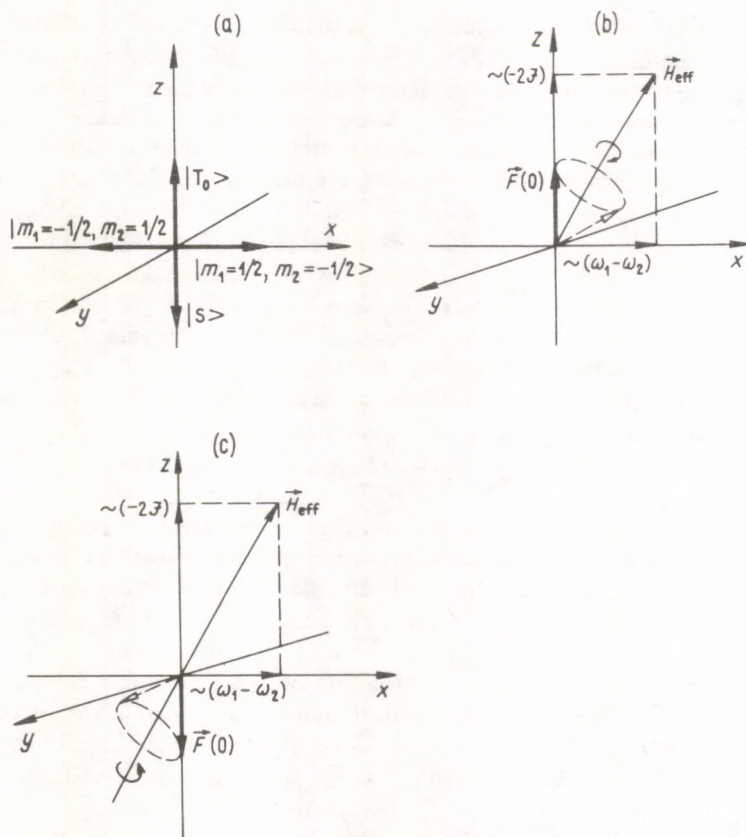


Fig. 4.21. One-to-one correspondence between the states of RP spins and those of the representative vector (a), and the motion of \vec{F} in the process of CIDEP arising (b), (c)

In terms of the effective spin the RP spin Hamiltonian (4.81) in the S-T₀ model has the form

$$\hat{H}_{\text{eff}} = -2\hbar \cdot J \cdot \hat{F}_z + \hbar \cdot (\omega_1 - \omega_2) \cdot \hat{F}_x.$$

It is thus seen that the F spin precesses in an effective magnetic field with a longitudinal component proportional to the exchange integral, and a transverse component proportional to the difference in the Larmor spin frequencies (see, e.g. Fig. 4.21 (b), (c)). The precession frequency of the F spin is

$$\omega_{\text{eff}} = [4 \cdot J^2 + (\omega_1 - \omega_2)^2]^{1/2}$$

The vector model of the effective spin motion allows one to follow the process of formation of RP unpaired electron polarization. Assume the exchange integral to be negative and the Larmor frequency of S_1 to exceed that of the other spin. The case under discussion conforms to the effective magnetic field as shown in Fig.

4.21 (b), (c). Let the RP be triplet-born, i.e. the effective spin is orientated along the positive z -semiaxis (Fig. 4.21 (b)). The vector \vec{F} precesses about the effective magnetic field \vec{H}_{eff} and thus deviates from z -axis, which results in a nonzero transverse component of \vec{F} directed along the positive x -semiaxis. This (see Fig. 4.21 (a)) is equivalent to an increase in the population of the state whose spin density is positive in one radical and negative in the other. If the RP is singlet-born then, according to Fig. 4.21 (c), the effective spin precession induces opposite spin polarizations: the spin density of the first radical being negative and that of the other positive.

The vector model of the effective spin motion readily yields a number of important conclusions concerning chemically induced dynamic electron polarizations one of which has already been obtained: the electrons of singlet- and triplet-born RPs are oppositely polarized. In the case of diffusion RP recombination the electron polarization sign is the same as that in triplet-born RP recombination. Figure 4.21 (b), (c) shows that the sign alteration of the exchange integral results in that of the spin polarization.

If the RP is either singlet- or triplet-born, i.e. the effective vector directed along z -axis, electron polarizations arise as a result of simultaneous effects of the difference in the Zeeman frequencies and the exchange radical interaction. To prove this remark, assume the exchange integral to be zero. The effective magnetic field \vec{H}_{eff} is then directed along x -axis, in which case the vector \vec{F} precesses in the yz -plane. This precession affects the y - and z -projections of the \vec{F} vector. Changes in the z -projection reflect singlet-triplet transitions induced by the difference in the Larmor electron frequencies. At the same time, the x -projection remains zero, and despite S-T₀ mixing no electron polarization arises. Likewise at $\omega_1 = \omega_2$, $J \neq 0$ the x -projection is zero and the spins are not polarized.

An optimum condition of CIDEP is

$$2|J| = |\omega_1 - \omega_2| \quad (4.82)$$

when the effective magnetic field is directed along the bisector of the angle between x - and z -axis and the vector \vec{F} can reach x -axis in the course of the precession. At $\omega_{\text{eff}} \cdot t = \pi$ the electron spins are either in $|m_1 = 1/2, m_2 = -1/2\rangle$ or $|m_1 = -1/2, m_2 = 1/2\rangle$ states, i.e. are completely polarized. Condition (4.82) was reported in ref. [4.28].

Note that chemical reactions play different roles in CIDNP and CIDEP. The former arises only in the course of the reaction, while the latter can also be observed in the absence of recombination, provided the initial RP is spin-correlated.

In the above considerations we assumed the exchange integral to have some fixed value. This is in fact impossible on account of mutual radical diffusion. In terms of the effective spin it means that the vector \vec{F} precesses in a magnetic field with the longitudinal component varying in time in a random manner. The greater part of the time is spent by radicals at the distances when the exchange integral is zero, while at contact moments it increases sharply. Adrian [4.29] has shown that in this case electron polarizations are also possible. The foregoing can be interpreted in terms of

the vector model. Assume two radicals are far from each other at the initial moment and the exchange integral is zero. At a moment t_1 they approach and the intensive exchange integral $|J| \gg |\omega_1 - \omega_2|$ starts functioning. When the radicals diffuse apart it stops working. Figure 4.22 shows the effective vector precession for this event sequence in the case of a triplet-born RP. No spin polarization arises before switching on the exchange integral (see Fig. 4.22 (a)). S-T₀ transitions result in a nonzero y-projection of the effective spin. For instance, Figure 4.22 (a) shows the vector at the moment when it is 90° turned about x-axis. With the exchange integral at work, within the time interval (t_1, t_2) the subsequent precession of the effective spin about the effective field gives a nonzero x-projection, i.e. electron polarizations arise (see Fig. 4.22(b)). With the exchange integral at rest, the effective spin starts precessing around the x-axis and its x-projection, i.e. spin polarization, does not change. Thus, for electron polarization to occur, the exchange integral and the difference in the Larmor frequencies must not necessarily work simultaneously, their action can be distributed in time.

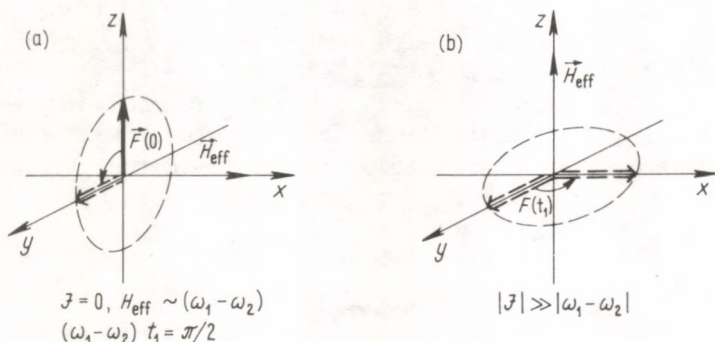


Fig. 4.22. CIDEP formation within the Adrian model [4.29]. A strong exchange interaction is switched on in the time interval (t_1, t_2)

Investigations of radical spin exchange during collisions in solutions [4.19] have shown the exchange integral to acquire values of an order of 10^{13} rad/s at radicals approaching at van der Waals distances. The analysis of the effective spin motion demonstrates RP contacts at van der Waals radii to completely destroy electron spin polarizations due to intensive exchange interactions. Indeed, assume that at a given moment a RP ensemble spins are polarized so that some orientation of the vector \vec{F} corresponds to their state (Fig. 4.23 (a)). With the radicals at the van der Waals distances, the intensive exchange interaction $|J| \gg |\omega_1 - \omega_2|$ begins working and the effective vectors of the RP ensemble begin precessing about z-axis. During the contact RP lifetime $\tau \sim 10^{-11} - 10^{-12}$ s the effective spins have enough time to repeatedly turn about z-axis. Due to the spread of contact times and RP exchange interaction values at a contact moment the effective spins appear, by the end of the contact, to uniformly distributed all over the surface of the cone formed by the effective vectors of different RPs of the ensemble (Fig. 4.23 (b)). As a result, the x-

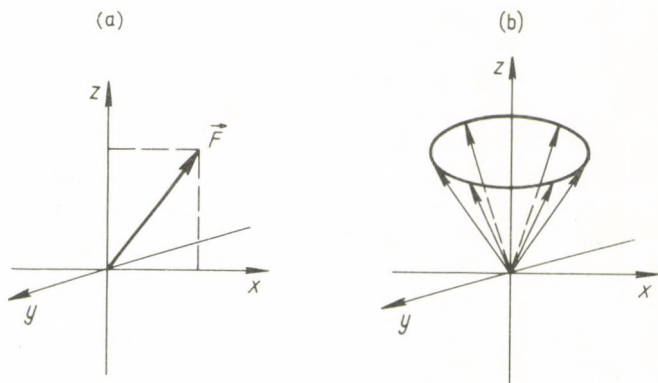


Fig. 4.23. RP electron spin depolarization due to strong exchange interactions

projection of \vec{F} averaged over the RP ensemble becomes zero and the spins are correspondingly depolarized. Such electron depolarization observed at radical contacts was established by Adrian [4.29].

At the interrational distances where the exchange integral is zero, electron polarizations do not arise. At the closest radical approach when the exchange integral is great, electrons are depolarized. Hence, RP electrons appear to be polarized at some intermediate interrational distances when the exchange integral is within the range $10^{12} > J \gtrsim 10^8$ rad/s.

While analyzing the effective vector motion under different conditions, in the case of short-lived RPs one can formulate the basic qualitative laws of CIDEP, the dependence of sign of CIDEP effects on that of magnetic-resonance RP parameters and RP precursor multiplicity. To analyze CIDEP multiplet effects, an RP ensemble must be divided into subensembles, each corresponding to a definite nuclear spin configuration and having its own effective vector \vec{F} . It seems to be more convenient to obtain laws of electron polarization sign in short-lived radicals using the operator formalism outlined in the beginning of the section.

The basic regularities of CIDEP in short-lived radicals. Consider the simplest case: a RP without magnetic nuclei with spin-Hamiltonian given by eq. (4.81). In this case the total spin projection of both unpaired electrons does not change as $\hat{S}_{1z} + \hat{S}_{2z}$ commutes with the system Hamiltonian which means that the electrons acquire polarizations which are equal in value but different in sign. Thus, it is sufficient to consider the polarization of one of the radicals, e.g., that denoted by subscript 1. The radical polarization of the type $M_{S_1} = -g_e \cdot \beta_e \cdot \langle \hat{S}_{1z} \rangle$ is given by the equations

$$\begin{aligned} \partial M_{S_1} / \partial t &= i\hbar^{-1} \cdot \langle [g_e \cdot \beta_e \hat{S}_{1z}, \hat{H}] \rangle \equiv -i \cdot g_e \cdot \beta_e \cdot J(t) \cdot Q, \\ \partial Q / \partial t &= -i\hbar^{-1} \langle [\hat{Q}, \hat{H}] \rangle \equiv i \cdot (\omega_1 - \omega_2) \cdot P_0 + i \cdot 2 \cdot J(t) \cdot Q_1, \\ \partial Q_1 / \partial t &= -i\hbar^{-1} \langle [\hat{Q}_1, \hat{H}] \rangle \equiv i \cdot 2 \cdot J(t) \cdot Q, \end{aligned} \quad (4.83)$$

where

$$\langle \hat{Q} \rangle = Q = \langle \hat{S}_1^+ \cdot \hat{S}_2^- - \hat{S}_1^- \cdot \hat{S}_2^+ \rangle, \quad \langle \hat{Q}_1 \rangle = Q_1 = \langle \hat{S}_{1z} - \hat{S}_{2z} \rangle.$$

At the initial moment the only nonzero value in (4.83) is P_0 which is +1 or -1 for a triplet T_0 or singlet RP precursor respectively. Solving these equations we obtain for short-lived radicals

$$M_{S_1} \approx g_e \cdot \beta_e \cdot (\omega_1 - \omega_2) \cdot P_0(0) \cdot \int_0^t \tau \cdot J(\tau) d\tau. \quad (4.84)$$

Thus, the net polarization sign of a given radical is determined by the sign of

$$\Gamma_{NE} = \mu \cdot \Delta g \cdot J \quad (4.85)$$

where $\mu = 1$ or -1 for a T_0 or S RP precursor. The polarization is positive if $\Gamma_{NE} > 0$ and negative if $\Gamma_{NE} < 0$. In eq. (4.85) the exchange integral sign is set constant in the course of mutual radical diffusion.

These results can be directly generalized for the case of RPs with any number of magnetic nuclei in high magnetic fields when the S- T_0 approximation can be applied. Equations similar to (4.83) give the following polarization of the hfs component of a radical ESR spectrum corresponding to a specified nuclear spin configuration

$$M_{S_1} \{m_{1k}\} \approx g_e \cdot \beta_e \cdot (\omega_1 - \omega_2 + \sum_k a_{1k} \cdot m_{1k}) \cdot P_0(0) \cdot \sum_0^t \tau \cdot J(\tau) d\tau. \quad (4.86)$$

Here a_{1k} is the isotropic hf constant of the radical under study, k is the number of the radical magnetic nucleus, m_k is the nuclear spin projection. Hence, the hf interaction induces not net but multiplet CIDEP effects. If the radical g -values are equal or their difference is negligible, the ESR spectral components are polarized antisymmetrically with respect to the spectrum centre. The multiplet effect sign is determined by the radical hf energy $E_{SI} = \hbar \cdot \langle \sum_k a_{1k} \hat{S}_{1z} \hat{I}_{kz} \rangle$ (4.5). On using eq. (4.86) we obtain the hf energy of a short-lived radical as

$$\begin{aligned} E_{SI} &\approx -\hbar \cdot \sum_k a_{1k}^2 \langle m_{1k}^2 \rangle \cdot P_0(0) \cdot \int_0^t \tau \cdot J(\tau) d\tau = \\ &= -(1/3) \cdot \hbar \cdot \sum_k I_{1k} \cdot (I_{1k} + 1) \cdot a_{1k}^2 \cdot P_0(0) \int_0^t \tau J(\tau) d\tau. \end{aligned}$$

It is interesting to note that the sign of the multiplet CIDEP effect is independent of that of the hf constant which may not hold for long-lived radicals. The multiplet CIDEP sign is determined by that of the product

$$\Gamma_{ME} = -\mu \cdot J \quad (4.87)$$

(Instead of eq. (4.87) ref. [4.37] gives the incorrect relation $\Gamma_{ME} = \mu \cdot J a$.) If the radical hf energy increases, i.e. E_{SI} , $\Gamma_{ME} > 0$, the polarization is of EA type, otherwise, when E_{SI} , $\Gamma_{ME} < 0$, the polarization is of the AE type.

In the majority of cases the exchange integral is expected to be negative. Then, according to eq. (4.87), the multiplet CIDEF effect is of AE type in a singlet-born RP and of EA type in a triplet-born RP. In the case of radical recombination in homogeneous solutions (diffusion RPs) EA polarizations should normally be observed.

In the case of short-lived radicals one can readily calculate CIDEF effects even in low fields when not only S-T₀ but also S-T₋, T₊ channels must be taken into account. For instance, consider electron polarizations in one-nucleus RPs with spin 1/2. To simplify the case, assume that the exchange integral does not change with time. In fact, the exchange integral changes at random during radical diffusion and thus *J* serves as an effective parameter. In low fields the difference in radical *g*-values is negligible and hence the spin-Hamiltonian can be expressed as in eq. (4.55).

In the case outlined the total projection of electron and nuclear spins is an integral of the motion, i.e. the spin moments of the electrons and the nucleus are oppositely polarized. The mean value of the nuclear spin projection on to *z*-axis is determined by eq. (4.60) and equals $\langle \hat{I}_z \rangle \approx \omega_0 \cdot a^2 \cdot J \cdot P_0(0) \cdot t^4/4!$. As a result of the conservation of the total spin projection the mean longitudinal component of the electron spins is

$$\langle \hat{S}_{1z} + \hat{S}_{2z} \rangle = -\langle \hat{I}_z \rangle. \quad (4.88)$$

In the case under discussion the electrons and nuclei are equally polarized since they have opposite signs of gyromagnetic ratios. In low fields the hf interaction of an unpaired electron with a magnetic nucleus induces the total polarization of both radicals

$$M_{S_1+S_2} = -g_e \cdot \beta_e \langle \hat{S}_{1z} + \hat{S}_{2z} \rangle \approx g_e \cdot \beta_e \cdot \omega_0 \cdot a^2 \cdot J \cdot P_0(0) \cdot t^4/4! \quad (4.89)$$

We now calculate the net electron polarization of each radical. Redifferentiate the radical spin moment operators again and obtain

$$\partial^{(4)} \langle \hat{S}_{1z} \rangle / \partial t^4 |_{t=0} = -(5/4) \cdot \omega_0 \cdot a^2 \cdot J \cdot P_0(0),$$

$$\partial^{(4)} \langle \hat{S}_{2z} \rangle / \partial t^4 |_{t=0} = (1/4) \cdot \omega_0 \cdot a^2 \cdot J \cdot P_0(0).$$

Hence in low fields, as well as within the S-T₀ approximation in high fields, the radicals are oppositely polarized. However, unlike the S-T₀ model, in low fields the electron polarization of the radical having a magnetic nucleus is five times higher than that of its partner. It can also be noted that the polarization sign is independent of the hf constant.

CIDEF effects of RPs with any number of magnetic nuclei can be calculated in a similar way [4.20]. The Zeeman energies of unpaired electrons are given by the relations:

$$E_{zS_1} \approx C \cdot P_0(0) \cdot J \cdot \left\{ -(5/3) \cdot \sum_n a_{1n}^2 \cdot I_{1n} \cdot (I_{1n} + 1) + \right. \\ \left. + (1/3) \cdot \sum_k a_{2k}^2 \cdot I_{2k} \cdot (I_{2k} + 1) \right\}, \quad (4.90)$$

$$E_{zS_2} \approx C \cdot P_0(0) \cdot J \cdot \left\{ (1/3) \cdot \sum_n a_{1n}^2 \cdot I_{1n} \cdot (I_{1n} + 1) - (5/3) \cdot \sum_k a_{2k}^2 \cdot I_{2k} \cdot (I_{2k} + 1) \right\},$$

where

$$C = g_e^2 \cdot \beta_e^2 \cdot \hbar^{-1} \cdot H_0^2 \cdot t^4/4! = \hbar \cdot \omega_0^2 \cdot t^4/4!,$$

a_{1n} and a_{2k} are hf constants of radicals with subscripts 1 and 2, respectively. According to (4.90), each nucleus contributes five times more to the electron polarization of its own radical than to that of the radical-partner.

Multiplet CIDEP is characterized by the mean value of the hf interaction:

$$E_{S_1, I_n} = \langle \hbar a_{1n} \hat{S}_1 \hat{I}_{1n} \rangle \approx -\hbar \cdot a_{1n}^2 \cdot I_{1n} \cdot (I_{1n} + 1) \cdot P_0(0) \cdot \int_0^t \tau J(\tau) d\tau.$$

Hence, in low magnetic fields the multiplet CIDEP sign is determined by the same eq. (4.87) as in the case of high fields.

Numerical calculations of CIDEP in high magnetic fields. The formal scheme to calculate magnetic and spin polarization effects, CIDEP included, was dwelt on in Section 2.3. The density matrix of *A* and *B* radicals constituting a pair is established by eqs (2.174, 178, 182, 204, 205). The mean value of the spin moment projection, e.g., of radical *A* on to the magnetic field direction (which determines the net CIDEP effect) and the mean value of the radical hf energy (which determines the multiplet CIDEP effect) are expressed through the radical density matrix σ_A by the relations

$$\langle \hat{S}_{Az} \rangle = Tr_A \{ \hat{S}_{Az} \cdot \sigma_A \}, \quad E_{S_A I} = Tr_A \{ \hat{H}_{hf} \cdot \sigma_A \}, \quad (4.91)$$

where \hat{H}_{hf} is the radical hf spin-Hamiltonian, Tr_A is the trace over the radical spin variables. The values characterizing the radical electron polarization (4.91) can be also expressed via the RP density matrix. For instance, the net radical electron polarization is $\langle S_{Az} \rangle = Tr \{ \hat{S}_{Az} \cdot \rho \}$ where Tr is the trace over the RP spin variables, ρ is the RP density matrix. If ρ is written in the singlet-triplet basis, then

$$\langle \hat{S}_{Az} \rangle = (1/2) \cdot (\rho_{T_+, T_+} - \rho_{T_-, T_-} + \rho_{ST_0} + \rho_{T_0S})$$

or in the S-T₀ approximation

$$\langle \hat{S}_{Az} \rangle = (1/2) \cdot (\rho_{ST_0} + \rho_{T_0S}) = \text{Re} \{ \rho_{ST_0} \}. \quad (4.92)$$

The electron spin polarization is proportional to the real part of the off-diagonal element of the RP density matrix in the singlet-triplet basis. This fact can be interpreted in terms of the vector model of effective spin *F* (See Fig. 4.21a). Indeed, for any spin 1/2 the mean values of its projection are expressed through the density matrix by the relations

$$\langle \hat{F}_z \rangle = (1/2) \cdot (\rho_{++} - \rho_{--}),$$

$$\langle \hat{F}_x \rangle = \text{Re} \{ \rho_{+-} \}, \quad \langle \hat{F}_y \rangle = \text{Im} \{ \rho_{+-} \},$$

where $|+\rangle, |-\rangle$ are the eigenstates of \hat{F}_z . For the effective spin *F*, T₀ and S serve as $|+\rangle$ and $|-\rangle$. One thus comes to the conclusion that eq. (4.92) expresses the fact that the radical electron spin polarization is proportional to the x-projection of the

effective spin F which is depicted in Fig. 4.21a. Note that eq. (4.92) was used to calculate electron polarizations in ref. [4.29, 32]. In ref. [4.32] CIDEP effects were analyzed with the RP kinetic equations (2.163–170) which were solved numerically in the S–T₀ approximation with different values of the mutual radical diffusion coefficient D , matrix elements of S–T₀ mixing (3.1), and singlet RP recombination rate constant (see (2.164)). The calculations were performed for two models of exchange interaction: when the exchange integral suddenly switches on at the moment of the closest radical approach and when it exponentially reduces with increasing interradsical distance. The data obtained can be summarized as follows. The principal theoretical conclusion is that at typical values of radical mobility ($D \approx 10^{-5}$ cm²/s), matrix element of singlet–triplet transitions ($\epsilon \approx 10^8$ rad/s), and exchange interaction parameters, the electron polarization is 30–40 times higher than its equilibrium value. Electron polarization increases proportionally to $\epsilon^{1/2}$ for liquids with radical diffusion coefficient $D \sim 10^{-5}$ cm²/s and $\epsilon \sim 10^8$ rad/s. This square-root dependence of magnetic and spin polarization effect scale on ϵ is typical of the diffusion RP model. Calculations reported in ref. [4.32] confirmed the conclusion [4.29] that in the model of a sudden switching on of the exchange interaction, the CIDEP effect sharply falls when the exchange integral exceeds 10^{12} rad/s. At such values of the exchange integral at a contact moment the electrons are depolarized (see Fig. 4.23). When the exchange integral is described by the exponential function and the exchange interaction increases, the CIDEP effects reach a kind of a plateau and no longer depends on the exchange integral unlike the model of a sudden switching on of exchange interaction. The scale of CIDEP effects increases with a decrease in the rate of exchange integral decay. These results obtained in the model of exponential decay of the exchange integral confirm qualitative data on CIDEP effects and approximate calculations made by Adrian [4.29] which demonstrate that electron polarizations arise when the radicals are at intermediate distances. A decrease in the rate of exchange integral decay results in the extension of the region of effective electron polarization and thus in an increase of the CIDEP effect.

CIDEP effects were analyzed taking into account the influence of radical exchange and ion-radical Coulomb interactions on the in-cage radical spatial diffusion [4.32]. Interradsical interaction potential in RP spin dynamics is allowed for by eqs (2.161, 170). It has been shown that the effect of the exchange interaction on the mutual radical diffusion can in fact be neglected when interpreting CIDEP effects. At the same time the long-range Coulomb interaction essentially influences the results.

The data published in ref. [4.32] make possible the quantitative analysis of both net and multiplet CIDEP effects in high magnetic fields. In ref. [4.32] electron polarizations have been calculated for the subensembles of RPs with an arbitrary number of magnetic nuclei and any nuclear spin configuration, i.e. the polarization of each hyperfine structure component of the radical ESR spectrum. A definite value of the matrix element of S–T₀ mixing, $\epsilon(m)$ (3.1), corresponds to each hf component of the ESR spectrum.

Thus the theory of CIDEP effects in radical reactions has been well understood qualitatively and elaborated quantitatively for a great number of RP parameters for high magnetic fields. Electron polarizations result from the simultaneous effects of singlet-triplet evolution and spin exchange induced by the exchange interaction. When two radicals are at van der Waals distances the electrons are depolarized provided their polarization was induced by $S-T_0$ mixing. Qualitatively this depolarization can be interpreted in the following way. In the $S-T_0$ approximation, unpaired electrons are oppositely polarized. When they are at van der Waals distances the partners exchange their spin polarizations as a result of spin exchange thus compensating opposite spin polarization. If electron polarizations are induced by $S-T_+$, T_+ transitions the polarization signs of both radicals coincide and radical spin exchange does not affect the process. In this case collisions at van der Waals distances do not result in electron depolarization. For the qualitative description of CIDEP effects the vector model of effective spin is convenient; the effective spin orientation is in one-to-one correspondence with definite states of two unpaired electrons of a pair.

Summarizing the results of the above discussion of chemically induced electron and nuclear polarizations, it is possible to conclude that the RP model gives an adequate description of a wide range of spin polarization effects in radical reactions. The scale of spin polarization depends on radical magnetic interaction parameters, radical mobility and reactivity. Quantitative analysis of CIDNP and CIDEP effects gives molecular kinetic characteristics of radicals (diffusion coefficients, in-cage RP lifetime) and magnetic resonance parameters (exchange integrals, hf constants and g -values of radicals, nuclear spin-spin interaction constants). Complementing each other, CIDNP and CIDEP investigations yield useful information on elementary steps of radical reactions and the structure of intermediate radicals. The basic conclusions of the theory of chemically induced polarization in the RP model have been widely confirmed experimentally. A detailed consideration of this problem is given below.

4.6 Spin polarizations in triplet molecule reactions

One of the main conclusions of the CIDEP theory within the RP model framework is the following: in high magnetic fields the total polarization of both unpaired electrons of a pair is expected to be zero and the polarizations of the partners must be opposite in sign. It is attributed to the fact that it is the $S-T_0$ spin evolution that makes the principal contribution to CIDEP while $S-T_+$, T_+ transitions are hardly probable. However, in photochemical reactions of unsaturated hydrocarbon compounds one can also observe radical pairs with both unpaired electrons equally polarized in sign (see, e.g. [4.33]). To account for these results Wong, Hutchinson and Wan [4.38] suggested the polarization mechanism which was called *triplet mechanism* or *triplet model*. In photochemical (and radiation-chemical) reactions, electron polarization does not arise in the RP after

the formation of radical particles, but in the stage preceding the RP generation. In many cases photochemical molecule transformations are known to originate from the triplet electron-excited state. For instance, a triplet molecule deprives a solvent molecule of a hydrogen atom, forming a RP by the scheme ${}^1M^* + RH \rightarrow \dot{M}H + \dot{R}$. The essence of the triplet spin polarization model is that the RP inherits the spin polarization of the triplet RP precursor.

Triplet molecule polarization in crystals. The triplet mechanism of CIDEP and CIDNP in solutions is based on the data of optical molecule polarization in crystals. Therefore, it is sensible to consider the optical spin polarization in molecular crystals before turning to the data on the theory of spin polarization by the triplet mechanism in photochemical reactions in solutions.

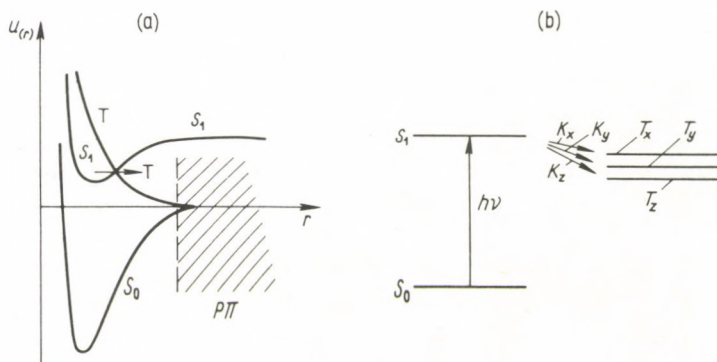


Fig. 4.24. Molecular terms (a) and transitions resulting in spin polarizations of the triplet state (b)

The scheme of electron transitions in a molecule leading to a triplet molecule with polarized spins is given in Fig. 4.24. Under light irradiation the molecule is excited to the singlet state S_1 . Then the intramolecular radiationless transition to the triplet state T occurs. In unsaturated hydrocarbons the intramolecular S_1 - T transition is induced by the spin-orbital interaction [4.39-41]. Because of magnetic interactions of the unpaired electrons, the term T splits into three sublevels (Fig. 4.24(b)). Experiments on luminescence in crystals [4.39, 40] and on the triplet state ESR (see, e.g. [4.41]) proved the intersystem transition to be of a selective character: the transition probabilities to different triplet sublevels are unequal. The S_1 - T transition selectivity follows the selective rules for the intersystem transition induced by the spin-orbital interaction and obeys the law of conservation of the symmetry of the total wave function of a molecule (see, e.g. [4.39]).

Triplet sublevel splitting is induced by spin-spin dipole-dipole or spin-orbital interactions of unpaired electrons or by their interaction with the external field. The spin Hamiltonian of a triplet molecule can be written in the form [4.42].

$$\hat{H}_T = \hat{H}_Z + \hat{H}_{SS} = g_e \cdot \beta_e \cdot H_0 \cdot \hat{S}_z + \hat{S} \cdot D \cdot \hat{S}, \quad (4.93)$$

where the first term describes the triplet Zeeman interaction, the second one

describes the triplet splitting in zero magnetic field, S is the total spin moment of the unpaired electrons, $S = S_1 + S_2$, D is the splitting tensor in zero magnetic field.

Triplet polarizations in crystals are usually investigated in zero field. The energy levels and the triplet eigenstates in zero field are well known. In terms of the principal axes of the tensor D , the Hamiltonian \hat{H}_{SS} can be presented as $\hat{H}_{SS} = D \cdot (\hat{S}_Z^2 - \hat{S}^2/3) + E \cdot (\hat{S}_X^2 - \hat{S}_Y^2)$, the eigenstates and energy levels are

$$\begin{aligned} |T_X\rangle &= (|-1/2, -1/2\rangle - |1/2, 1/2\rangle)/\sqrt{2}, \quad E_X = D/3 - E, \\ |T_Y\rangle &= i(|-1/2, -1/2\rangle + |1/2, 1/2\rangle)/\sqrt{2}, \quad E_Y = D/3 + E, \\ |T_Z\rangle &= (|1/2, -1/2\rangle + |-1/2, 1/2\rangle)/\sqrt{2}, \quad E_Z = -2 \cdot D/3. \end{aligned} \quad (4.94)$$

Here $|\pm \frac{1}{2}, \pm \frac{1}{2}\rangle$ conform to the spin states of the triplet unpaired electrons orientated either parallel or antiparallel to axis quantization. Note that the relative positions of the triplet levels depend on the signs of D and E . For example, when $D > 0$ and $E < 0$, the levels are arranged as given in Fig. 4.24b.

The selectivity of intramolecular intersystem transitions lies in the fact that the probabilities P_X, P_Y, P_Z of transitions to T_X, T_Y, T_Z levels, respectively, are unequal. Hence, the S_1-T transition (Fig. 4.24) results in a nonequilibrium population of the triplet spin sublevels: the spins prove to be mutually orientated in a definite way. In zero magnetic field no preferential direction and thus no prevailing spin orientation along any axis arises. In states (4.94) all the spin projections of the triplet unpaired electrons do equal zero. However populated these levels might be, no preferential spin orientation occurs. Whereas in zero field selective intersystem transitions give triplet molecules with polarizations of the type of multiplet effects conforming to a definite correlation of the spin states of two unpaired electrons. For instance, if $P_X \neq 0$ and $P_Y, P_Z = 0$, the triplet ESR spectrum shows one emission line at the T_Z-T_X transition instead of two absorption lines at transitions T_Z-T_X and T_Z-T_Y (see Fig. 4.24b). In non zero magnetic fields selective intersystem transitions afford triplet molecules whose spins are polarized with respect to the magnetic field direction. The general calculation scheme for unpaired electron spin polarizations is as follows [4.43]. Let $|n\rangle$ be eigenstates of triplet sublevels in an arbitrary magnetic field, P_n be the intersystem transition probability to the state $|n\rangle$. P_n is expressed through P_X, P_Y and P_Z as $P_n = \sum_q P_q \cdot |\langle q|n\rangle|^2$, where $q = X, Y, Z$. Hence, for the net polarization of triplet molecule spins we have

$$M_S = -g_e \cdot \beta_e \cdot \langle \hat{S}_{1H_0} + \hat{S}_{2H_0} \rangle = -g_e \cdot \beta_e \sum_n P_n \cdot \langle n | \hat{S}_{1H_0} + \hat{S}_{2H_0} | n \rangle, \quad (4.95)$$

where S_{H_0} is the spin projection to the field direction. The nuclear spin polarization induced by the hf interactions of unpaired electrons with magnetic nuclei can be calculated in a similar way [4.43].

Suppose that the transition probability solely to the state T_Y differs from zero, i.e. $P_Y \neq 0$. Suppose also that the tensor D is axially symmetrical, as it is observed in

the case of dipole-dipole interactions of unpaired electron spins in molecules with C_3 and higher rotational symmetry, and thus $E=0$. If the magnetic field is directed along the x -axis of the tensor D then the spin-Hamiltonian of the triplet becomes

$$\hat{H}_T = g_e \cdot \beta_e \cdot H_0 \hat{S}_x + D \cdot (\hat{S}_z^2 - \hat{S}^2/3).$$

Its eigenstates are

$$\begin{aligned} |1\rangle &= |T_x\rangle, \\ |2\rangle &= (2 \cdot R)^{-1/2} \cdot (-ia|T_y\rangle + b|T_z\rangle), \\ |3\rangle &= (2 \cdot R)^{-1/2} \cdot (ib|T_y\rangle + a|T_z\rangle), \end{aligned}$$

where $a = (R + D/2)^{1/2}$, $b = (R - D/2)^{1/2}$, $R^2 = (g_e \cdot \beta_e \cdot H_0)^2 + D^2/4$.

Use these functions and obtain

$$\begin{aligned} P_1 &= 0, \quad P_2 = a^2 \cdot P_Y, \quad P_3 = b^2 \cdot P_Y, \\ \langle 1 | \hat{S}_{H_0} | 1 \rangle &= 0, \quad \langle 2 | \hat{S}_{H_0} | 2 \rangle = g_e \cdot \beta_e \cdot H_0 / R, \quad \langle 3 | \hat{S}_{H_0} | 3 \rangle = -g_e \cdot \beta_e \cdot H_0 / R. \end{aligned}$$

Summing up the contributions of all triplet sublevels, we have the following spin polarization

$$M_S = -g_e^2 \cdot \beta_e^2 \cdot D \cdot (H_0/2 \cdot R^2) \cdot P_Y \sim -D \cdot P_Y. \quad (4.96)$$

Spin polarizations are greatly dependent on the molecule orientation with respect to the magnetic field. For instance, if in the above example the field is directed along the z -axis of the tensor of zero field splitting, then even selective intersystem transitions cannot induce polarization of triplet molecules.

Thus, in crystals with all molecules equally orientated with respect to the field, selective intersystem radiationless intramolecular transitions afford triplet molecules with polarized spins. If the triplet molecules take part in chemical reactions, the triplet polarization would be transferred to the reaction products. Triplet polarizations in crystals are of anisotropic character and depend on the molecule orientation with respect to the external field. Therefore, triplet molecule polarizations in liquids seem to be zero at average. However, optical polarizations of triplet excited molecule states has been shown [4.44] to take place not only in crystals but also in glasses and liquids.

Polarization of triplet molecules in liquids. With eq. (4.95) Wong *et al.* [4.44] calculated spin polarizations in triplet molecules arbitrary orientated in the external magnetic field and averaged the result over all possible molecule orientations. As a result, in the extreme case of high magnetic fields when $g_e \beta_e H_0 > D$ and $E=0$ they obtained

$$M_S = -(4/15) \cdot (D/H_0) \cdot (P_X + P_Y - 2P_Z). \quad (4.97)$$

In line with the experimental data on aromatic hydrocarbons $D > 0$, $P_X \gg P_Y$, P_Z (see, e.g. [4.44]). Then according to (4.97) electrons in triplet molecular states are negatively polarized. If a triplet molecule has time to react before paramagnetic

relaxation takes place, then the newly formed pair inherits the polarization of the triplet molecule. In case of aromatic molecules, RPs formed by this triplet molecule reactions display emission ESR lines. Note that for triplet molecules paramagnetic relaxation times are within nanosecond range [4.42]. Therefore, the triplet CIDEP mechanism would be sufficiently effective provided the triplet molecules are highly reactive and get into reactions at times of the order of either nanoseconds or less.

The theory of triplet CIDEP mechanism in solutions has been further developed by Atkins and Evans [4.45] and Pedersen and Freed [4.46]. They calculated the initial polarizations of RP electrons within the framework of the triplet model at different molecular orientational relaxation rates. The main steps of these calculations are as follows. Let $\rho_T(t)$ be the density matrix of triplet molecules, K_T be the rate constant of RP formation due to the triplet reaction. The polarization of any chosen RP is expressed by the equation

$$M_{S_1} = -g_e \cdot \beta_e \cdot \langle \hat{S}_{1z} \rangle = -g_e \cdot \beta_e \cdot \text{Tr} \left\{ \int_0^\infty dt \cdot K_T \rho_T(t) \hat{S}_{1z} \right\}, \quad (4.98)$$

where Tr means the trace over both spins. In fact, the RP polarization is contributed only by those triplets that have time to react before the paramagnetic relaxation in the triplet is over. Therefore, in (4.98) the upper limit can tend to infinity. For $\rho_T(t)$ we have the following equation of motion

$$\partial \rho_T / \partial t = -i\hbar^{-1} [\hat{H}_T(t), \rho_T] - K_T \cdot \rho_T + \hat{K} n_s(t). \quad (4.99)$$

Here the first term describes the density matrix variations induced by a Hamiltonian of the type (4.93). A molecular rotation changes the tensor D components in the laboratory coordinate system, therefore, \hat{H}_T in (4.99) is time dependent. The second term characterizes the triplet decay and RP formation. The last term corresponds to triplet origination from the singlet state, $n_s(t)$ being the singlet population and \hat{K} being the triplet formation rate operator which is diagonal on the basis T_x, T_y, T_z functions and has elements K_x, K_y, K_z (see Fig. 4.24b). Equation (4.99) must be averaged over all realizations of random triplet molecule rotations. In the case of sufficiently fast rotations, this averaging can be performed within time-dependent perturbation theory. In the case of arbitrary orientational relaxation rates of triplet molecules (see, e.g. [4.19]), one introduces a partial density matrix of the subensemble of triplet molecules having a certain spatial orientation. The molecule orientation will be characterized below by the position of a unit vector $\vec{\Omega}$. The full density matrix is

$$\rho_T(t) = \int d\Omega \cdot \rho_T(\vec{\Omega}, t).$$

The density matrix of the subensemble $\rho_T(\vec{\Omega}, t)$ obeys the equation

$$\begin{aligned} \partial \rho(\vec{\Omega}, t) / \partial t = & -i\hbar^{-1} [\hat{H}_T(\vec{\Omega}), \rho_T(\vec{\Omega})] - \\ & - K_T \cdot \rho_T(\vec{\Omega}) + \hat{K} \cdot n_s \cdot \varphi(\vec{\Omega}) + \hat{L}_\Omega \cdot \rho_T(\vec{\Omega}), \end{aligned} \quad (4.100)$$

where $\varphi(\vec{\Omega})$ is the statistical weight of molecules with assumed orientation, \hat{L}_Ω is the kinematic operator describing transitions of molecules from one subensemble to another due to their rotation.

The singlet state population decreases because of intersystem transitions to the triplet state

$$n_s(t) = \exp(-Kt) \quad (4.101)$$

where $K = K_X + K_Y + K_Z$.

Using equations (4.98–101), the initial electron polarizations have been obtained for a situation typical of liquids when the characteristic molecular rotation frequency exceeds the splitting energy in zero fields expressed in frequency units. At comparatively slow molecular rotations when $g_e \cdot \beta_e \cdot \hbar^{-1} \cdot H_0 \cdot \tau_0 > 1$ the polarization is [4.45]

$$M_{S_1} = -C_1 \cdot \{D \cdot (K_X + K_Y - 2K_Z) + 3E(K_Y - K_X)\} \quad (4.102)$$

where

$$C_1 = g_e^2 \cdot \beta_e^2 \cdot H_0 \cdot K_T \cdot K^{-1} \cdot \tau_0 \cdot \{2 \cdot [D^2 + 3E^2 + (15/4)K_T \cdot \tau_0 \cdot g_e^2 \cdot \beta_e^2 \cdot H_0^2]\}^{-1}.$$

In the case of extremely fast rotations, when $g_e \cdot \beta_e \cdot \hbar^{-1} \cdot H_0 \cdot \tau_0 < 1$,

$$M_{S_1} = -C_2 \cdot \{D \cdot (K_X + K_Y - 2K_Z) + 3E \cdot (K_Y - K_X)\}, \quad (4.103)$$

$$C_2 = g_e^2 \cdot \beta_e^2 \cdot H_0 \cdot K_T \cdot K^{-1} \cdot \tau_0 \cdot \{2 \cdot [D^2 + 3E^2 + 3K_T/2\tau_0]\}^{-1}.$$

When the rotation is "frozen" and $E=0$, eq. (2.102) yields the results reported in ref. [4.44]. The above formulas demonstrate the net polarization sign to be determined by the sign of the value

$$\Gamma_{NE} = -[D \cdot (K_X + K_Y - 2K_Z) + 3E \cdot (K_Y - K_X)] \quad (4.104)$$

or, viewing that $|D| \gg |E|$ in most systems, by the sign of

$$\Gamma_{NE} = -D \cdot (K_X + K_Y - 2K_Z). \quad (4.105)$$

Thus the triplet mechanism creates negative electron polarizations if $D > 0$ and $K_X + K_Y > 2K_Z$ or $D < 0$ and $K_X + K_Y < 2K_Z$, the polarization sign of both unpaired electrons of the RP being equal.

The triplet mechanism of CIDNP. During selective intersystem intramolecular transitions, the nuclear spins are being polarized simultaneously with the electrons. Colpa *et al.* [4.43] were the first to consider this mechanism of nuclear polarization as connected with optical nuclear polarization in molecular crystals. Nuclear polarizations of triplet molecules in photochemical reactions in solutions are discussed in refs. [4.17, 47]. The mathematical technique of the theory is the same as that in the CIDEP theory, i.e. equations of type (4.99) are to be solved, with nuclear spin states considered as well. Therefore, the hf interaction of unpaired electrons with magnetic nuclei must be added to \hat{H}_T . Nuclear polarizations in a triplet molecule are calculated by the formula (cf. (4.98)).

$$M_I = g_I \cdot \beta_I \cdot \langle \hat{I}_z \rangle = g_I \cdot \beta_I \cdot \text{Tr} \left\{ \int_0^\infty dt \cdot K_T \cdot \rho_T \cdot \hat{I}_z \right\} \quad (4.106)$$

where Tr denotes the trace over all spin, electronic and nuclear, triplet variables. Solving the equation of motion (4.99) in the second order of the time-dependent perturbation theory [4.45], the nuclear polarization of $I=1/2$ spin has been calculated [4.17, 47] for a triplet molecule with the spin Hamiltonian

$$\hat{H}_T = g_e \cdot \beta_e \cdot H_0 \hat{S}_z + \hat{S} \cdot \hat{D}(t) \cdot \hat{S} + \hbar a \hat{S}_z \hat{I}_z + \hbar b \cdot (\hat{S}_x \hat{I}_x + \hat{S}_y \hat{I}_y).$$

The nuclear polarization is

$$M_I = (1/20) \cdot g_I \cdot \beta_I \cdot b^2 \cdot \tau_0^2 \cdot K^{-1} \cdot \Gamma \cdot \{f(H_0) - f(-H_0)\}, \quad (4.107)$$

where

$$\Gamma = -[D \cdot (K_X + K_Y - 2K_Z) + 3E \cdot (K_Y - K_X)],$$

$$f(H_0) = (\omega_0 - a/2) \cdot \{[(\omega_0 - a/2)^2 + 2b^2] \cdot$$

$$\cdot [1 + \tau_0^2 \cdot ((\omega_0 - a/2)^2 + 2b^2)]\}^{-1},$$

$$\omega_0 = g_e \cdot \beta_e \cdot \hbar^{-1} \cdot H_0.$$

Hence, selective intersystem transitions induce nuclear polarizations which can be transferred to the reaction products of triplet molecules. The polarizations decrease with increasing molecular orientation relaxation rate $1/\tau_0$. Estimating nuclear polarizations in high and low magnetic fields by expanding eq. (4.107) into a series with respect to the small parameter a/ω_0 and taking into account that the condition $a \cdot \tau_0 \ll 1$ holds in liquids, we have for high magnetic fields

$$M_I \approx g_I \cdot \beta_I \cdot \Gamma \cdot a^2 \cdot \tau_0^2 \cdot [K \cdot \omega_0 \cdot (1 + \omega_0^2 \cdot \tau_0^2)]^{-1} \quad (4.108)$$

This formula indicates that the triplet mechanism contributes negligibly to the CIDNP in high magnetic fields. Indeed, on substituting typical parameters $a \approx 10^8$ rad/s, $\tau_0 \approx 10^{-10}$ s, $|\Gamma|/K \approx 10^8$ rad/s, $H_0 \approx 1$ kG one obtains from (4.108) $M_I \approx 10^{-6} \cdot g_I \cdot \beta_I$, i.e. it is comparable to equilibrium polarizations. The triplet mechanism of nuclear polarization is more effective in low magnetic fields when

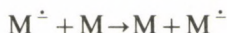
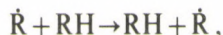
$$M_I \approx g_I \cdot \beta_I \cdot \Gamma \cdot K^{-1} \cdot \omega_0 \cdot \tau_0^2. \quad (4.109)$$

In low fields the nuclear spin polarization calculated by this formula can be about 100 times greater than the difference in the thermal equilibrium populations of spin states.

Nuclear polarization due to electron-nuclear cross-relaxation. One more mechanism of nuclear spin polarization [4.48, 49] induced by either electron-nuclear flip-flips or flip-flops is quite possible. Thus nuclear polarization mechanism of nuclear spin polarization [4.48, 49] induced by either electron-described in detail in monographs on magnetic resonance (see, e.g., [4.42]).

In most cases, however, this mechanism of nuclear polarization proves to be ineffective in chemical reactions. Electron-nuclear cross-relaxation occurs within a microsecond range which is also the time of electron and nuclear spin depolarization induced in radicals by spin-lattice relaxation. Thus, for this mechanism to manifest itself experimentally, certain fairly strict conditions must be fulfilled: radicals must be long-lived enough for the cross-relaxation to occur and polarized

nuclei must appear in diamagnetic products prior to radical spin-lattice relaxation. For instance, during an RP in-cage lifetime (subnanosecond and nanosecond ranges) the cross-relaxation has no time to occur and, hence, this nuclear polarization mechanism will not influence the CIDNP effect in the geminate recombination product. The nuclear polarizations induced by electron nuclear cross-relaxation can be accumulated in diamagnetic molecules provided fast reactions of unpaired electron transfer of the type



take place. Here the radicals turn into diamagnetic molecules inheriting the polarized radical nuclei, which results in the accumulation of nuclear polarizations in the diamagnetic molecules.

To summarize then one can conclude that the triplet mechanism creates the initial polarization of unpaired electrons in a RP, the polarization sign of both radicals being equal. For unsaturated hydrocarbons, as a rule, negative electron polarizations could be expected. In real systems both triplet and radical pair mechanisms can be realized simultaneously. The total result of both polarization mechanisms is asymmetry between the radicals of a pair. The RP spin evolution increases the initial electron polarization arising by the triplet mechanism in one-radical partner. In the other partner, the RP spin evolution induces polarization opposite in sign to the initial triplet polarization, the total polarization of this radical finally decreasing. Within the RP model, for a triplet precursor, the electron polarization in the radical with the larger g -value is negative, that in the radical with the smaller g -value is positive (see (4.85)). If the initial triplet polarization of the radicals is negative, both polarization mechanisms result in intensive emission in the ESR spectrum of the radical with a greater g -value and the ESR spectrum of the partner will be somewhat damped by the mutual compensation of the polarizations following both the triplet and RP mechanisms. These considerations might be useful to interpret the fact that CIDEP effects are often observed experimentally only in one of the partners.

CIDNP effects can also arise by the triplet mechanism. However, in high magnetic fields its contribution might be small and cannot compete with the nuclear polarization process within the RP model. In low fields the triplet mechanism can contribute to CIDNP effects.

Along with nuclear polarizations arising in the course of selective intramolecular S-T transitions, nuclear spins can also be polarized as a result of cross-relaxation transfer of radical electron polarizations to the nuclear spin subsystem.

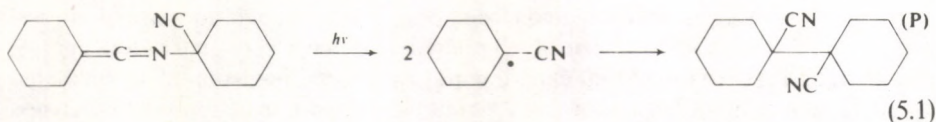
5 EXPERIMENTAL OBSERVATIONS OF MAGNETIC FIELD EFFECTS IN RADICAL REACTIONS

5.1 Spin effects

The assumption that the electron spin effects are of fundamental importance in radical reactions is the basis of theoretical models of the magnetic field influence on these reactions. We shall consider the experimental evidences for the manifestation of spin selection rule in free radical recombination reactions.

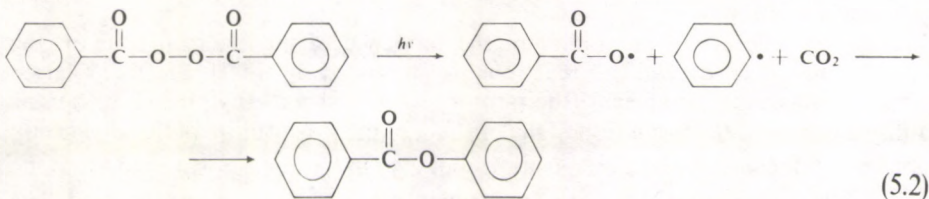
We shall consider in the first place the recombination of correlated radical pairs in the cage, where the recombination efficiency may be expected to depend on the spin multiplicity of the radical pair (in the absence of mechanisms of rapid transitions between different spin states).

The effects of RP spin multiplicity have been studied in a number of studies by comparing the reactions of direct and sensitized photolysis. Thus Fox and Hammond [5.1] observed an appreciable difference between the yields of the products of the recombination of two cyanocyclohexyl radicals in the photolysis of N-(1-cyanocyclohexyl)-pentamethylene-ketenimine,



In the direct photolysis (via an excited singlet state) in CCl_4 approximately 24% of succinonitrile (P) is formed. The triplet-sensitized decomposition under the same conditions gives only 8% of the compound (P). Thus the triplet RP recombination probability is in this case one-third of that for singlet pairs.

Similar effects have also been observed in the direct and sensitized photolyses of benzoyl peroxide [5.2],



The yield of phenyl benzoate was about 3% for triplet and about 8% for singlet pairs.

The influence of the sensitizer spin multiplicity on phenyl-benzoate formation has been recently studied for the same system [5.3]. Benzoyl peroxide solutions in toluene or benzene were irradiated by a high-pressure mercury lamp in the presence of aromatic hydrocarbons (naphthalene, fluorene, phenanthrene, etc.), which are singlet sensitizers, and also of aromatic ketones—acetophenone, benzophenone and 2-methyl-benzophenone—the latter being typical triplet sensitizers. The phenyl-benzoate yield was some 3.0% in the case of triplet sensitizers and some 10% in the case of singlet sensitizers.

The radical recombination in the bulk is another class of reactions characterized by the spin selection rule. When two radicals react at each encounter, the recombination rate is determined only by the diffusion rate. The rate constants for such diffusion-controlled reactions are determined by the expression

$$k_D = (4\pi N/1000)(\sigma_A + \sigma_B)(D_A + D_B), \quad (5.3)$$

where N is the Avogadro constant, D_A and D_B are the diffusion coefficients of A and B radicals in the reaction medium, σ_A and σ_B their reaction radii.

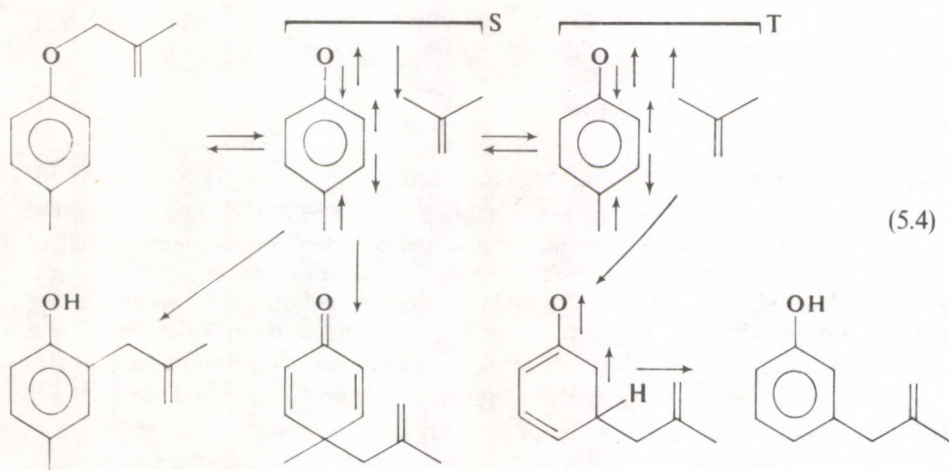
Note, however, that two radicals can recombine at an encounter only if the state of the radical pair is singlet. Since the probability of singlet encounters is 1/4, measured values of k_D must be expected to be 1/4 of the encounter rate constant predicted by relation (5.3). Experimental results on the basis of recombination kinetics of organic radicals do confirm this regularity. The k_D value calculated by eq. (5.3) for the most typical experimental conditions (solvent viscosity being about 1 cP) is near $8 \cdot 10^9 \text{ M}^{-1} \text{ s}^{-1}$ [5.4], while measured constants of bimolecular radical reactions as a rule, do not exceed $2 \cdot 10^9 \text{ M}^{-1} \text{ s}^{-1}$ [5.4].

The above regularity does not apparently obtain in reactions involving $\dot{\text{H}}$ atoms, $\dot{\text{O}}\text{H}$ and HO_2 radicals, and solvated electrons [5.5]. These reactions are of interest for us since they are not sterically hindered and have zero activation energy. However, it has been found that experimental k_D values differ from those calculated by eq. (5.3) by a factor between 1 and 2 but not 4. The spin selection rule is then less manifested. In a number of reactions, e.g., involving $\dot{\text{O}}\text{H}$ radicals, this fact can be associated with short electron relaxation times of one of the partners. However, in the case of reactions $\dot{\text{H}} + \dot{\text{H}}$, $\dot{\text{H}} + e_{\text{aq}}$, $e_{\text{aq}} + e_{\text{aq}}$ this explanation will not do. It is possible, that the reaction distance of a singlet pair exceeds the sum of the van der Waals radical radii [5.5].

Spin effects on spur dynamics in liquid phase radiolysis have been discussed in detail recently by Brocklehurst [5.6]. Fast spin relaxation of $\dot{\text{O}}\text{H}$ radicals was taken into consideration.

The very interesting possibility of the influence of the electron spin on the orientation effect in radical reactions is discussed in [5.7]. In the Claisen photochemical rearrangement (the photolysis of allyl *p*-methylphenyl ether), the authors observed the formation of the product of the substitution of the allyl group not only in the *ortho*- and *para*-positions but also in the *meta*-position in aromatic ring. In the analogous thermal rearrangement *meta*-products are not formed. The possibility of the formation of *meta*-products in the photochemical rearrangement

can be understood by examining the following mechanism which has been proposed on the basis of the analysis of the effects of CIDNP in this reaction:

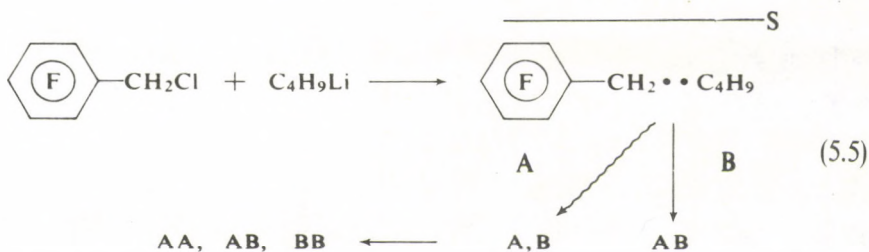


The radical pairs formed in the singlet state yield mainly *ortho*- and *para*-substitution products. For triplet pairs, *ortho*- and *para*-substitution is spin-prohibited. However, the spin density is negative in the *meta*-position, so that addition of the allyl radical in this position can occur in the triplet state. According to the authors [5.7], this in fact explains the formation of the *meta*-product.

The above examples show that the electron spin effects have in many instances a very marked influence on the kinetics of the recombination of free radicals. The conventional approach to radical reaction rates neglecting the spin selection rule cannot thus be considered valid.

5.2 Reactions of neutral radicals

A number of papers have been published, in which the effect of permanent magnetic field on radical reaction rate was observed. First, let us examine the reactions of neutral radicals. The authors of [5.8–10] were first to observe magnetic effects in liquid-phase radical reactions, specifically the reaction of pentafluorobenzyl chloride with C_4H_9Li in hexane. The basic mechanism of this reaction was determined by CIDNP and is described by the following scheme:



The ratio of the products AB and AA has been found [5.8–10] to increase by 30–40% when the reaction takes place in a 15 kG magnetic field in boiling hexane. The authors explained this effect in terms of the hf mechanism of the magnetic field effect. A pair of two alkyl radicals in the singlet-state is the direct precursor of the final product AB and AA. In this case AB results principally from an initial RP recombination, while AA results from radical reactions in the bulk. In consonance with the overall number of open S–T conversion channels in the pair (three channels in a low field and one S–T₀ channel in a high field), the probability of this conversion in high fields is less and hence the probability of RP recombination is higher as compared to lower fields. Thus the hf model predicts the increase of the ratio of the radical recombination products in the cage to that in the bulk, which is consistent with experiment.

To obtain additional evidence for the hf mechanism of field effects arising in the reaction of pentafluorobenzyl chloride with C₄H₉Li [5.11] the field dependence of the ratio between AB and AA products has been studied in detail (see Fig. 5.1).

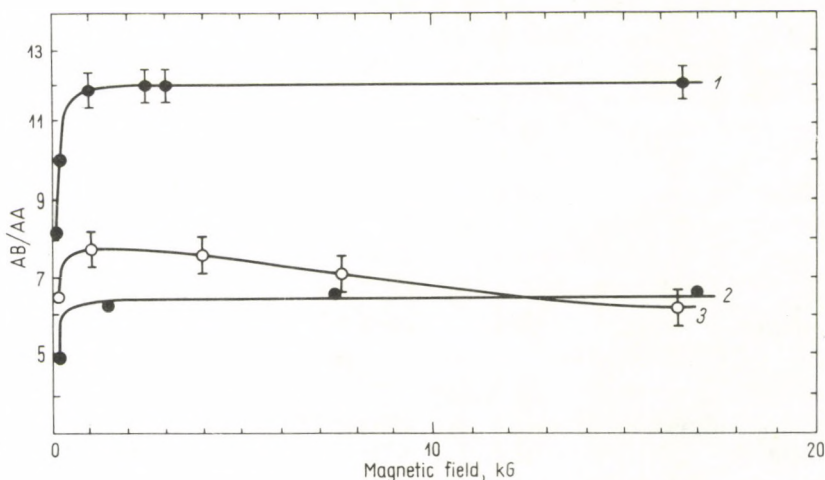


Fig. 5.1. Experimental dependences of the ratio of the reaction products AB and AA on magnetic field intensity in the C₄H₉Li reaction with pentafluorobenzyl chloride 1; *p*-fluorobenzyl chloride 2, and decafluorodiphenyl chloromethane 3

The field dependence reaches a plateau with the transition region at $H \approx 50\text{--}200$ Gauss. This is the field dependence of the singlet-state population predicted by theoretical computations for the hf model (see Fig. 5.2). In line with theory, a noticeable variation of P_s (transition region) must be observed at $H \approx A_{\text{eff}}/\gamma = (1/8)(\sum_i A_i^2)^{1/2}$ which in the reaction examined corresponds to $H \approx 60$ Gauss.

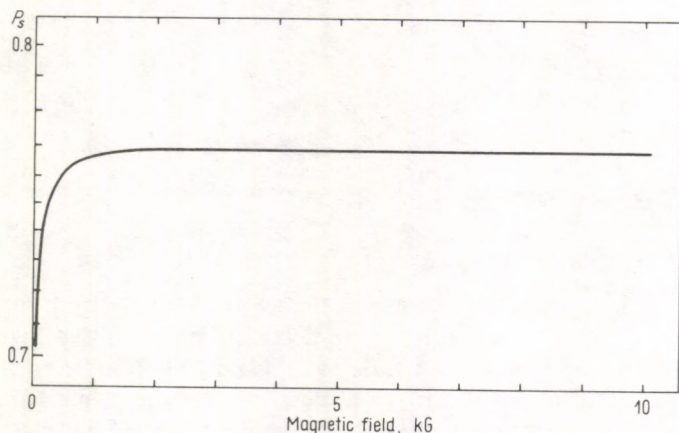


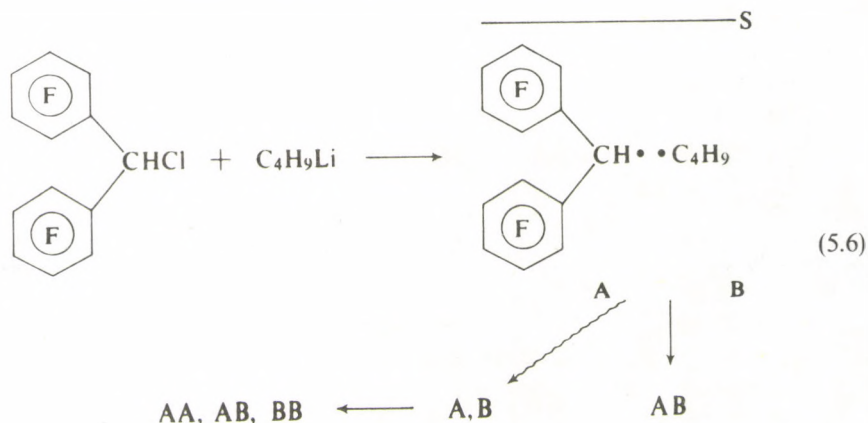
Fig. 5.2. Magnetic field dependence of the singlet-state recombination probability P_s for RP of pentafluorobenzyl (R_1) and butyl radicals (R_2) with the parameters: for 1 $A_x(H) = -16.80$ G, $A_0(F) = +9.5$ G, $A_m(F) = -4.9$ G, $A_p(F) = +17.1$ G, $g = 2.00278$; for 2 $A_x(\text{CH}_2) = -22.5$ G, $A_\beta(\text{CH}_2) = +27.0$ G, $A_\gamma(\text{CH}_2) = +1$ G, $g = 2.0025$

Subsequent studies of magnetic effects in reactions involving organolithium compounds [5.12–14] showed that the effect of the magnetic field can also be observed in the reactions of butyllithium with a number of other arylchloromethanes. Figure 5.1 (b) exemplifies the field dependence of AB/AA in the reaction of *p*-fluorobenzylchloride and butyllithium¹ [5.12]. The shape of the curve observed is well described by the hf model, as in the previous case.

Earlier we discussed another possibility for a magnetic field effect on radical recombination in solution, in which the singlet–triplet transitions were induced by the differences in the g -values. The difference in the Zeeman electron energies, $g_1\beta H - g_2\beta H$, and hence the S–T conversion rate increases with the field, which will result in a decrease of the geminate radical recombination probability.

This effect has been first observed experimentally by Podoplelov *et al.* [5.13] in the reaction of decafluorodiphenylchloromethane with $\text{C}_4\text{H}_9\text{Li}$. This reaction follows a scheme analogous to (5.5),

¹ The reaction scheme of *p*-fluorobenzyl chloride with $\text{C}_4\text{H}_9\text{Li}$ is completely analogous with Scheme (5.5).



A study of the magnetic field effects in this reaction showed that, instead of maintaining a plateau, the AB/AA ratio decreases noticeably in high fields (Fig. 5.1 (c)). An increase of the AB/AA ratio in fields ranging from 0.5 to 1000 G in the reactions discussed above is fairly well described by the hf mechanism. With a further increase in the magnetic field, the difference in the Zeeman electron energies becomes an additional mechanism of singlet-triplet mixing and results in a decrease of the AB/AA ratio. The theoretically calculated $P_S(H)$ dependence is presented in [5.13]. The analogy between the theoretical and experimental curves shows the Δg -mechanism of field effects on radical recombination to be realized in the reaction of decafluorodiphenylchloromethane with C_4H_9Li . Note that H^1 and F^{19} CIDNP effects in this reaction [5.15] indicate an appreciable difference in the g -values of decafluorodiphenylchloromethyl and butyl radicals, ($\Delta g \approx 1 \cdot 10^{-3}$), which is necessary for the Δg -mechanism to manifest itself.

Paper [5.11] discusses what values of the parameters employed in theoretical models correspond to the magnetic field effect observed. Using experimental values of $[AB]/[AA]$ in high and low fields (see Fig. 5.1) it has been found for the reaction of pentafluorobenzyl chloride, with C_4H_9Li in the diffusion RP model with $A_{eff} \approx 10^9$ rad/s, that the time of the diffusion jump $\tau = 6 \cdot 10^{-10}$ s. This value considerably exceeds the typical times of diffusion jump (10^{-11} s) in solvents with normal viscosities of some 1 centipoise. Anomalously low radical mobility in $C_6F_5CH_2Cl-C_4H_9Li$ reactions is associated [5.11] with the polymeric structure of butyllithium in solution. Indeed, it is well known [5.16], that C_4H_9Li exists in hydrocarbon solvents as a hexamer. The so-called "electron deficient structure", in which each lithium atom is bonded to three carbon atoms, is generally accepted [5.16]. The basis of this structure is a "chair" formed by six lithium atoms (Fig. 5.3). There are indications [5.17, 18] that in the reactions of lithiumalkyls with alkyl halides, the alkyl radicals formed from organolithium compounds participate in the reaction not in the free state but as complexes with the parent associates. It is

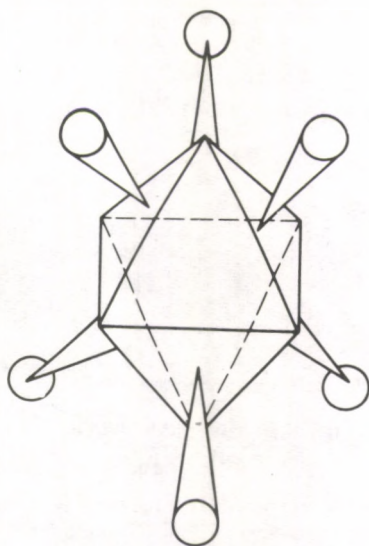


Fig. 5.3. Spatial structure of alkyl lithium hexamer in hydrocarbon solvents [5.16]

therefore natural to expect that the characteristic diffusion time of such a complex would be much longer than that of a typical RP.

If the hypothesis about the complexing between free radicals and organolithium compound associates participating in the reaction is correct, one must expect an appreciable influence of the sizes of the associate on the magnetic effects. Indeed, an increase in the associate size must lead to an increase in τ which is one of the parameters determining the scale of the magnetic effects. To support this hypothesis, the magnetic field effects arising in the reactions of pentafluorobenzyl chloride with some lithiumorganic compounds varying in associate sizes (Table 5.1) have been investigated experimentally [5.19]. The data listed in Table 5.1 are in a qualitative agreement with theoretical predictions. In fact, the field effect increases with the associate size (from isopropyl- to amyl-lithium). The disappearance of the effect with the further increase in the associate size (for the reaction with $C_7H_{15}Li$) is attributed [5.19] to the fact that in the last case the time τ is long enough for the interference of different channels of S-T conversion to become of importance. Sarvarov and Salikhov [5.20] predicted theoretically that in a number of cases at high values of $A\tau$, magnetic effects can vanish.

The papers discussed demonstrate that to obtain appreciable magnetic field effects on radical reactions (tens of percents) we have to study reactions in which the intermediate free radicals have an extremely low mobility (10^{-9} – 10^{-10} s). One of the ways to reduce diffusion mobility is to perform reactions in highly viscous solvents. The fact that a decrease in the solvent viscosity does reduce the magnetic effect was exemplified [5.10, 20] by the reactions of pentafluorobenzylchloride with butyllithium. When radical reactions are run in nonviscous solvents ($\tau \approx 10^{-11}$ s)

Table 5.1. Effects of magnetic field on the ratio of the principal products (AB and AA) in the reaction of pentafluorobenzyl chloride with lithium alkyls in hexane (Ref. [5.19])

RLi	$\epsilon_{\text{RLi}}/\epsilon_{\text{C}_4\text{H}_9\text{Li}}^a$
<i>i</i> -C ₃ H ₇ Li	0
<i>n</i> -C ₃ H ₇ Li	0.6
<i>n</i> -C ₄ H ₉ Li	1.0
<i>n</i> -C ₅ H ₁₁ Li	1.4
<i>n</i> -C ₇ H ₁₅ Li	0

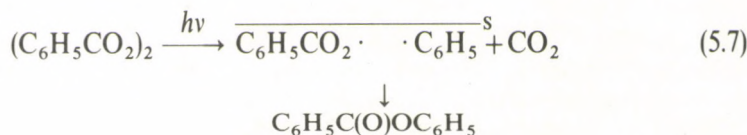
^a The field effect is expressed as

$$\epsilon = \frac{([\text{AB}]/[\text{AA}])_{\infty} - ([\text{AB}]/[\text{AA}]_0)}{([\text{AB}]/[\text{AA}]_0)}$$

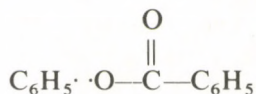
where $([\text{AB}]/[\text{AA}]_0)$ and $([\text{AB}]/[\text{AA}]_{\infty})$ are the ratios of the products in the earth's field and in a high field, respectively. The value of ϵ in the reaction of pentafluorobenzyl chloride with butyl lithium in hexane is taken as unity.

one must expect small effects (<10%), which may not be amenable to existing methods of analysis. The analysis of the literature shows that this is the case for all examples so far reported in which the magnetic field does not influence radical reactions in solutions [5.12].

One more way of increasing the scale of magnetic effects in liquid-phase radical reactions is to apply superhigh magnetic fields. In a case when the radical g -values differ appreciably, magnetic effects can be observed in high fields even in low viscous solvents. It can be illustrated by the sensitized photodecomposition of benzoylperoxide in fields up to 43,000 G (chrysene as a sensitizer, toluene as a solvent [5.21]). The general scheme of peroxide decomposition is



The effect of magnetic fields on the geminate recombination product of the intermediate RP (phenylbenzoate) and on the products of the escape free radicals (*o*-methyl-diphenyl, *p*-methyl-diphenyl and 1,2-diphenylethane) has been investigated [5.21]. The results of magnetic effect studies are given in Fig. 5.4. The phenylbenzoate yield is seen to decrease with increasing magnetic field which is in agreement with an increase of the S-T conversion rate in the pair



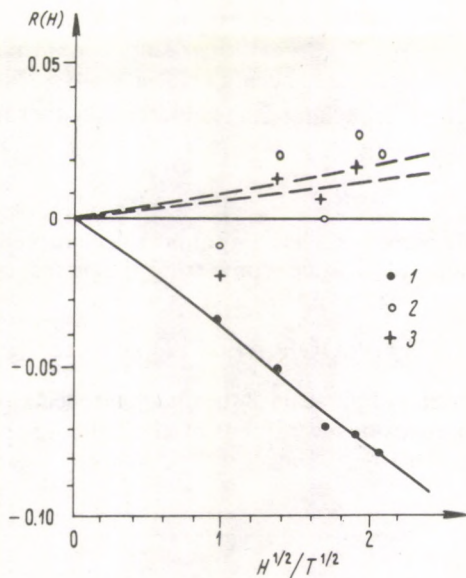


Fig. 5.4. Effect of magnetic field on the product yield of singlet sensitized photolysis of benzoyl peroxide (in toluene) [5.21]. $R(H) = P(H) - P(0)/P(0)$, where $P(H)$ and $P(0)$ are product yield in the magnetic field H and in the earth's magnetic field respectively; 1 — for phenyl benzoate; 2 — for *ortho*-methyldiphenyl, and 3 — for both *p*-methyldiphenyl and 1,2-diphenylethane

($\Delta g \approx 0.01$) expected by the Δg -mechanism. The product of escape radicals must naturally increase, which is observed experimentally (see Fig. 5.4). It should be noted that the field dependence of magnetic effects is described by the function $f \approx H^{1/2}$ obtained from studies on radical re-encounter dynamics. The scale of the effect observed is in good agreement with calculations.

Recently the magnetic field effect has been observed in a very important class of radical reactions, i.e., free-radical oxidation reactions [5.22]. Kadnikov [5.22] investigated radical oxidation of unsaturated aliphatic acids (e.g., linoleic and linolenic acids) in different magnetic fields. A characteristic feature of this complex chain process is an accompanying weak chemiluminescence in the visible region associated with disproportionation of peroxy radicals RO_2 . The molecules of the triplet-born ketone serve as a luminescence emitter. The luminescence intensity falls with increasing magnetic field [5.22]. Moreover, the oxidation product (hydroperoxides $ROOH$) yield is shown [5.22] to vary in a magnetic field too. Although the mechanism of the magnetic field effect observed has not yet been fully explained, it is possible to assume the magnetosensitive stage to be the intersystem crossing in a pair of paramagnetic particles including a triplet ketone molecule.

The possibility of magnetic field effects on the rate of chain liquid-phase oxidation has been discussed in ref. [5.23]. In branching chain reactions the magnetosensitive stage can be the branching reaction. In this case even negligible changes in the

branching rate can appreciably affect the reaction rate as a whole. The low temperature oxidation of hydrocarbons and liquid-phase oxidation of organometallic compounds have been explored in [5.23]. For hydrocarbon oxidation, disrupted chain branching can result from the thermal decomposition of hydroperoxides ROOH by the reaction



while for oxidation of organometallic compound, the disrupted chain branching is a result of organometallic peroxide decomposition. For instance, in the case of a Et_4Pb oxidation



The numerical estimates of the scale of the magnetic effects arising in this reaction showed [5.23] that in fields of several tens of kilogauss, the probability of radical escape can vary by some 10%.

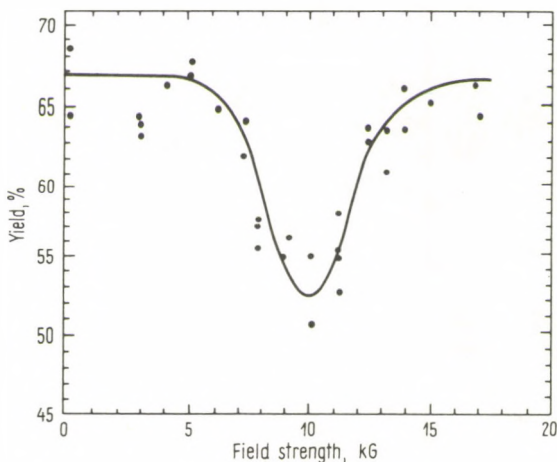
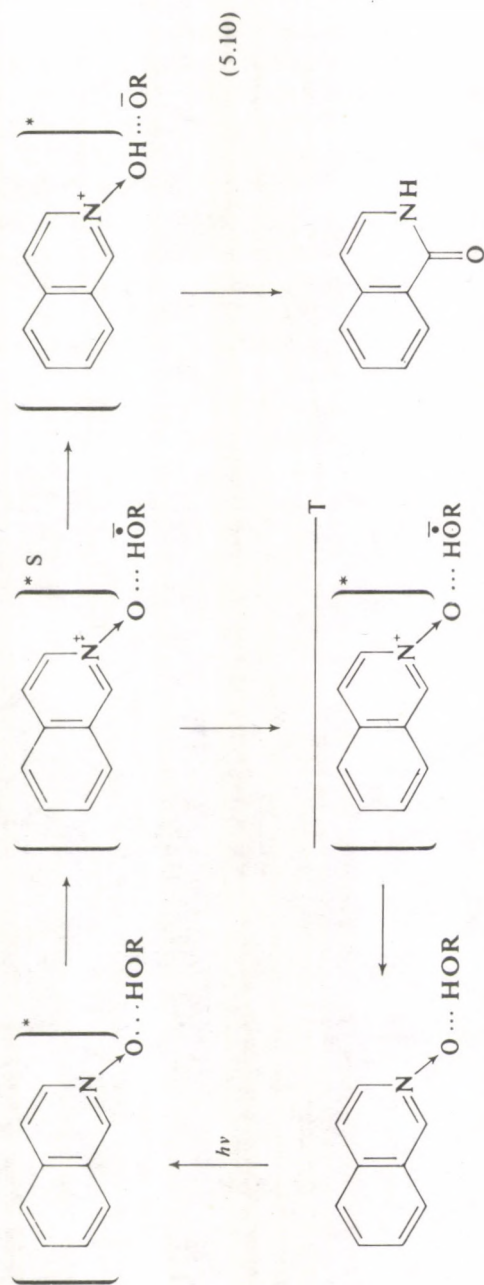


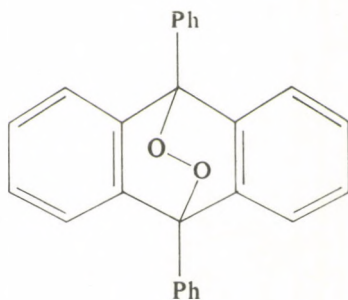
Fig. 5.5. The effect of magnetic field on the yield of lactam in the photochemical reaction of isoquinoline-N-oxide in ethanol [5.24]

A very interesting effect of the magnetic field has been observed in the photochemical reaction of isoquinoline-N-oxide in ethanol [5.24, 25]. The yield of the reaction product—lactam—proved to depend on magnetic field strength in a resonance manner (see Fig. 5.5). This effect has been interpreted by the following scheme of lactam generation [5.25]:

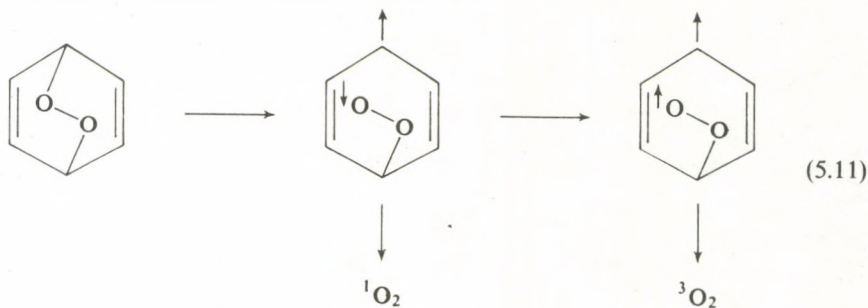


According to this scheme the isoquinoline-N-oxide molecule coupled to the solvent by a hydrogen bond becomes singlet-excited on absorption of a photon. It is followed by the electron transfer from the excited N-oxide molecule to a solvent molecule and the formation of a pair of radical-ions in the singlet state. The N→O-group of this molecule is protonated with subsequent formation of the final product, the lactam. Within the scheme proposed the magnetosensitive stage of the reaction is the singlet-triplet conversion in the radical-ion pair. The electron exchange integral J of the radical-ion pair coupled by a hydrogen bond is assumed [5.25] to be non-zero. In this case the shape of the experimental dependence observed can be interpreted as follows. For $|2J| > |A|$ in fields when $|2J + H| > |A|$, the isotropic hf interaction does not mix the S and T states and the probability of S-T conversion is zero. In intermediate fields, when $|2J + H| \lesssim |A|$, this probability has its maximum value. The singlet-triplet mixing is maximal in fields in which the singlet state is in resonance with one of the triplet states ($H \approx 2J$).

The influence of a magnetic field on S-T mixing in the intermediate biradical has been used to interpret the field effect [5.26] on the singlet oxygen yield in the thermolysis of endoperoxides of some aromatic compounds. It has shown [5.26] that the singlet oxygen yield decreases in a magnetic field (up to 14,000 G). The maximum effect (about 30%) is observed for the compound



According to [5.26], the process of hydroperoxide thermolysis includes biradical stages:



The biradical mentioned ensures favourable conditions for the Δg -mechanism of magnetic field effect ($\Delta g \approx 10^{-2}$). Studies on the field dependence of $^1\text{O}_2$ yield have shown the experimental data obtained do agree with this mechanism. Note, however, that the smooth trend of the field dependence (no maxima) is not quite understandable in terms of the above biradical scheme.

The greatest effect of a magnetic field on radical recombination has been reported recently by Turro *et al.* [5.27] who studied dibenzyl-ketone photolysis in micellar solutions. The escape product (dibenzyl) yield in presence of CuCl_2 as a radical acceptor in the liquid phase has been found to be one-third in a field $H = 13,400$ G as compared to the yield in the Earth's magnetic field. Such a great scale of the field effect is perhaps associated with two factors: (1) the triplet character of the primary

radical pairs $\text{C}_6\text{H}_5\text{CH}_2\overset{\text{O}}{\parallel}{\text{C}} \cdot \text{CH}_2\text{C}_6\text{H}_5$ and (2) the substantial increase of the cage effect in micelles.

Interesting magnetic field effects in photochemical experiment with neutral radicals have been obtained in [5.28]. The yield of the acyl radical in a benzophenone solution in hexane was measured after irradiation with a pulsed nitrogen laser. A second light pulse of lower intensity, with a delay of $\Delta t = 38$ ns, produced fluorescence of the ketyl radical. The processes in this system have the following sequence. Once excited, benzophenone in the triplet state abstracts a hydrogen atom from the hexane solvent. Thus a triplet radical pair consisting of ketyl and hexyl radicals is produced. Conversion of this pair to a singlet pair causes a back reaction, which diminishes the yield of the acyl radical.

The experiment showed that the luminescence intensity decreases approximately linearly with increasing magnetic field intensity and at 6 kG the decrease in intensity is $\approx 9\%$. The observed effect has the same sign as the Δg -mechanism. It is still unclear, however, why the hf mechanism is not evident under these conditions and also why the field dependence is linear rather than quadratic.

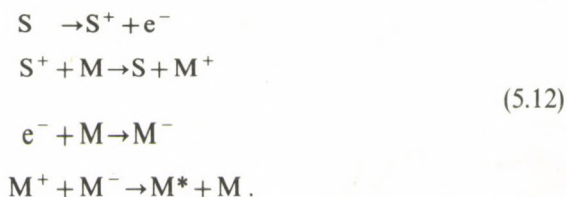
5.3 Recombination of radical-ions

Studies of magnetic field effects arising in radical-ion recombination are more advantageous as compared to those of neutral radical recombination. First, owing to the Coulomb attraction of oppositely charged radical-ions, the in-cage lifetime can increase considerably, which results in stronger magnetic effects. Second, the recombination of aromatic radical-ion pairs, which so far have been mainly investigated, gives electronically-excited molecules. The existing optical techniques allow high accuracy of fast detection of both singlet (by fluorescence) and triplet (by absorption) excited states. As a result, the accuracy of magnetic effect detection can be increased as compared to the methods based on measurements of the reaction product yield. Of primary importance is however the fact that optical methods

allow time-resolved experiments, i.e., make it possible observe the S-T evolution of a radical pair directly as well as the magnetic effect on its evolution and geminate recombination.

Radical-ion pairs were formed in solution by ionizing radiation or by light, the time resolved experiments employing the apparatus with RPs generated and detected within times less than the typical times of S-T evolution (several nanoseconds). For that purpose pulse electron accelerators, radioactive sources, and pulse lasers have been used to generate RPs, the recombination products detected either by their absorption or luminescence with nanosecond resolution.

Radiation-chemical generation of radical pairs. Magnetic effects arising in the recombination of a pair of positive and negative radical-ions produced by ionizing radiation have been explored by Brocklehurst and some Canadian investigators [5.29-35]. The idea behind the experiments is as follows [5.29]. Hydrocarbon solvent molecules are irradiated by fast electrons. The aromatic molecules present in solution in small concentrations capture both the electron and the hole of the parent positive ion. As a result, a singlet pair of radical-ions coupled by Coulomb forces, is formed and the S-T conversion can precede the recombination. The process of ion-radical generation and recombination follows the scheme:



Here S is a solvent molecule, M is an aromatic molecule, M* is either the excited singlet or triplet state of this molecule. Like the case of neutral free radical recombination, the magnetic field can be expected to influence the S-T conversion rate and hence the ratio of singlet and triplet excited molecules.

Note that unlike the case of the radical reactions considered above, the radical-ions constituting a pair cannot leave for the bulk but recombine with the probability approximately equal to unity since the initial interchange distance (50 to 150 Å) is less than the Onsager radius for a nonpolar solvent (300 Å). A large initial separation between the radical-ions results in a nanosecond range for their recombination time, and this becomes comparable to the typical time of S-T evolution. It favours the magnetic effect observation as compared to the case of neutral radical recombination.

Figure 5.6 depicts the fluorescence oscillogram observed on pulse radiolysis of 0.01 M fluorene solution in squalane (2,6,10,15,19,23-hexamethyl-tetracosane) [5.31] with a 3 MeV electron accelerator. A magnetic field ($H = 3000$ G) is seen to increase the emission intensity after the pulse. This effect shows that the population of the preceding singlet radical-ion pairs increases in a magnetic field, which can be qualitatively interpreted within the hf model. Studies on the field dependence of the fluorescence intensity [5.30, 31] have confirmed this conclusion. Figure 5.7 shows

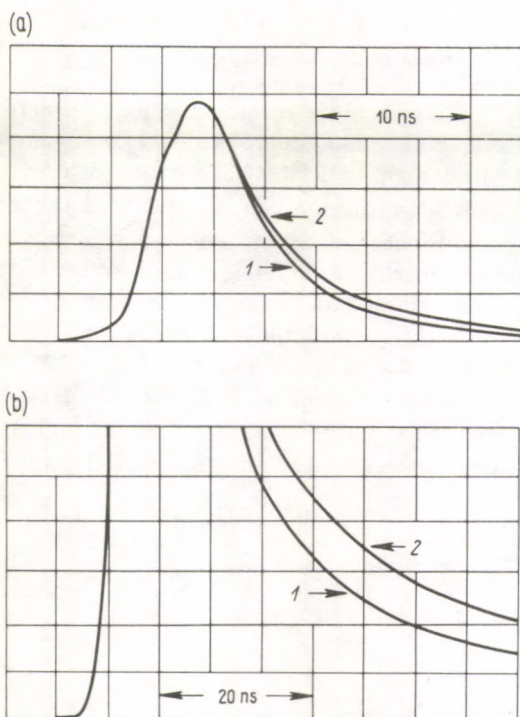


Fig. 5.6. Oscillogram of fluorescence observed under pulse radiolysis of 0.01 M fluorene solution in squalane; 1 – no magnetic field; 2 – in a field of 3000 G [5.31]

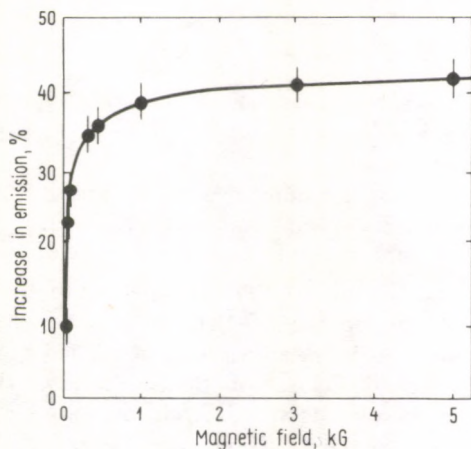


Fig. 5.7. Magnetic field effects on fluorescence intensity in 0.01 M fluorene solution in squalane 200 ns after the pulse [5.31]

the general trend of the experimental curve to be analogous to that calculated for the hf-mechanism. Since the singlet state yield increases in a magnetic field, the triplet excited state yield can be expected simultaneously to reduce. Though in the latter case the picture should be much more complex, a small reduction of the triplet concentration in a magnetic field has been observed experimentally [5.30].

Of special interest is the time dependence of magnetic effects which directly reflects the development of S-T evolution. This dependence has been obtained in the above experiments on pulse-excited fluorescence [5.31,35] and also from the scintillation pulse shape measured by the single-photon-counting technique [5.32]. Figure 5.8 depicts the data obtained by this technique in solutions of terphenyl- h_{14} and terphenyl- d_{14} in decalin. In line with theory, no effects are detected in the initial steps when S-T evolution has not yet developed. In further steps, when S-T mixing is over, the curves become saturated. The S-T evolution time is seen from Fig. 5.8 to increase noticeably when the RP partners (terphenyl cation- and anion-radicals) are deuterated. This is direct evidence that the magnetic effects in these systems arise from the hf-mechanism.

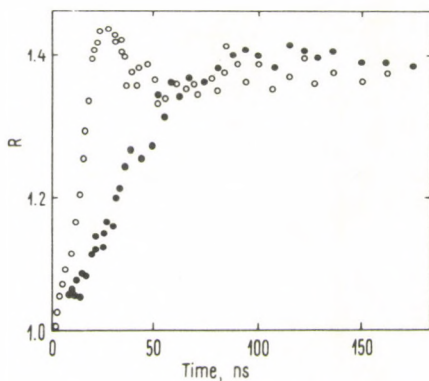


Fig. 5.8. Ratio R of fluorescence intensities of a scintillation pulse in a field 0.16 T and in zero field vs. time: (●), 0.005 M terphenyl- h_{14} in decalin; (○), 0.005 M terphenyl- d_{14} in decalin [5.32]

Alongside the pulse experiments, a number of experiments were performed under stationary conditions using a γ -radiation source [5.33–35]. The data on the fluorescence intensity measured in different magnetic fields (Fig. 5.9) show the absolute magnitude of magnetic effects to be less under continuous irradiation. This difference can be accounted for by the fact that under steady-state conditions the luminescence is contributed to by fast processes of excited molecule generation which are insensitive to magnetic fields. Note that in these experiments radical-ion recombination was studied in solvents with different viscosities (Fig. 5.9). In the case of the most viscous solvent—squalane—the magnetic field effect on the fluorescence yield and thus on the singlet RP population was maximum. In benzene (the least viscous solvent) the field produced no effect at all, while for cyclohexane the

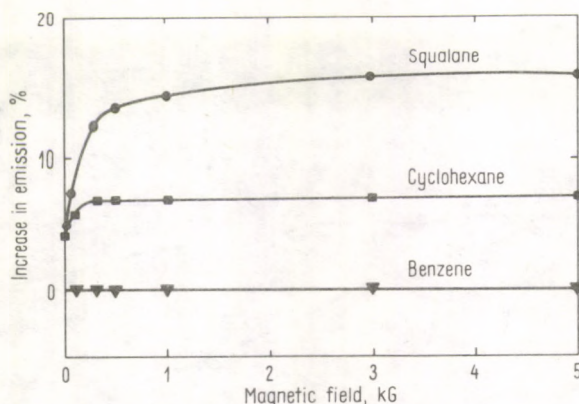


Fig. 5.9. The effect of an applied magnetic field on the intensity of fluorene singlet emission from various solvents containing 10^{-2} M fluorene, γ -irradiated at room temperature [5.33]

situation was intermediate. These results confirm the theoretical assumption that a rise in the solvent viscosity can result in an appreciable increase of the magnetic field effects arising in RP recombination. It is quite possible however [5.34] that in the above experiments the type of the solvent affected the mechanism of excited molecule formation and through that the magnetic effects. For instance, direct experiments [5.35] on radiolysis of anthracene solution in benzene have shown the absence of a slow stage in the geminate recombination of anthracene ions, the excited molecules resulting from faster processes which are insensitive to a magnetic field.

Additional evidence for magnetic effects arising from the hf-mechanism has been obtained in stationary state experiments [5.34, 35]. The deuteration of luminescent molecules of naphthalene or anthracene affected the trend of the fluorescence field dependence.

RP singlet-triplet evolution, as shown in Section 2.2, is oscillation between states with different multiplicity. These oscillations can be observed in time-resolved experiments by measuring the generation rate of the product with a definite multiplicity.

Klein and Voltz [5.36, 37] were the first to observe quantum singlet-triplet oscillations in experiments similar to those discussed above. Scintillator molecules (Fig. 5.10) with fluorescence lifetime 1.5 ns were used as electron and hole acceptors. A cyclohexane solution of this compound was ionized by fast electrons from a ^{90}Sr - ^{90}Y 0.1 μCi radioactive source and the radioluminescence was detected by the single-photon counting technique.

Figure 5.10 depicts the time evolution of magnetic effects for various magnetic fields. All the curves show damped oscillations. The frequency of these oscillations is about 8 MHz, which corresponds in order of magnitude to the hf coupling constants in aromatic radical-ions. The authors failed to detect distinct oscillations in

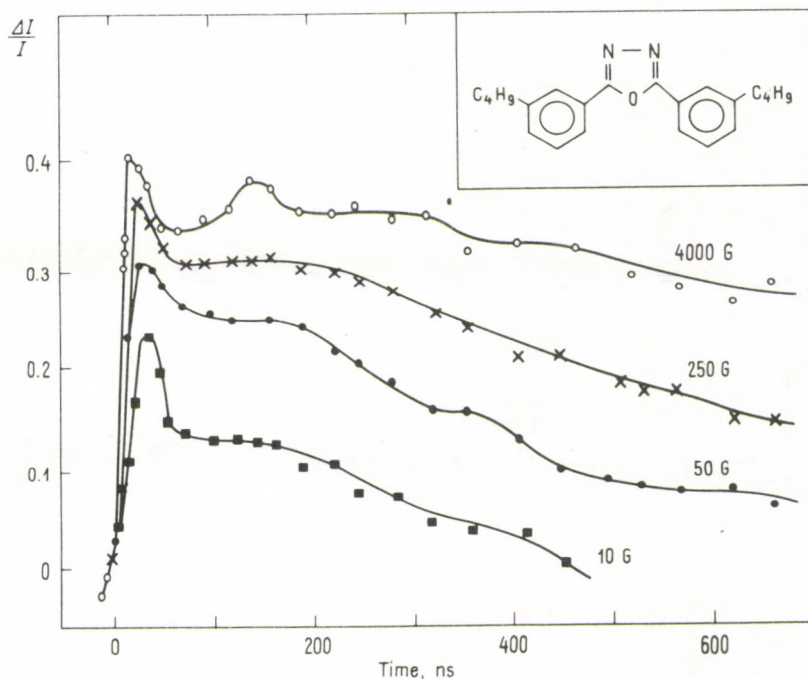


Fig. 5.10. Time evolution of the relative increase in radioluminescence intensity $\Delta I/I$ at different magnetic fields in $1.5 \cdot 10^{-3}$ M scintillator solution (see the formula given in figure) in cyclohexane under β -irradiation [5.37]

solutions of aromatic molecules such as anthracene and perylene. In the above system an unusual situation is perhaps realized: when the hf constants are connected by simple multiple ratios, and this favours the detection of the oscillations.

Figure 5.10 also demonstrates the increase in the magnetic effect with magnetic field and the exponential decay of the effect at long times. The latter is believed by the authors to be associated with irreversible processes of spin-spin and spin-lattice relaxation.

Radical-ion pairs produced by radiation-chemical means were used to verify one more theoretical prediction on the anomalous trend of the field dependence of S-T conversion in the simplest RP with one or several equivalent nuclei. As noted, in the case of a RP with many nonequivalent nuclei, an increase in the magnetic field results in a monotonic decrease in the S-T conversion probability starting with the lowest fields. A RP with either one or several equivalent nuclei is an important exception. According to the theory, the S-T conversion probability in such pairs first increases and then reduces as it becomes saturated.

To verify these conclusions, hexafluorobenzene radioluminescence has been studied in different hydrocarbon solvents [5.38]. Radioluminescence was excited by

a $1 \mu\text{Ci } ^{60}\text{Co}$ source. In the C_6F_6^- radical-ion the hf constant with six equivalent fluorine atoms, $A^- = 137 \text{ G}$, is very high. Therefore, the behaviour of this system is mainly determined by the large hf constant of the anion and hence should have the above mentioned peculiarities typical of the systems with equivalent nuclei.

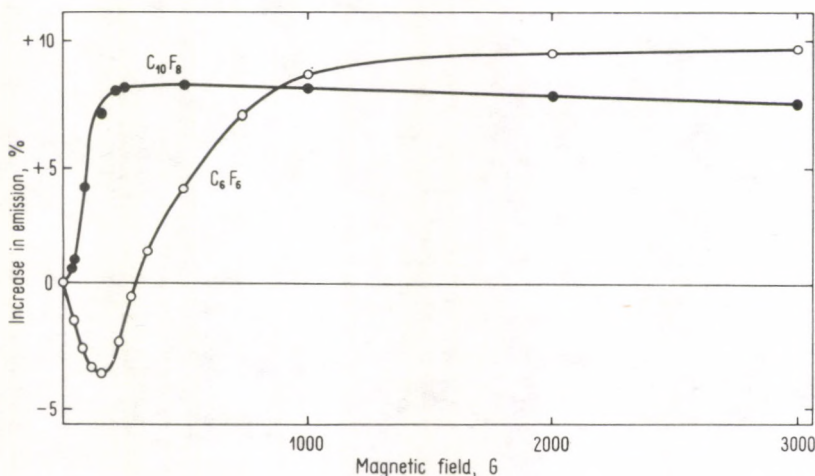


Fig. 5.11. Magnetic field dependence of radioluminescence intensity: (○), $3.5 \cdot 10^{-2} \text{ M C}_6\text{F}_6$ in hexane; (●) $10^{-2} \text{ M C}_{10}\text{F}_8$ in hexane [5.38]

The results given in Fig. 5.11 confirm this conclusion. The hexafluorobenzene luminescence intensity passes through a pronounced minimum in fields of about 100 G. This is not the case for perfluoronaphthalene where the anion and cation have two types of fluorine atoms. In the case of hexafluorobenzene, the anomalous field dependence has been observed not only in n-hexane but also in other solvents such as n-pentane, n-tetradecadene, and squalane. It is interesting to note that the depth of the minimum increases when benzene is added to the system. This is perhaps associated with the fact that in such system $\text{C}_6\text{F}_6^-/\text{C}_6\text{H}_6^+$ pairs recombine, the S-T evolution in the latter being less affected by the cation as a result of the small hf constant in C_6H_6^+ .

Figure 5.12 shows the theoretical field dependences of the probability of recombining to the singlet state for three values of the experimental parameters. Curve 2, calculated with account taken of the hf in both the hexafluorobenzene anion and cation is seen to be in qualitative agreement with experiment.

Photochemical generation of radical pairs. Two teams of West German scientists independently studied similar systems where radical-ion pairs were generated photochemically by the charge transfer from a donor molecule—substituted aniline—to a light-excited acceptor molecule—pyrene [5.39–43]. This reaction results in a singlet pair of radical-ions as in radiation-chemical reactions described in the above sections, its behaviour having however some peculiar features. First, in

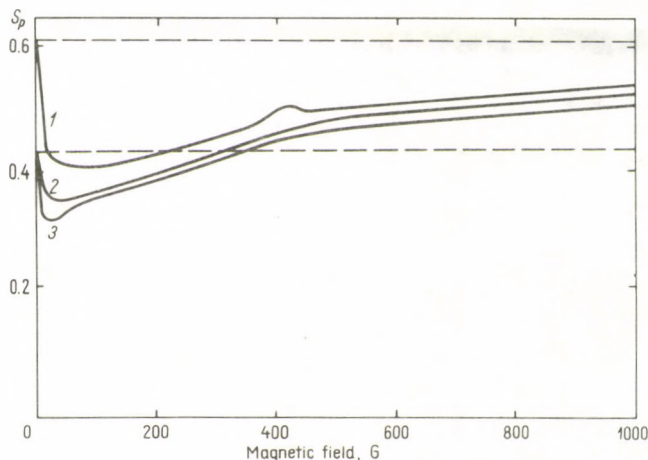
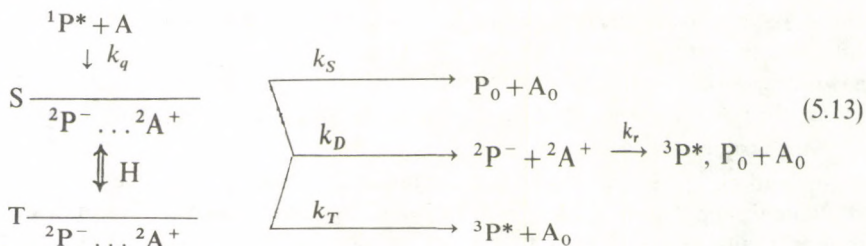


Fig. 5.12. Magnetic field dependence of the singlet state recombination probability S_p for a RP with the parameters: 1 $A^- = 137$ G, $A^+ = 0$, $\tau_r = 10^{-8}$ s; 2 $A^- = 137$ G, $A^+ = 15.9$ G, $\tau_r = 10^{-8}$ s; 3 $A^- = 137$ G, $A^+ = 15.9$ G, $\tau_r = 10^{-7}$ s [5.38]

the photochemical experiments discussed, radical-ions were generated in a direct contact but not at a greater distance from each other. Hence for the partners to separate, solvents with high dielectric constants—methanol and acetonitrile—were used in the experiments instead of nonpolar hydrocarbons which reduced the Coulomb interaction. Second, under these conditions the energy of charge neutralization was sufficient only for triplet-excited pyrene molecule generation, while singlet RPs could recombine to give molecules only in the ground state. Hence, only the triplet RP recombination channel was detected by triplet-triplet absorption of pyrene molecules. The reaction scheme of the system under study can be presented as follows [5.41]:



where P is a pyrene molecule and A is a substituted aniline molecule. The subscript "o" denotes neutral molecules in the ground singlet state; k_q is the rate constant of excited pyrene molecule quenching due to the charge transfer and the radical-ion

pair generation; the constants k_S , k_T , and k_D correspond to the three channels of RP decomposition: the recombination from the singlet (k_S) and triplet (k_T) states and separation of the pair by diffusion (k_D); k_r is the rate constant of bulk radical-ion recombination.

Radical-ion pair generation was achieved with a nitrogen laser with a pulse duration of the order of several nanoseconds; the triplet-triplet absorption was detected either by dye laser excited by the same pulse of the nitrogen laser [5.41, 42], or by a high pressure pulse xenon lamp [5.39, 40].

Consider the data on time-resolved experiments with the systems pyrene/N,N-dimethylaniline (Py/DMA), pyrene/3,5-dimethoxy-N,N-dimethylaniline (Py/DMDMA) and the perdeuterated system Py- d_{10} /DMA- d_{10} in different solvents [5.39, 40]. As an example, Fig. 5.13 gives the time dependence of the pyrene triplet molecule (E_T) and pyrene radical-ion (E_{ion}) absorption for the system Py/DMA in methanol. The triplet molecule signal first increases rapidly, which mainly corresponds to radical-ion geminate recombination, and then increases slowly, which is associated with radical-ion recombination in the bulk. The figure shows the magnetic field effect to arise in the initial stage of radical-ion geminate recombination, its further contribution remaining unchanged. The decrease in the triplet molecule yield observed experimentally in the magnetic field pertains to the hf mechanism of RP singlet-triplet conversion. The magnetic field also affects only slightly the yield of the separated ions. When analyzed by the scheme (5.13), this

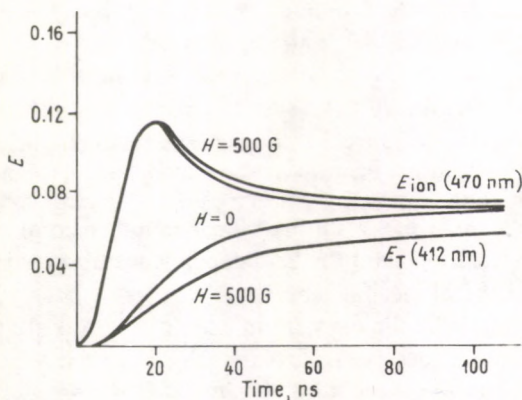
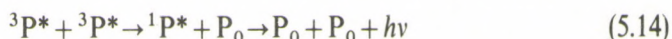


Fig. 5.13. Time evolution of ion-radical (E_{ion}) and triplet (E_T) extinction in the system Py/DMA in methanol [5.40]

result shows the singlet radical-ion pair recombination probability must be less than that of the triplet pair. Similar results were obtained in other polar solvents such as ethanol, acetonitrile, and dimethylformamide. A detailed analysis of the whole range of results obtained gives a quantitative estimation of the fraction of the singlet and triplet geminate recombination in each case [5.40].

Steady state experiments [5.39, 40] provide additional evidence for the hf mechanism of magnetic field effects in these systems. The triplet generation rate was determined by the intensity of the delayed fluorescence arising in the process



The delayed fluorescence intensity falls with increasing magnetic field and reaches a plateau in fields ≥ 100 G, which agrees with the theoretical dependence of the hf mechanism. The scale of the magnetic effect in these experiments was however less than that in time-resolved experiments performed in the nanosecond range. This difference can be attributed to the fact that under steady state conditions one could detect the triplet molecules resulting both from geminate and escape recombinations, the latter being only weakly sensitive to magnetic fields.

The fact that the transition region of the magnetic field strength $H_{1/2}$ changes with the hf constant in the series of the radical-ions studied (Fig. 5.14) is the most convincing evidence for the hf mechanism. Experimental values of $H_{1/2}$ are 55 G and 45 G for the systems Py/DMA and Py/DMDMA respectively. In the case of perdeuterated system Py- d_{10} /DMA- d_{10} the value of $H_{1/2}$ shows some two-fold decrease as compared to that in Py/DMA. It is possible to predict [5.40] that $H_{1/2}$ must be proportional to the sum of the hf constants with account taken of the spin value:

$$A_{\text{eff}} = \sum_k [A_k^2 I_k(I_k + 1)]^{1/2}. \quad (5.15)$$

Here A_k is the hf constant for the k -th nucleus having I_k spin. The computed values of $A_{\text{eff}}/2$ equal 59, 40 and 21 G for the systems Py/DMA, Py/DMDMA and Py- d_{10} /DMA- d_{10} respectively, which is a pleasing fit to the observed values of $H_{1/2}$.

Time-resolved experiments with the system pyrene-diethylaniline in methanol [5.41] afforded similar data. Figure 5.15 depicts the magnetic field dependence of the intermediate compound absorption at the wavelength 415 nm measured 8 ns after the system was acted upon by a laser pulse. The absorption was mainly attributed to the triplet molecules resulting from geminate recombination of pyrene and diethylaniline radical-ions and the field dependence observed was interpreted as a manifestation of the hf mechanism.

The anthracene/dimethylaniline system in acetonitrile was studied in a similar way [5.43]. As in the above case, the scale of the magnetic effect was about 10%. The half-decay region of the magnetic effect lay in fields $H_{1/2} = 50$ –70 G. A certain dependence of $H_{1/2}$ on the moment of triplet molecules detection following radical pair generation was of interest. It turned out that the shorter the time interval between the initiating and probing pulses, the greater the $H_{1/2}$ value. The energetic levels for short-lived RPs were assumed to be lifetime-broadened, this broadening hampering the removal of the S–T degeneracy by the external field. As a result, the shorter the time interval, the higher the field $H_{1/2}$ required to remove the S–T degeneracy and to affect the S–T evolution rate.

The hf mechanism was also confirmed by steady-state experiments on the system anthracene (perdeuteroanthracene)/diethylaniline in acetonitrile [5.42]. In this case

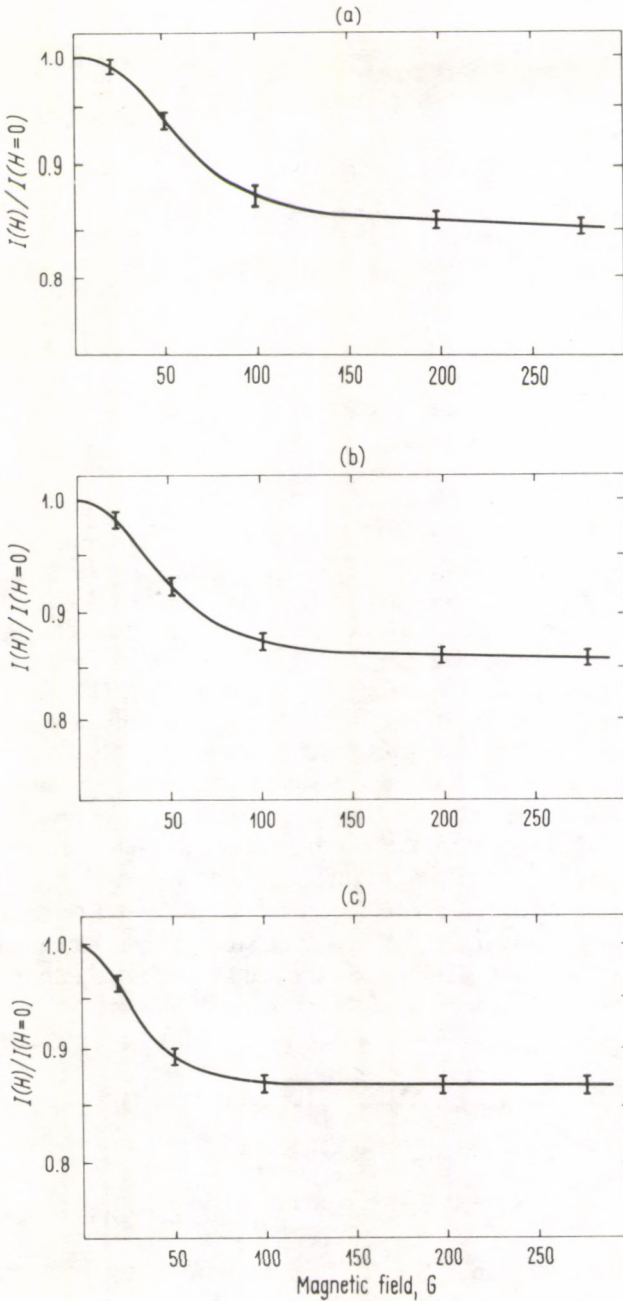


Fig. 5.14. Magnetic field dependence of the delayed pyrene fluorescence in the system (a) Py/DMA; (b) Py/DMDMA; and (c) Py- d_{10} /DMA- d_{10} in methanol [5.40]

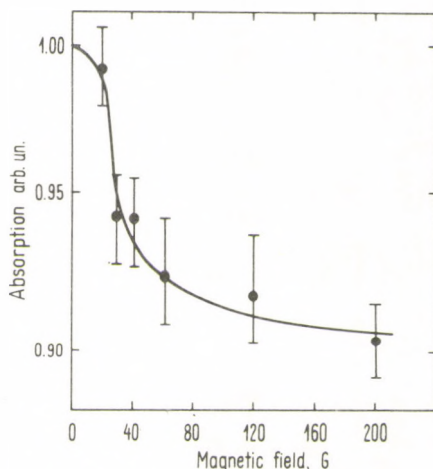
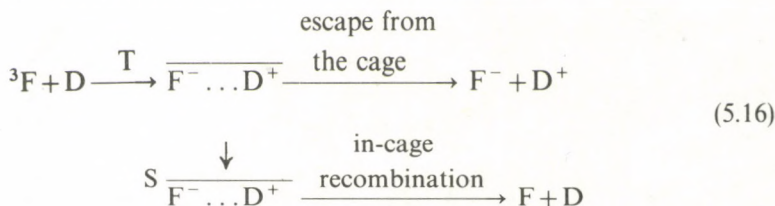


Fig. 5.15. Field dependence of nonstationary absorption at 415 nm in the system pyrene ($5 \cdot 10^{-4}$ M) diethylaniline (10^{-2} M) in methanol [5.41]

anthracene was excited by a CW krypton laser, the stationary state concentration of the anthracene ions being detected by the absorption spectrum. Since $K_T > K_S$, a decrease in K_T with growing magnetic field must increase the anthracene anion concentration in the bulk, which was confirmed by experiment. The relative scale of the magnetic effect was only 1.25%. Nevertheless, the high accuracy of the absorption measurements made it possible to detect reliably the difference in the trends of the curves for normal and deuterated anthracene. The magnetic effect reached half of its extreme value at $H_{1/2} = 75 \pm 3$ G in the former case and at $H_{1/2} = 62 \pm 3$ G in the latter. Within the hf mechanism this decrease is associated with a lower energy of hf interaction in the deuterated species.

In the investigation discussed above, the primary radical-ion pair was singlet-born. The case of the primary triplet-born pair was studied in the reaction of triplet-excited fluorenone (F) with diazabicyclooctane (D) as an electron donor in polar solvents [5.44]. The reaction scheme of this pair is as follows:



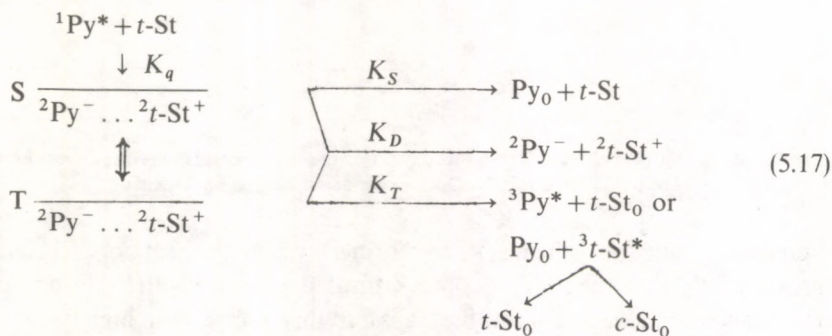
The singlet-triplet transition of the pair is brought about by the hf-mechanism and depends upon the magnetic field. The recombination occurs only in the singlet state and yields products in the ground state. The triplet pair dissociates and gives relatively long-lived radical-ions in the bulk solution.

The radical-ion concentration in the bulk was measured experimentally shortly after the exciting light pulse. The free ion yield in a magnetic field (270 G) was found to increase as compared to that in zero field. The relative increase grows with the solvent viscosity (1 to 75 cP), reaching 20–25% at high viscosities. These results are in full agreement with scheme (5.16) where the S–T mixing is conditioned by the hf-mechanism.

Photosensitized *cis*–*trans* isomerization of olefines was one more system where the magnetic effects associated with transformations of photochemically produced radical-ion pairs were observed. The field effect on the reaction rates of *cis*–*trans* isomerization was first reported as far back as 1972 [5.45]. In the case of isomerization of stilbene and piperylene sensitized by aromatic ketones, the external field (up to 9 kG) was reported to affect the reaction rate and the photostationary isomer ratio, the scale of the effect reaching some 10%. In the absence of the sensitizer the magnetic field produced no effect. These results however have not yet been confirmed and reliably interpreted as there were no grounds to suggest the presence of radical stages in the reactions.

Considerable CIDNP effects have however been recently observed in similar systems [5.46–47], which prompted a supposition on the presence of radical-ion stages in the processes of photosensitized *cis*–*trans* isomerization, allowing a new approach to the magnetic effects in such systems [5.48].

CIDNP effects were studied in the isomerization of *trans*-stilbene and decafluorodiphenylethylene-1,2 in the presence of sensitizers — pyrene, benzophenone, benzyl, octafluoronaphthalene — in different solvents. The analysis of CIDNP effects resulted in the following reaction scheme (with pyrene as a singlet sensitizer) [5.46]



The scheme employs the same symbols as those in the earlier schemes to demonstrate their analogy. Here *t*-St is *trans*-stilbene, *c*-St is *cis*-stilbene. Within this scheme the magnetic field reduces the *trans*–*cis* transition rate by decelerating the S–T conversion.

Experimental data obtained for the systems pyrene/*trans*-stilbene and pyrene *trans*-decafluorodiphenylethylene-1,2 in CH₃CN (Figs 5.16 and 5.17) are in full

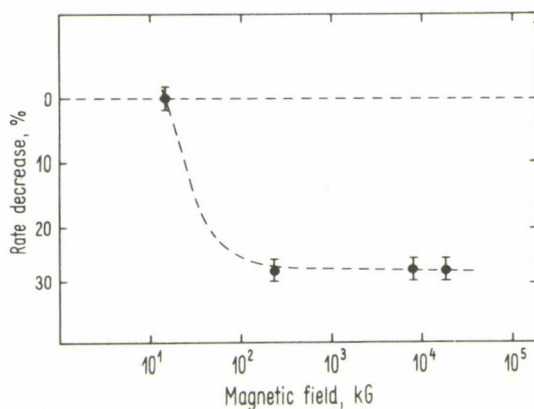


Fig. 5.16. Magnetic field effect on *trans*-stilbene photoisomerization rate in the presence of pyrene in CH_3CN . Dots, experiments; dashed lines, theory [5.48]

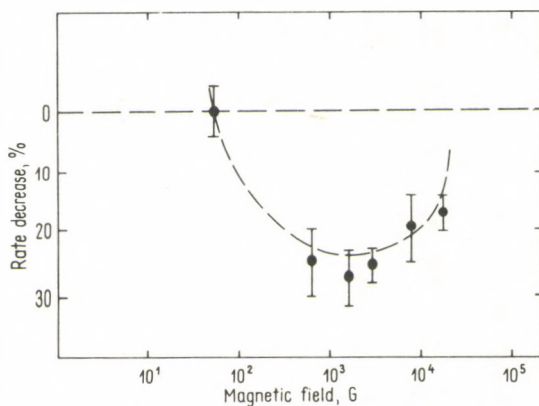


Fig. 5.17. Magnetic field effect on decafluorodiphenylethane -1,2 photoisomerization rate in the presence of pyrene in CH_3CN . Dots, experiment; dashed line, theory [5.48]

agreement with this scheme. In the former system the reaction decelerates with growing field, then the curve becomes saturated in accord with the hf-mechanism. In the latter case the reaction rate first falls and then increases in high fields which fact can be interpreted by a simultaneous action of the hf and Δg -mechanisms. This qualitative interpretation fits theoretical calculations as shown in Fig. 5.17 by a dashed line. These calculations were carried out in the semiclassical approximation (see Section 3.2.4) with use made of experimental hf constants and g -values.

The fit between experimental and theoretical curves of magnetic effects has led to the conclusion that the radical-ion path of *cis-trans* stilbene isomerization sensitized by pyrene is the basic one. This conclusion is also valid for octafluoronaphthalene which also shows large magnetic effects. Unlike the results

reported in ref. [5.45], no appreciable magnetic effect was observed in the system with benzophenone as a triplet sensitizer. Therefore, the problem of the radical stage in this case requires additional investigation.

The above example shows magnetic effects to be informative of the chemical reaction mechanism. Note that CIDNP studies alone, though suggesting radical-ion participation in isomerization reactions, do not answer the question whether that path is the basic one.

5.4 Optical detection of radical-ion pair ESR spectra

The magnetic effects in radical reaction considered in the present section and the possibility of resonance microwave radiation effects on RP reactions considered in Section 2.2 form the basis of optical methods to detect radical pair ESR spectra in liquids.

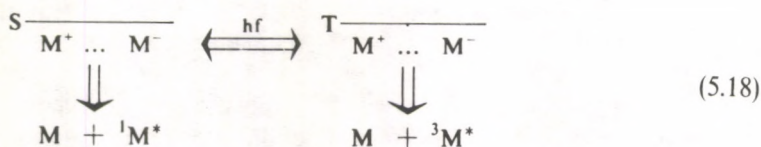
The optical detection of magnetic resonance (ODMR) was first proposed and applied [5.49] to the study of ESR spectra of isolated triplet-excited molecules in molecular crystals at low temperatures. Microwave radiation-induced transitions between triplet sublevels affect the fluorescence intensity since the light emission probabilities are unequal for different sublevels. Thus, detecting the magnetic field (or radiation frequency) dependence of the luminescence intensity one can indirectly detect the ESR spectrum of a triplet molecule.

Later on, the ODMR method was applied to observe the ESR spectra of short-lived pairs of paramagnetic particles in ionic [5.50] and molecular [5.51] crystals. One of the recombination channels of such pairs is accompanied by generation of singlet-excited molecules able to emit light. Resonance microwave radiation can affect the probability of recombination to this state by changing the mutual orientation of the electron spins during the pair lifetime.

A similar technique [5.52–54] has been recently applied to detect the ESR spectra of short-lived radical-ion pairs induced in liquids by ionizing radiation. The technique is marked by extremely high sensitivity and allows one to obtain ESR spectra with fairly well resolved hyperfine structure.

The principle of the method. Let us now discuss the principle of the method considering, as an example, the recombination of aromatic radical-ion pairs produced by ionizing radiation in a nonpolar solvent with a small admixture of aromatic molecules. As has been discussed in detail in Section 5.3, this system initially yields a singlet pair of aromatic radical-ions, M^+ and M^- , coupled by the Coulombic attraction and certain to recombine.

The transformation of this pair follows the scheme



The singlet-triplet evolution of such pairs is due to the hf-mechanism. The excited aromatic molecule M^* is formed either in a singlet state, and thus can emit light, or in triplet state which is nonluminescent, depending on the multiplicity of the pair at the recombination moment.

Figure 5.18 gives the energy level diagram showing why resonance microwave radiation affects RP S-T evolution. In high magnetic fields in the absence of microwave radiation, the hf-mechanism mixes only S and T_0 states. The sublevels T_+ and T_- are off-resonance with the S-level owing to the Zeeman splitting and thus cannot be populated by the hf-mechanism. In this case the pair would oscillate between the S and T_0 states and, at sufficiently long times, both states would be on average equally populated. If, however, microwave radiation induces resonant ESR transitions (Fig. 5.18b) all the three triplet sublevels can be populated. This must result in a cut in the singlet level population. If, for instance, all the four sublevels are equally populated, the singlet state population amounts to 25% instead of 50% in the absence of microwave radiation. Thus, the singlet recombination probability and hence the luminescence intensity under resonance microwave irradiation falls markedly, and this makes possible optical detection of ESR signals. Roughly speaking, the scale of the effect must be the same as that observed when zero magnetic field is used instead of high fields, i.e., tens of percent.

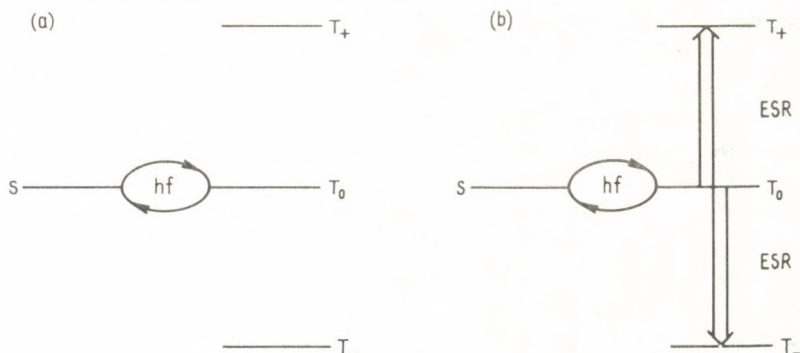


Fig. 5.18. Energy level diagram and S-T transitions in RP at a high external magnetic field and (a) $H_1 = 0$; (b) $H_1 \neq 0$; hf is S- T_0 mixing due to hyperfine interactions; ESR are resonance microwave transitions

A strong ODMR signal can perhaps be obtained if the orientation of the radical electron spins changes substantially during the pair lifetime τ_{RP} , that is if $(\gamma H_1)^{-1}$, the precession period of a spin in a resonance microwave magnetic field H_1 , is comparable to τ_{RP} . A typical RP lifetime in the system discussed is of the order of 10^{-7} - 10^{-8} s. It means that a microwave field of 1 to 10 G is required. Measurable signals can be obtained, however, in a lower field H_1 due to a very high sensitivity of the ODMR technique.

The qualitative picture discussed can be illustrated by numerical calculations of S-T evolution under microwave irradiation [5.54]. Figure 5.19 shows the S-T

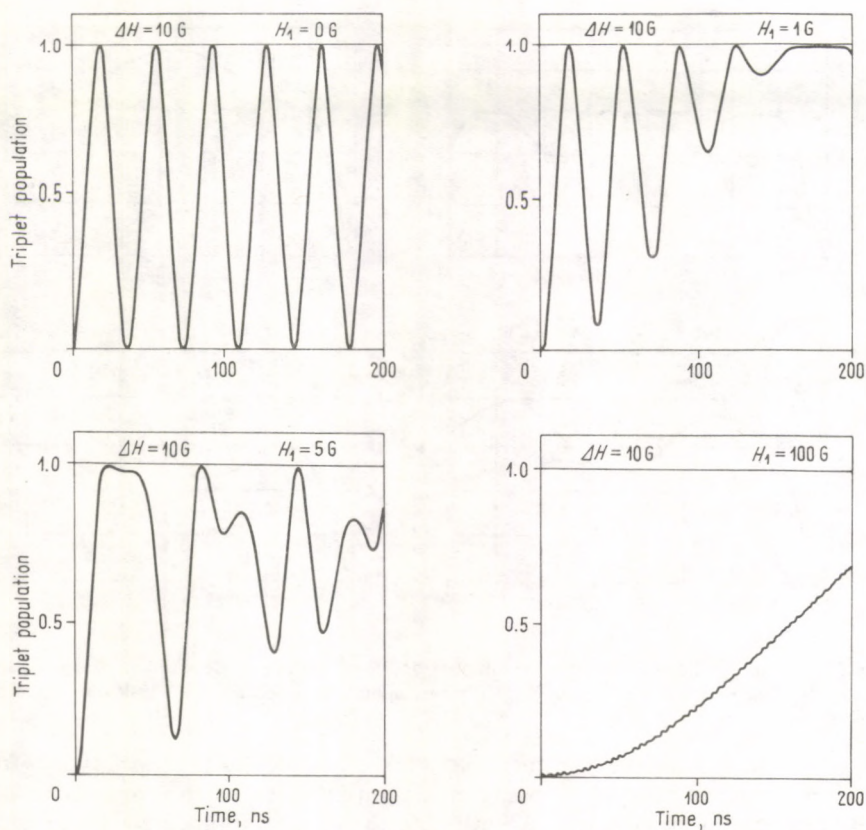


Fig. 5.19. Time dependence of triplet population for a singlet-born RP with the 10 G difference in the ESR line positions at various H_1 [5.54]

evolution of a radical pair whose radical lines are 10 G separated owing to the Δg -value. At zero H_1 this pair will oscillate between the S and T_0 levels with a frequency equal to the difference in the resonance frequencies of the two radicals. In this case the average population of the singlet state is one half. At H_1 comparable to the splitting, the S-T evolution becomes more complex but it can be readily seen that the average triplet population is in this case higher than it was at $H_1 = 0$. In fact, this is due to populating the T_+ and T_- sublevels along with the T_0 state.

Real systems contain a range of radical pairs which differ by the splitting between the resonance lines. The S-T mixing in such systems is more complex and involves the superposition of evolutions of various RP subensembles. Figure 5.20 presents an example of calculations of such a complex system consisting of negative and positive naphthalene ions. In our calculations the hf constants and the g -values of both ions were assumed equal. The microwave frequency corresponded to the center of the

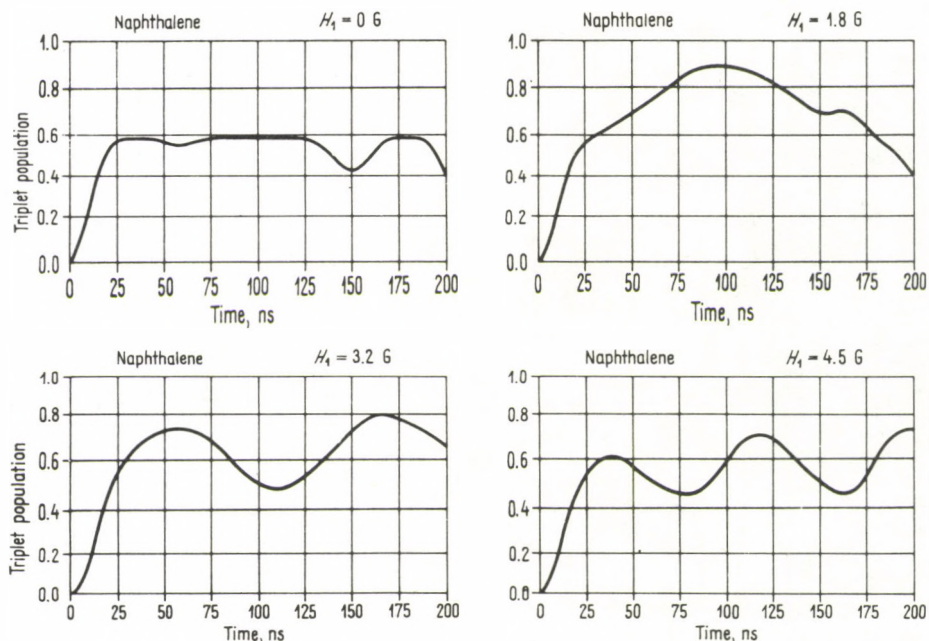


Fig. 5.20. Time dependence of triplet population for a naphthalene singlet-born radical ion pair at various H_1 . The microwave radiation frequency corresponds to the centre of the ESR spectrum [5.54]

spectrum. One can see that the microwave field influences the S-T evolution as well, the average triplet population being maximum at H_1 equal to several Gauss.

It is interesting to note that according to these calculations the average triplet level populations increase with H_1 up to maximum, then fall. This effect is associated with the fact that at $H_1 > A$ all the spins precess about H_1 (in a rotating frame) with approximately the same frequency. This synchronous precession does not violate the initial spin correlation and hence the triplet population probability decreases.

The technique of radical pair ODMR detection. To detect radical pair ESR spectra by the ODMR method one can use slightly modified standard ESR spectrometers. First, the microwave source must be sufficiently powerful. Second, a light detector, e.g., a photomultiplier, must be used instead of a microwave (crystal) detector. If the luminescence is sufficiently intensive, the signal can be detected with use made of the amplifying and detecting units of the spectrometer itself. The luminescence being low, it is expedient to detect it by the single-photon counting technique, i.e., the ESR spectrometer must be supplied with a number of special blocks.

A block-diagram of a ODMR spectrometer for RP investigations in the case of weak luminescence is given in Fig. 5.21 [5.33]. A quartz tube with the solution under study is placed into the spectrometer cavity in the range of the maximum microwave magnetic field. The solution is irradiated by the source introduced into the tube

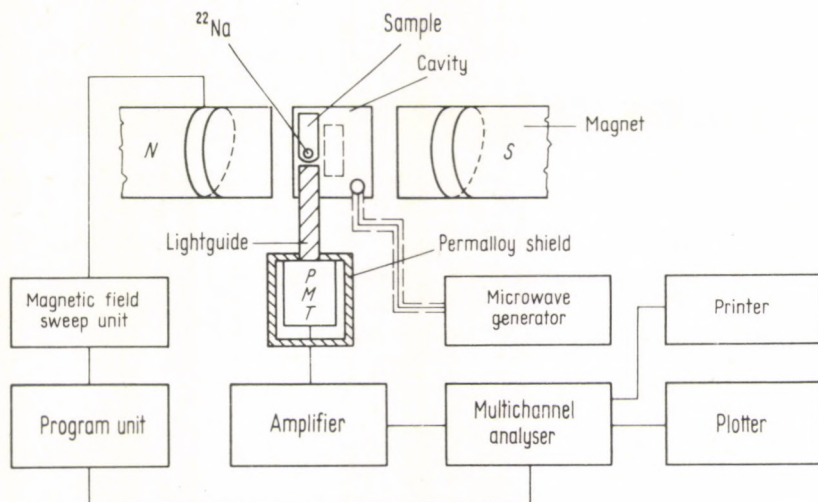


Fig. 5.21. Block-diagram of the spectrometer for optical detection of RP ESR spectra by the single-photon-counting (PMT = photo-multiplier tube) [5.53]

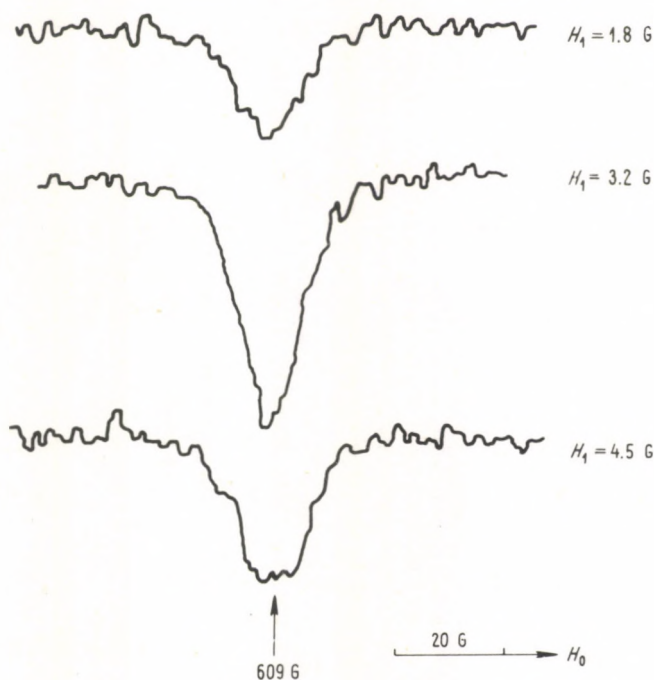


Fig. 5.22. Optically detected ESR spectrum of (naphthalene) $^-$ /(naphthalene) $^+$ radical ion pair in $1.15 \cdot 10^{-2} \text{ M}$ naphthalene solution in squalane at room temperature and various microwave fields H_1 . The time of spectrum recording is 12.5 min, the time average concentration is about 20 radical pairs per sample, the microwave generator frequency is 1700 MHz [5.53]

containing the sample. The light emitted by the sample is transferred through a light-guide to a permalloy-shielded photomultiplier. The program block governs the magnetic field sweep unit and the multichannel analyser. The luminescence intensity detected by the single-photon counting technique is stored in the analyser memory and extracted to the display, recorder, or type printer.

As an example illustrating the high sensitivity of the method, Fig. 5.22 depicts the ESR spectrum of (naphthalene)⁺/(naphthalene)⁻ pair in squalane taken with a powerful 1700 MHz generator as a microwave radiation source [5.53]. The spectrum is taken at various values of H_1 and the hyperfine structure unresolved. According to estimates [5.53] the time average concentration in this sample is some 20 radical pairs, the signal-to-noise ratio being approximately 10/1 at the detection time of 12.5 min. Thus, the sensitivity of the method is about ten orders higher than that of standard ESR spectrometers.

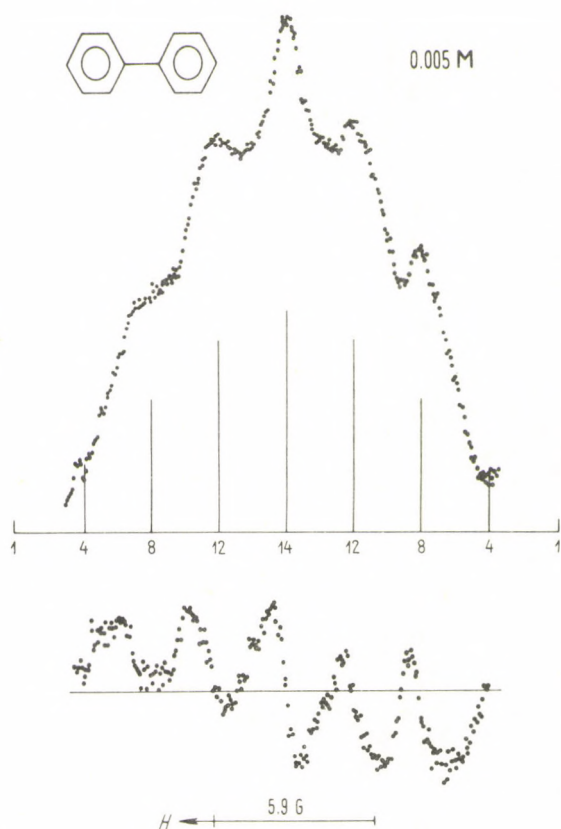


Fig. 5.23. Optically detected ESR spectrum of (diphenyl)⁻/(diphenyl)⁺ radical-ion pair and its first derivative in 0.005 M diphenyl solution in squalane at room temperature. The central part of the spectrum is given, the expected hyperfine structure is shown schematically. The spectrum is taken in the X-band, the recording time is 1 h, RP concentration is about 100 pairs per sample [5.55]

Detection of hyperfine structure. To obtain a well-resolved hyperfine structure in ODMR spectra it is necessary to reduce the two basic contributions to the line broadening characteristic of the method. First, this broadening is conditioned by short RP lifetimes, e.g., at a lifetime 100 ns it amounts to about 1 G. This contribution can be reduced by using more viscous liquids. The other considerable contribution to the line width is made by the microwave field H_1 . It can be reduced by decreasing H_1 provided this is permitted by the signal-to-noise ratio.

Figures 5.23 and 5.24 show examples of ESR spectra for short-lived radical-ion pairs with resolved hyperfine structure. In the ESR spectra of a (diphenyl)⁻/(diphenyl)⁺ pair [5.55] one can see a distinct hyperfine splitting resulting from *ortho*- and *para*-protons, the splitting of the *meta*-protons being small and unresolved. The spectrum observed results most probably from the overlap of the anion and cation spectra, which must have similar structure and splittings. When the diphenyl molecule concentration in the solution is increased, the hyperfine structure becomes smoothed and the spectrum narrows. In all likelihood, these changes are due to the charge transfer between ions and neutral molecules that takes place prior to the RP recombination, i.e., within times shorter than 100 ns.

The ESR spectrum depicted in Fig. 5.24 belongs to the radical pair (hexafluorobenzene)⁻/(anthracene)⁺ [5.56]. The anthracene cation signal is the intense line in the centre of the spectrum with unresolved hyperfine structure. The hexafluorobenzene anion spectrum is of interest due to its distinct second-order hyperfine structure given schematically under the spectrum, which fits the experimental spectrum perfectly.

To conclude, note that the technique under discussion can also be employed to observe the ESR spectra of short-lived radical pairs generated either in

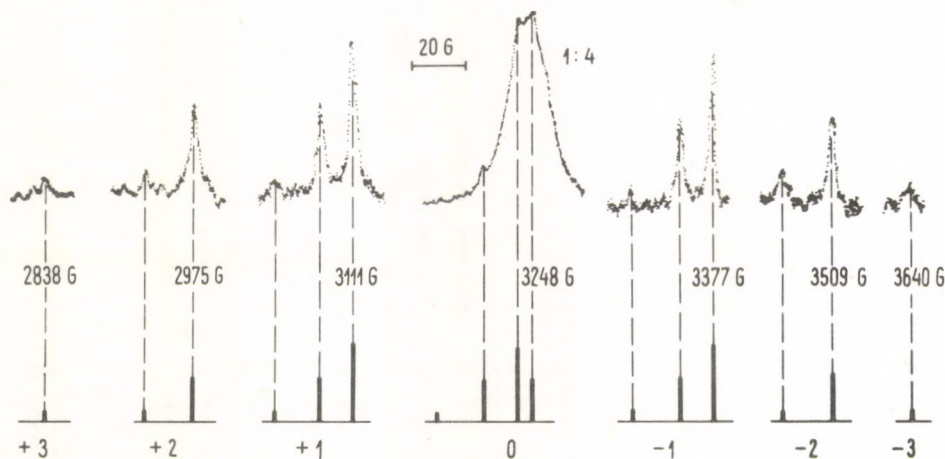


Fig. 5.24. Optically detected ESR spectrum of $C_6F_6^-/(anthracene)^+$ radical-ion pair in squalane at room temperature. The intense line in the centre is the ESR signal from the anthracene cation. In the $C_6F_6^-$ ESR spectrum the second order hyperfine structure given schematically under the spectrum, is resolved [5.56]

photochemical or thermal reactions provided the recombination product is electronically excited and can emit light. Owing to its high sensitivity this technique opens wide vistas in studying the nature, reactions, and molecular dynamics of short-lived RPs in different chemical processes.

5.5 Radical reactions in solids

We now consider the possibility of magnetic field effects in radical reactions in solids. In this case a decrease in diffusion mobility will, generally speaking, favour magnetic effects arising from RPs. Recently several reports of experimental observation of such effects have become available in the literature.

The influence of the magnetic field on the free radical concentration in the low-temperature photolysis of formaldehyde was studied by the ESR method [5.57]. This system is of interest because the pair formed as a result of the photolysis



contain radicals with extremely high hf constants, such as atomic hydrogen with $A = 500$ G and the formyl radical with $A = 132$ G. The ESR spectrum at 77 K shows only the formyl radical, the $\dot{\text{H}}$ atom being insufficiently stable under these conditions. The kinetics of $\text{H}\dot{\text{C}}\text{O}$ radical formation was studied in magnetic fields of 75 and 6200 G directly in a ESR spectrometer cavity (the residual field of the magnet was 75 G). The stationary concentration of formyl radicals was shown experimen-

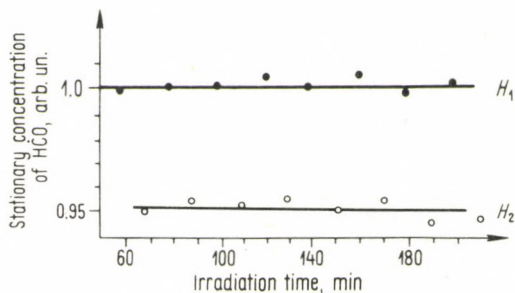


Fig. 5.25. Effect of the magnetic field on photostationary concentration of formyl radicals for low-temperature photolysis of formaldehyde at 77 K ($H_1 > H_2$)

tally to be higher in the high-field photolysis (Fig. 5.25). The basic mechanisms of $\text{H}\dot{\text{C}}\text{O}$ radical decay resulting in stationary concentration are associated with the following reactions



The magnetic field is assumed [5.57] to affect the recombination of the formyl radical and hydrogen atom at a random encounter in the matrix (reactions (5.21) and (5.22)). Indeed, the sign of the effect corresponds qualitatively to the hf-mechanism of the field effects upon F -pairs.

Similar experiments involving deuterioformaldehyde [5.57] showed no appreciable field effect on the photostationary concentration of $D\dot{C}O$ radicals. The authors attributed this to both the hf constant decrease in radicals \dot{D} and $D\dot{C}O$ as compared to \dot{H} and $H\dot{C}O$, and the reduced mobility of deuterium atom.

The magnetic effects on the radiation polymerization of acrylonitrile and acetaldehyde have been studied at low temperatures [5.58, 59]. The magnetic field appeared to affect both the polymerization rate and the molecular weights of the polymers formed. Since these processes can go by the free-radical mechanism, the field can be assumed to act by the mechanisms under discussion. Magnetosensitive stages of the radical polymerization process can be both the initiation and the bimolecular chain termination.

Note in conclusion that magnetic field effects on geminate radical-ion (dye and anthracene) recombination has been observed on the crystal surface in anthracene crystal photolysis sensitized by dyes [5.60]. The effect discovered has been interpreted in terms of the hf-mechanism [5.60].

5.6 Biochemical reactions

The discovery and studies of magnetic effects in radical reactions has recently stimulated investigations of the nature of magnetic field effects on biochemical processes. Magnetic effects in biology, and in biochemical reactions *in vitro*, in particular, have long been investigated [5.61]. The present book, however, does not consider investigations on magnetic effects in biology, because their number is ever increasing. Note, nevertheless, that the development of magnetobiology is hampered by a number of difficulties which results in a sceptical attitude towards the problem as a whole. The basic difficulties lie in obtaining reproducible results and in the absence of any physically substantiated mechanisms of biological effects of magnetic fields. It is quite possible that in at least some cases magnetic field effects upon biological systems are conditioned by the radical pair mechanism considered in this book. This mechanism can manifest itself in the reactions involving particles with unpaired electrons, e.g., the processes of electron transfer in cytochrome chains and related oxidative phosphorylation reactions, stages of photosynthesis, and certain enzymatic reactions. In this connection, the application of methods elaborated for simple radical reactions seems to be promising both for interpreting magnetic effects in biochemical reactions and for obtaining additional information on their mechanism.

This approach has been used to investigate, for example, magnetic effects on photochemical processes of reaction centres in the photosynthetic bacteria *Rhodospseudomonas sphaeroides* [5.62, 63]. Figure 5.26 presents a plausible

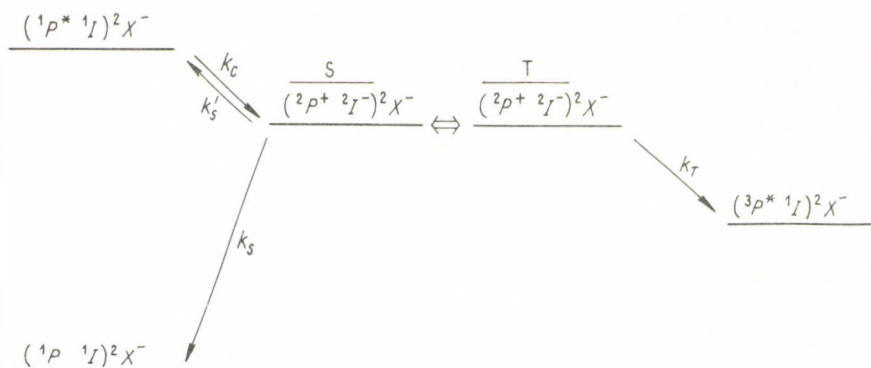


Fig. 5.26. Reaction scheme of the primary electron transfer in the reaction centre of bacteriochlorophyll with the second acceptor chemically reduced. 1P and 1I are donor and acceptor molecules in the ground singlet state. $^1P^*$ and $^3P^*$ are donor molecules in the singlet and triplet excited states, $^2P^+$ and $^2I^-$ are cation- and anion-radicals of the donor and acceptor, $^2X^-$ is the second acceptor in its reduced state [5.64]

scheme for the primary photochemical step in the photoreaction centre of these bacteria. The light having been absorbed by an antenna-pigment molecule (not shown in the scheme), the excitation energy is transferred to the primary donor P, presumably a bacteriochlorophyll dimer. The electron is then transferred from the excited bacteriochlorophyll dimer to the electron acceptor, bacteriopheophytin (I) (rate constant K_c). Under ordinary conditions the electron is then rapidly transferred to the second acceptor, i.e., an iron-ubiquinone complex (X). In the papers considered, the acceptor X was either previously chemically reduced to $^2X^-$, or withdrawn from the system with the further electron transfer blocked. The process of photosynthesis was thus stopped at the initial stage of radical-ion pair ($^2P^+/^2I^-$) formation. Being singlet-born from the singlet excited molecule $^1P^*$, this pair however can then turn into the triplet state due to hyperfine interactions. Depending upon the RP multiplicity at the recombination moment, the products can be either singlet (rate constant K_S), or triplet (rate constant K_T). Besides, a singlet RP can perhaps recombine into excited singlet state (rate constant K'_S), which requires the energy of activation.

In the experiments discussed the triplet recombination channel was detected by its characteristic triplet-triplet absorption after pulse irradiation. The external magnetic field was found in both cases to reduce the yield of triplet states φ_T , i.e., to inhibit conversion of a singlet-born RP into the triplet state, the triplet yield curves reaching plateaux in high fields. These results show a qualitative fit to the hf-mechanism of magnetic field effects.

The results depend upon the manner of preparing the reaction centre of the sample [5.63]; this influences both the scale of the magnetic effect

$$R = 1 - \frac{\varphi_T(\infty)}{\varphi_T(0)}, \quad (5.23)$$

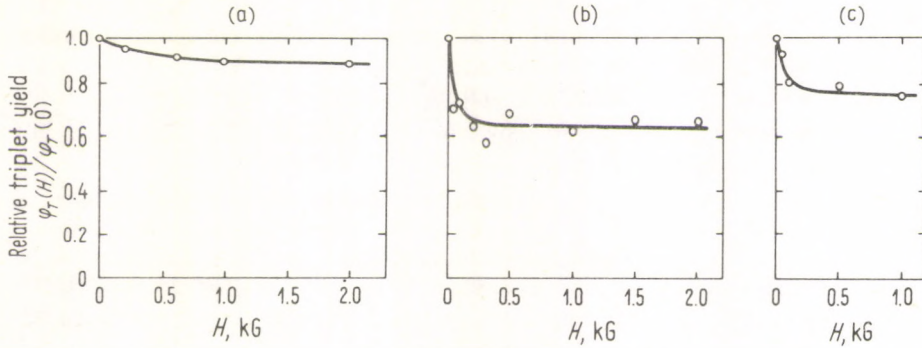


Fig. 5.27. Relative yield of triplet molecules vs. magnetic field for (a) chromatophore of RPs sphaeroides 2.4.1, (b) their reaction centres, (c) the reaction centres of RPs sphaeroides R-26 [5.63]

where $\varphi_T(0)$ and $\varphi_T(\infty)$ are the triplet yields in zero field and on the plateau respectively, and the field strength $H_{1/2}$ at which the decrease in the triplet yield is one-half of its maximum value (Fig. 5.27). For instance, in chromatophores of natural RP sphaeroides $R=0.15$ and $H_{1/2}=250$ G; in their reaction centres, in the absence of complexes of functional iron with ubiquinone, $R=0.4$, $H_{1/2}=35$ G; in the reaction centres of Rps. sphaeroides mutant R-26 with intact iron-ubiquinone complexes, $R=0.25$, $H_{1/2}=50$ G.

Considerable changes in $H_{1/2}$ value at a comparatively large scale of the magnetic effect, R , is a unique fact difficult to be explained within the simple hf-model, which connects the value of $H_{1/2}$ with the effective hf constant. On the other hand, the fact that R and $H_{1/2}$ are influenced by the manner of preparing the sample reflects subtle change in the reaction centre and is of great biophysical interest. Therefore, attempts have been undertaken to analyze theoretically in detail the influence of different factors, such as variations in kinetic rate constants and introduction of exchange interactions, on the shape of the field dependence of the triplet yield [5.64, 65]. Theoretical analysis of this problem is simpler than that of radical pairs in solution owing to the fact that the species ${}^2P^+$ and ${}^2I^-$ are immobilized and in permanent contact. Therefore, the exchange interactions, if any, can be considered constant in time, and the chemical reactions are of first order. At the same time, the situation is complicated by the fact that the anisotropic interactions are not averaged, but this complication so far has been neglected in calculations. To bring the analysis to the stage of numerical calculations, real hyperfine interactions in a bacteriochlorophyll cation and bacteriopheophytin anion were replaced by the effective hf interactions with one [5.65] or two [5.64] protons.

Detailed numerical calculations [5.64, 65] have shown that the values of $H_{1/2}$ and R vary for several reasons. For instance, at sufficiently high values of the constants K_T and K_S , the $H_{1/2}$ value is determined not by the effective hf constant but by the triplet and singlet level broadening ($\hbar K_T$ or $\hbar K_S$). Therefore, an increase in K_T or K_S results in an increase of $H_{1/2}$. The quantity R can vary as a result of RP exchange

interactions with the third paramagnetic particle—iron—ubiquinone complex located in the vicinity. This interaction results in the field-independent mechanism of ion-radical S-T relaxation and hence must reduce the scale of the magnetic effect. At the same time, the exchange interaction between ${}^2I^-$ and ${}^2P^+$ seems to be negligible. It should have resulted in characteristic maxima in the curve $\varphi_T(H)$, but this was not detected in experiment.

Of particular interest is the speculation [5.64] about the effect of reversibility of the electron transfer between ${}^2P^+$ and ${}^2I^-$ ($K'_S \neq 0$) which was confirmed by some published experimental data on fluorescence in such systems. The reversibility of the electron transfer reaction must influence the RP S-T evolution. Indeed, the electron spins become strongly coupled after the back transfer which in effect results in a fast relaxation of their phases and thus in the deceleration of the singlet-triplet mixing. At the same time, numerical calculations show the quantity $H_{1/2}$ to increase with K'_S ; Fig. 5.28 exemplifies this behaviour. The assumption based on the electron transfer reversibility leads to a number of testable predictions. For instance, according to the model, $H_{1/2}$ values must fall with falling temperature. The final solution of the problem of what induces $H_{1/2}$ and R changes obviously requires some additional experiments and their comparison with model theoretical calculations.

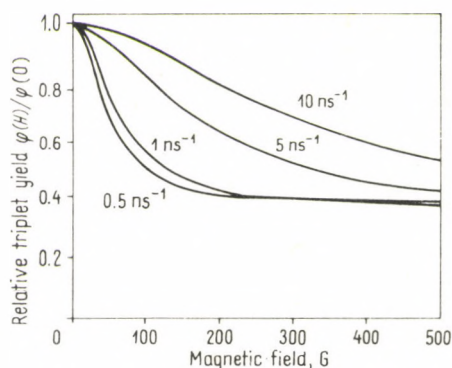


Fig. 5.28. Calculated magnetic field dependence of the relative triplet yield $\varphi_T(H)/\varphi_T(0)$ for different rate constants K'_S ($K_S=0.1 \text{ ns}^{-1}$, $K_T=1 \text{ ns}^{-1}$, $A_1=5 \text{ G}$, $A_2=10 \text{ G}$, $J_{PI}=J_{IX}=0$; A_1 and A_2 are effective hf constants for the pair ${}^2P^+ / {}^2I^-$) [5.64]

The above studies are closely connected with fluorescence investigations of *Rhodospseudomonas sphaeroides* at 1.4 K [5.66]. As in the above work, the electron acceptor X was chemically reduced. The fluorescence intensity of the antenna pigment was detected experimentally at 911 nm wavelength depending on the field strength. The luminescence intensity was found to reduce with increasing field, a constant level being reached for fields above 300 G. The overall decrease in the intensity was not great, being 1.1%. The effect observed is discussed in terms of the following model. The reaction centre $(PI)^2X^-$ is a trap for the electron excitation of

the antenna pigment and hence reduces its luminescence intensity. However, once in the triplet excited state, the centre stops functioning as an excitation acceptor and the pigment luminescence intensity must increase. Since magnetic fields influence the triplet concentration, as shown above, they must also affect the luminescence intensity. Estimations show both the sign and the scale of the effect to fit this model.

One more biochemical system in which magnetic field effects have been studied in detail, is hydrogen peroxide decomposition by catalase [5.67]. The acceleration effect of a magnetic field upon this reaction has been reported [5.67a]. There is no direct evidence for free radicals participating in this reaction. It is however, possible that redox processes result in certain intermediate radical pairs involving an active ferment centre—an iron ion—and a free radical formed from a peroxide molecule.

Note in conclusion that one of the problems of primary importance arising when discussing the mechanism of some enzymatic reactions is whether they run by the synchronous (nonradical) mechanism or by a sequence of redox (free radical) steps which are unobservable because free radicals do not leave enzyme active centres and are short-lived. The latter mechanism can be detected by the observation of magnetic effects.

5.7 Processes involving triplet molecules

The discovery and investigation of magnetic effects in radical reactions were preceded by studies of magnetic field effects upon processes involving excited triplet states. These effects were observed in solids prior to the discovery of CIDNP [5.68, 69]. Nowadays the number of papers devoted to examination of magnetic field effects on photoelectrical, luminescent, and photochemical properties of molecular crystals and organic semi-conductors goes on, and the scope of problems and objects under study constantly broadens (see, e.g., reviews by Sokolik, Frankevich [5.70], and Avakian [5.71]). These studies stimulated analogous research on fluid solutions. At first, studies on magnetic field effects upon processes involving triplet excited molecules and reactions of free radicals in solution were developed independently, the elaboration of the theory, however, showed the nature of the magnetic effects in the above processes to be similar. Intersystem crossing in pairs of reacting particles has been found to be the magnetosensitive stage of such processes. Thus reactions of triplet molecules (as well as of free radicals) can be spin-selective and hence applied field-dependent. We do not intend to give a thorough review of studies in this field but confine ourselves to the basic ones concerned with spin-selective processes involving triplet molecules studied experimentally in liquids and for which magnetic field effects have been observed.

1. *The quenching of the excited triplet states by a free radical* [5.72, 73]. This process has a doublet final state and the quenching step can therefore occur only in collisions where the triplet molecule and the radical are in a collective doublet state.

2. *Triplet-triplet annihilation* [5.74]. In a random encounter in solution a pair of triplet molecules can form singlet, triplet, and quintet states with respect to the total spin. Quenching takes place in the singlet state, since it leads to the formation of molecules in ground and excited singlet states.

3. *The quenching of excited triplet states by oxygen* [5.75]. Since oxygen has a triplet ground state, this process is analogous to the triplet-triplet annihilation and is also spin-selective.

4. *The photochemical oxidation of aromatic hydrocarbons* [5.76]. The primary stage in this reaction is the formation of an excited singlet oxygen molecule as a result of the collision of an excited triplet hydrocarbon molecule with oxygen in the ground state. The influence of the magnetic field on this process has so far been established only for the reaction in the solid state.

The influence of a magnetic field on the above processes is interpreted in terms of a mechanism formally identical to that examined for the recombination reactions of free radicals. According to the dominant view, the magnetic field influences the dynamics of the spins of two paramagnetic species, i.e. the rate of change of the multiplicity of the pair of paramagnetic species which have collided in solution. The change in multiplicity can occur both on direct contact of the species and during their lifetime in the cage, during the intervals between repeated collisions of a given pair of paramagnetic species.

As in the recombination of radicals, the change in spin multiplicity can be induced by the Δg - and hf-mechanisms. However, the transitions due to the dipole-dipole interaction of the unpaired electrons of each of the triplet molecules are more effective for the latter. In solutions, the thermal motion of triplet molecules modulates this dipole-dipole interaction in a random fashion, which leads to an effective paramagnetic relaxation of the triplet molecules. These relaxation transitions mix the states of two paramagnetic particles with different multiplicities. Thus the influence of the magnetic field on elementary processes involving triplet molecules in solutions is interpreted as the result of the field dependence of the relaxation transitions caused by the fluctuating dipole-dipole interaction in the triplet molecules. We point out yet again that this interpretation is equivalent to the mechanism proposed by Brocklehurst [5.77] to account for the effect of the magnetic field in radiation-chemical reactions. The influence of a magnetic field on processes involving triplet molecules in solutions has been examined theoretically by Atkins and Evans [5.78] who investigate comparatively nonviscous solutions where the molecular rotation is fairly rapid so that stochastic perturbation theory and the Redfield equation can be used to calculate the kinetic coefficients describing the relaxation transition.

A theory of the processes under consideration may be developed on the basis of the fundamental equations which were quoted above in the discussion of radical recombination reactions. The specific features of a real system are reflected in the formulation of the equations for the pair density matrix.

Atkins and Evans calculated the possibility of the triplet-triplet annihilation in arbitrary magnetic fields. The following expression has been obtained for the ratio of the intensities of the fluorescence accompanying with annihilation in high (approximately 10 kG) and zero magnetic field

$$I_n/I_0 = 1 - 0.61 \Phi_{TT}(K(0)\tau_a)^{1/2}, \quad (5.24)$$

where τ_a is the duration of the elementary step in transitional diffusion; Φ_{TT} is related to the probability λ_T , that the triplet which has collided will be annihilated subject to the condition that the pair was in the singlet state during the encounter, by the expression

$$\Phi_{TT} = \lambda_T / (1 - \lambda_T) \quad (5.25)$$

$K(0)$ is the spectral density of the dipole-dipole interaction at zero frequency

$$K(0) = (D^2 + 3E^2)\tau_r. \quad (5.26)$$

Here D and E are the principal values of the dipole-dipole interaction tensor and τ_r is the characteristic rotational relaxation time.

Analogous reasoning for the quenching of triplet molecules by radicals leads to the following results [5.78]

$$I_n/I_0 = 1 + 0.95 \Phi_{DT}(K(0)\tau_a)^{1/2}, \quad (5.27)$$

where Φ_{DT} is related to the probability of the quenching of the triplet λ_D in such a collision, where the pair was in the doublet state, by the expression

$$\Phi_{DT} = \lambda_D^2 / (1 - 4/3\lambda_D + \lambda_D^2) \quad (5.28)$$

Theoretical analysis shows that the probabilities of the triplet-triplet annihilation and of the quenching of the triplet biradicals in solutions should decrease with increasing magnetic field strength. The opposite variation with the field should be observed for the fluorescent intensity in such a case. The theory predicts in addition that the transitional region is located in fields corresponding to the equality of the Zeeman and rotational frequencies.

The theoretical results [5.78] are in good qualitative and quantitative agreement with numerous experiments [5.73-76, 79-85]. Tables 5.2-5.4 list systems in which the magnetic field has an effect on the elementary processes involving triplet molecules.

The first observation of the influence of the magnetic field was made in 1969 by Faulkner and Bard [5.74] in studies of the delayed fluorescence of anthracene in solution on photoexcitation. Delayed fluorescence (DF) is known to arise as a result of the formation of an excited singlet state on annihilation of the triplet states: $T + T \rightarrow S + S_0$ (T and S are the excited triplet and singlet states and S_0 is the ground state of the molecule). The DF intensity is then defined by the expression

$$I_{DF} = \frac{1}{2} \Phi_f K_A (I_a \Phi_T \tau)^2, \quad (5.29)$$

Table 5.2. Experimental results for the influence of the magnetic field on the rate of triplet-triplet annihilation in solutions (for delayed fluorescence)

Reaction	Change in luminescence intensity, % (for $H = 8 \text{ kG}$) ^b	References
$T + T \quad S + S_0$		
(Anthracene) ^T + (Anthracene) ^T in dimethylformamide	4-5	[5.74]
in acetonitrile	2	[5.75]
(Pyrene) ^T + (Pyrene) ^T in dimethylformamide	2-3	[5.75]
in acetonitrile	1-2	[5.75]
in cyclohexane	6-7	[5.79]
(1,2-Benzanthracene) ^T + (1,2-Benzanthracene) ^T in cyclohexane	4	[5.79]
(Anthracene) ^T + (Anthracene) ^T in CH_2Cl_2	5	[5.80]
$T + T = E^a + S_0$		
(Pyrene) ^T + (Pyrene) ^T in cyclohexane	6-7	[5.79]
(1,2-Benzanthracene) ^T + (1,2-Benzanthracene) ^T in cyclohexane	3	[5.79]

^a E = excimer^b in the magnetic field, the luminescence intensity diminishes, indicating a decrease in reaction rate

Table 5.3. Experimental results for the influence of the magnetic field on the quenching of triplet states by radical-ions

Reaction $R + T \rightarrow R + S_0$	Concentration of radicals (molecules), M	Change in luminescence intensity, % ($H = 8 \text{ kG}$) ^a	Method of registration	References
Radical-cation of Wurster's Blue + (Anthracene) ^T in CH_2Cl_2	$1.8 \cdot 10^{-7}$			
	$(8.0 \cdot 10^{-5})$	2%	DF	[5.73]
	$2.1 \cdot 10^{-7}$	6%	DF	[5.80]
	$(1.1 \cdot 10^{-3})$			
	$3.6 \cdot 10^{-7}$			
p -Benzoquinone radical-anion + (Anthracene) ^T in CH_2Cl_2	$(1.0 \cdot 10^{-7})$	9%	DF	
	$1.6 \cdot 10^{-7}$			
Radical-cation of Wurster's Blue + (Pyrene) ^T in dimethyl-formamide	$(1.0 \cdot 10^{-3})$	3%	DF	[5.80]
	$(5.0 \cdot 10^{-3})$			
	$1.0 \cdot 10^{-3}$	8%	ECL	[5.79]
	$(1.0 \cdot 10^{-3})$	20%	ECL	

Table 5.3. (continued)

Reaction $R + T \rightarrow R + S_0$	Concentration of radicals (molecules), M	Change in luminescence intensity, % ($H = 8 \text{ kG}$) ^a	Method of regis- tration	Refer- ences
Radical-cation of Wurster's Blue + (Rubrene) ^T in dimethyl-formamide	$1.5 \cdot 10^{-3}$ ($1.0 \cdot 10^{-3}$)	30%	ECL	[5.81]
<i>p</i> -Benzoquinone radical-anion + (Rubrene) ^T in dimethylformamide	$2.4 \cdot 10^{-3}$ ($1.0 \cdot 10^{-3}$)	12%	ECL	[5.81]
Rubrene radical-ion + (Rubrene) ^T in dimethylformamide	$1.0 \cdot 10^{-3}$	12%	ECL	[5.81]
Radical-cation of Wurster's Blue + (1,3,6,8-Tetraphenylpyrene) ^T in dimethylformamide	$0.23 \cdot 10^{-3}$ ($0.15 \cdot 10^{-3}$)	26% ^b	ECL	[5.81]
10-Methylphenothiazine radical-cation + (Fluor-anthene) ^T in dimethylformamide	$2.4 \cdot 10^{-3}$ ($3.0 \cdot 10^{-3}$)	14%	ECL	[5.81]
Radical-cation of Wurster's Blue + (Anthracene) ^T in dimethylformamide	$14.4 \cdot 10^{-3}$ ($10.3 \cdot 10^{-3}$)	18%	ECL	[5.82]
Radical-cation of Wurster's Blue + 9,10-Diphenylanthracene ^T in dimethylformamide	$14.6 \cdot 10^{-3}$ ($10.5 \cdot 10^{-3}$)	5%	ECL	[5.82]
Tri- <i>p</i> -tolylamine radical-cation + (9,10-Diphenylanthracene) ^T in tetrahydrofuran	$1.0 \cdot 10^{-3}$ ($1.0 \cdot 10^{-3}$)	15%	ECL	[5.82]

^a The DF and ECL intensity increases in the magnetic field indicating a decrease of the rate of reaction

^b $H = 6 \text{ kG}$

^c For the ECL experiments, the 'radical concentration' column lists the concentrations of the initial compounds from which the radical-ions are formed

Table 5.4. Experimental results for the influence of the magnetic field on the quenching of triplet states by oxygen [5.75]

Reaction $T + {}^1\text{O}_2 \rightarrow S + {}^3\text{O}_2$	Oxygen pressure, atm	Change in DF intensity, % ($H = 8 \text{ kG}$)
(Anthracene) ^T + (Anthracene) ^T in dimethylformamide ^a	0	-3
	$3.0 \cdot 10^{-3}$	+3
	$6.0 \cdot 10^{-3}$	+5
(Pyrene) ^T + (Pyrene) ^T in dimethylformamide ^b	0	-2
	$6.0 \cdot 10^{-3}$	+1

^a anthracene concentration $2.1 \cdot 10^{-4} \text{ M}$

^b pyrene concentration $2.6 \cdot 10^{-4} \text{ M}$

where Φ_f is the probability of fluorescence, K_A is the rate constant for the triplet-triplet annihilation, I_a is the rate of absorption of light, Φ_T is the probability of the formation of the triplet state, and τ is the lifetime of the triplet state. It has been observed [5.74] that the DF intensity decreases with increase of the magnetic field

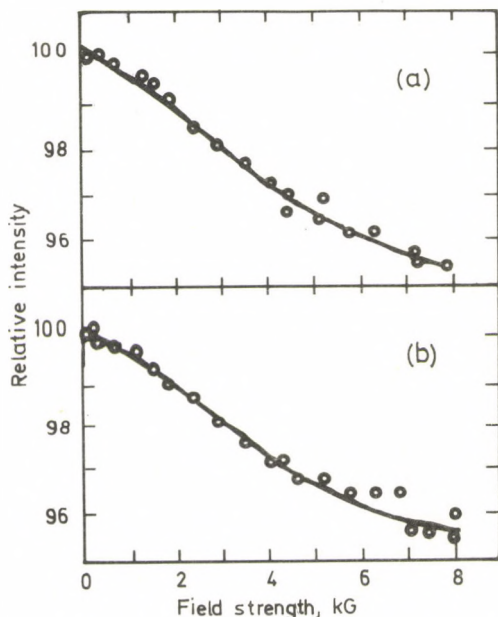


Fig. 5.29. Magnetic field effect on delayed fluorescence from anthracene solutions in DMF: (a) $5 \cdot 10^{-4}$ M, (b) $7 \cdot 10^{-5}$ M [5.74]

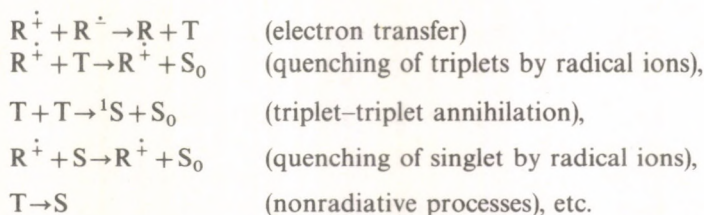
strength (see Fig. 5.29 and Table 5.2). In principle, both Φ_T and K_A are magnetically sensitive quantities. Experiments on sensitized photolysis permitted a more unambiguous solution of this problem. Whereas in direct photolysis the triplet states of anthracene arise by an intersystem crossing from excited singlet states, on sensitization they are populated in a triplet-triplet energy transfer process. Consequently, in such cases the efficiency of the formation of triplet states Φ_T is determined by different processes. It has been shown [5.74] that the variation of the DF intensity with the magnetic field is the same for both direct and sensitized photolysis. This enabled the authors [5.74] to conclude that the observed variation of the DF intensity in the magnetic field is due to the influence of the latter on the triplet-triplet annihilation rate constant. The decrease of the rate of the triplet-triplet annihilation in the magnetic field (to 7%), manifested in the DF spectra, was also subsequently observed for a number of other systems (see Table 5.2). It is noteworthy that the effect of the magnetic field depends strongly on the solvent, which apparently indicates a significant role of the medium of the annihilation processes. In a study of DF in pyrene and 1,2-benzanthracene solutions [5.79], it was possible to observe the influence of the magnetic field not only on the fluorescence of the monomeric molecules but also on that of dimers (exciplexes).

Numerous experimental studies have been devoted to the quenching of triplet states by free radicals (Table 5.3). In the presence of radicals, the DF lifetime is appreciably shortened and the effect of the magnetic field on the fluorescence intensity is of the opposite sign (the intensity increases with the field). The usual mechanism of the process is



where R is a quenching agent in a doublet state (free radical).

The magnetic field affects reactions (5.30) and (5.31) in the same way, decreasing the constants K_A and K_R . However, it is readily seen that, when reaction (5.31) predominates over reaction (5.30), the DF intensity determined by the overall concentration of triplets will decrease in the magnetic field. The change in the nature of the magnetic field effect upon DF can be readily traced when the relative concentration of radicals is varied (see Table 5.3): the effect increases with concentration of the radical-ions. Together with the DF method, electrogenerated chemiluminescence (ECL) has been widely used to investigate the effect of the magnetic field on elementary processes involving triplet states. The idea of such experiments is as follows. In an electrochemical cell containing an electrolyte (as a rule tetrabutylammonium perchlorate) and the test compound (e.g. anthracene), the radical ions R^+ and R^- are produced. The subsequent processes are listed below:



The luminescence intensity due to the excited singlet states is recorded in the experiments.

Virtually all the systems in which the influence of the magnetic field on ECL was observed belong to the class of reactions with an 'energy deficit', since the energy evolved on electron transfer is insufficient for the direct formation of the excited singlet state. It has been shown in a number of studies that in such systems the luminescence intensity increases with increasing magnetic field strength (by up to 30%). This effect is usually explained by the fact that radical ions play an important role in the reactions as triplet quenching agents, since the excited states generated in ECL processes are formed together with radical ions, the rate of quenching by the latter species undoubtedly constitutes the main factor influencing the luminescence intensity. The excited singlet states are quenched less effectively owing to their short lifetime. Table 5.3 presents the magnetic field effects for a single field strength $H \approx 8$ kG in the systems investigated. Figure 5.30 illustrates as an example the typical variation of the ECL intensity with the magnetic field. We may note that this type of variation is in full agreement with the theory of Atkins and Evans [5.78].

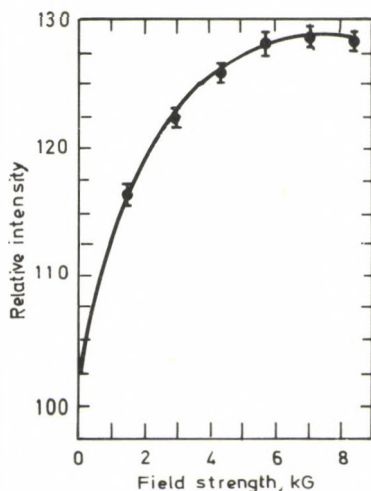


Fig. 5.30. The influence of the magnetic field on the intensity of the electrogenerated chemiluminescence in a system containing rubrene and the radical-cation of Wurster's Blue [5.81]

The influence of the magnetic field on the quenching of the delayed fluorescence of anthracene and pyrene by molecular oxygen has been observed [5.75] (see Table 5.4). As for quenching by radicals, the magnetic field increased the DF intensity. The observed effect has been explained [5.75] by the following mechanism



At high oxygen concentrations, reaction (5.34) predominates and the DF intensity should therefore increase. The formation of singlet oxygen as a result of the reaction with an excited triplet hydrocarbon molecule (a reaction of type (5.34)) is probably the primary stage of the photochemical oxidation reaction. Since this reaction depends on the magnetic field, presumably the rate of photochemical oxidation of aromatic hydrocarbons is also sensitive to the magnitude of the magnetic field. The effect of the magnetic field in the photochemical oxidation reaction has so far been observed only in the solid phase [5.76]. The influence of the magnetic field on the surface conductivity of solid tetracene has been noted in the presence of oxygen [5.76]. The observed effect has been explained by the influence of the field on the photochemical oxidation reaction, leading to an increase of photoconductivity.

5.8 Conclusion

We can conclude from the papers discussed above that the effect of the magnetic field on radical reactions in solutions has been well established and that the proposed theoretical models of this effect (hf and Δg) have been confirmed

experimentally. The experimental studies have identified the processes in which the magnetic effects are observed, the scale of these effects, and the most favourable conditions for their observation.

We can consider the characteristic structural parameters of the radical pairs (g -values of the radicals and the hyperfine coupling constants), which may be useful in estimating the magnetic effects (Tables 5.5 and 5.6). As can be seen from the tables both the difference between the g -values² and the hf constants as a rule are not large and hence large magnetic field effects can be expected to occur only at long lifetimes of the radical pairs or at very high field strength.

An analysis of the studies we have discussed confirms this viewpoint. Noticeable effects can be observed in systems having a relatively long lifetime of intermediate radical pairs. These systems differ only in the causes of the increased lifetimes. In some cases the recombination radius increases because of the electrostatic

Table 5.5. g -Values of some free radicals in solution (Ref. [5.86])

Radical	g -value
$\cdot\text{CH}_2\text{CH}_3$	2.00260
$\cdot\text{CH}_2\text{CH}_2\text{CH}_3$	2.00265
$\cdot\text{CH}_2\text{CH}_2\text{CH}_2\text{CH}_3$	2.00267
$\cdot\text{CH}_2\text{CH}_2\text{OH}$	2.00247
$\cdot\text{CH}_2\text{CHO}$	2.0045
$\text{H}\dot{\text{C}}\text{O}$	2.0003
$\text{CH}_3\dot{\text{C}}\text{O}$	2.0005
$(\text{CH}_3)_2\text{N}\cdot$	2.0044
$\cdot\text{CH}_2\text{NH}_2$	2.00282
$\cdot\text{CH}_2\text{SC}(\text{CH}_3)_3$	2.0049
$\text{C}_6\text{H}_5\text{CH}_2\cdot$	2.00263
$\cdot\text{CH}=\text{CH}_2$	2.00220
$\text{C}_6\text{H}_5\cdot$	2.0024 ^a
$\text{F}\dot{\text{C}}\text{O}$	2.0016
$(\text{Ph})_3\text{SiO}_2\cdot$	2.0277
$(\text{Me})_3\text{PbO}_2\cdot$	2.034
$\text{C}_6\text{H}_5\dot{\text{N}}\text{H}$	2.00324
$\cdot\text{SC}(\text{CH}_3)_3$	2.0262
$\cdot\text{C}(\text{Cl})_3$	2.0091
$\cdot\text{C}(\text{CH}_3)_3$	2.0170
$\cdot\text{Si}(\text{CH}_3)_3$	2.0031
$\cdot\text{Ge}(\text{CH}_3)_3$	2.0104
$\cdot\text{Sn}(\text{CH}_3)_3$	2.0389 ^a

^a measured in solid matrices

² In contrast to ordinary radical pairs, very large Δg -values (up to several units) can be observed in pairs containing paramagnetic ions.

interaction of charged particles; in other cases, complexes are formed among the radicals. The lifetime of the radical pairs can also be increased by decreasing the temperature or by increasing the solvent's viscosity.

There are also systems in which large magnetic effects can be predicted at normal radical mobilities. Specifically, these are reactions involving element-centred organic radicals³ or transition-metal paramagnetic ions in which the Δg -values and the hyperfine interaction can be anomalously large (see Tables 5.5 and 5.6).

Table 5.6. Values of hyperfine constants of some free radicals in solution (Ref. [5.86])

Radical	hf constant G
$\text{Me}_3\text{Sn}\cdot$	$A(^{119}\text{Sn}) = -1611$ $A(^{117}\text{Sn}) = -1530$ $A_{\text{H}}^{\text{CH}_3} = -2.5$
$\cdot\text{CH}_3$	$A_{\text{H}} = (-)23.04$
$\cdot\text{CH}_2\text{CH}_3$	$A_{\text{H}}^{\text{CH}_2} = (-)22.38$ $A_{\text{H}}^{\text{CH}_3} = (+)26.87$ $A_{\text{H}}(\alpha) = (+)13.40$
$\cdot\text{CH}=\text{CH}_2$	$A_{\text{H}}(\beta_1) = (+)65.00$ $A_{\text{H}}(\beta_2) = (+)37.00$
$\cdot\text{CH}_3$	$A_{\text{C}}^{13} = (+)38.34$
$\cdot\text{CF}_3$	$A_{\text{C}}^{13} = (+)271.60$
$\cdot\text{CF}_3$	$A_{\text{F}}^{19} = (+)142.40$
$(\text{C}_6\text{H}_5)_3\text{Ge}\cdot$	$A_{\text{Ge}}^{73} = 84$ $I(^{73}\text{Ge}) = 9/2$

Very promising but hardly explored subjects of experimental study are the magnetic effects on reactions in which the original radical pairs are triplet pairs. Much larger effects are predicted for these reactions than for those involving original singlet pairs with the same radical pair parameters.

It would be interesting to study further the magnetic effects in biological systems, to examine the experiments in terms of the mechanisms discussed here, to verify the predictions based on these mechanisms, and to set up new experiments for examining them at the molecular level.

It would also be interesting to use magnetic field effects to determine the radical stages of chemical and biochemical reactions. This method can be used if the EPR method and the method of chemical polarization of nuclei are impracticable for one reason or another, or if they fail to reveal the presence of any radical species.

³ Appreciable magnetic field effects on reactions with participation of germanium-organic radicals have been observed recently [5.87].

6 MAGNETIC ISOTOPE EFFECT

6.1 Introduction

Isotope effects observed in chemical reaction kinetics are usually associated with the isotope mass of the atoms which affects the mass of the molecules, the moments of inertia, and the vibrational frequencies. The theory of kinetic isotope effects allowing for variations of the mean vibrational energies of molecules and activated complexes gives in many cases a quantitative description of the effects observed [6.1].

The theoretical models of singlet-triplet evolution in a radical pair which we have described allow a new type of isotope effect based on the difference in magnetic isotopic properties. The above theoretical analysis demonstrates that the hyperfine interaction between the nuclei and electrons in a RP can result in singlet-triplet mixing, i.e. in changes of the RP multiplicity. Since the hf energies are unequal for different nuclear isotopes one can expect different recombination efficiencies for radical pairs containing these isotopes. This phenomenon will be called the *magnetic isotope effect* [6.2] in contrast to the common kinetic isotope effect.

Experimental studies on isotope effects in the liquid phase are not numerous and in fact are concerned with decomposition rates of organic peroxides and azo-compounds (see, e.g., [6.3, 4]). In a number of cases, unusually high secondary isotope effects were observed in the thermolysis of hydrogen- and deuterium containing compounds ($k_H/k_D \approx 1.3-1.4$) [6.4], which would be tempting to attribute to the difference in magnetic properties of hydrogen and deuterium. Indeed, the hf constants for H and D are known to differ approximately by a factor of 7. Hence, hydrogen-containing RPs are highly likely to change their spin states (from S to T), and so the efficiency of the back recombination of the primary pairs to give the initial compounds would be less than that for the deuterated analogue.

Unfortunately, in all the above cases one cannot exclude the possibility the isotope effect arises in the primary molecular decomposition but not in the RP reaction. This opens no alternative explanation of the observed isotope effects associated with the energy difference of zero vibrations [6.1].

Consider the conditions that ensure maximum magnetic isotope effects in radical reaction products. First, the hf constants with the magnetic nuclei in intermediate RPs must be markedly different on isotopic substitution. In this case free radical recombination reactions can be used to select magnetic isotopes and to distinguish them from nonmagnetic ones. From this standpoint, the most favourable pairs are

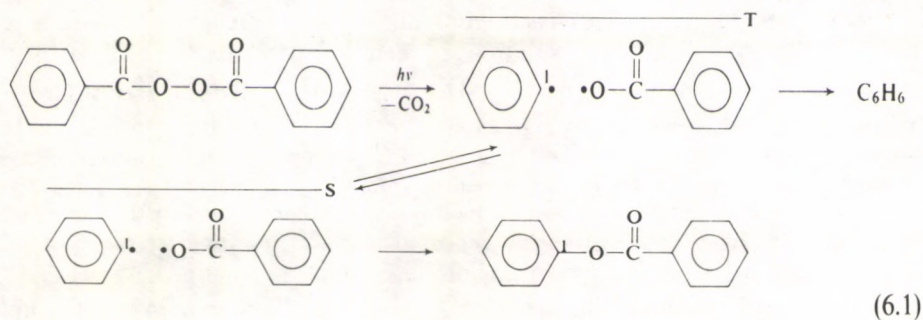
$^1\text{H}-^2\text{D}$, $^{12}\text{C}-^{13}\text{C}$, $^{16}\text{O}-^{17}\text{O}$, the last two pairs being especially convenient since ^{12}C and ^{16}O have no magnetic moments at all. Second, the hf constant for one of the isotopes must be sufficiently high for the S-T conversion processes to be effective. σ -radicals obey this condition. For example, the hf constants with ^{13}C in σ -radicals are

the following: $A = 150$ G in phenyl radicals, 160 G in the radical $\begin{array}{c} \text{H} \\ | \\ \cdot\text{C}=\text{C} \\ | \quad | \\ \text{H} \quad \text{H} \end{array}$ and

350 G in ethynyl radicals [6.5]. Third, the generation of triplet radical pairs is necessary since their recombination always follows singlet-triplet conversion and is most effective in isotope selection. To account for this, consider a RP with one of the partners containing a hydrogen nucleus. Radical pairs involving ^{13}C magnetic isotope are subjected to faster singlet-triplet conversions than those containing a ^{12}C nonmagnetic isotope. That is why pairs with ^{13}C become singlet and recombine more quickly than those with ^{12}C . Diffusion processes of triplet RPs (preferentially those with ^{12}C) and subsequent radical encounter in a solution can also yield recombination products, the latter decreasing the isotope effect. To exclude other ways of generating the RP recombination product, it is necessary to introduce radical traps which react efficiently with the escaping radicals. It is thus clear that if singlet RPs are generated, then due to the back singlet-triplet pair evolution, their RP recombination products will be impoverished by the magnetic isotope. This process, however, will be considerably less effective in the isotopic selection as a greater portion of the singlet pairs recombine without singlet-triplet conversion (primary recombination) and only a small fraction of singlet pairs are subjected to singlet-triplet evolution resulting in isotopic selection. Uncorrelated pairs formed by random encounters of independently generated radicals occupy an intermediate position as to the isotopic selection efficiency. And, finally, to observe magnetic isotope effects, electron and radical relaxation times must be sufficiently long. If electron (or nuclear) relaxation in radicals is fast (within a time less or comparable to that of the triplet-singlet evolution), the spin correlation in the pair is violated and the pair remains uncorrelated. In other words, fast relaxation results in randomization without electron precession and disrupts the triplet-singlet evolution. As a result, the reaction efficiency of magnetic isotope selection reduces. The fast relaxation in radicals can be attributed to strong spin orbital or spin rotational interactions (for electrons) and also to quadrupole interactions (for nuclei).

6.2 Reactions of neutral radicals

The first experimental evidence for magnetic isotope effects was reported in [6.6, 8]. Carbon isotope effects have been studied [6.6,7] in the reaction of sensitized photochemical decomposition of benzoyl peroxide in solution:



This system obeys all the forementioned requirements favouring the observation of such effects: (1) the phenyl radical belongs to the class of σ -radicals with higher hf constants at ^{13}C nuclei (in our case $2.4 \cdot 10^9$ rad/s); (2) the intermediate RP is triplet-born [6.9]. Note that magnetic effects of a similar nature, CIDNP and constant field effects on the product yield have been observed in the reaction discussed. Besides, as it has already been emphasized, this reaction provides us with direct experimental evidence for the spin selection rule in phenyl benzoate formation. Thus, with the magnetic isotope effect discovered, the benzoyl peroxide photolysis has become a unique process to detect and study all spin and magnetic effects in the free radical recombinations discussed in this book.

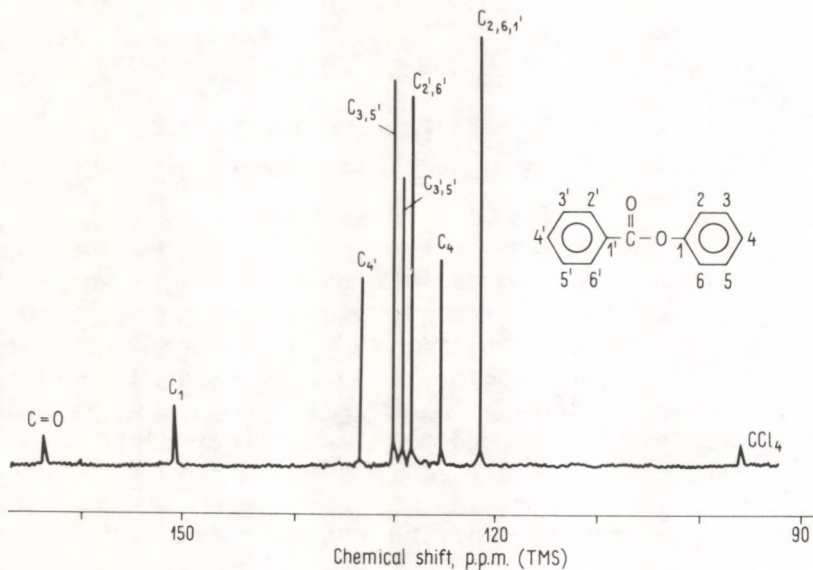


Fig. 6.1. ^{13}C NMR spectrum of phenylbenzoate isolated after completing of sensitized photolysis of benzoyl peroxide in CCl_4 (sensitizer: acetophenone)

Phenylbenzoate (2–3% yield) has been obtained from the reaction mixture after 30-hour photolysis of 0.1 M solution of benzoyl peroxide in CCl_4 (0.3 M acetophenone as a sensitizer) [6.6,7]. The ^{13}C NMR spectrum of the phenyl benzoate obtained as well as the signals assignment are given in Fig. 6.1. We have determined the relative content of ^{13}C in different phenylbenzoate positions on the ground of thorough analysis of relative line intensities in the NMR spectra; the results are listed in Ref. [6.2]. These show the ^{13}C content in position 1 to increase by $18 \pm 4\%$,⁴ which greatly exceeds the reported ^{12}C — ^{13}C isotopic effects [6.1] but is as expected on the basis of the ideas discussed and the reaction scheme.

The estimates show more than a two-fold increase in ^{13}C content in position 1 of product 1 in the system under investigation. Smaller isotope effects (about 18%) have been associated with the following factors [6.6,7]: (1) partial decomposition of peroxide from the excited singlet state resulting in singlet RPs; (2) the probability of product 1 formation at random encounters in the bulk.

So as to provide an additional evidence for the magnetic nature of the isotope effect, the thermal decomposition of benzoyl peroxide proceeding through singlet RPs has been studied [6.6, 7]. In this case the magnetic isotope effect must be much smaller. In full agreement with this theoretical prediction, no appreciable change of ^{13}C composition in position 1 has been detected [6.6, 7].

One more example of isotope effects has been obtained when studying photochemical decomposition of dibenzyl ketone (in benzene and hexane) [6.8]. The ketone photochemical decomposition occurs from the triplet state, giving a RP



Further transformations of the radicals are associated with the following reactions:



Mass-spectrometric analysis of dibenzyl ketone isotopic composition confirms [6.8] that the enrichment with ^{13}C isotope grows with the extent of ketone decomposition. According to the reaction scheme, isotope effects can arise in the pair $\text{C}_6\text{H}_5\text{CH}_2\dot{\text{C}}\text{O} \cdot \dot{\text{C}}\text{H}_2\text{C}_6\text{H}_5$. Here the “magnetic” pairs (involving ^{13}C magnetic isotopes) recombine faster than “nonmagnetic” ones involving ^{12}C . In agreement with the reported data [6.6, 7] the maximum enrichment with ^{13}C isotope will be observed for the central carbon atom since the hf interaction with the carbonyl carbon atom in the radical $\text{C}_6\text{H}_5\text{CH}_2\dot{\text{C}}\text{O}$ considerably exceeds all the other hf interactions in the pair ($A_c \approx 150$ G).

Experiments performed in magnetic fields of various strengths have provided additional evidence for the magnetic nature of the isotope effects [6.8]. The most

⁴ Analysis of ^{13}C NMR spectra for different species of commercial phenyl benzoate has been made for comparison.

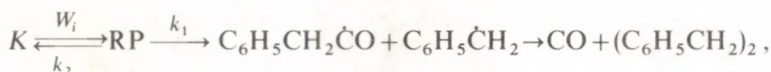
effective magnetic isotope enrichment is obtained in low magnetic fields when all the three singlet states contribute to singlet-triplet mixing; whereas in high fields only the S-T₀ channel is open. The effect of isotopic enrichment turns out to fall with increasing field intensity.

A remarkable ¹³C enrichment has been obtained in recovered dibenzyl ketone after partial photolysis in highly viscous solutions [6.10] and in micellar solution [6.11, 12]. This effect was interpreted in terms of an enhanced cage effect of radical pairs in micellar and viscous solutions.

We now discuss the relations between the magnetic isotope effect and isotope enrichment, which have been studied in most detail in dibenzyl ketone photolysis.

From qualitative considerations it transpires that the dibenzyl ketone isotope enrichment depends on the ketone conversion. We shall establish the quantitative ratio between these values.

The scheme of the photochemical decomposition of a ketone *K* can be presented as



where W_i is the rate of photochemical radical pair (RP) generation, k_1 is the RP dissociation rate constant, k_2 is the ketone regeneration rate constant.

The rate of RP generation is $W_i = n\nu$

where n is the number of the photons absorbed, $n = \Delta I = I_0 \{1 - \exp[-\epsilon l(K)]\}$, or, at low ketone concentrations when $\epsilon l(K) \ll 1$, $n = I_0 \epsilon l(K)$; ϵ is the molar extinction coefficient; l is the effective thickness of the sample; I_0 is the light intensity; ν is the quantum yield of RP generation; we set $I_0 \epsilon l \nu = \varphi$.

The photochemical decomposition rate of a nonmagnetic ketone is

$$-\frac{d(K)}{dt} = \frac{\varphi k_1}{k_1 + k_2} (K) = \psi(K)$$

that of a magnetic ketone (involving a ¹³C isotope in the carbonyl group) is

$$-\frac{d(K^*)}{dt} = \frac{\varphi k_1}{k_1 + k_2^*} (K^*) = \psi^*(K^*).$$

The only difference between magnetic and nonmagnetic radical pairs is that the former recombine faster than the latter, i.e. $k_2^* > k_2$. Let the ratio $k_2^*/k_2 = \gamma$, $\gamma > 1$. Then

$$(K) = (K_0) \exp(-\psi t)$$

$$(K^*) = (K_0^*) \exp(-\psi^* t)$$

and the enrichment δ is

$$\delta = (K^*/K) = (K_0^*/K_0) \exp[(\psi - \psi^*)t] = \delta_0 \exp[(\psi - \psi^*)t].$$

Substituting the expression for ψ gives

$$\lg S = \lg(\delta/\delta_0) = \left[\frac{k_2(1-\gamma)}{k_1 + \gamma k_2} \right] \lg(K/K_0)$$

or $\lg S = \alpha \lg F$, where S is the isotope enrichment, $F = (K/K_0)$, i.e. the fraction of unreacted nonmagnetic ketones.

The total conversion is measured by the ratio

$$f = \frac{(K) + (K^*)}{(K_0) + (K_0^*)}$$

where f is the total fraction of the unreacted ketones, the magnetic and nonmagnetic ketones included.

The quantities f and F are related by

$$F = \frac{1 + \delta_0}{1 + \delta} f.$$

It is obvious that $F = f$ for a natural isotope content in the ketone ($\delta \ll 1$, $\delta_0 \ll 1$); $F \neq f$ at the photolysis of enriched ketones.

Thus, the isotope enrichment and the conversion of a ketone must be connected by the universal relation

$$\lg S = \alpha \lg F.$$

The experimental data on isotope enrichment in dibenzyl ketone photolysis are summarized in Fig. 6.2; the universal dependence predicted theoretically is seen to be confirmed by experiment.

The value of α characterizes the efficiency of isotope enrichment; the absolute value of α is extremely small in nonviscous solvents and increases appreciably with viscosity and in micelles.

The expression for α is

$$\alpha = \frac{k_2(1-\gamma)}{k_1 + \gamma k_2}$$

or

$$\alpha = \frac{1-\gamma}{(k_1/k_2) + \gamma}.$$

The ratio k_1/k_2 characterizes the competition between the RP recombination and dissociation reactions

$$\gamma = (k_2^*/k_2) = (p^*/p),$$

where p^* and p are the probabilities of ketone generation from a magnetic and nonmagnetic radical pair which can be calculated theoretically from the S-T mixing rate.

For instance, for the pair $|\text{C}_6\text{H}_5\text{CH}_2^{12}\dot{\text{C}}\text{O}\dot{\text{C}}\text{H}_2\text{C}_6\text{H}_5|^{\text{T}}$ $p = 0.6 \cdot 10^{-3}$; for the pair $|\text{C}_6\text{H}_5\text{CH}_2^{13}\dot{\text{C}}\text{O}\dot{\text{C}}\text{H}_2\text{C}_6\text{H}_5|^{\text{T}}$ $p^* = 3.8 \cdot 10^{-3}$. Hence, $\gamma = 6$ and, setting $k_1/k_2 = 10^2$, we have $\alpha \approx -0.05$ which is in good agreement with experiment on benzene and hexane.

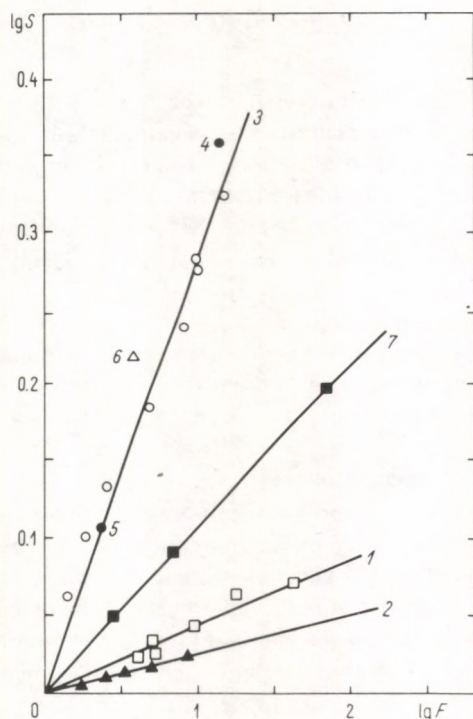


Fig. 6.2. Plots of isotope enrichment vs. conversion in coordinates $\log S/\lg F$ for dibenzylketone photolysis: 1 in hexane [6.11]; 2 in benzene [6.8]; 3 in hexadecyltrimethylammonium chloride micelles, ketone enriched with ^{13}C [6.11]; 4 in hexadecyltrimethylammonium chloride micelles, ketone with natural abundance of ^{13}C [6.11]; 5 in glycerol + tertbutanol (2:1) [6.12]; 6 in hexadecyltrimethylammonium bromide micelles [6.12]; 7 in hexadecyltrimethylammonium chloride micelles in 15 kG magnetic field [6.11]

The ratio k_1/k_2 can be computed from the RP molecular dynamics; it must reduce in viscous solutions and micelles. At $k_1/k_2=10$ and $\gamma=6$ $\alpha=-0.33$ which fits experiment on micelles and viscous solutions.

The theory discussed allows one to evaluate theoretically the magnitude of enrichment and to predict the requirements of maximum isotope enrichment.

Several experimental attempts to find isotope effects of magnetic nature for heavy elements were made according to [6.13].

In reactions investigated, magnetic effects may arise in the pair of two $(\text{CH}_3)_3\text{Sn}$ radicals.

The increasing of the magnetic isotope effect is favoured by the following factors: anomalous hf constants in trimethylstannyl radicals as compared to common organic radicals and relatively high natural contents of tin magnetic isotopes facilitating their analyses (see Table 5.6). Nevertheless, precise experiments did not indicate any isotope effects [6.13].

6.3 Reactions of radical-ions

Brocklehurst [6.14] did an interesting experiment detecting magnetic isotope effects immediately after an elementary step of geminate radical-ion recombination. The process of radical-ion formation was studied during radiolysis of aromatic molecules in hydrocarbon solvents (see Scheme 5.12). The fluorescence induced by the process $M^+ + M^- \rightarrow M + {}^1M^*$ (M and ${}^1M^*$ are the ground and singlet excited states of the aromatic molecules) was detected by scintillation pulse shapes measured by single-photon counting. By this technique one can measure the distribution of the time intervals between the moment of the scintillator excitation and that of single photoelectron formation at the photomultiplier cathode detecting scintillations. In other words, the frequency of photoelectron formation over a narrow time interval range is measured depending on the duration of a given time interval.

Brocklehurst [6.14] detected fluorescence of terphenyl- h_{14} and $-d_{14}$ in decalin and benzene. Figure 5.8 depicts plots of the fluorescence intensity ratio in a magnetic field (1600 G) and without it versus the time passed after the scintillator pulse. At short times the magnetic field effect is seen to be much higher in the case of terphenyl- h_{14} . This can be attributed to differences in the hf constants and thus the S-T conversion rates in radical-ion pairs of H- and D-containing terphenyls. The theoretical dependence of P_S (RP singlet character) is shown in Ref. [6.14]. The pleasing fit between the observed and calculated curves and also the trend of the field dependence is reliable evidence for the magnetic nature of the isotope effect.

Similar isotope effects on fluorescence have been observed in γ -radiolysis of solutions of naphthalene, anthracene, diphenyl, and their deuterated analogs (under stationary conditions) [6.15].

6.4 Conclusion

There are four remarkable features distinguishing the magnetic isotope effect from the ordinary classical isotope kinetic effect which arises due to the difference in isotopic nuclear masses.

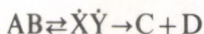
1. In contrast with the classical isotope effect, the magnetic isotope effect is manifested only in reactions involving RP formation and recombination.

2. The magnetic isotope effect can reach an order of several percentage units (an order of several percent for heavy nuclei of the type ${}^{13}\text{C}$, ${}^{17}\text{O}$, ${}^{15}\text{N}$, etc.) while the classical effect is usually much less.

3. The classical isotope effect is not sensitive to the magnetic field, while the magnetic effect shows a strong magnetic field dependence: it decreases with increasing of field because in high fields T_+ and T_- levels are switched off the singlet-triplet evolution. In high fields only the S- T_0 channel is effective, while in low fields all the three channels are open simultaneously.

4. The magnetic isotope effect depends on the hf energy, the spins and magnetic moments of the nuclei, and the parameters characterizing the RP molecular dynamics (solvent viscosity, radical diffusion coefficient, etc.).

The magnetic isotope effect can often influence the classical effect, distorting its magnitude. For instance, in the reaction $AB \rightarrow C + D$ the isotope effect is referred usually to the difference in masses. However, if the reaction goes via radicals according to the scheme



then the total isotope effect measured experimentally is in fact a superposition of both effects. Therefore, the conclusions drawn from the isotope effects (both primary and secondary) must be treated critically.

The discovery of magnetic isotope effects is of fundamental importance. The new isotope effect is sensitive not to the *mass* isotopic nuclei but to their *magnetic properties*. It is the basis of a new method of investigating mechanisms of chemical, geochemical, and biochemical processes [6.16].

This effect throws new light upon many problems of geochemical genesis of oils, minerals, and ores and also on the cosmogological problem of the origin and evolution of a substance.

Thus, the well-known anomalies in oxygen isotope contents in carbon chondrites [6.16] are perhaps associated with magnetic isotope effects rather than having a nuclear-genetic origin as it has been considered so far.

The well-known anomalies of ^{13}C isotope contents in a number of molecules discovered in interstellar space can be also explained in terms of magnetic isotope effects. These effects can take place in chemical reactions occurring on the surface of dust particles.

Note, in conclusion, that magnetic isotope effects can be applied to isotope separation. This method to separate isotopes differs essentially from the well-known techniques: none of them employs different magnetic isotope properties for enrichment. The proposed technique of isotope separation is especially useful in the case of heavy isotopes with small mass differences.

It should also be emphasized that the discovery of the magnetic isotope effect can be regarded as a unique possibility to separate nuclear isomers which are known to differ both in spins and hf energies, this difference sometimes being sufficiently great. For example, the spins of the isotope ^{119}Sn and its isomer $^{119\text{M}}\text{Sn}$ are equal to $1/2$ and $11/2$ respectively. Thus, according to theory, one can expect nuclear isomer selection effects in different radical reaction products. On the other hand, experimental investigations on the efficiency of nuclear isomer separation in such reactions can, probably, be of great help to determine the magnetic moments of nuclei in excited states [6.13].

7 CHEMICALLY INDUCED DYNAMIC NUCLEAR POLARIZATION

7.1 Experimental observations and detection of CIDNP

7.1.1 High magnetic fields

The nonequilibrium population of Zeeman nuclear levels is preserved in molecules for a time T_n (about 1–100 s). Hence, to observe and detect CIDNP, the reaction must be performed in the probe of an NMR spectrometer. Thermal reactions are the simplest for this purpose: in this case no new spectrometer modification is needed. The CIDNP kinetics are usually studied by repetitive scans of either the whole spectrum or some of its portions. An example of such a record is depicted in Fig. 7.1 (another one is in Fig. 7.2). The reaction rate constants, polarization coefficients, and relaxation times can be found by the CIDNP kinetic equations [7.1].

Buchachenko *et al.* [7.2] have proposed the technique of *pulse saturation and reversal* of the CIDNP signal which allows the nuclear relaxation times to be determined independently.

When studying photo-induced nuclear polarization, the light can be delivered to the sample either by light pipes (using a nonmodified NMR spectrometer) or through a special hole in the probe. A detailed description of this technique is reported in Refs [7.3–5].

Flow systems are often used to observe CIDNP; in this case, mixing the reagents and the reaction itself are performed in the same magnet and then a fast flow brings the mixture into the NMR spectrometer probe. The same technique is applied to observe CIDNP in fast reactions, e.g., in the redox system Ti^{3+} - H_2O_2 -*i*- $\text{C}_3\text{H}_7\text{OH}$ [7.6]. Since the field of the additional magnet, where the reaction runs, can be varied, this technique is used to study the field dependence of CIDNP. Lawler and Halfon [7.7] described a flow apparatus designed for this purpose.

Analogous equipment was used by Trifunac *et al.* [7.8–9] to investigate the CIDNP in radiation chemical processes. The additional magnet had a hole to introduce a beam of fast electrons (e.g. from a Van der Graaf accelerator). The only requirement general for all flow systems is that the time of the sample transfer from the additional magnet to that of the spectrometer must be shorter than the nuclear relaxation time.

Fisher and Laroff [7.10] proposed a unique method to observe CIDNP. It is known that if a two-level system is acted on by an instantaneous high coherent oscillating field at the frequency of transitions between the levels, then the system approaches a new stationary state through decaying oscillations (transient

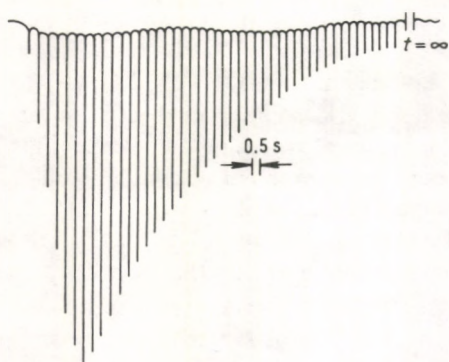


Fig. 7.1. ^{31}P phosphate CIDNP kinetics in cyclohexylperoxidicarbonate decomposition in the presence of phosphite [7.74]

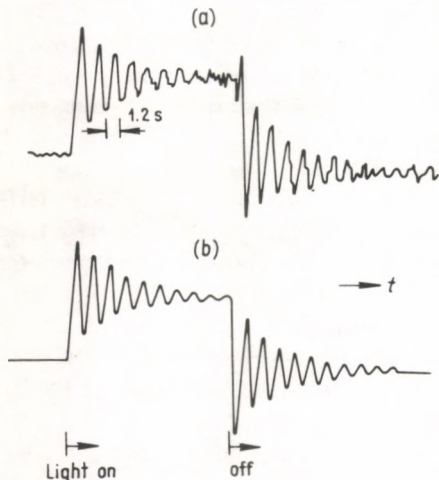


Fig. 7.2. Nonstationary emission signal mutations of tert-butyl chloride observed experimentally in course of photolysis of di-tert-butyl ketone (a); nonstationary nutations calculated by the Bloch equation (b) [7.10]

processes). Torrey [7.11] was the first to observe such oscillations in NMR spectroscopy, later they were discovered in lasers and in microwave spectroscopy. In NMR, the transition oscillations are the initial phase of the magnetic vector precessional motion and are manifested in transient nutations superimposed on the vector precession around the magnetic field direction.

NMR nutations can be induced by an instantaneous change of one of the three parameters: the external field H_0 , the radiofrequency field H_1 , and the resonant frequency ω . There is one more way to induce nutations proposed in Ref. [7.10]: a sudden change of the magnitude of magnetization vector by creating non-equilibrium level populations by CIDNP.

Figure 7.2 depicts the nutation signals for tert-butyl-chloride emission line at di-tert-butyl ketone photolysis in CCl_4 . These arise at the moment of switching on the light, i.e., when the nonequilibrium magnetization appears, then decay and reach their stationary values corresponding to the negative magnetization of tert-butyl chloride protons. After the irradiation is switched off, the CIDNP vanishes, the magnetization relaxes to a new stationary value and its fast changes again induce nutations. The nutations having decayed, the signal reaches an equilibrium value corresponding to zero magnetization. It means that no tert-butyl chloride is formed during the photolysis, and the nutations are induced only by the magnetization resulting from CIDNP.

The nutation frequency is determined by the equation

$$\rho\omega_1 = [\omega_1^2 - 0.25 \cdot (1/T_1 - 1/T_2)^2]^{1/2}$$

where $\omega_1 = \gamma H_1$ and T_1 and T_2 are nuclear relaxation times. If the generation of the nonequilibrium magnetization is not continuous, as in the above case, but occurs by periodic pulses with a frequency $\omega_m = \rho \omega_1$ the stationary nutations can be observed by phase sensitive detection. The pulse periodic conditions for the generation of nonequilibrium magnetization can be realized by way of the reaction rate modulation with the frequency ω_m (e.g., by intermittent irradiation). These conditions have been realized at di-tert-butyl ketone photolysis [7.10]. Figure 7.3(a) shows the change of the tert-butyl chloride NMR signal under continuous photolysis; the emission signal arising at the moment of switching on of the light is seen to gradually decrease and in fact disappear at the moment of switching off of the light. The signal intensity is then determined by the total contribution of the emission and absorption of the molecules formed. Figure 7.3(b) depicts the stationary nutation signals at the reaction modulation with the frequency of intermittent radiation $\omega_m = 0.92 \omega_1$. In this case the nutation signals correspond to the emission frequency and disappear just after the light is switched off.

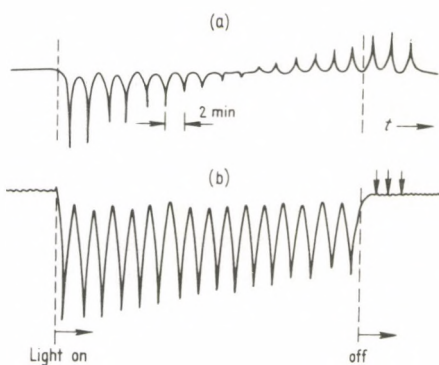


Fig. 7.3. Tert-butyl chloride CIDNP kinetics under stationary irradiation of di-tert-butyl ketone (a); and stationary nutations in discontinuous photolysis (b) [7.10]

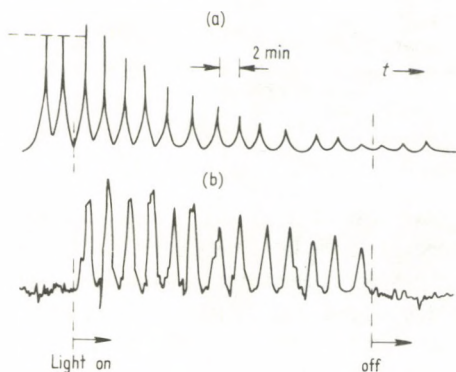


Fig. 7.4. NMR signal kinetics of di-tert-butyl ketone at its stationary photolysis (a) and its non-stationary nutations under discontinuous light (b) [7.10]

An analogous example is given in Fig. 7.4 for the case of the CIDNP of the starting material—di-tert-butyl ketone. Under steady-state irradiation, positive polarizations can barely be observed under intermittent irradiation (Fig. 7.4 (b)), but the stationary nutation signals induced by the CIDNP contribution to the magnetization are clearly seen.

The stationary nutation technique allows one to distinguish between the signals of polarized and nonpolarized nuclei in the CIDNP spectra. It is especially useful to detect weak CIDNP signals overlapped by intensive signals of solvent, starting reagents or nonpolarized products.

We now consider briefly the pulse NMR Fourier spectroscopy developed to detect CIDNP. It has some advantages over the standard stationary NMR technique.

The main peculiarity of the Fourier spectroscopy refers to the homonuclear spin systems interconnected by spin-spin coupling. If such systems are not in thermodynamic equilibrium the NMR signal intensity will be strongly dependent on the angle of rotation α of the magnetic vector induced by radiofrequent pulses. In conventional c.w. NMR, the signal intensity is proportional to the population difference of the levels connected by the transitions observed. In the case of Fourier spectroscopy, a pulse excites the spin system as a whole and, hence, the intensities of the lines depend on the populations of all the levels, the relationship between the line intensities and level populations being greatly complicated at large angles α . The intensities are directly proportional to the populations only at small α ; for the sake of accuracy, α must not exceed $10\text{--}20^\circ$.

The intensity distortions at large α greatly affect the multiplet CIDNP in homonuclear spin systems. At $\alpha = 90^\circ$ the multiplet CIDNP is completely averaged by the pulse and cannot be detected by Fourier spectroscopy.

However, this restriction has nothing to do with net and multiplet nuclear polarizations in heteronuclear spin systems (e.g., in the spin multiplet of the nucleus ^{13}C of a methane molecule). The advantages of Fourier spectroscopy are high sensitivity and the possibility of measuring nuclear relaxation times by CIDNP kinetics rapidly changing in time. Figure 7.5 depicts an example of ^{13}C CIDNP spectra of dibenzyl ketone photochemical decomposition products.

The theory and principles of the Fourier spectroscopy as applied to CIDNP have been explored in Refs [7.13–15].

CIDNP provides information on chemical events taking place on time scales ranging from 10^{-8} to 10^{-3} s. But the long relaxation times of diamagnetic reaction

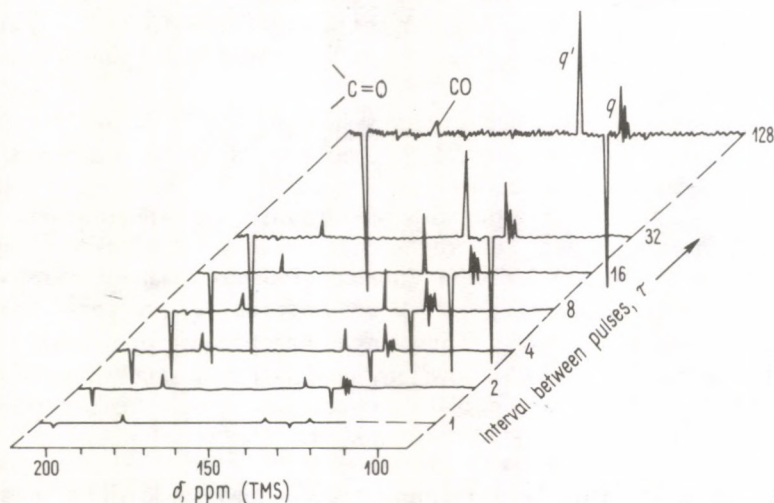


Fig. 7.5. Set of ^{13}C photo-CIDNP spectra in dibenzyl ketone decomposition obtained by the Fourier spectroscopy technique; τ is the time interval between pulses (q and q' are lines referring to quaternary carbon atoms of dibenzyl-ketone and dibenzyl) [7.12]

products under steady-state conditions hinder the carrying out of direct kinetic analysis. The first examples of time-resolved CIDNP with resolution of $1 \cdot 10^{-6}$ s were reported in [7.16]. The experimental procedure, which is applicable to any system in which photolysis creates a RP, is the following. The sample is placed in the probe of high resolution NMR spectrometer. The saturation pulse of ≈ 50 ms duration totally destroys the initial nuclear magnetization. The sample is then irradiated by a laser flash lasting several nanoseconds. The excited molecules generate RP's, which induce CIDNP by geminate or random recombination. The laser pulse is followed at any desired time interval τ , by an RF pulse creating a transverse magnetization. The resultant free induction decay of the polarized products formed on the application of the sampling radiofrequency pulse is collected and the entire sequence is repeated ($\geq 10^3$ times) to achieve a sufficient signal to noise ratio. The time resolution of these experiments is determined by the duration of the radiofrequency pulse, which is currently $1 \cdot 10^{-6}$ s. In order to obtain more detailed kinetic information it is necessary to reduce the duration of the RF pulse.

7.1.2 Low magnetic fields

In experimental studies of low field CIDNP one usually uses the technique of sample "transfer": reactions are carried out in a separate magnet, then the sample is rapidly transferred either by hand [7.17] or by a flow system [7.7] to a NMR spectrometer probe to detect the polarization. The rate of the sample "transfer" must exceed the nuclear relaxation rate in the reaction products. There are practical difficulties associated with rapid quenching of the reaction, i.e., with a fast cooling of the sample before its "transfer". Moreover, the process of transfer itself may distort the polarization pattern in low magnetic fields. Below we mention the main factors causing distortions.

First, the eigenstates of the nuclear spin system in the field where the reaction occurs can differ from those in the NMR spectrometer field. The sample transfer from H_p to H_0 field occurs adiabatically if the eigenstates of the spin system remain constant. For two groups of protons with the constant of spin-spin interaction J_{nn} , the nuclear-spin state mixing is determined by the values $1/2 J_{nn}$ (matrix element which mixes the two states). To observe the conditions of adiabatic transfer, the transfer time must exceed $\tau = (2\tau \cdot 1/2 J_{nn})^{-1}$. On substituting a typical value of $J_{nn} = 7$ Hz one obtains $\tau = 0.05$ s. Thus, this estimate shows the transfer to be practically always adiabatic. Deviations may appear either at small values of J_{nn} or at a high rate of transfer. When the adiabatic conditions are violated, the correlation diagrams, relating the nuclear spin states in H_p and H_0 fields, must be computed strictly.

The second factor is that a fast sample transfer may cause violation of the adiabatic conditions, and, thus, the total magnetization vector lags behind the direction of the external field which, in general, varies from 0.5 G to tens of thousands of Gauss. In this case an adiabatic change means that the field varies

negligibly within the Larmour precession period $(\gamma H)^{-1}$. It can be readily shown that even at $H=1$ G this can be realized provided the transfer time exceeds $3.7 \cdot 10^{-5}$ s which is practically always observed. Note that the adiabatic condition discussed has been corroborated experimentally [7.18]. For that purpose, a scheme involving a fast single-acting switch of magnetic field (13 G) direction was used. Thermal decomposition of benzoyl peroxide was performed in a constant magnetic field of 13 G. Then the magnetic field direction was altered within a short time and the sample was transferred to the probe of a NMR spectrometer. The CIDNP kinetics observed for various switching times τ is shown in Fig. 7.6. It is seen that the polarization sign alters at $\tau = 10 \pm 3 \mu\text{s}$, (4) whereas at $\tau = 40 \pm 3 \mu\text{s}$ (2) and $25 \pm 3 \mu\text{s}$ (3) a slight decrease in the intensity is observed. On the other hand, the adiabatic condition shows that, in this case, the magnetization vector direction and thus the polarization sign alternation must occur in $\tau < 20 \mu\text{s}$ (4). Thus, the experimental and theoretical data coincide.

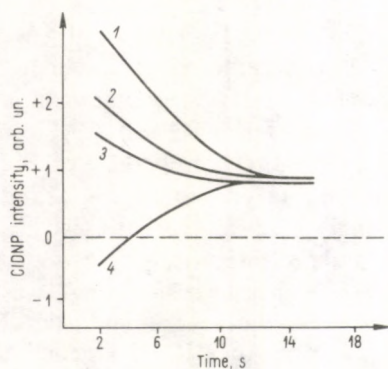


Fig. 7.6. Influence of the time of changing $H=13$ G field direction on ^1H CIDNP effects of benzene in thermal benzoyl peroxide decomposition in solutions [7.18]

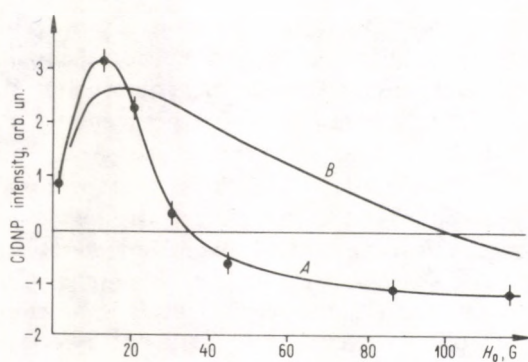


Fig. 7.7. Magnetic field effect on benzene ^1H CIDNP intensity in thermal benzoyl peroxide decomposition in solution: A — by direct observation; B — by the sample transfer method [7.21]

The above difficulties of experimental studies of low field CIDNP were obviated by direct detection of polarizations with a NMR spectrometer specially designed for that purpose (one which involved no sample transfer) [7.19–22]. The nuclear spin echo signal was observed either in the earth's field or in a field H_0 (0.2–10 G) created by Helmholtz coils. The homogeneity of the H_0 field ensures a signal echo duration of 100 ms. If necessary, another pair of Helmholtz coils could be used to create a "polarizing" field of 10–200 G. The reaction was performed in a field H_p , whereas during the echo registration cycle this field was cut off within a time 1 ms–5 s. In all experiments on direct observation of low field nuclear polarizations [7.19–22] the signal/noise ratio was not worse than 5–10:1 and the signal echo duration attributed to the inhomogeneity of the earth's magnetic field within the sample, was not less than 0.1 s.

The method of direct CIDNP observation allowed one to solve the problem of whether the techniques of sample transfer give an adequate picture of low field polarization. For that purpose the field dependences of the polarized signal intensity of benzene in the reaction of benzoyl peroxide thermolysis obtained by the direct technique were compared with those obtained by the sample transfer method. The curves obtained are plotted in Fig. 7.7. It is seen that in low fields in both cases an absorption signal is observed with the maxima approximately coinciding. At the same time, appreciable differences in the trends of the curves are observed in the region of the polarization sign alteration.

The above example, as well as a number of other experiments [7.23], shows that the sample transfer technique correctly depicts the position of CIDNP maxima; direct observation, however, is necessary to describe in detail the field dependence of low field polarizations. One must therefore be very careful in determining the g -values from the crossover point of low field CIDNP in transfer experiments (see [7.24]).

An important feature of the direct observation of low field CIDNP is the absence of the solvent signal which can distort the signal in the transfer technique. Note that in the experiments on the direct observation of low field CIDNP, large polarization coefficients were observed experimentally. For instance, in a field of 10 G the polarization coefficient reached $10^4-3 \cdot 10^4$. Such large values considerably exceed those observed in high fields and (without account taken of relaxation and generation and decay radical kinetics) convincingly confirm that the CIDNP mechanism cannot be explained by the Overhauser effect in radicals.

The technique of determining the absolute CIDNP amplification coefficient. As was noted, the absolute coefficient E is an important qualitative characteristic of CIDNP. To determine E experimentally, one usually studies the CIDNP kinetics. A disadvantage of this approach is, however, the requirement of precise control over the nuclear relaxation characteristics of the reaction products, and this is possible only for relatively simple spin systems. Hence, the E values obtained by this method are only estimates.

To overcome the above difficulties, one can employ pulse methods which allow one to obtain the desirable values directly from the polarized NMR signal intensity. In this case there is no necessity to control precisely the nuclear-relaxation parameters of the reaction products. The first version of this technique in low fields [7.22] includes pulse photo-excitation of the reaction realized by a pulsed ISP-2000 lamp with a flash energy of 1000–2000 J, and the subsequent detection of the polarized spin echo signal with an NMR spectrometer. The total excitation time, equal to the flash duration (2–5 ms) and the NMR signal detection (0.4 s), was much less than the nuclear relaxation time of a number of diamagnetic compounds (5–10 s). The value of E can be then determined directly by the intensity ratio between the polarized and equilibrium signals of the product.

7.2 Experimental basis of the CIDNP theory

7.2.1 High magnetic fields

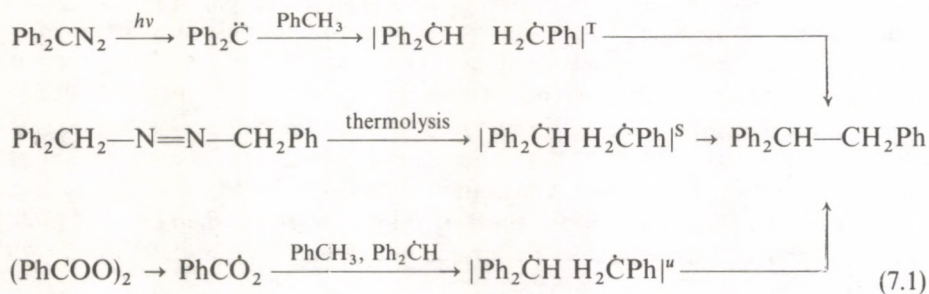
Singlet-triplet conversion of a radical pair involving S and T_0 states has been shown to be the most effective CIDNP mechanism in high magnetic fields, since the projection of the total electron spin of the radicals does not change during the conversion, that of the nuclear spin must not change either (as follows from the law of conservation of the electron-nuclear angular momentum). Hence, the nuclear spins do not reorientate in an S- T_0 transition but they are selectively distributed: radical pairs with one nuclear spin orientation preferentially recombine, those with the opposite orientation dissociate. Thus, the role of chemical reactions in high magnetic fields is to select the radicals by their nuclear spin states.

CIDNP theory in high magnetic fields predicts that the polarization sign must depend on the spin multiplicity of the radical pair and hence on the precursor spin multiplicity. It must also depend on the magnitude and the sign of the difference in the g -values, the sign of the hyperfine electron-nuclear interaction constant, the sign of the nuclear spin-spin coupling constant, and on the type of the radical pair.

Numerous experimental investigations confirm all the statements and conclusions of the theory. This section will consider only a few of these proofs.

Spin multiplicity. The first experimental evidence for the fact that the spin multiplicity of a radical pair determines the nuclear polarization sign was obtained by Closs [7.25, 26] and prompted the idea of singlet-triplet evolution in radical pairs which makes the basis of the modern CIDNP theory.

A radical pair $\text{Ph}_2\dot{\text{C}}\text{H H}_2\dot{\text{C}}\text{Ph}$ is formed in three ways (see the scheme): (a) diphenyldiazomethane photolysis in toluene with diphenylcarbene generation with triplet ground state; the subsequent reaction of triplet carbene with toluene gives a triplet radical pair; (b) thermal or photochemical azocompound decomposition occurs in the singlet state and gives a singlet radical pair; (c) finally, at the thermal decomposition of benzoyl peroxide in the mixture of toluene and benzoyloxy diphenylmethane, the radicals react with the solvent molecules giving radicals $\text{Ph}\dot{\text{C}}\text{H}_2$ and $\text{Ph}_2\dot{\text{C}}\text{H}$; the following random diffusion encounters of these radicals result in radical pairs with uncorrelated spins.



Since both radicals have almost equal g -factors, the molecule $\text{Ph}_2\text{CH}-\text{CH}_2\text{Ph}$ resulting from the pair recombination must, according to the theory, show a CIDNP multiplet effect with a sign that alters on varying the spin multiplicity. Indeed, experimental CIDNP spectra of $>\text{CH}-\text{CH}_2-$ fragment (Fig. 7.8) confirm these predictions: the molecule originated from a triplet pair carries AE polarization (Fig. 7.8 (a)), that from a singlet pair EA polarization (Fig. 7.8 (b)). The nuclear polarization of the molecule originated from an uncorrelated radical pair (Fig. 7.8 (c)) coincides in sign with that from a triplet pair (in line with the theory).

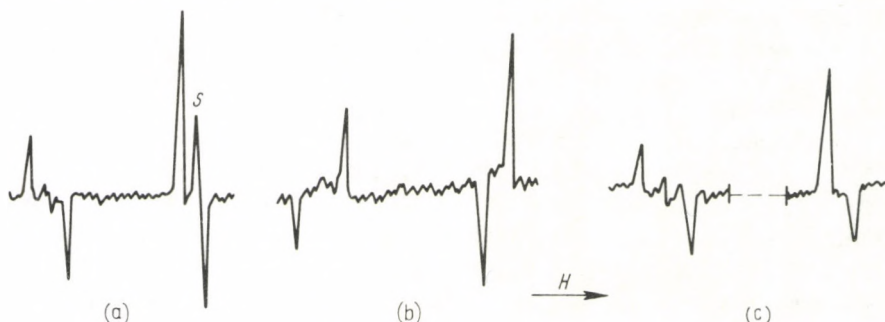
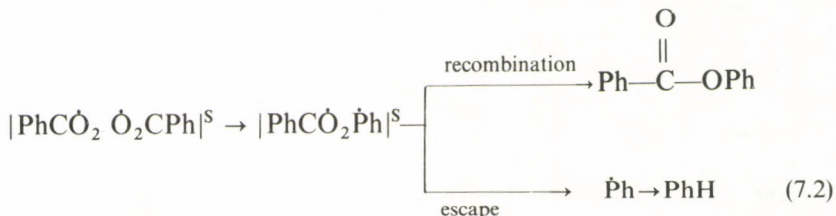


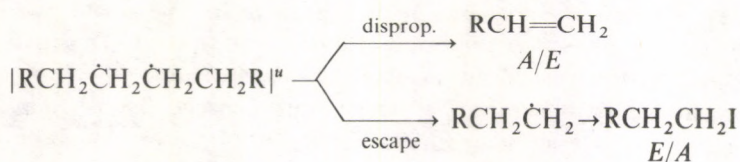
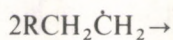
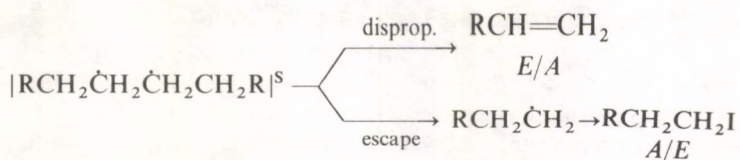
Fig. 7.8. NMR spectra for benzyl protons of 1,1,2-triphenyl-ethane molecules generated from triplet (a), singlet (b) and diffusion (c) pairs [7.25]. S denotes the NMR line of ^{13}C satellite of solvent

Benzene molecules formed on thermal and photochemical benzoyl peroxide decomposition induce emission in CIDNP spectra. Peroxide decomposition follows the scheme



Nuclear polarization arises in the secondary singlet radical pair ($\text{PhCOO} \dots \text{Ph}$) ^{S} where $\Delta g \neq 0$; as predicted by the theory, net polarization must be expected in the product. This prediction has been confirmed experimentally. Moreover, on peroxide photolysis in the presence of ketones, which sensitize peroxide decomposition via the triplet state and triplet radical pairs, the benzene molecules carry positive polarization [7.4, 27]. In this case the precursor's spin multiplicity alteration leads to the nuclear polarization sign reversion (Fig. 7.9).

A good example of the multiplet effect sign alteration is shown in Fig. 7.10 [7.28]. Molecules with polarized nuclei are formed in the reaction of n -butyllithium with n -butyl iodide which runs by the scheme:



(7.3)

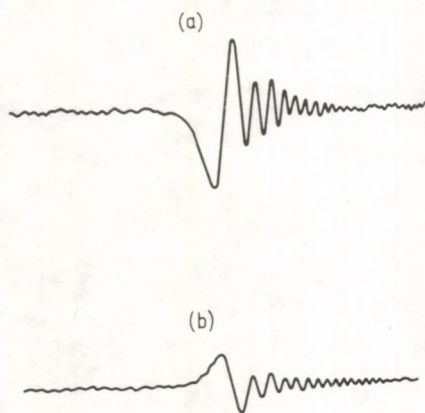


Fig. 7.9. NMR spectrum for benzene generated from benzoyl peroxide in direct photolysis (a) and photosensitized decomposition in presence of deuterioacetophenone (b). Emission in (a) is seen to be substituted by absorption in (b) [7.27]

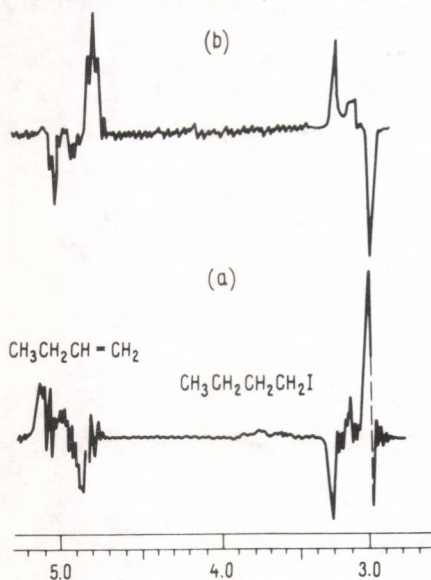
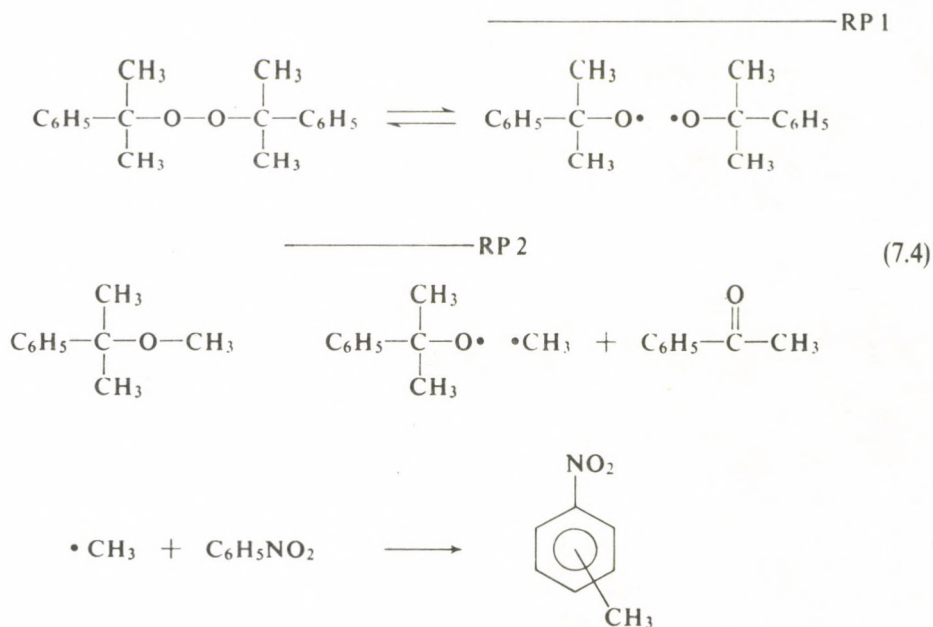


Fig. 7.10. CIDNP spectra of the reaction products of *n*-butyl-lithium with *n*-butyl iodide: (a) in the absence and (b) in the presence of radical acceptors [7.28]

In the primary singlet radical pair $\Delta g=0$ and, as expected, in the conversion products only multiplet CIDNP is observed: n-butylene formed by disproportionation carries *EA* polarization, while the escaping radicals transform into butyl iodide molecules with *AE* polarization. A portion of the escaping radicals experiences random encounters in pairs with uncorrelated spins and yields the same products, but oppositely polarized. In the absence of radical scavengers the experimentally observed polarization is the sum of both contributions that made by uncorrelated pairs being greater (Fig. 7.10a). In the presence of radical scavengers (2-hexene) the contribution of uncorrelated pairs vanishes, the polarization is created only in the primary singlet pairs (Fig. 7.10b), which causes the CIDNP sign inversion.

The possibility of the existence of spin-uncorrelated geminate radical pairs has been proved in [7.29]. If in a successive transformation of a radical pair, $R_1 \cdot \cdot R_2 \rightarrow R'_1 \cdot \cdot R'_2$, one of the partners of an initial pair (or both) has a short electron relaxation time, then the CIDNP sign will be independent of the initial multiplicity of the pair (S or T). To discriminate between such uncorrelated geminate pair ($R'_1 \cdot \cdot R'_2$) from random *F*-pairs, the symbol *F** has been proposed. The first experimental evidences for the existence of *F**-pair have been obtained in [7.30]. During thermal decomposition of cumene peroxide in nitrobenzene (0.5 M–1M) at temperature 150–170 °C, an overall polarization of the methyl protons has been observed. A maximum positive polarization has been registered for OCH_3 -protons of methyl ester. The signals from methyl protons of *ortho*- and *para*-nitro-toluenes are polarized negatively. The scheme of the above reaction can be represented as follows

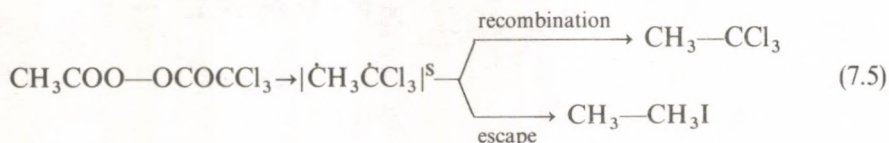


The CIDNP effects appear in RP 2, whose partners have quite different g -factors. The analysis of the CIDNP sign has shown that, unlike acyl peroxide thermolysis, RP 2 has triplet character. Note that the negative net polarization of methyl carbons in compound (1) observed in ^{13}C NMR spectrum corroborates this conclusion. The triplet character of RP 2 is associated with the fact that cumyloxy radicals have a short electron relaxation time T_2 (RP 2 is an F^* -pair). The CIDNP effects observed can be readily interpreted provided $\tau^{-1} < T_2^{-1} < \Delta g\beta H$ (τ — is the RP 1 lifetime, Δg — is the difference of g -values in RP 2).

The precursor spin multiplicity dependence of the sign of CIDNP is of fundamental importance for identifying chemical reaction mechanisms.

Nuclear polarization in geminate recombination and escape products. As predicted by the theory, the sign of nuclear polarization in geminate recombination (or disproportionation) escape products must be opposite. Indeed, in the above case, n -butyl radicals disproportionating in a singlet pair induce EA polarization in n -butylene, while the radicals avoiding both recombination and disproportionation in the primary pair escape into the bulk solution and induce AE polarization in the butyl iodide molecules (Fig. 7.10a). The same sign inversion is characteristic of CIDNP in uncorrelated pairs (Fig. 7.10b).

There are many such examples. Thus, at $\text{CH}_3\text{COO—OCOCCl}_3$ peroxide decomposition in the presence of iodine



the methyl group protons in the geminate recombination products are negatively polarized, while methyl iodide protons of escape products, are positively polarized (Fig. 7.11). In acetyl peroxide decomposition, the geminate recombination products (methyl acetate, ethane) show emission in the proton NMR spectra. The reaction products of the escaping radicals (methane, methyl chloride) are positively polarized (Fig. 7.12) [7.32].

In benzoyl peroxide decomposition opposite signs of ^{13}C nuclear polarization are observed in the recombination (phenyl benzoate, diphenyl) and escape (benzene, CO_2) products (Fig. 7.13) [7.33]. It is also the case for acetylbenzoyl peroxide decomposition [7.34]: in the recombination products (PhCOOCH_3 , PhCH_3) the methyl radicals induce a positive polarization of ^{13}C nuclei, in the escape products (CH_4 , CH_3Cl) the polarization is negative (Fig. 7.14). An analogous sign inversion is characteristic of proton polarization too: it is negative in the recombination products (PhCOOCH_3 , toluene, ethane), and positive in the escape products (benzene, methane, methyl chloride) (Fig. 7.15).

In the reaction of ethyl lithium with ethyl iodide occurring according to the scheme (7.10)

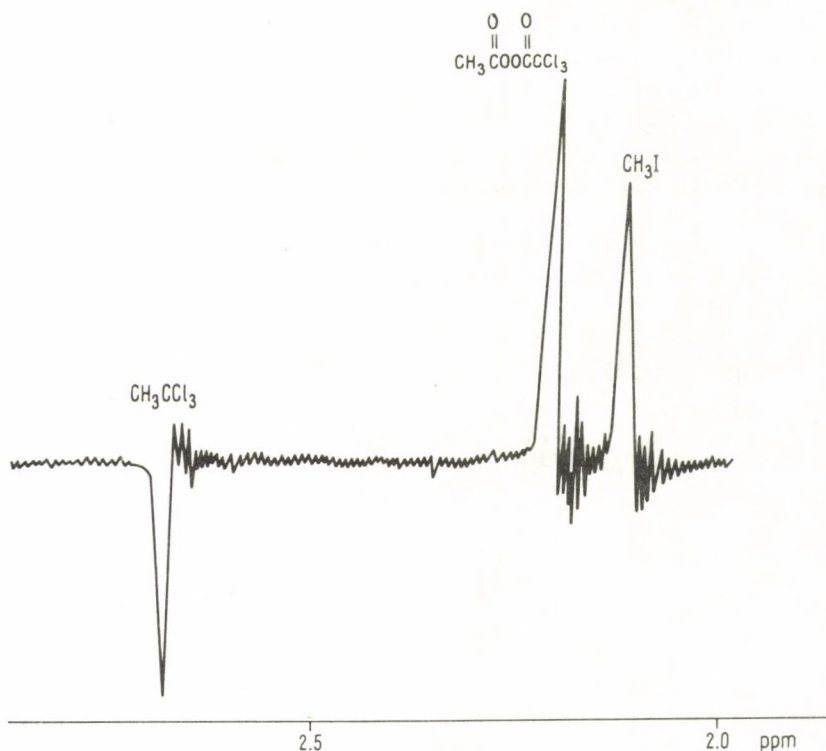
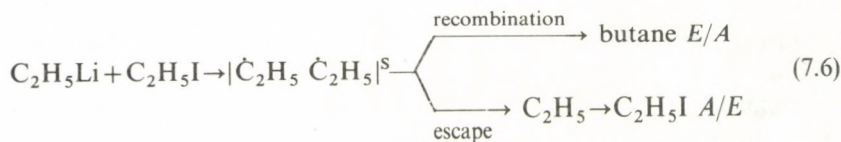


Fig. 7.11. CIDNP spectrum for the products of thermal decomposition of $\text{CH}_3\text{CO}_2\text{O}_2\text{CCCl}_3$ in CCl_4 in the presence of iodide [7.31]

the recombination product—butene—has *EA* polarization whereas ethyl iodide molecules, generated from the escaping radicals have *AE* polarization (Fig. 7.16).

The dependence of the nuclear polarization sign on the type of chemical reaction which yields molecules is an important property of CIDNP, and is used in chemistry to identify chemical reaction mechanisms and chemical transformation sequences.

CIDNP dependence on radical Zeeman energies. The theory predicts the dependence of CIDNP sign on the sign of Δg , which in turn determines the difference of Zeeman energies $\Delta g\beta H$ in the radical pair; the net polarization manifesting itself if $\Delta g \neq 0$. If $\Delta g = 0$ only the multiplet effect is observed. Indeed, in reactions of alkylhalides with alkyl lithium, CIDNP arises in alkyl radical pairs with

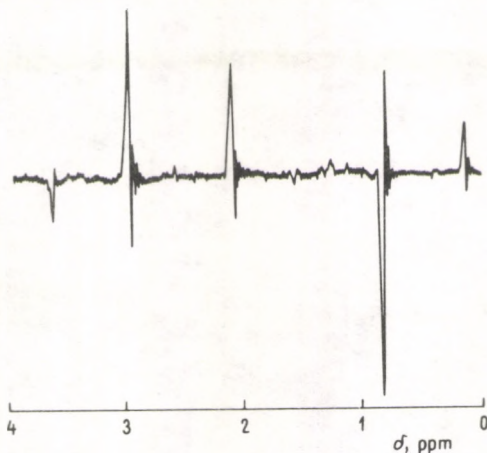


Fig. 7.12. 60 MHz spectrum taken during decomposition of 0.1 M acetyl peroxide in hexachloroacetone at 110°C [7.17]

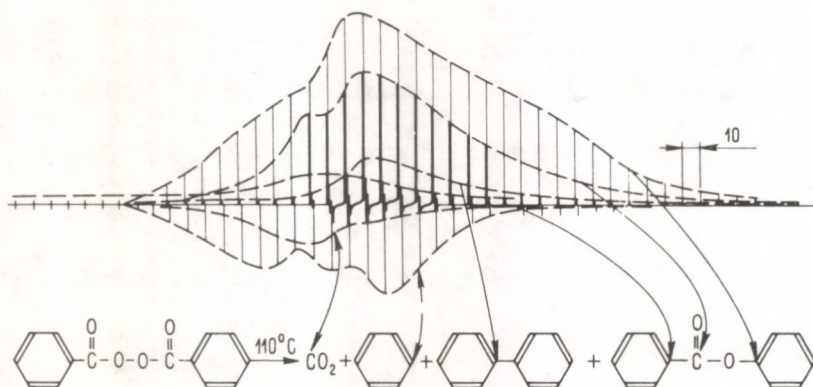


Fig. 7.13. ^{13}C CIDNP spectrum for the products of thermal benzoyl peroxide decomposition recorded repeatedly (10 s intervals) during the reaction [7.33]

similar g -factors; and it is only the multiplet polarization that is observed in the recombination products of these pairs (Figs 7.10, 7.16). In the decomposition of acetyl peroxides $\text{RCOO—OCOR}'$, the primary acyloxy radicals readily decompose yielding CO_2 ; hence, the main contribution to the CIDNP comes from the radical pairs $|\dot{\text{R}} \ \dot{\text{R}}'|$ with $\Delta g=0$. Thus the acylperoxide decomposition products show only multiplet CIDNP. Decomposition of benzoyl peroxide or peroxides of the type PhCOO—OCOR gives long-living $\text{PhCO}\dot{\text{O}}$ radicals, that is why the radical pairs $|\text{PhCO}\dot{\text{O}} \ \dot{\text{P}}\text{h}|$ or $|\text{PhCO}\dot{\text{O}} \ \dot{\text{R}}|$ with $\Delta g \neq 0$ make the basic contribution to CIDNP. The foregoing accounts for the net polarization in the radical recombination products (Figs. 7.9, 7.11–7.15).

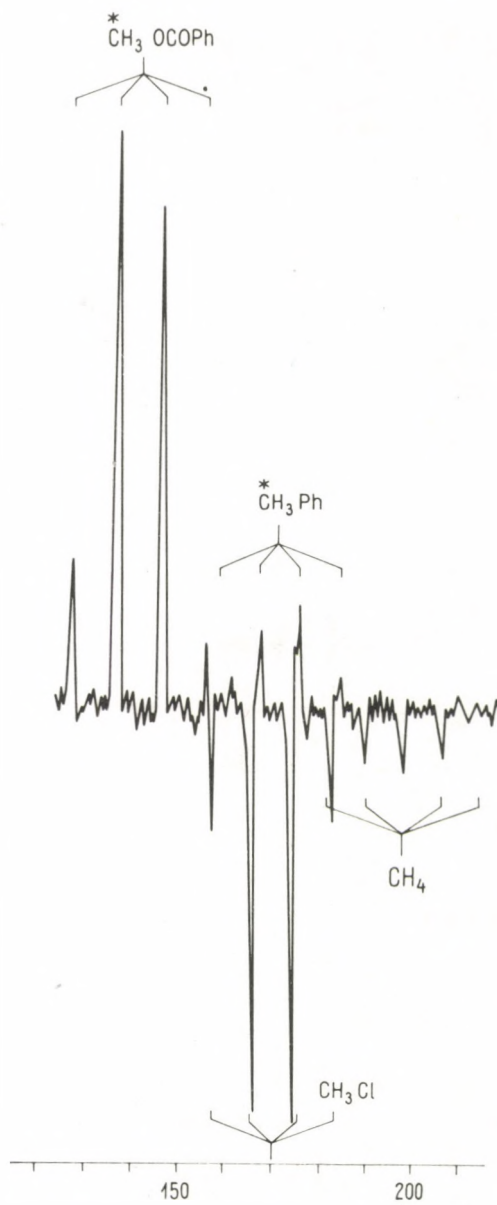


Fig. 7.14. ^{13}C CIDNP spectrum for the products of thermal acetylbenzoyl peroxide decomposition in tetrachloroethylene at 110°C [7.34]. Polarized nuclei are denoted by asterisks

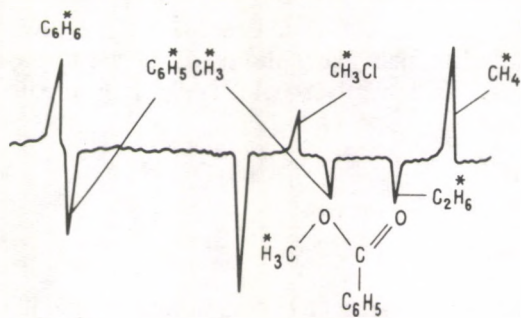


Fig. 7.15. CIDNP spectra for the products of thermal acetylbenzoyl peroxide decomposition recorded during the reactions [7.34]. Polarized protons are denoted by asterisks

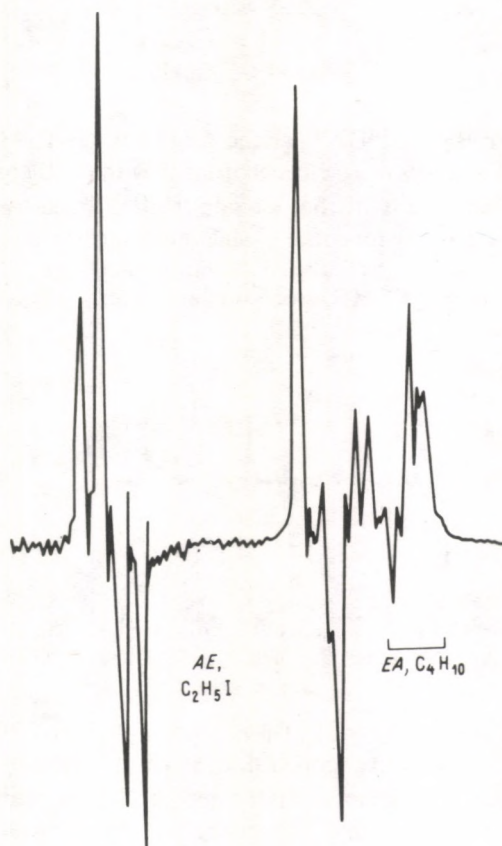


Fig. 7.16. CIDNP spectrum in the reaction of ethyllithium with ethyl iodide in benzene [7.10]

Closs *et al.* [7.36] clearly demonstrated the CIDNP sign inversion accompanying that of Δg in a radical pair. The photolysis of substituted benzaldehyde in diphenylmethane and its derivatives yields triplet radical pairs



In the series of substituted benzaldehyde and diphenylmethane the quantity $\Delta g = g(\text{Ar}\dot{\text{C}}\text{HOH}) - g(\text{Ar}'_2\dot{\text{C}}\text{H})$ changes in the following way

	Ar	Ar'	Δg	
(a)	<i>p</i> -Br—C ₆ H ₄ —	C ₆ H ₅ —	$1.8 \cdot 10^{-3}$	(7.8)
(b)	<i>p</i> -Cl—C ₆ H ₄ —	C ₆ H ₅	$1.3 \cdot 10^{-3}$	
(c)	C ₆ H ₅ —	C ₆ H ₅	$0.5 \cdot 10^{-3}$	
(d)	C ₆ H ₅ —	<i>p</i> -Cl—C ₆ H ₅	$0.3 \cdot 10^{-3}$	
(e)	C ₆ H ₅ —	<i>p</i> -Br—C ₆ H ₅	$-1.8 \cdot 10^{-3}$	

In the same series the CIDNP of the fragment >CH—CH< in the recombination products changes in a strict accordance with the theory (Fig. 7.17). In cases (a, b), $\Delta g > 0$, which results in the net polarization (negative for the protons of CHO group and positive for those of CHAR'₂ group). In cases (c, d) $\Delta g \approx 0$, hence, the multiplet polarization prevails. Finally, in case (e) $\Delta g < 0$ which results in the inverted sign (positive for CHO protons and negative for CHAR'₂ protons).

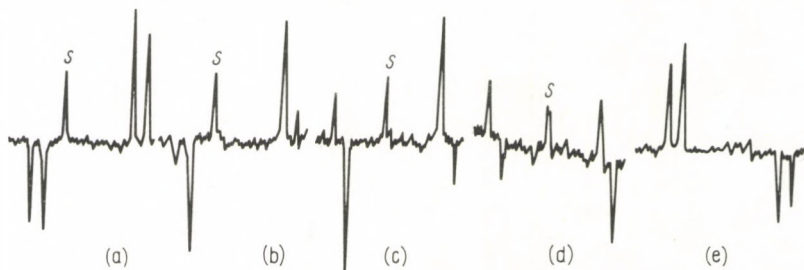


Fig. 7.17. CIDNP spectra for benzyl protons of 1,2,2-triaryl-ethanol. The indices a–e correspond to the numbers of the substituents in the text. *S* denotes the NMR line of ¹³C satellite of the solvent [7.36]

The hf energy dependence of CIDNP. The high field CIDNP theory predicts nuclear polarization sign inversion with the sign alteration of the hf constant; this has been confirmed by experiment. In the decomposition of acetylbenzoyl peroxide the methyl protons of methyl benzoate, the main product of the geminate recombination, are negatively polarized (Fig. 7.15), while ¹³C nuclei of the same group are polarized positively (Fig. 7.14). In both cases the polarization arises in the

radical pair $|\text{PhCO}\dot{\text{O}} \dot{\text{C}}\text{H}_3|^{\text{S}}$; the protons and ^{13}C nuclei being differently polarized because the hf constant in the radical $\dot{\text{C}}\text{H}_3$ is negative for the protons ($a_{\text{H}} = -22.5$ G), and positive for the ^{13}C nucleus ($a_{^{13}\text{C}} = 38$ G).

In benzoylpropionyl peroxide decomposition the proton polarization of CH_2 and CH_3 groups are opposite in sign in the recombination product $\text{PhCO}_2\text{CH}_2\text{CH}_3$ (Fig. 7.18), the polarization arising in the radical pair $|\text{PhCO}_2 \dot{\text{C}}\text{H}_2\text{CH}_3|^{\text{S}}$. The polarization sign inversion is caused by the hf constant sign change: it is known that in the radical $\dot{\text{C}}\text{H}_2\text{CH}_3$ $A_{\text{CH}_2} = -22.4$ G, $A_{\text{CH}_3} = +26.9$ G.

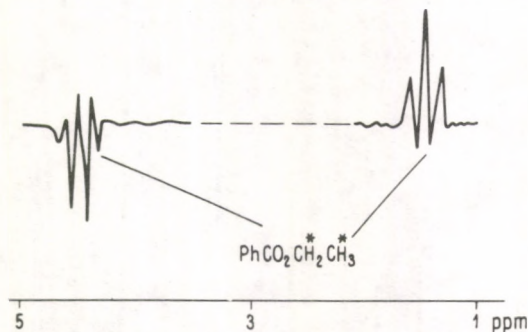


Fig. 7.18. $\text{C}_6\text{H}_5\text{CO}_2\text{CH}_2\text{CH}_3$ CIDNP spectrum in benzoylpropionyl peroxide decomposition [7.37]. Polarized protons are denoted by asterisks

The multiplet polarization sign must be dependent on that of the spin-spin nuclear coupling constant, this dependence being determined by the Kaptein rules (eq. (4.10), p. 175). This theoretical prediction has been fully confirmed by experiment.

Figure 7.19 depicts the CIDNP spectrum of the decomposition products of acetyl peroxide enriched with ^{13}C isotope (55%) in the methyl group. The net polarization of the protons in the molecules involving the nonmagnetic isotope of ^{12}C has already been discussed. It fully describes the polarization resulting from unlabelled peroxide decomposition (Fig. 7.12). In ^{13}C labelled molecules there is the geminal spin-spin interaction of ^{13}C nuclei and protons and, as a consequence, the proton multiplet polarization superimposed on the net polarization is observed. *EA* multiplet polarization is observed for the group O^{13}CH_3 in $\text{CH}_3\text{COOCH}_3$ and for ethane, whereas *AE* polarization is observed for methane and CH_3Cl . Both net and multiplet polarizations are in full accord with the Kaptein rules, bearing in mind that the sign of $J_{^{13}\text{C}-\text{H}}$ constant is positive ($J_{^{13}\text{C}-\text{H}} = 146$ Hz in OCH_3 methyl acetate group, $J_{^{13}\text{C}-\text{H}} = 150$ Hz in CH_3 and $J_{^{13}\text{C}-\text{H}} = 124$ Hz in CH_4).

The protons in the ethane molecule $^{13}\text{C}_2\text{H}_6$ have *EA* multiplet polarization (Fig. 7.19). The theoretical CIDNP spectrum shows a pleasing fit to the experimental one. Since ethane nuclear polarization arises in the radical pairs $|\text{CH}_3\text{CO}\dot{\text{O}} \dot{\text{C}}\text{H}_3|^{\text{S}}$ and $|\dot{\text{C}}\text{H}_3 \dot{\text{C}}\text{H}_3|^{\text{S}}$, in theoretical spectrum calculations the ratio of the contributions of these pairs was assumed to be 1.9.

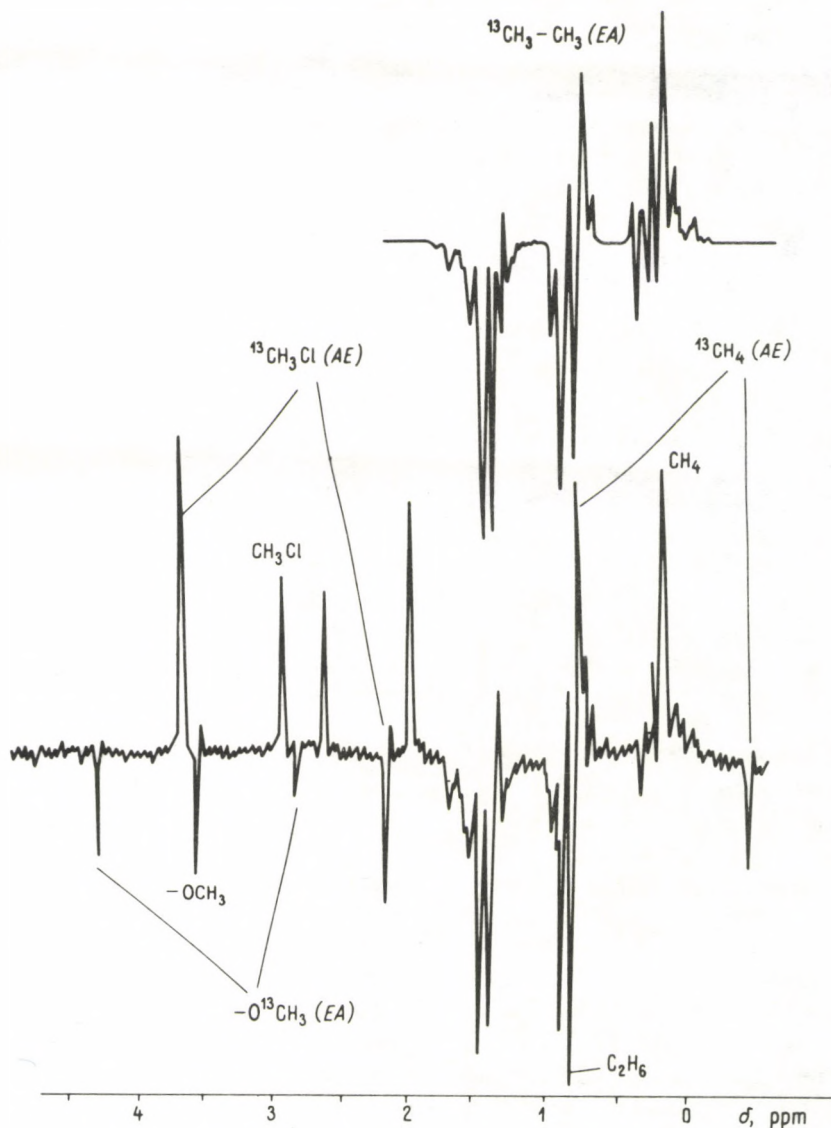


Fig. 7.19. CIDNP spectrum for the thermal decomposition products of acetyl peroxide ^{13}C labelled by 55% (hexachloroacetone, 110°C). Theoretical spectrum of $^{13}\text{CH}_3\text{-CH}_3$ molecule is shown above [7.38]

^{13}C nuclear polarization also fits experiment. Figure 7.20 shows experimental and theoretical ^{13}C CIDNP spectra for the $\text{H}_3^{13}\text{C-CH}_3$ molecule. The EA multiplet effect of ^{13}C nuclei coincides in sign with the proton multiplet effect (Fig. 7.19). Note that the geminal $^{13}\text{C-H}$ spin-spin interaction in ethane is positive.

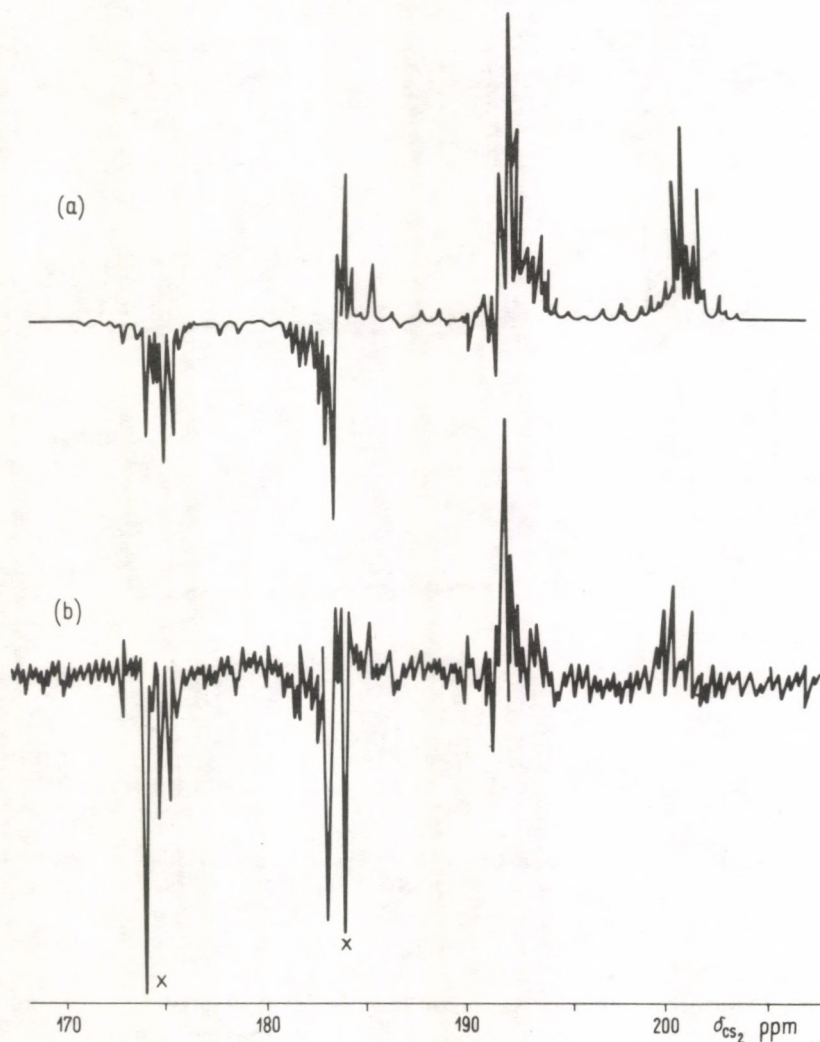


Fig. 7.20. ^{13}C CIDNP spectrum of $^{13}\text{CH}_3\text{—CH}_3$ molecules in acetyl peroxide decomposition in hexachloroacetone (124°): (a) experimental spectrum; (b) theoretical spectrum [7.38]. Lines not belonging to ethane are denoted by crosses

In the thermal decomposition of lauroyl peroxide $(\text{C}_{11}\text{H}_{23}\text{COO})_2$ in the presence of isopropyl iodide [7.39] one observes the multiplet polarization of the disproportionation product of the primary radical pair $|\text{C}_9\text{H}_{19}\text{CH}_2\dot{\text{C}}\text{H}_2 \quad \dot{\text{C}}\text{H}_2\text{CH}_2\text{C}_9\text{H}_{19}|^{\text{S}}$ and in the products formed from the escaping radicals (in $\text{C}_{11}\text{H}_{23}\text{I}$) (Fig. 7.21). In this case the CIDNP sign fits theory, when the fact that the spin-spin interaction constants in the fragments —CH=CH_2 and $\text{—CH}_2\text{CH}_2\text{I}$ are positive is taken into account.

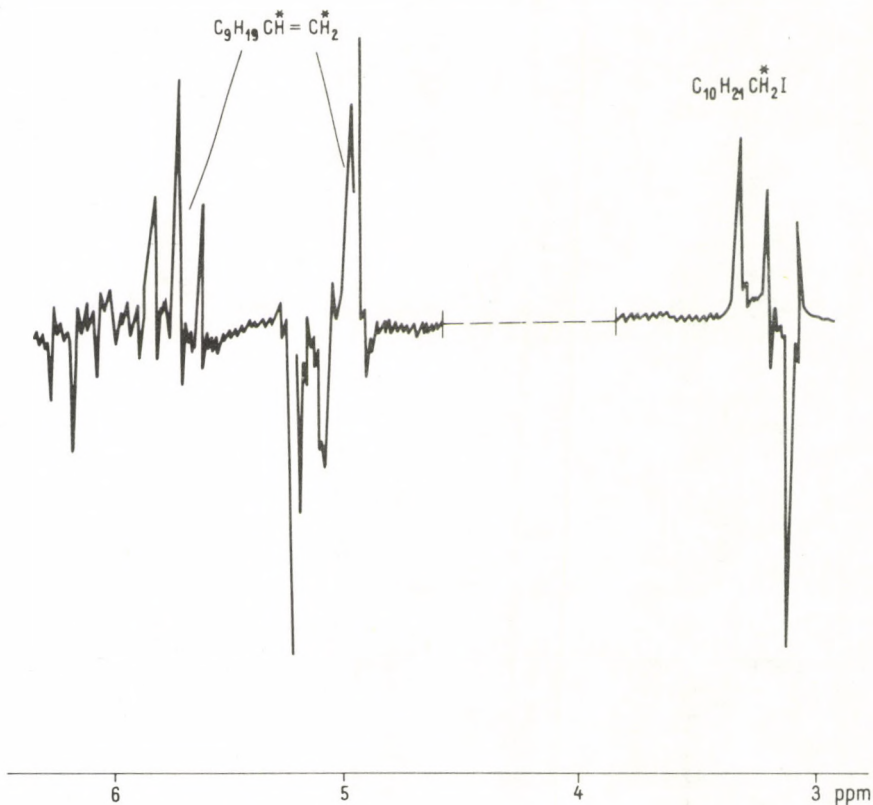


Fig. 7.21. CIDNP spectrum for the products of lauroyl peroxide decomposition in the presence of isopropyl iodide [7.39]

Much use in structural chemical studies is made of the dependence of the net and multiplet CIDNP signs on the signs of the hf constants. CIDNP spectra is of importance for obtaining information on the sign of the magnetic electron-nucleus (in radicals) and nucleus-nucleus (in molecules) interaction constants; we shall explore the subject in more details in the next section.

7.2.2 Low magnetic fields

In low magnetic fields the $S-T_0$ approximation is invalid, one must consider additional $S-T_+$, $S-T_-$ channels of intersystem crossing. These channels were shown above to be of a fundamental importance in CIDNP. Unlike $S-T_0$ transitions when the radical pairs are selected by their nuclear spin states and the total polarization is zero, $S-T_+$ and $S-T_-$ transitions do result in nonequilibrium spin state populations.

The theoretical difficulties and the experimental problems mentioned above (see Section 7.1) hampered low field CIDNP investigations. Nevertheless, the present state of the theory and the experimental data demonstrate that low field CIDNP can yield unique information on the properties of radical pairs in solution and add substantially to the conventional high field CIDNP technique.

As has been shown in the theoretical sections, nuclear polarization effects must depend on RP multiplicity, radical hf constants, the manner of generating reaction products and the electron exchange interaction energy in the RP. Below we consider a number of experimental examples confirming the above theoretical statements.

RP multiplicity. CIDNP sign alteration in low fields induced by RP multiplicity changes was observed experimentally when studying ^{19}F polarization in the reaction of pentafluorobenzyl chloride with butyllithium [7.40]

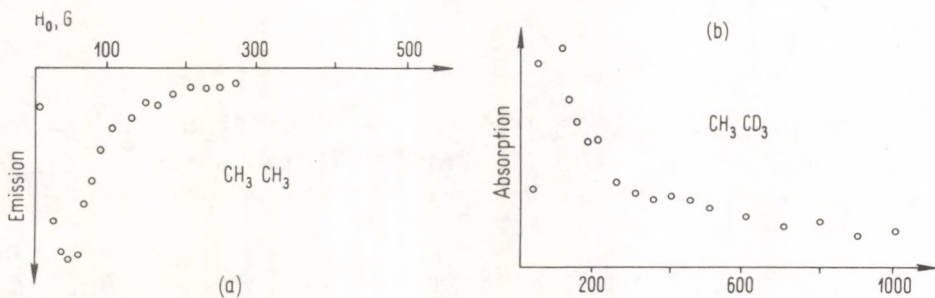
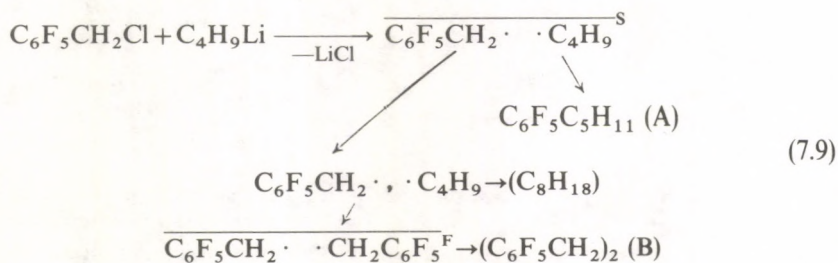
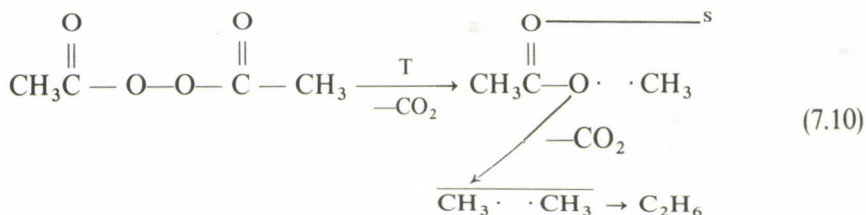


Fig. 7.22. Polarizations of ethanes CH_3CH_3 (a) and CD_3CH_3 (b) observed in thermal decomposition of acetyl peroxides $(\text{CH}_3\text{COO})_2$ and $(\text{CH}_3\text{CO}_2\text{CO}_2\text{CD}_3)$ respectively [7.41]

This reaction scheme shows the polarizations of the basic products, pentafluoroamylbenzene (A) and sym-pentafluorodiphenylethane (B), to originate in different radical pairs (S and F). In fields $H < 100$ G the products A and B reveal ^{19}F CIDNP (*ortho*-position) of different sign both in net polarization and the multiplet effect (E/A and I^+ for A; A/E and I^- for B) which is in a good agreement with theoretical predictions.

Hyperfine interaction constants. There are many examples confirming the interdependence of radical hf constants and CIDNP effects in low magnetic fields. Let us consider the most interesting example, which demonstrates the theoretically predicted influence of the effective hf constant in radical partner on net polarization. When studying CIDNP in the reaction of diacetyl peroxide thermal decomposition, den Hollander [7.41] discovered that ethane 1H polarization alters its sign in a partial isotope substitution of peroxide $CD_3(CO_2)_2CH_3$ in low fields (see Fig. 7.22). The conventional scheme of diacetyl peroxide decomposition is



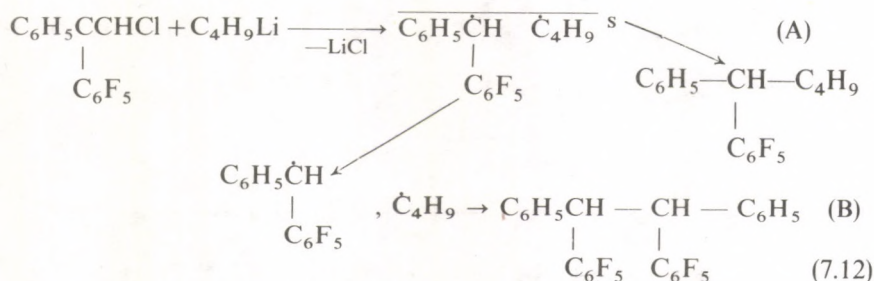
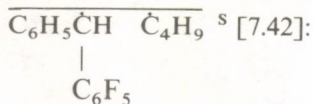
Thus, the ethane is the in-cage recombination product of a pair of methyl radicals in which the observed polarization arises. The fact that the ethanes C_2H_6 and $C_2H_3D_3$ are oppositely polarized is easily explained by the difference in the effective hf constants in the pairs $\dot{C}H_3 \dot{C}H_3$ and $\dot{C}D_3 \dot{C}H_3$. To show this, use relation (7.11) connecting the net polarization sign in low fields with the radical hf constants (see Section 4.3.)

$$\tilde{K}_u(I_i) \approx g_I \beta_I \omega_0 p_0 \{ B_{1i}^2 (J + A_{1i/4}) - 1/4 \cdot A_{1i} B_{2\text{eff}}^2 \} t / (2 \cdot 4!) \quad (7.11)$$

Substitute the known values of the hf constants for radicals $\dot{C}H_3$ and $\dot{C}D_3$ (-23.04 G and 3.3 G) into this relation and obtain $\tilde{K}_u(\dot{C}H_3 \dot{C}H_3) < 0$ and $\tilde{K}_u(\dot{C}H_3 \dot{C}D_3) > 0$, i.e. methyl proton polarization in the in-cage recombination products of radicals, CH_3CH_3 and CD_3CH_3 , must have opposite signs.

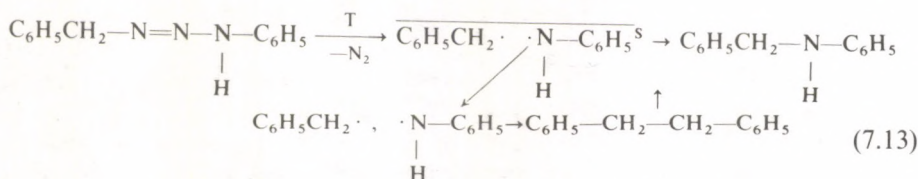
The origin of reaction products. In-cage and escape products. Unlike the simplicity of high magnetic fields where CIDNP results from nuclear spin states selection in low fields, the difference in polarization signs of in-cage and escape products is not inductable and depends on the electron exchange interaction energy in RP. As shown in Section 4.3 this difference can be observed only at small J . For $|J| > |A|/4$ the theory predicts the same CIDNP signs for different reaction products. We illustrate this by examples below.

In the reaction of pentafluorophenylphenylchloromethane with butyllithium the CIDNP effects of the basic products arise mainly in the pair



Here (A) is the in-cage recombination product and (B) is the escape product. CIDNP studies in the earth's magnetic field have shown ^{19}F CIDNP to be opposite in sign in these products. It is thus the case when $|J| < |A|/4$.

The thermal decomposition of benzyl phenyl triazene following the scheme [7.43]



is an example of reactions where nuclear polarization signs are the same in different products. In benzyl phenyl triazene thermolysis at 160°C (in hexaethylidisiloxane) the polarizations of N-benzylaniline and dibenzyl CH_2 -groups are suited to observation. In low fields (< 1000 G) both signals are negatively polarized (Fig. 7.23). The polarization both in N-benzyl aniline and dibenzyl has been shown [7.23] by the ^1H and ^{13}C CIDNP method to originate in the pair $\text{C}_6\text{H}_5\dot{\text{C}}\text{H}_2 \quad \dot{\text{N}}-\text{C}_6\text{H}_5$.

Thus benzylaniline and dibenzyl are in-cage and escape products, respectively.

The coincidence of CIDNP signs, according to theory, is indicative of a nonzero exchange integral J , as will be discussed below.

Electron exchange interaction. One of the most important conclusions of low field CIDNP theory is a high sensitivity of these effects to electron exchange interactions in the intermediate radical pairs. The experimental manifestations of these interactions are as follows.

The most systematic studies have been done in the reactions of triazene thermal decomposition [7.43, 44]. We consider the above example of benzylphenyltriazen

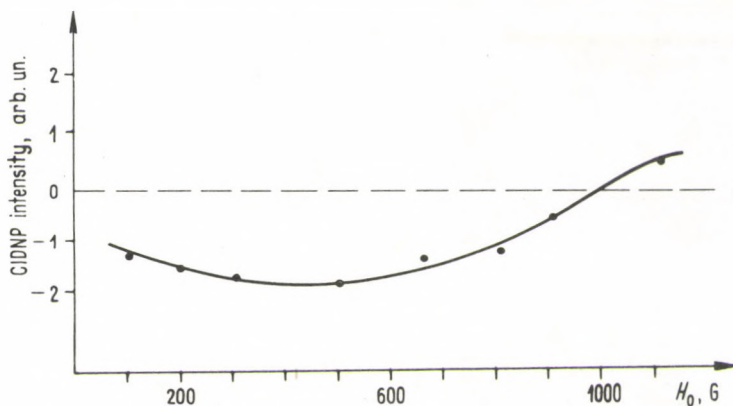


Fig. 7.23. Field dependence of ^1H CIDNP for dibenzyl (protons of CH_2 groups) in thermal decomposition of benzyl-phenyltriazenes in solution [7.43]

thermolysis. In this case the absolute value of J can be estimated by relations (4.67) and (4.68) and also by the position of the maximum in the low field dependence of CIDNP (Fig. 7.23). Since H_{max} considerably exceeds the hf constants in the pair $\text{C}_6\text{H}_5\dot{\text{C}}\text{H}_2 \quad \dot{\text{N}}-\text{C}_6\text{H}_5^{\text{S}}$ one can assume that $H_{\text{max}} \approx 2J$.

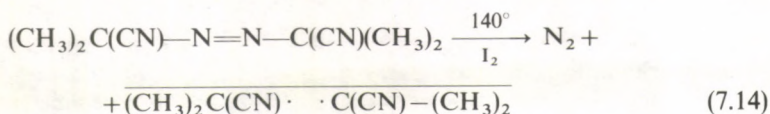
|
H

With the last relation we have $J \approx 250 \text{ G} = 5 \cdot 10^9 \text{ rad/s}$. The exchange integral sign can be readily obtained by relations (4.68) which show $J > 0$.

The fact is well known that values of J in a radical pair can change sign when two π -orbitals change their relative orientation [7.45]. However, positive values of J can be expected only within a narrow range of angles between interacting π -orbitals. Hence, when the radicals move independently in a solution, the mean value of J must be negative. The positive value obtained is perhaps informative of a certain correlation of the mutual radical motion in pairs of benzyl and aryl radicals. This can be connected with the radical association induced by π - π interactions involving the aromatic ring. Examples of stable radical π -complex formation are available in literature [7.46].

Low field CIDNP studies in thermolysis reactions of other triazenes proves that positive values of J can be observed only in RPs with π -radicals. Radical pairs containing σ -radicals (e.g. $\dot{\text{C}}_6\text{H}_5 \quad \dot{\text{N}}\text{HC}_6\text{H}_5$) show small negative absolute values of exchange integrals.

Generally speaking, the effective exchange integral, manifesting itself in low field nuclear polarizations, must depend on RP diffusion parameters. In this connection the problem of the influence of viscosity (which to a great extent determines radical mobility) on low field CIDNP effects is interesting. This problem has been investigated experimentally [7.23] in the thermal decomposition of bis-azo-diisobutyronitrile (AIBN). The initial thermolysis step results in a pair of 2-cyano-2-propyl radicals:



These radicals afford 2,4-dicyano-2,4-dimethylbutane (the basic reaction product) and the scavenging product 2-cyano-2-iodopropane. It is interesting to note that in high fields the CIDNP effects cannot be detected either in the absence of free radical scavengers or with I_2 . This can be attributed to the fact that in a pair of cyanopropyl radicals $\Delta g = 0$. In AIBN thermolysis (0.5 M solution in *o*-dichlorobenzene) in the presence of I_2 in fields 0.6–1000 G, the methyl protons of both products are positively polarized. As has been noted above, the coincidence of CIDNP signs of in-cage and escape products is indicative of a nonzero exchange integral. When estimated by relations (7.11), $J < -24.5$ G. Thus, a pair of cyanopropyl radicals has a negative exchange integral, its absolute value exceeding 25 G.

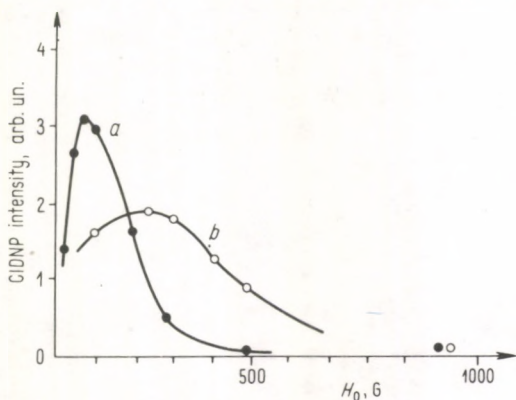


Fig. 7.24. Magnetic field dependence of the ^1H polarization of 2,4-dicyano-2,4-dimethylbutane in decomposition of azobis-iso-butyronitril in the presence of iodine at 1400°C in diphenylether (DPE) (a) and *p*-bis-(*p*-phenoxyphenoxy)-benzene (BPB) (b) [7.23]

In order to study viscosity effects, the field dependence of the CIDNP intensity has been measured [7.23] in thermolysis of AIBN in diphenylester (DPE) (a) and in *p*-bis-(*p*-phenoxyphenoxy)-benzene (BPB) (b) (Fig. 7.24). The viscosities of these solvents at 140°C differ by a factor of approximately 7 ($\eta = 0.6$ cP for DPE and $\eta \approx 4.0$ cP for BPB). The comparison of the curves (Fig. 7.24) shows the field dependences of CIDNP in DPE and BPB to differ markedly. In the former case the maximum CIDNP intensities are achieved in fields 50–70 G, in the latter at 200 G. The only source of this difference in RPs of the same structure is changes of the value of the exchange integral. The position of CIDNP maxima shows that the value of the exchange integral in BPB is 3–4 times greater (and has a negative sign) than that in DPE. Exchange interaction in RPs are well known to be induced by the overlap of unpaired electron orbitals. At $J < 0$ the absolute value is proportional to the squared

overlap integral S^2 , which is a function of the distance between the radicals and their mutual orientation for two interacting π -orbitals. Owing to radical rotation, in solutions it depends only upon separation. Thus, the observed increase in J with the solvent viscosity can be ascribed to a decrease of the mean interradsical distance.

To interpret this experiment, ref. [7.47] has considered a more realistic model in which the exchange integral is not constant but depends exponentially on the interradsical distance r $J(r) = J_0 e^{-ar}$. In point of fact, the theoretical approach employed is close to the diffusion CIDNP theory in biradicals [7.48], the only difference being in the description of the radical dynamics. Unlike biradicals, a change in interradsical distances in pairs is due to the Brownian motion with the diffusion coefficient D_A and D_B (where D_A and D_B are radical diffusion coefficients). To simplify computations, the simplest case of a one-nucleus RP with $I = 1/2$ ($\Delta g = 0$) has been considered [7.47]. Figure 7.25 shows CIDNP efficiency as a function of field. The curve is seen to shift towards high fields and to broaden with decreasing radical diffusion mobility. For experimental systems (see Fig. 7.24) the translational diffusion coefficients are governed by the Stoke's formula

$$D = kT/6\pi a_i \eta,$$

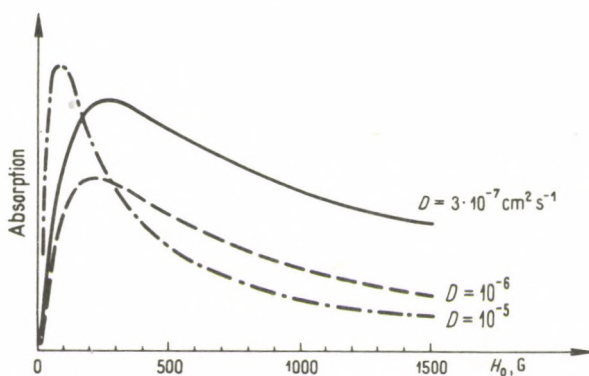


Fig. 7.25. Calculated magnetic field dependence of CIDNP for the recombination product from a singlet-born radical pair with one nuclear spin $I = 1/2$. Curves are calculated for some values of D for $A = -100$ G and $J < 0$ [7.47]

where a_i is the particle radius and η is the solvent viscosity. In the solvents used η equals 0.6 cP and 4 cP. The diffusion coefficient of 2-cyano-2-propyl radical ($a_i = 2.5$ Å) was estimated to be $2 \cdot 10^{-5} \text{ cm}^2 \text{ s}^{-1}$ and $3 \cdot 10^{-6} \text{ cm}^2 \text{ s}^{-1}$ for DPE and BPB respectively. The comparison of theoretical and experimental curves (Figs 7.25 and 7.24) demonstrates a good agreement between them. Thus, both theoretical analysis and experiment confirm that the relative contributions of short diffusion radical trajectories increase with the solvent viscosity. This in turn enhances the effective exchange integral, which is then manifested in the position of maxima in low magnetic fields.

Numerous results indicating the role of exchange interactions in inducing low field CIDNP have been obtained when studying field dependences of ^1H polarization in photolysis of some organic peroxides [7.49–53] and alkyl ketones [7.17, 24, 54–57]. In these studies exchange integrals were obtained by the comparison of experimental and theoretical dependencies, the calculated curves fitting experiment fairly well. A good example is the reaction of di-isopropyl ketone photodecomposition where an interesting case of a double change in chloroform polarization sign in low fields has been observed experimentally and reproduced by calculations [7.17] (see Fig. 7.26).

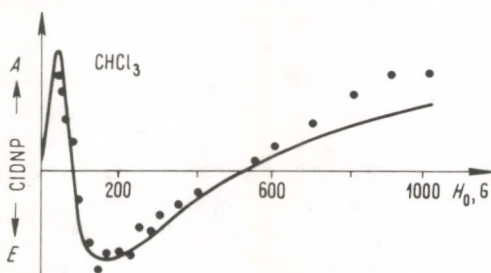


Fig. 7.26. Magnetic field effects on chloroform ^1H polarizations in di-isopropyl ketone photolysis in CCl_4 . Solid line is the result of theoretical calculations [7.17]

At the same time, it is necessary to note that to simplify practical CIDNP computations practically all investigators use the following approximations: (1) a reduced number of RP magnetic nuclei is considered, or (2) equivalent nuclei are replaced by one with an effective spin $I = \sum_i I_i$. As a result, the information on the exchange integral obtained is only an estimate. For instance, some values of the RP exchange integral in a number of photochemical reactions have been obtained in [7.17, 58]. However, in more recent publications [7.54, 59] these results have been explained on the basis that $J=0$.

The values of exchange integrals available in the literature that have been determined by low field CIDNP effects have been reviewed in [7.60]. It was found that the effective exchange integral is either close to zero or attains small negative values. the pair $\text{C}_6\text{H}_5\dot{\text{C}}\text{H}_2 \dot{\text{N}}-\text{C}_6\text{H}_5$ with a positive exchange integral being an



exception. As has been noted earlier, these anomalies are attributed to the formation of associates between radicals in pairs. Thus, the whole scope of the results allows one to conclude that the formation of nonequilibrium spin sublevel populations results, as a rule, from diffusional radical motion in solution (at rather long interradsical distances) when the radical exchange interaction can be neglected. On the other hand, studies of "anomalous" cases (either positive or large values of J) can turn out to be helpful in understanding subtle problems of the dynamics of mutual motion and interaction of radicals in solutions.

7.3 Chemical applications of CIDNP

Mechanisms of population redistribution (pumping) of the Zeeman nuclear levels of radicals and molecules are responsible for CIDNP. Theoretical CIDNP analysis and the data of numerous experimental investigations have unambiguously shown that the most effective pumping mechanism is the singlet-triplet mixing in radical pairs whose rate depends both on the radicals' nuclear spin and the energy of magnetic electron-nuclear interaction. This interaction connects two spin systems—electronic and nuclear—hence, a change of the angular momentum in the electron spin system (a singlet-triplet transition) is accompanied by a change of the angular momentum in the nuclear spin system, and that results in nuclear polarization. In high magnetic fields predominantly $S-T_0$ transitions occur, whereas in low and zero fields, $S-T_{\pm}$ mixing prevails. In the former case chemical reactions do not result in the spin reorientation but lead to the nuclear spin selection. In the latter case, however, the reaction is of importance since the singlet-triplet mixing in the pair results in the nuclear spin reorientation and thus in nuclear polarization and magnetization.

The efficiency of the pumping is determined, first, by the magnetic and exchange interactions in the pair which control the singlet-triplet mixing rate; second, by the dynamics of molecular motions which control the exchange interaction of the radical unpaired electrons; third, by the chemical dynamics which control the lifetime of radicals. The whole complex of these related processes forms the spin dynamics of the pair.

CIDNP is therefore a physical phenomenon with its origin and essence well understood and the theory developed quantitatively. Being a physical phenomenon, CIDNP serves as the basis of novel methods for studying and identifying chemical reaction mechanisms, the origin of active species and intermediate products in chemical reactions, radical properties, etc. This section treats the CIDNP applications that are the most important.

7.3.1 Identification of radical stages

The fact of CIDNP observation itself indicates radical stages and radical generation in the reaction irrespective of whether the radical route of the reaction is principal or only supplementary. CIDNP detection is a new and powerful method to observe radicals and radical stages (see, e.g., [7.1, 61–64] and thus is extremely popular and widely used in chemistry.

To be sure of observing CIDNP, the chemical pumping rates must be high and comparable to those of nuclear relaxation. Optimum conditions are when the reaction is over within 3–5 minutes or, even better, within seconds. This condition, however, is desirable but not indispensable. CIDNP can be observed even in slow reactions provided the polarization coefficients are sufficiently high. For example, in

acyl peroxide decomposition, an intensive CIDNP was observed within an hour without additional reagent supply. The strict requirement of CIDNP observation is that CIDNP kinetic curves should show maxima (which are the most reliable and unambiguous evidence of CIDNP observation) when the following conditions hold:

$$|E|k - \beta > 0 \text{ or } |E|kT_{1n} > 1. \quad (7.15)$$

These are the three parameters—the polarization coefficient, the reaction rate constant, and the nuclear relaxation time in the molecule—that determine the polarization magnitude, and their relationship (7.15) is the criterion for experimental CIDNP observation.

The problem is in what reactions CIDNP can be observed, and if any predictions are possible. This problem cannot be solved unambiguously, but there are some considerations. First of all, it is necessary that the reaction should yield radicals, in either the principal or the supplementary steps. This can be forecast by "chemical" intuition; however, this is no guarantee against mistakes because CIDNP is often observed in systems where no radical mechanisms are expected. This is a particular merit of the method.

Further, CIDNP arises only in the radicals whose fates are connected with radical pairs. The nuclear polarization occurs either in the recombination (disproportionation) or in the escape products. Addition, dissociation, and substitution elementary reactions of radicals are not accompanied by nuclear polarization because the angular momenta of electron and nuclear are preserved and the spins do not change. Therefore, in radical chain reactions the CIDNP arises only in the products resulting from termination of the kinetic chains. If these products are the same as those formed in the chain-propagation reactions and the chain length is great, then the portion of molecules with polarized nuclei is small. In fact, these molecules are strongly "diluted" by those formed in the chain propagation reactions (small polarization coefficient E). Therefore, the CIDNP in chain reactions with long chains is usually weak.

At present, CIDNP has been observed in various classes of reactions: peroxide and azocompound decomposition, molecular rearrangement and isomerization, photochemical decomposition, photosensitized reactions, reactions involving organometallic compounds of mercury, manganese, silicon, lithium, lead, tin, etc., reactions involving electron transfer, azocombination, oxidation, polymerization, chain halogenation, etc. CIDNP gives important information on the mechanisms, revealing new aspects. As to the novel results obtained by CIDNP technique one may refer to the detection of radical reactions of singlet carbenes and the orientation of nucleophilic reagents in aromatic radical reactions, identification of the stability of acyloxyradicals, the evidence of diazophenyl radical in a number of reactions of thermal decomposition and electron transfer, the detection of photochemical ketone decay in exciplexes, the identification of radical mechanisms in some reactions considered to be classical examples of nucleophilic and electrophilic substitution, etc.

The CIDNP method, as well as CIDNP phenomenon itself, is limited, however, and not generally applicable like other methods. The main restrictions of the CIDNP methods, as applied to investigations, are as follows.

The polarization is weak and hardly observable in reactions involving radicals with short lives ($\tau \lesssim 10^{-10}$ s). This time is too short for singlet-triplet mixing in a pair to take place, i.e. neither electron nor nuclear spin system changes within this time.

In general CIDNP observations unambiguously indicate radical generation in chemical reaction. However, the absence of CIDNP does not necessarily mean that the reaction yields no radicals. To observe CIDNP not only radical generation but also the condition (7.15) is needed. This is also the reason why polarizations are difficult to observe in systems with too short nuclear relaxation times in the molecules, when the depolarization rate is high (very viscous solutions, solids, glasses), as also follows from relation (7.15).

Pulse reaction conditions—pulse photolysis, radiolysis, laser irradiation—are of particular interest for CIDNP. CIDNP investigations in biochemical (in particular, enzymatic) processes are of no less interest.

7.3.2 Radical transformation genealogy

The signs of net and multiplet polarizations are firstly determined by the spin multiplicity of the radical pairs—molecule precursors—and, therefore, by the spin multiplicity of the reacting particles generating radical pairs. The spin states of reacting particles are the most important characteristics of the reaction mechanism.

With CIDNP it has been found that the majority of thermal reactions of decomposition, isomerization, electron transfer, oxidation, etc. occur in singlet state and, thus, the initial radical pairs are also singlet.

A number of direct photolysis reactions also takes place in the singlet state. Photochemical reactions involving ketones and also photosensitized reactions in the presence of triplet sensitizers go through triplet states.

Very often the same molecules are formed in chemical reactions either in the initial pairs (singlet or triplet) or in those of freely diffusing and randomly encountering radicals (the pairs with uncorrelated spins). The CIDNP observed in these molecules is a sum of both effects. Very often the contribution of diffusion pairs with uncorrelated spins to the CIDNP prevails and even if the reaction goes through a singlet state (i.e. the initial pairs are singlet) the total nuclear polarization indicates a triplet precursor. In these cases the only way to avoid erroneous conclusions is to study the influence of radical acceptors on CIDNP. In the presence of acceptors, free radicals are scavenged and the contribution of the diffusion pairs to the CIDNP vanishes; only the contribution of the initial radical pairs remains.

For instance, when lauroyl peroxide decomposes, in the presence of isopropyl iodide, the CIDNP intensity in the product increases with isopropyl iodide

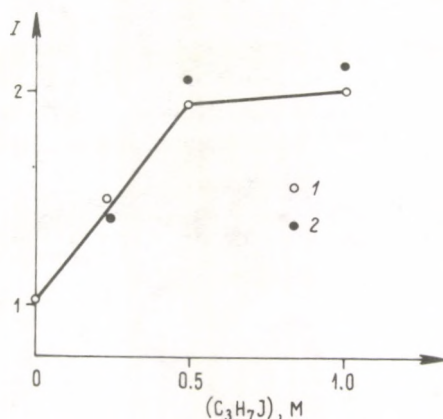
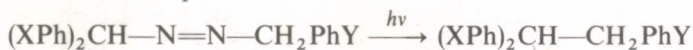


Fig. 7.27. Plots of undecene and undecylidide polarizations vs. isopropylidide concentration in lauroyl peroxide decomposition [7.64]: 1 — in freone; 2 — in octane

concentration [7.39] up to some limiting value (Fig. 7.27). At photochemical decomposition of azocompound



the polarization coefficient was found to be 90 ± 20 in the geminate recombination product. In the presence of acceptors (thiophenol) the polarization coefficient increases to 350 ± 70 ; simultaneously the recombination product yield shows a more than two-fold decrease [7.65]. Polarization of phenyl benzoate phenyl protons arising in benzoyl peroxide decomposition becomes twice as much when iodide is added [7.66].

In the above cases the reaction runs through the singlet state, the initial pairs are thus singlet. However, in the absence of acceptors the CIDNP contribution of opposite sign is observed in diffusion pairs, and this often compensates and reduces CIDNP from the initial pairs. When acceptors are added, this contribution disappears, with only the contribution of the initial singlet pairs remaining.

If the contribution of diffusion pairs becomes dominant, one can expect CIDNP sign alteration resulting from addition of acceptors. Quantitative CIDNP investigations allow one to distinguish between the contributions of the initial and diffusion radical pairs and to evaluate the relative product yields from these pairs.

By the sign of multiplet or net CIDNP one can judge what pairs dominate in the reaction. For instance, in acyl aliphatic peroxide decomposition, only multiplet polarization is observed in the products whereas in the products of aromatic or alkyl aromatic acyl peroxide decomposition net CIDNP arises. This means that in the former case the basic contribution to CIDNP is made by alkyl radicals and in the latter case by acyl radicals $\text{PhC}\dot{\text{O}}_2$, i.e. the lifetime of radicals $\text{PhC}\dot{\text{O}}_2$ ($\approx 10^{-7}$ s) greatly exceeds that of RCO_2 ($\tau \lesssim 10^{-10}$ s). Numerical data on lifetimes of acyl radicals are reported in ref. [7.1].

7.3.3 CIDNP kinetics

Even qualitative CIDNP observations are often sufficient to investigate reaction mechanisms. However, nuclear polarization kinetics gives reaction kinetic parameters: rate constants, activation energies, and, the most important characteristics, enhancement coefficients.

CIDNP kinetics are connected, first, with the chemical reaction kinetics and, second, with that of nuclear relaxation. In a general case it is described by the equation

$$\frac{dM}{dt} = E \cdot \frac{dM_0}{dt} - \beta(M - M_0) \quad (7.16)$$

or

$$\frac{dI}{dt} = E \cdot \frac{dI_0}{dt} - \beta(I - I_0) \quad (7.17)$$

where M is the total nuclear polarization of some kind of molecules or molecular groups; M_0 is the equilibrium nuclear polarization of the same molecules or groups; I and I_0 are the NMR signal intensities proportional to M and M_0 respectively.

The first term in eqs (7.16) and (7.17) determines the chemical pumping rate, the second term is the rate of depolarization disequilibrium polarization to its equilibrium value; E is the polarization coefficient; β is the relaxation rate, $\beta = T_1^{-1}$, T_1 is the nuclear relaxation time in the molecule.

Solutions of eqs (7.16) and (7.17) for different kinetic conditions have been obtained [7.1, 67, 68] and used by many investigators to analyze reaction kinetics and to determine rate constants, nuclear relaxation times, and polarization coefficients.

Note that the kinetic equations of CIDNP are independent of the physical polarization mechanism, they can be applied to describe the kinetics of chemically induced electron polarization (Chapter 8).

7.3.4 Radical and nonradical reaction routes

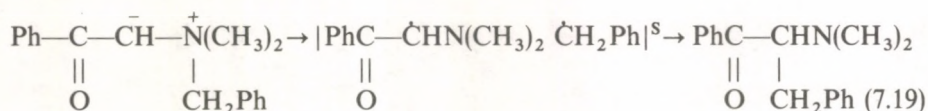
One must remember that the detection of nuclear polarization in reaction products does not necessarily mean that the radical mechanism is the main route of reaction. CIDNP is the only kinetic method which allows one to discriminate between radical and nonradical reaction mechanisms, especially in the case when both yield the same products. The method allows one not only to distinguish these mechanisms but also to estimate the extent of their competition quantitatively. For instance, if same product is formed in two ways with the rate constants k_1 and k_2 and the polarization coefficients E_1 and E_2 , then the experimentally obtained average polarization coefficient E is

$$E = (E_1 k_1 + E_2 k_2) / (k_1 + k_2) = E_1 p_1 + E_2 p_2, \quad (7.18)$$

where p_1 and p_2 are partial portions of both reaction routes. If the second way is nonradical, then $E_2=1$ and the second term can be neglected. Then with E_1 calculated theoretically one can easily find p_1 and p_2 (for more details see ref. [7.1]).

The problem of the relationship between radical and nonradical reaction pathways cannot always be solved unambiguously even by the CIDNP method. Reactions of intramolecular rearrangement (Wittig's, Meisenheimer's, Stevens etc.) can serve as an example. Until recently either ionic or molecular mechanism was ascribed to these reactions. However, CIDNP investigations have shown the products of these reactions have nuclear polarizations in almost all cases.

So, in the reaction

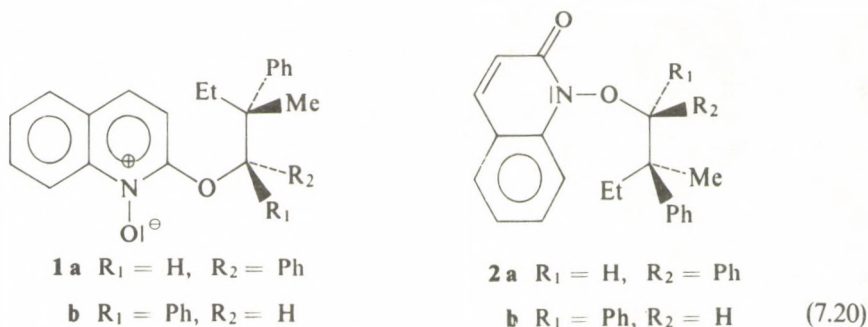


CH_2 protons of the benzyl group are negatively polarized [7.69]. This leads to the conclusion that the reaction follows a radical pathway through singlet radical pairs. However, in the case of the methyl-substituted analogue of imide, which shows stereochemical properties, the rearrangement product is 95% optically active, i.e., the rearrangement occurs with stereochemical conformation preservation of the migrating group. At first sight this result is not in accordance with the radical mechanism, as the radical centre is usually flat and hence product racemization and loss of optical activity are observed as a rule in radical reactions. An ionic rearrangement mechanism should also lead to the racemization. On the contrary, the molecular mechanism could ensure (via a three-membered transition complex) the conservation of optical activity, the product, however, having inverted conformation, but could not induce CIDNP. Thus, the arrangement mechanism still remains unclear.

The radical pathway of the reaction seems to be the basic one, however, the radical-partners are close enough to recombine at times less than the characteristic times of radical reorientation (10^{-12} – 10^{-11} s). Then the stereochemical properties of the starting yield are preserved in the product, however, at such lifetimes of the radical pairs that CIDNP can hardly arise in the product. Perhaps the reaction goes mainly through short-lived pairs and negligibly through long-lived ones (10^{-9} – 10^{-10} s). In this case the former pairs are responsible for the conservation of stereochemical configuration in the product, and the latter for the CIDNP.

In point of fact, it can be interpreted as follows. Stereochemical properties are preserved in the molecules generated by the initial recombinations, and CIDNP arises in those generated by the secondary recombination steps. Here one has to expect a certain relation between the degree of conservation of the initial stereochemical conformation and the CIDNP intensity: the greater the degree of conservation, the smaller the CIDNP and vice versa.

This conclusion has been corroborated qualitatively by experiment. In N-quinolones, isomerization products of N-oxide quinoline derivatives [7.70]



the initial stereochemical conformations are partially preserved and CIDNP arises. Thus, on 1a isomerization, the ratio between 2a and 2b products is 1.43, and the CIDNP intensity ratio is 0.8, i.e., less nuclear polarization is created in the product with the stereochemical conformation preserved. The same regularity is also observed in 1b isomerization.

The conservation of stereochemical conformation on initial recombination means that the characteristic times of molecular radical rotation in a pair are comparable to the recombination times (when applied to singlet pairs only). This conclusion is more reliable since the characteristic time scale of rotational and translational molecular diffusion in ordinary liquids are comparable.

More precise conclusions on the reaction mechanism can be made in the case considered by Baldwin *et al.* [7.71]. The Stevens rearrangement



proceeds with 36% of the initial configuration preserved and CIDNP is generated (emission in the CH group and absorption in the CHD group). Though the above problems are still applicable to this reaction too, the probability of radical reaction is much higher. (CIDNP in other intramolecular rearrangement reactions is discussed in ref. [7.1].)

Note, that nuclear polarizations are not observed in all rearrangement reactions. A systematic CIDNP analysis [7.72] shows that a successive detection of CIDNP in rearrangement reactions is possible only in cases when the molecular mechanism is formally forbidden by the rules of conservation of orbital symmetry (the Woodward-Hoffmann rules). However, on the basis of only qualitative CIDNP observations one cannot unambiguously deduce whether the nuclear polarization is evidence for the radical route as the basic transformation mechanism or the radical pathway is supplementary. This conclusion, as shown above, can be made only on the basis of quantitative CIDNP investigations.

In some cases, however, even at the qualitative level, the certain conclusion can be made that CIDNP arises in supplementary reactions or in a process imitating the

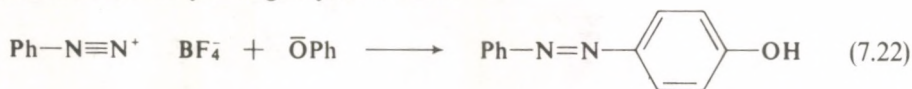
basic one and contributing only negligibly. For example, with ^{31}P CIDNP it has been shown that the reactions of organic phosphites with hydroperoxides follow two competitive mechanisms, one radical and one nonradical (ionic or molecular), the radical pathway which induces ^{31}P nuclear polarization, gives a negligible contribution (10^{-2} – 10^{-4}) [7.73]. In reactions of hydroperoxides with organic phosphites catalyzed by transition metal ions it has been found that the radical pathway is also negligible [7.74]. When studying CIDNP in the products of a rather uncommon reaction of tetraalkylammonium salts with carbon tetrachloride it has been concluded [7.75] that this reaction follows either an ionic or a molecular mechanism and is accompanied by the generation of unstable intermediates which initiate secondary reactions of a radical nature, the observed CIDNP arising therein.

In the analysis of ^{13}C CIDNP in the reaction of quinone diazide with cyclohexylamine, a strong nuclear polarization of the intermediate unstable triazene has been discovered [7.76]. The conclusion was made that triazene was formed in the nonradical reaction stages and its polarization resulted from the reversible decomposition of triazene by a radical mechanism. The conclusion on the competition between two mechanisms—radical and nonradical—of phenylacetyl peroxide $(\text{PhCH}_2\text{COO})_2$ decomposition was made on the basis of the data on CIDNP and the product composition [7.1, 77].

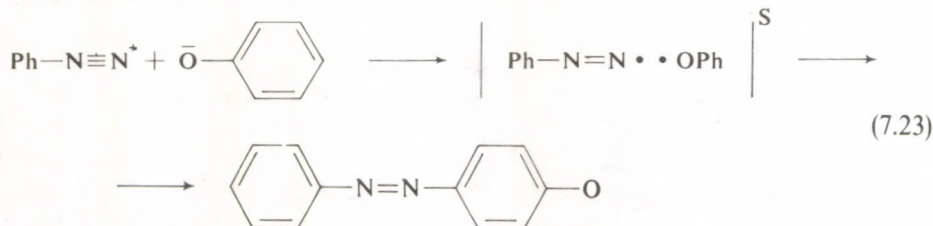
The general feature of these examples is that the radical mechanism resulting in nuclear polarization is either minor or supplementary.

CIDNP observed in some reactions, the mechanisms of which had been regarded as established, made scientists reconsider their traditional interpretation. To illustrate this, consider two reactions whose mechanisms were misinterpreted by methods other than CIDNP.

The first reaction, that of phenyl diazonium salt with phenolate ion, occurs in alkaline solutions yielding oxyazobenzene



This reaction was considered to follow an ionic mechanism. However, the detection of nuclear polarizations of ^1H , ^{13}C , and ^{15}N [7.78–81] (Fig. 7.28) in oxyazobenzene which is the main product of the reaction, and in the initial phenyl diazonium salt, allowed Bubnov *et al.* [7.80] to propose a radical mechanism with electron transfer



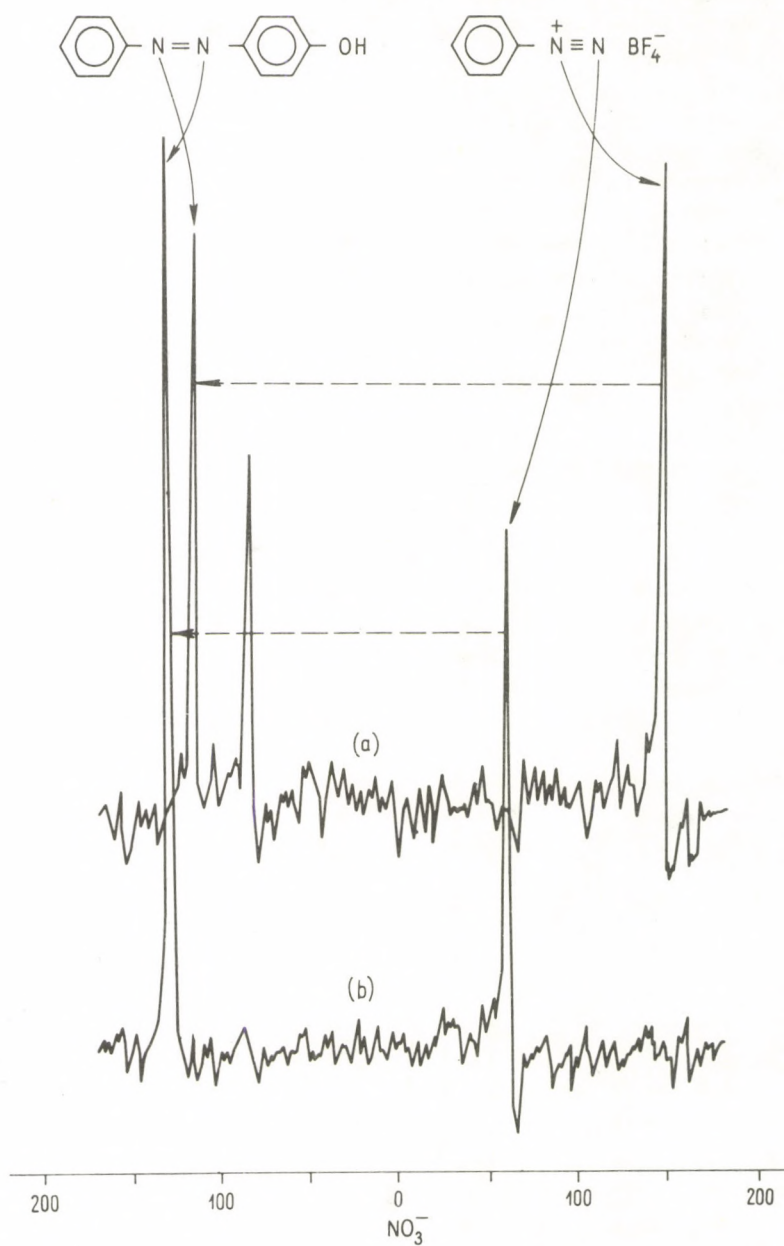
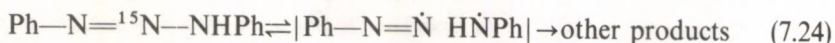


Fig. 7.28. ^{15}N CIDNP spectra observed in the reaction of phenyl diazonium salts with sodium phenolate [7.81]. Reagents: $\text{C}_6\text{H}_5\text{}^{15}\text{N}_2^+\equiv\text{N BF}_4^-$ (a) and $\text{C}_6\text{H}_5\text{N}^+\equiv^{15}\text{N BF}_4^-$ (b)

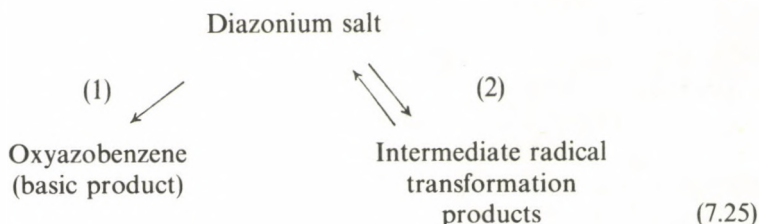
and the participation of the radical pair formed by phenyl diazonium radical and phenoxy. However, such a simple mechanism was criticized by Lippmaa *et al.* [7.81, 82] as it contradicted experimental data.

First, two nitrogen nuclei, both in the initial salt and the product, are positively and equally polarized. This fact disagrees with the representation of CIDNP as arising in a radical pair $|\text{Ph}\dot{\text{N}}_2 \ \dot{\text{O}}\text{Ph}|$ since the hf constants on the nitrogen atoms in the radical $\text{Ph}-\text{N}=\dot{\text{N}}$ differ greatly: they are large at the terminal atom and small at the nitrogen atom attached to the phenyl ring. Hence, one should expect a strong polarization of only one of the nitrogen nuclei. Indeed, in decomposition of diazoaminobenzene labelled with ^{15}N at the central position



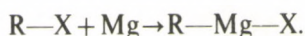
strong polarization of the central ^{15}N nucleus arises in the starting compound. In the decomposition of diazoaminobenzene labelled with ^{15}N in the position next to the phenyl ring no polarization of this nucleus is observed in the starting compound [7.83]. This fact is a reliable experimental evidence for the fact that in the radical $\text{Ph}\dot{\text{N}}_2$ a large hf constant is characteristic only of the terminal nitrogen atom. It is this nitrogen nucleus that must be strongly polarized in the transformation products of $\text{Ph}\dot{\text{N}}_2$ radical.

Second, it follows from the radical scheme suggested by Bubnov *et al.* [7.78] that the carbon nuclei of the phenoxy ring must be polarized. However, neither in the product, nor in the initial diazonium salt does this polarization arise, though the carbon nuclei of the phenyl ring are found to be polarized in diazonium salt, oxyazobenzene, and the by-product, benzene. It is characteristic that the nuclear polarization in the products precisely coincides with the nuclear polarization in the starting diazonium salt. The nuclear polarization seems to arise first in the starting salt and then to be fully transferred to the reaction product—oxyazobenzene. This fact allowed Lippmaa *et al.* to suggest that the transformation of diazonium salt in oxyazobenzene does not include radical stages and the basic mechanism of the diazocombination reaction is ionic. As to the nuclear polarization in diazonium salt, it seems to be formed in supplementary radical stages with the participation of radicals of the type $\text{Ph}-\text{N}=\text{N}\dot{\text{O}}$ or radical-ions. These supplementary stages are in many aspects vague, they can also include radical transformations proposed by Bubnov *et al.* (This is proved by a strong nitrogen nuclear polarization in non-identified intermediate products which can be induced either by $\text{Ph}-\text{N}=\text{N}-\text{OPh}$ or a similar substance, the substance being not observed in the final products [7.81].) It is important that the products of the radical stages do not transform into oxyazobenzene, but go back into diazonium salt. Thus, the way of forming the final product and inducing the nuclear polarization coexist independently. In general the transformation scheme of this system would be:



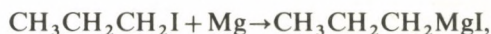
Path 1 results in the product, path 2 results in the nuclear polarization.

Now consider one more interesting example, the interaction of alkylhalogens with metallic magnesium. It is well known and important for organic chemistry the Grignard synthesis. This reaction was always considered to be ionic, resulting in the insertion of magnesium atom in the carbon—halogen bond:



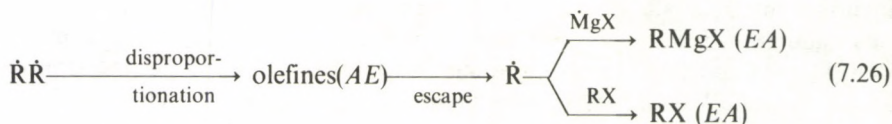
The reaction was also known to be followed by hydrocarbon formation. Hence, it was supposed that radicals participate in the reactions.

Evidence of radical generation in the Grignard synthesis has been obtained with CIDNP. Bodewitz *et al.* [7.84–86] performed the Grignard synthesis in the probe of an NMR spectrometer and observed CIDNP both in the Grignard reagent and in the hydrocarbon products from the recombination and disproportionation of alkyl radicals (Figs 7.29–30). For instance, in the reaction

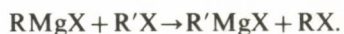


α -methylene protons in the $\text{CH}_3\text{CH}_2\text{CH}_2\text{MgI}$ carry *EA* polarization, the propylene protons are *AE* polarized. Polarization is also observed in $\text{C}_2\text{H}_5\text{MgBr}$ and $\text{C}_2\text{H}_5\text{MgI}$; in both cases the protons carry *EA* polarization. In the reaction with isopropyl iodide the protons are *EA* polarized.

The point is important that only multiplet CIDNP is observed in Grignard systems, and that net polarization has never been found. This means that the CIDNP observed does not arise in radical pairs $|\dot{\text{R}} \ \dot{\text{MgX}}|$ since in these pairs $\Delta g \neq 0$, which results in net CIDNP. Further, from the CIDNP signs in propylene and isopropyl iodide (Fig. 7.30) it follows unambiguously that the polarization arises in the diffusion radical pairs of alkyl radicals:



The CIDNP was shown by experiments not to arise in exchange reactions of the type



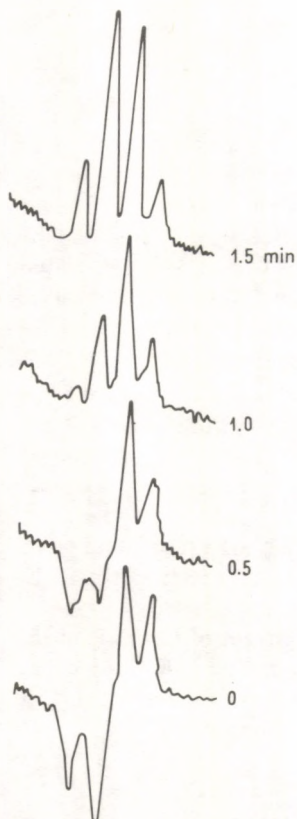


Fig. 7.29. CIDNP spectra of CH_2 protons of ethylmagnesium iodide in reaction of ethyl iodide with magnesium [7.84]

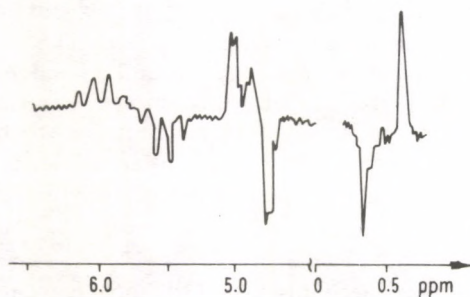
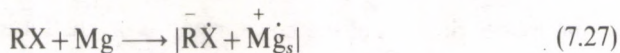


Fig. 7.30. CIDNP spectra of CH_2 and CH -protons of propylene (4.70–6.15 p.p.m.) and α -protons of propyl magnesium bromide (–0.35–0.65 p.p.m.) in reaction of isopropyl iodide with magnesium [7.85]

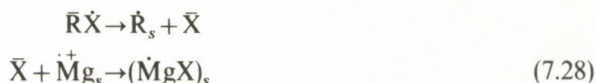
From these results it has been inferred [7.84–86] that the radicals are formed in the Grignard synthesis and they are of fundamental importance in its mechanism.

The following radical scheme of synthesis is proposed. The first stage is the electron transfer from metallic magnesium to the alkylhalogen molecule adsorbed



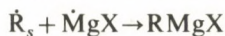
where Mg_s is a magnesium cation radical on the metallic magnesium surface. As a result of electron delocalization in metals, this radical is an electron-deficient surface defect.

The further reactions are



which result in adsorbed radicals \dot{R}_s and $(MgX)_s$; their recombination gives Grignard products.

However, the CIDNP in dibutyl ether was observed to be 5–30 times stronger than that in tetrahydrofuran, though the basicity of the latter is much higher. The Grignard reagent yield is approximately the same in both solvents. It is associated with the fact that the solvation of magnesium atoms and ions on the surface increases with the basicity (in tetrahydrofuran) which facilitates the escape of magnesium ions from the metallic surface. In tetrahydrofuran the CIDNP is weaker, i.e., the portion of pairs $|\dot{R} \dot{R}|^F$ is less than in dibutylether. It means that a considerable portion of alkyl radicals in tetrahydrofuran reacts not in the bulk but on the surface. Hence, the interaction



is the basic reaction of Grignard reagent formation. Here $\overset{\cdot}{Mg}X$ is a radical taken off the magnesium metallic surface. This is the main route of reaction since the Grignard reagent yields reach high values (up to 90%).

However, the above reactions do not account for the origin of CIDNP in the Grignard reagent. As it has been shown above, CIDNP arises in $|\dot{R} \dot{R}|^F$ pairs. The escaping radicals \dot{R}^* with polarized nuclei are adsorbed on the magnesium surface and bring their polarization to the final product by the reaction



This mechanism of Grignard reagent formation and CIDNP arising is, in principle, quite logical and convincing. The question remains why the recombination of \dot{R} and MgX radicals and the preceding radical pairs $|\dot{R} \overset{\cdot}{Mg}X|$ do not contribute to the nuclear polarization. As has been shown above for radical pairs with short electron relaxation times, the spin correlation is lost very quickly, the singlet–triplet evolution is violated and CIDNP does not arise. The pairs $|\dot{R} \overset{\cdot}{Mg}X|$ quite probably conform to this type since the electron relaxation time in the radical MgX can be very short.

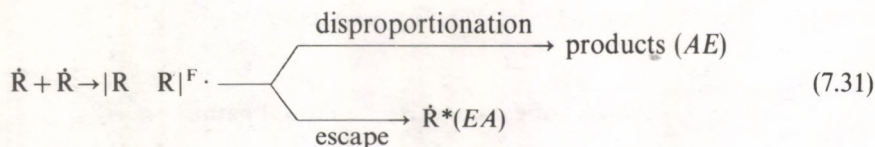
Quite recently Lawler *et al.* [7.87] have discovered that the presence of the catalyst $FeCl_2$ facilitates the reaction of alkylhalogen with the Grignard reagent, the reaction being accompanied by CIDNP. For example, in the reaction



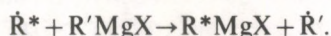
α -methylene protons of the new Grignard product are *EA* polarized. This allowed them to conclude that the radicals in such systems are generated in catalytic redox reactions having nothing to do with the Grignard synthesis at all, e.g., by the scheme



Furthermore, in the pairs with uncorrelated spins, the radicals acquire nuclear polarization:

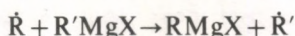


which is transferred to the Grignard reagent by the reaction



Thus, if there are some admixtures of iron or its salts or some other redox admixtures in the metallic magnesium, they can generate alkyl radicals and imitate the observed nuclear polarization in the products. According to this viewpoint radicals do not take part in the basic reaction of the Grignard synthesis at all, CIDNP being created only in the supplementary reactions.

However, Bodewitz *et al.* [7.88] opposed this viewpoint putting forward a number of arguments, the following being the most important. Leeuwen and Roobek investigated lead tetraacetate photolysis in the mixture of C_6D_6 and tetrahydrofuran in the presence of C_2H_5MgI . In the system ethyl radicals were generated and an intensive nuclear polarization was observed in the products of their transformation. However, no polarization was found in C_2H_5MgI . It means that the reaction suggested by Lawler



does not take place.

On the other hand, in a number of investigations CIDNP has been observed in reactions of haloidalkyls with organic magnesium compounds. Thus, isobutylene (6%), isobutane (39%) and tetramethylbutane (6%) are formed in tetrahydrofuran in the reaction of tert-butylmagnesium chloride with tert-butyl bromide [7.89]. The polarization observed in isobutane and isobutylene (AE) confirms the formation of tert-butyl radicals by electron transfer from the Grignard reagent to the alkylhalogen molecules. Vinyl proton polarization was also observed in 1-butene formed in the reaction of *n*-butylmagnesium iodide with *n*-butyl iodide [7.89].

The CIDNP in the reaction of diethylmagnesium with ethyl iodide and isopropyl iodide has been studied in [7.90]. It was observed in propylene (AE), propane (AE), isopropyl iodide (EA) and ethyl iodide (EA), and arises in pairs with uncorrelated spins, $|\dot{C}_2H_5 \quad \dot{C}_3H_7|$. It is interesting that ethane and ethylene have net polarization this is perhaps created in pairs $|(C_2H_5)_2\dot{Mg} \quad C_2H_5I|$ or $|(C_2H_5)_2\dot{M} \quad \dot{C}_2H_5|$ which are formed at the electron transfer between the reagents. Addition of two-valent cobalt and nickel salts accelerate the reaction and enhances the CIDNP (in accordance with the data by Ward *et al.* [7.89]).

These data prove that both the radicals and CIDNP can arise in reactions which are not connected with the Grignard synthesis, i.e., CIDNP is likely to arise in

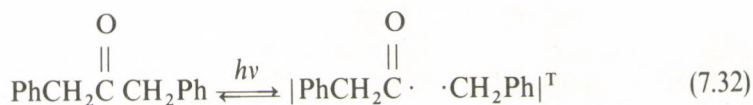
supplementary processes. Thus, the problem of the mechanism of Grignard synthesis remains unsolved.

These examples show how difficult and sometimes even impossible it is to interpret CIDNP and reaction mechanisms unambiguously.

7.3.5 Identification of crypto-radical pathways

One of the most exciting CIDNP features is its ability to detect crypto radical pathways which are impossible to detect by conventional methods. These pathways are usually connected with reversible transitions of radical pairs resulting in regeneration of the starting molecules. The examples of such transformations are quite numerous.

Dibenzyl ketone photolysis is accompanied with positive polarization of CH₂ protons and negative polarization of ¹³C keto-group [7.91–92]. It unambiguously indicated the partial regeneration of the primary ketone by the scheme



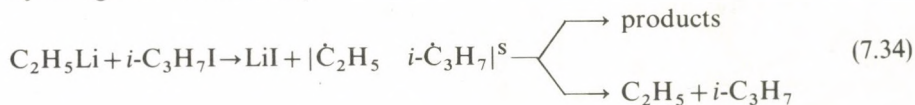
The same regeneration of the starting compounds was observed in the photolysis of di-*tert*-butyl ketone, deoxybenzoin, benzoin and other ketones subjected to Norrish type 1 photodecomposition [7.93, 94]. Nuclear polarization in the molecules of the starting material means that the reaction that follows decomposition, back recombination, contributes to the radiationless deactivation of electron excited molecules, this contribution being negligible, however, since the probability of triplet pair recombination does not exceed several percent.

The same regeneration takes place in azocompound photolysis [7.95]

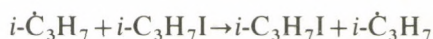


and is accompanied by nuclear polarization in the starting compound.

CIDNP is observed in alkylhalogen molecules in the reaction of alkyllithium with alkylhalogens. For instance,



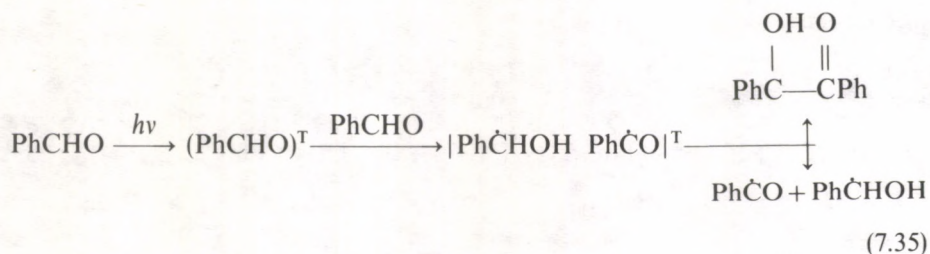
Radicals with polarized nuclei escaping the initial pairs take part in free valence migration reactions



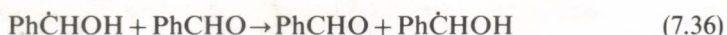
and transfer polarization to isopropyl iodide molecules.

Free valence migration reactions are usually detected by laborious isotopic techniques. However, one has no trouble in detecting such reactions with CIDNP.

Benzaldehyde photolysis in inert solvents, a strong nuclear polarization arises not only in the photolysis product—benzoin—but also in the aldehyde itself [7.93, 94]. Its formation follows the scheme

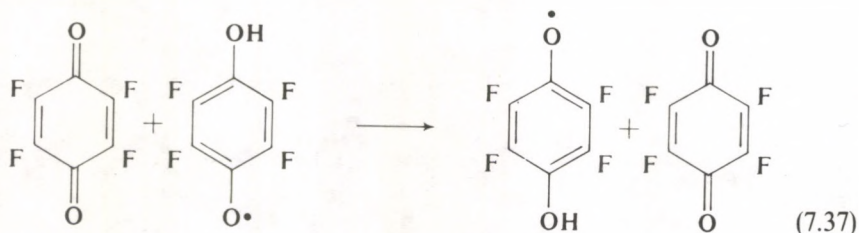


The radicals escaping the initial triplet pair participate in the hydrogen atom transfer reaction



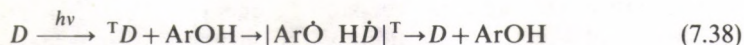
and confer nuclear polarization on the molecules of the starting aldehyde. The existence of this reaction, in which both the initial reagents and the final products are identical, is proved by the concentration dependence of the benzaldehyde CIDNP intensity. The reaction rate constant is about 10^5 l m s^{-1} .

Hydrogen atom transfer similarly inaccessible to observation by ordinary physical and kinetic techniques was observed in tetrafluoroquinone photolysis [7.96]:



It was accompanied by ^{19}F nuclear polarization in the primary quinone.

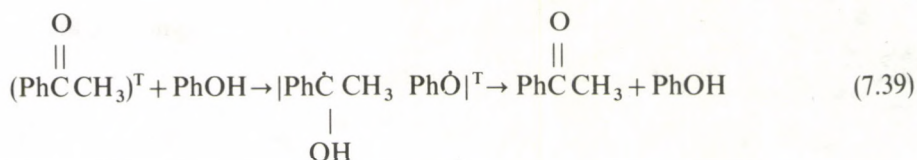
Photo-reversible hydrogen atom transfer was detected in reactions of dyes with phenols [7.97]



The initial photo-oxidation stage of phenol sensitized by dyes (for instance, Bengal rose) was shown by CIDNP to include the reversible hydrogen atom transfer between the hydroxyl phenol group and the oxygen atom of keto-group in the sensitizer molecule. Such reactions are almost completely reversible, i.e., the

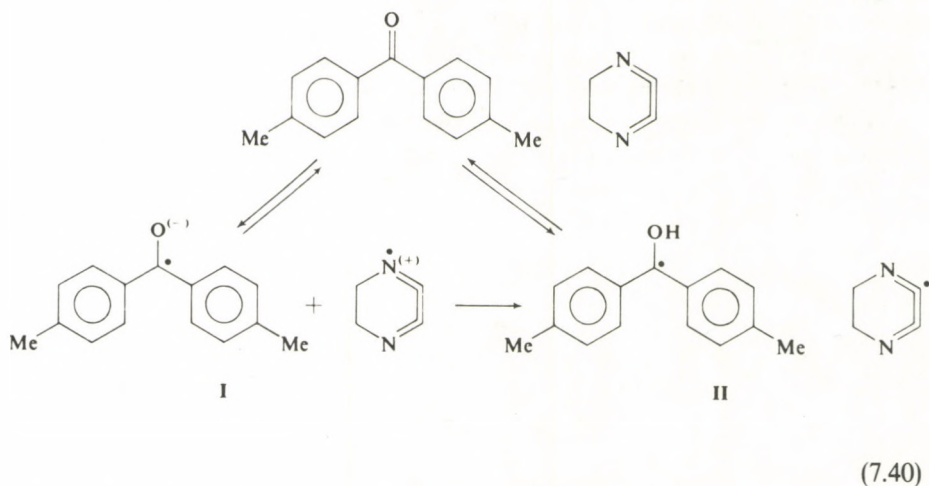
quantum yield of the irreversible pathways is very low. It shows the photoreversible hydrogen atom transfer is one of the main mechanisms of the degradation of electron excitation energy.

The quenching of acetophenol triplet states by phenols follows the same mechanism



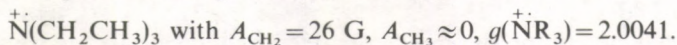
and is accompanied by a strong nuclear polarization in the starting molecules [7.5]. The excited states are also quenched by nitroaromatic compounds via photoreversible hydrogen atom transfer [7.98].

An interesting case of excited triplet state quenching of aromatic ketones by aliphatic amines was considered by Roth *et al.* [7.99, 100]:



The quenching can follow two paths: (1) reversible electron transfer resulting in the formation of intermediate radical-ion pair (I); (2) reversible hydrogen atom transfer with intermediate radical pair II. Under photoirradiation the system ketone + amine shows net polarization of the aromatic ketone protons whose sign corresponds to the regeneration of the initial ketone molecule from a pair with $\Delta g < 0$. For pair (I) $\Delta g = g(\text{Ph}_2\dot{\text{C}}\text{O}^-) - g(\equiv\dot{\text{N}}^+) \approx (2.003 - 2.0044) < 0$, for pair (II) $\Delta g = g(\text{Ph}_2\dot{\text{C}}\text{OH}) - g(-\dot{\text{C}}\text{HN} \leftarrow) \approx (2.0030 - 2.0028) > 0$. It means that the initial ketone regenerates from pair (I), i.e. the reversible electron transfer is the basic mechanism of excited ketone molecule quenching.

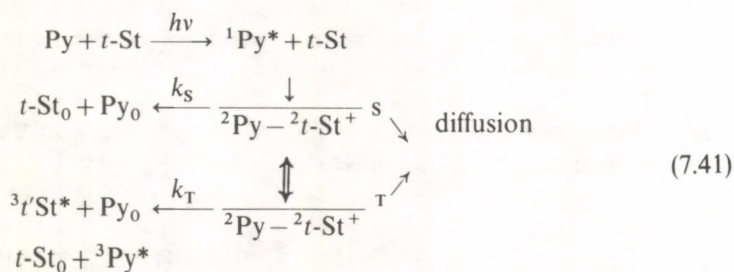
Reversible electron transfer is often also a quenching mechanism for excited singlet states. Direct evidence of the intermediate singlet radical-ion pairs in these processes has been obtained with CIDNP. For instance, when naphthalene is irradiated in deuterioacetonitrile in the presence of triethylamine, the amine methylene protons show strong negative polarizations, while the methyl protons are not polarized [7.100]. This proves that polarization arises in the radical-ion pair with one of the partners being an amine-cation radical



The other partner is a naphthalene radical anion with $g = 2.003$. The expected polarization sign coincides with experiment, provided the radical pair is in the singlet state, i.e., the reversible electron transfer is accompanied by quenching of the excited singlet state of the naphthalene molecule.

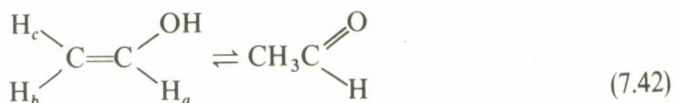
The reversible radical stages of electron and hydrogen atom transfer have been suggested earlier, unambiguous evidence of their existence being, however, obtained only with CIDNP. Photochemical reactions are the clearest examples of these radical stages where they are of fundamental importance in the processes of electron energy degradation and excited state quenching.

Interesting examples of electron transfer in the processes of photosensitized isomerization of olefins (in polar solvents) have been obtained in [7.101, 102]. Consider the classical process of *cis-trans* geometrical isomerization of stilbene. The conventional mechanism of the sensitized isomerization of stilbene deals with the triplet excitation transfer from the sensitizer to stilbene and does not include radical pathways. However, the detection and analysis of CIDNP effects in both isomers [7.102] show that the formation of excited stilbene is preceded by radical-ion pairs of stilbene and the sensitizer (pyrene):



7.3.6 Identification of unstable intermediates

CIDNP allows one to detect unstable intermediates which are formed in negligible quantities and are quickly transformed so that they cannot be observed among the final products. An example is vinyl alcohol, i.e. acetaldehyde enol form, which is in equilibrium with the ketoform



At room temperature the equilibrium is almost completely shifted to the right, so that the enol concentration is at least seven orders of magnitude lower than that of acetaldehyde. That is the reason why enol cannot be detected by conventional physical methods.

In acetaldehyde photolysis, enol is obtained by radical disproportionation



and, as these radicals escape from the radical pairs,

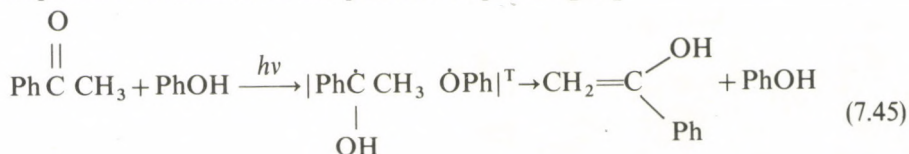


they carry nuclear polarization, transferring it to the enol molecules. On account of the strong polarization, one can detect the NMR spectrum of enol in small concentrations and determine the parameters of this unique molecule: the proton chemical shifts H_a , H_b and H_c being 6.27, 3.91, and 4.13 ppm respectively, and $J_{ab} = 6.5$ Hz, $J_{ac} = 14.0$ Hz, $J_{bc} = 1.8$ Hz [7.103].

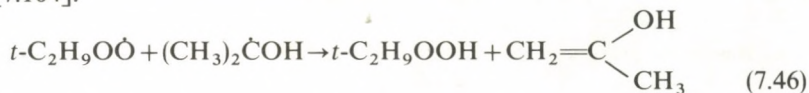
The CIDNP of ^{13}C neighbouring the hydroxyl group is negative [7.104]. This is in accordance with the fact that enol is formed by disproportionation in the diffusion pair $|t\text{-C}_4\text{H}_9\text{OO}\dot{\text{O}} \text{ HO}\dot{\text{C}}(\text{CH}_3)_2|^{\text{F}}$ with $\Delta g = g(\text{HO}\dot{\text{C}}\text{<}) - g(t\text{-C}_4\text{H}_9\text{OO}\dot{\text{O}}) < 0$ and the hf constant $A_{^{13}\text{C}}$ for the central carbon atom in the radical $(\text{CH}_3)_2\text{COH}$ being positive.

Photochemical reactions of tert-butyl hydroperoxide with different alcohols were used to synthesize different enols [7.105]. In all cases emission in the CIDNP spectra of ^{13}C neighbouring the hydroxyl group was observed, and the chemical shift of this nucleus was investigated in terms of the enol structure [7.105]. The CIDNP spectra made it also possible to detect the enol form in acetone photolysis (see [7.6]).

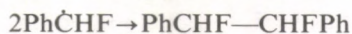
The acetophenone enol form was discovered by CIDNP in the photolysis of acetophenone in acetone in the presence of phenol [7.5]



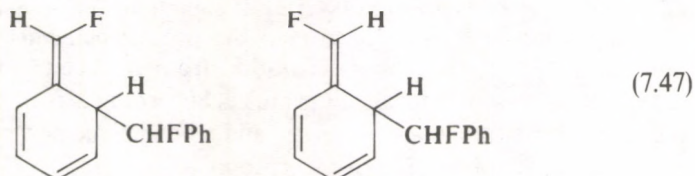
In the photolysis of tert-butyl hydroperoxide in isopropanol, the CIDNP spectrum showed the acetone enol form generated in the disproportionation reaction [7.104]:



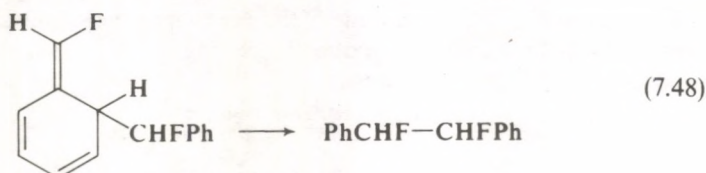
1,2-Difluorodibenzyl generated from α -fluorobenzyl radicals



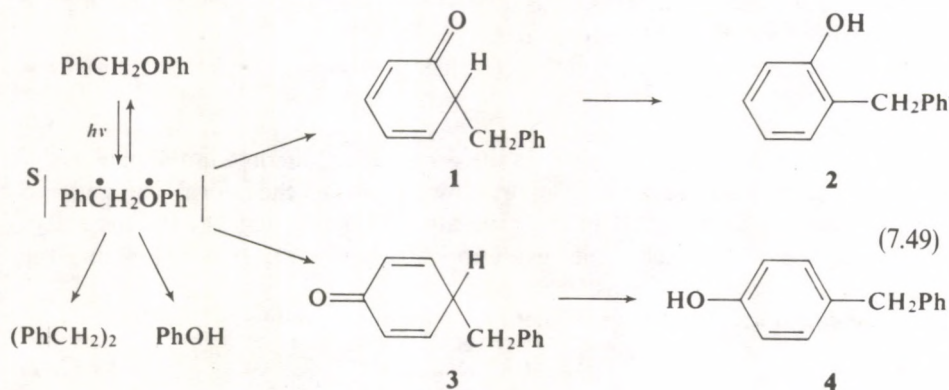
is one of the products of diphenylcarbene reaction with benzylfluoride. While not displayed in difluorobenzyl, ^{19}F nuclear polarization manifests itself in another product—difluorobenzyl precursor [7.106]. The CIDNP spectra showed that this product was fluoromethylenecyclohexa-2,4-diene in two diastereoisomeric forms



Thus, the α -fluorobenzyl radical recombination occurs with formation of the primary unstable product, substituted cyclohexadiene, which is then isomerized in dibenzyl with benzyl group migration



The intermediate unstable molecular product was also discovered by CIDNP in phenylbenzyl ether photolysis [7.107]. The reaction scheme describing the product composition and their nuclear polarization is



The intermediate unstable products (1) and (3) have the same structure as in the previous case (fluorobenzyl radical recombination). Here they are formed by the attachment of benzyl radical to phenoxyl in the *ortho*- and *para*-positions

respectively. In the product (3) the vinyl protons in 2 and 6 positions are positively polarized which corresponds to the product formation from a singlet pair, i.e., the ether photochemical decomposition runs via the singlet excited state. On switching off the light the vinyl molecule (3) proton polarization becomes half as big within 4 s, while it takes much longer (20 s and more) for the polarized nuclear signals of other molecules to reduce. It means that the nuclear relaxation time exceeds the lifetime of molecule (3). The CIDNP signal of these molecules are completely suppressed by addition of an acid, phenol (4) CIDNP signals being observed. Thus, (3) and (4) transformations are catalyzed by acid, this process being fast and accompanied by full transfer of the nuclear polarization from molecules (3) to phenol (4). The detection of unstable intermediate molecular products is of great interest as far as the reaction mechanism is concerned and reveals some new and unusual pathways of radical and molecular transformation.

7.3.7 Fast reaction kinetics in radical pairs

Singlet-triplet radical pair evolution leads to radical selection by the spin-nuclear states and, hence, to the pumping of the Zeeman nuclear levels. As it has been shown above the characteristic time of S-T₀ mixing is

$$t_{s-T_0} \approx (\Delta g \beta H + \sum_i A_i m_i^a - \sum_j A_j m_j^b)^{-1} \quad (7.50)$$

At ordinary values of Δg -factors and hf constants in organic radicals, $t \approx 10^{-9}$ – 10^{-7} s. The molecular dynamics of a pair are described by a dynamic model which suggests the radicals can escape the pair, travel apart, and then reencounter and form the initial pair again. The probability, $f(t)$ of the reencounter gradually decreases with increasing diffusion travel trajectory. However, it gives enough time for the singlet-triplet mixing in the pair to occur.

In the dynamic model the function $f(t)$ has the simplest form

$$f(t) = mt^{-3/2}. \quad (7.51)$$

In this form the function $f(t)$ neglects the finite radical lifetime in the pair (i.e., it supposes the radicals live infinitely long). However, in fact the radicals can undergo transformations which result in the generation of a new pair; at the instant of transformation the singlet-triplet evolution of the primary pair ceases and the evolution of a new pair begins.

To take into account the finite lifetime of the pair a modified function

$$f(t) = mt^{-3/2} \exp(-t/\tau) \quad (7.52)$$

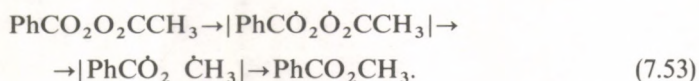
was introduced for the quantitative description of CIDNP. Here is the lifetime of the pair from the moment of its formation to the moment of its transformation into a new pair. This function takes into account the exponential time distribution of diffusion trajectories and restricts the singlet-triplet mixing time of the pair. The

degree of the singlet-triplet evolution, the pumping efficiency and the radical nuclear polarization acquired by the pair reduces as the time decreases.

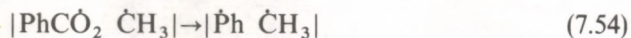
Thus any processes, physical and chemical, resulting in transformation of one radical pair into another and possessing a time scale less or comparable to the singlet-triplet evolution reduces the nuclear polarization. It is clear that by measuring the polarization one can estimate the kinetics of fast processes in radical pairs running with characteristic times t_{S-T_0} , i.e. 10^{-9} – 10^{-7} s.

Below we consider the basic processes of radical pair transformation.

1. *Radical decomposition.* A typical example is acyloxyradical decarboxylation in acyl peroxide decomposition

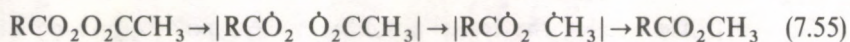


In the primary pair the hf constants on the protons of acyl radicals $\text{PhC}\dot{\text{O}}_2$ and $\text{CH}_3\dot{\text{C}}\text{O}_2$ are small, the difference of g -factors is negligible, hence, the S – T_0 mixing in this pair is slow. The time necessary to complete the S – T_0 transformations is great. Therefore, no nuclear polarization arises in fact in the primary pair. The main polarization of the protons of the methyl benzoate methyl group arises in the secondary pair. The singlet-triplet evolution of this pair stops when the radical $\text{PhC}\dot{\text{O}}_2$ decomposes, leading to new pair



The magnitude of the methyl benzoate polarization depends on the lifetime of the $\text{PhC}\dot{\text{O}}_2$ radical with respect to its decomposition: the shorter the lifetime, the less the polarization.

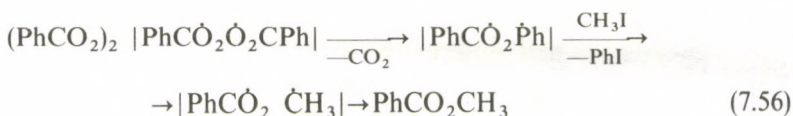
Using the modified function $f(t)$ in the form (7.52) we can calculate the value of polarization as a function of the radical lifetime τ . These calculations have been carried out for a number of pairs of the type $|\text{RC}\dot{\text{O}}_2\dot{\text{C}}\text{H}_3|$ resulting from peroxide decomposition



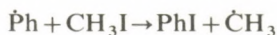
The nuclear polarization coefficients E for methyl protons are given in [7.60] at different times $T_{\text{RC}\dot{\text{O}}_2}$, a good agreement between theory and experiment being obtained at these times.

For the listed molecules the polarization coefficients, the lifetimes and the stability of acyloxyradicals gradually decrease. The lifetime of $\text{CH}_3\dot{\text{C}}\text{O}_2$ radical computed from the polarization coefficients coincides with that measured independently by other methods, this coincidence confirming the reliability of CIDNP as a quantitative method of chemical kinetics.

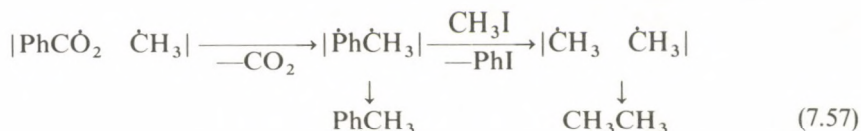
2. *Substitution reactions in radical pairs* also result in transformation of one radical pair into another. For instance, benzoyl peroxide decomposition in the presence of CH_3I ,



The radical pair $\mid \text{PhC}\dot{\text{O}}_2 \dot{\text{P}}\text{h} \mid$ transforms into a new pair $\mid \text{PhC}\dot{\text{O}}_2 \dot{\text{C}}\text{H}_3 \mid$ by the substitution reaction



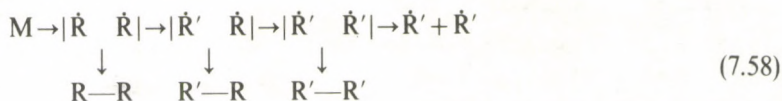
$\text{PhC}\dot{\text{O}}_2$ radical decarboxylation and the following substitution reactions are accompanied by new pair transformations



A remarkable feature of CIDNP in such systems is that in the products originating from new pairs (methyl benzoate, toluene, ethane) the methyl protons are *negatively* polarized. This means, that the pairs preserve the initial singlet pair spin multiplicity, and, furthermore, that the methyl proton polarization created in the pair $\mid \text{PhC}\dot{\text{O}}_2 \dot{\text{C}}\text{H}_3 \mid$ is preserved in further transformations and detected in toluene and even in ethane. The ability of the transformed pairs to preserve their spin multiplicity and the nuclear polarization conserved in the radicals is also confirmed by ^{13}C CIDNP.

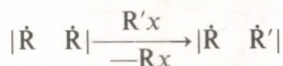
The conservation of the spin multiplicity in successive pairs means that their electron spin remains unchanged throughout the transformations; the conservation of nuclear polarization means that in decomposition and substitution reactions the nuclear spin does not change either. This property to conserve electron and nuclear spins is consistent with CIDNP experimental data, and is a general property of elementary processes of dissociation, recombination, and atom and electron transfer.

Kaptein [7.108] called the conservation of nuclear polarization both in the transformed pairs and in the molecules originated from them the *memory effect*. To describe it quantitatively, the following general scheme of radical transformation was considered



where a number of successive transformations of each radical, $\dot{\text{R}}$ and $\dot{\text{R}}'$, was assumed. The singlet-triplet evolutions in each of these pairs was supposed to occur independently and the polarization of each product, $\text{R}-\text{R}$, $\text{R}'-\text{R}$, and $\text{R}'-\text{R}'$, was calculated as the sum of the polarizations acquired in the preceding pairs. The quantitative results obtained were used to evaluate the radical pair lifetimes τ and the rate constants k of the successive transformations. It is evident that for

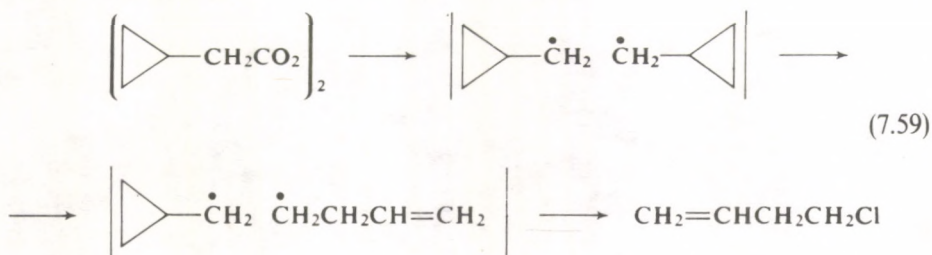
monomolecular decomposition reactions $\tau = k^{-1}$, for pair transformations by the bimolecular substitution reaction



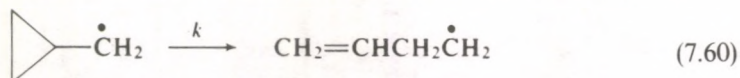
$\tau = k(R'X)^{-1}$ where k is the rate constant of the bimolecular reaction $\dot{R} + R'X \rightarrow RX + \dot{R}'$ leading to the transformation of one pair into another.

Using this approach and comparing theoretical CIDNP spectra with experimental ones, Kaptein determined the decomposition rate constant for the radical CH_3CO_2 to be $(2.5 \pm) \cdot 10^9 \text{ s}^{-1}$ (at 110°C), this value fitting fairly well with the value of $\tau_{\text{CH}_3\text{CO}_2}$ given in Table 7.1.

One more example is acetylcyclopropyl peroxide decomposition in hexachloroacetone



Transformation of one pair into another occurs by radical rearrangement

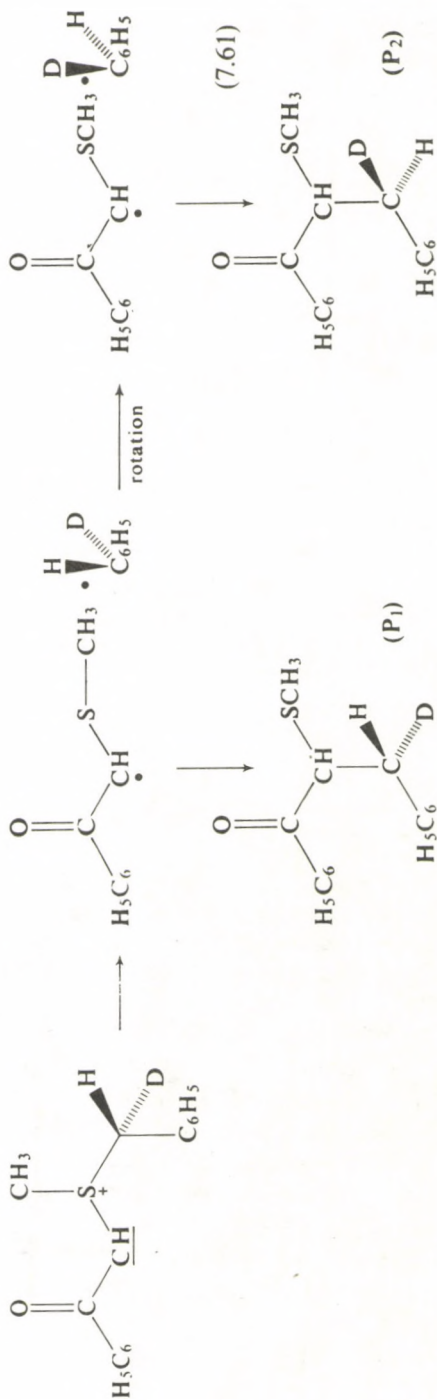


The CIDNP spectrum of one of the peroxide decomposition products—chlorobutylene—coincides with the theoretical prediction, provided that both pairs contribute to the nuclear polarization in the ratio 8:1; hence, the rate constant of cyclopropyl carbinyl radical rearrangement is determined to be $3 \cdot 10^7 \text{ s}^{-1}$ (at 80°) [7.108].

However, the authors of [7.109] showed that this approach, based on the additivity of singlet-triplet evolution of the successive radical pairs and hence on the additivity of their contributions to the CIDNP, is erroneous. The nonadditivity effects, called cooperative effects by den Hollander, are of fundamental importance for successive RPs with varying g -factors and hf constants. The origin of these effects will be considered below, but now consider some other RP transformation processes.

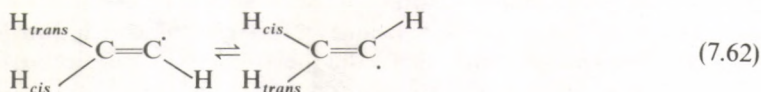
3. *Racemization* of RPs generated by optically active precursors is a physical process involving the molecular reconfiguration of one of the partners with respect to the other.

For example see equation (7.61):

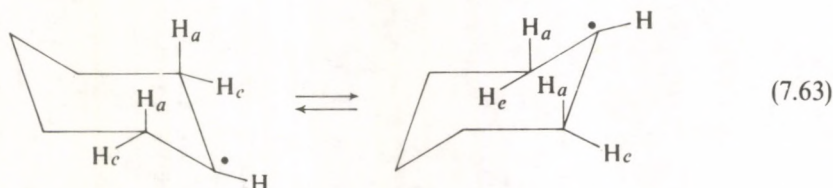


The products P_1 and P_2 are optical isomers originating from different pairs with different partner orientations. CIDNP in such systems has already been discussed; the conservation of optical activity is determined by the ratio of the time of the $S-T_0$ evolution in the pair to the time of molecular rotation, and by the relative contributions of the initial and secondary recombinations.

4. Conformational radical transformations

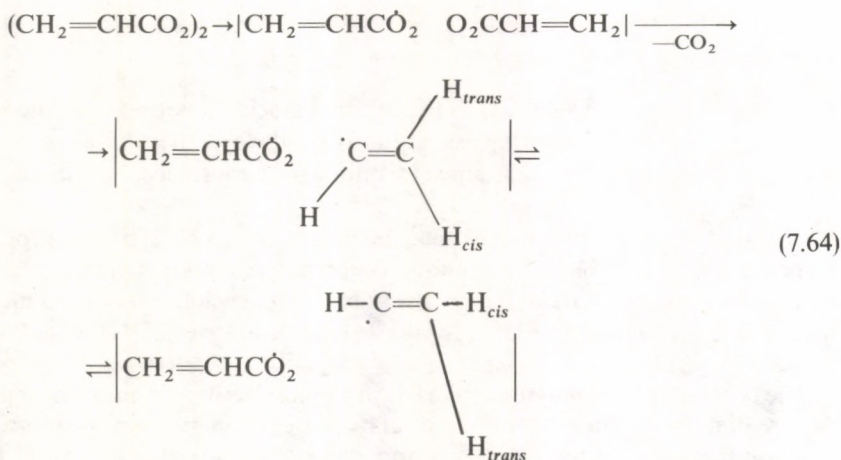


or



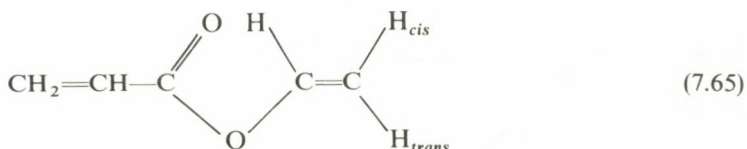
result in interchange of the radical hf constants. In the former case, the hydrogen atom inversion in the vinyl radical causes proton exchange between *cis*- and *trans*-positions with hf constants $A_{H_{cis}} = 34.2 \text{ G}$ $A_{H_{trans}} = 68.5 \text{ G}$. In the latter case the chair-chair inversion in the cyclohexyl radical causes the exchange of hydrogen atoms between axial and equatorial positions, with hf constants 41 G and 5 G respectively.

If these radicals form radical pairs, their inversion is in fact pair transformation (the radicals remaining chemically identical though) and the hf constants and thus the singlet-triplet evolution rates are changed. For example, acrylyl peroxide decomposition follows the scheme



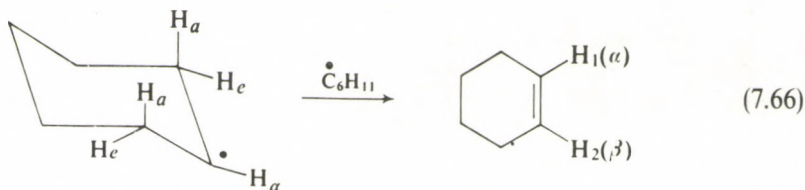
The last two pairs are chemically identical, the S-T₀ evolution rates being different with respect to the β-protons.

Two cases are possible here. If the radical inversion is slow (exceeding the S-T₀ mixing time), S-T₀ mixing is realized in radical pairs with fixed radical configuration. In this case the nuclear polarization in the recombination product must be different for H_{cis} and H_{trans} and proportional to A_{cis} and A_{trans}. If the inversion is fast (the inversion time is much less than that of the S-T₀ evolution), then S-T₀ evolution takes place in an averaged radical pair, and an average H_{cis} and H_{trans} are magnetically equivalent, and the average hf constant is (A_{H_{cis}} + A_{H_{trans}})/2. The CIDNP in the recombination products must be of equal magnitude and sign for both protons. This is the case that was observed for acrylyl peroxide decomposition in the recombination product



CIDNP effects for H_{cis} and H_{trans} protons were equal both in magnitude and in sign. This means that the vinyl radical inversion is fast with a rate greatly exceeding that of S-T₀ evolution ($k_{inv} > 10^{10} \text{ s}^{-1}$).

Quite a different situation was observed in RPs with cyclohexyl radicals. Livant and Lawler studied CIDNP in the disproportionation product of these radicals—in cyclohexene [7.110]:



Experimental cyclohexene CIDNP spectra coincided with those theoretically calculated under two following assumptions: (a) the cyclohexyl radical has a fixed geometry in a RP; (b) the radical disproportionation occurs with equatorial hydrogen atom abstraction.

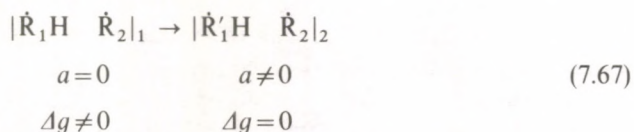
The former assumption means that the radical inversion is a slow process with respect to the S-T₀ evolution, i.e., the inversion frequency is less than 10^{-9} s^{-1} . This is consistent with ESR data: the inversion barrier in cyclohexyl is 21 kJ mol^{-1} , the inversion frequency recalculated for 40 °C (conditions of CIDNP experiments) is $5 \cdot 10^8 \text{ s}^{-1}$ [7.111].

The latter assumption points to reaction stereoselectivity in the radical pair. The preferential abstraction of the equatorial hydrogen atom in the disproportionation reaction is somewhat unexpected; a priori, the reaction seems to involve an axial

proton whose hf constant is 41 G and the carbon bonding is more repulsive as a result of the higher spin density concentrated on it as compared to a C—H_{eq.} bond. One of the possible interpretations of this fact is that the steric reaction limitations with respect to the axial atoms are more strict than those with respect to equatorial atoms.

We have considered the basic processes of radical pair transformations. Below we discuss cooperative effects in radical pairs. As has already been mentioned, if g -factors and radical hf constants are changed in pair transformations, the CIDNP in the products originating from these pairs cannot be calculated as the sum of CIDNP arising in all the preceding pairs. In these cases nonadditivity, or the cooperative effect, first mentioned in [7.109] proves to be important.

Consider the origin of these effects. Suppose we have a sequence of two pairs with one proton



Let $\Delta g \neq 0$ in pair, and the radical hf constants be equal to zero; in pair 2 the hf constants are large and $\Delta g = 0$. It is evident that no CIDNP arises in either pair, and the total effect is zero, i.e., no nuclear polarization can be observed in the product $R'_1 H - R_2$. This consideration however is invalid. To make this clear, it is sufficient

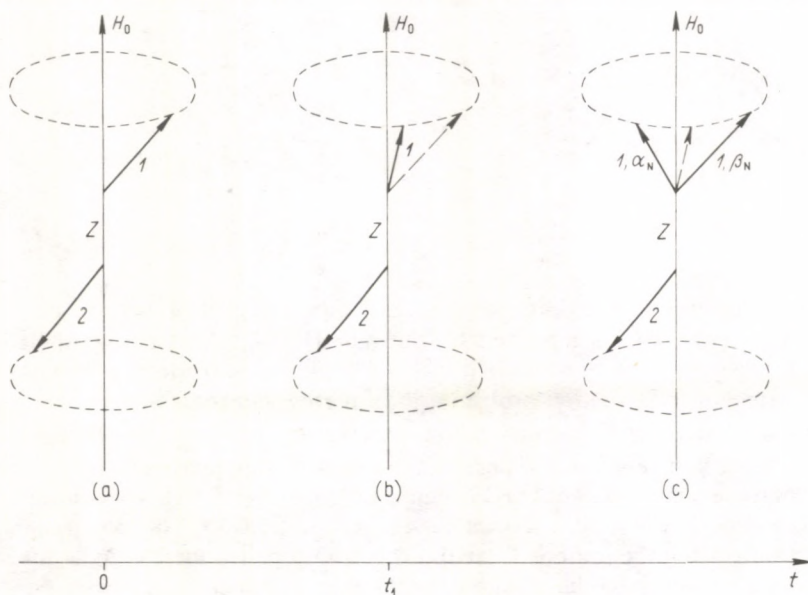
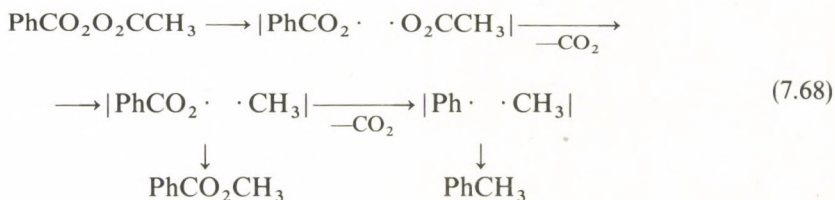


Fig. 7.31. Vector model of RP electron spins and singlet-triplet evolution: (a) initial state; (b) at the moment of transformation of pair 1 into pair 2; (c) pair 2 state. Z —axis is directed along magnetic field H

to consider the time evolution of the singlet-triplet mixing in terms of the vector model of pair electron spins. At $t=0$, pair 1 is singlet-born (Fig. 7.31 (a)). In this pair the precession frequencies of each spin differ because of the difference of g -factors. Therefore, by the moment of transformation of pair 1 into pair 2, t_1 , the difference in the spin precession phases appears, i.e., a triplet state admixture independent of the nuclear spin orientation occur (the hf constant in pair 1 is zero). At the time t_1 pair 1 is replaced by pair 2; the spin precession goes on, the difference in the precession frequencies now results from the hyperfine interaction: the electron spin associated with the α -proton precesses faster than that associated with the β -proton (provided the hf constant is positive). As a result, pair 2 with α -spin of proton becomes triplet more quickly, and the singlet-triplet mixing of the pair with β -spin is retarded, the pair thus becoming triplet more slowly (Fig. 7.31 (c)). Hence, the recombination product $R_1^{\cdot}H-R_2$ will be enriched with proton β -spins, while the pairs with α -spins, which become triplet (more quickly), are more likely to dissociate. Emission is detected in the CIDNP spectrum of the recombination product.

In the CIDNP analysis of the recombination products of successive radical pairs, it is necessary to consider the total singlet-triplet evolution of the whole pair sequence. In this case, the total CIDNP effect is the same as that of the CIDNP arising in a single pair in which Δg and the hf constants of all the preceding pairs are summed. This conclusion has been confirmed and theoretically substantiated in [7.109].

Examples of cooperative effect manifestations are quite numerous, acetylbenzoyl peroxide decomposition being the clearest

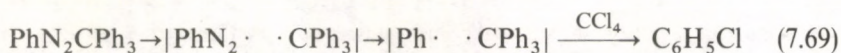


Methyl proton CIDNP has been discussed already; it arises in the pair $|\text{PhCO}_2\cdot \cdot \text{CH}_3|$, then is inherited by the pair $|\text{Ph}\cdot \cdot \text{CH}_3|$ and observed in toluene (this is called the *spin memory effect*). That is why emission in the CIDNP spectra corresponds to methyl proton both of methyl benzoate and of toluene.

The strong emission of phenyl protons in toluene is unexpected. In a radical $\text{PhCO}_2\cdot$ the hf constants at the phenyl protons are negligible; therefore the net CIDNP of these protons cannot arise in the pair $|\text{PhCO}_2\cdot \cdot \text{CH}_3|$. It cannot arise in the pair $|\text{Ph}\cdot \cdot \text{CH}_3|$ either, since $\Delta g \approx 0$. The net CIDNP of toluene phenyl protons results from the joint S-T₀ evolution of both pairs, one having a nonzero Δg , the other having large hf constants in the phenyl radical.

If no account is taken of cooperative effects, in erroneous conclusions can result for the signs and relative values of radical hf constants and radical transformation

rate constants. For instance, in phenylazotriphenylmethane decomposition in CCl_4 [7.112]



CIDNP was observed in chlorobenzene; it was suggested that it originated from the initial pair with the participation of diazophenyl radical $\text{PhN}_2 \cdot$. The signs of the hf constants at the protons of this radical were obtained from the CIDNP signs. However, the reliability of these data is doubtful. The CIDNP in chlorobenzene results from the $S-T_0$ mixing in both pairs—in the first pair Δg is large, in the second the hf constants in the phenyl radical are significant. The total CIDNP is associated with the cooperative effect of $S-T_0$ mixing in both pairs. The quantitative estimates of the diazophenyl radical lifetime [7.113] are perhaps invalid for the same reason: the net CIDNP was supposed to arise in the initial pair with the participation of PhN_2 radical, cooperative effects being neglected.

Now consider RP spin correlation. As noted above, the spin multiplicity of pairs does not change in the process of their transformation. It means that, first, in dissociations and substitutions, electron spins do not change, second, radical pairs have some spin memory and preserve their electron spin correlation.

The problem is how long the spin correlation can be preserved in pairs or, in other words, how much time it takes for a pair to be transformed into the doublet states of individual radicals. The loss of spin correlation does not exclude the possibility of the radicals forming the initial pair again, with a new random electron spin correlation (as in diffusion pairs formed by random encounters of independently generated radicals).

Function (7.52) describes all the diffusion trajectories of radicals in a pair; whereas the function

$$F(t) = mt^{-3/2} \exp(-t/T_2^*) \quad (7.70)$$

describes the trajectory of those diffusion paths in which the radicals preserve their correlation; here T_2^* is the characteristic time of correlation losses.

Comparing $f(t)$ and $F(t)$ one can see that if $T_2^* < \tau$ then the radicals return from their short diffusion paths ($t \lesssim T_2^*$) to form the initial pair with preserved spin correlation, and from long travels ($t > T_2^*$) to form uncorrelated pairs. In this case it is clear that the nuclear polarization is the sum of two parts: one arising in pairs with preserved correlation, the other in those having lost correlation. If $T_2^* \gg \tau$ all the pairs preserve their spin correlation.

There are some experimental data on CIDNP in the presence of radical acceptors [7.114] from which T_2^* was qualitatively evaluated, the ontime being 10^{-7} – 10^{-6} s, i.e., the RP spin correlation is preserved for a long time.

There are, however, cases when the spin correlation vanishes quickly. The reasons for this are, first, short electron relaxation time T_1 and T_2 in radicals, second, a large Δg for the pair. In the former case, the electron relaxation results in randomization of the electron phase precession in the pair and violation of the state mixing, these

pairs constantly being in a state with uncorrelated spins. Fast electron relaxation is supposed to take place in organometallic radicals of the type RHg , RMg , R_3Pb , etc. [7.115–117], and also in alkoxy radicals RO . Recently, however, nuclear polarization arising in radical pairs with the participation of RO , has been discovered in quinone photochemical reactions, i.e., the electron relaxation time in this radical exceeds that of S-T_0 evolution, $T_1 \gtrsim 10^{-10}$ s [7.118].

When the Δg of a pair is large, the time of S-T_0 mixing is small, and thus during the RP lifetime transitions S-T_0 and $\text{T}_0\text{-S}$ occur periodically and repeatedly; this results in spin correlation loss. CIDNP (and other magnetic effects) can be observed in such systems only in short-lived radical pairs with the lifetime $\tau \approx t_{\text{S-T}_0}$. The quantitative theory of these effects is given in ref. [7.29].

7.3.8 "Hot radicals"

The problem of hot radicals, i.e., those carrying excess energy in their internal degrees of freedom (either rotational or vibrational), is very often discussed in the literature. The existence of hot radicals in the gas phase at low pressures has been proved. The existence and possible participation of hot radicals in condensed phase reactions is often called in question since the strong intermolecular interactions in liquids or solids must lead to rapid, almost instantaneous, excess energy loss and scattering in the lattice. Nevertheless, speculations on the participation of hot radicals in reactions are widespread.

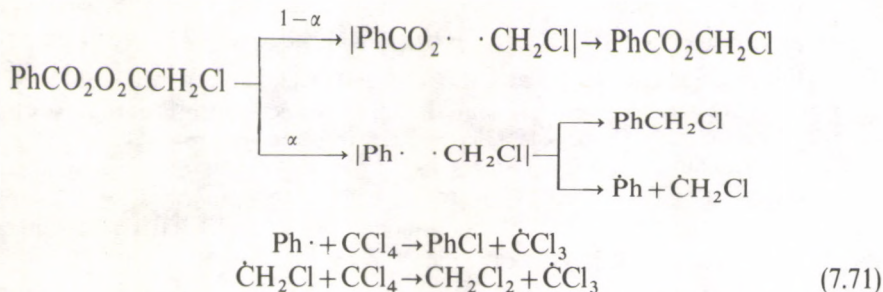
CIDNP allows one in principle to determine whether hot radicals are present in the process under study and whether they play any role. The idea of their observation is simple: if hot radicals do exist and possess a high reactivity, then the pairs including hot radicals transform into other pairs much faster than those whose radicals have no excess energy.

As shown above, the sign and the magnitude of CIDNP depend on the rate of RP transformation and thus will be sensitive to the presence of hot radicals. Consider some illustrations of this idea.

The first evidence for hot radicals has been obtained by Kaptein [7.17]: in acetyl peroxide thermal decomposition the net polarization of methyl acetate OCH_3 protons was observed and ascribed to the radical pair $|\text{CH}_3\text{CO}_2 \cdot \cdot \text{CH}_3|$. No net polarization was observed in the peroxide photolysis, i.e., the lifetime of the photogenerated pair $|\text{CH}_3\text{CO}_2 \cdot \cdot \text{CH}_3|$ is much shorter than that of the thermally generated pair. This difference was accounted for by the fact that, in photolysis, the radicals $\text{CH}_3\text{CO}_2 \cdot$ carry excess energy and decompose faster than those thermally generated.

A more detailed CIDNP investigation into the processes of peroxide decomposition involving hot radicals has been carried out by den Hollander *et al.* [7.119]. $\text{PhCO}_2\text{O}_2\text{OCH}_2\text{Cl}$ peroxide decomposition under thermally equilibrium conditions (CCl_4 , 120°), in direct photolysis, and in the presence of photosensitizers—anthracene and benzophenone—has been studied.

The CIDNP of the basic products of thermal decomposition is explained by the following reaction sequence



(The scheme does not consider pairs including $\text{CH}_2\text{ClCO}_2 \cdot$ radicals, which rapidly decarboxylate and have no influence on the CIDNP.)

The g -factor for benzoyloxyradical is 2.0117, for phenyl it is 2.00234, for $\dot{\text{C}}\text{H}_2\text{Cl}$ radical 2.0065; hf constants for phenyl $A_{\text{H}(\text{ortho})} = +17.4$ G, $A_{\text{H}(\text{meta})} = +5.9$ G and $A_{\text{H}(\text{para})} = +1.9$ G; for $\dot{\text{C}}\text{H}_2\text{Cl}$ $A_{\text{H}} = -20.7$ G. Hence, CH_2 protons of chloromethyl benzoate should carry negative polarization and CH_2Cl_2 positive, in accord with experiment. The emission line of CH_2 protons in PhCH_2Cl illustrates the memory effect: the negative polarization of CH_2 protons arises in the initial pair $|\text{PhCO}_2 \cdot \cdot \text{CH}_2\text{Cl}|$ then it is inherited by the secondary pair $|\text{Ph} \cdot \cdot \text{CH}_2\text{Cl}|$ and further in the molecule PhCH_2Cl . In the secondary pair $|\text{Ph} \cdot \cdot \text{CH}_2\text{Cl}|$ Δg has an opposite sign compared to the Δg in the initial pair; its CIDNP should be thus of an opposite sign. However, Δg of the initial pair is much higher than that of the secondary pair, hence the polarization arising in the initial pair predominates in the molecule PhCH_2Cl . Thus, the peroxide thermal decomposition occurs via radical pairs $|\text{PhCO}_2 \cdot \cdot \text{CH}_2\text{Cl}|$ and $|\text{Ph} \cdot \cdot \text{CH}_2\text{Cl}|$.

The CIDNP arising in the peroxide photolysis has a number of peculiarities. The CIDNP sign of chloromethyl benzoate CH_2 protons remains unchanged, i.e. the direct peroxide photolysis occurs in the singlet state (as well as the thermolysis). The CIDNP signs of CH_2 protons in PhCH_2Cl and CH_2Cl_2 molecules are inverted. It means that the greatest portion of polarization arises in the pair $|\text{Ph} \cdot \cdot \text{CH}_2\text{Cl}|$ and considerably exceeds that which could arise in the initial pair $|\text{PhCO}_2 \cdot \cdot \text{CH}_2\text{Cl}|$. This situation is in contrast to that observed in thermolysis.

The only possible explanation of this principal difference is that in photolysis the greatest portion of pairs $|\text{Ph} \cdot \cdot \text{CH}_2\text{Cl}|$ originates directly from the peroxide avoiding the initial pair stage; this reaction undoubtedly occurs with the participation of hot $\text{PhCO}_2 \cdot$ radicals, which so rapidly decarboxylate that the initial pairs with hot $\text{PhCO}_2 \cdot$ radicals do not contribute to the CIDNP at all. Thus the peroxide photolysis follows two channels: with the participation of hot radicals (with probability α) and by the normal path of thermolysis (with probability $1-\alpha$). The ratio of the CIDNP signal intensities of benzene chloride and chloromethyl benzoate CH_2 protons reflects the ratio of these two paths. This ratio was found to depend on the wavelength of the photolytic light: for $\lambda > 240$ nm this ratio is 5.0; for

$\lambda > 290$ nm it is 3.5. In other words, the shorter the wavelength, i.e. the higher the energy of photolytic quanta, the greater the probability α .

The peroxide decomposition sensitized by anthracene goes via the singlet state (like thermolysis); the CIDNP signs of benzyl chloride and CH_2Cl_2 protons show that in this case α is also large. The CIDNP signal ratio between benzyl chloride and chloromethylbenzoate is here less than that in the direct photolysis. It means that α is lower in sensitized photolysis as compared to direct photolysis.

The peroxide photodecomposition sensitized by benzophenone goes through the triplet state; in PhCH_2Cl the CH_2 protons are negatively polarized, i.e., even in this case the contribution to the CIDNP made by $|\text{Ph}\cdot \cdot \text{CH}_2\text{Cl}|$ pairs, generated directly from the peroxide via hot radicals, prevails.

The α values can be calculated from the CIDNP signal intensity ratio of chloromethyl benzoate and benzyl chloride (for thermal decomposition $\alpha = 0$); they are given below:

- Direct photolysis 0.75
- Sensitized by anthracene 0.25
- Sensitized by benzophenone 0.07
- Thermal decomposition 0.0.

In photolysis, 3/4 of the peroxide molecules decompose with the participation of hot PhCO_2 radicals, which quickly decarboxylate; only 1/4 of the radicals have enough time to lose the excess energy, to be stabilized, and to follow an ordinary reaction path as in thermolysis.

In the photolysis sensitized by anthracene the energy excess is less and so α decreases. The difference in α for photolysis sensitized by anthracene and benzophenone corresponds to that in the energy of their excited states; anthracene singlet state having the energy 320 kJ mol^{-1} , benzophenone triplet state 290 kJ mol^{-1} .

The energy excess is less in the case of benzophenone and, hence, the participation of hot radicals in the reaction decreases.

The above results prove that hot radicals do play an important role even in condensed phases, and strongly affect the reaction channel and the product yield. The CIDNP data give the lifetimes of hot PhCO_2 radicals. τ as $\lesssim 10^{-10}$ s; in principle, CIDNP comparison in thermal and photochemical processes of the same type can be used to identify hot radicals in other systems.

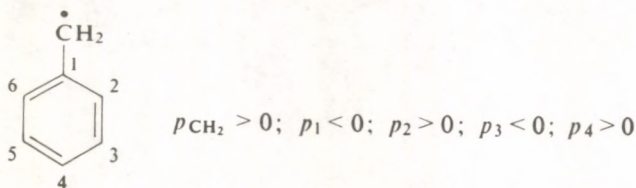
7.3.9 CIDNP applications in structural chemistry

CIDNP is of great importance as a method of structural chemistry, and adds considerably to the method of electron paramagnetic resonance and also to standard nuclear magnetic resonance. CIDNP allows one to determine the signs of radical hf constants, the g -factor, exchange interaction energies in RPs, the values and the signs of molecular spin-spin interaction constants, and radical nuclear

relaxation times. This section considers the most interesting and latest structural information obtained by CIDNP.

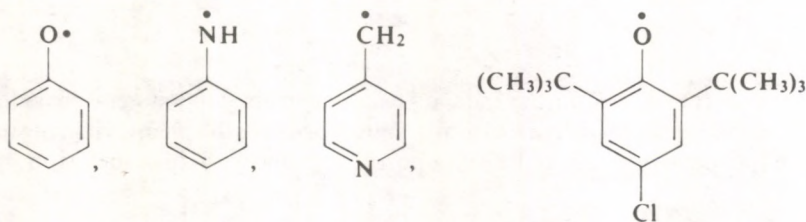
The signs of radical hf constants are of primary interest as they give information on the unpaired electron spin density distribution in the radical and also on which of the two distribution mechanisms—spin delocalization or spin polarization—prevail [7.46].

The sign of π -electron spin density in π -system in radicals of benzyl type is known from ESR and quantum chemistry to alternate:



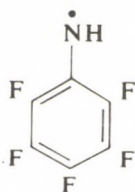
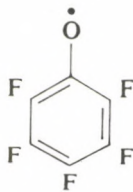
Hence, $A_{\text{H}}(\text{CH}_2) < 0$; $A_{\text{H}}(2, 6) < 0$; $A_{\text{H}}(3, 5) > 0$; $A_{\text{H}}(4) < 0$; hf signs for ^{13}C nuclei are opposite: $A_{\text{C}}(\text{CH}_2) > 0$; $A_{\text{C}}(1) < 0$; $A_{\text{C}}(2, 6) > 0$; $A_{\text{C}}(3, 5) < 0$; $A_{\text{C}}(4) > 0$. These results are obtained by CIDNP in dibenzyl ketone photolysis [7.91, 92] and are in full accord with theory.

The hf constant signs for H and ^{13}C in radicals [7.92, 120, 121]



alter in the same order. In the last radical the positive spin density starts from *ortho*-position of the phenyl ring into the tert-butyl group and results in the following hf constant signs: $A_{\text{C}}(\text{C}) < 0$; $A_{\text{C}}(\text{CH}_3) > 0$ [7.121].

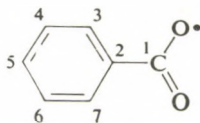
From the π -system of the phenyl ring the spin density penetrates to the hydrogen atoms, attached to the ring, by the mechanism of spin (or exchange) polarization; hence the hf constant signs are opposite to those on the neighbouring carbon atoms. In analogous fluoro-substituted radicals, the spin density propagates from the ring to the fluorine atoms by the direct delocalization mechanism, and has the same sign as that on the neighbouring carbon atoms; this explains why the signs of the hf constants on ^{19}F nuclei obtained by CIDNP [7.122] coincide with those on ^{13}C



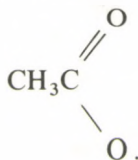
$$A_F(2,6) > 0; A_F(3,5) < 0; A_F(4) > 0$$

Now consider $\text{PhCO}_2\cdot$ and $\text{CH}_3\text{CO}_2\cdot$ radicals which, when studied by ESR, yield no information on the spin densities.

In the benzoyloxyl radical

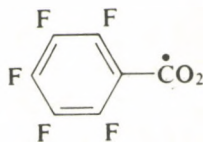


$A_C(1) < 0; A_C(2) < 0; A_C(3, 7) > 0$; in the radical



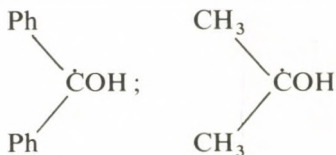
$A_C(\text{CO}_2) < 0; A_C(\text{CH}_3) > 0$.

The fragment $\text{O}-\text{C}-\text{O}$ in the radical is similar to the allyl system provided the oxygen atoms possess positive π -electron spin density. In the phenyl ring, positive π -electron spin density gets into the *ortho*-position; in line with this conclusion $A_F(3, 7) > 0$ in the radical



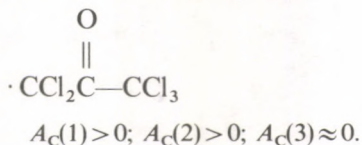
The sign of the hf constants for ^{13}C and ^{19}F in these radicals was obtained from CIDNP in the decomposition of the corresponding acyl peroxides [7.120, 123, 124].

The hf sign on the central carbon atom in the radical



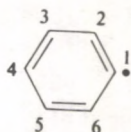
was found to be positive from ^{13}C CIDNP of enols generated in ketone photolysis [7.104]. The hf constant of the hydroxyl proton was found from the proton polarization in the photolysis of benzophenone in isopropanol [7.41] to be positive in the radical $\text{Ph}_2\dot{\text{C}}\text{OH}$ and negative in $(\text{CH}_3)_2\dot{\text{C}}\text{OH}$. This means that the OH group in the radical $(\text{CH}_3)_2\dot{\text{C}}\text{OH}$ is located in the radical plane, while in the radical $\text{Ph}_2\dot{\text{C}}\text{OH}$ it is outside the plane.

In the radical $\text{H}-\dot{\text{N}}-\text{COOC}_2\text{H}_5$ $A_{\text{H}}(\text{N}) < 0$, i.e., the π -electron is localized on the nitrogen atom [7.125], in $\dot{\text{C}}\text{HCl}_2$ and $\dot{\text{C}}\text{H}_3$ $A_{\text{C}} > 0$, $A_{\text{H}} < 0$, in keeping accordance with the theory of electronic structure of these radicals. In the radical



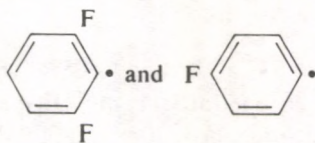
Now consider hf interactions in π -electron radicals in which the unpaired electron is located in a σ -orbital.

In the phenyl radical



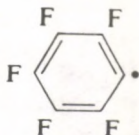
the unpaired electron occupies sp^2 -hybrid orbital and spreads through the ring through the σ -bond system. Therefore, all the hf constants on the protons are positive: $A_{\text{H}}(2,6) = +17.4$ G; $A_{\text{H}}(3,5) = +5.9$ G; $A_{\text{H}}(4) = +1.9$ G [7.126]; from the CIDNP spectra it follows that $A_{\text{C}}(1) > 0$ in agreement with theory.

In fluoro-substituted radicals



$A_{\text{F}}(2) > 0$ and $A_{\text{F}}(4) > 0$ (like on the phenyl radical protons).

In the radical

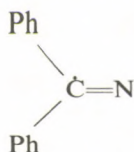


$A_F(2.6) > 0$, $A_F(3.5) > 0$, however, unexpectedly $A_F(4) < 0$; here $|A_F(2.6)| > |A_F(3.5)| > |A_F(4)|$. These data are obtained from the CIDNP spectra of the decomposition products of benzoylfluoro-substituted peroxides [7.124].

In vinyl radicals $\dot{C}H=CH_2$ and $CH_3-\dot{C}=CH_2$ the unpaired electron also occupies a σ -orbital and the theory predicts positive signs of the CIDNP constants on α - and β -protons. These predictions have been confirmed by the CIDNP spectra of decomposition products of corresponding acylperoxides [7.38]. In the last radical $A_H(CH_3) > 0$; this result has been obtained only by CIDNP.

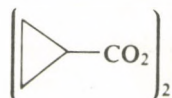
In the radical $CH_3-CH=\dot{C}H$ it has been obtained by CIDNP that $A_H(CH_3) < 0$ [7.38].

In the radical $PhCH_2\dot{C}O$, $A_C(CO) > 0$ according to ^{13}C CIDNP spectra obtained in dibenzyl ketone photolysis [7.92]. In the radical



$A_C(CN) < 0$; in the phenyl rings on the carbon atoms, to which the CN group is attached, $A_C > 0$; it is evident that the spin density spreads from the nitrogen σ -orbital along the σ -bonds alternating its sign [7.127].

From the CIDNP spectra of the decomposition product of peroxide



it has been found [7.38] that in cyclopropyl radical



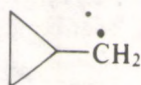
$A_H(\alpha) < 0$, $A_H(\beta) > 0$; $|A_H(\alpha)| = 6.5$ G according to ESR. The value of $A_H(\alpha) = -6.5$ G is small compared to $A_H = -23$ G in the CH_3 radical; it means that the cyclopropyl radical is bent and the α -proton is located outside the three-member cycle plane.

From the sign of the multiplet CIDNP in a propene molecule

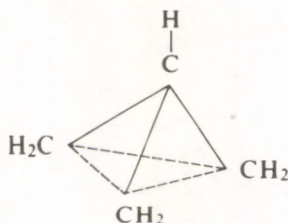


it has been found that the sign of the constant of the proton spin-spin vicinal interaction is positive ($J_{HH} = +1.8$ Hz) [7.38]. The positive sign of this constant is confirmed by CIDNP spectra in a large number of examples, as well as the negative sign of the geminate spin-spin interaction constants.

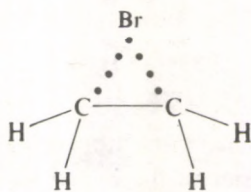
In the radical



the α -proton hf constant is negative and the β -proton hf constant is positive (+ 2.55 G). Hence, the radical conformation in which the π -orbital is almost parallel to the cyclopropyl ring plane and directed along the radical symmetry axis is more preferable. Besides, the CIDNP spectra entirely exclude the non-classical pyramidal structure of cyclopropylmethyl radical



The CIDNP spectra of $\text{PhCO}_2\text{O}_2\text{CCH}_2\text{CH}_2\text{Br}$ peroxide decomposition products unambiguously exclude the non-classical structure ascribed to the radical $\dot{\text{C}}\text{H}_2\text{CH}_2\text{Br}$,



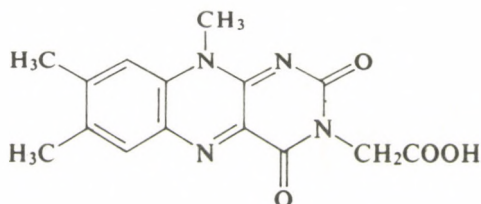
in which the Br atom is assumed to belong to both carbon atoms [7.128].

CIDNP affords unique information on nuclear relaxation times T_{1n}^R in short-living radicals inaccessible by other methods. The idea of T_{1n}^R determination is based on the comparison of the polarization coefficients in RP recombination and escape products. The initial polarizations arising in the radicals that have recombined and escaped from the pair are equal. However, the escaping radicals during the lifetime τ lose their polarization due to nuclear relaxation according to $\exp(-\tau/T_{1n}^R)$. With τ known, one can readily find T_{1n}^R ; thus, in the radical $\text{Ph}\dot{\text{C}}\text{H}_2$ $T_{1n}^R = 3.5 \cdot 10^{-4}$ s for CH_2 protons [7.65], in the radical $\dot{\text{C}}\text{HCl}_2$ $T_{1n}^R = 4.5 \cdot 10^{-4}$ s [7.129], in $\dot{\text{C}}(\text{CH}_3)_3$ $T_{1n}^R \approx 2.4 \cdot 10^{-4}$ s [7.130].

A new approach to the study of the structure of biomolecules employing CIDNP has been proposed by Kaptein *et al.* [7.131–133]. Some biological macromolecules (e.g. proteins, enzymes) possess globular structure in which some amino acid residues are on the globular surface and thus can get into contact with molecules in the solution, while other amino acid residues are “hidden” in the interior of the globule and thus unable to come into contact. If molecules of a substance capable to

react with the surface amino acid groups and to give rise to CIDNP are added to the solution of such a globular protein or enzyme, then the NMR spectra allow one to detect these surface groups and to distinguish them from the interior ones.

To create CIDNP, Kaptein *et al.* have used the photochemical reaction of 3-carboxymethylflavin dye



with amino acid residues of histidine(his), triptophane(trp) and tyrosine(tyr).

The photoreaction of flavin (F) with these amino acid groups follows the scheme (e.g., tyr)



The triplet flavin abstracts a hydrogen atom from tyr by reaction (7.73) and forms a radical pair; the back transfer of the hydrogen atom regenerates the starting molecules tyrH* and F. The CIDNP arising in the RP is detected in the amino acid residue tyrH*. Figure 7.32 depicts the CIDNP spectra for tyr, trp and his. In the aromatic region of his and trp, positive polarizations are observed, while the protons 3,5 tyr are negatively polarized. The CIDNP sign alteration is also observed for CH₂ protons which results from the sign alteration of Δg in the RP; flavosemiquinone g -factor ($g=2.0030$) is less than tyr g -factor ($g=2.0041$) but exceeds those of his and trp radicals.

NMR spectra of biomolecules contain a great number of overlapping lines. Therefore, to detect CIDNP, Kaptein *et al.*, have developed a special technique employing the methods of *preliminary line saturation* and *differential spectra*. Figure 7.33 presents pulse sequence. On preliminary saturation (pulse duration 1 s) a light pulse of an argon laser (pulse power 5–7 W, duration 0.4 s) and radio-frequency 90° pulses are switched on with 6 s intervals to detect the free induction signal decay. Then the same sequence is repeated, but without the light pulse. Alternating the light and dark sequences and subtracting the Fourier transforms of the free induction decays, one obtains the CIDNP signals as differential spectra. That was the method to study CIDNP of surface amino acid groups of some biomolecules.

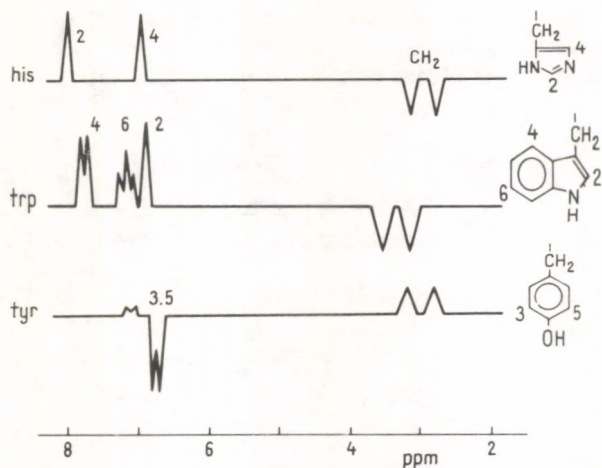


Fig. 7.32. The scheme of photo-CIDNP spectra of his, trp, and tyr amino acid residues in the presence of flavin [7.133]

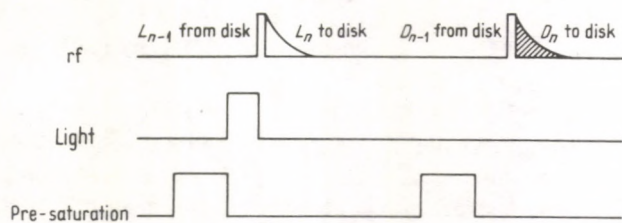


Fig. 7.33. Pulse sequence for the CIDNP detection by the differential spectra method, L and D denote light and dark periods [7.132]

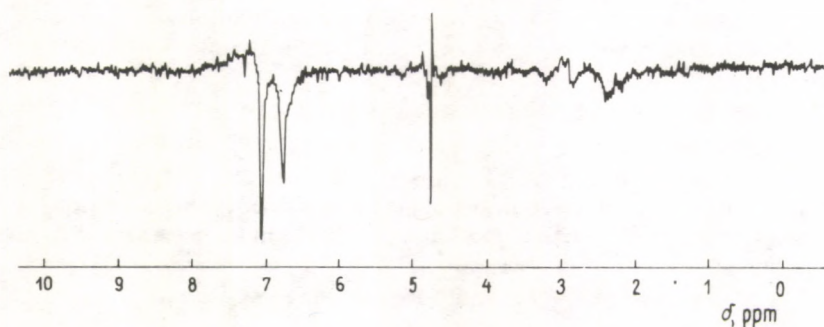


Fig. 7.34. Photo-CIDNP spectrum of bovine pancreatic trypsin inhibitor (360 MHz, D_2O , pH ~ 5.6) [7.133]

Bovine pancreatic trypsin inhibitor is a globular protein (molar mass 6500) containing only 8 aromatic amino acid residues: 4 tyrosines and 4 phenylalanines. On photolysis of solutions of this protein in the presence of flavin, the CIDNP spectrum shows two emission lines at 7.04 and 6.74 ppm (Fig. 7.34). They conform to the signals from tyr 10 and tyr 21; the other residues, tyr 23 and tyr 35, give no CIDNP signals. It is a direct evidence for tyr 10 and tyr 21 being located on the globule surface and tyr 23, tyr 35 in the interior. X-ray studies have demonstrated tyr 10 and tyr 21 to be on the globule surface in crystals. The coincidence of X-ray and photo-CIDNP data indicates that the protein macromolecule conformation is mainly preserved both in crystals and solutions.

Polarizations are also observed in the region 3 ppm (Fig. 7.34): positively polarized lines belong to the protons of β -CH₂ groups, while the weak emission at 2.91 ppm belongs to the ϵ -CH₂ groups of lys 41. It means that tyr 10 and lys 41 are close-spaced and the polarization of tyr 10 is transferred to lys 41 protons by the dipolar cross-relaxation mechanism.

The neighbourhood of lys 41 side group to tyr 10 aromatic ring is an example of local conformation variations of a macromolecule in solution as compared to crystal.

When investigating bovine pancreatic ribonuclease *A* (13,700 molar mass) the CIDNP of one histidine and two tyrosine residues have been observed: the first belongs to his 119 and is located in the active centre of enzyme, the CIDNP signals from tyrosine residue belong to tyr 76 and tyr 115. The CIDNP of tyr 25 protons has been observed in ribonuclease *S* obtained from ribonuclease *A* by breaking the bonding between the 21 and 22 residues. Thus, using CIDNP labelling, one can come to a conclusion about the availability of amino acid residues. The fact that the CIDNP of his 119 protons also vanished in the presence of the ribonuclease *A* inhibitor which blocks the enzyme active centre and makes his 119 inaccessible, agrees with the above conclusion.

Using CIDNP, one can also study macromolecule conformation changes induced by the solution composition, temperature, etc. For instance, in egg protein lysozyme, amino acid radicals trp 62 and trp 63 show CIDNP with temperature-dependent intensity because the macromolecule conformation and the possibility of getting into contact with amino acid residues trp 62 and trp 63 changes with temperature.

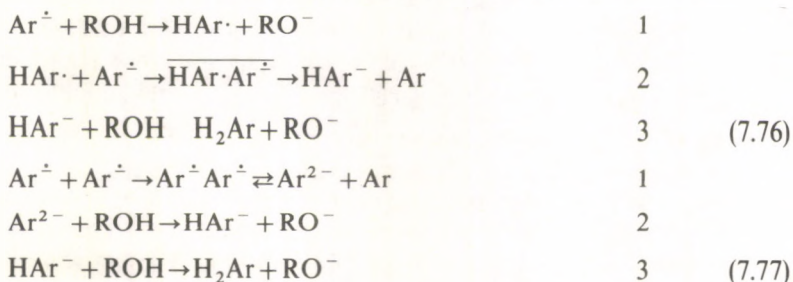
The method advanced by Kaptein *et al.* allows one to identify the surface amino acid residues of tyrosine, histidine, and tryptophane. It can be applied to investigation of rigid molecules whose conformation in a solution remains unchanged for at least 10 s. A number of biomolecules obey this condition (globular proteins, protein-nucleic acid complexes, etc.) and can be investigated by CIDNP technique.

7.3.10 Chemical applications of low field CIDNP

The above examples have demonstrated the wide vistas opened by chemical polarization investigations in high magnetic fields. The present section considers the problem of what additional information about chemical reaction mechanisms can be obtained from low field CIDNP studies.

Note first that there are cases when CIDNP, in principle, cannot be detected in high magnetic fields but only in low fields. This is so in the following situations: (1) the intermediate RPs contain radicals of the same type with $\Delta g = 0$ and the lines of the reaction product NMR spectra have no fine structure, (2) the exchange integral in the RP appreciably exceeds the hf constants, (3) the reaction yields only one product (cage or escape). In all these cases $S-T_0$ transitions in RPs cannot result in nuclear polarization: in the first case no multiplet effect is observed and the net effect equals zero; in the second case $S-T_0$ conversion does not take place at all, and in the last case there are no nuclear spin selection conditions necessary to create polarization in terms of the $S-T_0$ approximation. On the other hand, as follows from the above CIDNP theory, in all the situations under discussion there are no actual limitations (due to the important role of $S-T_{+, -}$ conversion processes) to observe CIDNP in low magnetic fields. Thus, in practical applications of the CIDNP method it is necessary to remember that when no CIDNP effects are detected in high magnetic fields, they can be found in a wide range of magnetic fields (including low fields).

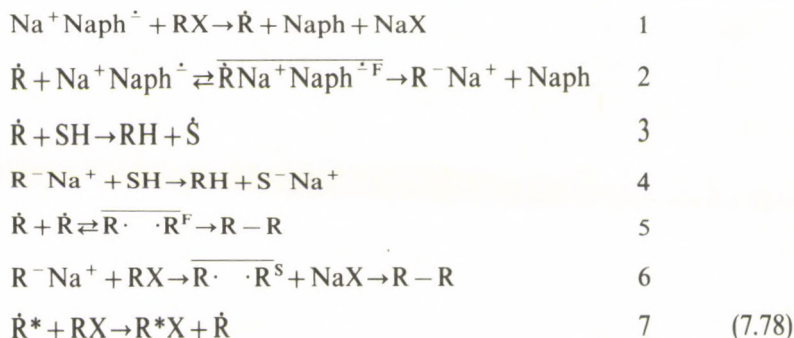
Much use was made of low field CIDNP effect investigations by Garst *et al.* (7.134–138] to study the mechanisms of the reactions involving radical-ions. These studies greatly stimulated the development of low field CIDNP theory. In the reactions of aromatic radical-ions with water and alcohols [7.134] CIDNP effects (emission) of the dihydroaromatic hydrocarbon reaction products can be observed only when the reaction is carried out in fields as high as some 60 G (neither in high nor in the earth's magnetic fields was the polarization detected). Two alternative mechanisms of these reactions were discussed in the literature:



where Ar is an aromatic hydrocarbon—naphthalene, perylene, anthracene; H_2Ar is a dihydroaromatic hydrocarbon; HAr^- is an anion formed by H-abstraction from H_2Ar ; HAr^{\cdot} is a radical formed by $\dot{\text{H}}$ -abstraction from H_2Ar ; Ar^{\cdot} is an anion-radical; Ar^{2-} is a dianion formed by attachment of two electrons to Ar.

CIDNP effect observation in the reaction under discussion allows one unambiguously to identify its mechanism. In fact, polarization can arise only in pair $\overline{\text{HAr}} \cdot \text{Ar}^{\cdot-}$. Stage 1 of Scheme (7.77) is a thermodynamic equilibrium, no CIDNP arises there. The presence of CIDNP of dihydro anthracene aliphatic protons in the reaction of D₁₀-anthracene with H₂O is an additional proof of the above conclusion.

Another series of papers of Garst *et al.* [7.135–138] explored the reaction of sodium naphthalenide with isopropyl chloride, isopropyl iodide, and 1,4-di-iodide butane. The schemes of these reactions can be presented as follows:



SH is the solvent, the polarized radical is marked by an asterisk. Ref. [7.135–138] report the polarization of 2,3-dimethylbutane at $\text{RX} = (\text{CH}_3)_2\text{CHCl}$ and that of cyclobutane at $\text{RX} = \text{I}(\text{CH}_2)_4\text{I}$. CIDNP was detected only in low fields (20–60 G). This interesting fact made Garst conclude that this reaction does not provide the nuclear spin selection conditions necessary for CIDNP to arise in high fields, and to reject the most probable, according to chemical data [7.137], path of R–R dimer formation (reaction 5 in Scheme (7.78)). In this connection, CIDNP in the reaction of sodium naphthalenide with $\text{C}_2\text{H}_5\text{Br}$, $(\text{CH}_3)_2\text{CHI}$, $(\text{CH}_3)_2\text{CHBr}$, $(\text{CH}_3)_2\text{CHCH}_2\text{I}$ was thoroughly investigated [7.139]. Unlike [7.135, 138] the polarization effects were detected over all range of magnetic fields from 0.5 to 23,000 G. High field CIDNP effects proved to be described within the limits of S–T₀ transitions and to follow the above scheme. Multiplet effects arise in $\overline{\text{R} \cdot \cdot \text{R}^{\text{F}}}$ and $\overline{\text{R} \cdot \cdot \text{R}^{\text{S}}}$ pairs, while net effects in $\overline{\text{RNa}^+ \text{Naph}^{\cdot-}}$ pairs.

This example can be treated as a warning for CIDNP investigators applying the method of sample transfer (see 7.1). The fact is that this method results in mixing the reagents outside the NMR spectrometer probe and the process of sample transfer can eliminate the polarization. Unlike [7.135, 138], in paper [7.139] the reaction was carried out inside the NMR spectrometer probe.

The reaction of phenyldiazonium fluoroborate with sodium methylate and alkali still attracts much attention of investigators. In spite of high field CIDNP effect studies and intensive kinetic studies [7.80, 81, 140–145], there is no common viewpoint on the free radical formation mechanism in these reactions. Some authors

suppose that the CIDNP effects in these reactions appear in those radical pairs including $\dot{\text{O}}\text{CH}_3$, $\dot{\text{O}}\text{H}$, etc. radicals [7.140, 141, 145]. An alternative viewpoint is that the free radical generation occurs during the homolytic decomposition of the intermediate product, diazo oxide $\text{Ar}-\text{N}=\text{N}-\text{O}-\text{N}=\text{N}-\text{Ar}$ [7.146]. On the other hand, the last mechanism takes place during the thermal decomposition of N-nitrozoacetanilide (NNA) [7.1]. In this connection unequivocal choice of the reaction mechanism could be made when studying low-field CIDNP [7.20]. Here, together with the diazonium fluoroborate reactions, N-nitroazoacetanilide thermolysis was studied, since one of the free radical formation mechanisms suggested for diazonium salts, namely diazo oxide decomposition, was proved to be realized in the latter reaction.

Figure 7.35 shows the ^1H CIDNP intensity for benzene plotted as a function of magnetic field for the reaction of $\text{C}_6\text{H}_5\text{N}_2^+\text{BF}_4^-$ with CH_3ONa . The field dependence of CIDNP for benzene as a product of NNA thermolysis has a similar form. A unique phenomenon of the low field CIDNP sign alteration was observed in these systems. The theoretical interpretation of the low field CIDNP mechanism developed in Section 4.3, enables us to solve the problem of the composition of radical pair—the reaction product precursor. In line with the foregoing, the low field polarization sign alteration (i.e., a double change of the CIDNP dependence) must be observed under the following conditions

$$JA_1 \approx 1/4 \cdot (\sum_j A_j^2 - A_1^2). \quad (7.79)$$

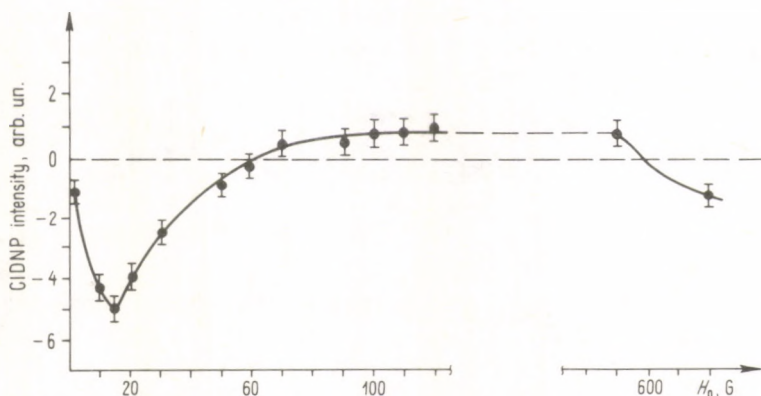
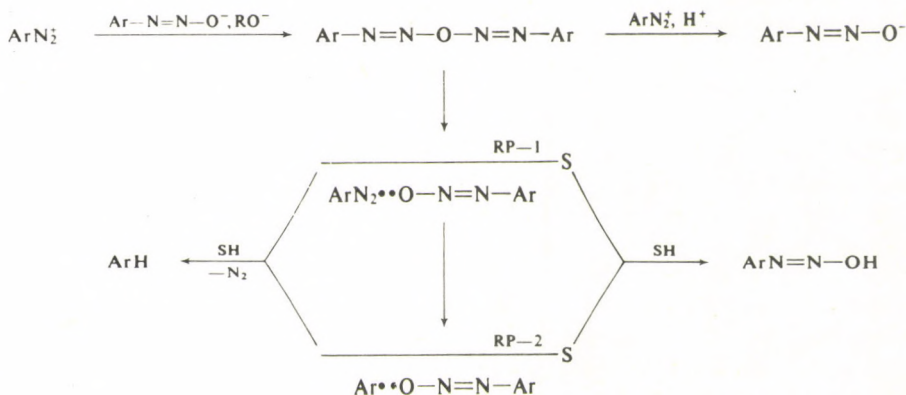


Fig. 7.35. Plots of ^1H CIDNP intensity of benzene vs. magnetic field in course of reaction of $\text{C}_6\text{H}_5\text{N}_2^+\text{BF}_4^-$ with CH_3ONa [7.20]

Note that the polarization sign alteration can take place only at comparatively small deviations from the precise equality (7.79), i.e., over a narrow range of relative changes in A_1 , $\sum_j A_j^2$ and J . For instance, one proton RP calculations show that the low field CIDNP sign does not alter when J and A change by 20%.

The field dependence of benzene CIDNP in the reaction of $C_6H_5N_2^+BF_4^-$ with CH_3ONa and $NaOH$ and in NNA thermolysis allows one to choose the scheme where CIDNP appears in identical radical pairs, i.e.,



(7.80)

Thus, the analysis of the field dependence of the CIDNP enables us to conclude that CIDNP effects arise in those RPs containing no $\dot{O}H$ and $\dot{O}CH_3$ radicals.

Within the framework of the last scheme, CIDNP can arise both in RP-1 and RP-2. Evaluations of the exchange integrals made by formulae (4.67, 68) are as follows

$$\text{for RP-1 } J < -395 \text{ G,}$$

$$\text{for RP-2 } J < -27.5 \text{ G.}$$

The analysis of the calculated exchange integral shows which RP makes the basic contribution to the CIDNP effects observed. The value of J observed in CIDNP usually does not exceed 10^2 G except for RPs involving π -radicals with a high degree of unpaired electron delocalization (e.g. benzyl radicals). Hence, the value of $J < -27.5$ G seems to be more reasonable with the above statements taken into consideration.

The above examples demonstrate that low field CIDNP is in some cases more applicable than the traditional methods of high field polarization and can be recommended for more extensive use in physicochemical studies.

7.4 CIDNP in the gas phase

An appreciable cage effect is a necessary condition to observe CIDNP. Cage effects are conventionally thought to be negligible in gas phase radical reactions and hence until recently there were no attempts to observe CIDNP in such reactions.

There are, however, at least two types of gas phase radical processes where the cage effect can be strong.

First, the reactions involving short-lived biradicals. The characteristic feature of biradical reactions lies in the fact that radical centres cannot diffuse far from each other and thus it is natural to expect that liquid gas transition negligibly affects the biradical recombination probability.

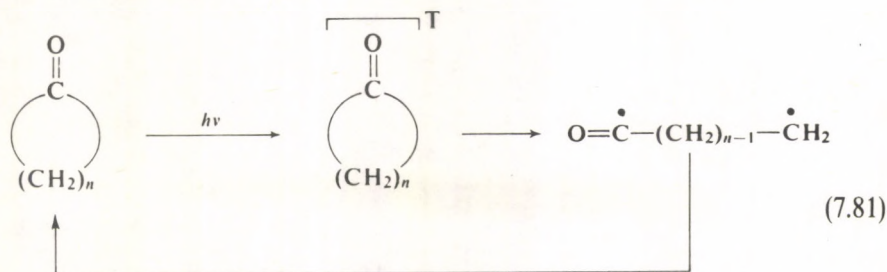
Second, gas phase radical-ion reactions. In this case the Coulomb interaction can induce the necessary cage effects. It is known, e.g., that in gas phase photo- and radiation-chemical ionization processes even at 10^{-10} atm the ion recombination probability becomes rather high and can reach some 10%.

Third, it is necessary to note that gas phase CIDNP can arise by the triplet mechanism, nonequilibrium population of nuclear spin levels result from selective intersystem crossing in the excited molecule and require no cage effect. In this case nuclear polarization in gases can be observed even in the absence of radical processes.

At the present time there are the first experimental observations of CIDNP in gas phase biradical reactions [7.147–148] and preliminary results on CIDNP in radical-ion reactions.

7.4.1 CIDNP in biradical reactions

A classic example of biradical reactions is the photolysis of aliphatic cyclic ketones following the scheme



Cycloheptanone is the most suited compound for CIDNP studies in gas phase for two reasons. First, CIDNP studies (at least in liquids) can be done in the probe of a commercial NMR spectrometer (14–20 kG). On the other hand, a comparatively low boiling point, $T_b = 179^\circ\text{C}$, favours detecting the NMR spectrum of gas phase cycloheptanone.

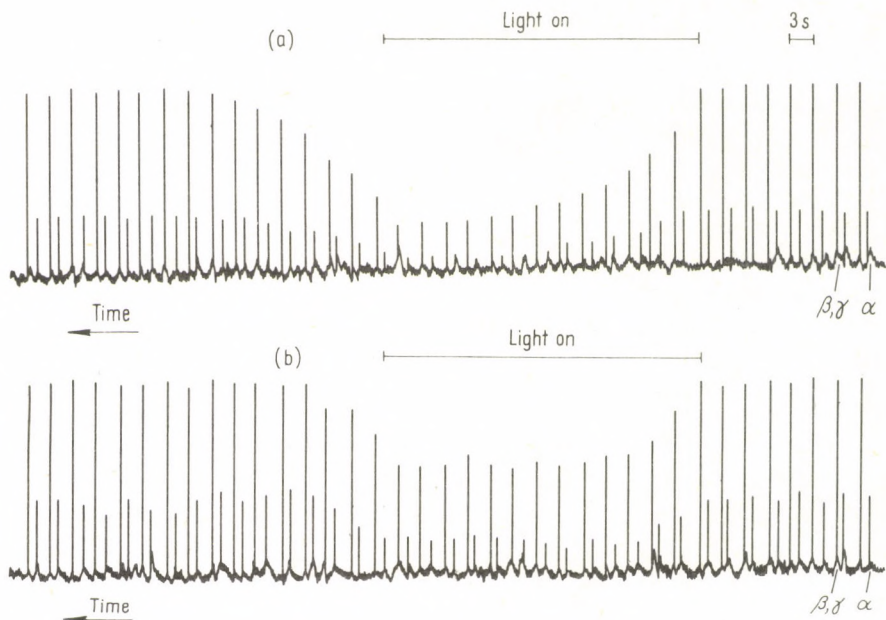


Fig. 7.36. Light effect on the NMR spectral line intensities for cycloheptanone in 0.05 M solution in CHCl_3 (a) and in the gas phase (b). Observations were carried out with periodic scanning of the spectra [7.148]

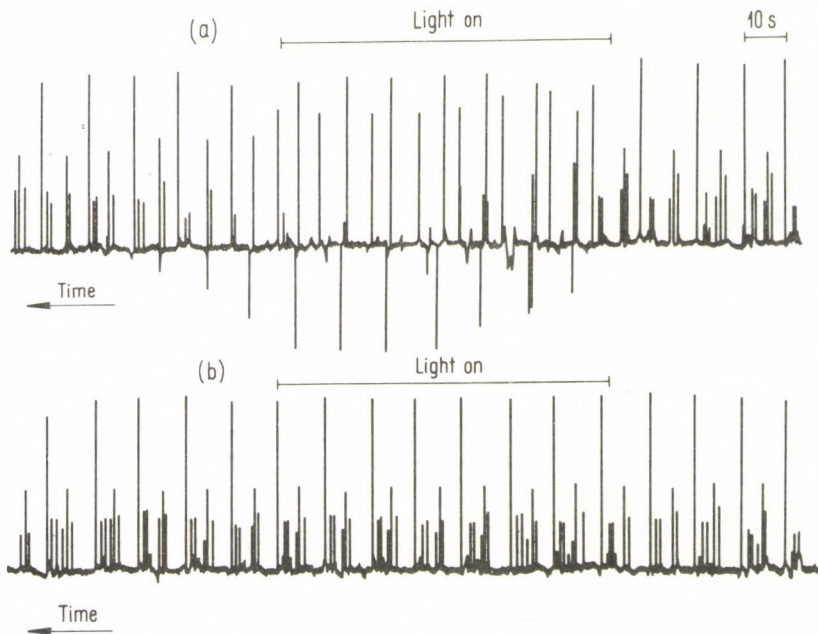
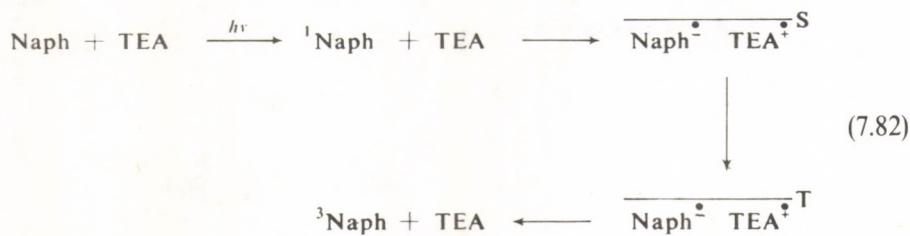


Fig. 7.37. Light effect on the NMR line intensities for methylethylketone in 0.05 M solution in CHCl_3 (a) and in the gas phase (b) [7.148]

Cycloheptanone was irradiated [7.148] under the conditions of complete sample evaporation and equilibrium of the saturated vapours with the liquid phase (120–200 °C) in a special sample tube. The ^1H NMR spectrum consists of two lines belonging to $\alpha\text{-CH}_2$ and $\beta, \gamma\text{-CH}_2$ groups (Fig. 7.36). In the gas phase under irradiation the net intensities of both lines reduce, which corresponds to a negative sign of the net CIDNP effect. An analogous (however more pronounced) decrease in the signal intensity of cycloheptanone has been observed in solution (CHCl_3). Figure 7.37 depicts the NMR spectra of methyl ethyl ketone (MEK) obtained under photolysis. In this reaction, involving monoradicals, CIDNP effects arise only in solution. Thus, this experiment shows once again the importance of cage effects for CIDNP manifestations in common radical reactions.

7.4.2 CIDNP in radical-ion reactions

The photooxidation of tertiary amines by aromatic compounds has been studied in liquids. This has been found to occur via electron transfer from an amine molecule to an aromatic molecule. For instance, in the simplest case of naphthalene and triethylamine in a polar solvent (acetonitrile), the following processes take place



This reaction was studied in [7.147] in the gas phase. The samples containing $1\text{--}2 \cdot 10^{-3}$ g naphthalene and $1\text{--}3 \cdot 10^{-3}$ g triethylamine were heated to 220 °C to ensure complete evaporation of naphthalene. Under irradiation with the full light of a high pressure mercury lamp, the intensities of CH_2 - and CH_3 -lines of the ^1H NMR spectrum for triethylamine decreased (Fig. 7.38) which corresponded to a negative net CIDNP (in solution the CIDNP was of an opposite sign).

Direct evidence for charged particles in the reaction under study was provided by photoconductivity measurements of the sample. The results obtained are demonstrative of the fact that charge carriers in irradiated mixtures of naphthalene and triethylamine vapours result mainly from photochemical interactions between the initial reagents. Studies of the photocurrent dependence on the exciting light intensity show that radical ions arise in two-photon processes. The second photon must be absorbed by naphthalene T_1 state with a long lifetime. The values of the $\text{N}(\text{CH}_2\text{CH}_3)_3$ ionization potential (7.85 eV) and C_{10}H_8 electron affinity (0.65 eV) prove that the energy of the excited state participating in the electron transfer

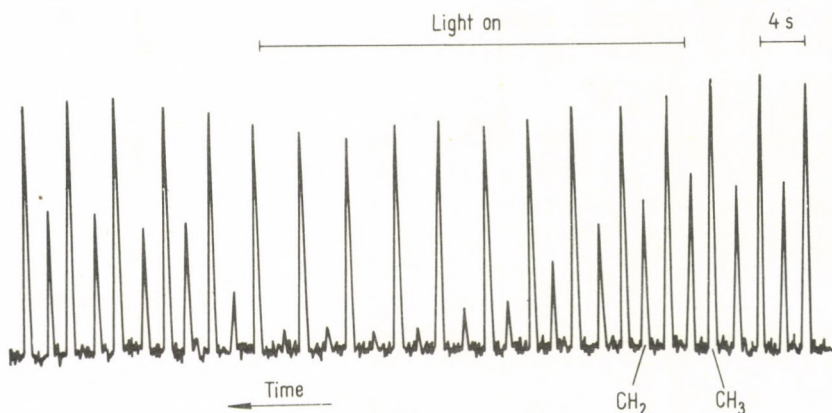
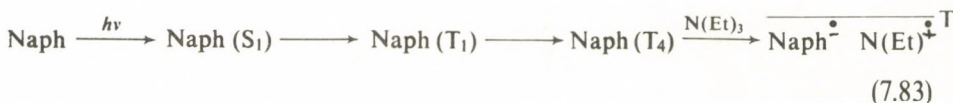


Fig. 7.38. Light effects on the line intensity in ^1H NMR spectra of triethylamine in the presence of naphthalene at $+220^\circ\text{C}$. The spectrum was scanned periodically [7.147]

reaction not less than 7.2 eV. The T_4 state of naphthalene with energy 7.4 eV obeys this requirement. A T_4-T_1 transition is realized by absorption of a $\lesssim 260$ nm photon. Therefore, no photocurrent arises in the sample irradiated through a glass filter for $\lambda > 310$ nm light. It is necessary to note that in this case CIDNP effects do not arise either.

The above results afford the following reaction scheme



The sign alternation of the net ^1H CIDNP in triethylamine in the liquid phase can be explained by this scheme, which shows that the multiplicity of the primary radical-ion pair in liquid differs from that in gas (see Schemes (7.82) and (7.83)).

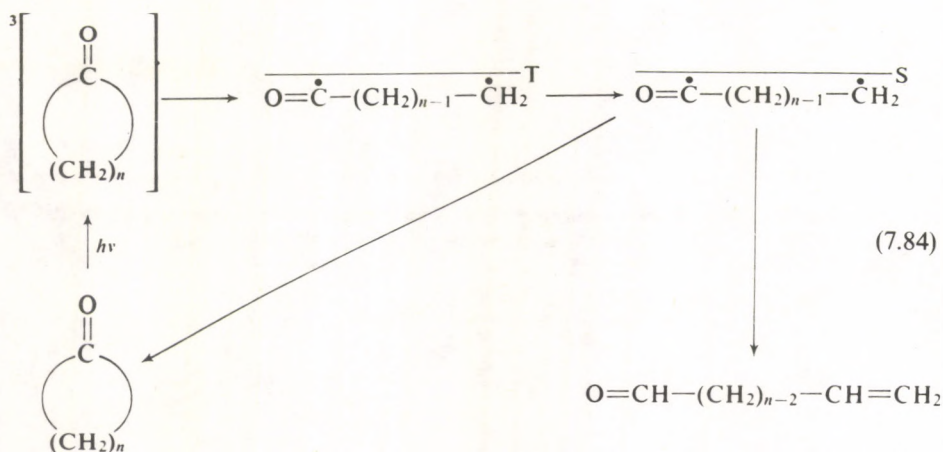
It is necessary to note that the results obtained [7.148] allow one to expect appreciable magnetic field and magnetic isotope effects in gas phase radical-ion reactions. The quantitative analysis of spin polarization and magnetic effects in these reactions demands detailed understanding of the generation, diffusion, and recombination of radical-ions in the gas phase.

7.5 CIDNP in biradicals

The characteristic features of biradicals, as compared to common RPs, are twofold. First, the substantial exchange interaction results in the fact that singlet-triplet transitions in biradicals are effective only in magnetic fields when the Zeeman

splitting of the triplet terms is comparable to the S-T splitting. As a result, the CIDNP effects must have a maximum in fields $H \approx 2|J|$. As a rule, the exchange integral is negative, and the singlet term crosses the triplet one as the field grows. If biradicals are born from any electronically excited triplet states, a S-T transition results in negative nuclear polarizations. In the general case, the nuclear polarization sign in a biradical is determined by the sign of $\Gamma = \mu J$ (cf. Eq. (4.73)). The other characteristic feature of biradicals is that the radical centres are permanently coupled. This increase in the lifetime of the "radical pair" can essentially affect the CIDNP enhancement factor.

Let us consider some basic experimental results on CIDNP in biradical reactions which illustrate these features. A classic example of the reaction involving biradicals is photochemical decomposition of saturated cyclic ketones:



The break of the C—C bond resulting in biradical formation is known [7.26] to occur in the triplet $n-\pi^*$ -state. The subsequent transformations of the biradical $\text{O}=\dot{\text{C}}-(\text{CH}_2)_{n-1}-\dot{\text{C}}\text{H}_2$ are associated with two reactions; recombination yielding the initial ketone and disproportionation yielding the aldehyde $\text{O}=\text{CH}-(\text{CH}_2)_{n-2}-\text{CH}=\text{CH}_2$.

In the photolysis of the above compounds, the CIDNP arises in both the initial ketone and the aldehyde [7.26, 149, 150]. As an example, Figure 7.39 depicts the NMR spectrum taken during cycloheptanone photolysis. All the signals are seen to be negatively polarized regardless of the signs of the hf constants in the intermediate biradical. Analogous results have been obtained in ^{13}C CIDNP studies on the same reaction [7.151], which is consistent with the S-T₋ model of CIDNP. The emission character of the polarization is informative of the fact that in this case the exchange integral takes negative values. To determine the absolute value of J , it is necessary to examine the field dependence of the CIDNP enhancement. Figure 7.40 shows these dependences obtained by Closs *et al.* [7.26, 150] for the series of ketones C₇ to C₁₁. The curves are seen to be characterized by two peculiar features: the maxima are

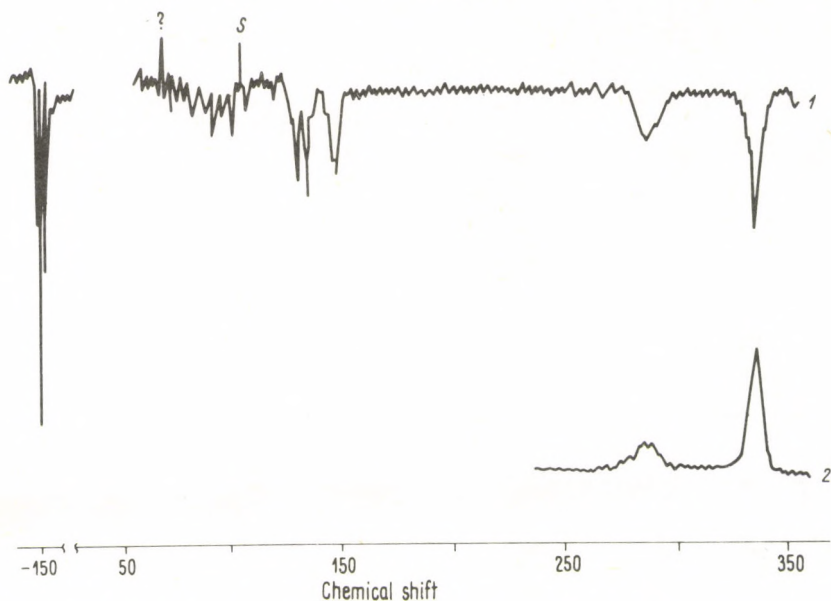


Fig. 7.39. ^1H NMR spectrum observed in course of cycloheptanone photolysis 1—in solution in CHCl_3 , 2—after photolysis [7.26]

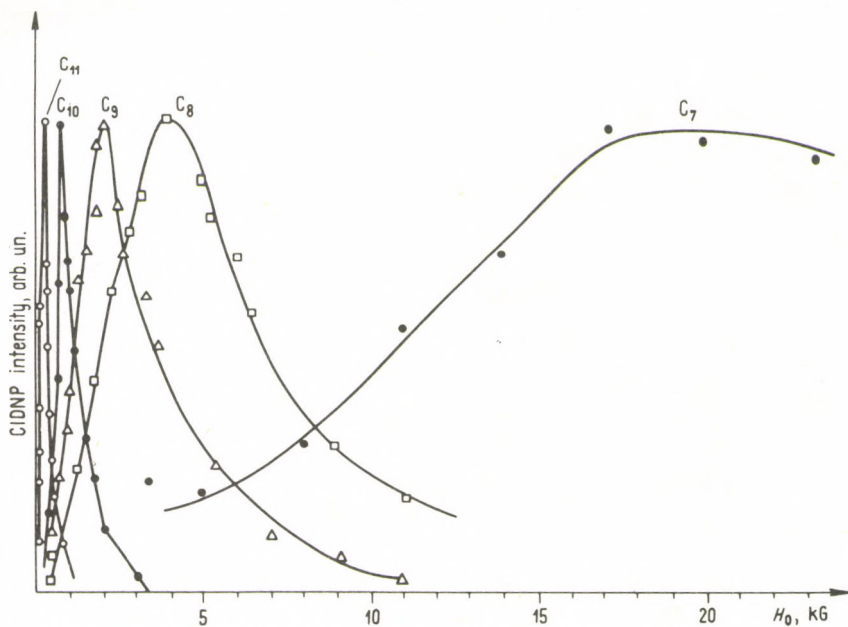


Fig. 7.40. Influence of the cycle size on the field dependence of ^1H CIDNP in cyclic ketones photolysis in solution by the $\text{H}-\overset{\text{O}}{\parallel}{\text{C}}$ -proton signal in aldehydes [7.26]

shifted towards low fields with growing length of the cycle, and the curve width is inversely proportional to the length of the chain. The position of the maxima has been shown [7.26, 150] to be determined by the average value of $|J|$. In this way, the results obtained show that the exchange integral falls in value with increasing length of the chain, which pertains to an increase of the mean distance between the radical centres with growing length of the carbon chain in the biradical $O=\dot{C}-(CH_2)_{n-1}-\dot{C}H_2$.

The decrease in the curve width (Fig. 7.39) due to increasing biradical length is interpreted in the literature in different ways. For instance, Closs ascribed this phenomenon to a reduction in the lifetime of biradicals in the singlet state [7.26]. Atkins and Evans proposed the jump model which asserts that the transitions occur between two biradical conformations possessing certain exchange interaction energies and lifetimes [7.152]. In [7.153] field dependence of CIDNP have been calculated by a stochastic Liouville method, in which the dynamics of the polymethylene chains is incorporated. The experimental field dependencies of 1H CIDNP for series of biradicals have been accounted by using a single exponential for the exchange interaction, which is function of the end-to-end distance [7.153]. Magnetic field dependent biradical CIDNP has been obtained in natural abundance ^{13}C NMR spectra taken immediately after irradiation of cyclic ketones in an auxiliary magnet [7.154]. The ^{13}C field dependence curves differ from the corresponding 1H curves: the maxima of the curves for the C_{11} and C_{12} biradicals appear at higher magnetic field strengths, and the ^{13}C curves are broader than the 1H curves. The authors of [7.154] showed that these differences are due to the different magnitudes of the hyperfine coupling constants for ^{13}C and 1H .

Absolute measurements of the NMR signal intensities in the course of photolysis of cyclic ketones showed an anomalously high CIDNP enhancement factor in these systems [7.22, 155]. For example, for cyclododecanone the CIDNP enhancement factor equals $3.6 \cdot 10^6$ at $H = 125$ G. However, the quantum yield of CIDNP, Φ , is a more informative characteristic of polarization efficiency. This characterizes the probability of a nuclear spin flip ($\alpha \rightarrow \beta$) per photon absorbed. The value of $\Phi = 0.3 \pm 0.05$ has been measured for the system discussed. According to experiment, this value can be even higher in some other biradicals (up to 0.7).

7.6 Technical applications of CIDNP

The substantial nuclear polarization arising in radical reactions open up wide vistas for its practical applications.

7.6.1 Nuclear magnetometry

Magnetometers employing free nuclear precession are widely used in all fields of measuring technique associated with evaluation of the Earth's magnetic field. They are employed in both ground measurements (to make up magnetic charts) and space

investigations. The main advantage of nuclear magnetometers, the possibility to make absolute measurements of the Earth's magnetic field, is based on the strict linear dependence of the precession frequency on the strength of the external magnetic field. The comparatively large sizes of the probes can be considered a serious disadvantage of these devices since they demand high homogeneity of the magnetic field inside the probe, because of a low equilibrium polarization of the working substance in low magnetic fields. Different ways of inducing non-equilibrium polarization are currently used to increase the sensitivity of the devices: prior application of a high magnetic field, microwave pumping, etc. All these means, however, fail to reduce the volume of the probe substantially (in modern magnetometers the volume of the working substance amounts to some 100 ml).

As stated in Section 7.5, in low field photochemical reactions involving biradicals the absolute value of the NMR signal has been observed to increase by 10^6 . It is the fact that the nonequilibrium polarization of the working substance arising in photochemical reactions running via biradicals (especially in case of full reversibility of the reaction) that allows one to reduce the working volume of the probe (≤ 1 ml) [7.156]. As a result, nuclear precession magnetometers can be successfully used also in inhomogeneous magnetic fields, which appreciably broadens the area of their application.

7.6.2 Oriented polarized targets

The creation of such polarized targets is of particular interest for nuclear physics since studies on reactions involving polarized nuclei provide unique information on spin dependencies of nuclear forces, spins, parities, and magnetic moments of excited nuclear states, etc. A target with polarization degree $\geq 10\%$ is therefore of practical interest. The conventional methods of producing such polarization are based on the use of extremely low temperatures (below 1K) and high polarizing magnetic fields (hundreds of thousands of gauss). As shown in Sec. 7.5., the CIDNP method can in fact ensure some 70% degree of polarization at room temperature in extremely low magnetic fields, which seems promising as applied to nuclear physics.

7.6.3 Radio-frequency generation with chemical pumping (chemical RASER)

Negative CIDNP corresponds to inverse population of the upper Zeeman level. The excess energy of negatively polarized nuclear spins can release its energy as electromagnetic radiation. However, the probability of spontaneous radiation of an isolated nuclear spin is negligible, about 10^{-25} s^{-1} and corresponds to a radiative relaxation time of 10^{25} s. Radiationless relaxation processes plainly occur much faster, and this excludes the possibility at detecting spontaneous incoherent electromagnetic radiation.

Nuclear magnetic moments contribute to the total nuclear moment creating the total nuclear magnetization of the sample. The coherent motion of nuclear magnetic moments is the Larmor precession of the total nuclear moment around the external field direction. This results in a transverse non-zero component of the nuclear

magnetic moment. The greater the transverse component of the precessing magnetic moment, the higher the degree of coherence of the nuclear spin motion. The loss in coherence, i.e. the disappearance of the transverse component of the magnetic moment, occurs with the transverse relaxation time T_2 and is caused by the distribution of the nuclear spin precession frequencies. As a result, the nuclear spin precession phases are randomized and the vector of the total transverse magnetization decomposes. The absence of the transverse components (M_x or M_y) of the magnetic moment conforms to incoherent spin motion.

Negatively polarized nuclei can radiate their excess energy provided their motion is coherent. This is associated with the fact that only the transverse components of the magnetic moment precessing with the Larmor frequency induce high-frequency EMF in the coil of a resonant oscillatory circuit*. So, to make a system of negatively polarized nuclei to radiate, it is necessary to ensure coherent motion of their magnetic moments.

In standard NMR spectrometers detection is achieved by applying an external radio-frequency field H_1 . Ordinary NMR spectra are detected as absorption of the energy of this field, while negative CIDNP spectra are detected as radiation induced by the field H_1 . The field H_1 may be applied not continuously (as in standard NMR spectrometers) but as pulses. The pulse duration τ being chosen so that $\gamma_1 H_1 \tau = \pi/2$, the total magnetic moment is turned through $\pi/2$ by this pulse and lies in the xy plane. Its precession induces an EMF in the coil with an initial amplitude proportional to the moment, and decaying exponentially with the characteristic time T_2 .

Can a system of negatively polarized nuclei supply its own coherence spontaneously without an external magnetic field H_1 ? Self-excitation of the coherency corresponds to that of the radiofrequency generation and the system of negatively polarized nuclei can thus serve as a quantum radiofrequency oscillator—a chemical RASER (the analogue of LASER and MASER). The mechanism of coherence self-excitation is as follows. The total magnetic moment of negatively polarized nuclei can slightly diverge from the z -axis due to random fluctuations of local magnetic fields (*magnetic noise* fluctuations). This results in a small transverse component of the magnetic moment inducing a small EMF in the coil. The electromagnetic field resulting from this EMF is called a *reaction field*. It interacts with the magnetic moment and turns it towards the xy -plane. As a result, the transverse component increases, thus inducing a higher reaction field, etc. Thus, the interaction between the magnetic moment and the reactive field of the oscillatory circuit induces coherence in the magnetic motion precession and a cascade increase in the EMF. If the magnetic moment is so large that the energy induced in the oscillatory circuit by the nuclear system exceeds the losses in the circuit, the system becomes a radiofrequency oscillator—a RASER.

* This process is in fact analogous to EMF excitation in the coil of any electric generator, the only difference being that it is the magnet but not the coil that rotates. Here the transverse component of the nuclear magnetic moment serves as the rotating magnet.

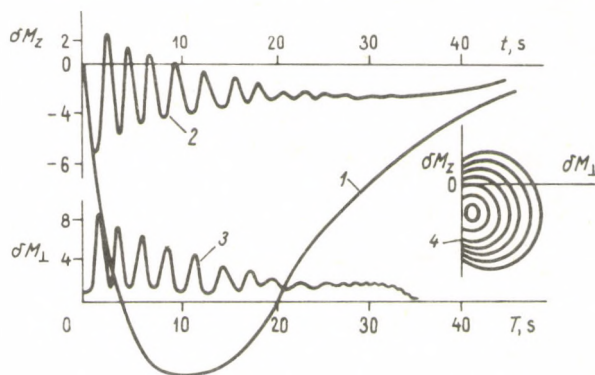


Fig. 7.41. Polarization component behaviour: 1 $M_\perp(t)$ dependence in the absence of reaction field; 2 $M_z(t)$ dependence with reaction field taken into account; 3 $M_\perp(t)$ dependence; 4 phase diagram of polarization vector behaviour [7.157]

The conditions of chemical pumping and self-excitation of a RASER have been analyzed theoretically [7.157]. The spin system dynamics in the case of chemical pumping has been calculated in terms of the phenomenological Bloch equations. Figure 7.41 shows the kinetics of changes of the transverse component of the nuclear polarization M_z with no account taken of the reaction field (Curve 1), which corresponds to the generally observed CIDNP kinetics. When the reaction field is taken into consideration, the kinetics take on a periodic character (Curve 2) and the transverse magnetization component M_\perp arises and induces a high-frequency EMF in the coil (Curve 3). The M_z and M_\perp oscillations depend on the generation threshold; the reaction field destroys the polarization and diminishes M_z . However, the chemical reaction induces new negative polarizations, which, in turn, result in reaching the generation threshold, and so on. Figure 7.41 (on the right 4) shows the dynamics of the M_z and M_\perp variations (the *phase diagram* of the process). The dynamics have been calculated under various conditions of chemical pumping [7.157].

Radiofrequency generation arising in chemical reactions was first observed experimentally by Zhuravlev *et al.* [7.158]. The photoreversible electron transfer in the system porphyrinquinone is accompanied by a strong negative polarization of quinone protons generating high-frequency EMF and, therefore, high-frequency current in the oscillatory circuit. Figure 7.42 depicts the record of low-frequency pulses between the frequencies of the generation and the reference oscillator of the recording system. With the light switched on, negative nuclear polarization arises and it takes the system 5–10 s to reach the generation threshold. The transient process being over, the generation and thus the high-frequency current becomes stationary. On switching off the light (no chemical pumping), the coherence is destroyed and the generation amplitude falls (Fig. 7.42). The reaction is practically reversible, which allows the generation to proceed for a long time. In this case the

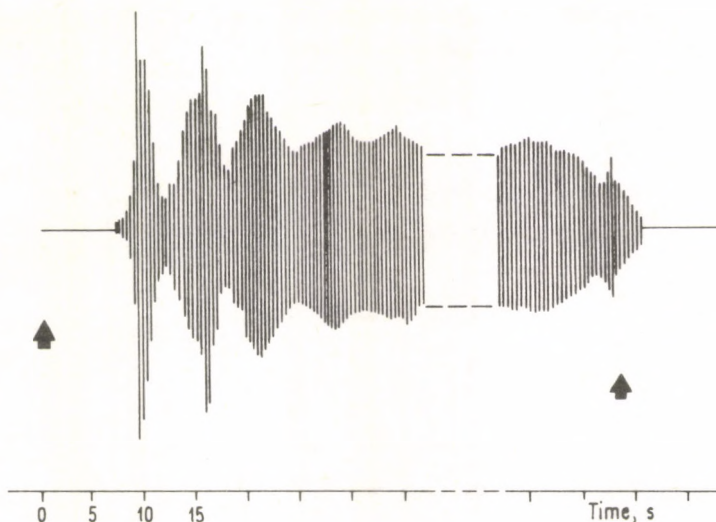


Fig. 7.42 Generation of high-frequency current in resonance circuit of NMR probe in course of photolysis of 10^{-3} M solution of porphyrine and quinone. Light switching on and off are indicated by arrows [7.158]

generation can run either under continuous (*continuous photolysis*) or pulse (*pulse photolysis*) conditions.

Thus, a radical reaction is in fact a quantum generator of electromagnetic radio-frequency oscillations, a kind of a molecular radio broadcasting system, this being a new physical manifestation of chemical reactions.

7.7 CIDNP detected magnetic resonance

CIDNP effects are determined by a complex of molecular kinetic and magnetic resonance RP parameters. Radical g -values and hf constants can be found from the analysis of the NMR spectra of RP reaction products and thus it is possible to construct the ESR spectra of these intermediate reactive species. CIDNP effects, however, can be used to detect directly radical ESR spectra in RPs. The point is that the microwave pumping affects the singlet-triplet mixing in RPs resonantly, the microwave field effects being large when the frequencies coincide with those of the ESR transitions in the RPs. CIDNP detection of radical ESR spectra in short-lived RPs is quite analogous to the method of optical detection of ESR spectra for short-lived RPs (Section 5.4).

As an example, consider the simplest case of a one-nucleus RP with spin $1/2$. Assume that the radical g -values are equal. In high magnetic fields according to the above theory no CIDNP effect arises in such a pair. The situation changes when a

microwave field is applied. Let the RP be singlet-born. Using the data adduced in Section 2.2 we can find the singlet RP term population at any time. For the RP subensemble with negative nuclear polarizations ($m_1 = -1/2$) we have (see eq. 2.150)

$$p_s^-(t) = \left(\cos \frac{\omega_{eff}^-(1)t}{2} \cos \frac{\omega_{eff}(2)t}{2} + (\vec{n}_1^- \cdot \vec{n}_2) \sin \frac{\omega_{eff}^-(1)t}{2} \sin \frac{\omega_{eff}(2)t}{2} \right)^2 \quad (7.85)$$

and for that with positive nuclear polarizations

$$p_s^+(t) = \left(\cos \frac{\omega_{eff}^+(1)t}{2} \cos \frac{\omega_{eff}(2)t}{2} + (\vec{n}_1^+ \cdot \vec{n}_2) \sin \frac{\omega_{eff}^+(1)t}{2} \sin \frac{\omega_{eff}(2)t}{2} \right)^2 \quad (7.86)$$

These formulas employ the same symbols as in Section 2.2.6:

$$\begin{aligned} \omega_{eff}^\pm(1) &= \left[\left(\gamma H_0 \pm \frac{a}{2} - \omega \right)^2 + \gamma^2 H_1^2 \right]^{1/2} \\ \omega_{eff}(2) &= [(\gamma H_0 - \omega)^2 + \gamma^2 H_1^2]^{1/2} \end{aligned} \quad (7.87)$$

\vec{n}_1^\pm are unit vectors with components

$$\left(\frac{\gamma H_1}{\omega_{eff}^\pm(1)}, 0, \frac{\gamma H_0 \pm \frac{a}{2} - \omega}{\omega_{eff}^\pm(1)} \right) \quad (7.88)$$

and the vector \vec{n}_2 has the components

$$\left(\frac{\gamma H_1}{\omega_{eff}(2)}, 0, \frac{\gamma H_0 - \omega}{\omega_{eff}(2)} \right)$$

The value of $\Delta\omega \equiv \gamma H_0 - \omega$ is the frequency difference between the microwave field and the resonance frequency of the ESR transition for the radical denoted 2; the value of a is the hyperfine splitting of the ESR spectrum for the radical labelled 1; H_1 is the microwave field amplitude. The nuclear polarization in the recombination product is determined by the difference in the values of p_s^+ and p_s^- ,

$$\Delta p_s(t) = p_s^+(t) - p_s^-(t). \quad (7.89)$$

Figure 7.43 gives the nuclear spin polarization in the subensemble of singlet RPs calculated by these formulas. The nuclear polarization is seen to arise in the presence of microwave pumping. The polarization sign depends upon that of the frequency difference of the microwave pumping from the centre of the radical ESR spectrum. It follows that microwave pumping influences CIDNP effects, which can then be used to detect ESR spectra of short-lived RPs.

Some intermediate values of the field H_1 are optimal for the successful CIDNP detection of ESR spectra. If $H_1 \ll 1$ G the microwave field has no time to manifest itself in the RP spin dynamics. If $H_1 > A$, as shown in Section 2.2.6, the RP spins in fact precess about the field H_1 , the dependence of the singlet-triplet transitions upon the nuclear spin configurations, and hence the CIDNP effects themselves, are reduced. The optimum values of H_1 must lie at $H_1 \approx A/2$.

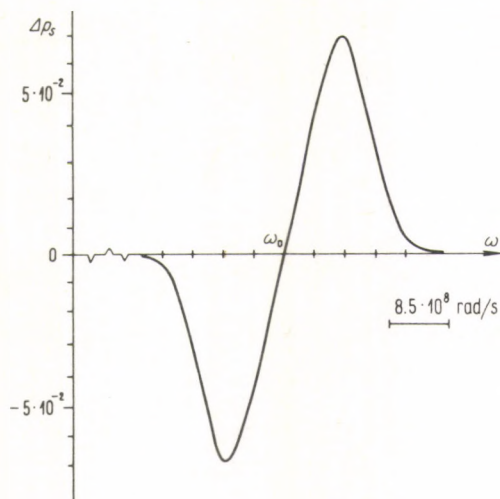


Fig. 7.43. Difference in nuclear sublevels population in the recombination product of RP with single nucleus ($I = 1/2$) vs. frequency of microwave pumping. Parameters: $g_1 = g_2 = 2.001$, $A = 100 \text{ G}$, $H_1 = 10 \text{ G}$, probability of singlet RP recombination $\lambda = 0.9090$...

CIDNP effects can also be used to observe the NMR spectra of short-lived RPs, as Sagdeev *et al.* [7.159, 160] were first to demonstrate. The idea of method proposed is as follows. Free radicals are generated in a system (with light, irradiation, or heat) and CIDNP effects are observed in the escape products. The latter means that the free radicals, \dot{R} , polarized in RPs, have lifetimes sufficiently short to conserve the nuclear polarization by the time of diamagnetic product (e.g. of RX type) generation. If the resonance transitions in the NMR spectra of intermediate radicals (a doublet for each group of equivalent nuclei) are saturated within the radical lifetime τ , the CIDNP effect will be changed in the NMR spectrum of the reaction product. Thus, the radical NMR spectra is, in this case, a dependence of CIDNP intensity on the frequency ω_2 of the saturating field.

The technique can be realized under the condition

$$(\gamma H_2)^{-1} < \tau < T_1^n, \quad (7.90)$$

where H_2 is the saturating field amplitude and T_1^n is the radical nuclear relaxation time.

The method proposed has been verified experimentally for benzyl radicals generated during dibenzyl ketone photolysis directly in a NMR spectrometer probe (with operating frequency 80 MHz). The signal from CH_2 -protons of the escape product—dibenzyl—was positively polarized. When a radiofrequency power from a RF generator ($\omega_2 = 30\text{--}60 \text{ MHz}$, $H_{2\text{max}} = 15 \text{ G}$) was applied to specially constructed coils, the polarized signal intensity changed in a resonance manner (see Fig. 7.44). The hf constant for the CH_2 -group of benzyl radicals can easily be found from

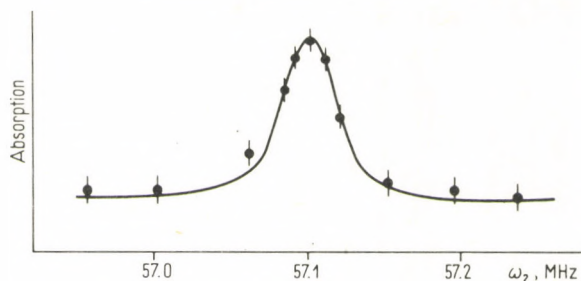


Fig. 7.44. CIDNP detected NMR spectrum of benzyl radical in solution [7.160]

the spectrum depicted, $a_h = (80 \text{ MHz} - 57.1 \text{ MHz}) \cdot 2 = 45.8 \text{ MHz}$, which is a good fit to the well known data on benzyl radical ESR spectra at low temperatures.

The fact that the polarization intensity increases with saturation of a resonance transition in benzyl radicals is associated with multiplet effects arising in the electron-nucleus system. These effects are manifested in ESR spectra as CIDEP and have never been observed in NMR spectra [7.159, 160].

Note in conclusion that the method proposed is highly sensitive (even more sensitive than the ESR method), highly resolved, and allows hf parameters to be found easily.

8 CHEMICALLY INDUCED DYNAMIC ELECTRON POLARIZATION

8.1 Experimental methods of CIDEP observation and analysis

Nonequilibrium populations of Zeeman electron levels tend to their equilibrium values with the characteristic time of electron relaxation $T_1 \approx 10^{-7}$ – 10^{-5} s. Therefore, to detect CIDEP, one needs a suitable technique of CIDEP spectroscopy.

Three types of experimental methods are used to study CIDEP. The simplest one is that of stationary observation of signals from the radicals formed in thermal, photo-, or radiation-induced chemical reactions. The ESR signal is a sum over radicals carrying polarization and those that have lost it. Under the conditions of stationary observations, a large contribution to the ESR signal is usually made by the latter radicals. Therefore, CIDEP effects manifest themselves weakly, and are usually detected as ESR spectrum distortion (e.g., deviations of the intensity distribution of the hyperfine structure components from that in the usual equilibrium spectrum). Under the most favourable conditions, however, some lines appear in emission; usually this is observed at high pumping rates, i.e., at high rates of radical formation (examples are given below).

The relative fraction of nonpolarized radicals can be reduced by decreasing the radical lifetime (e.g., by addition of scavengers or by some other chemical means). This increases the sensitivity of the CIDEP stationary technique. However, the radical lifetime cannot be shortened without limit since it results in a simultaneous decrease of the absolute radical concentration, the limit being determined by the ESR spectrometer.

One more difficulty of the stationary observation technique is that it is almost impossible to obtain quantitative information on CIDEP parameters and to establish the origin of the polarization.

More appropriate and reliable are methods involving *pulse detection* of CIDEP. There are two versions of pulse technique differing in the resolution time τ : in the first method $\tau < T_1$, in the second one $\tau > T_1$. The quantity τ is determined by the spectrometer bandpass.

The low resolution pulse technique ($\tau < T_1$) is the best one for quantitative investigations of CIDEP. In typical experiments short (20 ns–2 μ s) photo- or radiation pulses generate radicals in a sample placed in the cavity of a ESR spectrometer, and the signal variation versus electron and magnetic susceptibility of the sample is detected during the time of radical generation and decay using the

accumulating technique [8.1-4]. The signal is recorded as a function of time at a fixed magnetic field (Fig. 8.1). Detecting the signal in various magnetic fields, one can reproduce the whole ESR spectrum at any instant from the time decay profiles (Fig. 8.2). A disadvantage of the method is a bad signal-to-noise ratio which inevitably results from the wide bandpass of the spectrometer.

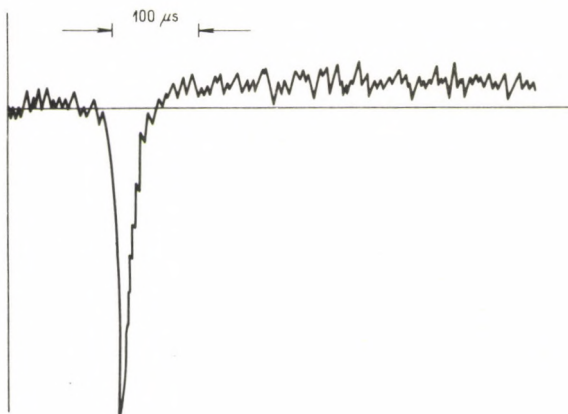


Fig. 8.1. Time dependence of the ESR signal in a fixed magnetic field of 2-chlorobenzaldehyde radicals in liquid paraffin. At the irradiation moment emission arises, then rapidly falls and, in $14 \mu\text{s}$, turns into a signal of radical equilibrium absorption: the absorption decays slowly, with the radical lifetime $2.4 \mu\text{s}$ [8.5]

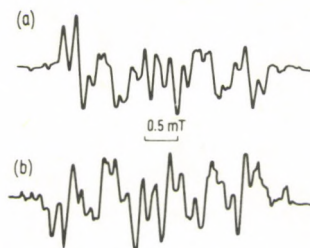


Fig. 8.2. ESR spectrum of 2-chlorobenzaldehyde radical plotted by time profiles of the signal decay: (a) in emission; (b) in absorption. The spectra are almost completely identical [8.5]

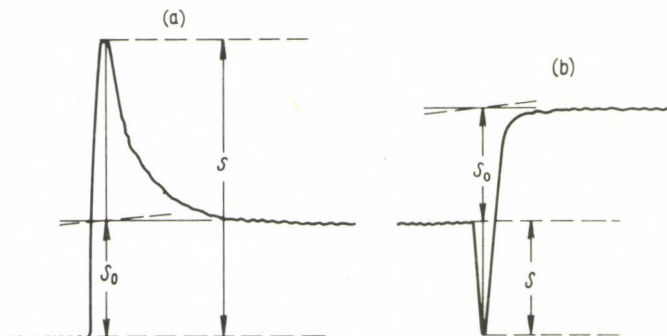


Fig. 8.3. Time dependence of CIDEP signal with pumping in radical formation acts: (a) positive polarization; (b) negative polarization

A compromise between the signal-to-noise ratio (i.e., a low sensibility) and the bandpass width (i.e., resolution) is achieved in the high resolution pulse technique ($\tau > T_1$); here $\tau \approx 100\text{--}200 \mu\text{s}$. A large value of τ reduces the requirements for a precise form of the pulse used to generate the radicals. Under these conditions, radicals are often generated by interrupted light (rotating sector method). However, in this version of the pulse technique, the magnitude and the form of the signal at the spectrometer outlet is determined not only by the actual signal but also by the spectrometer detecting system response and the form of the generating pulse. Hence, it is more difficult to obtain quantitative information by this technique; its reliability must be carefully examined.

A typical example of the pulse technique CIDEP detection is shown in Fig. 8.1. Other examples are given in Fig. 8.3. In these cases the electrons were polarized in the radical formation reactions. Hence, the CIDEP signal first sharply increases, reaches its maximum, then, with the spin-lattice relaxation rate, tends to the equilibrium signal which slowly decreases as a result of radical decay by chemical reaction. Experimental values of polarization coefficient γ are determined by the relations

$$\gamma = (|S| - |S_0|) / |S_0| \quad \text{for absorption}$$

and

$$\gamma = -(|S| + |S_0|) / |S_0| \quad \text{for emission.}$$

S and S_0 refer to the same instant; and so to find S_0 one must extrapolate the equilibrium signal to the time of S determination.

If the electron polarization arises in the radical decay reaction, it then decays with a rate that is the rate of destruction of the radicals: in this case the system is in stationary state with the pumping rate equal to that of relaxation. It is then impossible to measure S_0 directly and thus $\gamma \cdot S_0$ has to be determined from the ESR signal of unpolarized radicals having the same concentration. The situation is simplified in the case of the multiplet effect. Then S_0 can be found either from the central component of the spectrum (which is unpolarized) or by the mean of any two spectral lines symmetrical with respect to the centre (the lines are supposed to be equally and oppositely polarized). More detailed examples of different situations will be given while discussing experimental results.

8.2 Experimental CIDEP investigations

Since 1963, when CIDEP was observed for the first time, about one hundred reports on CIDEP in different processes have appeared in literature. CIDEP became of great interest after the discovery of CIDNP. We consider the main experimental results on CIDEP, their classification being based on the physical mechanisms of CIDNP whose theory has been developed above (Chapter 4).

8.2.1 CIDEP in radical pairs

The basic mechanism of electron polarization in radical pairs is singlet-triplet mixing induced by the difference of Larmor precession frequencies of the unpaired electrons. Such a difference may arise either because the radicals have different g -factors or due to hyperfine electron-nuclear interaction.

In $S-T_0$ evolution, the total number of electrons with α and β spins is preserved, i.e., the $S-T_0$ evolution in the radical pair does not create any excess number of electrons with α and β spins, it simply rearranges the electron spin populations between the radicals of the pair. Thus, the net polarization means that one of the radicals has an excess of α (or β) spins, while the other has the same excess of β (or α) spins. The electron polarizations of the radicals are equal in magnitude but opposite in sign.

If the polarization is multiplet, then α and β spins are distributed equally between the radical partners, the distribution in each depending on the radical nuclear spin state. So, in an escaping hydrogen atom, α spin belongs preferably to the nucleus α_n , and β spin to the nucleus β_n . Preferable population of the spin states $\alpha\alpha_n$ and $\beta\beta_n$ leads to multiplet effects EA in the hydrogen atom ESR spectrum [8.6].

Note that the net polarization arises if the main contribution to the $S-T_0$ evolution is made by the difference in the g -factors; the multiplet polarization arises when the main contribution is made by the hyperfine interaction.

Radical pairs can be generated in two ways; although the polarization mechanism is the same for both, the time behaviour of the polarization is different. Radical pairs formed by bond rupture are in a definite electronic state; these are pairs with correlated spins and electron polarization may arise immediately during the pair lifetimes (about 10^{-10} – 10^{-8} s), then vanish at the rate of electron spin-lattice relaxation.

In reactions involving independently generated radicals the electron polarization first increases with the rate of the RP generation (i.e., the rate of diffusion encounters), then reaches the stationary value when the RP generation rate (pumping rate) equals that of the electron relaxation. Later the polarization slowly decreases with the rate of the radical decay.

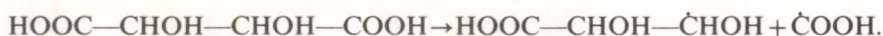
The analysis of the time dependence of CIDEP gives information on the origin of the polarization, while characteristic features of the CIDEP are informative of the polarization mechanisms.

We now consider experimental CIDEP studies.

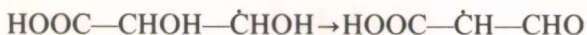
The photolysis of acetone in isopropanol gives multiplet effects EA observed in $(CH_3)_2\dot{C}OH$ ESR spectrum. The polarization was detected by the stationary technique in standard ESR spectroscopy (8.7–8). The multiplet effect sign shows that the radicals acquire polarization either in triplet or in diffusion pairs with $\Delta g = 0$. In line with the rule (4.87) $\Gamma = -\mu J = - + - = +$ which corresponds to EA. This result was then corroborated by the pulse technique [8.9]. Intensity changes of one of the ESR spectral components during one cycle of switching on and off the light (using the sector technique) is shown in [8.9]. At the moment of switching on,

the absorption signal rises sharply, it corresponds to the absorption by the newly formed radicals with equilibrium polarizations. Further, when diffusional radical encounters begin, negative polarizations arise in the diffusion pairs and compensate the primary absorption. Hence, the initial signal reduces to a definite stationary magnitude when the pumping rate in the diffusion pairs is equal to the rate of relaxation. The shorter the radical lifetime, the greater the contribution of the emission. On switching off the light, the stationary signal decreases with the rate of the radical decay by chemical reaction. Thus, in the photolysis of acetone in isopropanol, the pumping of $(\text{CH}_3)_2\dot{\text{C}}\text{OH}$ radical electron polarization is realized due to the $S-T_0$ mixing in diffusion pairs.

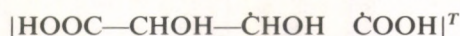
The photolysis of tartaric acid is quite different [8.7]. In the ESR spectrum, only the radical $\text{HOOC}-\text{CHOH}-\dot{\text{C}}\text{HOH}$ was observed, and was formed by the scheme:



The other partner, $\dot{\text{C}}\text{OOH}$, was not detected in the ESR spectrum. In highly acidic media ($\text{pH} < 1.5$), when the radical lifetime is shortened by the reaction



and becomes comparable to the spin-lattice relaxation time, the NMR spectral lines of the radical $\text{HOOC}-\text{CHOH}-\dot{\text{C}}\text{HOH}$ correspond to emission. The negative polarization can be supposed to originate from the initial triplet pair



during the $S-T_0$ mixing; indeed, emission can be expected for the radical $\text{HOOC}-\text{CHOH}-\dot{\text{C}}\text{HOH}$ in the pair with $\Delta g > 0$, where according to the rule (4.85) $\Gamma = \mu J$ $\Delta g = + - + = -$. However, the hf constant in the radical is comparable to $\Delta g \beta H$, and thus the multiplet polarization, comparable in value to the net polarization, should be detected in the spectrum along with the latter. Experimental spectra reveal no traces of multiplet effect (Fig. 8.4) which contradicts the conventional understanding of CIDEP in radical pairs.

Use made of the pulse technique showed the pumping to be realized in this case not in radical pairs but in the triplet state of the precursor molecule [8.9]. Unlike in radicals the polarization here reaches its maximum in the very beginning of irradiation, then reduces to the stationary state as a result of relaxation. The irradiation cut off, the signal reaches its equilibrium value because of relaxation, then falls with the rate of the radical decay.


This result unequivocally proves that the pumping occurs in the radical generation steps, i.e., by the triplet mechanism.

The multiplet CIDEP effect is often detected in thermally generated radicals. Thus, the multiplet EA polarization was observed in the radicals $\text{CH}_3\dot{\text{C}}\text{HCO}_2^-$, $\dot{\text{C}}\text{H}_2\text{CH}_2\text{CO}_2^-$, $(\text{CH}_3)_2\dot{\text{C}}\text{CH}_2^-$, $\dot{\text{C}}\text{H}_2\text{CH}(\text{CH}_3)\text{CO}_2^-$, and $(\text{CH}_3)_2\dot{\text{C}}\text{OH}$ in the redox generation in the flow system $\text{Ti}-\text{H}_2\text{O}_2$ in the presence of organic substances (propionic and isobutyric acids [8.10], and isobutyric acid and isopropanol [8.11]).



Fig. 8.4. ESR spectrum of radicals originated in photolysis of aqueous solution of vnic acid at pH ~ 1.5 and 31°C . Emission lines *A* belong to radical $\text{HOOC}-\dot{\text{C}}\text{HOH}-\dot{\text{C}}\text{HOH}$, equilibrium absorption lines *C* to radical $\text{HOOC}-\dot{\text{C}}\text{H}-\text{CHO}$, line *D* to radical of oxalic acid whose admixture is present in vnic acid [8.7]

CIDEP undoubtedly originates from diffusion pairs due to the $S-T_0$ transitions. In accord with theory, the magnitude of the polarization arising by this mechanism must be proportional to the square root of the hyperfine interaction energy, this prediction being confirmed by experiment (Fig. 8.5).

The CIDEP multiplet *EA* observed in the radical  is of the same origin [8.12]. The polarization value was calculated by the method of Freed and Pedersen; at $d=p=6.3 \text{ \AA}$, $D=3 \cdot 10^{-6} \text{ cm}^2 \cdot \text{s}^{-1}$, $J_0 > 8 \cdot 10^9 \text{ s}^{-1}$, $\tau_j=6 \cdot 10^{-11} \text{ s}$ the theoretical calculations differed from experiment by a factor of 2–3. This discrepancy is negligible, since the calculations were carried out assuming the radicals to be spherical. Account taken of the nonsphericity gives a 2–3-fold correction. Thus, the $S-T_0$ theory accounts for this CIDEP both qualitatively and quantitatively.

Multiplet polarization of the same origin was detected in hydrogen and deuterium atoms [8.6, 13–15], cyclohexadienyl [8.16], $\dot{\text{C}}\text{H}_2\text{CO}_2^-$ and $\dot{\text{C}}\text{H}(\text{CO}_2^-)_2$ radicals, and hydroxycyclohexadienyl [8.17].

In all the above cases the radicals were generated by radiolysis under either stationary or pulse irradiation. The CIDEP kinetics were studied by the pulse technique, and the nonequilibrium population was unambiguously shown to be created by $S-T_0$ transitions in diffusing radical pairs. First, after the pulse that

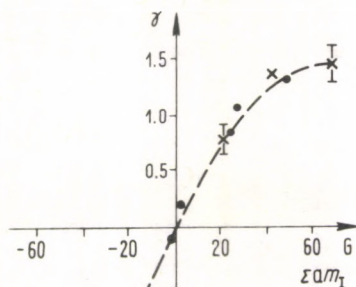


Fig. 8.5. Plots of γ vs. the total hf energy [8.10]

generates radicals, the CIDEP does not change for a long time (some 100 μ s) comparable to the radical lifetime; second, the CIDEP signal decays by the same kinetic law and with the same rate as the radicals; third, the CIDEP kinetics are independent of the microwave power level. If the radicals were formed with nonequilibrium populations, they would lose the latter within $T_1 \approx 1.4-2.8 \mu$ s, the decay rate being dependent on the microwave power.

For the radicals $\dot{\text{C}}\text{H}_2\text{CO}_2^-$, $\dot{\text{C}}\text{H}(\text{CO}_2^-)_2$, and $\dot{\text{C}}_6\text{H}_6\text{OH}$ the polarization coefficients were calculated by the equation

$$V = \gamma \tau_{1/2} T_1$$

where $\tau_{1/2} = \tau \ln 2$, τ is the radical lifetime. V values equal 30–100 and, within an order of magnitude, are close to those calculated theoretically by the Freed and Pedersen model (see Chapter 4).

The CIDEP of hydrogen atoms generated by radiolysis has the same properties and is of the same origin as that of radicals. The only difference is that the polarization observed is much higher for two reasons. First, the rate constant of diffusion encounters of hydrogen atoms is about $10^{10} \text{ l} \cdot \text{mole}^{-1} \cdot \text{s}^{-1}$, i.e., an order of magnitude higher than that of the radical collisions (some 10^9), which increases the pumping rate. Second, the spin-lattice relaxation time in the hydrogen atom is long (about 100 μ s) and hence the depolarization rate is small. The polarization coefficients V are the same as those in radicals (some 50–100) [8.14–15].

In the pulse radiolysis of liquid hydrocarbons, the alkyl radicals formed were also shown to have multiplet EA polarization [8.13, 18]. The polarization magnitude is approximately proportional to the square root of the hf energy, as it should be expected for the CIDEP created in diffusing pairs; CIDEP kinetics measured by the pulse technique also agree with this mechanism.

Direct evidence for the radical pair mechanism of CIDEP was obtained by Trifunac *et al.* [8.19]. In the pulse radiolysis of methanol, the radicals $\dot{\text{C}}\text{H}_2\text{OH}$

reveal pure multiplet polarization, its decay taking 10–20 μs , which greatly exceeds T_1 . Both facts demonstrate that CIDEP arises in the pairs $|\dot{\text{C}}\text{H}_2\text{OH } \dot{\text{C}}\text{H}_2\text{OH}|$. In the presence of $\text{CCl}_3\text{CH}_2\text{OH}$, together with these pairs, $|\dot{\text{C}}\text{H}_2\text{OH } \text{CCl}_3\dot{\text{C}}\text{HOH}|$ pairs with $\Delta g < 0$ are generated. As a result, the net polarization is contributed to the multiplet *EA* effect. The presence of $\text{CBr}_3\text{CH}_2\text{OH}$ results in pairs $|\dot{\text{C}}\text{H}_2\text{OH } \text{CBr}_3\dot{\text{C}}\text{HOH}|$ with Δg increased compared to the previous pair. Moreover, the radical $\text{CBr}_3\dot{\text{C}}\text{HOH}$ rapidly eliminates HBr and converts to $\dot{\text{C}}\text{Br}_2\text{CHO}$. The Δg -value in the new pair $|\dot{\text{C}}\text{H}_2\text{OH } \dot{\text{C}}\text{Br}_2\text{CHO}|$ is even greater. As a result, the contribution of the positive net polarization to CIDEP increases. Both contributions become comparable for CH_3OH radiolysis in the presence of $\text{CBr}_3\text{CH}_2\text{OH}$. This is also the situation with the CIDEP of other alcohol radicals [8.20].

In pulse radiolysis of slightly acidic alcohol solutions, net *EA* polarization is observed in $\dot{\text{C}}\text{H}_2\text{OH}$, $\text{CH}_3\dot{\text{C}}\text{HOH}$, $\text{CH}_3\text{CH}_2\dot{\text{C}}\text{HOH}$ and $(\text{CH}_3)_2\dot{\text{C}}\text{OH}$, its magnitude increasing gradually with increasing hf energy of the hyperfine structure components (i.e., approaching the edges of the ESR spectrum) [8.3]. Thus, in this case also, the CIDEP originates from diffusion pairs and $\text{S}-\text{T}_0$ transitions. The same polarization arises by the same mechanism in radicals $(\text{CH}_3)_2\dot{\text{C}}\text{OH}$, $\text{CH}_3\dot{\text{C}}\text{HOH}$, $\text{HOCH}_2\dot{\text{C}}\text{HOH}$, and $\dot{\text{C}}_6\text{H}_5\text{OH}$ in the photolysis of tert-butyl peroxide, hydrogen peroxide, acetone, and acetaldehyde in alcohols [8.22]. The polarization is proportional to the radical concentration, i.e., the pumping arises in diffusing radical pairs.

CIDEP responds to the influence of electrostatic interactions on the CIDEP of charged radicals. This assumption has been verified experimentally [8.23]. In the pulse radiolysis of sodium acetate and malonate, the radicals $\dot{\text{C}}\text{H}_2\text{CO}_2^-$ and $\dot{\text{C}}\text{H}(\text{CO}_2^-)_2$ demonstrate multiplet *EA* polarizations, which increase with the solution ionic strength (in qualitative agreement with theory).

In benzaldehyde- d_5 photolysis in fluorinated hydrocarbons, the pulse ESR technique detects positive polarization of the benzoyl radical $\text{Ph}\dot{\text{C}}\text{O}$ and negative polarization of hydroxybenzyl radical $\text{Ph}\dot{\text{C}}\text{HOH}$ [8.24]. The CIDEP signal decays in a time much shorter than the radical lifetime, these facts demonstrating that the CIDEP arises in the initial triplet radical pair $|\text{Ph}\dot{\text{C}}\text{O } \text{Ph}\dot{\text{C}}\text{HOH}|$ due to the $\text{S}-\text{T}_0$ transitions induced by the difference of g -values.

Next, we refer to the magnetic polarization of solvated electrons generated in photolysis or radiolysis. Glarum and Marshall [8.25] observed emission ESR spectra of solvated electrons in the photolysis of ether solutions of some alkali metals. In the photolysis of K , Cs , and Rb dissolved in tetrahydrofuran in the presence of dicyclohexyl-18-crown-6 [8.26], the multiplet polarization of K atoms (nuclear spin $3/2$, $g = 2.0010$) was observed together with the emission ESR spectra of solvated electrons. The solvated electron g -factor was 2.0021; the authors suggested that the CIDEP in this system arises in the diffusing radical pairs. However, the CIDEP behaviour within the irradiation cycle time (rotating sector technique) demonstrates that the pumping occurs in the elementary steps of solvated electron generation (Fig. 8.6). In this case the triplet mechanism perhaps also contributes principally to

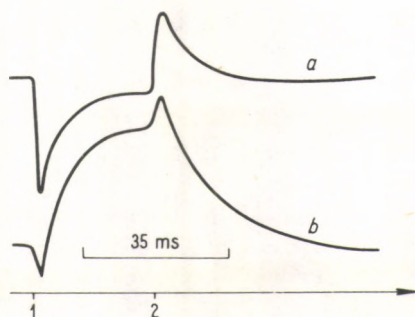
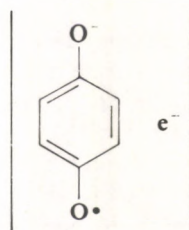


Fig. 8.6. CIDEP kinetics of solvated electron photolysis of rubidium solutions in tetrahydrofuran; at time 1 light is on, at time 2 it is off. In case (a), flux intensity is 10 times greater than that in case (b) [8.26]

the CIDEP. Examples of the simultaneous action of both mechanisms will be discussed below.

Fessenden [8.27] observed an interesting case of CIDEP radiolysis of aqueous-alcoholic solutions of *n*-benzoquinone: the positive electron polarization was shown by semiquinone radical-anion and negative polarization by the solvated electron. According to the CIDEP theory, in the diffusion mechanism, the radical with a lower g -factor must carry positive polarization and that with a higher g -factor negative (provided the molecules are singlet born). However, the situation observed was opposite since the semiquinone g -factor exceeded that of the solvated electron. An extra assumption that the recombination (or disproportionation) of a radical pair



yields a triplet molecule has been put forward. This hypothesis needs to be experimentally verified. If confirmed, the interest in such an elementary step will increase greatly. Perhaps the triplet molecule arises from two coupled solvated electrons, one having come from an anion radical.

In principle, CIDEP can arise in radical pairs by S-T transitions; however, no experimental evidence for this effect has so far been obtained. The only exception is, perhaps, the detection of hydrogen atoms in the radiolysis of slightly acidic frozen water solutions [8.28]. The atoms are $EA + E$ polarized; the emission admixture observed in the multiplet CIDEP can be accounted for by the contribution of the S-T₋ transitions. It is not yet time, however, for definite conclusions to be made.

8.2.2 CIDEP in reactions of triplet molecules

The polarization of electrons caused by the triplet mechanism is not, strictly speaking, chemical. It arises in triplet molecules due to the fact that in the transitions of molecules from the excited singlet into the triplet state populate the substates T_+ , T_- and T_0 with different rates. Moreover, the deactivation rates of these substates also differ. This results in the nonequilibrium population of T_{\pm} and T_0 substates of the triplet molecule. If this molecule reacts yielding two radicals, i.e. two doublet states, the nonequilibrium population is carried into the radicals and is manifested in their ESR spectra. The only condition is, however, that the characteristic time of triplet molecule chemical reaction must be shorter than that of its spin-lattice electron relaxation. The physical mechanisms of pumping in triplet states have been discussed in Chapter 4.

Characteristic features of triplet CIDEP are as follows. First, both radicals have polarizations equal in magnitude and sign; second, the polarization is independent of the radical hf energy; third, the polarization falls with the radical spin-lattice relaxation time, i.e., by the same kinetic law as in a radical pair with uncorrelated spins.

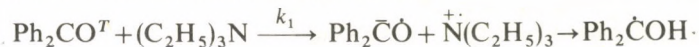
These features taken into account, one can easily distinguish between triplet born CIDEP and that generated from radical pairs.

In liquids, the influence of triplet molecule rotations on the population rate of the substates T_+ , T_- , and T_0 and also on the relaxation rate must be taken into consideration. Then the polarization coefficient observed experimentally can be determined by the expression [8.29]

$$3\gamma - 1 = 4\gamma_0^T k^3 T_1 (1 + k^3 T_1)^{-1} \quad (8.1)$$

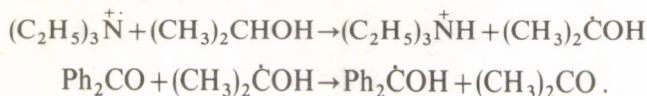
where 3T_1 is the spin-lattice relaxation time of the triplet molecule, γ_0^T is the polarization of this molecule, k is the rate constant of the reaction of the triplet molecule to give two radicals. Relation (8.1) is of use for quantitative CIDEP analysis, and to identify its origin reliably.

Strong emission of carbonyl compound radicals (e.g., semiquinone or $\text{Ph}_2\dot{\text{C}}\text{OH}$) has been observed in the photolysis of carbonyl compounds (duroquinone or benzoquinone) in alcohol solutions in the presence of triethylamine [8.30–33]. The radical generation includes the electron transfer:



The first interpretation of the CIDEP in such systems was given in terms of the pumping taking place in the radical-ion pair by means of $S-T_-$ transitions. Later a quantitative CIDEP analysis was carried out which showed the CIDEP to be described by eq. (8.1). In this case $k = k_1 [(\text{C}_2\text{H}_5)_3\text{N}]$ and the quantity $(3\gamma - 1)^{-1}$ is linearly dependent on the reciprocal amine concentration. This linearity was confirmed experimentally. Though expected within the RP model, the slope of this dependence is in better agreement with quantitative predictions of the triplet model. (Furthermore it gives ${}^3T_1 \approx 10^{-8}$ s, which fits theoretical estimates.)

As it was not detected in these experiments, the radical-cation $(C_2H_5)_3\dot{N}^+$ was supposed to react readily by the scheme



The result of these fast reactions was that the expected radical-cation polarization was transferred to the radical $Ph_2\dot{C}OH$. There is some evidence to support this viewpoint [8.31, 32]. However, some additional CIDEP investigations are required to solve the problem of the radical-cation behaviour unambiguously.

The triplet mechanisms of CIDEP in the system carbonyl compound/triethylamine was also demonstrated by the dependence of the polarization coefficient γ on the concentration of triplet state quenchers. Moreover, these measurements show that the three substates T_+ , T_- , and T_0 react with equal rate constants for converting the triplet state into a RP. If the rates were different, they could account for electron polarization. It can be proved by the following considerations. In the presence of quenchers (e.g. naphthalene) eq. (8.1) takes the form

$$3\gamma - 1 = \frac{4\gamma_0^T k [{}^3T_1 + (k_q Q)^{-1}]}{1 + k [{}^3T_1 + (k_q Q)^{-1}]} \quad (8.2)$$

where Q is the quencher concentration, k_q is the quenching rate constant, $k = k_1 [(C_2H_5)_3N]$. This equation is obtained under the assumption that the three substates T_+ , T_- , and T_0 react and are quenched with equal rate constants. The expression can be derived easily by substituting ${}^3T_1 + (k_q Q)^{-1}$, which is the effective lifetime of the triplet states, into eq. (8.1) instead of 3T_1 . Transforming eq. (8.2), one can easily prove that, all the suppositions being true, the coefficient $(3\gamma - 1)^{-1}$ must be linearly dependent on the quencher concentration Q . This dependence was obtained experimentally and the constant ratio k_1/k_q was found to be 0.8 [8.33], this value being reasonable since the rates of both processes—reaction and quenching—are diffusion controlled.

The radical CIDEP arising in the pulse photolysis of carbonyl compounds (benzophenone, dibenzyl, benzaldehyde and its chloro-substituted derivatives, acetophenone, anthraquinone, etc.) in paraffin also follows the triplet mechanism [8.5]. The radical ESR spectra correspond to pure emission (e.g., see Fig. 8.2) and reveal no traces of multiplet effects (the latter means that in these systems the RP contribution to the CIDEP is negligible). The magnitude of $(C_6H_5)_2\dot{C}OH$ radical polarization is proportional to $(\eta/T)^{-1/2}$, in accordance with the triplet model.

The pulse photolysis of duroquinone and naphthaquinone in isopropanol in the presence of 2,6-di-tert-butylphenol generates semiquinone and phenoxyl radicals whose ESR spectra show strong emission [8.34–37]. The negative polarization of both radicals unambiguously demonstrates the importance of the triplet mechanism of CIDEP in this system. Moreover, in the photolysis of 1,4-naphthoquinone in the presence of 1,4-naphtho-hydroxyquinone, strong emission of 1,4-naph-

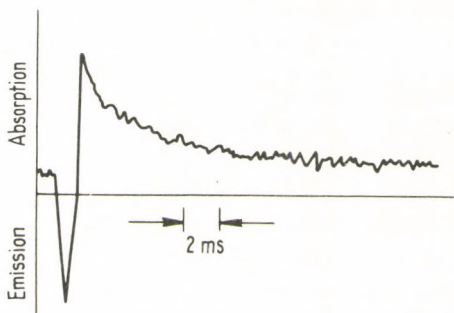
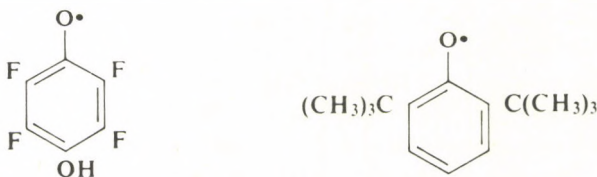


Fig. 8.7. ESR signal intensity variations for 1,4-naphthoquinone radical in pulse photolysis of naphthoquinone in isopropanol [8.35]

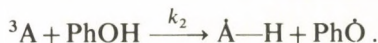
thosemiquinone radicals is observed. In this case it cannot arise from the RP mechanism at all, since in a pair of identical radicals, $\Delta g = 0$. The polarization increases with the viscosity and phenol concentration, in accordance with the triplet model of CIDEP. Finally, the time behaviour of the CIDEP signal (Fig. 8.7) is also evidence for the triplet born polarization.

In the photolysis of fluoroanyl in the presence of 2,6-di-*tert*-butyl the ESR spectrum of 2,6-di-*tert*-butylphenoxy shows a strong emission [8.38]. The CIDEP cannot arise by the RP mechanism since in the radical pair



$\Delta g \approx 0$. The triplet mechanism of the CIDEP is also of no doubt here.

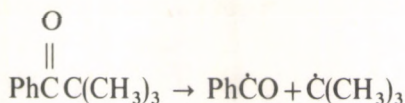
In a number of systems the CIDEP arises from both mechanisms. For instance, in the photolysis of duroquinone and anthraquinone in the presence of 2,6-di-*tert*-butylphenol (DTBP), both radicals demonstrate emission in the ESR spectra irrespective of the hf energy [8.33]. This is of importance, since it allows one to eliminate the CIDEP induced by the $S-T_-$ transition. By this mechanism, both radical partners carry negative polarization, its magnitude depending on the hf energy, since the probability of $S-T_-$ transitions is proportional to a^2 . The polarization of the anthrasemiquinone radical in benzene was shown to obey eq. (8.1) with $k = k_2(\text{DTBP})$, where k_2 is the rate constant of the reaction



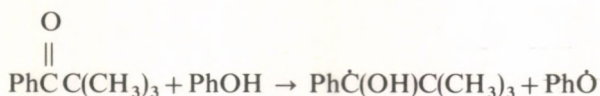
The phenoxy radical polarization also decreases with the phenol concentration, however, the polarization magnitude extrapolated to zero concentration does not prove to be zero. This means that at low phenol concentrations the polarization also arises in triplet RPs $[\dot{A}H \text{ Ph}\dot{O}]^T$ due to $S-T_0$ transitions. Indeed, at low phenol concentrations, the lifetime of a triplet anthraquinone molecule becomes long (exceeding the spin-lattice relaxation time 3T_1), and the triplet molecule polarization vanishes by the time the molecule reacts with phenol. Thus, both mechanisms contribute to the CIDEP: at high phenol concentrations the triplet mechanism dominates, at low concentrations the radical pair mechanism dominates.

The coexistence of both CIDEP mechanisms was confirmed in the photolysis of substituted benzoquinones and naphthoquinones in presence of 2,6-di-tert-butylphenol [8.39] and also in the photolysis of β -diketones $CH_3COCOCH_3$ and $CH_3COCOOH$ in isopropanol and cyclohexanol [8.40]. In both cases the initial photochemical reactions of excited triplet molecules contribute to the magnetic nuclear polarization by the triplet mechanism, while the secondary reactions in the RPs make an additional contribution to the CIDEP by the radical pair mechanism.

In the photolysis of pivalophenone in the presence of 2,6-di-tert-butylphenol, the contribution of both mechanisms is determined by two the competing reactions [8.33, 41]

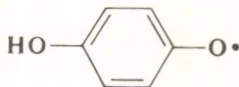


and



At high phenol concentrations, when the latter reaction is faster than the triplet molecule photo-decomposition, the contribution of the triplet mechanism dominates; at low phenol concentrations, the CIDEP is created in the radical pairs (multiplet EA polarization of tert-butyl radicals), the ketone decomposition predominating. The radical pair contribution to CIDEP also increases in low viscous solvents, for there the triplet molecules tumble more quickly and hence lose their polarization sooner (3T_1 becomes shorter).

Both contributions of the radical



generated by the pulse photolysis of benzoquinone in alcohols have been quantitatively distinguished [8.42]. The CIDEP kinetics of the one of the ESR spectrum components is shown in Fig. 8.8.

The triplet mechanism dominates in ethyleneglycol and is as much as 2/3; in a solvent with a lower viscosity (isopropanol) this contribution, as expected,

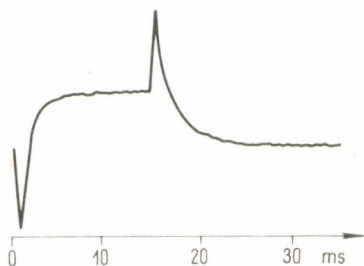


Fig. 8.8. CIDNP kinetics of semiquinone radical in photolysis of quinone in ethylenglycol; flush duration is 15 ms

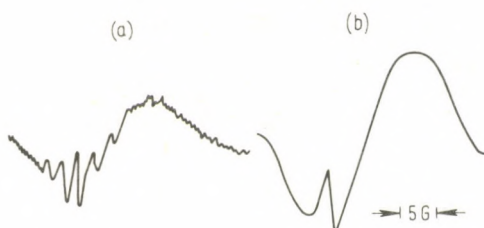
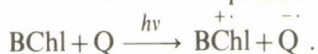


Fig. 8.9. ESR spectra of bacteriochlorophyll radical-cation (absorption) and semiquinone radical-anion (emission): (a) protiated semiquinone; (b) deuterated semiquinone

decreases. The polarization observed experimentally in radical pairs agrees with that calculated theoretically by the Freed and Pedersen model with the following parameters: $J_0 > 10^9$ rad/s, $r_{ex} = d = 0.64$ nm, $\tau_j \approx 4 \cdot 10^{-10}$ s. The triplet contribution fits theory provided the triplet molecule has a lifetime in the nanosecond range and the zero field splitting D is not less than 700 G, these parameters being quite reasonable.

The first example of CIDEP observations in biological systems [8.43] is interesting; this comes from bacteriochlorophyll irradiated with red light in the presence of quinone in dry acetone at low temperatures (-100 to -150 °C), giving bacteriochlorophyll radical-cation and benzoquinone radical-anion



Under steady-state conditions at -120 °C, both radicals have standard absorption ESR spectra. At -120 °C the semiquinone ESR spectrum vanishes, at -105 °C– -110 °C the semiquinone emission appeared (Fig. 8.9). The nonequilibrium population is supposed to originate from the bacteriochlorophyll triplet state and to appear in the semiquinone as a result of electron transfer. The emission in the BChl radical-cation ESR spectrum should also be observed; however, the absorption signal intensity of this radical is high and the line is broad, which explains why the emission cannot be observed by a stationary method against a background of strong absorption.

Photolysis by polarized light gives some additional evidence for the triplet CIDEP mechanism. Polarized light excites only those molecules whose optical transition dipolar moments are oriented along the electric vector of the exciting light. It results in an anisotropic distribution of singlet excited molecule orientations, and the S–T mixing populates the substates T_+ , T_0 , T_- in different ways depending on this distribution.

Adrian [8.44] was first to propose to use polarized light to test the triplet mechanism. He showed the magnitude of triplet spin polarization (and thus the

radical CIDEP) to change by $3(\cos^2 \chi - 1)$, where χ is the angle between the polarized light electric vector and the magnetic field direction.

This prediction was tested experimentally in the photolysis of duroquinone in the presence of triethylamine with polarized light. The difference in the polarization coefficients γ_{\parallel} and γ_{\perp} (at $\chi=0^\circ$ and 90° respectively), though small (about 5%) qualitatively corresponded to theory [8.45].

More distinct quantitative differences in γ_{\parallel} and γ_{\perp} were obtained in benzoquinone photolysis in the presence of 2,6-di-tert-butylphenol in tert-butanol [8.45]. Both semiquinone and phenyl radicals showed emission ESR spectra, γ_{\perp} exceeding γ_{\parallel} by 20%, in accord with theory. In the benzoquinone photolysis in the presence of triethylamine, only the semiquinone ESR spectrum was observed; its emission signal magnitude depended on the orientation of the light polarization plane: γ_{\perp} exceeded γ_{\parallel} by 30%. This value is greater than that (20%) predicted theoretically by Adrian.

Thus, in the photolysis of carbonyl and aromatic compounds the basic CIDEP mechanism is optical spin polarization in triplet molecules.

8.3 Conclusion

The comparison of experimental and theoretical results confirms the main ideas concerning the origin of CIDEP and its mechanism. Theory also predicts how CIDEP should depend on a number of parameters characterizing the details of particle interactions in elementary chemical reactions (lifetimes, molecular diffusion, exchange and Coulomb intermolecular potentials, radical recombination cross sections, spin-lattice relaxation times, dipolar interactions in triplet molecules, etc.). This information can be obtained by comparing the experimental and theoretical results, but in fact this problem is complicated since the number of parameters determining CIDEP is great. Quantitative CIDEP investigations are faced with considerable experimental difficulties. One sometimes fails to observe CIDEP of both radicals, to determine spin-lattice relaxation times, to detect the time dependence of CIDEP, etc. The technique of pulse ESR and photochemical experiments in nanosecond and picosecond ranges is complicated and not always available.

However, the prospects of emission ESR spectroscopy are quite promising, and this field undoubtedly will be extensively developed.

REFERENCES

- 1.1. A. R. Lepley and G. L. Closs (Editors), *Chemically Induced Magnetic Polarization*. Wiley, New York, 1973.
- 1.2. R. G. Lawler, *Progress in Nuclear Magnetic Resonance Spectroscopy*, **9**, 147 (1973).
- 1.3. G. L. Closs, *Adv. in Magn. Resonance*, **7**, 157 (1974).
- 1.4. A. L. Buchachenko, *Chemically Induced Polarizations of Electrons and Nuclei*. Nauka, Moscow, 1974.
- 1.5. L. T. Muus, P. W. Atkins, K. A. McLauchlan and J. B. Pedersen (Editors), *Chemically Induced Magnetic Polarization*. D. Reidel, Dordrecht, 1977.
- 1.6. J. H. Freed and J. B. Pedersen, *Adv. Magn. Resonance*, **8**, 1 (1976).
- 1.7. P. W. Atkins and G. T. Evans, *Adv. Chem. Phys.*, **35**, 1 (1976).
- 1.8. A. L. Buchachenko, *Usp. Khim.*, **45**, 761 (1976).
- 1.9. R. Z. Sagdeev, K. M. Salikhov and Yu. N. Molin, *Usp. Khim.* **46**, 569 (1977).
- 1.10. Yu. N. Molin, R. Z. Sagdeev and K. M. Salikhov, *Rev. of Soviet Authors, Chem. ser.*, **1**, 1 (1979).
- 1.11. A. Carrington and A. D. McLachlan, *Introduction to Magnetic Resonance*. Harper and Row, New York, Evanston and London, 1967.
- 1.12. J. Bargon, H. Fischer and U. Johnsen, *Z. Naturforsch.*, **22a**, 1551 (1967).
- 1.13. H. R. Ward and R. G. Lawler, *J. Amer. Chem. Soc.*, **89**, 5518 (1967).
- 1.14. R. Kaptein and L. J. Oosterhoff, *Chem. Phys. Lett.*, **4**, 195 (1969).
- 1.15. R. Kaptein and L. J. Oosterhoff, *Chem. Phys. Lett.*, **4**, 214 (1969).
- 1.16. G. L. Closs, *J. Amer. Chem. Soc.*, **91**, 4552 (1969).
- 1.17. G. L. Closs and A. D. Trifunac, *J. Amer. Chem. Soc.*, **92**, 2183 (1970).
- 1.18. F. J. Adrian, *J. Chem. Phys.*, **53**, 3374 (1970); **54**, 3912 (1971).
- 1.19. R. W. Fessenden and R. H. Schuler, *J. Chem. Phys.*, **39**, 2147 (1963).
- 1.20. B. Smaller, J. R. Remko and E. C. Avery, *J. Chem. Phys.*, **48**, 5174 (1968).
- 1.21. F. J. Adrian, *J. Chem. Phys.*, **54**, 3918 (1971).
- 1.22. P. W. Atkins, I. C. Buchanan, R. C. Gurd, K. A. McLauchlan and A. F. Simpson, *Chem. Commun.*, **9**, 513 (1970).
- 1.23. R. Livingstone and H. Zeldes, *J. Chem. Phys.*, **53**, 1406 (1970).
- 1.24. P. W. Atkins and K. A. McLauchlan, in *Chemically Induced Magnetic Polarization*. A. R. Lepley and G. L. Closs (Editors) Wiley, New York, 1973.
- 1.25. S. K. Wong, D. A. Hutchinson and J. K. S. Wan, *J. Chem. Phys.*, **58**, 985 (1973).
- 1.26. B. Brocklehurst, *Nature*, **221**, 921 (1969).
- 1.27. R. G. Lawler and G. T. Evans, *Ind. Chim. Belg.*, **36**, 1087 (1971).
- 1.28. R. Z. Sagdeev, K. M. Salikhov, T. V. Leshina, M. A. Kamkha, S. M. Shein and Yu. N. Molin, *Pis'ma ZhETF*, **16**, 599 (1972).
- 1.29. K. M. Salikhov, F. S. Sarvarov, R. Z. Sagdeev, Yu. N. Molin, T. V. Leshina, M. A. Kamkha and S. M. Shein, *Proc. of XI European Congress on Molecular Spectroscopy, Tallin, 1973*, p. 363.
- 1.30. A. V. Podoplelov, R. Z. Sagdeev, T. V. Leshina, Yu. N. Molin and Yu. A. Grishin, *Dokl. AN SSSR*, **225**, 855 (1975).

- 1.31. Y. Tanimoto, H. Hayashi, S. Nagakura, H. Sakuragi and K. Tokumaru, *Chem. Phys. Lett.*, **41**, 687 (1976).
- 1.32. A. L. Buchachenko, E. M. Galimov, V. V. Ershov, G. A. Nikiforov and A. D. Pershin, *Dokl. AN SSSR*, **228**, 379 (1976).
- 1.33. Yu. N. Molin and R. Z. Sagdeev, *Lecture on All-Union Conference on Chemical Kinetics Dedicated to the 80th Anniversary of Academician N. N. Semenov*, Moscow, 1976.
- 1.34. B. Brocklehurst, R. S. Dixon, E. M. Gardy, V. J. Lopata, M. J. Quinn, A. Singh and F. P. Sargent, *Chem. Phys. Lett.*, **28**, 361 (1974).
- 1.35. K. Schulten, H. Staerk, A. Weller, H.-J. Werner and B. Nickel, *Z. Phys. Chem. N. F.*, **101**, 371 (1976).
- 1.36. M. E. Michel-Beyerle, R. Haberkorn, W. Bube, E. Steffens, H. Schröder, H. J. Neusser, E. W. Schlag and H. Seidltz, *Chem. Phys.*, **17**, 139 (1976).
- 1.37. N. J. Turro and B. Kraeutler, *J. Amer. Chem. Soc.*, **100**, 7432 (1978).
- 2.1. J. Franck and E. Rabinowitch, *Trans. Far. Soc.*, **30**, 120 (1934).
- 2.2. R. M. Noyes, *J. Amer. Chem. Soc.*, **77**, 2042 (1954).
- 2.3. E. Rabinowitch and W. C. Wood, *Trans. Far. Soc.*, **32**, 1381 (1936).
- 2.4. R. M. Noyes, *Effects of Diffusion Rates on Chemical Kinetics*, in: *Progress in Reaction Kinetics*. G. Porter (Editor) Pergamon Press, Oxford, London, New York, Paris, 1961, **1**, pp. 129-161.
- 2.5. V. I. Goldansky, K. I. Zamaraev, A. I. Mikhailov and R. F. Khairutdinov, *Tunnel transitions in electron transfer reactions*, in *Problems of elementary chemical reaction kinetics*. Nauka, Moscow, 1973, pp. 68-80.
- 2.6. L. Onsager, *Phys. Rev.*, **54**, 554 (1938).
- 2.7. Ya. S. Lebedev, *Dokl. AN SSSR*, **171**, 378 (1966).
- 2.8. Ya. I. Frenkel, *Kinetic Theory of Liquids*. AN SSSR, Moscow, Leningrad, 1959.
- 2.9. S. Chandrasekhar, *Rev. Mod. Phys.*, **15**, 1 (1943).
- 2.10. R. M. Noyes, *J. Chem. Phys.*, **22**, 1349 (1954).
- 2.11. R. M. Noyes, *J. Amer. Chem. Soc.*, **78**, 5486 (1956).
- 2.12. F. J. Adrian, *J. Chem. Phys.*, **53**, 3374 (1970).
- 2.13. T. J. Chuang, G. W. Hoffman and K. B. Eisenthal, *Chem. Phys. Lett.*, **25**, 201 (1974).
- 2.14. J. M. Deutch, *J. Chem. Phys.*, **56**, 6076 (1972).
- 2.15. L. Monchick, *J. Chem. Phys.*, **24**, 381 (1956).
- 2.16. Z. Schulten and K. Schulten, *J. Chem. Phys.*, **66**, 4616 (1977).
- 2.17. T. R. Waite, *J. Chem. Phys.*, **32**, 21 (1960).
- 2.18. E. Rabinowitch, *Trans. Far. Soc.*, **33**, 1225 (1937).
- 2.19. A. M. North, *The Collision Theory of Chemical Reactions in Liquids*. John Wiley, London, Methuen and New York, 1964.
- 2.20. R. Kaptein and J. L. Oosterhoff, *Chem. Phys. Lett.*, **4**, 195 (1969).
- 2.21. G. L. Closs, *J. Amer. Chem. Soc.*, **91**, 4552 (1969).
- 2.22. T. R. Waite, *Phys. Rev.*, **107**, 463 (1957).
- 2.23. S. G. Entelis and R. P. Tiger, *The Kinetics of Reactions in Liquid State*. Khimia, Moscow, 1973.
- 2.24. B. Stevens and R. R. Williams, *Chem. Phys. Lett.*, **36**, 100 (1975).
- 2.25. K. S. Schmitz and J. M. Schurr, *J. Phys. Chem.* **76**, 534 (1972).
- 2.26. Yu. N. Molin, K. M. Salikhov and K. I. Zamaraev, *Spin Exchange. Principles and Applications in Chemistry and Biology*. Springer Verlag, Heidelberg, 1980.
- 2.27. K. M. Salikhov, *Teor. Eksp. Khim.*, **13**, 732 (1977).
- 2.28. A. Carrington and A. D. McLachlan, *Introduction to Magnetic Resonance with Applications to Chemistry and Chemical Physics*. Harper and Row, New York, Evanson, London, 1967.
- 2.29. B. Brocklehurst, *J. Chem. Soc., Faraday Trans.*, II, **72**, 1869 (1976).
- 2.30. K. M. Salikhov, D. Sc. Thesis, Kazan, 1974.
- 2.31. F. S. Sarvarov and K. M. Salikhov, *Teor. Eksp. Khim.*, **11**, 435 (1975).
- 2.32. R. Haberkorn, Doctoral Thesis, München, 1977.
- 2.33. K. Schulten and P. G. Wolynes, *J. Chem. Phys.*, **68**, 3292 (1978).
- 2.34. R. Z. Sagdeev, K. M. Salikhov and Yu. N. Molin: *Usp. Khim.*, **46**, 569 (1977).

- 2.35. Yu. N. Molin, R. Z. Sagdeev and K. M. Salikhov, *Rev. of Soviet Authors, Chem. ser.*, **1**, 1 (1979).
- 2.36. G. T. Evans and R. G. Lawler, *Mol. Phys.*, **30**, 1085 (1975).
- 2.37. H.-J. Werner, Z. Schulten and K. Schulten, *J. Chem. Phys.* **67**, 646 (1977).
- 2.38. K. M. Salikhov, A. G. Semenov and Yu. D. Tsvetkov, *Electron Spin Echo and Its Application*. Nauka, Novosibirsk, 1976.
- 2.39. G. M. Zhidomirov and K. M. Salikhov, *ZhETF*, **56**, 1933 (1969).
- 2.40. K. Schulten and I. R. Epshtein, *J. Chem. Phys.*, **71**, 309 (1979).
- 2.41. S. I. Kubarev and E. A. Pschenichnov, *Chem. Phys. Lett.*, **28**, 66 (1974).
- 2.42. S. I. Kubarev, E. A. Pschenichnov and A. S. Schustov, *Teor. Eksp. Khim.*, **12**, 435 (1976).
- 2.43. A. Abragam, *The Principles of Nuclear Magnetism*. Clarendon Press, Oxford, 1961.
- 2.44. L. D. Landau and E. M. Lifschitz, *Quantum Mechanics*. Nauka, Moscow, 1974.
- 2.45. J. B. Pedersen and J. H. Freed, *J. Chem. Phys.*, **58**, 2746 (1973).
- 2.46. J. B. Pedersen and J. H. Freed, *J. Chem. Phys.*, **59**, 2869 (1973).
- 2.47. J. B. Pedersen and J. H. Freed, *J. Chem. Phys.*, **61**, 1517 (1974).
- 2.48. K. M. Salikhov, F. S. Sarvarov, R. Z. Sagdeev, Yu. N. Molin, T. V. Leschina, M. A. Kamkha and S. M. Schein, *XI European Congress on Molecular Spectroscopy, Tallin, 1973*. Abstracts, p. 363.
- 2.49. K. M. Salikhov, F. S. Sarvarov, R. Z. Sagdeev and Yu. N. Molin, *Kinet. i Katal.*, **16**, 279 (1975).
- 2.50. F. S. Sarvarov and K. M. Salikhov, *React. Kinetics and Catal. Lett.*, **4**, 33 (1976).
- 2.51. F. S. Sarvarov, C. Sc. Thesis, Novosibirsk, 1977.
- 2.52. G. T. Evans, P. D. Fleming and R. G. Lawler, *J. Chem. Phys.*, **58**, 2071 (1973).
- 2.53. R. Haberkorn, *Chem. Phys.*, **19**, 165 (1977).
- 2.54. R. Kaptein and J. L. Oosterhoff, *Chem. Phys. Lett.*, **4**, 214 (1969).
- 2.55. R. Z. Sagdeev, K. M. Salikhov, T. V. Leschina, M. A. Kamkha, S. M. Schein and Yu. N. Molin, *Pis'ma ZhETF*, **16**, 599 (1972).
- 2.56. R. G. Lawler and G. T. Evans, *Ind. Chim. Belg.*, **36**, 1087 (1971).
- 2.57. F. J. Adrian, *J. Chem. Phys.*, **54**, 3912 (1971).
- 2.58. R. Kaptein, Ph. D. Thesis, Leiden, 1971.
- 2.59. F. J. Adrian, *Chem. Phys. Lett.*, **10**, 70 (1971).
- 2.60. R. Z. Sagdeev, Yu. N. Molin, K. M. Salikhov, M. A. Kamkha, T. V. Leschina and S. M. Schein, *Org. Magn. Resonance*, **5**, 603 (1973).
- 2.61. J. I. Morris, R. C. Morrison, D. W. Smith and J. F. Garst, *J. Amer. Chem. Soc.*, **94**, 2406 (1972).
- 2.62. P. W. Atkins and G. T. Evans, *Chem. Phys. Lett.*, **24**, 45 (1974).
- 2.63. B. Brocklehurst, *Chem. Phys. Lett.*, **28**, 357 (1974).
- 2.64. J. A. den Hollander, Ph. D. Thesis, Leiden, 1976.
- 2.65. R. C. Johnson and R. E. Merrifield, *Phys. Rev.*, **1B**, 896 (1970).
- 2.66. M. Tomkiewicz, A. Groen and M. Cocivera, *J. Chem. Phys.*, **56**, 5850 (1972).
- 2.67. R. M. Lynden-Bell, *Mol. Phys.*, **8**, 71 (1964).
- 2.68. R. Haberkorn, *Mol. Phys.*, **32**, 1491 (1976).
- 2.69. A. B. Doktorov, *Physica*, **90A**, 109 (1978).
- 2.70. N. N. Bogolubov, *Problems of the Dynamic Theory in Statistical Physics*. Fizmatgiz, Moscow, Leningrad, 1946.
- 2.71. P. A. Purtov and K. M. Salikhov, *Teor. Eksp. Khim.*, **15**, 121 (1979).
- 2.72. P. A. Purtov and K. M. Salikhov, *Teor. Eksp. Khim.*, **15**, 234 (1979).
- 2.73. P. A. Purtov and K. M. Salikhov, *Teor. Eksp. Khim.*, **16**, 579 (1980).
- 2.74. P. A. Purtov, C. Sc. Thesis, Novosibirsk, 1981.
- 2.75. S. A. Sukhenko, P. A. Purtov, K. M. Salikhov, *Khim. Fiz.*, **3**, 21 (1983).
- 2.76. P. J. Hore, K. A. McLauchlan, *Mol. Phys.*, **42**, 533 (1981).
- 2.77. K. M. Salikhov, F. S. Sarvarov, *Teor. Eksp. Khim.*, **18**, 146 (1982).
- 2.78. A. I. Kruppa, T. V. Leschina, R. Z. Sagdeev, K. M. Salikhov, F. S. Sarvarov, *Chem. Phys.*, **67**, 27 (1982).
- 3.1. R. G. Lawler and G. T. Evans, *Ind. Chim. Belg.*, **36**, 1087 (1971).
- 3.2. R. Z. Sagdeev, K. M. Salikhov, T. V. Leshina, M. A. Kamkha, S. M. Shein and Yu. N. Molin, *Pis'ma ZhETF*, **16**, 599 (1972).

- 3.3. R. Z. Sagdeev, Yu. N. Molin, K. M. Salikhov, M. A. Kamkha, T. V. Leshina and S. M. Shein, *Org. Magn. Resonance*, **5**, 603 (1973).
- 3.4. K. M. Salikhov, F. S. Sarvarov, R. Z. Sagdeev, Yu. N. Molin, T. V. Leshina, M. A. Kamkha and S. M. Shein, *XI European Congress on Molecular Spectroscopy, Tallin, 1973*, Abstracts, p. 363.
- 3.5. K. M. Salikhov, D. Sc. Thesis, Kazan 1974.
- 3.6. K. M. Salikhov, F. S. Sarvarov, R. Z. Sagdeev and Yu. N. Molin, *Kinet. i Kat.*, **16**, 279 (1975).
- 3.7. F. S. Sarvarov and K. M. Salikhov, *React. Kinetics and Catal. Lett.*, **4**, 33 (1976).
- 3.8. F. S. Sarvarov, C. Sc. Thesis, Novosibirsk 1977.
- 3.9. P. A. Purtov and K. M. Salikhov, *Teor. Eksp. Khim.*, **15**, 121 (1979).
- 3.10. R. Haberkorn, D. Sc. Thesis, München, 1977.
- 3.11. Z. Schulten and K. Schulten, *J. Chem. Phys.*, **66**, 4616 (1977).
- 3.12. H.-J. Werner, Z. Schulten and K. Schulten, *J. Chem. Phys.*, **67**, 646 (1977).
- 3.13. J. B. Pedersen and J. H. Freed, *J. Chem. Phys.*, (a) **58**, 2746 (1973); (b) **59**, 2869 (1973); (c) **61**, 1517 (1974).
- 3.14. J. B. Pedersen, *J. Chem. Phys.*, **67**, 4097 (1977).
- 3.15. G. T. Evans, P. D. Fleming and R. G. Lawler, *J. Chem. Phys.*, **58**, 2071 (1973).
- 3.16. R. Kaptein, Ph. D. Thesis, Leiden 1971.
- 3.17. M. Tomkiewicz, A. Groen and M. Cocivera, *J. Chem. Phys.*, **56**, 5850 (1972).
- 3.18. Yu. N. Molin, K. M. Salikhov and K. I. Zamaraev, *Spin Exchange. Principles and Applications in Chemistry and Biology*. Springer Verlag, Heidelberg, (1980).
- 3.19. J. A. den Hollander, Ph. D. Thesis, Leiden 1976.
- 3.20. K. M. Salikhov, *Teor. Eksp. Khim.*, **13**, 732 (1977).
- 3.21. L. D. Landau and E. M. Lifshitz, *Quantum Mechanics*. Fizmatgiz, Moscow, 1963, pp. 380-391.
- 3.22. G. L. Closs and C. E. Doubleday, *J. Amer. Chem. Soc.*, **95**, 2735 (1973).
- 3.23. W. A. Pryor, *Free Radicals*. McGraw-Hill Book Company, New York, Toronto, London, Sydney, 1964.
- 3.24. F. S. Sarvarov, V. N. Schmidt, V. A. Kobzareva and K. M. Salikhov, *Zhurnal Fizich. Khimii*, **56**, 1585 (1982).
- 3.25. F. S. Sarvarov and K. M. Salikhov, *Teor. Eksp. Khim.*, **11**, 435 (1975).
- 3.26. R. Haberkorn, *Chem. Phys.*, **19**, 165 (1977).
- 3.27. F. J. J. de Kanter, R. Z. Sagdeev and R. Kaptein, in F. J. J. de Kanter, D. Sc. Thesis, Holland, 1978.
- 3.28. G. P. Zientara and J. H. Freed, *J. Chem. Phys.*, **70**, 1359 (1979).
- 3.29. K. Schulten and I. P. Epstein, *J. Chem. Phys.*, **71**, 309 (1979).
- 3.30. P. A. Purtov and K. M. Salikhov, *Teor. Eksp. Khim.*, **16**, 579 (1980).
- 3.31. B. Brocklehurst, *Chem. Phys. Lett.*, **28**, 357 (1974); *J. Chem. Soc. Far. Trans.*, II, **72**, 1869 (1976).
- 3.32. P. A. Purtov and K. M. Salikhov, *Teor. Eksp. Khim.*, **16**, 737 (1980).
- 3.33. K. Schulten and P. G. Wolynes, *J. Chem. Phys.*, **68**, 3292 (1978).
- 3.34. R. Haberkorn, private communication
- 4.1. R. Kaptein, *Chemically Induced Dynamic Nuclear Polarization*. Ph. D. Thesis, Leiden, 1971.
- 4.2. F. S. Sarvarov, K. M. Salikhov and R. Z. Sagdeev, *Chem. Phys.*, **16**, 41 (1976).
- 4.3. J. B. Pedersen and J. H. Freed, *J. Chem. Phys.*, **61**, 1517 (1974).
- 4.4. F. J. Adrian, *J. Chem. Phys.*, **53**, 3374 (1970).
- 4.5. P. A. Purtov and K. M. Salikhov, *Teor. Eksp. Khim.*, **15**, 234 (1979).
- 4.6. A. L. Buchachenko, *Chemically Induced Polarizations of Electrons and Nuclei*, Nauka, Moscow, 1974.
- 4.7. J. H. Freed, *Lecture at the International Symposium on Magnetic Resonance in Physics, Chemistry and Biology*. Argonne National Laboratory, Illinois, USA, 1979.
- 4.8. J. A. den Hollander, *CIDNP and Rate Processes of Radicals*. Ph. D. Thesis, Leiden, 1976.
- 4.9. F. S. Sarvarov, V. N. Schmidt, V. A. Kobzareva and K. M. Salikhov, *Zhurnal Fizich. Khimii*, **56**, 1585 (1982).
- 4.10. A. Abragam, *The Principles of Nuclear Magnetism*. Clarendon Press, Oxford, 1961.
- 4.11. G. L. Closs, *Lecture at the International Symposium on Magnetic Resonance in Physics, Chemistry and Biology*. Argonne National Laboratory, Illinois, USA, 1979.

- 4.12. G. L. Closs, *J. Amer. Chem. Soc.*, **93**, 1546 (1971).
- 4.13. L. M. Wainer, A. V. Podoplelov, T. V. Leshina, R. Z. Sagdeev and Yu. N. Molin, *Biofizika*, **2**, 234 (1978).
- 4.14. F. J. Adrian, *Chem. Phys. Lett.*, **10**, 70 (1971).
- 4.15. G. L. Closs and C. E. Doubleday, *J. Amer. Chem. Soc.*, **94**, 9248 (1972); **95**, 2735 (1973).
- 4.16. J. I. Morris, R. C. Morrison, D. W. Smith and J. F. Garst, *J. Amer. Chem. Soc.*, **94**, 2406 (1972).
- 4.17. R. Z. Sagdeev, Yu. N. Molin, K. M. Salikhov, T. V. Leshina, M. A. Kamkha and S. M. Shein, *Org. Magn. Resonance*, **5**, 599 (1973).
- 4.18. F. S. Sarvarov, C. Sc. Thesis, Novosibirsk, 1977.
- 4.19. Yu. N. Molin, K. M. Salikhov and K. I. Zamaraev, *Spin Exchange. Principles and Applications*. Springer Verlag, Heidelberg, 1980.
- 4.20. K. M. Salikhov, *Proceedings of the XX Ampere Colloque*. Tallin, 1978.
- 4.21. F. J. J. de Kanter, R. Z. Sagdeev and R. Kaptein, in press, see also ref. [4.27].
- 4.22. G. P. Zientara and J. H. Freed, *J. Chem. Phys.*, **70**, 1359 (1979).
- 4.23. P. A. Purtov and K. M. Salikhov, *Teor. Eksp. Khim.*, **16**, 737 (1980).
- 4.24. G. T. Evans and R. G. Lawler, *Mol. Phys.*, **30**, 1085 (1975).
- 4.25. F. J. J. De Kanter, R. Kaptein and R. A. Van Santen, *Chem. Phys. Lett.*, **45**, 13 (1977).
- 4.26. P. W. Atkins and G. T. Evans, *Chem. Phys. Lett.*, **24**, 45 (1974).
- 4.27. F. J. J. De Kanter, *Biradical CIDNP*. Ph. D. Thesis, Leiden, 1978.
- 4.28. R. Kaptein and J. L. Oosterhoff, *Chem. Phys. Lett.*, **4**, 195 (1969).
- 4.29. F. J. Adrian, *J. Chem. Phys.*, **54**, 3918 (1971); **57**, 5107 (1972).
- 4.30. P. W. Atkins, R. C. Gurd, K. A. McLauchlan and A. F. Simpson, *Chem. Phys. Lett.*, **8**, 55 (1971).
- 4.31. P. W. Atkins, *Chem. Phys. Lett.*, **18**, 290 (1973).
- 4.32. J. B. Pedersen and J. H. Freed, *J. Chem. Phys.*, **58**, 2746 (1973); **59**, 2869 (1973).
- 4.33. A. J. Dobbs, *Mol. Phys.*, **30**, 1073 (1975).
- 4.34. A. D. Trifunac and D. J. Nelson, *J. Amer. Chem. Soc.* **99**, 289 (1977).
- 4.35. L. Monchick and F. J. Adrian, *J. Chem. Phys.*, **68**, 4376 (1978).
- 4.36. A. L. Buchachenko, R. Z. Sagdeev and K. M. Salikhov, *Magnetic and Spin Effects in Chemical Reactions*. Nauka, Novosibirsk, 1978, Ch. 4, § 4.
- 4.37. R. G. Lawler, *Chemically Induced Dynamic Nuclear Polarization*, in *Progress in Nuclear Magnetic Resonance Spectroscopy*. Pergamon Press, Oxford, New York, Toronto, Sydney, Braunschweig, 1973, v. 9, pp. 147-206.
- 4.38. S. K. Wong, D. A. Hutchinson and J. K. S. Wan, *J. Amer. Chem. Soc.*, **95**, 622 (1973).
- 4.39. M. S. De Groot, I. A. M. Hesselmann and J. H. Van der Waals, *Mol. Phys.*, **12**, 259 (1967).
- 4.40. L. Hall, A. Armstrong, W. R. Moomaw and M. A. El-Sayed, *J. Chem. Phys.*, **48**, 1395 (1968).
- 4.41. J. Schmidt, *Chem. Phys. Lett.*, **14**, 411 (1970).
- 4.42. A. Carrington and A. D. McLachlan, *Introduction to Magnetic Resonance with Applications to Chemistry and Chemical Physics*. Harper and Row, New York, Evanston, London, 1967.
- 4.43. J. P. Colpa, K. H. Hausser and D. Stehlik, *Z. Naturforsch.*, **26a**, 1792 (1971).
- 4.44. S. K. Wong, D. A. Hutchinson and J. K. S. Wan, *J. Chem. Phys.*, **58**, 985 (1973).
- 4.45. P. W. Atkins and G. T. Evans, *Mol. Phys.*, **27**, 1633 (1974).
- 4.46. J. B. Pedersen and J. H. Freed, *J. Chem. Phys.*, **62**, 1706 (1975).
- 4.47. F. S. Sarvarov and K. M. Salikhov, *Proc. All-Union Conference on Nuclear and Electron Polarization and Magnetic Field Effects in Chemical Reactions*, Novosibirsk, 1975, p. 46.
- 4.48. J. Bargon, H. Fischer and U. Johnsen, *Z. Naturforsch.* **22a**, 1551 (1967).
- 4.49. F. J. Adrian, H. M. Vyas and J. K. S. Wan, *J. Chem. Phys.*, **65**, 1454 (1976).
- 4.50. K. M. Salikhov, *Chem. Phys.*, **64**, 371 (1982).
- 4.51. P. A. Purtov, K. M. Salikhov, *All-Union Conference on Chemical Physics Dedicated to the Memory of Academician V. V. Voievodsky*, Novosibirsk, 1982.
- 4.52. S. A. Sukhenko, P. A. Purtov and K. M. Salikhov, *Khim. Fizika*, **3**, 21 (1983).
- 5.1. J. R. Fox and G. S. Hammond, *J. Amer. Chem. Soc.*, **86**, 4031 (1964).
- 5.2. T. Nakata and K. Tokumaru, *Bull. Chem. Soc. Japan*, **43**, 3315 (1970).
- 5.3. K. Tokumaru, A. Onshima, T. Nakata, H. Sakuragi and T. Mishima, *Chemistry Lett.*, 571 (1974).
- 5.4. K. U. Ingold, in *Free Radicals*. J. K. Kochi (Editor), Interscience, New York, 1973, 1, 37.

- 5.5. V. M. Berdnikov and Yu. N. Molin, in *Vsesoyuznaya konferentsiya "Polyarizatsiya yader i elektronov i efekty magnitnogo polya v khimicheskikh reaktivnykh"*. Tezisy dokladov. (Abstracts of papers presented at the All-Union Conference on Polarization of Nuclei and Electrons and Effects of Magnetic Field in Chemical Reactions), R. Z. Sagdeev (Editor) Novosibirsk, 1975, p. 44.
- 5.6. B. Brocklehurst, *J. Chem. Soc. Faraday Trans.*, II, **75**, 123 (1979).
- 5.7. W. Adam, H. Fischer, H. J. Hansen, H. Heimgartner, H. Schmid, and H. R. Woespe, *Angew. Chemie*, **85**, 669 (1973).
- 5.8. R. Z. Sagdeev, T. V. Leshina, M. A. Kamkha, S. M. Shein, and Yu. N. Molin, *Izv. AN SSSR, Ser. khim.*, 2128 (1972).
- 5.9. R. Z. Sagdeev, K. M. Salikhov, T. V. Leshina, M. A. Kamkha, S. M. Shein, and Yu. N. Molin, *Pis'ma ZhETF*, **16**, 599 (1972).
- 5.10. R. Z. Sagdeev, Yu. N. Molin, K. M. Salikhov, T. V. Leshina, M. A. Kamkha, and S. M. Shein, *Org. Magn. Resonance*, **5**, 603 (1973).
- 5.11. R. Z. Sagdeev, T. V. Leshina, A. V. Podoplelov, K. M. Salikhov, F. S. Sarvarov, Yu. A. Grishin and Yu. N. Molin, in *Radiospektroskopiya tvyordogo tela*. A. G. Lindin (Editor) Institut fiziki, Krasnoyarsk, 1976, 2,9.
- 5.12. R. Z. Sagdeev, K. M. Salikhov, and Yu. N. Molin, *Usp. Khim.*, **46**, 569 (1977).
- 5.13. A. V. Podoplelov, R. Z. Sagdeev, T. V. Leshina, Yu. A. Grishin and Yu. N. Molin, *Dokl. AN SSSR*, **225**, 866 (1975).
- 5.14. R. Z. Sagdeev, T. V. Leshina, A. V. Podoplelov, Yu. N. Molin, F. S. Sarvarov, K. M. Salikhov and Yu. A. Grishin, in Ref. 5.5, p. 34.
- 5.15. A. V. Podoplelov, T. V. Leshina, R. Z. Sagdeev, M. A. Kamkha and S. M. Shein, *Zh. Org. Khim.*, **12**, 495 (1976).
- 5.16. T. V. Talalayeva and K. A. Kocheshkov, *Metody elementoorganicheskoy khimii, Li, Na, K, Rb, Cs*. Nauka, Moscow, 1971.
- 5.17. F. S. D'yachkovskiy and A. E. Shilov, *Usp. Khim.*, **35**, 699 (1966).
- 5.18. H. R. Ward, R. G. Lawler and R. A. Cooper, in *Chemically Induced Magnetic Polarisation*. A. R. Lepley and G. T. Closs (Editors), Wiley, New York, London, Sydney, Toronto, 1973, p. 281.
- 5.19. A. V. Podoplelov, T. V. Leshina, R. Z. Sagdeev and Yu. N. Molin, *Dokl. AN SSSR*, **230**, 150 (1976).
- 5.20. F. S. Sarvarov and K. M. Salikhov, *Teor. Eksp. Khim.*, **11**, 435 (1975).
- 5.21. Y. Tanimoto, H. Hayashi, S. Nagakura, H. Sakuragi and K. Tokumaru, *Chem. Phys. Lett.*, **41**, 267 (1976).
- 5.22. O. G. Kadnikov, *Pis'ma ZhETF*, **4**, 32 (1978).
- 5.23. S. I. Kubarev, Ye. A. Pshenichnov and A. S. Shustov, *Teor. Eksp. Khim.*, **15**, 16 (1979).
- 5.24. N. Hata, *Chemistry Lett.*, 547 (1976).
- 5.25. N. Hata, *Chemistry Lett.*, 1359 (1978).
- 5.26. N. J. Turro and M.-F. Chow, *J. Amer. Chem. Soc.*, **101**, 3701 (1979).
- 5.27. N. J. Turro, N. Kraeutler and D. R. Anderson, *J. Amer. Chem. Soc.*, **102**, (1980).
- 5.28. H. Staerk and K. Razi Naqvi, *Chem. Phys. Lett.*, **50**, 386 (1977).
- 5.29. B. Brocklehurst, *Chem. Phys. Lett.*, **28**, 357 (1974).
- 5.30. B. Brocklehurst, R. S. Dixon, E. M. Gardy, V. J. Lopata, M. J. Quinn, A. Singh and F. P. Sargent, *Chem. Phys. Lett.*, **28**, 361 (1974).
- 5.31. F. P. Sargent, B. Brocklehurst, R. S. Dixon, E. M. Gardy, V. J. Lopata and A. Singh, *J. Phys. Chem.*, **81**, 815 (1977).
- 5.32. B. Brocklehurst, *Chem. Phys. Lett.*, **44**, 245 (1976).
- 5.33. R. S. Dixon, E. M. Gardy, V. J. Lopata and F. P. Sargent, *Chem. Phys. Lett.*, **30**, 463 (1975).
- 5.34. R. S. Dixon, F. P. Sargent, V. J. Lopata and E. M. Gardy, *Chem. Phys. Lett.*, **47**, 108 (1977).
- 5.35. R. S. Dixon, F. P. Sargent, V. J. Lopata, E. M. Gardy and B. Brocklehurst, *Canad. J. Chem.*, **55**, 2093 (1977).
- 5.36. J. Klein and R. Voltz, *Phys. Rev. Lett.*, **36**, 1214 (1976).
- 5.37. J. Klein and R. Voltz, *Canad. J. Chem.*, **55**, 2102 (1977).
- 5.38. O. A. Anisimov, V. M. Grigoryants, S. V. Kiyanov, K. M. Salikhov, S. A. Sukhenko and Yu. N. Molin, *Teor. Eksp. Khim.*, **18**, 292 (1982).

- 5.39. K. Schulten, H. Staerk, A. Weller, H.-J. Werner and B. Nickel, *Z. Phys. Chem. N. F.* **101**, 371 (1976).
- 5.40. H.-J. Werner, H. Staerk and A. Weller, *J. Chem. Phys.*, **68**, 2419 (1978).
- 5.41. M. E. Michel-Beyerle, R. Haberkorn, W. Bube, E. Steffens, H. Schröder, H. J. Neusser, E. W. Schlag and H. Seidlitz, *Chem. Phys.*, **17**, 139 (1976).
- 5.42. W. Bube, R. Haberkorn and M. E. Michel-Beyerle, *J. Amer. Chem. Soc.*, **100**, 5993 (1978).
- 5.43. M. E. Michel-Beyerle, H. M. Kruger, R. Haberkorn and H. Seidlitz, *Chem. Phys.*, **42**, 441 (1979).
- 5.44. N. Deriasamy and H. Linschitz, *Chem. Phys. Lett.*, **64**, 281 (1979).
- 5.45. A. Gupta and G. S. Hammond, *J. Chem. Phys.*, **57**, 1789 (1972).
- 5.46. T. V. Leshina, S. G. Belyaeva, V. I. Maryasova, R. Z. Sagdeev, and Yu. N. Molin, *Chem. Phys. Lett.*, **75**, 438 (1980).
- 5.47. H. D. Roth and L. M. Manion Schilling, *J. Amer. Chem. Soc.*, **101**, 1898 (1979).
- 5.48. T. V. Leshina, K. M. Salikhov, R. Z. Sagdeev, S. G. Belyaeva, V. I. Maryasova, P. A. Purtov and Yu. N. Molin, *Chem. Phys. Lett.*, **70**, 228 (1980).
- 5.49. M. Sharnoff, *J. Chem. Phys.*, **46**, 3263 (1967).
- 5.50. Y. Ruedin, P. A. Schnegg, C. Jaccard and N. Aegerter, *Phys. Stat. Sol. (b)* — **54**, 565 (1972).
- 5.51. E. L. Frankevich and A. I. Pristupa, *Pis'ma ZhETF*, **24**, 397 (1976).
- 5.52. O. A. Anisimov, V. M. Grigoryants, V. K. Molchanov and Yu. N. Molin, *Dokl. AN SSSR*, **248**, 380 (1979).
- 5.53. O. A. Anisimov, V. M. Grigoryants, V. K. Molchanov and Yu. N. Molin, *Chem. Phys. Lett.*, **66**, 265 (1979).
- 5.54. Yu. N. Molin, O. A. Anisimov, V. M. Grigoryants, V. K. Molchanov and K. M. Salikhov, *J. Phys. Chem.*, **84**, 1853 (1980).
- 5.55. O. A. Anisimov, V. M. Grigoryants and Yu. N. Molin, *Pis'ma ZhETF*, **30**, 589 (1979).
- 5.56. O. A. Anisimov and Yu. N. Molin, *Khim. Vysok. Energ.*, **14**, 307 (1980).
- 5.57. V. I. Pervukhin, R. Z. Sagdeev, A. A. Obynochnyy and Yu. N. Molin, in Ref. 5.5, p. 43.
- 5.58. K. Mori, Y. Tabata and K. Oshima, *Kogyo Kagaku Zasshi*, **73**, 815 (1970).
- 5.59. K. Mori, Y. Tabata and K. Oshima, *Kogyo Kagaku Zasshi*, **73**, 1215 (1970).
- 5.60. R. P. Groff, R. E. Merrifield, A. Suna and P. Avakian, *Phys. Rev. Lett.*, **29**, 429 (1972).
- 5.61. M. F. Barnothy (Editor), *Biological Effects of Magnetic Fields*. Plenum Press, New York, vol. 1 (1964); vol. 2 (1969).
- 5.62. R. E. Blankenship, T. J. Schaafsma and W. W. Parson, *Biochim. Biophys. Acta*, **461**, 297 (1977).
- 5.63. A. J. Hoff, H. Rademaker, R. van Grondelle and L. N. M. Duysens, *Biochim. Biophys. Acta*, **460**, 547 (1977).
- 5.64. H.-J. Werner, K. Schulten and A. Weller, *Biochim. Biophys. Acta*, **502**, 255 (1978).
- 5.65. R. Haberkorn and M. E. Michel-Beyerle, *Biophys. J.*, **26**, 489 (1979).
- 5.66. H. Gorter de Vries and A. J. Hoff, *Chem. Phys. Lett.*, **55**, 395 (1978).
- 5.67. (a) W. Haberditzl, *Nature*, **213**, 72 (1967); (b) L. M. Weiner, A. V. Podoplelov, T. V. Leshina, R. Z. Sagdeev and Yu. N. Molin, *Biofizika*, **23**, 234 (1978).
- 5.68. Ye. L. Frankevich and B. M. Romyantsev, *Pis'ma ZhETF*, **6**, 553 (1967).
- 5.69. R. C. Johnson, R. E. Merrifield, P. Avakian and R. B. Flippen, *Phys. Rev. Lett.*, **19**, 285 (1967).
- 5.70. I. A. Sokolik and Ye. L. Frankevich, *Usp. Fiz. Nauk*, **111**, 261 (1973).
- 5.71. P. Avakian, *Pure Appl. Chem.*, **37**, 1 (1974).
- 5.72. G. J. Hoytink, *Disc. Faraday Soc.*, **45**, 14 (1968).
- 5.73. L. R. Faulkner and A. J. Bard, *J. Amer. Chem. Soc.*, **91**, 6497 (1969).
- 5.74. L. R. Faulkner and A. J. Bard, *J. Amer. Chem. Soc.*, **91**, 6495 (1969).
- 5.75. H. Tachikawa and A. J. Bard, *J. Amer. Chem. Soc.*, **95**, 1672 (1973).
- 5.76. Ye. L. Frankevich and I. A. Sokolik, *Khim. Vysok. Energ.*, **6**, 433 (1972).
- 5.77. B. Brocklehurst, *Nature*, **221**, 921 (1969).
- 5.78. P. W. Atkins and G. T. Evans, *Mol. Phys.*, **29**, 921 (1975).
- 5.79. H. Tachikawa and A. J. Bard, *Chem. Phys. Lett.*, **26**, 563 (1974).
- 5.80. H. Tachikawa and A. J. Bard, *Chem. Phys. Lett.*, **26**, 10 (1974).
- 5.81. L. R. Faulkner, H. Tachikawa and A. J. Bard, *J. Amer. Chem. Soc.*, **94**, 691 (1972).
- 5.82. L. X. Faulkner and A. J. Bard, *J. Amer. Chem. Soc.*, **91**, 209 (1969).

- 5.83. G. P. Keszthelyi, N. E. Tokel-Takvoryan, H. Tachikawa and A. J. Bard, *Chem. Phys. Lett.*, **23**, 219 (1973).
- 5.84. H. Tachikawa and A. J. Bard, *Chem. Phys. Lett.*, **19**, 287 (1973).
- 5.85. H. Tachikawa and A. J. Bard, *Chem. Phys. Lett.*, **26**, 246 (1974).
- 5.86. A. L. Buchachenko, R. Z. Sagdeev and K. M. Salikhov, *Magnitnyye i spinovyye efekty v khimicheskikh reaktivakh*. Nauka, Novosibirsk, 1978, p. 190.
- 5.87. T. V. Leshina, V. I. Maryasova, R. Z. Sagdeev, O. I. Margorskaya, D. A. Bravo-Zhivotovskiy, O. A. Kruglaya and N. S. Vyazankin, *React. Kinet. Catal. Lett.*, **12**, 491 (1979).
- 6.1. L. Melander, *Isotope Effects on Reaction Rates*, Ronald Press Co., New York, 1960.
- 6.2. Yu. N. Molin, R. Z. Sagdeev and K. M. Salikhov, *Soviet Sci. Rev. sect. B Chem. Rev.*, **1**, 1 (1979).
- 6.3. S. Seltzer and E. J. Hamilton, Jr., *J. Amer. Chem. Soc.*, **88**, 3775 (1966).
- 6.4. S. Rummel, H. Hubner and P. Krumbiegel, *Z. Chem.*, **7**, 351 (1967).
- 6.5. J. A. Pople, D. L. Beveridge and P. A. Dobosh, *J. Amer. Chem. Soc.*, **90**, 4201 (1968).
- 6.6. Yu. N. Molin and R. Z. Sagdeev, *Lecture at the All-Union Conference on Chemical Kinetics Dedicated to 80th Birthday of Academician N. N. Semenov*, Moscow, 1976.
- 6.7. R. Z. Sagdeev, T. V. Leshina, M. A. Kamkha, O. I. Belchenko, Yu. N. Molin and A. I. Rezvukhin, *Chem. Phys. Lett.*, **48**, 89 (1977).
- 6.8. A. L. Buchachenko, E. M. Galimov, V. V. Yershov, G. A. Nikiforov and A. D. Pershin, *Dokl. AN SSSR*, **228**, 379 (1976).
- 6.9. R. Kaptein, J. A. den Hollander, D. Antheunis and L. J. Oosterhoff, *J. Chem. Soc. Chem. Commun.*, 1687 (1970).
- 6.10. L. Sterna and A. Pines, *Annual Report of Materials and Molecular Research Division of Lawrence Berkeley Laboratory*, University of California, LBL-7355, HC-13, TID-4500-R66, 1977.
- 6.11. N. J. Turro and B. Kraeutler, *J. Amer. Chem. Soc.*, **100**, 7432 (1978).
- 6.12. V. F. Tarasov, A. D. Pershin and A. L. Buchachenko, *Izv. AN SSSR ser. khim.*, (1980).
- 6.13a. A. V. Podoplelov, T. V. Leshina, R. Z. Sagdeev, Yu. N. Molin and V. I. Goldanskiy, *Pis'ma ZhETF*, **29**, 419 (1979).
- 6.13b. A. V. Podoplelov, V. I. Medvedev, R. Z. Sagdeev, K. M. Salikhov, Yu. N. Molin, V. M. Moralev and I. N. Misko, *Abstracts of Conference on Chemically Induced Spin Polarization and Magnetic Effects in Chemical Reactions*, Novosibirsk, 1981, p. 81.
- 6.14. B. Brocklehurst, *Chem. Phys. Lett.*, **44**, 245 (1976).
- 6.15. R. S. Dixon, F. P. Sargent, V. J. Lopata and E. M. Gardy, *Chem. Phys. Lett.*, **47**, 108 (1977).
- 6.16. A. L. Buchachenko, *Zh. Fiz. Khim.*, **51**, 2461 (1977).
- 6.17. R. N. Clayton, L. Grossman and T. K. Mayeda, *Science*, **182**, 485 (1973).
- 7.1. A. L. Buchachenko, *Khimicheskaya polyarizatsiya elektronov i yader*. Nauka, Moscow, 1974.
- 7.2. A. L. Buchachenko, A. V. Kessenikh and S. V. Rykov, *Teor. Eksp. Khim.*, **6**, 677 (1970).
- 7.3. G. L. Closs and L. E. Closs, *J. Amer. Chem. Soc.*, **91**, 4549 (1969).
- 7.4. R. Kaptein, J. A. den Hollander, D. Antheunis and L. J. Oosterhoff, *J. Chem. Soc. Chem. Commun.*, 1687 (1970).
- 7.5. S. M. Rosenfeld, R. G. Lawler and H. R. Ward, *J. Amer. Chem. Soc.*, **95**, 946 (1973).
- 7.6. M. Cocivera, C. A. Fyfe, Sh. P. Vaish and H. E. Chen, *J. Amer. Chem. Soc.*, **96**, 1611 (1974).
- 7.7. R. G. Lawler and M. Halfon, *Rev. Sci. Instrum.*, **45**, 84 (1974).
- 7.8. A. D. Trifunac, K. W. Johnson and R. H. Lowers, *J. Amer. Chem. Soc.*, **98**, 6067 (1976).
- 7.9. A. D. Trifunac and D. J. Nelson, *Chem. Phys. Lett.*, **46**, 346 (1977).
- 7.10. H. Fischer and G. P. Laroff, *Chem. Phys.*, **3**, 217 (1974).
- 7.11. H. C. Torrey, *Phys. Rev.*, **76**, 1059 (1949).
- 7.12. R. Kaptein, *Adv. Free-Radic. Chem.*, **5**, 319 (1975).
- 7.13. S. Schaublin, A. Hohener and R. R. Ernst, *J. Magn. Resonance*, **13**, 196 (1974).
- 7.14. C. F. Poranski Jr., S. A. Sojka and W. B. Monitz, *J. Amer. Chem. Soc.*, **98**, 1337 (1976).
- 7.15. K. A. Christensen, D. M. Grant, E. M. Schulman and Ch. Walling, *J. Phys. Chem.*, **78**, 1971 (1974).
- 7.16. G. L. Closs and R. J. Miller, *J. Amer. Chem. Soc.*, **101**, 1639 (1979).
- 7.17. R. Kaptein, Thesis, Leiden, 1971.
- 7.18. Yu. G. Gladkiy, R. Z. Sagdeev, Yu. N. Molin, V. D. Zhidkov and V. V. Pervukhin, in *Vsesoyuznaya Konferentsiya "Polyarizatsiya yader i elektronov i efekty magnitnogo polya v khimicheskikh*

- reaktsiyakh". Tezisy doklada* (Abstracts of papers presented at the All-Union Conference on Polarization of Nuclei and Electrons and Effects of Magnetic Fields in Chemical Reactions). R. Z. Sagdeev (Editor) Novosibirsk, 1975, p. 24.
- 7.19. Yu. A. Grishin, B. D. Naumov and R. Z. Sagdeev, *Radiospektroskopiya (Perm')*, **11**, 83 (1978).
- 7.20. A. V. Dushkin, Yu. A. Grishin, T. V. Leshina and R. Z. Sagdeev, *Tetrahedron Lett.*, 1309 (1977).
- 7.21. R. Z. Sagdeev, Yu. A. Grishin and A. V. Dushkin, *Chem. Phys. Lett.*, **46**, 343 (1977).
- 7.22. Yu. A. Grishin, A. V. Dushkin and R. Z. Sagdeev, *Khim. Vysok. Energ.*, **12**, 278 (1978).
- 7.23. R. Z. Sagdeev, Thesis, Novosibirsk, 1977.
- 7.24. D. A. Hutchinson, H. M. Vyas, S. K. Wong and J. K. S. Wan, *Mol. Phys.*, **29**, 1767 (1975).
- 7.25. G. L. Closs, *J. Amer. Chem. Soc.*, **91**, 4552 (1969).
- 7.26. G. L. Closs, *Adv. Magn. Resonance*, **7**, 157 (1974).
- 7.27. S. R. Fahrenholtz and A. M. Trozzolo, *J. Amer. Chem. Soc.*, **93**, 251 (1971).
- 7.28. R. G. Lawler, *Progr. NMR Spectr.*, **9**, 147 (1973).
- 7.29. J. A. den Hollander and R. Kaptein, *Chem. Phys. Lett.*, **41**, 257 (1976).
- 7.30. Yu. A. Grishin, A. V. Dushkin, T. V. Leshina, Yu. N. Molin, R. Z. Sagdeev and R. Kaptein, in *Magnetic Resonance and Related Phenomena*. Proceedings of the XXth Congress AMPERE, E. Kundla, E. Lippmaa and T. Saluvere, (Editors) Springer, Berlin, Heidelberg, New York, 1979, p. 158.
- 7.31. H. R. Ward, *Accounts Chem. Res.*, **5**, 18 (1972).
- 7.32. R. Kaptein, J. Brokken-Zijp and F. J. J. de Kanter, *J. Amer. Chem. Soc.*, **94**, 6280 (1972).
- 7.33. E. Lippmaa, T. Pehk, A. L. Buchachenko and S. V. Rykov, *Chem. Phys. Lett.*, **5**, 521 (1970).
- 7.34. A. L. Buchachenko, S. V. Rykov, A. V. Kessenikh and G. S. Bylina, *Dokl. AN SSSR*, **190**, 839 (1970).
- 7.35. H. R. Ward, R. G. Lawler and R. A. Cooper, *J. Amer. Chem. Soc.*, **91**, 746 (1969).
- 7.36. G. L. Closs, C. E. Doubleday and D. R. Paulson, *J. Amer. Chem. Soc.*, **92**, 2185 (1970).
- 7.37. R. A. Cooper, R. G. Lawler and H. R. Ward, *J. Amer. Chem. Soc.*, **94**, 552 (1972).
- 7.38. R. Kaptein, in *Chemically Induced Magnetic Polarization*. A. R. Lepley, G. L. Closs (Editors) Wiley, New York, London, Sydney, Toronto, 1973, p. 137.
- 7.39. R. A. Cooper, R. G. Lawler and H. R. Ward, *J. Amer. Chem. Soc.*, **94**, 545 (1972).
- 7.40. R. Z. Sagdeev, Yu. N. Molin, K. M. Salikhov, T. V. Leshina, M. A. Kamkha and S. M. Shein, *Org. Magn. Resonance*, **5**, 599 (1973).
- 7.41. J. A. den Hollander, Thesis, Leiden, 1976.
- 7.42. A. V. Podoplelov, T. V. Leshina, R. Z. Sagdeev, M. A. Kamkha and S. M. Shein, *Zh. Org. Khim.*, **12**, 495 (1976).
- 7.43. A. V. Dushkin, I. M. Sychova, T. V. Lyoshina and R. Z. Sagdeev, *Izv. AN SSSR, ser. khim.*, 559 (1977).
- 7.44. A. V. Dushkin, T. V. Leshina, I. M. Sychova and R. Z. Sagdeev, Ref. 7.18, p. 22.
- 7.45. R. N. Musin and P. V. Schastnev, *Zh. Strukt. Khim.*, **17**, 419 (1976).
- 7.46. A. L. Buchachenko and A. M. Vasserman, *Stabil'nyye Radikaly*. Khimiya, Moscow, 1973.
- 7.47. F. J. J. de Kanter, Thesis, Leiden, 1978.
- 7.48. F. J. J. de Kanter, R. Kaptein and R. A. van Santen, *Chem. Phys. Lett.*, **45**, 575 (1977).
- 7.49. I. Ya. Slonim, Ya. G. Urman and A. G. Konovalov, *Dokl. AN SSSR*, **195**, 1153 (1970).
- 7.50. M. Lehnig and H. Fischer, *Z. Naturforsch.*, **24a**, 1771 (1969).
- 7.51. H. Fischer and M. Lehnig, *J. Phys. Chem.*, **75**, 3410 (1971).
- 7.52. H. Fischer, In. Ref. 7.38, p. 197.
- 7.53. S. V. Rykov, A. L. Buchachenko and V. I. Baldin, *Zh. Strukt. Khim.*, **10**, 928 (1969).
- 7.54. R. Kaptein and J. A. den Hollander, *J. Amer. Chem. Soc.*, **94**, 6269 (1972).
- 7.55. G. T. Evans and R. G. Lawler, *Mol. Phys.*, **30**, 1085 (1975).
- 7.56. H. M. Vyas, S. K. Wong, B. B. Adeleke and J. K. S. Wan, *J. Amer. Chem. Soc.*, **97**, 1385 (1975).
- 7.57. K. Y. Choo and J. K. S. Wan, *J. Amer. Chem. Soc.*, **97**, 7127 (1975).
- 7.58. H. Fischer, *Ind. Chim. Belg.* **36**, 1054 (1971).
- 7.59. M. Lehnig and H. Fischer, *Z. Naturforsch.*, **27a**, 1300 (1972).

- 7.60. A. L. Buchachenko, R. Z. Sagdeev and K. M. Salikhov, *Magnitnyye i spinovyye efekty v khimicheskikh reaktsiyakh*. Nauka, Novosibirsk, 1978, p. 217.
- 7.61. D. Bethell and M. R. Brinkman, *Adv. Phys. Org. Chem.*, **10**, 53 (1973).
- 7.62. A. L. Buchachenko, *Zh. Vses. Khim. Obshchest.*, **19**, 250 (1974).
- 7.63. A. L. Buchachenko, *Usp. Khim.*, **45**, 761 (1976).
- 7.64. G. L. Closs, *Proc. 23rd International Congress of Pure and Applied Chemistry*, **4**, 19 (1971).
- 7.65. G. L. Closs and A. D. Trifunac, *J. Amer. Chem. Soc.*, **92**, 7227 (1970).
- 7.66. B. Blank and H. Fischer, *Helv. Chim. Acta*, **54**, 905 (1971).
- 7.67. A. L. Buchachenko and Sh. A. Markarian, *Int. J. Chem. Kinet.*, **4**, 513 (1971).
- 7.68. A. L. Buchachenko, *Ind. Chim. Belge*, **36**, 1065 (1971).
- 7.69. U. Schollkopf, U. Ludwig, G. Ostermann and M. Patsch, *Tetrahedron Lett.*, 3415 (1969).
- 7.70. F. Gerhart and L. Wilde, *Tetrahedron Lett.*, 475 (1974).
- 7.71. J. E. Baldwin, W. F. Erickson, R. E. Hackler and R. M. Scott, *J. Chem. Soc. Chem. Commun.*, 576 (1970).
- 7.72. H. Iwamura, M. Iwamura, T. Nishida and Sh. Sato, *J. Amer. Chem. Soc.*, **92**, 7474 (1970).
- 7.73. A. D. Pershin, D. G. Pobedimskiy, V. A. Kurbatov and A. L. Buchachenko, *Izv. AN SSSR ser. khim.*, 581 (1975).
- 7.74. D. G. Pobedimskiy, A. D. Pershin, Sh. A. Nasybullin and A. L. Buchachenko, *Izv. AN SSSR ser. khim.*, 79 (1976).
- 7.75. A. D. Pershin, N. M. Lapshin and A. L. Buchachenko, *Izv. AN SSSR*, 1001 (1976).
- 7.76. G. A. Nikiforov, A. D. Pershin, A. L. Buchachenko and V. V. Yershov, Ref. 7.18, p. 17.
- 7.77. Ch. Walling and A. R. Lepley, *J. Amer. Chem. Soc.*, **94**, 2007 (1972).
- 7.78. N. N. Bubnov, K. A. Bilevich and O. Yu. Okhlobystin, *Priroda*, **5**, 4 (1971).
- 7.79. E. Lippmaa, T. Pehk and T. Saluvere, *Ind. Chim. Belge*, **36**, 1070 (1971).
- 7.80. N. N. Bubnov, B. Ya. Medvedev, L. A. Polyakova, K. A. Bilevich and O. Yu. Okhlobystin, *Org. Magn. Resonance*, **5**, 437 (1973).
- 7.81. E. Lippmaa, T. Pehk, T. Saluvere and M. Magi, *Org. Magn. Resonance*, **5**, 441 (1973).
- 7.82. A. L. Buchachenko and E. T. Lippmaa, *Vestn. AN SSSR*, No 1, p. 120 (1973).
- 7.83. E. Lippmaa, T. Saluvere, T. Pehk and A. Olivson, *Org. Magn. Resonance*, **5**, 429 (1973).
- 7.84. H. W. H. J. Bodewitz, C. Blomberg and F. Bickelhaupt, *Tetrahedron Lett.*, 281 (1972).
- 7.85. H. W. H. J. Bodewitz, C. Blomberg and F. Bickelhaupt, *Tetrahedron*, **29**, 719 (1973); **31**, 1053 (1975).
- 7.86. H. W. H. J. Bodewitz, C. Blomberg and F. Bickelhaupt, *Tetrahedron Lett.*, 2003 (1975).
- 7.87. R. G. Lawler and P. Livant, *J. Amer. Chem. Soc.*, **98**, 3710 (1976).
- 7.88. B. J. Schaart, H. W. H. J. Bodewitz, C. Blomberg and F. Bickelhaupt, *J. Amer. Chem. Soc.*, **98**, 3712 (1976).
- 7.89. H. R. Ward, R. G. Lawler and Th. A. Marzli, *Tetrahedron Lett.*, 521 (1970).
- 7.90. L. F. Kasukhin, M. P. Ponomarchuk and Zh. F. Buteyko, *Zh. Org. Khim.*, **8**, 665 (1972).
- 7.91. B. Blank, P. Mennitt and H. Fischer, *Proc. 23rd International Congress of Pure and Applied Chemistry*, **4**, 1 (1971).
- 7.92. Ref. 7.60, p. 235.
- 7.93. M. Cocivera and A. M. Trozzolo, *J. Amer. Chem. Soc.*, **92**, 1772 (1970).
- 7.94. G. L. Closs and D. R. Paulson, *J. Amer. Chem. Soc.*, **92**, 7229 (1970).
- 7.95. N. A. Porter, L. J. Marnett, C. H. Lochmüller, G. L. Closs and M. Shobataki, *J. Amer. Chem. Soc.*, **94**, 3664 (1972).
- 7.96. H. M. Vyas and J. K. S. Wan, *Canad. J. Chem.*, **54**, 979 (1976).
- 7.97. K. A. Muszkat and M. Weinstein, *J. Chem. Soc. Chem. Commun.*, 143 (1975).
- 7.98. K. A. Muszkat and M. Weinstein, *J. Chem. Soc. Perkin Trans.*, 1072 (1976).
- 7.99. H. D. Roth and A. A. Lamola, *J. Amer. Chem. Soc.*, **96**, 6270 (1974).
- 7.100. H. D. Roth, *Mol. Photochem.*, **5**, 91 (1973).
- 7.101. H. D. Roth and M. L. Manion Schilling, *J. Amer. Chem. Soc.*, **101**, 1898 (1979).
- 7.102. T. V. Leshina, S. G. Belyaeva, V. I. Maryasova, R. Z. Sagdeev and Yu. N. Molin, *Chem. Phys. Lett.*, **75**, 438 (1980).

- 7.103. B. Blank, A. Henne, G. P. Laroff and H. Fischer, *Pure Appl. Chem.*, **41**, 475 (1975).
- 7.104. S. A. Sojka, C. F. Poranski Jr. and W. B. Moniz, *J. Amer. Chem. Soc.*, **97**, 5953 (1975).
- 7.105. S. A. Sojka, C. F. Poranski Jr. and W. B. Moniz, *J. Magn. Resonance*, **23**, 417 (1976).
- 7.106. D. Bethell, M. R. Brinkman and J. Hayes, *J. Chem. Soc. Chem. Commun.*, 475 (1972).
- 7.107. R. Bausch, H.-P. Schuchmann, C. van Sonntag, R. Benn and H. Dreeskamp, *J. Chem. Soc. Chem. Commun.*, 418 (1976).
- 7.108. R. Kaptein, *J. Amer. Chem. Soc.*, **94**, 6262 (1972).
- 7.109. J. A. den Hollander, *Chem. Phys.*, **10**, 167 (1975).
- 7.110. P. Livant and R. G. Lawler, *J. Amer. Chem. Soc.*, **98**, 6044 (1976).
- 7.111. S. Ogawa and R. W. Fessenden, *J. Chem. Phys.*, **41**, 994 (1964).
- 7.112. K. G. Seifert and F. Gerhart, *Tetrahedron Lett.*, 829 (1974).
- 7.113. L. F. Kasukhin, M. P. Ponomarchuk and A. L. Buchachenko, *Chem. Phys.*, **3**, 136 (1974).
- 7.114. R. Kaptein, F. M. Verheus and L. J. Oosterhoff, *J. Chem. Soc. Chem. Commun.*, 877 (1971).
- 7.115. F. J. J. de Kanter, *Org. Magn. Resonance*, **8**, 129 (1976).
- 7.116. R. Benn, *Chem. Phys.*, **15**, 369 (1976).
- 7.117. P. W. N. M. Leeuwen, R. Kaptein, R. Huis and C. F. Roobek, *J. Organometal. Chem.*, **104**, C44 (1976).
- 7.118. V. M. Kuznets, D. N. Shigorin and A. L. Buchachenko, *Dokl. AN SSSR*, **234**, 1112 (1977).
- 7.119. J. A. den Hollander and J. P. M. van der Ploeg, *Tetrahedron*, **32**, 2433 (1976).
- 7.120. H. Iwamura, M. Iwamura, M. Imanari and M. Takeuchi, *Tetrahedron Lett.*, 2325 (1973).
- 7.121. G. A. Nikiforov, Sh. A. Markaryan, L. G. Plekhanova, B. D. Sviridov, S. V. Rykov, V. V. Ershov, A. L. Buchachenko, T. Pehk, T. Saluvere and E. Lippmaa, *Org. Magn. Resonance*, **5**, 339 (1973).
- 7.122. M. L. Kaplan, M. L. Manion and H. D. Roth, *J. Phys. Chem.*, **78**, 1837 (1974).
- 7.123. E. T. Lippmaa, T. I. Pehk, A. L. Buchachenko and S. V. Rykov, *Dokl. AN SSSR*, **195**, 632 (1970).
- 7.124. H. D. Roth and M. L. Kaplan, *J. Amer. Chem. Soc.*, **95**, 262 (1973).
- 7.125. M. R. Brinkman, D. Bethell and J. Hayes, *Tetrahedron Lett.*, 989 (1973).
- 7.126. P. H. Kasai, E. Hedaya and E. B. Whipple, *J. Amer. Chem. Soc.*, **91**, 4364 (1969).
- 7.127. Ch. Brown, R. F. Hudson and A. J. Lawson, *J. Amer. Chem. Soc.*, **95**, 6500 (1973).
- 7.128. J. H. Hargis and Ph. B. Shevlin, *J. Chem. Soc. Chem. Commun.*, 179 (1973).
- 7.129. M. Lehnig and H. Fischer, *Z. Naturforsch.*, **25a**, 1963 (1970).
- 7.130. D. J. Carlsson and K. U. Ingold, *J. Amer. Chem. Soc.*, **90**, 7074 (1968).
- 7.131. R. Kaptein, K. Dijkstra and K. Nicolay, *Nature*, **274**, 293 (1978).
- 7.132. R. Kaptein, K. Dijkstra, F. Muller, C. G. van Schagen and A. J. W. G. Visser, *J. Magn. Resonance*, **31**, 171, (1978).
- 7.133. R. Kaptein, *Proc. European Conference on NMR of Macromolecules*, Sassari, Sardinia, 1978.
- 7.134. J. F. Garst and J. A. Pacifici, *J. Amer. Chem. Soc.*, **27**, 1802 (1975).
- 7.135. J. F. Garst, R. H. Cox, J. T. Barbas, R. D. Roberts, J. I. Morris and R. C. Morrison, *J. Amer. Chem. Soc.*, **92**, 5761 (1970).
- 7.136. J. F. Garst, F. E. Barton II and J. I. Morris, *J. Amer. Chem. Soc.*, **93**, 4310 (1971).
- 7.137. J. F. Garst, *Free Radicals*, **1**, 503 (1973).
- 7.138. J. F. Garst, In Ref. 7.38, p. 223.
- 7.139. M. A. Kamkha, N. M. Katkova, T. V. Leshina, R. Z. Sagdeev and S. M. Shein, *Tetrahedron Lett.*, 1313 (1977).
- 7.140. A. Rieker, P. Niederer and H. B. Stegmann, *Tetrahedron Lett.*, 3873 (1971).
- 7.141. K. A. Bilevich, N. N. Bubnov, B. Ya. Medvedev, O. Yu. Okhlobystin and L. V. Ermanson, *Dokl. AN SSSR*, **193**, 583 (1970).
- 7.142. A. F. Levit, A. L. Buchachenko, L. A. Kiprianova and I. P. Gragerov, *Dokl. AN SSSR*, **203**, 628 (1972).
- 7.143. T. G. Sterlyova, L. A. Kiprianova, A. F. Levit and I. P. Gragerov, *Dokl. AN SSSR*, **219**, 1140 (1974).
- 7.144. I. P. Gragerov, A. F. Levit, L. A. Kiprianova, A. L. Buchachenko and T. G. Sterlyova, *Ukr. Khim. Zh.*, **41**, 570 (1975).
- 7.145. N. N. Bubnov, K. A. Bilevich, L. A. Poljakova and O. Yu. Okhlobystin, *J. Chem. Soc. Chem. Commun.*, 1058 (1972).

- 7.146. Ch. Buchardt and E. Merz, *Tetrahedron Lett.*, 2431 (1964).
- 7.147. A. V. Dushkin, Yu. A. Grishin, A. V. Yurkovskaya, R. Z. Sagdeev, F. J. J. de Kanter and R. Kaptein, *Abstracts of Lectures and Posters of the 4th Specialized Colloque Ampere on Dynamical Processes in Molecular Systems Studied by rf-Spectroscopy*. (Karl-Marx-University, Leipzig, 1979, p. 139).
- 7.148. A. V. Dushkin, A. V. Yurkovskaya and R. Z. Sagdeev, *Zh. Fiz. Khim.*, **53**, 2643 (1979); *Chem. Phys. Lett.*, **67**, 524 (1979).
- 7.149. G. L. Closs and C. E. Doubleday, *J. Amer. Chem. Soc.*, **94**, 9248 (1972).
- 7.150. G. L. Closs and C. E. Doubleday, *J. Amer. Chem. Soc.*, **95**, 2735 (1973).
- 7.151. R. Kaptein, R. Freeman and H. D. Hill, *Chem. Phys. Lett.*, **26**, 104 (1974).
- 7.152. P. W. Atkins and G. T. Evans, *Chem. Phys. Lett.*, **24**, 45 (1974).
- 7.153. F. J. J. de Kanter, J. A. den Hollander, A. H. Huizer and R. Kaptein, *Mol. Phys.*, **34**, 857 (1977).
- 7.154. F. J. J. de Kanter, R. Z. Sagdeev and R. Kaptein, *Chem. Phys. Lett.*, **58**, 334 (1978).
- 7.155. Yu. A. Grishin, A. V. Dushkin, R. Z. Sagdeev, Yu. G. Gladky and R. Kaptein, Ref. 7.147, p. 140.
- 7.156. Yu. A. Grishin, A. V. Dushkin and R. Z. Sagdeev, U.S.S.R. patent No. 594469 (Official Bulletin 1978, N. 7., p. 177).
- 7.157. V. L. Berdinskiy, A. L. Buchachenko and A. D. Pershin, *Teor. Eksp. Khim.*, **12**, 666 (1976).
- 7.158. A. G. Zhuravlev, V. L. Berdinskiy and A. L. Buchachenko, *Pis'ma ZhETF*, **28**, 150 (1978).
- 7.159. R. Z. Sagdeev, *Lecture at the International Symposium on Magnetic Resonance in Physics Chemistry and Biology*, Argonn, National Laboratory, Illinois, USA 1979.
- 7.160. R. Z. Sagdeev, Yu. A. Grishin, A. Z. Gogolev, A. V. Dushkin, A. G. Semyonov and Yu. N. Molin, *Zh. Strukt. Khim.*, **20**, 1132 (1979).
- 8.1. P. J. Hore, C. G. Joslin and K. A. McLauchlan, *Chem. Soc. Rev.* **8**, 29 (1979).
- 8.2. P. W. Atkins, K. A. McLauchlan and A. F. Simpson, *Nature*, **219**, 927 (1968).
- 8.3. K. Y. Choo and J. K. S. Wan, *J. Amer. Chem. Soc.*, **97**, 7127 (1975).
- 8.4. H. M. Vyas, S. K. Wong, B. B. Adeleke and J. K. S. Wan, *J. Amer. Chem. Soc.*, **97**, 1385 (1975).
- 8.5. P. W. Atkins, I. C. Buchanan, R. C. Gurd, K. A. McLauchlan and A. F. Simpson, *J. Chem. Soc. Chem. Commun.*, 513 (1970).
- 8.6. R. W. Fessenden and R. H. Schuler, *J. Chem. Phys.*, **39**, 2147 (1963).
- 8.7. H. Zeldes and R. Livingston, *J. Phys. Chem.*, **74**, 3336 (1970).
- 8.8. H. Zeldes and R. Livingston, *J. Chem. Phys.*, **53**, 1406 (1970).
- 8.9. R. Livingston and H. Zeldes, *J. Magn. Resonance*, **9**, 331 (1973).
- 8.10. H. Paul and H. Fischer, *Z. Naturforsch.*, **25a**, 443 (1970).
- 8.11. V. F. Shuvalov, P. A. Stunzhas and A. P. Moravskiskii, *Org. Magn. Resonance*, **5**, 347 (1973).
- 8.12. H. Paul, *Chem. Phys.*, **15**, 115 (1976).
- 8.13. B. Smaller, E. C. Avery and J. R. Remko, *J. Chem. Phys.*, **55**, 2414 (1971).
- 8.14. P. Neta, R. W. Fessende and R. H. Schuler, *J. Phys. Chem.*, **75**, 1654 (1971).
- 8.15. N. C. Verma and R. W. Fessenden, *J. Chem. Phys.*, **58**, 2501 (1973).
- 8.16. K. Eiben and R. W. Fessenden, *J. Phys. Chem.*, **75**, 1186 (1971).
- 8.17. R. W. Fessenden, *J. Chem. Phys.*, **58**, 2489 (1973).
- 8.18. B. Smaller, J. R. Remko, E. C. Avery, *J. Chem. Phys.*, **48**, 5174 (1968).
- 8.19. A. D. Trifunac and E. C. Avery, *Chem. Phys. Lett.*, **27**, 141 (1974).
- 8.20. A. D. Trifunac and M. C. Thurnauer, *J. Chem. Phys.*, **62**, 4889 (1975).
- 8.21. A. D. Trifunac and E. C. Avery, *Chem. Phys. Lett.*, **28**, 294 (1974).
- 8.22. P. B. Ayscough, T. H. English, G. Lambert and A. J. Elliot, *Chem. Phys. Lett.*, **34**, 557 (1975).
- 8.23. A. D. Trifunac, *J. Amer. Chem. Soc.*, **98**, 5202 (1976).
- 8.24. P. W. Atkins, J. M. Frimston, P. G. Frith, R. C. Gurd and K. A. McLauchlan, *J. Chem. Soc. Faraday Trans. II*, **69**, 1542 (1973).
- 8.25. S. H. Glarum and J. H. Marshall, *J. Chem. Phys.*, **52**, 5555 (1970).
- 8.26. A. Friedenberg and H. Levanon, *Chem. Phys. Lett.*, **41**, 84 (1976).
- 8.27. R. W. Fessenden and N. C. Verma, *J. Amer. Chem. Soc.*, **98**, 243 (1976).
- 8.28. H. Shiraishi, H. Kadoi, Y. Katsumura, Y. Tabata and K. Oshima, *J. Phys. Chem.*, **78**, (1336) 1974.
- 8.29. P. W. Atkins and G. T. Evans, *Mol. Phys.*, **27**, 1633 (1974).

- 8.30. P. W. Atkins, K. A. McLauchlan and P. W. Percival, *J. Chem. Soc. Chem. Commun.*, 121 (1973).
- 8.31. P. W. Atkins, A. J. Dobbs, G. T. Evans, K. A. McLauchlan and P. W. Percival, *Mol. Phys.*, **27**, 769 (1974).
- 8.32. P. W. Atkins, A. J. Dobbs and K. A. McLauchlan, *Chem. Phys. Lett.*, **29**, 616 (1974).
- 8.33. A. J. Dobbs, *Mol. Phys.*, **30**, 1073 (1975).
- 8.34. S. K. Wong and J. K. S. Wan, *J. Amer. Chem. Soc.*, **94**, 7197 (1972).
- 8.35. S. K. Wong, D. A. Hutchinson and J. K. S. Wan, *J. Amer. Chem. Soc.*, **95**, 622 (1973).
- 8.36. S.-K. Wong, D. A. Hutchinson and J. K. S. Wan, *Canad. J. Chem.*, **52**, 251 (1974).
- 8.37. J. K. S. Wan, S.-K. Wong and D. A. Hutchinson, *Acc. Chem. Res.*, **7**, 58 (1974).
- 8.38. H. M. Vyas and J. K. S. Wan, *Canad. J. Chem.*, **54**, 979 (1976).
- 8.39. B. B. Adeleke and J. K. S. Wan, *J. Chem. Soc. Faraday Trans.*, **1**, **72**, 1799 (1976).
- 8.40. P. B. Aysough, G. Lambert and A. J. Elliot, *J. Chem. Soc. Faraday Trans.*, **1**, **72**, 1770 (1976).
- 8.41. P. W. Atkins, A. J. Dobbs and K. A. McLauchlan, *J. Chem. Soc. Faraday Trans.*, **2**, **71**, 1269 (1975).
- 8.42. J. B. Pederson, C. E. M. Hansen, H. Parbo and L. T. Muus, *J. Chem. Phys.*, **63**, 2398 (1975).
- 8.43. J. R. Harbour and G. Tollin, *Photochem. Photobiol.*, **19**, 163 (1974).
- 8.44. F. J. Adrian, *J. Chem. Phys.*, **61**, 4875 (1974)474).
- 8.45. A. J. Dobbs and K. A. McLauchlan, *Chem. Phys. Lett.*, **30**, 257 (1975).
- 8.46. B. B. Adeleke, K. Y. Choo and J. K. S. Wan, *J. Chem. Phys.*, **62**, 3882 (1975).

SUBJECT INDEX

- acetylbenzoyl peroxide 311, 316, 356
acetylcyclopropyl peroxide 351
acetyl peroxide 190, 311, 317, 358
acrylyl peroxide 353
acyl peroxide 329, 362
- bacteriochlorophyll 400
benzaldehydes 316, 343
benzoin 342
benzoyl peroxide 243, 244, 292-294, 305, 307, 308, 311
benzoylpropionyl peroxide 317
biomolecules 365-368
biradicals 51, 139, 205
biradical recombination 199
boundary conditions 100-106
butyllithium
 CIDNP 321, 322
 magnetic field effect 245-250
- cage 13, 33, 34
 primary 34
 secondary 34
cage effect 32, 33
¹³C CIDNP 311, 316-318, 335, 342, 346, 350, 362-364
CIDEP
 discovery of 29
 optimum condition of 228
 origin of 226, 236
CIDNP
 discovery of 29
 multiplet effect 26, 28
 net effect 26, 27
 optimum condition of 329
 origin of 26
cis-trans photoisomerization 267-269, 345
Cross-Kaptein-Oosterhoff (CKO) model 113
- contact
 radius 35
 time 48
continuous diffusion model 99, 103, 104, 110, 118, 179, 186
cooperative effect 191, 351, 355-357
cumene peroxide 310
- delayed fluorescence 283, 287
differential spectra 366
diffusion flux 100, 224
deoxybenzoin 342
diazoaminobenzene 337
dibenzyl ketone 296, 297, 303
diphenyldiazomethane 307
diphenylmethanes 316
diphenyl radical-ions 274
ditert-butyl ketone 301, 342
- electrogenerated chemiluminescence 287, 288
electron spin density distribution 361
electron transfer 90, 101, 344, 345, 396, 400
encounter efficiency tensor 108, 110
energy level broadening 138, 139
energy level crossing 71, 77, 138, 139, 226
exchange integral 64
excited singlet state quenching 345
excited triplet state quenching 344
exponential model 44, 46, 103, 110, 136, 155
- fast reaction 397
¹⁹F CIDNP 362
first contact 39
 distribution of 36
 probability of 37, 40
 recombination probability at 112
 time of 40, 43

- flow systems 300
 fluorescence 298
 formaldehyde 276
 Fourier spectroscopy 303
 free valence migration 342
- geminate recombination 33
 Δg -mechanism 18, 66, 96, 247, 248, 251
- hexafluorobenzene anion 275
 hf-mechanism 18, 66, 96, 246, 247
 hole transfer 90
 hydrogen atom transfer 343, 344
- interradical interactions 99, 101, 102
 Coulomb 42, 48, 134, 139, 184, 234
 dipole-dipole 64
 exchange 48, 64, 97, 111, 125, 155, 159, 184,
 213, 214, 217, 229, 234, 360
- isomers
 nuclear 299
 optical 353
- isotope
 enrichment 295
 separation 299
- kinematic operator 99
- lauroyl peroxide 319
- lifetime
 between encounters 108
 contact 48
 distribution of 44
 in-cage 34, 108, 309
 "settled" 35
- magnetically equivalent nuclei 78, 96
 magnetically non-equivalent nuclei 84, 89
 magnetic field effect
 discovery of 30
 in butyl lithium reaction 245-250
 in *cis-trans* photoisomerization 267-269
 in photolysis of donor/acceptor solutions
 261-267
 in photolysis of formaldehyde 276
 in radiation polymerization 277
 in radioluminescence 256-261
 origin of 13, 22
- magnetic isotope effect
 discovery of 30
 origin of 13, 22
 magnetization 169
 memory effect 350, 356
 micelles 296
- naphthalene radical-ions 273
 ^{15}N CIDNP 335
- numerical calculations of
 CIDEP in high fields 233
 CIDNP in biradicals 224
 CIDNP in high fields 184
 CIDNP in low fields 213, 216
 magnetic isotope effect 115, 167
 magnetic field effect 115, 125-128, 135, 157,
 162, 166
- one re-encounter approximation 114
 Onsager radius 42
- optical deflection of ESR of RP
 principles of 269
 sensitivity of 274
 technique of 272
- optically detected ESR of
 hexafluorobenzene anion 275
 naphthalene radical-ions 273
 in photosynthetic processes 277
- optimum condition of
 CIDEP 228
 CIDNP 329
- oscillating of geminate recombination 120, 184
- paramagnetic relaxation 62, 106, 140, 168, 310,
 340, 357, 365, 390
- ^{31}P CIDNP
- phenylbenzyl ether 347
- photolysis
 direct 243, 244, 252
 sensitized 243
- polarization
 in a primary pair 194
 in a secondary pair 194, 195, 349
 negative 169-173
 optical 236
 positive 169, 173
 redistribution 198
 relaxation 197
 transfer 342
- probability of
 diffusion radical pair recombination 106, 112,
 122, 129, 131, 133, 136, 141

- formation of a molecule with a set nuclear spin configuration 118, 119, 136, 144
- geminate recombination 47, 102, 105, 112, 118, 129, 131, 136, 141, 160
- primary pair recombination 145
- RP escape from a cage 51
- secondary pair recombination 145
- the first contact 40
- triplet product formation 146, 161
- product
 - bulk recombination 34
 - escape 33
 - geminate 33
- projection operator 100

- quantum yield of RP generation 295
- quenching of triplet states 286–288

- radical interactions
 - anisotropic 62
 - isotropic 61
- radical-ion pairs
 - effect of deuteration in recombination of 258, 263–266
 - in *cis-trans* photoisomerization 267–269
 - in photosynthetic processes 277
 - photochemical generation of 261
 - quantum oscillations in recombination of 259
 - radiation-chemical generation of 256
- radical pairs 34
 - correlated 14, 59, 60, 390
 - diffusion 34, 338
 - F*-pairs 173
 - initial state of 101
 - one-nucleus 26
 - secondary 349–351
 - short-lived 178, 230–232
 - singlet-triplet transitions in 15, 59, 61
 - spin states of 14
 - uncorrelated 14, 59, 60, 173, 311, 338, 341, 390
- radical rotation 334
- rate constant of diffusional encounters 43, 44, 51
- reaction
 - fast 300
 - geminate 33
 - layer thickness 46, 47, 57
 - of rearrangement 334
 - with acceptors 45
- reaction field 381
- reactivity anisotropy 54, 60, 106, 131
- recombination
 - bulk 43, 51
 - geminate 33, 34, 46
 - non-stationary 52, 123
- re-encounters 33, 130
 - number of 36, 39
 - probability distribution 36–39
- rotating sector technique 390

- singlet-triplet transitions in radical pairs
 - Ag*-mechanism of 18, 66, 96
 - hf-mechanism of 18, 66, 96
 - interference of 156, 203, 205, 207, 212
 - mechanisms of 16, 236
 - relaxation mechanism of 19
 - transition frequency 22
 - under microwave irradiation 270–272
 - vector model for 17
- slow reaction 328
- solvated electron 394, 395
- spin delocalization 361
- spin exchange 235
- spin polarization 361
- spin selection rule 58, 141, 146
- stilbene 345

- tartaric acid 391
- tetrafluoroquinone 343
- time-resolved CIDNP 304
- total spin 64
- triazene 335
- trimolecular reactions 199

- vector models 17, 226, 355
- violation of Kaptein rules 175, 180–184

- zero field splitting 237

